INFLAMMATORY MECHANISMS OF HEMOLYTIC DISEASES

EDITED BY: Renata Sesti-Costa, Caroline Le Van Kim, Nicola Conran, João Luiz Silva-Filho and Wilma Barcellini

PUBLISHED IN: Frontiers in Immunology

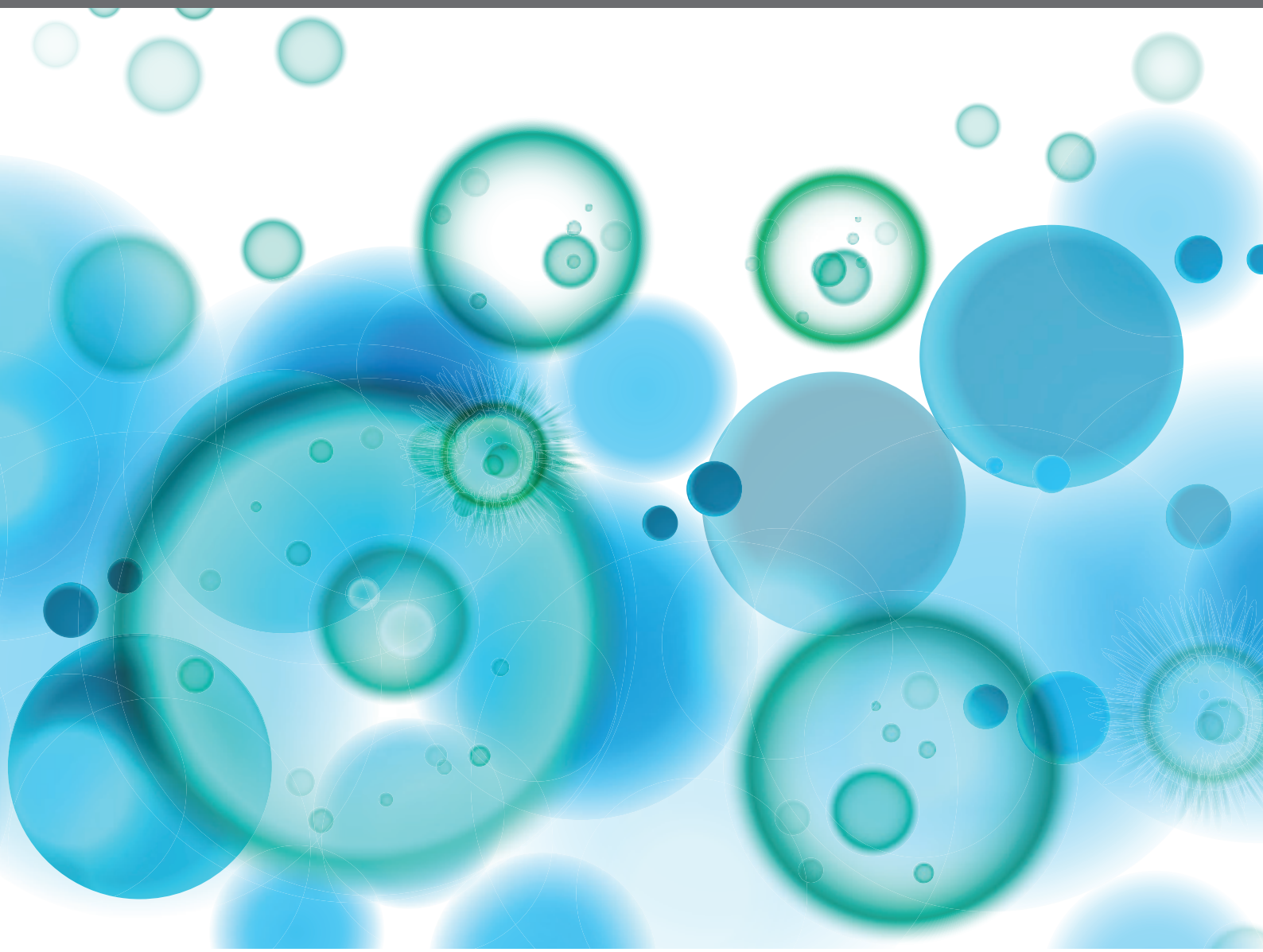

frontiers Research Topics

ISSN 1664-8714
ISBN 978-2-88974-427-5
DOI 10.3389/978-2-88974-427-5

About Frontiers

Frontiers is more than just an open-access publisher of scholarly articles: it is a pioneering approach to the world of academia, radically improving the way scholarly research is managed. The grand vision of Frontiers is a world where all people have an equal opportunity to seek, share and generate knowledge. Frontiers provides immediate and permanent online open access to all its publications, but this alone is not enough to realize our grand goals.

Frontiers Journal Series

The Frontiers Journal Series is a multi-tier and interdisciplinary set of open-access, online journals, promising a paradigm shift from the current review, selection and dissemination processes in academic publishing. All Frontiers journals are driven by researchers for researchers; therefore, they constitute a service to the scholarly community. At the same time, the Frontiers Journal Series operates on a revolutionary invention, the tiered publishing system, initially addressing specific communities of scholars, and gradually climbing up to broader public understanding, thus serving the interests of the lay society, too.

Dedication to Quality

Each Frontiers article is a landmark of the highest quality, thanks to genuinely collaborative interactions between authors and review editors, who include some of the world's best academicians. Research must be certified by peers before entering a stream of knowledge that may eventually reach the public - and shape society; therefore, Frontiers only applies the most rigorous and unbiased reviews.
Frontiers revolutionizes research publishing by freely delivering the most outstanding research, evaluated with no bias from both the academic and social point of view. By applying the most advanced information technologies, Frontiers is catapulting scholarly publishing into a new generation.

What are Frontiers Research Topics?

Frontiers Research Topics are very popular trademarks of the Frontiers Journals Series: they are collections of at least ten articles, all centered on a particular subject. With their unique mix of varied contributions from Original Research to Review Articles, Frontiers Research Topics unify the most influential researchers, the latest key findings and historical advances in a hot research area! Find out more on how to host your own Frontiers Research Topic or contribute to one as an author by contacting the Frontiers Editorial Office: frontiersin.org/about/contact

INFLAMMATORY MECHANISMS OF HEMOLYTIC DISEASES

Topic Editors:
Renata Sesti-Costa, State University of Campinas, Brazil
Caroline Le Van Kim, Université Paris Diderot, France
Nicola Conran, State University of Campinas, Brazil
João Luiz Silva-Filho, University of Glasgow, United Kingdom
Wilma Barcellini, IRCCS Ca 'Granda Foundation Maggiore Policlinico Hospital, Italy

Citation: Sesti-Costa, R., Van Kim, C. L., Conran, N., Silva-Filho, J. L., Barcellini, W., eds. (2022). Inflammatory Mechanisms of Hemolytic Diseases. Lausanne: Frontiers Media SA. doi: 10.3389/978-2-88974-427-5

Table of Contents

05 ***Editorial: Inflammatory Mechanisms of Hemolytic Diseases***
Renata Sesti-Costa, João Luiz Silva-Filho, Wilma Barcellini, Caroline Le Van Kim and Nicola Conran

08 ***The Role of Hemoglobin Oxidation Products in Triggering Inflammatory Response Upon Intraventricular Hemorrhage in Premature Infants***
Judit Erdei, Andrea Tóth, Andrea Nagy, Benard Bogonko Nyakundi, Zsolt Fejes, Béla Nagy Jr., László Novák, László Bognár, Enikö Balogh, György Paragh, János Kappelmayer, Attila Bácsi and Viktória Jeney

22 ***The Red Blood Cell—Inflammation Vicious Circle in Sickle Cell Disease***
Elie Nader, Marc Romana and Philippe Connes

33 ***New Insights in the Pathogenesis and Therapy of Cold Agglutinin-Mediated Autoimmune Hemolytic Anemia***
Sigbjørn Berentsen

46 ***The Changing Landscape of Autoimmune Hemolytic Anemia***
Wilma Barcellini and Bruno Fattizzo

58 ***Small Paroxysmal Nocturnal Hemoglobinuria Clones in Autoimmune Hemolytic Anemia: Clinical Implications and Different Cytokine Patterns in Positive and Negative Patients***
Bruno Fattizzo, Juri Giannotta, Anna Zaninoni, Austin Kulasekararaj, Lilla Cro and Wilma Barcellini

65 ***Congenital Hemolytic Anemias: Is There a Role for the Immune System?***
Anna Zaninoni, Elisa Fermo, Cristina Vercellati, Anna Paola Marcello, Wilma Barcellini and Paola Bianchi

77 ***Identification of a Heme Activation Site on the MD-2/TLR4 Complex***
John D. Belcher, Ping Zhang, Julia Nguyen, Zachary M. Kiser, Karl A. Nath, Jianjun Hu, John O. Trent and Gregory M. Vercellotti

87 ***Pro-inflammatory Actions of Heme and Other Hemoglobin-Derived DAMPs***
Marcelo T. Bozza and Viktória Jeney

100 ***Hydroxyurea Scavenges Free Radicals and Induces the Expression of Antioxidant Genes in Human Cell Cultures Treated With Hemin***
Sânzio Silva Santana, Thassila Nogueira Pitanga, Jeanne Machado de Santana, Dalila Lucíola Zanette, Jamile de Jesus Vieira, Sètondji Cocou Modeste Alexandre Yahouédéhou, Corynne Stéphanie Ahouefa Adanho, Sayonara de Melo Viana, Nivea Farias Luz, Valeria Matos Borges and Marilda Souza Goncalves

112 ***Hemopexin as an Inhibitor of Hemolysis-Induced Complement Activation***
Victoria Poillerat, Thomas Gentinetta, Juliette Leon, Andreas Wassmer, Monika Edler, Carine Torset, Dandan Luo, Gerald Tuffin and Lubka T. Roumenina

124 ***Heme Induces IL-6 and Cardiac Hypertrophy Genes Transcripts in Sickle Cell Mice***
Oluwabukola T. Gbotosho, Maria G. Kapetanaki, Samit Ghosh, Flordeliza S. Villanueva, Solomon F. Ofori-Acquah and Gregory J. Kato

132 ***Heme on Pulmonary Malaria: Friend or Foe?***
Tatiana Almeida Pádua and Mariana Conceição Souza

138 ***Spatiotemporal Alterations in Gait in Humanized Transgenic Sickle Mice***
Stacy Kiven, Ying Wang, Anupam Aich, Donovan A. Argueta, Jianxun Lei, Varun Sagi, Madhushan Tennakoon, Saad J. Bedros, Nils Lambrecht and Kalpna Gupta

152 ***Association Between Nitric Oxide, Oxidative Stress, Eryptosis, Red Blood Cell Microparticles, and Vascular Function in Sickle Cell Anemia***
Elie Nader, Marc Romana, Nicolas Guillot, Romain Fort, Emeric Stauffer, Nathalie Lemonne, Yohann Garnier, Sarah Chambers Skinner, Maryse Etienne-Julan, Mélanie Robert, Alexandra Gauthier, Giovanna Cannas, Sophie Antoine-Jonville, Benoît Tressières, Marie-Dominique Hardy-Dessources, Yves Bertrand, Cyril Martin, Céline Renoux, Philippe Joly, Marijke Grau and Philippe Connes

165 ***Endothelial Barrier Integrity Is Disrupted* In Vitro *by Heme and by Serum From Sickle Cell Disease Patients***
Vanessa Araujo Gomes Santaterra, Maiara Marx Luz Fiusa, Bidossessi Wilfried Hounkpe, Francine Chenou, Wouitchekpo Vincent Tonasse, Loredana Nilkenes Gomes da Costa, Diego Garcia-Weber, Igor de Farias Domingos, Franciele de Lima, Ivanio Teixeira Borba-Junior, Aderson da Silva Araújo, Antonio Roberto Lucena-Araújo, Marcos André Cavalcante Bezerra, Magnun Nueldo Nunes dos Santos, Fernando Ferreira Costa, Jaime Millán and Erich Vinicius De Paula

175 ***Endothelial TLR4 Expression Mediates Vaso-Occlusive Crisis in Sickle Cell Disease***
Joan D. Beckman†, Fuad Abdullah, Chunsheng Chen, Rachel Kirchner, Dormarie Rivera-Rodriguez, Zachary M. Kiser, Aithanh Nguyen, Ping Zhang, Julia Nguyen, Robert P. Hebbel, John D. Belcher and Gregory M. Vercellotti

185 ***The Worst Things in Life are Free: The Role of Free Heme in Sickle Cell Disease***
Oluwabukola T. Gbotosho, Maria G. Kapetanaki and Gregory J. Kato

207 ***Inflammatory Dendritic Cells Contribute to Regulate the Immune Response in Sickle Cell Disease***
Renata Sesti-Costa, Marina Dorigatti Borges, Carolina Lanaro, Dulcinéia Martins de Albuquerque, Sara Terezinha Olalla Saad and Fernando Ferreira Costa

219 ***Immunological Hallmarks of Inflammatory Status in Vaso-Occlusive Crisis of Sickle Cell Anemia Patients***
Alexander Leonardo Silva-Junior, Nadja Pinto Garcia, Evilázio Cunha Cardoso, Stephanny Dias, Andrea Monteiro Tarragô, Nelson Abrahim Fraiji, Matheus Souza Gomes, Laurence Rodrigues Amaral, Andréa Teixeira-Carvalho, Olindo Assis Martins-Filho, Erich Vinicius De Paula, Allyson Guimarães Costa and Adriana Malheiro

233 ***Soluble MD-2 and Heme in Sickle Cell Disease Plasma Promote Pro-Inflammatory Signaling in Endothelial Cells***
Ping Zhang, Julia Nguyen, Fuad Abdulla, Alexander T. Nelson, Joan D. Beckman, Gregory M. Vercellotti and John D. Belcher

frontiers in Immunology

EDITORIAL
published: 12 January 2022
doi: 10.3389/fimmu.2021.834527

Editorial: Inflammatory Mechanisms of Hemolytic Diseases

Renata Sesti-Costa[1], João Luiz Silva-Filho[2], Wilma Barcellini[3], Caroline Le Van Kim[4] and Nicola Conran[1]*

[1] Hematology and Hemotherapy Center, University of Campinas (UNICAMP), Campinas, Brazil, [2] Wellcome Centre for Molecular Parasitology, Institute of Infection, Immunity and Inflammation, University of Glasgow, Glasgow, United Kingdom, [3] Hematology Unit, Fondazione Istituto di Ricovero e Cura a Carattere Scientifico (IRCCS) Ca' Granda Ospedale Maggiore Policlinico Hospital, Milan, Italy, [4] Université de Paris and Université des Antilles, INSERM, BIGR, Paris, France

Keywords: hemolysis, inflammation, anemia, DAMP, immune response

Editorial on the Research Topic

Inflammatory Mechanisms of Hemolytic Diseases

Hemolytic diseases have several underlying causes and result in reduced red blood cell (RBC) counts due to the destruction of these cells in the circulation. Under homeostatic conditions or mild hemolysis, free hemoglobin (Hb), heme or iron, released by RBCs in the intravascular environment, are neutralized by haptoglobin, hemopexin and transferrin, respectively. These plasmatic complexes are cellularly interiorized, degraded and the iron is recycled for use in new erythroblasts. However, during acute or chronic hemolytic diseases, intravascular scavenger molecules saturate resulting in the accumulation of free RBC components, which are potent danger-associated molecular patterns (DAMPs) sensed by endothelial and innate immune cells that trigger a cascade of oxidative and inflammatory processes. This Research Topic assembles 13 original research and 7 review articles that focus on the mechanisms inducing inflammation and how it contributes to the pathology of acute and chronic hemolytic diseases in human patients and animal models.

Recognized experts in the field contributed review articles to this issue that shed light on the heme-induced mechanisms that lead to tissue damage and disorders. Bozza and Jeney meticulously reviewed the mechanisms by which Hb-derived DAMPS, such as free heme, metHb and ferrylHb, act as proinflammatory triggers. They elucidate the cascade of Hb and heme oxidation, which leads to reactive and damaging molecules, and clarify the knowledge gathered so far about the ligands and the pathways that directly stimulate the activation of endothelial and innate immune cells, promoting endothelial barrier permeability, leukocytes recruitment, secretion of proinflammatory cytokines, the generation of reactive oxygen species (ROS), neutrophil extracellular traps (NET) formation, cell death and trained immunity. Jeney et al. reported that oxidized Hb forms, free heme and a product of heme catabolism, bilirubin, were found in the cerebrospinal fluid from infants with intraventricular hemorrhage (IVH), which correlated with VCAM-1, ICAM-1 and IL-8 levels. The direct effect of Hb products was shown by the treatment of a human brain endothelial cell line with heme, which induced significant production of ROS and decreased cell viability. Furthermore, treatment with either heme or ferrylHb up-regulated VCAM-1, ICAM-1 and IL-8 expression, which was not achieved by native Hb or even metHb, revealing specific functions of the different products of oxidized Hb in endothelial cells.

Pádua and Souza focused their review on the role of heme in pulmonary malaria, a disease characterized by the presence of free heme and heme oxidation due to hemolysis caused by RBC-infected *Plasmodium* sp. The system involved in the clearance of heme has been shown to play a

OPEN ACCESS

Edited and reviewed by:
Pietro Ghezzi,
Brighton and Sussex Medical School, United Kingdom

****Correspondence:***
Renata Sesti-Costa
renata.sesti@gmail.com

Specialty section:
This article was submitted to Inflammation, a section of the journal Frontiers in Immunology

Received: *13 December 2021*
Accepted: *23 December 2021*
Published: *12 January 2022*

Citation:
Sesti-Costa R, Silva-Filho JL, Barcellini W, Le Van Kim C and Conran N (2022) Editorial: Inflammatory Mechanisms of Hemolytic Diseases. Front. Immunol. 12:834527. doi: 10.3389/fimmu.2021.834527

protective role in malaria outcomes, since the level of hemeoxygenase-1 (HO-1), the enzyme responsible for heme detoxification, is positively correlated with protection from multi-organ dysfunction and survival. A peculiar feature of plasmodium infection is the hemozoin, a bio-crystallized structure produced by the parasites after digestion of Hb from infected-RBCs, thus another form of heme derivative that is not present in other hemolytic disorders. Some data show that hemozoin is phagocyted together with the RBCs content mainly by macrophages and monocytes, which become activated to produce proinflammatory cytokines and chemokines, leading to pneumocyte apoptosis and loss of alveolar integrity.

Free heme and iron are extremely oxidative, generating ROS in the vascular milieu by different mechanisms. This oxidative stress has a direct cytotoxic effect, causing the oxidation of proteins, lipids, and DNA, which culminates in tissue damage, as well as an indirect effect by generating and releasing new DAMPs. Thus, ROS seem to be a key player in a great feedforward loop that is activated by RBC products and, in turn, is able to generate even more reactive mediators, amplifying the inflammatory response. This can be exemplified by sickle cell disease (SCD), as widely reviewed by Connes's and Kato's groups. As precisely covered by Nader et al., SCD is a disease characterized by a vicious circle between abnormality in RBCs and inflammation. A genetic single mutation in the β-globin gene leads to an anomalous hemoglobin (HbS), which polymerizes under deoxygenation, changing the deformability and fragility of the RBCs and, consequently, causing intravascular hemolysis. In sequence, cell free hemoglobin and heme induce ROS production and deplete nitric oxide (NO) from the microenvironment. The pro-oxidative milieu created is responsible for oxidation of several compounds, and may further increase RBC death and inflammation, amplifying the damage. Indeed, Connes's group (Nader et al.) demonstrated the effects of ROS and NO on RBC deformability and eryptosis. ROS was also involved in sickle RBC-derived microparticle (MP) release. The levels of circulating RBC-MPs correlated with arterial stiffness in SCD patients and were able to activate a human endothelial cell line, inducing secretion of proinflammatory cytokines through a TLR4-dependent mechanism. In line with that, Santana et al. showed that hydroxyurea (HU), a FDA approved drug for SCD, induces antioxidant gene expression, such as superoxide dismutase-1 and glutathione disulfide-reductase. Moreover, HU was able to reduce ROS production induced by hemin treatment, suggesting that HU acts by an additional and previously unappreciated role in SCD disease by inducing antioxidant proteins and, hence scavenging free radicals.

In their review article, Gbotosho et al. decipher each of the heme-induced pathways that lead to the complications of SCD, where excessive ROS are generated by RBCs due to the unstable nature of HbS and to a greater percentage of NADPH oxidase and mitochondria retention in mature RBCs. The RBCs-derived microparticles generated in SCD are also able to deliver heme to endothelial cells, mediating additional oxidative stress. Besides the role of heme as pro-oxidative mediator and a DAMP, the authors emphasize its ability to induce PlGF and IL-6 and discuss several pathways by which these mediators can contribute to the multiple pathophysiology of SCD. The direct link between free heme in the bloodstream with IL-6 production and with tissue damage is shown in a mice model by another article from the group Gbotosho et al. By injection of heme in the mice, they demonstrated, *in vivo*, the expression of IL-6 and markers of cardiac stress and hypertrophy in Townes mice, a model of SCD, through a pathway independent of Nrf2, the canonical transcription factor activated by HO-1.

Belcher and Vercellotti's groups investigated different aspects of TLR4 signaling induced by heme. Although TLR4 is a well described heme ligand and it is widely expressed, it is not completely clear which cells are the TLR4-expressed effectors of the heme-induced proinflammatory disorders. By generating a bone marrow chimera deficient in TLR4 in a murine model of SCD, Beckman et al. elegantly demonstrated that endothelial, but not hematopoietic, TLR4 expression is necessary for the microvascular stasis presented in the disease. In order to understand how TLR4-dependent heme stimulation occurs, Belcher et al. performed a detailed investigation on this matter. Through pull-down and reporter assays they demonstrated that, similarly to LPS, heme binds to the adaptor molecule myeloid differentiation factor-2 (MD-2) to initiate NF-kB signaling, a process that is dependent on TLR4 and CD14. Interestingly, by generating MD-2 mutants, they were able to identify possible binding sites for heme in the MD-2 molecule, which they found to be different to the binding sites for LPS. Although MD-2 is often co-expressed with TLR4 on the cell surface, Zhang et al. showed high levels of the soluble form of MD-2 (sMD-2) in human and murine sickle plasma, which was shown to induce IL-8 secretion by human endothelial cells, suggesting that heme bound to sMD-2 is also able to promote endothelial cell activation in SCD.

Santaterra et al. showed that besides the induction of inflammatory cytokines, heme present in the serum of SCD patients promotes endothelial barrier disruption *in vitro* in a manner dependent on hemopexin levels in serum, indicating that when the free heme clearance system is overwhelmed, heme is able to cause injury. In line with this observation, Poillerat et al. demonstrated the pharmacokinetic properties of hemopexin in mice in order to guide future therapy for hemolytic diseases by scavenging free heme from the bloodstream.

Neutrophils and monocytes are recognized as major producers of inflammatory cytokines in the vascular microenvironment during hemolysis. However, other cells may play a role in this process. As evidence of this, HO-1was shown to be involved in inflammatory dendritic cell (DC) differentiation from circulating monocytes by Sesti-Costa et al., suggesting a role for heme or its derivatives in the generation of these immune cells. Accordingly, SCD patients had higher circulating inflammatory DCs, and monocyte-derived DCs from patients were able to produce MCP-1, IL-6 and IL-8 in culture and induce Th17 and Tc17 profile skewing, indicating that hemolysis may also alter the response of a previously unappreciated immune cell subset.

The inflammatory cytokine and chemokine landscape of SCD patients in different statuses was carefully analyzed by Silva-Junior et al., who observed that patients have a proinflammatory profile even in steady state. Interestingly, some of the secreted mediators are decreased upon vaso-oclusive crisis (VOC), which is mainly marked by cytokines involved with lymphocyte proliferation, Th2 responses, and high levels of G-CSF, an important growth factor for neutrophil development. PDGF-BB and IL-1ra were pointed out as important hallmarks of clinical recovery post-VOC, as they are strikingly high during crisis and were the ones that significantly declined in the convalescent stage, representing potential markers for prognosis. A novel potential approach for managing SCD is also brought by Kiven et al. with a new way to evaluate pain status in SCD. Using an automated gait measurement method, the authors accessed gait patterns in a mouse model of SCD and found alterations in stance instability and spatial and temporal gait parameters. Interestingly, changes in gait correlated with mechanical and deep tissue hyperalgesia. In addition, purkinje cells, which are associated with movement and neural function, were shown to undergo apoptosis in the cerebella of SCD mice, suggesting that neuronal damage and chronic pain may incite compensatory gait alterations in SCD.

Two complete reviews in this Research Topic bring novel insights on the landscape of autoimmune hemolytic anemia (AIHA). Barcellini and Fattizzo underscored the heterogeneity of the disease, as the pathology depends on the isotype and complement-induced ability of the autoantibodies specific to the RBCs developed. The outcome is also reflected by the effectiveness of the compensatory erythropoiesis and whether the cause is either primary or secondary. The authors critically discuss the currently available therapies, the ones in development and the challenges encountered to obtain accurate treatment and diagnosis. In line with the underappreciated heterogeneity of the disease, the prevalence of a PNH clone in AIHA patients was found to be higher than expected (37.4%) by Fattizzo et al. In addition, the hemolytic pattern and cytokine profile differed between PNH positive versus negative in AIHA patients, suggesting that they may be in need of different therapy indications and that testing for PNH may be beneficial especially in cases unresponsive to current AIHA treatment.

The differences in the pathogenesis of AIHA mediated by cold agglutinins is another instance of the heterogeneity of outcomes in the disease, as covered by Berentsen. In this case, cold-reactive antibodies that are able to agglutinate RBCs arise from either a clonal lymphoproliferative source, such as in cold agglutinin disease (CAD), or a secondary clinical disorder, as seen in secondary cold agglutinin syndrome (CAS). The author extensively reviews the immune pathogenesis of both diseases, covering the origin and role of the agglutinins, the activation of complement and induction of inflammation, which considerably impact the chosen treatment. Finally, Zaninoni et al. discuss the poorly studied role of the immune system in congenital hemolytic anemia (CHA), especially the levels of naturally occurring antibodies that can play different roles in health and disorders, and are involved both positively and negatively in autoimmune disease. The authors highlighted the evidence so far that suggests that these antibodies may have a pathogenic role in CHA by inducing removal of RBCs in the spleen, and also the implications of splenectomy for the immune response in CHA patients.

We hope the readers enjoy this Research Topic issue that contains a relevant update on the consequences of hemolytic anemia from different causes, and we thank all authors that provided their valuable contributions to this collection.

AUTHOR CONTRIBUTIONS

All authors contributed to the article and approved the submitted version.

FUNDING

RS-C and NC are funded by FAPESP, grant numbers 2019/09704-7 and 2021/05191-5 granted to RS-C, and 2019/18886-1 granted to NC.

Conflict of Interest: The authors declare that the research was conducted in the absence of any commercial or financial relationships that could be construed as a potential conflict of interest.

Publisher's Note: All claims expressed in this article are solely those of the authors and do not necessarily represent those of their affiliated organizations, or those of the publisher, the editors and the reviewers. Any product that may be evaluated in this article, or claim that may be made by its manufacturer, is not guaranteed or endorsed by the publisher.

frontiers in Immunology

ORIGINAL RESEARCH
published: 06 March 2020
doi: 10.3389/fimmu.2020.00228

The Role of Hemoglobin Oxidation Products in Triggering Inflammatory Response Upon Intraventricular Hemorrhage in Premature Infants

*Judit Erdei[1,2], Andrea Tóth[1,2], Andrea Nagy[3], Benard Bogonko Nyakundi[1,2], Zsolt Fejes[4], Béla Nagy Jr.[4], László Novák[5], László Bognár[5], Enikö Balogh[1], György Paragh[6], János Kappelmayer[4], Attila Bácsi[7] and Viktória Jeney[1]**

[1] MTA-DE Lendület Vascular Pathophysiology Research Group, Research Centre for Molecular Medicine, Faculty of Medicine, University of Debrecen, Debrecen, Hungary, [2] Doctoral School of Molecular Cell and Immune Biology, Faculty of Medicine, University of Debrecen, Debrecen, Hungary, [3] Department of Pediatrics, Faculty of Medicine, University of Debrecen, Debrecen, Hungary, [4] Department of Laboratory Medicine, Faculty of Medicine, University of Debrecen, Debrecen, Hungary, [5] Department of Neurosurgery, Faculty of Medicine, University of Debrecen, Debrecen, Hungary, [6] Department of Internal Medicine, Faculty of Medicine, University of Debrecen, Debrecen, Hungary, [7] Department of Immunology, Faculty of Medicine, University of Debrecen, Debrecen, Hungary

OPEN ACCESS

Edited by:
Nicola Conran,
Campinas State University, Brazil

Reviewed by:
Richard F. Keep,
University of Michigan, United States
John D. Belcher,
University of Minnesota Twin Cities, United States

***Correspondence:**
Viktória Jeney
jeney.viktoria@med.unideb.hu

Specialty section:
This article was submitted to Inflammation, a section of the journal Frontiers in Immunology

Received: 25 November 2019
Accepted: 28 January 2020
Published: 06 March 2020

Citation:
Erdei J, Tóth A, Nagy A, Nyakundi BB, Fejes Z, Nagy B Jr, Novák L, Bognár L, Balogh E, Paragh G, Kappelmayer J, Bácsi A and Jeney V (2020) The Role of Hemoglobin Oxidation Products in Triggering Inflammatory Response Upon Intraventricular Hemorrhage in Premature Infants. Front. Immunol. 11:228. doi: 10.3389/fimmu.2020.00228

Intraventricular hemorrhage (IVH) is a frequent complication of prematurity that is associated with high neonatal mortality and morbidity. IVH is accompanied by red blood cell (RBC) lysis, hemoglobin (Hb) oxidation, and sterile inflammation. Here we investigated whether extracellular Hb, metHb, ferrylHb, and heme contribute to the inflammatory response after IVH. We collected cerebrospinal fluid (CSF) (n = 20) from premature infants with grade III IVH at different time points after the onset of IVH. Levels of Hb, metHb, total heme, and free heme were the highest in CSF samples obtained between days 0 and 20 after the onset of IVH and were mostly non-detectable in CSF collected between days 41 and 60 of post-IVH. Besides Hb monomers, we detected cross-linked Hb dimers and tetramers in post-IVH CSF samples obtained in days 0–20 and 21–40, but only Hb tetramers were present in CSF samples obtained after 41–60 days. Vascular cell adhesion molecule-1 (VCAM-1) and interleukin-8 (IL-8) levels were higher in CSF samples obtained between days 0 and 20 than in CSF collected between days 41 and 60 of post-IVH. Concentrations of VCAM-1, intercellular adhesion molecule-1 (ICAM-1), and IL-8 strongly correlated with total heme levels in CSF. Applying the identified heme sources on human brain microvascular endothelial cells revealed that Hb oxidation products and free heme contribute to the inflammatory response. We concluded that RBC lysis, Hb oxidation, and heme release are important components of the inflammatory response in IVH. Pharmacological interventions targeting cell-free Hb, Hb oxidation products, and free heme could have potential to limit the neuroinflammatory response following IVH.

Keywords: intraventricular hemorrhage, hemoglobin, heme, premature infants, cerebrospinal fluid, adhesion molecules, brain endothelial cell, inflammation

INTRODUCTION

Intraventricular hemorrhage (IVH) is a frequent complication of prematurity, occurring in about 15% to 20% of very low birth-weight (<1,500 g) preterm infants, and its incidence is even higher (∼45%) in extremely low birth-weight infants (500–750 g) (1–3). IVH is associated with high neonatal mortality (20–50%) and increases the risk of neurodevelopmental impairment in the surviving infants beyond the risk associated with prematurity alone (4).

During fetal brain development, neurons and glial cells migrate out from the germinal matrix (GM), a highly cellular and vascularized layer of the brain. The GM is most active between 8 and 28 gestational weeks, and generally absent in term infants (5). In preterm infants, IVH results from bleeding of the GM, because its capillary network is extremely fragile, and unable to regulate cerebral blood flow (6).

IVH in preterm infants leads to systemic inflammation, characterized by elevation of pro-inflammatory cytokines, e.g., tumor necrosis factor alpha (TNF-α), interleukin-8 (IL-8), IL-1β, chemokines such as monocyte adhesion molecule-1, and increased levels of adhesion molecules, i.e., vascular cell adhesion molecule-1 (VCAM-1) and intercellular adhesion molecule-1 (ICAM-1) (7). As a sign of local inflammatory response, the levels of E-selectin, VCAM-1, ICAM-1, and L-selectin were found to be elevated in the cerebrospinal fluid (CSF) of patients after subarachnoid hemorrhage (8).

Rupture of the microvasculature of the GM causes extravasation of red blood cells (RBCs) in the CSF followed by lysis of RBCs. While hemoglobin (Hb) is compartmentalized in RBCs, its oxidation is prevented by a highly effective antioxidant defense system including enzymatic (Cu/Zn superoxide dismutase, catalase, glutathione peroxidase, and peroxiredoxins) and non-enzymatic (glutathione) scavengers [reviewed in Jeney et al. (9)]. In contrast, outside RBCs, Hb is prone to oxidation, giving rise to the formation of different Hb oxidation products [metHb (Fe^{3+}), ferrylHb ($Fe^{4+} = O^{2-}$)] and subsequent release of heme. The formed high-valence (Fe^{4+}) iron compounds are reactive intermediates and decay quickly via intramolecular electron transfer between the ferryl iron and specific amino acid residues of the globin chains resulting in the formation of globin radicals (10). Then the termination of the reaction occurs when these globin radicals react with each other leading to the formation of covalently cross-linked Hb multimers [reviewed in Jeney et al. (9)]. Covalently cross-linked oxidized Hb forms have been detected in different biological samples including plasma following intravascular hemolysis as well as in human complicated atherosclerotic lesions with intraplaque hemorrhage (11, 12).

Oxidized Hb forms (metHb, ferrylHb) and labile heme exert diverse pro-oxidant and pro-inflammatory activities toward different cell types including endothelial cells (ECs). As pro-oxidants, they induce lipid peroxidation and sensitize ECs to oxidant-mediated killing (13, 14). Heme induces toll-like receptor 4 (TLR4) activation and subsequent upregulation of adhesion molecules VCAM-1, ICAM-1, and E-selectin in ECs (15).

Besides heme, ferrylHb but not Hb or metHb induces upregulation of adhesion molecules in ECs, but interestingly, this response is not dependent on TLR4 activation (16). Increased endothelial permeability contributes to inflammatory cell extravasation upon hemolysis, and previous studies showed that ferrylHb and free heme induce the loss of endothelial integrity (16–20).

The goal of the present study was to perform a qualitative and quantitative analysis of the Hb content of human CSF samples obtained from premature infants following IVH with a special interest in detecting ferrylHb/covalently cross-linked Hb species. We also aimed to investigate the pro-oxidant and pro-inflammatory effects of these Hb forms on human brain microvascular endothelial cells (HBECs). We determined the levels of inflammatory markers in post-IVH CSF samples and correlated their values to the heme content of CSF samples to further understand the role of heme in triggering the inflammatory response following IVH. We believe that a better understanding of the molecular mechanism of the post-IVH inflammatory response is critical in tailoring therapeutic tools to avoid these infants from the development of the life-long neurological effects of IVH.

MATERIALS AND METHODS

Materials

Reagents were purchased from Sigma-Aldrich (St. Louis, MO, United States) unless otherwise specified.

Patient Selection and CSF Collection

In this study, we used the leftover of CSF samples that were collected by spinal tap or ventricular reservoir puncture for diagnostic purposes at the Department of Neurosurgery, University of Debrecen. Preterm infants (n = 20) diagnosed with grade III IVH with a mean gestational age at birth of 27.9 ± 2.2 weeks were involved in the study. CSF samples were collected at 26.6 ± 16.4 days after the onset of IVH. No CSF was obtained exclusively for inclusion in this study. Within 30 min of collection, CSF samples were centrifuged (2,000 g, 4°C, 15 min), and supernatants were stored aliquoted at −70°C until analysis. The procedures were approved by the Scientific and Research Ethics Committee of the University of Debrecen and the Ministry of Human Capacities under the registration number of 1770-5/2018/EÜIG. Parental consent forms were signed by the parents of the infants involved in this study.

Determination of Hb, metHb, ferrylHb, Total Heme, Free Heme, and Bilirubin Levels in CSF

The absorbance spectra (250–700 nm) of CSF samples were taken with a spectrophotometer (NanoDrop 2000, Thermo Fisher Scientific, MA, United States). Concentrations of Hb, metHb, and ferrylHb were calculated from the absorbance values measured at 541, 576, and 630 nm, using the absorption coefficients and equations determined previously by Meng and Alayash (21). The

total heme concentration of CSF samples was determined by using a QuantiChrom Heme Assay Kit (Gentaur Ltd., London, United Kingdom) according to the manufacturer's instructions. Concentration of non-Hb bound heme was calculated by the following equation: [free heme] = [total heme] – [Hb-heme] – [metHb-heme] – [ferrylHb]. Bilirubin levels in CSF samples were measured by a colorimetric assay on a Cobas 6000 analyzer (Roche Diagnostics, Mannheim, Germany).

Cell Culture

HBEC cell line was purchased from ATCC (CRL-3245, Manassas, VA, United States). Cells were cultured in Media 199, supplemented with 10% fetal bovine serum (Gibco, Waltham, MA, United States), 40 μg/ml EC growth supplement, and 1% penicillin/streptomycin in 5% CO_2 humidified atmosphere at 37°C. HBECs were used at passages 5 and 8.

Hemoglobin Preparation

We prepared Hb, metHb, and ferrylHb from fresh blood obtained from healthy volunteers as described in detail in our previous work (12). Briefly, Hb was isolated from fresh blood drawn from healthy volunteers using ion-exchange chromatography on a DEAE Sepharose CL-6B column. metHb was generated by incubation (30 min, 25°C) of purified Hb with a 1.5-fold molar excess of $K_3Fe(CN)_6$ over heme. FerrylHb was obtained by incubation (1 h, 37°C) of Hb with a 10:1 ratio of H_2O_2 to heme. The ferryl state of iron is highly unstable and therefore ferrylHb transiently forms. During stabilization of ferryl iron, different chemically heterogeneous oxidized Hb molecules are formed, which we refer to as ferrylHb to reflect rather the way of their formation than their actual oxidation status. After oxidation, both metHb and ferrylHb were dialyzed against saline (three times for 3 h at 4°C) and concentrated using Amicon Ultra centrifugal filter tubes (10,000 MWCO, Millipore Corp., Billerica, MA, United States). Aliquots were snap-frozen in liquid nitrogen and stored at −70°C until use.

Cell Viability Assay

Confluent HBECs grown in 96-well tissue-culture plates were washed twice with Hank's Balanced Salt Solution (HBSS) and exposed to heme and different Hb species (Hb, metHb, or ferrylHb at a concentration of 10–100 μmol/L heme group) for 24 h. Then cells were washed with HBSS, and 100 μl of 3-[4,5-dimethylthiazol-2-yl]-2,5-diphenyl-tetrazolium bromide (MTT) (0.5 mg/ml) solution in HBSS was added. After a 4-h incubation, the MTT solution was removed, formazan crystals were dissolved in 100 μl of dimethyl sulfoxide, and optical density was determined at 570 nm.

Endothelial Cell Monolayer Integrity Assay

The electric cell-substrate impedance sensing (ECIS) method was used to measure the endothelial monolayer integrity. HBECs were cultured in 8-well electrode arrays (8W 10E, Applied BioPhysics Inc., Troy, NY, United States). After reaching confluence, cells were treated with different Hb species (Hb, metHb, and ferrylHb at a concentration of 50 μmol/L heme), and the complex impedance spectrum was monitored with an ECIS Zθ instrument (Applied BioPhysics Inc., Troy, NY, United States) for 4 h. Results are shown as the difference between monolayer resistance at 4,000 Hz at 0 time point and 4 h.

Quantitative Real-Time PCR

Total RNA was isolated from HBECs using TRizol (RNA-STAT60, Tel-Test Inc., Friendswood, TX, United States) according to the manufacturer's protocol. Two micrograms of RNA was reverse-transcribed to cDNA with a High-Capacity cDNA Reverse Transcription Kit (Applied Biosystems, Waltham, MA, United States). PCR was performed using iTaq Universal Probes Supermix (BioRad Laboratories, Hercules, CA, United States) and predesigned primers and probes (TaqMan® Gene Expression Assays) VCAM-1 (Hs01003372), ICAM-1 (Hs00164932), HO-1 (Hs01110250), IL-8 (Hs00174103), and GAPDH (Hs0278624). Relative mRNA expressions were calculated with the ΔΔCt method using GAPDH as an internal control.

Intracellular ROS Measurement

ROS production was monitored by using the 5-(and-6)-chloromethyl-2',7'-dichlorodihydrofluorescein diacetate, acetyl ester (CM-H2DCFDA) assay (Life Technologies, Carlsbad, CA, United States). Confluent HBECs were exposed to the Hb forms Hb, metHb, ferrylHb, and heme (10, 25, 50, and 100 μmol/L heme) for 4 h in M199 media supplemented with 1% FBS. Then cells were loaded with CM-H2DCFDA (10 μmol/L, 30 min, at 37°C in the dark), followed by three washes with HBSS. Fluorescence intensity was measured every 30 min for 4 h applying 488-nm excitation and 533-nm emission wavelengths.

Western Blot

Whole cell lysates (20 μg/lane) or CSF samples (5 μl/lane) were resolved on 10% SDS-PAGE, then blotted onto a nitrocellulose membrane (Amersham Proton 1060003, GE Healthcare, Chicago, IL, United States). Western blot was performed with the use of the following polyclonal antibodies: anti-HO-1 antibody (70081, Cell Signaling Technology Inc., Danvers, MA, United States) at a concentration of 50 ng/ml and anti-VCAM-1 antibody (Sc-8304, Santa Cruz Biotechnology, Inc., Dallas, TX, United States) at a concentration of 1 μg/ml. We used peroxidase labeled anti-rabbit IgG (NA931, Amersham Bioscience, Piscataway, NJ, United States) as a secondary antibody at a concentration of 20 ng/ml. For Hb detection, we used an HRP-conjugated goat antihuman Hb polyclonal antibody (ab19362-1, Abcam Plc., Cambridge, United Kingdom) at a concentration of 0.1 μg/ml. Antigen–antibody complexes were visualized with the horseradish peroxidase chemiluminescence system (Amersham Biosciences Corp., Piscataway, NJ, United States). Chemiluminescent signals were detected conventionally on an X-ray film or digitally by using a C-DiGit Blot Scanner (LI-COR Biosciences, Lincoln, NE, United States). After detection, the membranes were stripped and re-probed for β-actin using HRP-conjugated anti-β-actin antibody (Sc-47778, Santa Cruz Biotechnology, Inc., Dallas, TX, United States) at a concentration

of 0.13 μg/ml. Blots were quantified by using the inbuilt software of the C-DiGit Blot Scanner (LI-COR Biosciences, Lincoln, NE, United States).

Measurement of Soluble VCAM-1, ICAM-1, and IL-8 Levels in CSF Samples

To perform enzyme-linked immunosorbent assay (ELISA), CSF samples were first centrifuged at 10,000 *g* for 1 min. Soluble VCAM-1 and ICAM-1 protein concentrations were quantitatively measured by ELISA as described in the manufacturer protocol (R&D Systems, Minneapolis, MN, United States). Levels of IL-8 were determined by ELISA (BD OptEIA; BD Biosciences, San Diego, CA, United States).

Statistical Analysis

Results are expressed as mean ± SD. At least three independent experiments were performed for all *in vitro* studies. Statistical analyses were performed with GraphPad Prism software (version 8.01, San Diego, CA, United States). Comparisons between more than two groups were carried out by ordinary one-way ANOVA followed by *post hoc* Tukey's multiple-comparisons test. We applied one-way ANOVA followed by Dunnett's *post hoc* test when experimental groups were compared to a control. A value of $p < 0.05$ was considered significant. To measure the strength of the association between two variables, we performed Pearson's correlation analysis. A strong positive correlation was defined as a value of Pearson's correlation coefficient (r) > 0.4.

RESULTS

Time-Dependent Accumulation of Different Oxidized Hb Forms, Free Heme, and Bilirubin in Post-IVH CSF Samples

In this study, we have analyzed 20 CSF samples that were collected by spinal tap or ventricular reservoir puncture from preterm infants diagnosed with grade III IVH. The main characteristics of the patients are summarized in **Table 1**. All patients were preterm infants with a median gestational age of 28 weeks at delivery (**Table 1**). The mean birth weight of the infants was 1,094 ± 282 g (**Table 1**). Out of the 20 infants, 10 did not receive steroid prophylaxis, and 8 obtained partial steroid prophylaxis. In addition, 14 infants were born via Cesarean section, 18 developed hydrocephalus, and 2 of them died before 6 months of age (**Table 1**).

Because CSF samples were taken for diagnostic purposes, we obtained CSF samples at different time points after the onset of IVH (days 14–60, mean: 27.6 ± 15.6 days, median: 21 days). Based on the elapsed time between the onset of IVH and CSF sampling, we divided the samples into three groups, 0–20 days, 21–40 days, and 41–60 days. CSF samples obtained at different time intervals after the onset of the IVH had different colors, i.e., 0–20 days CSF samples had brownish discoloration, 21–40 days CSF samples were yellowish, whereas 41–60 days CSF samples were colorless similar to a normal CSF specimen (**Figure 1A**). To evaluate Hb, metHb, and ferrylHb concentrations in CSF, we took the visible absorption spectra of the samples and calculated Hb concentrations with the use of molar extinction coefficients as determined previously (21). The Hb levels of CSF samples obtained 0–20 days after the onset of IVH showed a big variation from 13.08 up to 228.12 μmol/L, with an average of 85.04 ± 72.38 μmol/L. The Hb concentration in CSF samples obtained at later time points, i.e., 21–40 days after IVH onset, was significantly lower (7.61 ± 10.32 μmol/L), and Hb was undetectable in CSF samples collected 41–60 days following IVH (**Figure 1B**).

One-electron oxidation of Hb leads to the formation of metHb. Similarly to that of Hb, we found high amounts of metHb in CSF samples obtained at 0–20 days (80.51 ± 77.65 μmol/L), which decreased gradually during the study period (**Figure 1C**). On average, metHb concentration was 9.65 ± 10.77 μmol/L in CSF samples obtained at 21–40 days after the onset of IVH and was below the detection limit in CSF samples collected after 41–60 days of IVH (**Figure 1C**). Two-electron oxidation of Hb by

TABLE 1 | Characteristics of the patients.

Characteristic	Grade III IVH (*n* = 20)
Male sex - no./total no.	11/20
Gestational age at delivery	
Median - week	28
Distribution	
23 week 0 days to 25 week 6 days	4
26 week 0 days to 27 week 6 days	4
28 week 0 days to 29 week 6 days	6
30 week 0 days to 31 week 6 days	6
Birth weight	
Mean ± s.d. - g	1094 ± 282
Distribution	
≥500 to <750 g	3
≥750 to <1000 g	6
≥1000 to <1250 g	4
≥1250 to <1500 g	7
Apgar 5 min	
Median	5
Distribution	
0–3	4
4–6	13
7–8	3
9–10	0
Apgar 10 min	
Median	8
Distribution	
0–3	0
4–6	7
7–8	9
9–10	4
Steroid prophylaxis - yes/partial/no	2/8/10
Multiply pregnancy - no./total no.	5/20
Cesarean section delivery - no./total no.	14/20
Hydrocephalus - no./total no.	18/20
Death - no./total no.	2/20
Timing of the CSF samples [days after the onset of IVH, (*n*)]	14(1), 15(1), 16(1), 17(2), 19(1), 20(2), 21(4), 24(1), 25(1), 28(1), 32(1), 45(1), 60(3)

CSF samples were collected from premature infants (n = 20) diagnosed with grade III IVH.

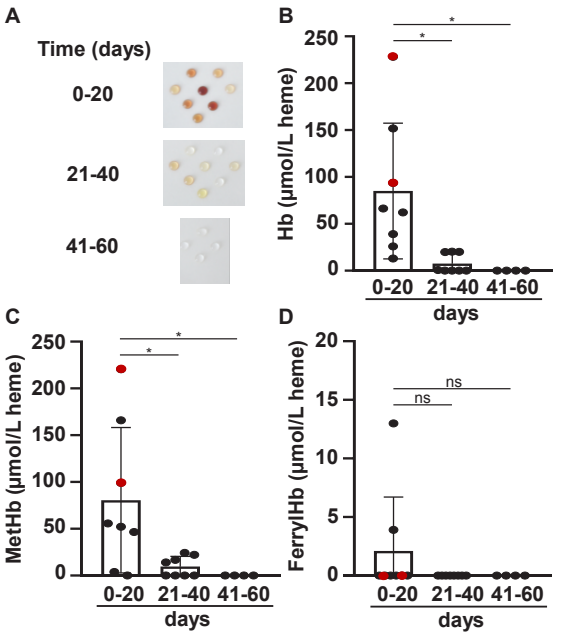

FIGURE 1 | Time-dependent accumulation of Hb, metHb, and ferrylHb in post-IVH CSF samples. CSF samples (n = 20) were obtained from preterm infants diagnosed with grade III IVH at different time intervals after the onset of IVH. **(A)** Physical appearance of CSF samples obtained at different time intervals after the onset of IVH (days 0–20, 21–40, 41–60). **(B–D)** Concentrations of Hb, metHb, and ferrylHb were quantified spectrophotometrically in CSF samples. Closed circles represent individual samples, red circles represent patients that died before 6 months of age, and bars represent mean ± SD values. P-values were calculated using one-way ANOVA followed by Tukey's multiple comparison analysis. *$p < 0.05$.

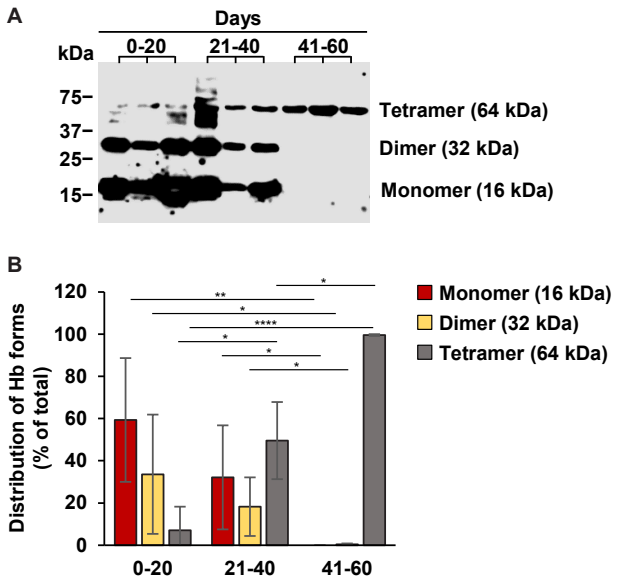

FIGURE 2 | Time-dependent accumulation of covalently cross-linked globin multimers in post-IVH CSF samples. Hb contents of CSF samples (n = 20) obtained from preterm infants diagnosed with grade III IVH at different time intervals after the onset of IVH were analyzed by western blot. **(A)** Representative western blot is shown. **(B)** Densitometric analysis of western blots of all samples (n = 20) was performed and percentage of globin monomers, dimers, and tetramers (Hb) is presented as mean ± SD. P-values were calculated using one-way ANOVA followed by Tukey's multiple comparison analysis. *$p < 0.05$, **$p < 0.01$, ****$p < 0.001$.

peroxides, for instance, could lead to the formation of ferrylHb. Interestingly, we could hardly detect any ferrylHb in the CSF samples, which could be explained by the highly unstable nature of this Hb species (**Figure 1D**).

FerrylHb is a reactive intermediate that decays quickly via intramolecular electron transfer between the ferryl iron and specific amino acid residues of the globin chains. In this reaction, globin radicals are produced, which are still unstable and react with each other to get stabilized via the formation of covalent bonds between the globin subunits (9). Next we addressed whether this occurs following IVH in the CSF. We have analyzed all the CSF samples by western blot under reducing conditions and detected Hb forms with different molecular weights that corresponded as globin monomers (16 kDa), dimers (32 kDa), and tetramers (Hb) (64 kDa). A representative western blot is shown in **Figure 2A**. Densitometric analysis of the western blots revealed that in CSF samples obtained at 0–20 days after the onset of IVH contained predominantly globin monomers (59.3 ± 29.3% of total Hb), less globin dimers (33.6 ± 28.2% of total Hb), and very low amounts of Hb tetramers (7.03 ± 11.1% of total Hb) (**Figures 2A,B**). Interestingly, we observed a shift toward the formation of globin dimers and tetramers in CSF samples obtained at 21–40 days post-IVH (**Figures 2A,B**). This change becomes highly remarkable in CSF samples obtained after 41–60 days of IVH, as these samples contained neither monomers nor dimers but contained Hb tetramers (**Figures 2A,B**).

Hb oxidation can lead to the dissociation of the heme group from the globin giving a rise in the formation of non Hb-bound (free) heme. To see whether this occurred following IVH, first we determined total heme levels in CSF samples. Total heme levels were very high in CSF obtained at 0–20 days after the onset of IVH ranging from 120.02 up to 1,035.27 µmol/L with an average of 463.01 ± 303.39 µmol/L (**Figure 3A**). Total heme levels were significantly lower in CSF samples obtained at 21–40 days after the onset of IVH (64.98 ± 73.50 µmol/L) and was below 1 µmol/L in CSF samples collected 41–60 days post-IVH (**Figure 3A**). Correlation analysis between Hb and total heme levels revealed a very strong linear correlation (r = 0.7296) between the two variables, suggesting that Hb is the major source of heme in CSF as we expected (**Figure 3B**). Next we calculated the concentration of free heme as described in the methods. Free heme concentrations were high in CSF collected at 0–20 days after the onset of IVH ranging from 41.99 to 717.39 µmol/L with an average of 295.34 ± 259.80 µmol/L (**Figure 3C**). Free heme levels were significantly lower in CSF samples obtained at 21–40 days after the onset of IVH (47.73 ± 57.50 µmol/L) and was below 1 µmol/L in CSF samples collected 41–60 days post-IVH (**Figure 3C**). We looked at the correlation between the concentration of oxidized Hb (metHb + ferrylHb) and free heme and found a strong positive

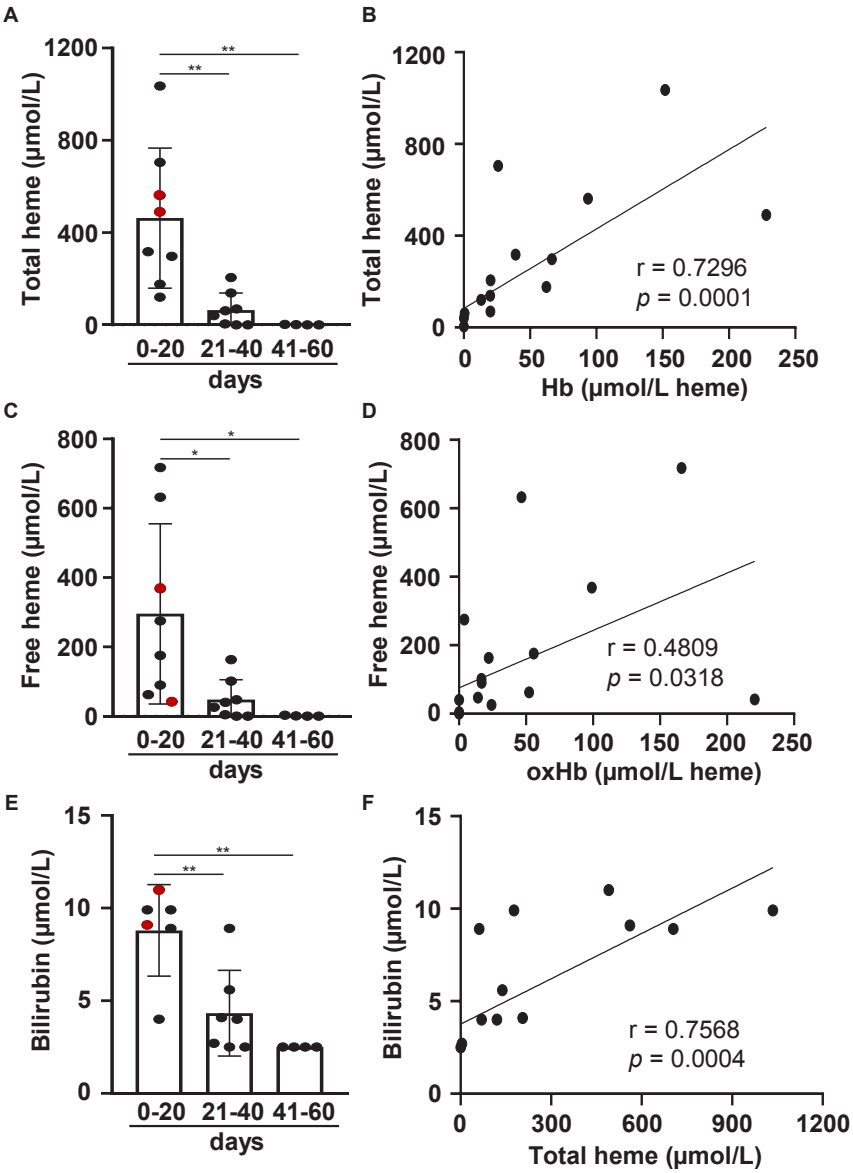

FIGURE 3 | Time-dependent accumulation of total heme, free heme, and bilirubin in post-IVH CSF samples. CSF samples (n = 20) were obtained from preterm infants diagnosed with grade III IVH at different time intervals (days 0–20, 21–40, 41–60) after the onset of IVH. **(A,C,E)** Total heme, free heme, and bilirubin levels of CSF samples were determined. Closed circles represent individual samples, red circles represent patients that died before 6 months of age, and bars represent mean ± SD. P-values were calculated using one-way ANOVA followed by Tukey's multiple comparison analysis. *$p < 0.05$, **$p < 0.01$. **(B,D,E)** Correlation between **(B)** Hb and total heme concentrations, **(D)** oxidized Hb forms (MHb + FHb) and free heme concentrations, and **(F)** total heme and bilirubin concentrations in post-IVH CSF samples (n = 20) is shown. R represents Pearson's correlation coefficient.

correlation (r = 0.4809) between the two variables, which supports the concept that oxidized Hb forms can release their heme prosthetic groups (**Figure 3D**). Additionally, we measured the concentration of bilirubin, one of the end-products of heme catabolism in CSF samples. We found that bilirubin levels were the highest (8.8 ± 2.47 μmol/L) in CSF collected at 0–20 days after the onset of IVH, and then it gradually decreased in time (**Figure 3E**). We found that bilirubin levels strongly correlated to the total heme levels in post-IVH CSF samples (r = 0.7568) (**Figure 3F**).

Pro-oxidant and Pro-inflammatory Effects of Hb Forms and Free Heme Toward Human Brain Microvascular Endothelial Cells

IVH in preterm infants leads to systemic inflammation characterized by increased levels of pro-inflammatory cytokines and cellular adhesion molecules. ECs play a critical role in the pro-inflammatory responses, and Hb oxidation products have been shown to be implicated in diverse hemolysis-associated

sterile inflammatory reactions. Therefore, next we have addressed the pro-oxidant and pro-inflammatory effects of the different Hb oxidation products that were identified in post-IVH CSF samples toward HBECs.

First we have addressed whether the different Hb forms induce heme oxygenase-1 (HO-1), the stress-responsive inducible enzyme that catalyzes heme degradation upon heme overload conditions. We exposed HBECs to Hb, metHb (MHb), ferrylHb (FHb), and free heme (25 μmol/L heme group). Oxidized Hb forms, i.e., metHb and ferrylHb, induced an 18.2 ± 2.6-fold and a 12.1 ± 3.1-fold elevation of HO-1 mRNA levels (4 h), respectively (**Figure 4A**). In contrast, native Hb did not cause an elevation of HO-1 mRNA (**Figure 4A**). Free heme was a highly more potent inducer of HO-1 in HBECs in comparison with metHb and ferrylHb triggering a more than 1,000-fold elevation of the HO-1 mRNA level after a 4-h exposure (**Figure 4A**). In parallel with the changes of the HO-1 mRNA level, both metHb and ferrylHb induced an about 20-fold elevation of the HO-1 protein expression, whereas free heme increased the HO-1 expression by about 200-fold (**Figure 4B**).

Heme is a catalyst of the Fenton reaction and therefore is implicated in the sustained production of reactive oxygen species (ROS) under hemolytic conditions. Next we investigated whether the Hb oxidation products found in post-IVH CSF samples induce ROS production in HBECs. HBECs were treated with Hb, metHb, ferrylHb, and heme (10, 25, 50, 100 μmol/L heme group) for 4 h, and ROS formation was measured as described in the methods. Heme at concentrations of 50 and 100 μmol/L induced substantial production of ROS (**Figure 5A**). In contrast, neither native Hb nor oxidized Hb forms (metHb and ferrylHb) increased ROS production in HBECs (**Figure 5A**). To see whether Hb oxidation products induce HBEC death, we exposed the cells to Hb, metHb, ferrylHb, and free heme (10, 25, 50, 100 μmol/L heme group) for 24 h. Heme at concentrations of 50 and 100 μmol/L induced a substantial reduction in cell viability (**Figure 5B**). On the contrary, cell viability was unaffected by the Hb forms, even when they were applied at the highest concentration (**Figure 5B**). A previous study on human umbilical vein ECs showed that oxidized Hb increased endothelial monolayer permeability (16). Therefore, we investigated whether the Hb forms impair HBEC monolayer integrity. We exposed HBECs to Hb, metHb, and ferrylHb (50 μmol/L heme group) and measured the changes of monolayer resistance over a 4-h period of time (**Figure 5C**). HBEC monolayer integrity was unaffected by native Hb or metHb treatment. In contrast, ferrylHb treatment largely impaired HBEC monolayer integrity (**Figure 5C**).

Heme and oxidized Hb forms have been shown to be implicated in the immune response in hemolytic diseases. More specifically, heme and ferrylHb have been shown to upregulate the expression of cellular adhesion molecules including VCAM-1 and ICAM-1 in human umbilical vein ECs. Here we treated HBECs with Hb, metHb, ferrylHb, and heme (25 μmol/L heme group) and measured mRNA expressions (4 h) of VCAM-1, ICAM-1, and the pro-inflammatory cytokine IL-8 (**Figures 6A–D**). We used LPS (100 ng/ml) as a positive control in these experiments. Free heme and ferrylHb triggered marked elevations of VCAM-1 mRNA (∼15–20-fold), whereas the effect of native Hb and metHb was milder inducing about 5-fold increases of VCAM-1 (**Figure 6A**). We observed a similar trend on the protein level, namely, ferrylHb and free heme were more potent in inducing VCAM-1 expression than native Hb and metHb (**Figure 6B**). Additionally, free heme and ferrylHb but not native Hb and metHb induced elevations of ICAM-1 and IL-8 mRNA levels (**Figures 6C,D**). We have to note that the bioavailable heme concentrations in these experiments were much lower than 25 μmol/L due to the presence of specific (Hx) and non-specific (albumin) heme-binding proteins present in the serum, which was applied at 1% in these experiments.

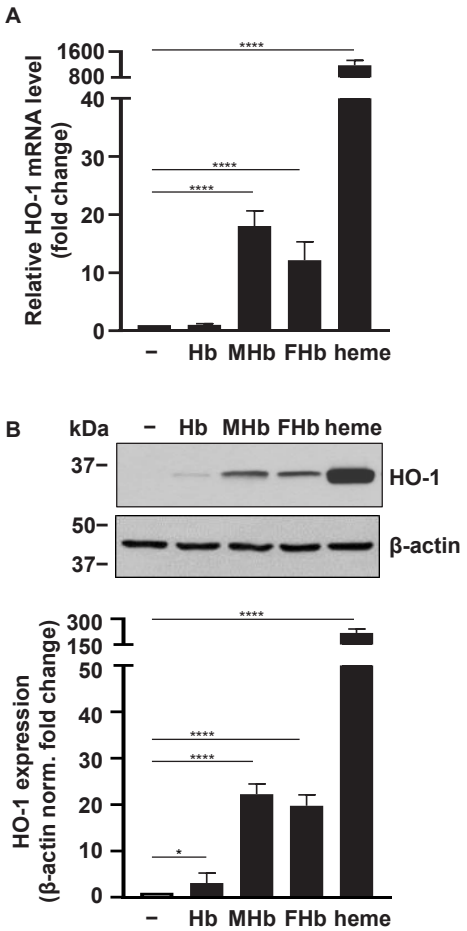

FIGURE 4 | Induction of HO-1 mRNA and protein expression by different Hb forms in HBECs. Confluent HBECs (P5-8) were exposed to vehicle, Hb, MetHb (MHb), ferrylHb (FHb), and heme (25 μmol/L heme group) in 1% FBS. **(A)** Relative mRNA expression (4 h, mean ± SD) of HO-1 normalized to GAPDH from three independent experiments performed in triplicates. **(B)** HO-1 protein levels (16 h) were analyzed by western blot from whole cell lysates. Membranes were re-probed for β-actin. Representative blots of three independent experiments are shown. Densitometry analysis (mean ± SD) of three independent experiments. **(A,B)** *P*-values were calculated using one-way ANOVA followed by Dunnett's *post hoc* analysis. $^{*}p < 0.05$ and $^{****}p < 0.001$.

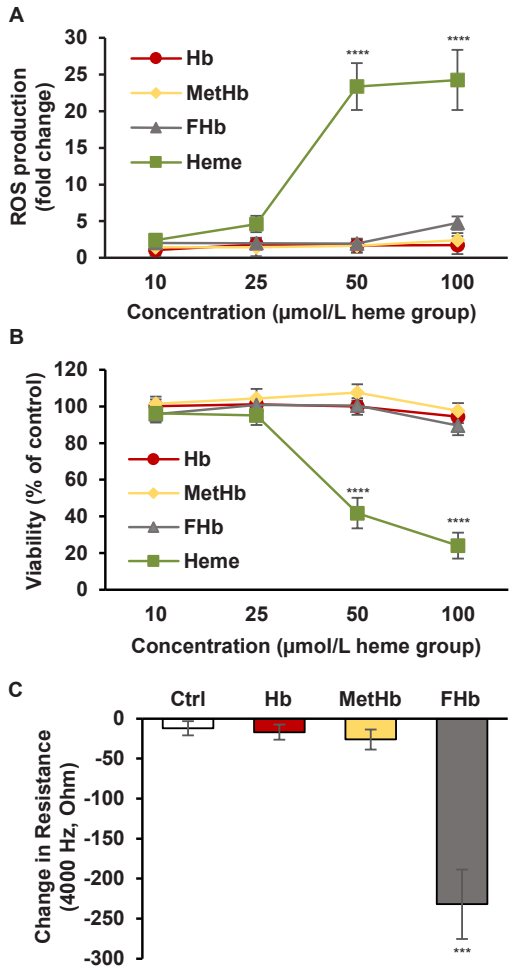

FIGURE 5 | Induction of ROS production and cell death by different Hb forms in HBECs. **(A)** Confluent HBECs (P5-8) were exposed to vehicle, Hb, MetHb, ferrylHb (FHb), and heme (10, 25, 50, 100 μmol/L heme group) in 1% FBS for 4 h, then ROS production was monitored by DCFDA assay for an additional 4 h. Graph shows ROS production (mean ± SD) at 4-h time point from three independent experiments performed in quadruplicates. **(B)** Confluent HBECs (P5-8) were exposed to vehicle, Hb, MetHb, ferrylHb (FHb), and heme (10, 25, 50, 100 μmol/L heme group) in 1% FBS and cellular viability (24 h) was assessed by MTT assay. Graph shows cell viability as a percentage of viability of vehicle-treated cells (mean ± SD) from three independent experiments performed in quadruplicates. **(C)** HBECs cultured in 8-well ECIS plates were exposed to Hb, metHb, and ferrylHb (FHb) (50 μmol/L heme group) in 1% FBS containing media. The complex impedance spectrum was monitored with an ECIS Zθ instrument for 4 h. Change in resistance (mean ± SD) was calculated based on the difference between monolayer resistance at 4,000 Hz at 0 time point and 4 h from three independent experiments performed in triplicates. **(A–C)** *P*-values were calculated using one-way ANOVA followed by Tukey's multiple comparison analysis. ***$p < 0.005$, ****$p < 0.001$.

Correlations Between Levels of Heme and Pro-inflammatory Markers in Post-IVH CSF Samples

Previous studies showed that the levels of pro-inflammatory markers including soluble adhesion molecules and inflammatory cytokines are elevated in post-IVH CSF samples. Our *in vitro* data suggested that Hb-derived heme may play a critical role in the induction of the pro-inflammatory response. To address this question, we measured VCAM-1, ICAM-1, and IL-8 levels in post-IVH CSF samples (N = 20). VCAM-1 levels were the highest in CSF samples obtained between 0 and 20 days after the onset of IVH (305.11 ± 120.12 ng/ml) (**Figure 7A**). Comparing to these samples, VCAM-1 levels were significantly lower in CSF samples obtained at 41–60 days after the onset of IVH (165.31 ± 56.51 ng/ml) (**Figure 7A**). Then we analyzed whether there is a correlation between heme and VCAM-1 levels in the post-IVH CSF samples, and we found a strong linear correlation between the two variables (r = 0.5603) (**Figure 7B**). Next, we determined the level of soluble ICAM-1 in post-IVH CSF samples. We observed a decreasing trend of ICAM-1 levels, but the differences were not significant (**Figure 7C**). On the other hand, ICAM-1 levels correlated strongly (r = 0.5864) with total heme concentrations in post-IVH CSF samples (**Figure 7D**). Finally, we have measured the level of the pro-inflammatory cytokine IL-8 in the post-IVH CSF samples. We found that IL-8 levels were the highest in CSF samples obtained at 0–20 days after the onset of IVH (3.92 ± 0.85 μg/ml), and then we observed a gradual decrease in IL-8 levels at 21–40 and 41–60 days after the onset of IVH resulting in 2.19 ± 1.5 and 0.2 ± 0.29 μg/ml IL-8 concentrations, respectively (**Figure 7E**). Additionally, we found a strong positive correlation between total heme concentration and IL-8 levels in post-IVH CFS samples (r = 0.6768) (**Figure 7F**).

DISCUSSION

IVH is a frequent complication of prematurity that associates with high neonatal mortality and increased risk of neurodevelopmental impairment in the surviving infants (1–4). It is known for a long time that inflammation plays a critical role in the pathophysiology of IVH-induced brain damage; however, the molecular mechanism by which IVH stimulates the inflammatory response is not fully understood. Extravasation of blood into the intraventricular space triggers a cascade of events including the release of various vasoactive and pro-inflammatory molecules from blood and the vascular system [reviewed in Sercombe et al. (22)].

In this study, we performed a qualitative and quantitative analysis of Hb content of human CSF samples obtained from premature infants following IVH at different time points after the onset of IVH to understand the kinetics of Hb release, oxidation, and clearance. We investigated the pro-oxidant and pro-inflammatory effects of the identified Hb forms on HBECs to extend our understanding of the particular roles that these species may play in the neuroinflammatory response following IVH. We measured the levels of pro-inflammatory markers in post-IVH CSF samples at different time points after the onset of IVH to explore the kinetics of the inflammatory response and investigated whether the inflammatory response correlates to the extent of hemolysis.

We showed that after IVH Hb is released into the CSF and Hb oxidation occurs leading to the formation of metHb,

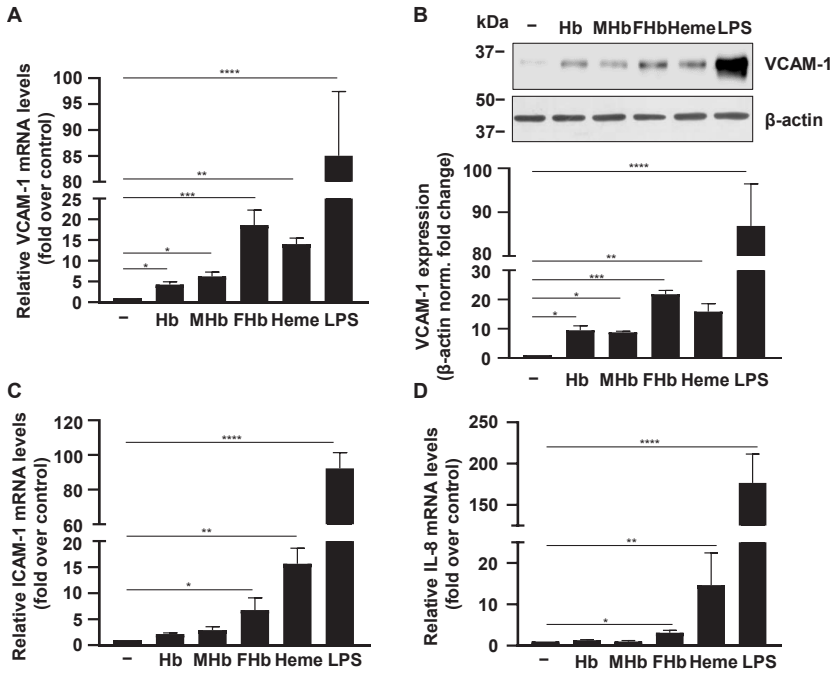

FIGURE 6 | Pro-inflammatory effects of different Hb forms in HBECs. **(A–D)** Confluent HBECs (P5-8) were exposed to vehicle, Hb, metHb (MHb), ferrylHb (FHb), heme (25 μmol/L heme group), and LPS (100 ng/ml) in 1% FBS. Relative mRNA expression (4 h, mean ± SD) of VCAM-1, ICAM-1, and IL-8 normalized to GAPDH from three independent experiments performed in triplicates are shown. **(B)** VCAM-1 protein levels (16 h) were analyzed by western blot from whole cell lysate. Membranes were re-probed for β-actin. Representative blots of three independent experiments are shown. Densitometry analysis (mean ± SD) of three independent experiments. **(A–D)** *P*-values were calculated using one-way ANOVA followed by Dunnett's *post hoc* analysis. $^{*}p < 0.05$, $^{**}p < 0.01$, $^{***}p < 0.005$, $^{****}p < 0.001$.

ferrylHb, and covalently cross-linked oxidized globin multimers. Previous studies showed that cell-free Hb and Hb metabolites are present in CSF following different types of intracranial hemorrhage including IVH (23–25). Particularly, metHb that is produced in a one-electron oxidation of Hb was detected in CSF samples obtained following IVH in preterm infants as well as in an experimental rabbit model of IVH (23). On average, the metHb level in the CSF samples obtained between days 0 and 20 after the onset of IVH was 80.51 ± 77.65 μmol/L, which is in good agreement with the previously reported level of metHb in CSF (∼ 40 μmol/L) on day 3 post-IVH in a rabbit model (23).

Peroxides trigger a two-electron oxidation of Hb, leading to the generation of ferrylHb in which the oxidation state of iron is +4. This unstable form of oxidized Hb was detected in human blood under physiologic and pathophysiologic conditions, but whether this form is produced following IVH has never been addressed (26–28). We could detect ferrylHb only in two out of eight CSF samples obtained between days 0 and 20 after the onset of IVH, which might be explained by the highly reactive nature of the ferryl iron.

High-valent iron in ferrylHb promotes the oxidation of definite amino acids of the globin chains and the subsequent intermolecular cross-linking of the globin subunits (9, 29, 30). Under *in vivo* conditions, these covalently cross-linked ferrylHb species were detected in different biological samples including plasma and urine following intravascular hemolysis as well as in human complicated atherosclerotic lesions with intraplaque hemorrhage (11, 12, 31). Here we showed for the first time that covalently cross-linked oxidized globin multimers, i.e., dimers and tetramers, are present in the CSF samples following IVH.

In the circulation, extracellular Hb is eliminated through the haptoglobin (Hp)–CD163 scavenger pathway (32). First extracellular Hb binds to Hp with extremely high affinity (Kd ∼ 10-12 mol/L) (33), then Hb–Hp complexes are internalized via CD163 receptors expressed on macrophages and monocytes (34). Regarding the CNS, Hp is present in CSF, but because of its low concentration, the Hb-binding capacity of CSF (∼100 μg Hb in adults) is far below the Hb-binding capacity of plasma (∼5 g Hb) (35). It has been shown that following IVH, Hb penetrates from the intraventricular space to the periventricular white matter and contributes to the development of IVH-associated brain injury.

Hb concentration of CSF samples obtained between days 0 and 20 after the onset of IVH showed a huge variation ranging from 13 up to 228 μmol/L with an average of 85 μmol heme groups/L. This corresponds to 10–530 mg of Hb in the 50-ml volume of CSF in the infants, and although we are lacking information about Hp levels in the CSF of premature infants, we assume that in most CSF samples, the level of cell-free Hb exceeds the Hb-binding capacity of CSF.

Once bound to Hp, Hb is protected from oxidation; therefore, the presence of oxidized Hb forms, i.e., metHb and ferrylHb in the post-IVH CSF samples support the idea that the level of Hb overwhelms the Hb binding capacity of Hp in CSF following

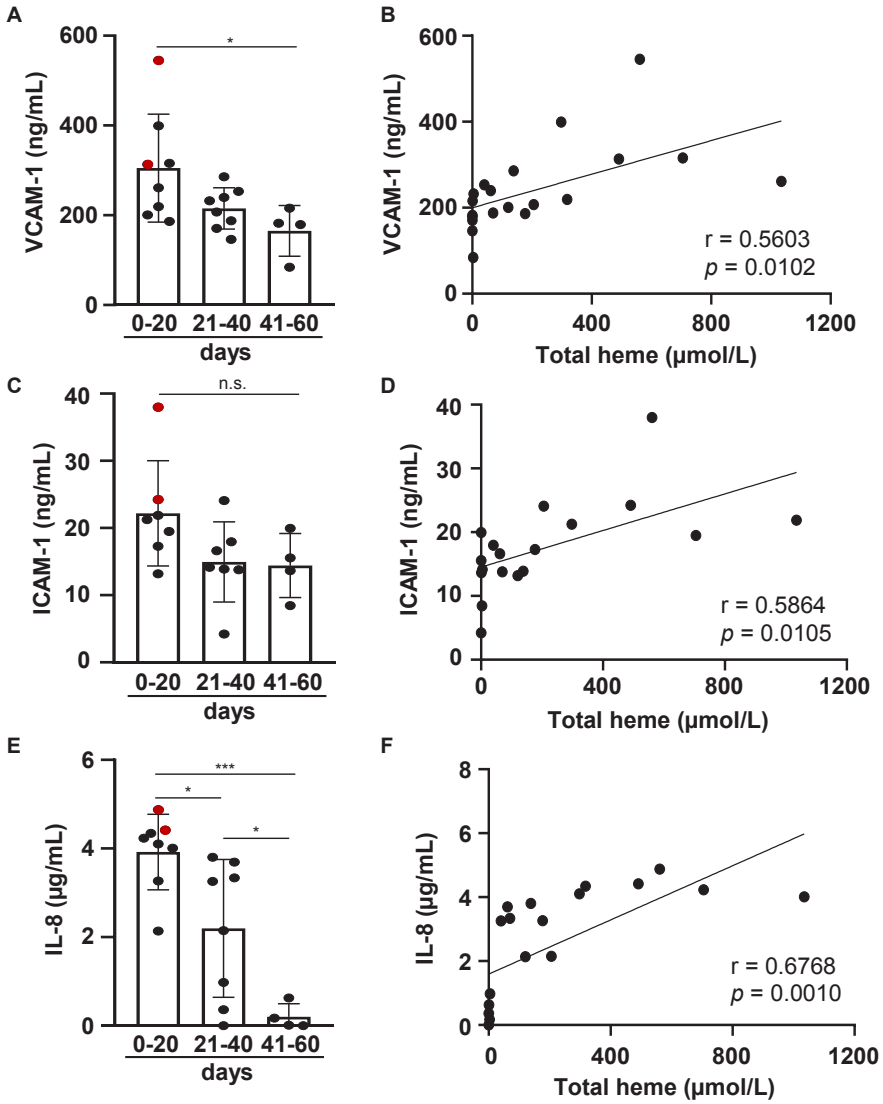

FIGURE 7 | Level of soluble VCAM-1, soluble ICAM-1, and IL-8 in post-IVH CSF samples. CSF samples (n = 20) were obtained from preterm infants diagnosed with grade III IVH at different time intervals after the onset of IVH. **(A,C,E)** Soluble VCAM-1, ICAM-1, and IL-8 levels of CSF samples obtained at different time intervals after the onset of IVH (days 0–20, 21–40, 41–60) were determined by ELISA in duplicates. Closed circles represent individual samples, red circles represent patients that died before 6 months of age, and bars represent mean ± SD. P-values were calculated using one-way ANOVA followed by Tukey's multiple comparison analysis. Correlation between **(B)** total heme and soluble VCAM-1, **(D)** total heme and soluble ICAM-1, and **(F)** total heme and IL-8 levels in post-IVH CSF samples is shown. R represents Pearson's correlation coefficient. $^{*}p < 0.05$, $^{***}p < 0.005$.

IVH. Moreover, covalently cross-linked oxidized Hb multimers that formed upon Hb oxidation have limited affinity toward Hp; therefore, these species might bypass the homeostatic control of cell-free Hb (36).

In contrast to native Hb, MetHb as well as ferrylHb can release their heme prosthetic groups (13, 14, 37). Heme is a hydrophobic molecule, which allows its penetration through cell membranes by passive diffusion, although recently, cell surface and organelle-associated transporters were discovered to facilitate the movement of heme between the different cellular compartments [reviewed in Gozzelino (38)]. Heme has long been considered as a pro-oxidant molecule (39), and recently, its pro-inflammatory nature has been recognized as well (40). The pro-oxidant reactivity of heme relies on the ability of its iron atom to exchange electrons with a variety of substrates. For example, interaction of heme with H_2O_2 results in the formation of the highly reactive hydroxyl radical in the Fenton reaction. Consequently, heme sensitizes various cells to oxidant- or cytokine-mediated killing (41, 42). Regarding cells of the central nervous system (CNS), heme (5–40 μmol/L) has been shown to be cytotoxic toward astrocytes (43) and neurons (44), and sensitize oligodendrocytes to TNF-α mediated programmed cell death (42).

To see whether there is any non Hb-bound, so-called "free" heme in the post-IVH CSF samples, first we determined the total heme concentration in CSF (total heme = heme in all Hb forms + free heme), and then calculated the amount of free heme. We found a big individual variation in free heme levels in CSF samples obtained between days 0 and 20 after the onset of IVH ranging from 42 up to 717 μmol/L.

Intravascular free heme is eliminated by the CD91–heme–hemopexin scavenging system [reviewed in Smith and McCulloh (45)]. Hemopexin binds heme with the highest affinity of any known protein (46), inhibits its catalytic activity, and facilitates its removal via the CD91 receptor (47). The same CD91–heme–hemopexin route exists in the CNS and plays an important role in heme detoxification after subarachnoid hemorrhage in adults influencing the clinical outcome (48). We have no information whether the CD91–heme–hemopexin scavenging system has evolved fully in preterm infants or the heme removal capacity of such a system upon IVH, but in any case, we assume that the system is oversaturated and this contributes to the accumulation of free heme in the CSF after IVH.

Hb, metHb, total heme, and free heme levels were lower in CSF samples collected at later time points between days 21 and 40 after the onset of IVH in comparison to CSF samples collected during the first 20 days following IVH. This suggests that although the Hb and heme scavenging capacity of the CSF was overwhelmed right after the onset of IVH, a slow clearing procedure took place afterward. In CSF samples collected between days 41 and 60 after the onset of IVH, we could hardly detect heme in any form. CSF is renewed four to five times a day in adults, and this rate is considered to be even higher in neonates. CSF is cleared via the blood–CSF barrier through specific proteins that are expressed in the choroid plexus epithelial cells that provide transport of nutrients and ions into the CNS and removal of waste products and ions from the CSF. Clearance for Hb and its derivatives from CSF via the blood–CSF barrier could be an option following IVH, but this mechanism has not yet been characterized.

FerrylHb is stabilized by intermolecular electron transfer between the ferryl iron and an adjacent amino acid of the globin chain resulting in globin radicals. The formed globin-based radicals react with each other and form covalently cross-linked Hb multimers that we could detect in CSF samples. Interestingly, we found a clear shift toward the formation of higher multimers at later time points after the onset of IVH. In CSF obtained between days 21 and 40 after the onset of IVH, we found significantly more covalently cross-linked oxidized globin tetramers than in CSF collected earlier (days 0–20). Moreover, in the CSF samples collected between days 41 and 60 after the onset of IVH, we could detect exclusively the covalently cross-linked oxidized globin tetramers. Considering that we could not detect any heme in these samples, we concluded that these globin tetramers have already released their heme prosthetic groups. The presence of this form of Hb at days 41–60 after the onset of IVH suggests that there is no efficient mechanism in the CNS for the elimination of this oxidized Hb form.

The blood–brain barrier (BBB) prevents blood cells and pathogens from entering the brain parenchyma and regulates the transport of molecules between the plasma and the CNS (49). Intracerebral hemorrhage (ICH) is associated with BBB dysfunction, and several studies showed that blood components (e.g., thrombin, Hb, iron) play a major role in ICH-induced BBB dysfunction (50). The BMEC monolayer is an important component of the BBB, and in a critical manner contributes to the neuroinflammatory response mainly by inducing the leukocyte adhesion cascade to facilitate the transmigration of inflammatory cells into the CNS. Therefore, we investigated the effect of the identified Hb forms in post-IVH CSF samples on BMECs.

Free heme content of CSF obtained between days 0 and 20 after the onset of IVH was particularly high; only one out of eight CSF samples had a free heme content below 50 μmol/L, three samples had high free heme content (50–250 μmol/L), and four out of the eight CSF samples had very high free heme content that exceeded 250 μmol/L. We showed here that heme at the concentration of 50 μmol/L or higher causes BMEC death due to elevated production of ROS. On the other hand, neither native Hb nor the oxidized Hb forms triggered ROS production or EC death.

With the use of a guinea pig exchange transfusion model, it was previously shown that polymerized cell-free Hb triggers BBB disruption (51). Additionally, we showed earlier that ferrylHb induces intermolecular gap formation in HUVECs leading to decreased endothelial monolayer integrity (16). In agreement with the previous study, here we found that ferrylHb but not native Hb or metHb impairs BMEC monolayer integrity.

HO-1, the oxidative stress-responsive enzyme that catalyzes heme degradation, is induced following ICH in different cells of the CNS including astrocytes, microglia, and ECs (52). Here we showed that besides sublethal concentration of heme, oxidized Hb forms, i.e., metHb and ferrylHb induce HO-1 expression. HO-1 has antioxidant and anti-inflammatory actions and affords protection against programmed cell death and inhibits the pathogenesis of a variety of immune-mediated inflammatory diseases (42). In line with this notion, it was shown that the upregulation of HO-1 prevents the development of experimental cerebral malaria in mice and attenuates BBB disruption and neuroinflammation (53). These beneficial effects are considered to be mediated by the binding of carbon monoxide (CO) – the end-product of HO-1 activity – to Hb, preventing its oxidation and the generation of free heme (53).

Recent studies showed the beneficial effect of CO gas as well as CO releasing molecules (CORMs) in ICH. CO/CORM treatment alters the inflammatory response, attenuates vasospasm, improves neurobehavioral function, preserves the circadian rhythm, and overall reduces the severity of brain damage in experimental models of ICH (54–56). Further studies are needed to understand whether the beneficial effect of CO on ICH-induced brain damage relies on its ability to prevent oxidation of cell-free Hb and subsequent heme release.

Adhesion molecules mediate the inflammatory cell response to injury through adherence to the vascular endothelium, diapedesis through the endothelial barrier, and migration into the tissues. Normally, vascular endothelium is in a quiescent state characterized by low expression of adhesion molecules. In contrast, upon insult, endothelial dysfunction develops,

characterized by elevated expression of adhesion molecules and pro-inflammatory cytokines. Brain hemorrhage triggers a local inflammatory response, and consequently, the levels of soluble adhesion molecules (i.e., E-selectin, ICAM-1, VCAM-1, and L-selectin) and inflammatory cytokines are elevated in the CSF of patients after subarachnoid hemorrhage (8, 57). IVH is followed by a systemic inflammatory response as well, and the extent of this response seems to be associated with white matter injury (7). ICAM-1 is a potential therapeutic target to attenuate cerebral vasospasm after subarachnoid hemorrhage (58).

Heme and oxidized Hb forms (i.e., metHb and ferrylHb) have been previously shown to induce adhesion molecules as well as pro-inflammatory cytokines (e.g., IL-6, IL-8, IL-1β) in human umbilical vein ECs (16, 59–61). Here we showed that heme and ferrylHb are the most potent inducers of the expression of adhesion molecules and IL-8 in BMECs, and that the levels of VCAM-1, ICAM-1, and IL-8 in CSF gradually decreased following the onset of IVH and correlated to total heme concentration of CSF.

Overall our study suggests that RBC destruction, Hb oxidation, and heme release are important pathogenic factors in IVH. On the other hand, this work also has some limitations. The study examined a very fragile group of patients: preterm babies with IVH grade III. The work is based on the examination of CSF samples obtained for diagnostic purposes; therefore, we could not influence the time of sampling. The earliest time point when we obtained CSF was day 14 after the onset of IVH, leaving us without information about the critically important first 2 weeks following IVH. We can speculate that in the first 2 weeks after IVH, we could have seen even higher amounts of Hb and its derivatives in the CSF. Another limitation of this work is that we have focused on only Hb and its derivatives, although it is very likely that the IVH-associated inflammatory response is much more complex. The major determinant of the inflammatory response and the outcome of IVH is the volume of bleeding, which likely correlates with the levels of Hb and its derivatives in the CSF. Despite these limitations, we believe that extracellular Hb and its derivatives contribute to the pathogenesis of IVH and pharmacological interventions targeting extracellular Hb, Hb oxidation, and heme could have a potential to limit the neuroinflammatory response following IVH.

DATA AVAILABILITY STATEMENT

All datasets generated for this study are included in the article/supplementary material.

ETHICS STATEMENT

The procedures were approved by the Scientific and Research Ethics Committee of the University of Debrecen and the Ministry of Human Capacities under the registration number of 1770-5/2018/EÜIG. Parental consent forms were signed by the parents of the eight infants involved in this study.

AUTHOR CONTRIBUTIONS

JE: collection and assembly of data and participation in drafting the manuscript writing. AN, LN, and LB: patient selection, sample collection, and revision of the manuscript. AT, BNy, EB, and ZF: data collection and analysis. BNa, JK, AB, and GP: data analysis and interpretation, and revision of the manuscript. VJ: conception and design, data analysis and interpretation, and drafting the manuscript. All authors agreed to be accountable for all aspects of the work in ensuring that questions related to the accuracy or integrity of any part of the work are appropriately investigated and resolved. All authors approved the manuscript submission.

FUNDING

This research was funded by the Hungarian National Research, Development and Innovation Office (NKFIH), grant numbers K116024 and K131535, Hungarian Academy of Sciences, MTA-DE Lendület Vascular Pathophysiology Research Group, grant number 96050, and European Union and the European Social Fund, grant number GINOP-2.3.2-15-2016-00005. BNa is a recipient of the Lajos Szodoray Grant (University of Debrecen).

REFERENCES

1. Sheth RD. Trends in incidence and severity of intraventricular hemorrhage. *J Child Neurol*. (1998) 13:261–4.
2. Wilson-Costello D, Friedman H, Minich N, Fanaroff AA, Hack M. Improved survival rates with increased neurodevelopmental disability for extremely low birth weight infants in the 1990s. *Pediatrics*. (2005) 115:997–1003. doi: 10.1542/peds.2004-0221
3. Stoll BJ, Hansen NI, Bell EF, Shankaran S, Laptook AR, Walsh MC, et al. Neonatal outcomes of extremely preterm infants from the NICHD Neonatal Research Network. *Pediatrics*. (2010) 126:443–56. doi: 10.1542/peds.2009-2959
4. Mukerji A, Shah V, Shah PS. Periventricular/intraventricular hemorrhage and neurodevelopmental outcomes: a meta-analysis. *Pediatrics*. (2015) 136:1132–43. doi: 10.1542/peds.2015-0944
5. Perlman JM. The relationship between systemic hemodynamic perturbations and periventricular-intraventricular hemorrhage-a historical perspective. *Semin Pediatr Neurol*. (2009) 16:191–9. doi: 10.1016/j.spen.2009.09.006
6. Milligan DW. Failure of autoregulation and intraventricular haemorrhage in preterm infants. *Lancet*. (1980) 1:896–8.
7. Leviton A, Allred EN, Dammann O, Engelke S, Fichorova RN, Hirtz D, et al. Systemic inflammation, intraventricular hemorrhage, and white matter injury. *J Child Neurol*. (2013) 28:1637–45. doi: 10.1177/0883073812463068
8. Polin RS, Bavbek M, Shaffrey ME, Billups K, Bogaev CA, Kassell NF, et al. Detection of soluble E-selectin, ICAM-1, VCAM-1, and L-selectin in the cerebrospinal fluid of patients after subarachnoid hemorrhage. *J Neurosurg*. (1998) 89:559–67. doi: 10.3171/jns.1998.89.4.0559
9. Jeney V, Eaton JW, Balla G, Balla J. Natural history of the bruise: formation, elimination, and biological effects of oxidized hemoglobin. *Oxid Med Cell Longev*. (2013) 2013:703571. doi: 10.1155/2013/703571

10. Reeder BJ, Cutruzzola F, Bigotti MG, Hider RC, Wilson MT. Tyrosine as a redox-active center in electron transfer to ferryl heme in globins. *Free Radic Biol Med*. (2008) 44:274–83. doi: 10.1016/j.freeradbiomed.2007.06.030
11. Nagy E, Eaton JW, Jeney V, Soares MP, Varga Z, Galajda Z, et al. Red cells, hemoglobin, heme, iron, and atherogenesis. *Arterioscler Thromb Vasc Biol*. (2010) 30:1347–53. doi: 10.1161/ATVBAHA.110.206433
12. Nyakundi BB, Toth A, Balogh E, Nagy B, Erdei J, Ryffel B, et al. Oxidized hemoglobin forms contribute to NLRP3 inflammasome-driven IL-1beta production upon intravascular hemolysis. *Biochim Biophys Acta Mol Basis Dis*. (2019) 1865:464–75. doi: 10.1016/j.bbadis.2018.10.030
13. Jeney V, Balla J, Yachie A, Varga Z, Vercellotti GM, Eaton JW, et al. Pro-oxidant and cytotoxic effects of circulating heme. *Blood*. (2002) 100:879–87. doi: 10.1182/blood.v100.3.879
14. Potor L, Banyai E, Becs G, Soares MP, Balla G, Balla J, et al. Atherogenesis may involve the prooxidant and proinflammatory effects of ferryl hemoglobin. *Oxid Med Cell Longev*. (2013) 2013:676425. doi: 10.1155/2013/676425
15. Belcher JD, Chen C, Nguyen J, Milbauer L, Abdulla F, Alayash AI, et al. Heme triggers TLR4 signaling leading to endothelial cell activation and vaso-occlusion in murine sickle cell disease. *Blood*. (2014) 123:377–90. doi: 10.1182/blood-2013-04-495887
16. Silva G, Jeney V, Chora A, Larsen R, Balla J, Soares MP. Oxidized hemoglobin is an endogenous proinflammatory agonist that targets vascular endothelial cells. *J Biol Chem*. (2009) 284:29582–95. doi: 10.1074/jbc.M109.045344
17. Singla S, Sysol JR, Dille B, Jones N, Chen J, Machado RF. Hemin causes lung microvascular endothelial barrier dysfunction by necroptotic cell death. *Am J Respir Cell Mol Biol*. (2017) 57:307–14. doi: 10.1165/rcmb.2016-0287OC
18. Kuck JL, Bastarache JA, Shaver CM, Fessel JP, Dikalov SI, May JM, et al. Ascorbic acid attenuates endothelial permeability triggered by cell-free hemoglobin. *Biochem Biophys Res Commun*. (2018) 495:433–7. doi: 10.1016/j.bbrc.2017.11.058
19. Rafikova O, Williams ER, McBride ML, Zemskova M, Srivastava A, Nair V, et al. Hemolysis-induced lung vascular leakage contributes to the development of pulmonary hypertension. *Am J Respir Cell Mol Biol*. (2018) 59:334–45. doi: 10.1165/rcmb.2017-0308OC
20. Wagener BM, Hu PJ, Oh JY, Evans CA, Richter JR, Honavar J, et al. Role of heme in lung bacterial infection after trauma hemorrhage and stored red blood cell transfusion: a preclinical experimental study. *PLoS Med*. (2018) 15:e1002522. doi: 10.1371/journal.pmed.1002522
21. Meng FT, Alayash AI. Determination of extinction coefficients of human hemoglobin in various redox states. *Anal Biochem*. (2017) 521:11–9. doi: 10.1016/j.ab.2017.01.002
22. Sercombe R, Dinh YR, Gomis P. Cerebrovascular inflammation following subarachnoid hemorrhage. *Jpn J Pharmacol*. (2002) 88:227–49. doi: 10.1254/jjp.88.227
23. Gram M, Sveinsdottir S, Ruscher K, Hansson SR, Cinthio M, Akerstrom B, et al. Hemoglobin induces inflammation after preterm intraventricular hemorrhage by methemoglobin formation. *J Neuroinflammation*. (2013) 10:100. doi: 10.1186/1742-2094-10-100
24. Hugelshofer M, Sikorski CM, Seule M, Deuel J, Muroi CI, Seboek M, et al. Cell-free oxyhemoglobin in cerebrospinal fluid after aneurysmal subarachnoid hemorrhage: biomarker and potential therapeutic target. *World Neurosurg*. (2018) 120:e660–6. doi: 10.1016/j.wneu.2018.08.141
25. Righy C, Turon R, Freitas G, Japiassu AM, Faria Neto HCC, Bozza M, et al. Hemoglobin metabolism by-products are associated with an inflammatory response in patients with hemorrhagic stroke. *Rev Bras Ter Intensiva*. (2018) 30:21–7. doi: 10.5935/0103-507x.20180003
26. Svistunenko DA, Patel RP, Voloshchenko SV, Wilson MT. The globin-based free radical of ferryl hemoglobin is detected in normal human blood. *J Biol Chem*. (1997) 272:7114–21.
27. Reeder BJ, Sharpe MA, Kay AD, Kerr M, Moore K, Wilson MT. Toxicity of myoglobin and haemoglobin: oxidative stress in patients with rhabdomyolysis and subarachnoid haemorrhage. *Biochem Soc Trans*. (2002) 30:745–8. doi: 10.1042/bst0300745
28. Vollaard NB, Reeder BJ, Shearman JP, Menu P, Wilson MT, Cooper CE. A new sensitive assay reveals that hemoglobin is oxidatively modified in vivo. *Free Radic Biol Med*. (2005) 39:1216–28. doi: 10.1016/j.freeradbiomed.2005.06.012
29. Ramirez DC, Chen Y-R, Mason RP. Immunochemical detection of hemoglobin-derived radicals formed by reaction with hydrogen peroxide: involvement of a protein-tyrosyl radical. *Free Radic Biol Med*. (2003) 34:830–9. doi: 10.1016/s0891-5849(02)01437-5
30. Deterding LJ, Ramirez DC, Dubin JR, Mason RP, Tomer KB. Identification of free radicals on hemoglobin from its self-peroxidation using mass spectrometry and immuno-spin trapping: observation of a histidinyl radical. *J Biol Chem*. (2004) 279:11600–7. doi: 10.1074/jbc.M310704200
31. Deuel JW, Schaer CA, Boretti FS, Opitz L, Garcia-Rubio I, Baek JH, et al. Hemoglobinuria-related acute kidney injury is driven by intrarenal oxidative reactions triggering a heme toxicity response. *Cell Death Dis*. (2016) 7:e2064. doi: 10.1038/cddis.2015.392
32. Thomsen JH, Etzerodt A, Svendsen P, Moestrup SK. The haptoglobin-CD163-heme oxygenase-1 pathway for hemoglobin scavenging. *Oxid Med Cell Longev*. (2013) 2013:523652. doi: 10.1155/2013/523652
33. Hwang PK, Greer J. Interaction between hemoglobin subunits in the hemoglobin. Haptoglobin complex. *J Biol Chem*. (1980) 255:3038–41.
34. Kristiansen M, Graversen JH, Jacobsen C, Sonne O, Hoffman HJ, Law SK, et al. Identification of the haemoglobin scavenger receptor. *Nature* (2001) 409:198–201. doi: 10.1038/35051594
35. Galea J, Cruickshank G, Teeling JL, Boche D, Garland P, Perry VH, et al. The intrathecal CD163-haptoglobin-hemoglobin scavenging system in subarachnoid hemorrhage. *J Neurochem*. (2012) 121:785–92. doi: 10.1111/j.1471-4159.2012.07716.x
36. Vallelian F, Pimenova T, Pereira CP, Abraham B, Mikolajczyk MG, Schoedon G, et al. The reaction of hydrogen peroxide with hemoglobin induces extensive alpha-globin crosslinking and impairs the interaction of hemoglobin with endogenous scavenger pathways. *Free Radic Biol Med*. (2008) 45:1150–8. doi: 10.1016/j.freeradbiomed.2008.07.013
37. Balla J, Jacob HS, Balla G, Nath K, Eaton JW, Vercellotti GM. Endothelial-cell heme uptake from heme proteins: induction of sensitization and desensitization to oxidant damage. *Proc Natl Acad Sci USA*. (1993) 90:9285–9.
38. Gozzelino R. The pathophysiology of heme in the brain. *Curr Alzheimer Res*. (2016) 13:174–84. doi: 10.2174/1567205012666150921103304
39. Balla G, Vercellotti GM, Muller-Eberhard U, Eaton J, Jacob HS. Exposure of endothelial cells to free heme potentiates damage mediated by granulocytes and toxic oxygen species. *Lab Investigation*. (1991) 64:648–55.
40. Dutra FF, Bozza MT. Heme on innate immunity and inflammation. *Front Pharmacol*. (2014) 5:115. doi: 10.3389/fphar.2014.00115
41. Balla J, Vercellotti GM, Jeney V, Yachie A, Varga Z, Jacob HS, et al. Heme, heme oxygenase, and ferritin: how the vascular endothelium survives (and dies) in an iron-rich environment. *Antioxid Redox Signal*. (2007) 9:2119–37. doi: 10.1089/ars.2007.1787
42. Gozzelino R, Jeney V, Soares MP. Mechanisms of cell protection by heme oxygenase-1. *Annu Rev Pharmacol Toxicol*. (2010) 50:323–54. doi: 10.1146/annurev.pharmtox.010909.105600
43. Dang TN, Bishop GM, Dringen R, Robinson SR. The metabolism and toxicity of hemin in astrocytes. *Glia*. (2011) 59:1540–50. doi: 10.1002/glia.21198
44. Dang TN, Robinson SR, Dringen R, Bishop GM. Uptake, metabolism and toxicity of hemin in cultured neurons. *Neurochem Int*. (2011) 58:804–11. doi: 10.1016/j.neuint.2011.03.006
45. Smith A, McCulloh RJ. Hemopexin and haptoglobin: allies against heme toxicity from hemoglobin not contenders. *Front Physiol*. (2015) 6:187. doi: 10.3389/fphys.2015.00187
46. Hrkal Z, Vodrazka Z, Kalousek I. Transfer of heme from ferrihemoglobin and ferrihemoglobin isolated chains to hemopexin. *Eur J Biochem*. (1974) 43:73–8.
47. Hvidberg V, Maniecki MB, Jacobsen C, Hojrup P, Moller HJ, Moestrup SK. Identification of the receptor scavenging hemopexin-heme complexes. *Blood*. (2005) 106:2572–9. doi: 10.1182/blood-2005-03-1185
48. Garland P, Durnford AJ, Okemefuna AI, Dunbar J, Nicoll JA, Galea J, et al. Heme-hemopexin scavenging is active in the brain and associates with outcome after subarachnoid hemorrhage. *Stroke*. (2016) 47:872–6. doi: 10.1161/STROKEAHA.115.011956
49. Sweeney MD, Zhao Z, Montagne A, Nelson AR, Zlokovic BV. Blood-brain barrier: from physiology to disease and back. *Physiol Rev*. (2019) 99:21–78. doi: 10.1152/physrev.00050.2017

50. Keep RF, Zhou N, Xiang J, Andjelkovic AV, Hua Y, Xi G. Vascular disruption and blood-brain barrier dysfunction in intracerebral hemorrhage. *Fluids Barriers CNS*. (2014) 11:18. doi: 10.1186/2045-8118-11-18
51. Butt OI, Buehler PW, D'Agnillo F. Blood-brain barrier disruption and oxidative stress in guinea pig after systemic exposure to modified cell-free hemoglobin. *Am J Pathol*. (2011) 178:1316–28. doi: 10.1016/j.ajpath.2010.12.006
52. Li QQ, Li LJ, Wang XY, Sun YY, Wu J. Research progress in understanding the relationship between heme oxygenase-1 and intracerebral hemorrhage. *Front Neurol*. (2018) 9:682. doi: 10.3389/fneur.2018.00682
53. Pamplona A, Ferreira A, Balla J, Jeney V, Balla G, Epiphanio S, et al. Heme oxygenase-1 and carbon monoxide suppress the pathogenesis of experimental cerebral malaria. *Nat Med*. (2007) 13:703–10. doi: 10.1038/nm1586
54. Yabluchanskiy A, Sawle P, Homer-Vanniasinkam S, Green CJ, Foresti R, Motterlini R. CORM-3, a carbon monoxide-releasing molecule, alters the inflammatory response and reduces brain damage in a rat model of hemorrhagic stroke. *Crit Care Med*. (2012) 40:544–52. doi: 10.1097/CCM.0b013e31822f0d64
55. Schallner N, Lieberum JL, Gallo D, LeBlanc RH III, Fuller PM, Hanafy KA, et al. Carbon monoxide preserves circadian rhythm to reduce the severity of subarachnoid hemorrhage in mice. *Stroke*. (2017) 48:2565–73. doi: 10.1161/STROKEAHA.116.016165
56. Kamat PK, Ahmad AS, Dore S. Carbon monoxide attenuates vasospasm and improves neurobehavioral function after subarachnoid hemorrhage. *Arch Biochem Biophys*. (2019) 676:108117. doi: 10.1016/j.abb.2019.108117
57. Gaetani P, Tartara F, Pignatti P, Tancioni F, Rodriguez y Baena R, De Benedetti F. Cisternal CSF levels of cytokines after subarachnoid hemorrhage. *Neurol Res*. (1998) 20:337–42. doi: 10.1080/01616412.1998.11740528
58. Bavbek M, Polin R, Kwan AL, Arthur AS, Kassell NF, Lee KS. Monoclonal antibodies against ICAM-1 and CD18 attenuate cerebral vasospasm after experimental subarachnoid hemorrhage in rabbits. *Stroke*. (1998) 29:1930–5; discussion 1935–6. doi: 10.1161/01.str.29.9.1930
59. Wagener FA, Feldman E, de Witte T, Abraham NG. Heme induces the expression of adhesion molecules ICAM-1, VCAM-1, and E selectin in vascular endothelial cells. *Proc Soc Exp Biol Med*. (1997) 216:456–63.
60. Liu XY, Spolarics Z. Methemoglobin is a potent activator of endothelial cells by stimulating IL-6 and IL-8 production and E-selectin membrane expression. *Am J Physiol Cell Physiol*. (2003) 285:C1036–46. doi: 10.1152/ajpcell.00164.2003
61. Erdei J, Toth A, Balogh E, Nyakundi BB, Banyai E, Ryffel B, et al. Induction of NLRP3 Inflammasome activation by heme in human endothelial cells. *Oxid Med Cell Longev*. (2018) 2018:4310816. doi: 10.1155/2018/4310816

Conflict of Interest: The authors declare that the research was conducted in the absence of any commercial or financial relationships that could be construed as a potential conflict of interest.

frontiers in Immunology

REVIEW
published: 13 March 2020
doi: 10.3389/fimmu.2020.00454

The Red Blood Cell—Inflammation Vicious Circle in Sickle Cell Disease

Elie Nader[1,2], *Marc Romana*[2,3,4] *and Philippe Connes*[1,2]*

[1] Laboratoire Interuniversitaire de Biologie de la Motricité (LIBM) EA7424, Team Vascular Biology and Red Blood Cell, Université Claude Bernard Lyon 1, Université de Lyon, Lyon, France, [2] Laboratoire d'Excellence du Globule Rouge (Labex GR-Ex), PRES Sorbonne, Paris, France, [3] Université des Antilles, UMR_S1134, BIGR, Pointe-à-Pitre, France, [4] Université de Paris, UMR_S1134, BIGR, INSERM, Paris, France

Sickle cell disease (SCD) is a genetic disease caused by a single mutation in the β-globin gene, leading to the production of an abnormal hemoglobin called hemoglobin S (HbS), which polymerizes under deoxygenation, and induces the sickling of red blood cells (RBCs). Sickled RBCs are very fragile and rigid, and patients consequently become anemic and develop frequent and recurrent vaso-occlusive crises. However, it is now evident that SCD is not only a RBC rheological disease. Accumulating evidence shows that SCD is also characterized by the presence of chronic inflammation and oxidative stress, participating in the development of chronic vasculopathy and several chronic complications. The accumulation of hemoglobin and heme in the plasma, as a consequence of enhanced intravascular hemolysis, decreases nitric oxide bioavailability and enhances the production of reactive oxygen species (ROS). Heme and hemoglobin also represent erythrocytic danger-associated molecular pattern molecules (eDAMPs), which may activate endothelial inflammation through TLR-4 signaling and promote the development of complications, such as acute chest syndrome. It is also suspected that heme may activate the innate immune complement system and stimulate neutrophils to release neutrophil extracellular traps. A large amount of microparticles (MPs) from various cellular origins (platelets, RBCs, white blood cells, endothelial cells) is also released into the plasma of SCD patients and participate in the inflammation and oxidative stress in SCD. In turn, this pro-inflammatory and oxidative stress environment further alters the RBC properties. Increased pro-inflammatory cytokine concentrations promote the activation of RBC NADPH oxidase and, thus, raise the production of intra-erythrocyte ROS. Such enhanced oxidative stress causes deleterious damage to the RBC membrane and further alters the deformability of the cells, modifying their aggregation properties. These RBC rheological alterations have been shown to be associated to specific SCD complications, such as leg ulcers, priapism, and glomerulopathy. Moreover, RBCs positive for the Duffy antigen receptor for chemokines may be very sensitive to various inflammatory molecules that promote RBC dehydration and increase RBC adhesiveness to the vascular wall. In summary, SCD is characterized by a vicious circle between abnormal RBC rheology and inflammation, which modulates the clinical severity of patients.

Keywords: sickle cell disease, inflammation, red blood cell, oxidative stress, heme

OPEN ACCESS

Edited by:
Nicola Conran,
Campinas State University, Brazil

Reviewed by:
Samit Ghosh,
University of Pittsburgh, United States
Erich Vinicius De Paula,
Campinas State University, Brazil

***Correspondence:**
Philippe Connes
pconnes@yahoo.fr;
philippe.connes@univ-lyon1.fr

Specialty section:
This article was submitted to Inflammation, a section of the journal Frontiers in Immunology

Received: *04 December 2019*
Accepted: *27 February 2020*
Published: *13 March 2020*

Citation:
Nader E, Romana M and Connes P (2020) The Red Blood Cell—Inflammation Vicious Circle in Sickle Cell Disease. Front. Immunol. 11:454. doi: 10.3389/fimmu.2020.00454

INTRODUCTION

Sickle cell disease (SCD) is a genetic disease caused by a single mutation in the β-globin gene, leading to the production of an abnormal hemoglobin called hemoglobin S (HbS). Under deoxygenation, the HbS polymerizes, which causes the sickling of red blood cells (RBCs). Sickled RBCs are very fragile and rigid. These abnormal features of sickle RBCs are believed to be responsible for chronic anemia and frequent and recurrent painful vaso-occlusive crises, respectively. However, although the molecular defects at the origin of the disease have been well-described, patients with SCD may exhibit various acute and/or chronic complications, which may affect several organs, such as the lungs, heart, kidney, brain, skin, bones, and eyes, for example. It is worth noting that this genetic disorder is associated with an extreme inter-individual variability of its clinical presentation (1). In addition, while it is easy to consider that rigid RBCs could obstruct the microcirculation and trigger the onset of vaso-occlusive like events, it has been demonstrated that the transit time of RBCs in deoxygenated vascular areas would be theoretically too short to allow RBCs to spend enough time to sickle (2, 3). This means that other biological mechanisms participate in the pathophysiological processes of the disease. Activation and increased adhesiveness of neutrophils, monocytes and platelets to the endothelium, mainly in post-capillary venules, may initiate vaso-occlusion (4–7). The resulting decreased blood flow induces a longer transit time of RBCs in vascular areas with poor oxygen content, hence promoting HbS polymerization and RBC sickling (6). The accumulation of rigid RBCs and adherent circulating cells into the microcirculation is responsible for vaso-occlusion (6). Mounting evidence shows that SCD is characterized by the presence of chronic inflammation and oxidative stress, participating in the development of chronic vasculopathy, endothelial dysfunction and several chronic complications. In addition, this pro-oxidative and pro-inflammatory environment further impairs the rheological properties of RBCs, hence further impacting the clinical severity of disease in patients.

THE ROLE OF HEMOLYSIS IN INFLAMMATION AND VASCULAR DYSFUNCTION

Although chronic anemia is fairly well-tolerated by SCD patients, the severity of anemia modulates their aerobic fitness and quality of life (8, 9). Moreover, levels of anemia, partly determined by the rate of intravascular hemolysis in SCD patients, influences their survival rate (9). In addition, intravascular hemolysis also plays a key role in the pathophysiology of SCD, independently of its effects on anemia. Patients with the highest rate of hemolysis are at risk of earlier mortality, compared to those with less pronounced hemolysis (10). This section will discuss the consequences of enhanced hemolysis on inflammation, oxidative stress and the vascular function in SCD (11).

Hemolysis and Nitric Oxide (NO) Bioavailability

NO produced by the endothelial NO-synthase (eNOS) is a strong modulator of vascular physiology. Through its effects on the vascular smooth cells, NO plays a key role in vasodilation. Moreover, NO has been shown to downregulate the transcription of several endothelial adhesion molecules of both the CAM (ICAM-1, VCAM-1) and selectin (E- and P-selectin) families (12) and to inhibit platelet activation (13). Accumulating evidence strongly supports a key role of hemolysis in the decrease of NO bioactivity/bioavailability in SCD (14, 15). The accumulation of hemoglobin in the plasma affects the bioavailability of nitric oxide (NO). Cell-free hemoglobin destroys NO at a rate of 1,000-fold faster than hemoglobin encapsulated in the RBCs (16). Moreover, hemolysis leads to the release of the arginase contained in erythrocytes into the plasma. The free arginase hydrolyzes arginine, which is the precursor to NO, to ornithine and urea, thereby exacerbating the decrease in NO bioavailability (11). Indeed, any decrease in NO bioactivity/bioavailability would result in vascular dysfunction.

Blood flow responses to sodium nitroprusside (a NO donor) or to L-NMMA (a NO-synthase inhibitor) are abolished in patients with SCD (17). Flow-mediated dilation response using nitroglycerin (a NO donor) is impaired in patients with SCD, compared to a control group (18). Belhassen et al. (19) reported increased diameter in the brachial artery at baseline in SCD patients, compared to a control group, but the vessel was not able to further dilate in response to a flow-mediated dilation procedure. At the microcirculatory level, Moeckesch et al. (20) reported decreased hyperemic response to skin heating localized stress in children with SCD, compared to healthy children, suggesting impaired microcirculatory NO-driven vasodilation in the former population.

The decrease in NO bioavailability could also be responsible for the enhanced platelet activation (13) observed in SCD patients, as documented by increased expression of platelet activation markers, such as P-selectin, CD63, activated glycoprotein IIb/IIIa, plasma soluble factor-3 and factor-4, β-thromboglobulin, and platelet-derived soluble CD40 ligand (21, 22). Such abnormal platelet activation has been associated with thrombosis and pulmonary hypertension, a clinical manifestation of endothelial dysfunction, in SCD patients (23). Kato et al. (24) also reported positive associations between the level of plasma soluble adhesion molecules and the severity of pulmonary hypertension.

On the whole, these studies strongly support a key role of hemolysis on endothelial/vascular dysfunction through its effects on NO bioactivity/availability.

Hemolysis, Oxidative Stress, and Inflammation

The accumulation of extracellular hemoglobin and heme in SCD, which cannot be fully neutralized by haptoglobin and hemopexin, respectively (14), is a major source of oxidative stress. Hemoglobin may react with hydrogen peroxide through the Fenton reaction to form hydroxyl free radical and

methemoglobin. The rate of autooxidation of Hb is greatly enhanced when released into the plasma, where it is partially oxygenated, and more particularly when the Hb tetramer dissociates into dimers (25). In addition, the repeated episodes of ischemia-reperfusion, such as those that occur during vaso-occlusive crises, induce the release of plasma xanthine oxidase (XO) (26). The released XO can impair vascular function by binding to the luminal cells of the vessel. This oxidative milieu results in exacerbated NO scavenging via an oxygen free radical-dependent mechanism, and further affects the vascular system. Mockesch et al. (20) recently showed that the impairment of microvascular regulation in children with SCD was significantly associated with both nitrotyrosine and markers of systemic oxidative stress, confirming the important roles of oxidative stress and NO scavenging in the development of vascular dysfunction in SCD.

Excessive production of reactive oxygen species (ROS) leads to endothelial damage, through peroxidation of the lipid membrane and/or DNA fragmentation, potentially leading to cellular apoptosis (27, 28). In addition, ROS play a central role in promoting vascular inflammation and endothelial activation through the activation of redox-sensitive transcription factors in the endothelium, such as NF-κB (29). The increased expression of several vascular cell adhesion molecules, such as VCAM-1, ICAM-1, L-, P-, and E-selectins, may then facilitate the binding of sickle RBCs, platelets and white blood cells (WBCs) to endothelial cells, which would trigger the onset of vaso-occlusion (30–32). Marui et al. (30) demonstrated that the use of pyrrolidine dithiocarbamate (an antioxidant) on cultured endothelial cells (HUVEC) was able to decrease the expression of VCAM-1 induced by IL-1β. There is clearly an interplay between oxidative stress and inflammation, which participates in the pathogenesis of SCD (33). Additionally, Belcher et al. (34) demonstrated that the administration of dimethyl fumarate (a drug activating Nrf2 expression and increasing the transcription and expression of several genes involved in antioxidant defenses) for several days in sickle cell mice decreased the hepatic expression of TLR4, NF-κB activation, VCAM-1, ICAM-1 and E-selectin mRNA levels, and hepatic necrosis.

Seminal work from Wagener et al. (35) showed that *in vitro* incubation of endothelial cells with heme led to a rise in adhesion molecule expression. Furthermore, the same group (36) reported that injection of heme in mice increased vascular permeability, adhesion molecule expression and leucocyte extravasation. Another group reported that incubation of endothelial cells with hemin (i.e., heme oxidized in its ferric form) increased the production of IL-8 (37). Although most of these inflammatory effects could be partly driven by the resulting enhanced oxidative stress caused by heme accumulation, heme would also directly activate the immune innate system (38).

Ghosh et al. (39) showed that hemin administration in sickle mice enhanced intravascular hemolysis, which further increased the amount of extracellular hemin, caused lung injuries typical of acute chest syndrome and decreased their survival rate. However, TLR4 inhibition (by the use of TAK-242) and hemopexin replacement therapy, prior to hemin infusion, protected sickle mice from developing acute chest syndrome. Chimeric sickle cell mice, knocked out for TLR4, did not develop extensive lung injury and were able to survive after infusion of hemin. Belcher et al. (40) investigated the role of heme in SCD vaso-occlusion and showed that administration of heme to SCD mice caused increased endothelial P-selectin and vWF expression, enhanced leucocyte rolling and adhesion and blood flow stasis. When treated with TAK-242 (an inhibitor of TLR4), blood stasis, leucocyte rolling and adhesion were decreased in mice injected with heme.

Adisa et al. (41) reported an association between plasma free heme concentration and the incidence of vaso-occlusive crises, in children with SCD. More recently, Pitanga et al. (42) reported a 4-fold higher level of circulating IL-1β in SCD patients at steady state, compared to healthy individuals. The authors also observed higher mRNA expressions of NLRP3 and IL-1β in the peripheral blood mononuclear cells (PBMC) of SCD patients, suggesting the activation of the NLRP3 inflammasome. Subsequently, they showed that incubation of PBMC with sickle RBCs induced higher mRNA expression of the genes encoding IL-1β, leukotriene, TLR9, NLRP3, caspase 1, and IL-18 in the supernatant, as compared to PBMC that were incubated with healthy RBCs. The authors did not look for the RBC element/molecule that could trigger the activation of the inflammasome and one could suggest that RBCs may contain several molecules that can act as eDAMPs. Hemolysis-related products are now considered as important eDAMPs that could trigger inflammasome activation in the context of SCD and participate in the pathophysiology of several complications (15, 43). Collectively, these findings suggest that hemolysis-related products could play a major role in the pathophysiology of several complications in SCD, through their binding to TLR4 and the activation of NF-κB and NLRP3 pathways and the enhanced production of pro-inflammatory cytokines, such as IL1β and IL18 (15). Other potent eDAMPs that may be released by RBCs during hemolysis include heat shock proteins (Hsp), such as Hsp70, IL-33, and adenosine 5′ triphosphate (43).

Hemolysis, Neutrophil Extracellular Traps (NETs), and Inflammation

Heme/hemin have also been shown to activate neutrophils (44) and promote the release of NETs in SCD (45). Schimmel et al. (46) reported higher nucleosome levels in SCD patients at steady state, compared to healthy individuals, with a further increase during crisis. In addition, the authors reported a correlation between the levels of nucleosomes and the length of hospital stay in patients developing acute chest syndrome. NETs are composed of decondensed chromatin fibers coated with antimicrobial granular and cytoplasmic proteins, such as myeloperoxidase (MPO), neutrophil elastase, and alpha defensin. These NETs are able to promote endothelial activation, thus increasing VCAM-1 and ICAM-1 expression (47). It has also been suggested that NETs could promote vessel occlusion by providing a scaffold for platelets, RBCs and pro-coagulant molecules (48). Recent studies also demonstrated that NETs induced the activation of the NLRP3 inflammasome in macrophages through TLR4/TLR9 signaling pathways, leading to higher production of IL-1β in the

context of diabetes and atherosclerosis (49, 50). Indeed, one may suspect a role of NETs in SCD pathogenesis through an activation of the immune innate system (15).

Hemolysis and the Alternative Complement Pathway

Hemolysis activates the alternative complement pathway. In atypical uremic hemolytic syndrome, heme has been shown to activate the complement system in plasma and on endothelial cells (51). Heme-induced exocytosis of Weibel-Palade bodies from endothelial cells induces the expression of P-selectin, which is known to bind C3b and trigger complement activation (51). In addition, heme can trigger the release of C5a and C5b9, leading to the activation and permeabilization of endothelial cells (51). The attachment of membrane attack complexes to the endothelial cells may promote inflammation through NF-κB signaling (52).

Increased soluble C5b-9 levels have been reported in SCD patients (53, 54). Vercellotti et al. (55) demonstrated increased C3 activation fragments and C5b-9 in the kidneys, lungs and liver of sickle cell mice, compared to control mice, and Lombardi et al. (56) found increased microvascular deposition of C5b-9 on skin biopsies in SCD patients. Increased alternative pathway Bb fragments have also been reported in the plasma of both sickle cell mice and sickle cell patients (55, 57). The infusion of recombinant C5a has been shown to cause blood stasis and inflammation in the liver of sickle cell mice (through NF-κB activation and increased expression of TLR4 and several adhesion molecules), but this response was reversed by an anti-C5a receptor IgG (55). The increased externalization of phosphatidylethanolamine and phosphatidylserine at the membrane of sickle RBCs is also suspected to induce complement activation with increased C3 and C3b binding (56, 57). A very recent work investigated the role of heme on complement activation in the context of SCD (58). The authors showed increased C3 and C9 deposition in the kidneys of both sickle cell mice and SCD patients and demonstrated that C3 fragment deposition was increased in the kidney of normal mice receiving phenylhydrazine to promote intravascular hemolysis. The effects of hemin were tested on endothelial cells and it was shown that heme triggered rapid P-selectin, C3aR and C5aR expression, C3 and C5b9 deposition, and downregulated CD46, a transmembrane protein able to bind and inactivate C3b and C4b. The use of hemopexin with hemin reduced the deposition of C3 and C5b9 on endothelial cells. Merle et al. (59) demonstrated that P-selectin drives complement attack on endothelial cells during intravascular hemolysis in a TLR-4/heme-dependent manner. Altogether, these studies support a key role for hemolysis in endothelial dysfunction in SCD with implications for the participation of the alternative complement pathway.

Hemolysis, Microparticles, Inflammation, and Oxidative Stress

Circulating extra-cellular vesicles (EV), such as microparticles (MPs, 0.1–1 μm) and exosomes (30–100 nm), are thought to play a role in the pathogenesis of SCD (60, 61). Several groups reported a 3- to 4-fold increase of plasma MPs (mainly originating from platelets and RBCs) in SCD patients at steady-state compared to healthy individuals (62–66), with a further rise during vaso-occlusive crises (62, 67, 68). Khalyfa et al. (69) reported increased levels of circulating exosomes in SCD patients compared to healthy individuals, with the most severe patients (i.e., with the highest rate of painful vaso-occlusive crises) exhibiting the highest levels.

MPs and exosomes carry diverse cargoes including proteins, RNA species, such as mRNA and miRNA and lipids that can be transported and exchanged between cells, strongly suggesting that EV play key roles in cell-cell communication at both paracrine and systemic levels (61, 70). Not specific to SCD, these EV may promote inflammation, oxidative stress, coagulation, and endothelial activation. The high amount of externalized phosphatidylserine at the surface of most of the MPs is responsible for their pro-coagulant property while others express tissue factor (60, 61). Various blood cell-derived MPs have also been shown to regulate the production of reactive oxygen species and promote endothelial activation (61, 71). MPs shed by endothelial cells (71), monocytes (72), and lymphocytes (73) induce endothelial O_2^- and H_2O_2 production in cultured endothelial cells through processes involving different enzymatic systems, and thus may lead to apoptosis (74). Treatment of endothelial cells with platelet- and endothelial cell-derived MPs were associated with increased expression of cell adhesion molecules and monocyte-endothelial cell interactions (74, 75).

However, only a few studies have investigated the effects of EV in the context of SCD, and more particularly the effects of RBC-derived MPs. It seems that the amount of circulating RBC-derived MPs is directly related to the degree of hemolysis (64, 76, 77). Several authors reported strong associations between various markers of hemolysis, such as heme, lactate dehydrogenase, plasma hemoglobin, serum bilirubin, reticulocyte count, fetal Hb or hemoglobin concentration, and RBC-MPs (76, 77). Camus et al. (78, 79) previously demonstrated that *ex-vivo* generated sickle RBC-MPs, when infused in sickle cell mice, promoted kidney vaso-occlusions. The authors further demonstrated that these RBC-MPs delivered toxic heme to endothelial cells, which increased the production of reactive oxygen species and the expression of endothelial cell adhesion molecules, and promoted apoptosis. Interestingly, heme-loaded MPs were also shown to activate the alternative and terminal complement pathway at the surface of the endothelial cells (58). Khalyfa et al. (69) demonstrated that exosomes isolated from SCA patients with frequent vaso-occlusive crises, for which RBC-derived exosomes being the most abundant, decreased endothelial permeability and promoted P-selectin expression on cultured endothelial cells. These exosomes also significantly increased the adhesion of monocytes to the vascular wall in mice, compared with exosomes isolated from SCA patients with a less severe phenotype.

Taken together, these findings suggest that the accumulation of RBC-MPs, consecutive to enhanced hemolysis, in SCD could cause serious damage to the vascular system and modulate clinical severity.

HOW DO SICKLE RBCs REACT TO THIS PRO-INFLAMMATORY AND PRO-OXIDATIVE ENVIRONMENT?

Because RBCs are very fragile and prone to lysis, SCD patients are characterized by chronic anemia. We previously discussed the consequences of enhanced hemolysis in SCD on the reduction of NO bioavailability, the increase in oxidative stress and inflammation, the production of NETs, the activation of the alternative complement pathway and the release of RBC-derived MPs, which all lead to endothelial activation and vascular dysfunction. However, this pro-inflammatory and pro-oxidative environment may further damage the RBCs, which could further alter their rheological properties and increase their fragility.

Nitric Oxide and RBCs

The effects of NO on the vascular system have been well-described in the literature, but NO may also affect the mechanical properties of RBCs. One of the first reports suggesting that NO could affect RBC deformability was the study of Starzyk et al. (80), which demonstrated that intravenous infusion of L-NAME (an eNOS inhibitor) in rats caused a reduction in RBC deformability. Bor-Kucukatay et al. (81) then demonstrated that several eNOS inhibitors decreased RBC deformability. A recent work conducted in SCD showed that *in vitro* incubation of RBCs with sodium nitroprusside (a NO donor) decreased the amount of intracellular reactive oxygen species and increased RBC deformability (82). This study also demonstrated that, in addition to its effects on HbF production and the reduction of HbS polymerization, the positive effects of hydroxycarbamide treatment on SCD RBC deformability could be related to the increased NO delivery from the drug to sickle RBCs.

It has been suggested that the effect of NO on RBC deformability could be partially mediated by soluble guanylyl cyclase (sGC) (83), but studies by Bor-Kucukatay et al. (81) and Baskurt et al. (84) also support a role for NO in potassium permeability. In addition, NO could decrease the risk for hemolysis and increase RBC survival rate through its effects on eryptosis since NO is able to down-regulate caspase 3 activity through S-nitrosylation (85). More recently, another group demonstrated that the NO donor, sodium nitroprusside, inhibited the decrease in RBC deformability induced by ionophore A23187-mediated calcium influx in RBC (86). Increased intracellular calcium concentration activates calcium-sensitive K^+ (Gárdos) channels, resulting in potassium-efflux and decreased cell volume, which in turn increases the stiffness of RBC; however, the presence of sodium nitroprusside abolished this calcium-induced impairment in RBC deformability (86). Barodka et al. (86) suggested that sodium nitroprusside may have limited calcium influx, thereby inhibiting the activation of Gárdos channels, and thus, maintaining cell volume and RBC deformability. However, the effects of NO on RBC rheology may not be limited only to its effects on RBC deformability. For instance, Bor-Kucukatay et al. (87) demonstrated that incubation of RBC with sodium nitroprusside decreased RBC aggregation, while giving L-NAME to rats resulted in a rise in their RBC aggregation. The underlying mechanisms at the origin of these findings are unclear, but might involve membrane/cytoskeletal protein nitrosylation or oxidative stress modulation. In conclusion, the reduction of NO bioavailability in SCD probably plays a role in the modulation of RBC rheology (82, 88).

Oxidative Stress and RBCs

As previously discussed, oxidative stress is increased in SCD, both in plasma and RBC (15, 82, 89–92), with a further rise during painful vaso-occlusive crises (68). Through its effects on the membrane of RBCs (i.e., lipid peroxidation and protein oxidation) and caspase 3 activation (93, 94), oxidative stress is a key modulator of RBC rheological properties. Moreover, oxidative stress is able to activate Ca^{2+}-permeable non-selective cation channels in the RBC membrane, leading to the accumulation of Ca^{2+} within RBCs, which can trigger RBC membrane scrambling, resulting in phosphatidylserine exposure and possibly in membrane bubbling and emission of MPs (95). In addition, the activation of Ca^{2+}-sensitive K^+ channels can lead to K^+ exit, hyperpolarization, Cl^- exit and cell shrinkage (95).

Baskurt et al. (96) demonstrated that superoxide anion caused a decrease in RBC deformability, a slight decrease in RBC aggregation and a large increase in RBC aggregates strength, meaning that the RBC aggregates formed are more robust upon oxidative stress. Depending on the concentration used, hydrogen peroxide may decrease RBC deformability (high concentration) or increase RBC adhesion to endothelial cells (low concentration) (97). Using atomic force microscopy, Sinha et al. (98) demonstrated the deleterious effects of several oxidant molecules (hydrogen peroxide, diamide, primaquine bisphophate, and cumene hydroperoxide) on RBC cytoskeletal architecture and membrane stiffness. All these changes may affect the fragility of RBCs. For instance, McNamee et al. (99) recently showed that phenazine methosulfate (an agent that generates superoxide anion within RBCs) decreased RBC deformability and increased the sensitivity of RBCs to shear-mediated damage. Hierso et al. (100) compared the biophysical response of healthy and SCD RBCs to *in-vitro* oxidative stress, using t-butyl hydroperoxide (TBHP). TBHP increased the production of ROS and decreased GSH content within the RBCs of both SCD and healthy individuals. In addition, the molecule decreased RBC deformability and RBC aggregation, and increased the strength of RBC aggregates in the two populations. However, the magnitude of changes in RBC rheology was 2- to 3-fold higher in SCD patients than in healthy individuals, indicating that RBC from SCD patients are more susceptible to oxidative stress than RBC from healthy individuals. The decrease in RBC antioxidant defenses in SCD could account for these differences (100).

Inflammation and RBCs

SCD is characterized by a pro-inflammatory state leading to high plasma cytokines levels. Karsten et al. (101) recently showed that 46 cytokines can be detected in RBCs lysates of healthy individuals, and their median concentrations in

RBCs were 12-fold higher than in plasma. Among them, the authors reported the presence of IFN-γ, IL-1β, IL-18, TNF-α as well as several chemokines, such as IL-8 and RANTES. The mean IL-1β and IL-18 concentrations in whole blood were 0.5 and 13.3 pg/ml, respectively, but the concentrations reached 4.2 and 657.6 pg/ml in RBCs, respectively (after correction for white blood cell contamination). When incubated in a protein-free media, the authors demonstrated that RBCs were able to release TNF-α, RANTES, IL-6, IL-8, and other molecules. It was also demonstrated that RBCs were able to capture various recombinant cytokines by using a recombinant standard cytokine mix. This study concluded that RBCs are dynamic reservoirs of cytokines, preventing chemokine clearance and thereby prolonging chemokine half-life in the blood. One major locus for cytokines binding is the Duffy Antigen receptor for chemokines (DARC) (102). Instead of acting as a reservoir, Darbonne et al. (102) proposed that RBCs act as a sink for IL-8, thereby inactivating the IL-8-dependent gradient and preventing neutrophil recruitment. DARC may also capture other chemokines of the CXC and CC families (103). Lee et al. demonstrated that patients lacking erythroid DARC expression exhibited higher plasma chemokine levels following LPS exposure, suggesting that DARC could act as chemokine scavengers to decrease immune-activating signals (sink hypothesis). The two models for RBC regulation of cytokines and chemokines levels could appear contradictory, but they may be not mutually exclusive. Fukuma et al. (104) proposed that RBCs would scavenge chemokines/cytokines from sites of inflammation, but could eventually release them in response to a reduction of plasma levels, effectively maintaining homeostasis. The degree of rupture of this homeostasis is unknown in SCD, but some studies have investigated the consequences of various inflammatory molecules on RBC properties. Bester et al. (105, 106) recently demonstrated that IL-8 affects the shape of healthy RBCs with morphological changes typical of those occurring during eryptosis. Circulating extracellular histones (i.e., a marker of NETosis) have recently been reported to promote eryptosis in healthy donors, ending with increased RBC phosphatidylserine externalization and RBC shrinkage (107). Test et al. (108) demonstrated increased binding of C5-b7 and of C9 to dense sickle RBCs, increasing the susceptibility of these cells to C5b-9-mediated reactive lysis initiated by C5b6. George et al. (109) tested the effects of transforming growth factor β1 and endothelin-1 (two cytokines known to be elevated in the context of SCD) on healthy RBCs. They demonstrated that these two inflammatory molecules stimulated RBC NADPH oxidase activity, leading to the accumulation of reactive oxygen species, which are known to damage the membrane of RBCs and increase their rigidity when produced in excess. In addition, endothelin-1 has been shown to promote dehydration of sickle RBCs through an activation of the Gárdos Channel, leading to a rise in RBC density (110). Durpes et al. (111) showed that the percentage of RBCs with densities higher than 1.12 (i.e., irreversibly sickle dehydrated RBCs) was 17-fold higher in sickle cell patients expressing DARC, compared to Duffy-negative patients. Since chemokines and cytokines would be able to bind to DARC, these results suggest a link between inflammation and sickle RBC dehydration. Furthermore, the authors demonstrated that both IL-8 and RANTES promoted dehydration in sickle RBC expressing DARC, through an activation of the Gárdos pathway. The same group (112) reported an effect of these two chemokines on the activation of α4β1 integrin in sickle reticulocytes expressing DARC, resulting in a greater adhesion of sickle RBCs to immobilized VCAM-1 and fibronectin. These findings could partly explain why Drasar et al. (113) reported that SCD patients with RBCs expressing DARC could be more prone to developing leg ulcers and kidney disease than Duffy-negative SCD patients, although this association between Duffy phenotype and SCD clinical severity is still debated (114, 115). Nebor et al. (116) failed to find an association between Duffy phenotype and the clinical severity in a large cohort of SCD patients, but they reported higher plasma IL-8 and RANTES levels in Duffy-positive vs. Duffy-negative patients, suggesting that RBCs can clearly modulate the level of inflammation in SCD. Although the exact mechanisms by which RBCs can modulate inflammation in SCD are not fully understood, these findings support the fact that pro-inflammatory molecules may promote sickle RBC dehydration and increase RBC density/rigidity through increased Gárdos channel activity, as well as increase RBC adhesiveness to endothelial cells through α4β1 clustering.

IMPAIRED RBC RHEOLOGY IS INVOLVED IN THE PATHOPHYSIOLOGY OF SCD

As previously discussed, enhanced hemolysis, due to the decreased deformability and increased fragility of sickle RBC, disturbs NO metabolism and promotes oxidative stress and inflammation through various mechanisms. In turn, this pro-inflammatory and pro-oxidative environment may further impair the rheological properties of RBCs and increase their fragility, further impacting on the clinical expression of the disease. For instance, SCD patients with the lowest RBC deformability have been reported to be at higher risk of developing priapism, leg ulcers and glomerulopathy than those with the highest RBC deformability (117–119). There is a clear relationship between RBC deformability, RBC fragility and the extent of hemolysis in SCD (120). Patients with the lowest deformability have higher hemolytic rates, which may increase their risk of developing hemolytic-like complications, such as those cited above (14, 121, 122). Moreover, abnormal RBC aggregation properties may also play a role in SCD pathogenesis and are modulated by both oxidative stress and inflammation. Lamarre et al. (123) found an association between increased RBC aggregation strength and the occurrence of acute chest syndrome. More recently, Lapouméroulie et al. (124) observed a rise of RBC aggregation and of the robustness of RBC aggregates in SCD patients during vaso-occlusive crisis compared to the steady-state condition. Abnormal RBC aggregation may both disturb blood flow in the microcirculation and microcirculation (125). In the microcirculation, increased RBC aggregate strength may increase vascular resistance and decrease blood flow at the entry of capillaries (88). In the

macrocirculation, the different hemodynamic re-arrangements between flowing RBC aggregates and single flowing RBCs create a situation where the width of the cell free layer close to the vascular wall is larger when RBC aggregates are flowing, leading to a decrease in wall shear stress, and reductions in eNOS activation and NO production, thus impacting on the ability of the vessels to adapt their diameters (125–127).

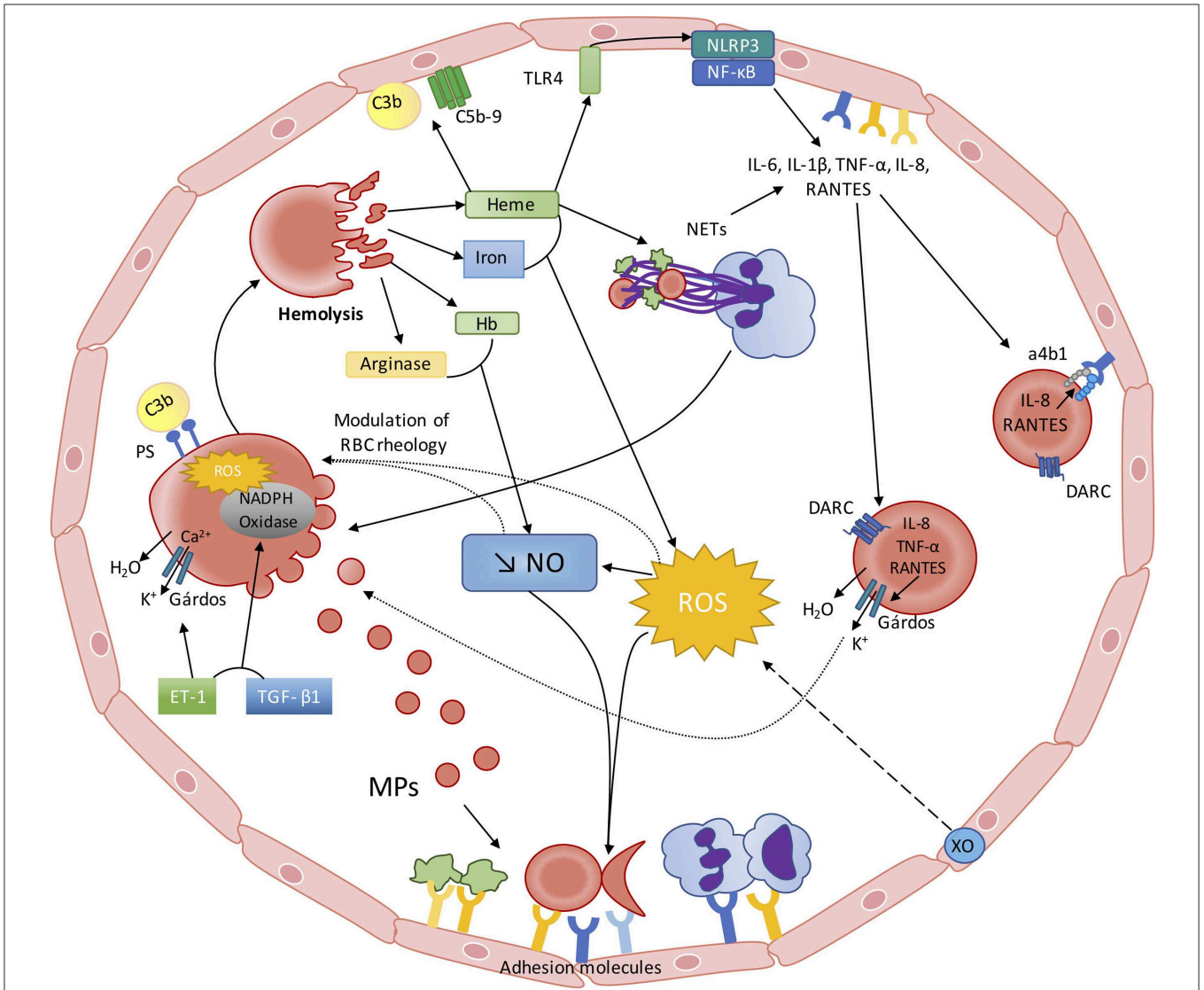

FIGURE 1 | The red blood cell—inflammation vicious circle in sickle cell disease. *From RBC alterations to oxidative stress, inflammation and endothelial dysfunction*: Sickled RBC are very fragile and prone to hemolyze. Hemolysis leads to the release of heme, iron, Hb and arginase into the plasma, which interfere with the metabolism/bioavailability of NO: (I) free arginase may hydrolyze the NO precursor Arginine; (II) free Hb scavenges NO at a rate of 1,000-fold faster than Hb encapsulated in the RBCs; (III) heme and iron increase ROS generation, which lead to the production of peroxynitrite. ROS production is also enhanced by Xanthine Oxidase activation, caused by the repetition of ischemic/reperfusion events. Decreased NO bioavailability and increased ROS activate endothelial cells, which in turn express adhesion molecules of both the CAM and Selectin families, promoting cell-cell interactions. Free heme is able to activate endothelial TLR4, which promotes inflammasome activation and cytokines production through NF-κB activation. Heme may also activate neutrophils, which would release NETs that can also affect endothelial cells and act as a scaffold for platelets and RBCs. Recent evidence also showed that free heme could stimulate the complement pathway with potential consequences at the endothelial cell level. *From inflammation and oxidative stress to RBC alterations*: This pro-inflammatory and pro-oxidative environment, resulting from sickle RBCs alterations, also impacts on RBC rheology and physiology. Increased ROS production may lower RBC deformability and increase RBC aggregation. Decreased NO bioavailability could also participate in the decrease of RBC deformability and promote eryptosis. NETs could also promote RBC eryptosis. Circulating inflammatory molecules, such as ET-1 and TGF-β, may activate RBC NADPH Oxidase, which in turn would produce ROS and further alter RBC. ROS and ET-1 are known to activate the RBC Gárdos channel, which could favor RBC dehydration and further promote HbS polymerization. The enhanced release of MP by sickled RBCs could further exacerbate inflammation and oxidative stress. Increased RBC phosphatidylserine exposure may favor the binding of complement proteins at the surface of RBCs, which can induce their lysis. RBCs also act as a reservoir and/or a sink for pro-inflammatory cytokines/chemokines. IL-8, TNF-α, and RANTES promote RBC dehydration through Gárdos channel activation in RBCs expressing DARC. IL-8 and RANTES can also lead to the activation of α4β1 integrin in sickle reticulocytes expressing DARC, contributing to the adhesion of these cells to the endothelium.

CONCLUSION

While SCD is the first disease for which the molecular basis has been identified (128), the pathophysiology of this disorder remains not fully understood despite decades of extensive studies dedicated to decipher these complex mechanisms. While the consequences of the polymerization of abnormal hemoglobin S were originally described to result in RBC deformability impairment and increased fragility, a large number of abnormalities have been described more recently, such as: the consequences of enhanced hemolysis on decreased NO bioactivity/bioavailability, the consequences of hemolysis and other factors on oxidative stress, the activation of inflammation, the release of NETosis products into the blood, the activation of the alternative complement pathway and the production of deleterious extracellular vesicles. All these biological abnormalities modulate and reflect the clinical severity of the patients. But, during the last years, accumulating evidence shows that each of these abnormalities impacts on RBC physiology and biophysical behavior: NO modulates directly the rheology of RBCs, increased oxidative stress may cause damage to the RBC membrane, accumulation of cytokines in the RBCs may further promote their dehydration and increase their adhesiveness to the vascular wall, accumulation of NETs could participate in hetero-cellular aggregation and accumulation of fragments of the alternative complement pathway may fragilize RBCs. Indeed, one may assume that these recent data suggest a new vicious circle in SCD, starting with impaired RBC rheology and increased RBC fragility and ending with further impairment of RBC, which would further worsen the clinical condition of SCD patients (**Figure 1**). As our understanding of the complex pathophysiological scheme of SCD has clearly improved during the last decade, further studies are warranted to better describe the relationships between the various abnormalities associated with the most frequently encountered genetic disease worldwide.

AUTHOR CONTRIBUTIONS

EN, MR, and PC reviewed the literature, wrote the manuscript, and drew the figure. All authors approved the final version of the manuscript.

REFERENCES

1. Lettre G. The search for genetic modifiers of disease severity in the beta-hemoglobinopathies. *Cold Spring Harb Perspect Med*. (2012) 2:a015032. doi: 10.1101/cshperspect.a015032
2. Ferrone FA. The delay time in sickle cell disease after 40 years: a paradigm assessed. *Am J Hematol*. (2015) 90:438–45. doi: 10.1002/ajh.23958
3. Coates TD, Chalacheva P, Zeltzer L, Khoo MCK. Autonomic nervous system involvement in sickle cell disease. *Clin Hemorheol Microcirc*. (2018) 68:251–62. doi: 10.3233/CH-189011
4. Kaul DK, Fabry ME, Nagel RL. Microvascular sites and characteristics of sickle cell adhesion to vascular endothelium in shear flow conditions: pathophysiological implications. *Proc Natl Acad Sci USA*. (1989) 86:3356–60. doi: 10.1073/pnas.86.9.3356
5. Belcher JD, Marker PH, Weber JP, Hebbel RP, Vercellotti GM. Activated monocytes in sickle cell disease: potential role in the activation of vascular endothelium and vaso-occlusion. *Blood*. (2000) 96:2451–9. doi: 10.1182/blood.V96.7.2451
6. Zhang D, Xu C, Manwani D, Frenette PS. Neutrophils, platelets, and inflammatory pathways at the nexus of sickle cell disease pathophysiology. *Blood*. (2016) 127:801–9. doi: 10.1182/blood-2015-09-618538
7. Koehl B, Nivoit P, El Nemer W, Lenoir O, Hermand P, Pereira C, et al. The endothelin B receptor plays a crucial role in the adhesion of neutrophils to the endothelium in sickle cell disease. *Haematologica*. (2017) 102:1161–72. doi: 10.3324/haematol.2016.156869
8. Connes P, Machado R, Hue O, Reid H. Exercise limitation, exercise testing and exercise recommendations in sickle cell anemia. *Clin Hemorheol Microcirc*. (2011) 49:151–63. doi: 10.3233/CH-2011-1465
9. Elmariah H, Garrett ME, De Castro LM, Jonassaint JC, Ataga KI, Eckman JR, et al. Factors associated with survival in a contemporary adult sickle cell disease cohort. *Am J Hematol*. (2014) 89:530–5. doi: 10.1002/ajh.23683
10. Taylor JGT, Nolan VG, Mendelsohn L, Kato GJ, Gladwin MT, Steinberg MH. Chronic hyper-hemolysis in sickle cell anemia: association of vascular complications and mortality with less frequent vasoocclusive pain. *PLoS ONE*. (2008) 3:e2095. doi: 10.1371/journal.pone.0002095
11. Kato GJ, Gladwin MT, Steinberg MH. Deconstructing sickle cell disease: reappraisal of the role of hemolysis in the development of clinical subphenotypes. *Blood Rev*. (2007) 21:37–47. doi: 10.1016/j.blre.2006.07.001
12. De Caterina R, Libby P, Peng HB, Thannickal VJ, Rajavashisth TB, Gimbrone MA, et al. Nitric oxide decreases cytokine-induced endothelial activation. Nitric oxide selectively reduces endothelial expression of adhesion molecules and proinflammatory cytokines. *J Clin Invest*. (1995) 96:60–8. doi: 10.1172/JCI118074
13. Radomski MW, Moncada S. The biological and pharmacological role of nitric oxide in platelet function. *Adv Exp Med Biol*. (1993) 344:251–64. doi: 10.1007/978-1-4615-2994-1_20
14. Kato GJ, Steinberg MH, Gladwin MT. Intravascular hemolysis and the pathophysiology of sickle cell disease. *J Clin Invest*. (2017) 127:750–60. doi: 10.1172/JCI89741
15. Kato GJ, Piel FB, Reid CD, Gaston MH, Ohene-Frempong K, Krishnamurti L, et al. Sickle cell disease. *Nat Rev Dis Primers*. (2018) 4:18010. doi: 10.1038/nrdp.2018.10
16. Rother RP, Bell L, Hillmen P, Gladwin MT. The clinical sequelae of intravascular hemolysis and extracellular plasma hemoglobin: a novel mechanism of human disease. *JAMA*. (2005) 293:1653–62. doi: 10.1001/jama.293.13.1653
17. Reiter CD, Wang X, Tanus-Santos JE, Hogg N, Cannon RO III, Schechter AN, et al. Cell-free hemoglobin limits nitric oxide bioavailability in sickle-cell disease. *Nat Med*. (2002) 8:1383–9. doi: 10.1038/nm1202-799
18. Eberhardt RT, Mcmahon L, Duffy SJ, Steinberg MH, Perrine SP, Loscalzo J, et al. Sickle cell anemia is associated with reduced nitric oxide bioactivity in peripheral conduit and resistance vessels. *Am J Hematol*. (2003) 74:104–11. doi: 10.1002/ajh.10387
19. Belhassen L, Pelle G, Sediame S, Bachir D, Carville C, Bucherer C, et al. Endothelial dysfunction in patients with sickle cell disease is related to selective impairment of shear stress-mediated vasodilation. *Blood*. (2001) 97:1584–9. doi: 10.1182/blood.V97.6.1584
20. Mockesch B, Charlot K, Jumet S, Romana M, Divialle-Doumdo L, Hardy-Dessources MD, et al. Micro- and macrovascular function in children with sickle cell anaemia and sickle cell haemoglobin C disease. *Blood Cells Mol Dis*. (2017) 64:23–9. doi: 10.1016/j.bcmd.2017.02.001
21. Pakbaz Z, Wun T. Role of the hemostatic system on sickle cell disease pathophysiology and potential therapeutics. *Hematol Oncol Clin North Am*. (2014) 28:355–74. doi: 10.1016/j.hoc.2013.11.011
22. Noubouossie D, Key NS, Ataga KI. Coagulation abnormalities of sickle cell disease: Relationship with clinical outcomes and the effect of disease modifying therapies. *Blood Rev*. (2016) 30:245–56. doi: 10.1016/j.blre.2015.12.003

23. Villagra J, Shiva S, Hunter LA, Machado RF, Gladwin MT, Kato GJ. Platelet activation in patients with sickle disease, hemolysis-associated pulmonary hypertension, and nitric oxide scavenging by cell-free hemoglobin. *Blood*. (2007) 110:2166–72. doi: 10.1182/blood-2006-12-061697
24. Kato GJ, Martyr S, Blackwelder WC, Nichols JS, Coles WA, Hunter LA, et al. Levels of soluble endothelium-derived adhesion molecules in patients with sickle cell disease are associated with pulmonary hypertension, organ dysfunction, and mortality. *Br J Haematol*. (2005) 130:943–53. doi: 10.1111/j.1365-2141.2005.05701.x
25. Zhang L, Levy A, Rifkind JM. Autoxidation of hemoglobin enhanced by dissociation into dimers. *J Biol Chem*. (1991) 266:24698–701.
26. Aslan M, Ryan TM, Adler B, Townes TM, Parks DA, Thompson JA, et al. Oxygen radical inhibition of nitric oxide-dependent vascular function in sickle cell disease. *Proc Natl Acad Sci USA*. (2001) 98:15215–20. doi: 10.1073/pnas.221292098
27. Radi R, Beckman JS, Bush KM, Freeman BA. Peroxynitrite-induced membrane lipid peroxidation: the cytotoxic potential of superoxide and nitric oxide. *Arch Biochem Biophys*. (1991) 288:481–7. doi: 10.1016/0003-9861(91)90224-7
28. Pohlman TH, Harlan JM. Adaptive responses of the endothelium to stress. *J Surg Res*. (2000) 89:85–119. doi: 10.1006/jsre.1999.5801
29. Lavrovsky Y, Chatterjee B, Clark RA, Roy AK. Role of redox-regulated transcription factors in inflammation, aging and age-related diseases. *Exp Gerontol*. (2000) 35:521–32. doi: 10.1016/S0531-5565(00)00118-2
30. Marui N, Offermann MK, Swerlick R, Kunsch C, Rosen CA, Ahmad M, et al. Vascular cell adhesion molecule-1 (VCAM-1) gene transcription and expression are regulated through an antioxidant-sensitive mechanism in human vascular endothelial cells. *J Clin Invest*. (1993) 92:1866–74. doi: 10.1172/JCI116778
31. Gee BE, Platt OS. Sickle reticulocytes adhere to VCAM-1. *Blood*. (1995) 85:268–74. doi: 10.1182/blood.V85.1.268.bloodjournal851268
32. Sultana C, Shen Y, Rattan V, Johnson C, Kalra VK. Interaction of sickle erythrocytes with endothelial cells in the presence of endothelial cell conditioned medium induces oxidant stress leading to transendothelial migration of monocytes. *Blood*. (1998) 92:3924–35. doi: 10.1182/blood.V92.10.3924
33. Conran N, Belcher JD. Inflammation in sickle cell disease. *Clin Hemorheol Microcirc*. (2018) 68:263–99. doi: 10.3233/CH-189012
34. Belcher JD, Chen C, Nguyen J, Zhang P, Abdulla F, Nguyen P, et al. Control of oxidative stress and inflammation in sickle cell disease with the Nrf2 activator dimethyl fumarate. *Antioxid Redox Signal*. (2017) 26:748–62. doi: 10.1089/ars.2015.6571
35. Wagener FA, Feldman E, De Witte T, Abraham NG. Heme induces the expression of adhesion molecules ICAM-1, VCAM-1, and E selectin in vascular endothelial cells. *Proc Soc Exp Biol Med*. (1997) 216:456–63. doi: 10.3181/00379727-216-44197
36. Wagener FA, Eggert A, Boerman OC, Oyen WJ, Verhofstad A, Abraham NG, et al. Heme is a potent inducer of inflammation in mice and is counteracted by heme oxygenase. *Blood*. (2001) 98:1802–11. doi: 10.1182/blood.V98.6.1802
37. Natarajan R, Fisher BJ, Fowler AA III. Hypoxia inducible factor-1 modulates hemin-induced IL-8 secretion in microvascular endothelium. *Microvasc Res*. (2007) 73:163–72. doi: 10.1016/j.mvr.2007.01.002
38. Dutra FF, Bozza MT. Heme on innate immunity and inflammation. *Front Pharmacol*. (2014) 5:115. doi: 10.3389/fphar.2014.00115
39. Ghosh S, Adisa OA, Chappa P, Tan F, Jackson KA, Archer DR, et al. Extracellular hemin crisis triggers acute chest syndrome in sickle mice. *J Clin Invest*. (2013) 123:4809–20. doi: 10.1172/JCI64578
40. Belcher JD, Chen C, Nguyen J, Milbauer L, Abdulla F, Alayash AI, et al. Heme triggers TLR4 signaling leading to endothelial cell activation and vaso-occlusion in murine sickle cell disease. *Blood*. (2014) 123:377–90. doi: 10.1182/blood-2013-04-495887
41. Adisa OA, Hu Y, Ghosh S, Aryee D, Osunkwo I, Ofori-Acquah SF. Association between plasma free haem and incidence of vaso-occlusive episodes and acute chest syndrome in children with sickle cell disease. *Br J Haematol*. (2013) 162:702–5. doi: 10.1111/bjh.12445
42. Pitanga TN, Oliveira RR, Zanette DL, Guarda CC, Santiago RP, Santana SS, et al. Sickle red cells as danger signals on proinflammatory gene expression, leukotriene B4 and interleukin-1 beta production in peripheral blood mononuclear cell. *Cytokine*. (2016) 83:75–84. doi: 10.1016/j.cyto.2016.03.016
43. Mendonca R, Silveira AA, Conran N. Red cell DAMPs and inflammation. *Inflamm Res*. (2016) 65:665–78. doi: 10.1007/s00011-016-0955-9
44. Graca-Souza AV, Arruda MA, De Freitas MS, Barja-Fidalgo C, Oliveira PL. Neutrophil activation by heme: implications for inflammatory processes. *Blood*. (2002) 99:4160–5. doi: 10.1182/blood.V99.11.4160
45. Chen G, Zhang D, Fuchs TA, Manwani D, Wagner DD, Frenette PS. Heme-induced neutrophil extracellular traps contribute to the pathogenesis of sickle cell disease. *Blood*. (2014) 123:3818–27. doi: 10.1182/blood-2013-10-529982
46. Schimmel M, Nur E, Biemond BJ, Van Mierlo GJ, Solati S, Brandjes DP, et al. Nucleosomes and neutrophil activation in sickle cell disease painful crisis. *Haematologica*. (2013) 98:1797–803. doi: 10.3324/haematol.2013.088021
47. Folco EJ, Mawson TL, Vromman A, Bernardes-Souza B, Franck G, Persson O, et al. Neutrophil extracellular traps induce endothelial cell activation and tissue factor production through interleukin-1alpha and cathepsin G. *Arterioscler Thromb Vasc Biol*. (2018) 38:1901–12. doi: 10.1161/ATVBAHA.118.311150
48. Thalin C, Hisada Y, Lundstrom S, Mackman N, Wallen H. Neutrophil extracellular traps: villains and targets in arterial, venous, and cancer-associated thrombosis. *Arterioscler Thromb Vasc Biol*. (2019) 39:1724–38. doi: 10.1161/ATVBAHA.119.312463
49. Warnatsch A, Ioannou M, Wang Q, Papayannopoulos V. Inflammation. Neutrophil extracellular traps license macrophages for cytokine production in atherosclerosis. *Science*. (2015) 349:316–20. doi: 10.1126/science.aaa8064
50. Liu D, Yang P, Gao M, Yu T, Shi Y, Zhang M, et al. NLRP3 activation induced by neutrophil extracellular traps sustains inflammatory response in the diabetic wound. *Clin Sci (Lond)*. (2019) 133:565–82. doi: 10.1042/CS20180600
51. Frimat M, Tabarin F, Dimitrov JD, Poitou C, Halbwachs-Mecarelli L, Fremeaux-Bacchi V, et al. Complement activation by heme as a secondary hit for atypical hemolytic uremic syndrome. *Blood*. (2013) 122:282–92. doi: 10.1182/blood-2013-03-489245
52. Jane-Wit D, Surovtseva YV, Qin L, Li G, Liu R, Clark P, et al. Complement membrane attack complexes activate noncanonical NF-κB by forming an Akt^+ NIK^+ signalosome on $Rab5^+$ endosomes. *Proc Natl Acad Sci USA*. (2015) 112:9686–91. doi: 10.1073/pnas.1503535112
53. Chapin J, Terry HS, Kleinert D, Laurence J. The role of complement activation in thrombosis and hemolytic anemias. *Transfus Apher Sci*. (2016) 54:191–8. doi: 10.1016/j.transci.2016.04.008
54. Gavriilaki E, Mainou M, Christodoulou I, Koravou EE, Paleta A, Touloumenidou T, et al. *In vitro* evidence of complement activation in patients with sickle cell disease. *Haematologica*. (2017) 102:e481–2. doi: 10.3324/haematol.2017.174201
55. Vercellotti GM, Dalmasso AP, Schaid TR Jr, Nguyen J, Chen C, et al. Critical role of C5a in sickle cell disease. *Am J Hematol*. (2019) 94:327–37. doi: 10.1002/ajh.25384
56. Lombardi E, Matte A, Risitano AM, Ricklin D, Lambris JD, De Zanet D, et al. Factor H interferes with the adhesion of sickle red cells to vascular endothelium: a novel disease-modulating molecule. *Haematologica*. (2019) 104:919–28. doi: 10.3324/haematol.2018.198622
57. Wang RH, Phillips G Jr, Medof ME, Mold C. Activation of the alternative complement pathway by exposure of phosphatidylethanolamine and phosphatidylserine on erythrocytes from sickle cell disease patients. *J Clin Invest*. (1993) 92:1326–35. doi: 10.1172/JCI116706
58. Merle NS, Grunenwald A, Rajaratnam H, Gnemmi V, Frimat M, Figueres ML, et al. Intravascular hemolysis activates complement via cell-free heme and heme-loaded microvesicles. *JCI Insight*. (2018) 3:96910. doi: 10.1172/jci.insight.96910
59. Merle NS, Paule R, Leon J, Daugan M, Robe-Rybkine T, Poillerat V, et al. P-selectin drives complement attack on endothelium during intravascular hemolysis in TLR-4/heme-dependent manner. *Proc Natl Acad Sci USA*. (2019) 116:6280–5. doi: 10.1073/pnas.1814797116
60. Hebbel RP, Key NS. Microparticles in sickle cell anaemia: promise and pitfalls. *Br J Haematol*. (2016) 174:16–29. doi: 10.1111/bjh.14112

61. Romana M, Connes P, Key NS. Microparticles in sickle cell disease. *Clin Hemorheol Microcirc*. (2018) 68:319–29. doi: 10.3233/CH-189014
62. Shet AS, Aras O, Gupta K, Hass MJ, Rausch DJ, Saba N, et al. Sickle blood contains tissue factor-positive microparticles derived from endothelial cells and monocytes. *Blood*. (2003) 102:2678–83. doi: 10.1182/blood-2003-03-0693
63. Van Beers EJ, Schaap MC, Berckmans RJ, Nieuwland R, Sturk A, Van Doormaal FF, et al. Circulating erythrocyte-derived microparticles are associated with coagulation activation in sickle cell disease. *Haematologica*. (2009) 94:1513–9. doi: 10.3324/haematol.2009.008938
64. Nebor D, Romana M, Santiago R, Vachiery N, Picot J, Broquere C, et al. Fetal hemoglobin and hydroxycarbamide moduate both plasma concentration and cellular origin of circulating microparticles in sickle cell anemia children. *Haematologica*. (2013) 98:862–7. doi: 10.3324/haematol.2012.073619
65. Tantawy AA, Adly AA, Ismail EA, Habeeb NM, Farouk A. Circulating platelet and erythrocyte microparticles in young children and adolescents with sickle cell disease: Relation to cardiovascular complications. *Platelets*. (2013) 24:605–14. doi: 10.3109/09537104.2012.749397
66. Nebor D, Bowers A, Connes P, Hardy-Dessources MD, Knight-Madden J, Cumming V, et al. Plasma concentration of platelet-derived microparticles is related to painful vaso-occlusive phenotype severity in sickle cell anemia. *PLoS ONE*. (2014) 9:e87243. doi: 10.1371/journal.pone.0087243
67. Van Tits LJ, Van Heerde WL, Landburg PP, Boderie MJ, Muskiet FA, Jacobs N, et al. Plasma annexin A5 and microparticle phosphatidylserine levels are elevated in sickle cell disease and increase further during painful crisis. *Biochem Biophys Res Commun*. (2009) 390:161–4. doi: 10.1016/j.bbrc.2009.09.102
68. Hierso R, Lemonne N, Villaescusa R, Lalanne-Mistrih ML, Charlot K, Etienne-Julan M, et al. Exacerbation of oxidative stress during sickle vaso-occlusive crisis is associated with decreased anti-band 3 autoantibodies rate and increased red blood cell-derived microparticle level: a prospective study. *Br J Haematol*. (2017) 176:805–13. doi: 10.1111/bjh.14476
69. Khalyfa A, Khalyfa AA, Akbarpour M, Connes P, Romana M, Lapping-Carr G, et al. Extracellular microvesicle microRNAs in children with sickle cell anaemia with divergent clinical phenotypes. *Br J Haematol*. (2016) 174:786–98. doi: 10.1111/bjh.14104
70. Colombo M, Raposo G, Thery C. Biogenesis, secretion, and intercellular interactions of exosomes and other extracellular vesicles. *Annu Rev Cell Dev Biol*. (2014) 30:255–89. doi: 10.1146/annurev-cellbio-101512-122326
71. Burger D, Montezano AC, Nishigaki N, He Y, Carter A, Touyz RM. Endothelial microparticle formation by angiotensin II is mediated via Ang II receptor type I/NADPH oxidase/Rho kinase pathways targeted to lipid rafts. *Arterioscler Thromb Vasc Biol*. (2011) 31:1898–907. doi: 10.1161/ATVBAHA.110.222703
72. Essayagh S, Xuereb JM, Terrisse AD, Tellier-Cirioni L, Pipy B, Sie P. Microparticles from apoptotic monocytes induce transient platelet recruitment and tissue factor expression by cultured human vascular endothelial cells via a redox-sensitive mechanism. *Thromb Haemost*. (2007) 98:831–7. doi: 10.1160/TH07-02-0082
73. Yang C, Mwaikambo BR, Zhu T, Gagnon C, Lafleur J, Seshadri S, et al. Lymphocytic microparticles inhibit angiogenesis by stimulating oxidative stress and negatively regulating VEGF-induced pathways. *Am J Physiol Regul Integr Comp Physiol*. (2008) 294:R467–476. doi: 10.1152/ajpregu.00432.2007
74. Distler JH, Akhmetshina A, Dees C, Jungel A, Sturzl M, Gay S, et al. Induction of apoptosis in circulating angiogenic cells by microparticles. *Arthritis Rheum*. (2011) 63:2067–77. doi: 10.1002/art.30361
75. Barry OP, Pratico D, Savani RC, Fitzgerald GA. Modulation of monocyte-endothelial cell interactions by platelet microparticles. *J Clin Invest*. (1998) 102:136–44. doi: 10.1172/JCI2592
76. Nouraie M, Lee JS, Zhang Y, Kanias T, Zhao X, Xiong Z, et al. The relationship between the severity of hemolysis, clinical manifestations and risk of death in 415 patients with sickle cell anemia in the US and Europe. *Haematologica*. (2013) 98:464–72. doi: 10.3324/haematol.2012.068965
77. Olatunya OS, Lanaro C, Longhini AL, Penteado CFF, Fertrin KY, Adekile A, et al. Red blood cells microparticles are associated with hemolysis markers and may contribute to clinical events among sickle cell disease patients. *Ann Hematol*. (2019) 98:2507–21. doi: 10.1007/s00277-019-03792-x
78. Camus SM, Gausseres B, Bonnin P, Loufrani L, Grimaud L, Charue D, et al. Erythrocyte microparticles can induce kidney vaso-occlusions in a murine model of sickle cell disease. *Blood*. (2012) 120:5050–8. doi: 10.1182/blood-2012-02-413138
79. Camus SM, De Moraes JA, Bonnin P, Abbyad P, Le Jeune S, Lionnet F, et al. Circulating cell membrane microparticles transfer heme to endothelial cells and trigger vasoocclusions in sickle cell disease. *Blood*. (2015) 125:3805–14. doi: 10.1182/blood-2014-07-589283
80. Starzyk D, Korbut R, Gryglewski RJ. The role of nitric oxide in regulation of deformability of red blood cells in acute phase of endotoxaemia in rats. *J Physiol Pharmacol*. (1997) 48:731–5.
81. Bor-Kucukatay M, Wenby RB, Meiselman HJ, Baskurt OK. Effects of nitric oxide on red blood cell deformability. *Am J Physiol Heart Circ Physiol*. (2003) 284:H1577–84. doi: 10.1152/ajpheart.00665.2002
82. Nader E, Grau M, Fort R, Collins B, Cannas G, Gauthier A, et al. Hydroxyurea therapy modulates sickle cell anemia red blood cell physiology: Impact on RBC deformability, oxidative stress, nitrite levels and nitric oxide synthase signalling pathway. *Nitric Oxide*. (2018) 81:28–35. doi: 10.1016/j.niox.2018.10.003
83. Simmonds MJ, Detterich JA, Connes P. Nitric oxide, vasodilation and the red blood cell. *Biorheology*. (2014) 51:121–34. doi: 10.3233/BIR-140653
84. Baskurt OK, Uyuklu M, Meiselman HJ. Protection of erythrocytes from sub-hemolytic mechanical damage by nitric oxide mediated inhibition of potassium leakage. *Biorheology*. (2004) 41:79–89.
85. Chowdhury KD, Sen G, Biswas T. Regulatory role of nitric oxide in the reduced survival of erythrocytes in visceral leishmaniasis. *Biochim Biophys Acta*. (2010) 1800:964–76. doi: 10.1016/j.bbagen.2010.05.008
86. Barodka V, Mohanty JG, Mustafa AK, Santhanam L, Nyhan A, Bhunia AK, et al. Nitroprusside inhibits calcium-induced impairment of red blood cell deformability. *Transfusion*. (2014) 54:434–44. doi: 10.1111/trf.12291
87. Bor-Kucukatay M, Yalcin O, Gokalp O, Kipmen-Korgun D, Yesilkaya A, Baykal A, et al. Red blood cell rheological alterations in hypertension induced by chronic inhibition of nitric oxide synthesis in rats. *Clin Hemorheol Microcirc*. (2000) 22:267–75.
88. Tripette J, Alexy T, Hardy-Dessources MD, Mougenel D, Beltan E, Chalabi T, et al. Red blood cell aggregation, aggregate strength and oxygen transport potential of blood are abnormal in both homozygous sickle cell anemia and sickle-hemoglobin C disease. *Haematologica*. (2009) 94:1060–5. doi: 10.3324/haematol.2008.005371
89. Nur E, Brandjes DP, Teerlink T, Otten HM, Oude Elferink RP, Muskiet F, et al. N-acetylcysteine reduces oxidative stress in sickle cell patients. *Ann Hematol*. (2012) 91:1097–105. doi: 10.1007/s00277-011-1404-z
90. Silva DGH, Belini Junior E, De Almeida EA, Bonini-Domingos CR. Oxidative stress in sickle cell disease: an overview of erythrocyte redox metabolism and current antioxidant therapeutic strategies. *Free Radic Biol Med*. (2013) 65:1101–9. doi: 10.1016/j.freeradbiomed.2013.08.181
91. Mockesch B, Connes P, Charlot K, Skinner S, Hardy-Dessources MD, Romana M, et al. Association between oxidative stress and vascular reactivity in children with sickle cell anaemia and sickle haemoglobin C disease. *Br J Haematol*. (2017) 178:468–75. doi: 10.1111/bjh.14693
92. Van Beers EJ, Van Wijk R. Oxidative stress in sickle cell disease; more than a DAMP squib. *Clin Hemorheol Microcirc*. (2018) 68:239–50. doi: 10.3233/CH-189010
93. Suzuki Y, Ohkubo N, Aoto M, Maeda N, Cicha I, Miki T, et al. Participation of caspase-3-like protease in oxidation-induced impairment of erythrocyte membrane properties. *Biorheology*. (2007) 44:179–90.
94. Nur E, Biemond BJ, Otten HM, Brandjes DP, Schnog JJ, Group CS. Oxidative stress in sickle cell disease; pathophysiology and potential implications for disease management. *Am J Hematol*. (2011) 86:484–9. doi: 10.1002/ajh.22012
95. Bissinger R, Bhuyan AAM, Qadri SM, Lang F. Oxidative stress, eryptosis and anemia: a pivotal mechanistic nexus in systemic diseases. *FEBS J*. (2019) 286:826–54. doi: 10.1111/febs.14606
96. Baskurt OK, Temiz A, Meiselman HJ. Effect of superoxide anions on red blood cell rheologic properties. *Free Radic Biol Med*. (1998) 24:102–10. doi: 10.1016/S0891-5849(97)00169-X
97. Kaul DK, Koshkaryev A, Artmann G, Barshtein G, Yedgar S. Additive effect of red blood cell rigidity and adherence to endothelial cells in inducing

vascular resistance. *Am J Physiol Heart Circ Physiol*. (2008) 295:H1788–1793. doi: 10.1152/ajpheart.253.2008
98. Sinha A, Chu TT, Dao M, Chandramohanadas R. Single-cell evaluation of red blood cell bio-mechanical and nano-structural alterations upon chemically induced oxidative stress. *Sci Rep*. (2015) 5:9768. doi: 10.1038/srep09768
99. McNamee AP, Horobin JT, Tansley GD, Simmonds MJ. Oxidative stress increases erythrocyte sensitivity to shear-mediated damage. *Artif Organs*. (2018) 42:184–92. doi: 10.1111/aor.12997
100. Hierso R, Waltz X, Mora P, Romana M, Lemonne N, Connes P, et al. Effects of oxidative stress on red blood cell rheology in sickle cell patients. *Br J Haematol*. (2014) 166:601–6. doi: 10.1111/bjh.12912
101. Karsten E, Breen E, Herbert BR. Red blood cells are dynamic reservoirs of cytokines. *Sci Rep*. (2018) 8:3101. doi: 10.1038/s41598-018-21387-w
102. Darbonne WC, Rice GC, Mohler MA, Apple T, Hebert CA, Valente AJ, et al. Red blood cells are a sink for interleukin 8, a leukocyte chemotaxin. *J Clin Invest*. (1991) 88:1362–9. doi: 10.1172/JCI115442
103. Lee JS, Wurfel MM, Matute-Bello G, Frevert CW, Rosengart MR, Ranganathan M, et al. The Duffy antigen modifies systemic and local tissue chemokine responses following lipopolysaccharide stimulation. *J Immunol*. (2006) 177:8086–94. doi: 10.4049/jimmunol.177.11.8086
104. Fukuma N, Akimitsu N, Hamamoto H, Kusuhara H, Sugiyama Y, Sekimizu K. A role of the Duffy antigen for the maintenance of plasma chemokine concentrations. *Biochem Biophys Res Commun*. (2003) 303:137–9. doi: 10.1016/S0006-291X(03)00293-6
105. Bester J, Pretorius E. Effects of IL-1beta, IL-6 and IL-8 on erythrocytes, platelets and clot viscoelasticity. *Sci Rep*. (2016) 6:32188. doi: 10.1038/srep32188
106. Bester J, Matshailwe C, Pretorius E. Simultaneous presence of hypercoagulation and increased clot lysis time due to IL-1beta, IL-6 and IL-8. *Cytokine*. (2018) 110:237–42. doi: 10.1016/j.cyto.2018.01.007
107. Yeung KW, Lau PM, Tsang HL, Ho HP, Kwan YW, Kong SK. Extracellular histones induced eryptotic death in human erythrocytes. *Cell Physiol Biochem*. (2019) 53:229–41. doi: 10.33594/000000132
108. Test ST, Woolworth VS. Defective regulation of complement by the sickle erythrocyte: evidence for a defect in control of membrane attack complex formation. *Blood.* (1994) 83:842–52. doi: 10.1182/blood.V83.3.842.842
109. George A, Pushkaran S, Konstantinidis DG, Koochaki S, Malik P, Mohandas N, et al. Erythrocyte NADPH oxidase activity modulated by Rac GTPases, PKC, and plasma cytokines contributes to oxidative stress in sickle cell disease. *Blood*. (2013) 121:2099–107. doi: 10.1182/blood-2012-07-441188
110. Rivera A, Jarolim P, Brugnara C. Modulation of Gardos channel activity by cytokines in sickle erythrocytes. *Blood*. (2002) 99:357–603. doi: 10.1182/blood.V99.1.357
111. Durpes MC, Nebor D, Du Mesnil PC, Mougenel D, Decastel M, Elion J, et al. Effect of interleukin-8 and RANTES on the Gardos channel activity in sickle human red blood cells: role of the Duffy antigen receptor for chemokines. *Blood Cells Mol Dis*. (2010) 44:219–23. doi: 10.1016/j.bcmd.2010.02.001
112. Durpes MC, Hardy-Dessources MD, El Nemer W, Picot J, Lemonne N, Elion J, et al. Activation state of alpha4beta1 integrin on sickle red blood cells is linked to the duffy antigen receptor for chemokines (DARC) expression. *J Biol Chem*. (2011) 286:3057–64. doi: 10.1074/jbc.M110.173229
113. Drasar ER, Menzel S, Fulford T, Thein SL. The effect of Duffy antigen receptor for chemokines on severity in sickle cell disease. *Haematologica*. (2013) 98:e87–89. doi: 10.3324/haematol.2013.089243
114. Afenyi-Annan A, Kail M, Combs MR, Orringer EP, Ashley-Koch A, Telen MJ. Lack of Duffy antigen expression is associated with organ damage in patients with sickle cell disease. *Transfusion*. (2008) 48:917–24. doi: 10.1111/j.1537-2995.2007.01622.x
115. Araujo NB, Domingos IF, Medeiros FS, Hatzlhofer BL, Mendonca TF, Vasconcelos LR, et al. Lack of association between the Duffy antigen receptor for chemokines (DARC) expression and clinical outcome of children with sickle cell anemia. *Immunol Lett*. (2015) 166:140–2. doi: 10.1016/j.imlet.2015.05.015
116. Nebor D, Durpes MC, Mougenel D, Mukisi-Mukaza M, Elion J, Hardy-Dessources MD, et al. Association between Duffy antigen receptor for chemokines expression and levels of inflammation markers in sickle cell anemia patients. *Clin Immunol*. (2010) 136:116–22. doi: 10.1016/j.clim.2010.02.023
117. Connes P, Lamarre Y, Hardy-Dessources MD, Lemonne N, Waltz X, Mougenel D, et al. Decreased hematocrit-to-viscosity ratio and increased lactate dehydrogenase level in patients with sickle cell anemia and recurrent leg ulcers. *PLoS ONE*. (2013) 8:e79680. doi: 10.1371/journal.pone.0079680
118. Lamarre Y, Romana M, Lemonne N, Hardy-Dessources MD, Tarer V, Mougenel D, et al. Alpha thalassemia protects sickle cell anemia patients from macro-albuminuria through its effects on red blood cell rheological properties. *Clin Hemorheol Microcirc*. (2014) 57:63–72. doi: 10.3233/CH-131772
119. Cita KC, Brureau L, Lemonne N, Billaud M, Connes P, Ferdinand S, et al. Men with sickle cell anemia and priapism exhibit increased hemolytic rate, decreased red blood cell deformability and increased red blood cell aggregate strength. *PLoS ONE*. (2016) 11:e0154866. doi: 10.1371/journal.pone.0154866
120. Connes P, Lamarre Y, Waltz X, Ballas SK, Lemonne N, Etienne-Julan M, et al. Haemolysis and abnormal haemorheology in sickle cell anaemia. *Br J Haematol*. (2014) 165:564–72. doi: 10.1111/bjh.12786
121. Connes P, Alexy T, Detterich J, Romana M, Hardy-Dessources MD, Ballas SK. The role of blood rheology in sickle cell disease. *Blood Rev*. (2016) 30:111–8. doi: 10.1016/j.blre.2015.08.005
122. Connes P, Renoux C, Romana M, Abkarian M, Joly P, Martin C, et al. Blood rheological abnormalities in sickle cell anemia. *Clin Hemorheol Microcirc*. (2018) 68:165–72. doi: 10.3233/CH-189005
123. Lamarre Y, Romana M, Waltz X, Lalanne-Mistrih ML, Tressieres B, Divialle-Doumdo L, et al. Hemorheological risk factors of acute chest syndrome and painful vaso-occlusive crisis in children with sickle cell disease. *Haematologica*. (2012) 97:1641–7. doi: 10.3324/haematol.2012.066670
124. Lapoumeroulie C, Connes P, El Hoss S, Hierso R, Charlot K, Lemonne N, et al. New insights into red cell rheology and adhesion in patients with sickle cell anaemia during vaso-occlusive crises. *Br J Haematol*. (2019) 185:991–4. doi: 10.1111/bjh.15686
125. Nader E, Skinner S, Romana M, Fort R, Lemonne N, Guillot N, et al. Blood rheology: key parameters, impact on blood flow, role in sickle cell disease and effects of exercise. *Front Physiol*. (2019) 10:1329. doi: 10.3389/fphys.2019.01329
126. Baskurt OK, Yalcin O, Meiselman HJ. Hemorheology and vascular control mechanisms. *Clin Hemorheol Microcirc*. (2004) 30:169–78.
127. Yalcin O, Meiselman HJ, Armstrong JK, Baskurt OK. Effect of enhanced red blood cell aggregation on blood flow resistance in an isolated-perfused guinea pig heart preparation. *Biorheology*. (2005) 42:511–20.
128. Pauling L, Itano HA, Singer SJ, Wells IC. Sickle cell anemia a molecular disease. *Science*. (1949) 110:543–8. doi: 10.1126/science.110.2865.543

Conflict of Interest: The authors declare that the research was conducted in the absence of any commercial or financial relationships that could be construed as a potential conflict of interest.

frontiers in Immunology

REVIEW
published: 07 April 2020
doi: 10.3389/fimmu.2020.00590

New Insights in the Pathogenesis and Therapy of Cold Agglutinin-Mediated Autoimmune Hemolytic Anemia

*Sigbjørn Berentsen**

Department of Research and Innovation, Haugesund Hospital, Haugesund, Norway

Autoimmune hemolytic anemias mediated by cold agglutinins can be divided into cold agglutinin disease (CAD), which is a well-defined clinicopathologic entity and a clonal lymphoproliferative disorder, and secondary cold agglutinin syndrome (CAS), in which a similar picture of cold-hemolytic anemia occurs secondary to another distinct clinical disease. Thus, the pathogenesis in CAD is quite different from that of polyclonal autoimmune diseases such as warm-antibody AIHA. In both CAD and CAS, hemolysis is mediated by the classical complement pathway and therefore can result in generation of anaphylotoxins, such as complement split product 3a (C3a) and, to some extent, C5a. On the other hand, infection and inflammation can act as triggers and drivers of hemolysis, exemplified by exacerbation of CAD in situations with acute phase reaction and the role of specific infections (particularly *Mycoplasma pneumoniae* and Epstein-Barr virus) as causes of CAS. In this review, the putative mechanisms behind these phenomena will be explained along with other recent achievements in the understanding of pathogenesis in these disorders. Therapeutic approaches have been directed against the clonal lymphoproliferation in CAD or the underlying disease in CAS. Currently, novel targeted treatments, in particular complement-directed therapies, are also being rapidly developed and will be reviewed.

Keywords: autoimmune hemolytic anemia, cold agglutinin disease, lymphoproliferative, complement, inflammation, therapy

OPEN ACCESS

Edited by:
Wilma Barcellini, Foundation Ca Granda Maggiore Hospital (IRCCS), Italy

Reviewed by:
Bruno Fattizzo, IRCCS Ca 'Granda Foundation Maggiore Policlinico Hospital, Italy
Geir Erland Tjønnfjord, Oslo University Hospital, Norway

***Correspondence:**
Sigbjørn Berentsen
sigbjorn.berentsen@haugnett.no

Specialty section:
This article was submitted to Inflammation, a section of the journal Frontiers in Immunology

Received: *16 February 2020*
Accepted: *13 March 2020*
Published: *07 April 2020*

Citation:
Berentsen S (2020) New Insights in the Pathogenesis and Therapy of Cold Agglutinin-Mediated Autoimmune Hemolytic Anemia. Front. Immunol. 11:590. doi: 10.3389/fimmu.2020.00590

INTRODUCTION

Cold-antibody autoimmune hemolytic anemias (cAIHAs) are mediated by autoantibodies characterized by a temperature optimum of the antigen-antibody (AgAb) reaction at 0-4°C. These hemolytic disorders account for ∼25–30% of autoimmune hemolytic anemias (AIHAs) (1). **Table 1** shows a further classification of cAIHAs (1–7). Cold agglutinins (CAs) are cold-reactive antibodies that are able to agglutinate red blood cells (RBCs) (8–10). Only CA-mediated AIHAs, i.e., cold agglutinin disease (CAD) and cold agglutinin syndrome (CAS), will be further addressed in this review. Although the term CAD, as coined by Schubothe in 1952 (11), originally included both these concepts, CAD should be distinguished from CAS (2, 3).

According to the recent international AIHA consensus document (3), CAD is defined as "an AIHA characterized by a monospecific direct antiglobulin test (DAT) strongly positive for complement fragment C3d and a cold agglutinin (CA) titer of 64 or higher at 4°C (3, 12–14). DAT for IgG is usually negative, but can be weakly positive in up to 20% of the patients (15, 16). There may be occasional cases with CA titer < 64 (3, 16)." By definition, "patients may have a

TABLE 1 | Cold-antibody mediated autoimmune hemolytic anemias.

Entity	Etiology	Autoantibody properties	Ig class	Complement activation	Predominant type of hemolysis	Incidence
Cold agglutinin disease (CAD)	Primary (low-grade LPD)	Cold agglutinins, anti-I (rarely anti-Pr or anti-IH)	IgM	Classical pathway ++, terminal pathway (+)	Extravascular	Uncommon, mainly elderly people
Cold agglutinin syndrome (CAS)	Secondary (Mycoplasma, EBV; aggressive lymphoma)	Cold agglutinins, anti-I or anti-i (rarely anti-IH?)	IgM or IgG	Classical pathway ++, terminal pathway (+)	Extravascular	Rare, any age
Paroxysmal cold hemoglobin-uria (PCH)	Children: Mostly postviral. Adults: Tertiary syphilis or hematologic malignancy.	Non-agglutinating biphasic Ab, anti-P	IgG	Classical pathway +++, terminal pathway +++	Intravascular	Rare in children, ultra-rare in adults

Ab, antibody; EBV, Epstein-Barr virus; Ig, immunoglobulin; LPD, lymphoproliferative disorder.
Based on data from Sokol et al. (1), Berentsen and Tjønnfjord (2), Jäger et al. (3), Barcellini et al. (4), Randen et al. (5), and Shanbhag and Spivak (6).

TABLE 2 | Diagnostic criteria for cold agglutinin disease.

Level	Criteria	Procedures, comments and reminders
Required for diagnosis	Chronic hemolysis	As assessed by hemoglobin levels and biochemical markers of hemolysis
	Polyspecific DAT positive	Performed in most laboratories but insufficient for diagnosis
	Monospecific DAT strongly positive for C3d	DAT is usually negative for IgG, but occasionally weakly positive
	CA titer $\geq$ 64 at 4°C	Blood specimen must be kept at 37-38°C from sampling until serum/plasma has been removed from the clot/cells
	No overt malignant disease or relevant infection	Clinical assessment for malignancy. Radiology as required. Exclusion of recent infection with *Mycoplasma* or EBV
Confirmatory but not required for diagnosis	Monoclonal IgMκ in serum (or, rarely, IgG or λ phenotype)	Blood specimen must be kept at 37-38°C from sampling until serum/plasma has been removed from the clot/cells
	Ratio between κ and λ positive B-cells > 3.5 (or, rarely, < 0.9)	Flow cytometry in bone marrow aspirate
	'CA-associated lymphoproliferative disorder' by histology	Bone marrow biopsy

CA, cold agglutinin; DAT, direct antiglobulin test; EBV, Epstein-Barr virus; Ig, immunoglobulin. Previously published by Berentsen (23), reused under general permission, slightly modified. Copyright: The American Society of Hematology.

B-cell clonal lymphoproliferative disorder (LPD) detectable in blood or marrow but no clinical or radiological evidence of malignancy" (3), and there is evidence that CAD is a clonal LPD of the bone marrow in most, probably all cases (5, 17–19). This distinct clinicopathological entity should be called a disease, not syndrome (3, 20). These patients are obviously identical with those previously described as having "idiopathic" or primary CAD (21, 22). **Table 2** summarizes the diagnostic criteria for CAD.

CAS is a similar clinical-hematological syndrome further defined by "the presence of an associated clinical disease, for example infection, autoimmune disorder, overt evidence of a lymphoma (clinical or radiological), or other malignancy" (3, 20). Typical underlying infections are *Mycoplasma pneumoniae* pneumonia, Epstein Barr virus (EBV) infection, or, rarely, other specific infections (2, 24, 25).

IMMUNE PATHOGENESIS IN CAD AND CAS

Origin of Cold Agglutinins

Like other IgM, CAs are produced by B-cells, predominantly at the lymphoplasmacytic cell stage (5, 26). However, IgM can also be produced by a smaller compartment of plasma cells that are long-lived and not targeted by chemoimmunotherapy (26, 27). The CA-producing cells are monoclonal in CAD as well as in CAS secondary to lymphoma, but polyclonal in CAS secondary to infection (2, 9).

The *IGVH4-34* gene, originally named V_H4-21, is located on the q arm of chromosome 14. In CAD, this gene encodes for the CA IgM heavy chain in more than 85% (9, 28, 29). In contrast, the monoclonal IgM heavy chain molecule found in Waldenström macroglobulinemia (WM) is usually encoded by the *IGHV3* gene (30). Framework region 1 (FR1) of the heavy gene variable region is essential for recognition of the I antigen (31, 32); however, the affinity and specificity for I antigen binding also depends on the heavy chain complementarity determining region 3 (CDR3) and the light chain variable region (29, 33). Recent data suggest that "subtle differences in light chain multiple binding sequences may contribute to differences in thermal amplitude and clinical phenotype" (29).

The first cytogenetic change observed in CAD was complete or partial trisomy 3 (34). A recent study found trisomy 3 (+3 or +3q) in all of 12 samples from CAD patients who participated in a clinical trial. Nine of these had an additional trisomy 12 or 18, but never both (19). Malecka et al. also found that the Ig light chain gene *IGKV3-20* and, to lesser extent, the similar *IGHV3-15* gene are used in most patients (74%) and might contribute to the I antigen binding. The *IGKV3-20* CDR3 region is highly homologous in a subgroup of patients and correlated with younger age at diagnosis (29). This finding is consistent with specific antigen selection in this group of patients. **Table 3** summarizes the heavy and light chain gene usage. Next

generation sequencing together with flow cytometry-assisted cell sorting of bone marrow from 16 patients enabled Malecka and coworkers to identify recurrent mutations of *KMT2D* (69%) and *CARD11* (31%) (36, 37). In diffuse large B-cell lymphoma, *CARD11* mutations have been shown to induce constitutive activation of the NF-κB pathway (29, 38).

Evidence of a clonal lymphoproliferative disorder (LPD) of the bone marrow has been recognized for decades (21). This LPD was previously perceived as being heterogeneous and was classified into several entities of low-grade LPD, frequently interpreted as lymphoplasmacytic lymphoma (LPL) or marginal zone lymphoma (MZL) (16, 18, 21, 39). A comprehensive histopathology study of 54 patients with CAD, however, showed a surprisingly homogenous type of lymphoid infiltration that has been termed "CAD-associated LPD" (5, 40).

The lymphoid infiltration usually consists of nodular B-cell aggregates, but some biopsies show only scattered B-cells (**Figure 1**). Involvement can vary between 5 and 80% of the intertrabecular surface, median 10% (5, 41). Mature plasma cells are seen surrounding the lymphoid nodular aggregates and throughout the marrow in between, but only few plasma cells are usually seen within the aggregates. The plasma cells have the same heavy and light chain restriction as the B-cells, consistent with a plasmacytoid differentiation of the B-cell clone. The histological pattern does not display features typically found in LPL (39), such as fibrosis, paratrabecular location of lymphoid infiltrates, lymphoplasmacytoid cell morphology, or infiltration by mast cells (5). The lymphoid infiltration mimics that of MZL by morphology; the immune phenotype is not distinct, and some similarities in molecular genetic features have also been identified (5). However, CAD patients do not have an extramedullary marginal zone lymphoma, and therefore, bone marrow involvement of MZL can be ruled out. In summary, CAD-associated LPD does not display the features of other indolent B-cell lymphomas types as described by the WHO classification. Therefore, it should be considered a distinct entity (5, 14, 39, 40). Development of diffuse large B-cell lymphoma is uncommon, probably occurring in less than 4% of the patients during 10 years (18).

Although cold hemagglutination was described in mammals already in 1903 and a CA was discovered in human serum in 1918 (8, 42), the physiological function of CAs has not been clarified. It is difficult to envision a functional role of antibodies with a temperature optimum way below body temperature. Comparative studies, however, have strongly indicated that the evolution of the adaptive immune system began with the jawed vertebrates (43–46). Cartilaginous fish, which are phylogenetically ancient and considered closely related to the first jawed vertebrates, have only one immunoglobulin class in common with humans: IgM (43, 46). The V, D, and J gene sequences, known to undergo rearrangement during B-lymphocyte maturation in humans (47), have also been identified in sharks, however in the form of preformed combinations

TABLE 3 | Immunoglobulin heavy and light chain V gene usage in cold agglutinin disease and Waldenström macroglobulinemia.

Gene	Cold agglutinin disease	Waldenström macroglobulinemia/ lymphoplasmacytic lymphoma
Heavy chain gene	*IGHV4-34* (>85%) (5, 9, 28, 29)	*IGHV3* (83%) (*IGHV3-23*, 24%) (5, 30)
Light chain gene	*IGKV3-20* (59%) (29, 35)	Not determined

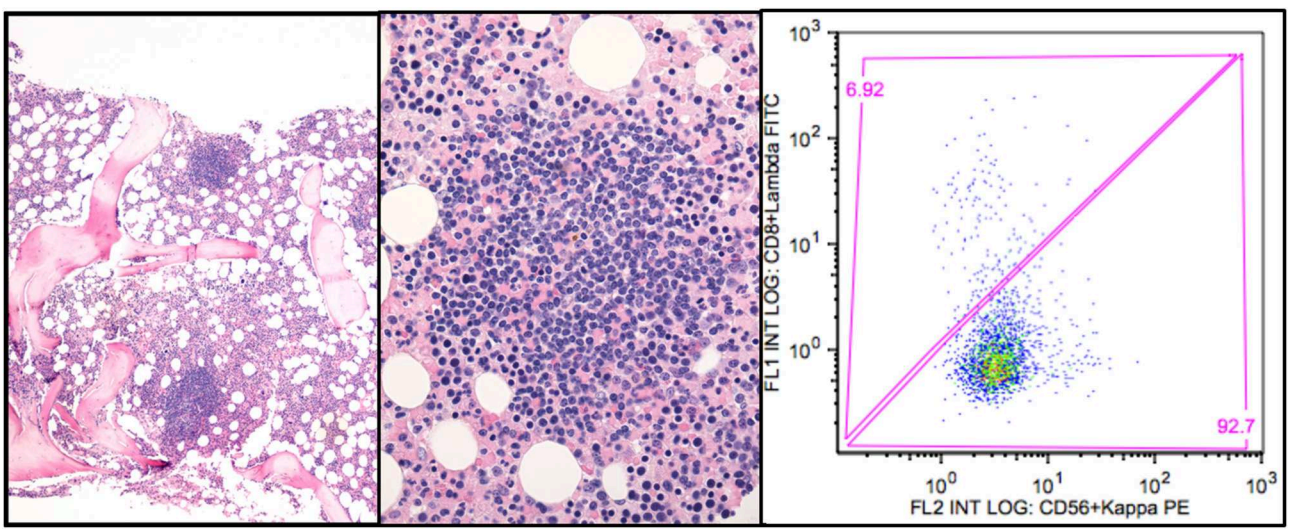

FIGURE 1 | CAD-associated lymphoproliferative disorder. **(A)** shows the nodular infiltration pattern. **(B)** highlights the resemblance to marginal zone B cell infiltration. **(C)** shows the typical flow cytometry finding of a monoclonal κ+ B-cell population (gated on CD19+ B-cells). Courtesy of U. Randen. First published in Clin Adv Hematol Oncol 2020 by S. Berentsen et al. (41), reused under Creative Commons Attribution Non-Commercial License. Copyright: S. Berentsen, A. Malecka, U. Randen, and G.E. Tjønnfjord.

TABLE 4 | Cold agglutinin disease: handling of samples.

Analysis	Material	Sampling	Handling of sample
Hemoglobin, blood cell counts	Blood	EDTA vacutainer	Prewarm at 37–38°C before analysis if problems with agglutination
Cold agglutinin titer, thermal amplitude, immunoglobulin quantification, electrophoresis, immune fixation	Serum or plasma	Blood is drawn into prewarmed vacutainers (For serum: No gel or additive). Place in warming cabinet or water bath at 37-38°C	Keep at 37–38°C until serum/plasma has been removed from the clot/cells, after which the sample can be handled at room temperature
Flow cytometry	Bone marrow aspirate (Too low sensitivity if performed in peripheral blood)	Add EDTA or heparin	Prewarming before analysis will often be sufficient. If not, wash cells at 37-38°C. For description, see Ulvestad et al. (9)

EDTA, ethylenediamine-tetraacetic acid.

Table first published in Journal of Blood Medicine 2019 by Berentsen et al. (14), reused under general permission (Creative Commons Attribution Non-Commercial License). Copyright: Berentsen et al.

located on several chromosomes (43). While the *IGHV4-34* gene is not known to produce any physiologically functional antibody in man, the temperature optimum of CAs is much closer to the environmental and body temperature of non-mammal sea vertebrates. Furthermore, CAs can react with antigens other than RBC surface macromolecules, and structures closely related to the I antigen are present on some microorganisms such as *Streptococcus* and *Listeria* species (48, 49). Thus, one might explain human CAs as remnants of a primitive vertebrate immune system (45, 46, 50).

Immunological Properties of Cold Agglutinins

Most CAs have specificity for the Ii blood group system of carbohydrate antigens (51, 52). The densities of I and i antigens on the RBC surface are inversely proportional. Only the i antigen is expressed on neonatal RBCs, whereas the I antigen predominates from 18 months-age and onwards (51). Hence, in most subjects but infants, CAs specific for the I antigen are more pathogenic than those with anti-i specificity (53, 54). Occasionally, CAs are specific for the RBC surface protein antigen Pr, and these CAs can be highly pathogenic (54, 55). Antigen specificities in CAD and CAS are listed in **Table 2**. CAs in CAD are usually anti-I specific.

Most CAs in CAD are monoclonal IgMκ (18, 56). Only ∼7% of the cases show λ light chain restriction, while CA of the IgG class occurs in less than 5% (18, 57). Monoclonal IgA is even rarer and may not be identical to the CA but rather a bystander (58–60). In CAS secondary to aggressive B-cell lymphoma, the light chain phenotype can be λ as well as κ (61). CAs in infection-associated CAS are polyclonal (2). These CAs are anti-I specific IgM in *Mycoplasma* pneumonia (62, 63) and IgG or IgM with anti-i specificity in EBV or cytomegalovirus infection (25, 64–66). In CAS following infection with EBV, a rheumatoid factor-like IgM-IgG complex has been reported to act as a CA in single case (66).

The activity of a CA is usually assessed by the titer, measured at 4°C and defined as the inverse of the maximum serum dilution at which agglutination can be seen. Nearly all patients with CAD have a CA titer $\geq$ 64; we found a median titer of 512 (range, 16–819200) (3, 13, 18, 67). A titer as high as 168 million has been reported (68). In older publications, titers tended to be higher than reported in more recent literature (9, 11, 18, 21, 69), probably because of an underestimation in clinical practice and some recent studies. Titration can be time-consuming, and some laboratories discontinue the serial dilution when a clearly pathological titer has been reached.

The thermal amplitude (TA) is defined as the highest temperature at which the CA will react with the antigen (9, 70). The pathogenicity of CA depends on the TA more than on the titer (70, 71). If the TA exceeds 28-30°C, RBCs will agglutinate in the cooler parts of the circulation even at mild ambient temperatures, often followed by complement activation and hemolysis. In some patients, the TA can approach 37°C (53).

For CA detection, serum protein electrophoresis, and assessments of CA titer, TA and IgM levels, samples must be obtained and handled as indicated in **Table 4** (10, 13). Detectable CA is present in serum in a proportion of the adult population without any hemolysis or clinical symptoms, although reported percentages are highly variable (53, 72). These individuals do not have CAD or CAS. The normally occurring CAs are present in low titers, in most cases below 64 and nearly always below 256, have low TA, and are polyclonal (53). In contrast, significant CA activity was found in 8.5% of 172 consecutive individuals with a monoclonal IgM (69). Titers were between 512 and 65,500, and all individuals with detectable CA had hemolysis. Therefore, monoclonal CA are generally more pathogenic than polyclonal CA.

The ability of CAs to agglutinate RBCs after binding to the cell surface (**Figure 2**) can be attributed to the pentameric structure and large molecule size of IgM (8, 11, 41). Agglutination-mediated, cold-induced ischemic symptoms from the acral capillary circulation have been reported in 40–90% of patients with CAD. Severity can range from slight acrocyanosis to disabling Raynaud phenomena and, in rare cases, even gangrene (16, 18). Atypical circulatory features include dermatologic manifestations, sometimes described as livedo reticularis and sometimes as livedo racemosa (73–75). On rewarming in the central circulation, CA detaches from the cells and the aggregates disintegrate. Complement protein complex C1, which has bound to the AgAb complex before the CA detaches, remains cell-bound and complement activation ensues.

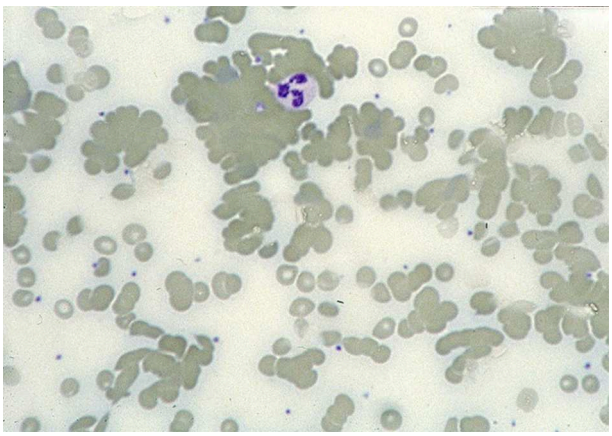

FIGURE 2 | Blood smear in a patient with CAD. Agglutination of erythrocytes dominates the picture. Courtesy of G.E. Tjønnfjord. First published in Clin Adv Hematol Oncol 2020 by S. Berentsen et al. (41), reused under Creative Commons Attribution Non-Commercial License. Copyright: S. Berentsen, A. Malecka, U. Randen, and G.E. Tjønnfjord.

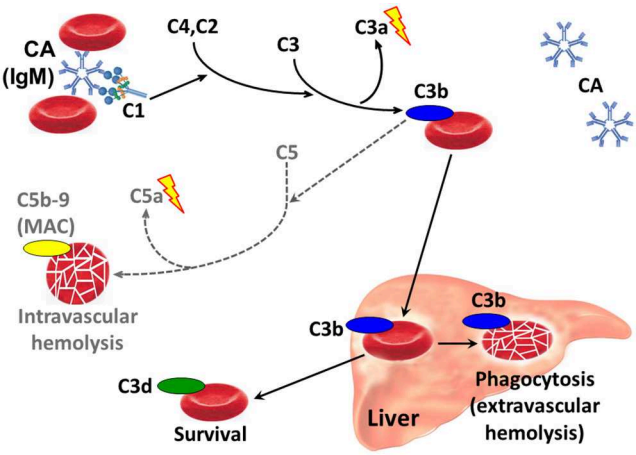

FIGURE 3 | Classical complement pathway-mediated hemolysis in CAD. Only relevant steps and components are shown. Black arrows, major pathways. Gray/dotted arrows, minor pathways. Lightning symbol indicates anaphylotoxin properties. C1, C2, etc., complement proteins; CA, cold agglutinin; Ig, immunoglobulin; MAC, membrane attack complex.

CAs should be distinguished from cryoglobulins (76). Rarely, however, cold-reactive immunoglobulins have been described that exhibited both CA and cryoglobulin properties (68, 76, 77). The Ii antigen system is also present on granulocytes, monocytes, lymphocytes, and thrombocytes (78–80). While aggregation of neutrophils has been observed in rare cases (78, 81), patients with CAD are not known to have an increased frequency of thrombocytopenia (9).

Complement Activation and Hemolysis

Antigen-bound IgM is a potent complement activator (82–84). Following cold-induced binding of CA to the RBCs during passage through the acral parts of the circulation, the AgAb complex induces fixation of complement protein C1q and, thereby, complement activation by the classical pathway (**Figure 3**) (84–88). C1 esterase activates C4 and C2, thus generating C3 convertase which results in the formation of C3a, a soluble anaphylotoxin, and C3b, an opsonin with enzymatic activity (84, 89). On rewarming to 37°C in the central circulation and detachment of CA, C3b remains bound and C3b-opsonized RBCs undergo phagocytosis by the mononuclear phagocytic system, mainly in the liver (84, 87, 90, 91). This process is also known as extravascular hemolysis. On the surviving cells, surface-bound C3b is degraded into its more or less inactive split products iC3b, C3c, and C3d.

Complement activation may proceed beyond the C3b formation step by binding of the C4bC2a complex to C3b, thus generating C5 convertase (89, 92). This enzyme initiates the terminal complement cascade by cleaving C5 into C5a, a potent anaphylotoxin, and C5b, which remains cell-bound. C5b is able to bind C6, C7, C8 and C9, resulting in formation of the membrane attack complex (MAC) and intravascular hemolysis. Due to inhibition by surface-bound regulatory proteins such as CD55 and CD59, however, complement activation is often not sufficient to produce clinically significant activation of the terminal complement pathway (73, 87, 93).

The major mechanism of hemolysis in stable disease, therefore, is the extravascular destruction of C3b-coated erythrocytes by the mononuclear phagocytic system. In severe disease and acute exacerbation, however, there can be a substantial component of intravascular hemolysis, as evidenced by the occurrence of hemoglobinuria in 15% of the patients (16), the observation of hemosiderinuria (76), and the modest but significant effect of treatment with eculizumab (73).

IgG is a weaker complement activator than IgM (82, 83), and the rare cases of IgG mediated CAD behave differently from IgM mediated disease in terms of effect of therapy (57). Among the IgG subclasses, IgG3 activates complement more efficiently than does IgG1, whereas IgG2 is a still weaker activator and IgG4 does not trigger the complement system (94). Thus, the mechanisms of hemolysis may be different in IgG mediated disease as compared with typical IgM mediated CAD.

In a retrospective cohort of patients with CAD, we found a median hemoglobin level (Hb) of 9.2 g/dL (range, 4.5–15.3 g/dL) (18). Hemolytic anemia was slight (or sometimes even compensated) in 36% of the patients (Hb $>$ 10.0 g/dL), moderate (Hb 8.0–10.0 g/dL) in 37%, and severe (Hb $<$ 8.0 g/dL) in 27%. Severity of anemia correlated with markers of hemolysis, but not with IgM levels, which may be associated with complement-independent RBC agglutinating activity as well (**Figure 4**).

Direct Antiglobulin Test

DAT detects immunoglobulin and/or complement components on the RBC surface (3, 95). When markers of hemolysis (lactate dehydrogenase, haptoglobin, bilirubin, and absolute reticulocyte count) show that an anemia is hemolytic, DAT is performed to demonstrate autoimmune pathogenesis. In many laboratories, DAT is first done by using a polyspecific antibody reagent. If

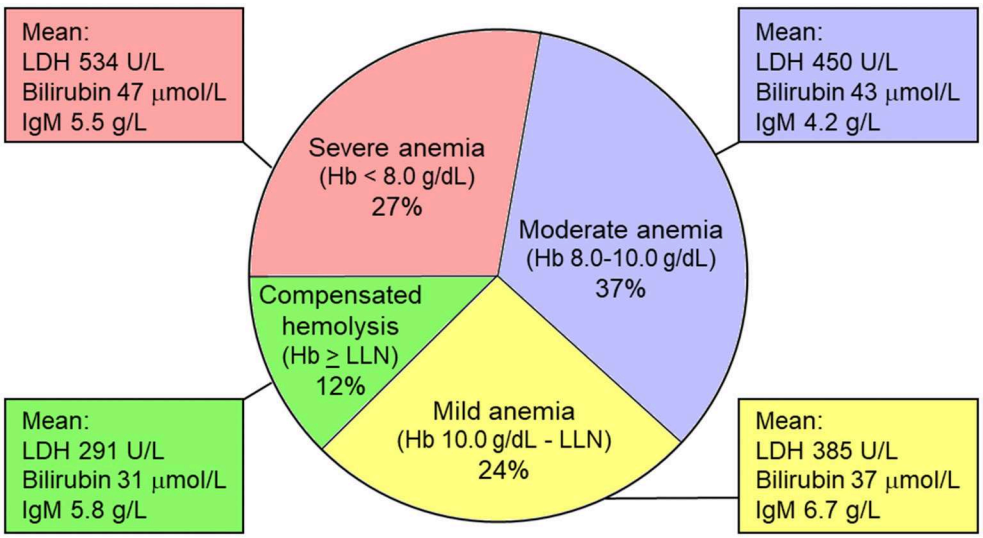

FIGURE 4 | Severity of anemia in cold agglutinin disease (percentages of patients). Severity of anemia correlates nicely with markers of hemolysis (LDH and bilirubin levels), but not with IgM levels, which may be associated with complement-independent RBC agglutinating activity as well as complement-mediated hemolysis. Hb, hemoglobin level; LDH, lactate dehydrogenase; LLN, lower limit of normal (Hb 11.5 g/dL in women and 12.5 g/dL in men). Based on data from Berentsen et al. (18).

AIHA is confirmed, a monospecific DAT must be performed, i.e., by using antibodies against specific immunoglobulin classes and complement proteins. Despite the IgM mediated pathogenesis in CAD and CAS, monospecific DAT is usually negative for IgM because the CA detaches from the RBC surface before it can be identified by DAT (**Figure 3**). As mentioned above, however, the classical pathway activation and C3b opsonization of RBCs will result in a strongly positive DAT for C3 components, in particular C3d (13, 84). For reasons that are incompletely understood, monospecific DAT is also weakly positive for IgG in up to 20% of the patients (16, 18).

COLD-ANTIBODY AIHA AND INFLAMMATION

Impact of cAIHA on Inflammation

The production of CA by an autonomous B-cell clone explains why CAD does not seem to be associated with other autoimmune diseases (9, 18). Still, serum levels of C-reactive protein (CRP) > 5 mg/L occur in ∼25% of the patients in the absence of any identifiable infection, consistent with some kind of proinflammatory state.

Complement activation is closely linked to inflammatory responses and, often, part of these responses (89, 96–99). It has been shown that persistent complement activation is associated with a proinflammatory state in some hemolytic disorders. Interactions between the complement system, inflammatory cytokines, and coagulation was investigated in an *in vitro* model using inhibition of *E. coli*-induced complement activation in human blood (100). The investigators found that complement activation resulted in increased expression of pro-inflammatory cytokines and upregulating of tissue factor mRNA levels. This upregulation, whether induced by *E. coli* or purified lipopolysaccharide, was efficiently blocked by C1 inhibition and, to a lesser extent, by C3 inhibition.

In CAD and CAS, complement activation results in production of C3a, an anaphylotoxin, and, in cases with terminal pathway activation, release of the potent anaphylotoxin C5a (**Figure 3**) (89, 99). The strong classical pathway activation in CAD is reflected by low serum levels of C4 because of continuous consumption; median level was 0.07 g/L in a large descriptive study (reference range, 0.13–0.32 g/L), and 72% of the patients had levels below 0.13 g/L (18). To a smaller extent, CAD patients also tend to have low levels of C1s, C2, C3, and C5 (18, 87). In a follow-up study of a single patient with CAD, temporarily raised levels of interleukin(IL)-1β, IL-6, tumor necrosis factor(TNF)-α, and interferon(INF)-γ were found to be associated with elevated CRP (101, 102). Other immunoregulatory cytokines may also be involved, as discussed in the next subsection, "Impact of inflammation and infection on cAIHA" (103–105).

In polyclonal autoimmune disorders, release of proinflammatory cytokines have been associated with fatigue, which is a bothersome symptom in many patients with CAD (106, 107). Therapeutic classical pathway inhibition in CAD has been shown to impressively relieve the fatigue, although an effect on fatigue of improved Hb levels cannot be ruled out (107).

In theory, the cross-talk between the complement system, inflammatory processes, and the coagulation cascade (100, 108, 109) might result in an increased frequency of thrombosis in CAD and CAS. Such a risk is definitely present in wAIHA (110, 111). In CAD, this risk has been clearly documented in the most severely affected patients (73), and recent registry-based studies have found a slightly increased frequency of thrombosis in unselected CAD cohorts as well (112, 113). According to one AIHA study, leukocytes influenced the risk of thrombosis

(111), and the tissue factor expression by granulocytes has been implicated as one of the links between inflammation and thrombosis (114). The role of this interaction is more unclear in CAD, however, due to the different immune pathogenesis and because CAD patients usually do not have elevated leukocyte counts (9).

Impact of Inflammation and Infection on cAIHA

Exacerbation of hemolytic anemia during febrile illness in a patient with CAD was described in 1999 as "paradoxical hemolysis" (115). Subsequently, descriptive studies showed that this occurs in 40–70% of the patients (18), and exacerbations have also been described after major trauma or major surgery (101, 116). The phenomenon is best explained by the low levels of classical pathway components, in particular C4, caused by continuous consumption in steady-state patients as already discussed. Probably, C4 activation is rate-limiting for complement-mediated hemolysis because of these low levels. When an acute phase reaction occurs, increased amounts of complement proteins are produced, and exacerbation will ensue. This causal relationship has been documented in a single patient (101). Direct complement activation, for example by microbial agents, may also contribute to the exacerbation in some situations.

In a mouse model of systemic autoimmunity with AIHA as a major component, elimination of the proinflammatory cytokine INF-γ was found to delay AIHA development (102). Moreover, a role of several immunoregulatory cytokines (IL-1α, IL-2, IL-6, IL-10, IL-12, IL-13, IL-17, IL-21, INF-γ, and tumor growth factor(TGF)-β) has been found or implicated in wAIHA (103–105). However, the relevance for CAD of these observations is unclear because of its distinct immune pathogenesis.

In infection-associated CAS, the causal relationship between infection and complement mediated hemolytic anemia is different. In *Mycoplasma pneumoniae* pneumonia, IgM-CA is produced by polyclonal lymphoplasmacytoid cells, probably as part of the physiological immune response (62, 63, 117). In fact, a qualitative test for CA was used as a diagnostic test for *Mycoplasma* infection before specific serology was clinically available, but its usefulness was limited because of low specificity and sensitivity (2). Most of these CAs do not cause hemolysis, but occasionally, profound hemolytic anemia can occur because of high-titer, anti-I specific CAs (62, 63). The temporal course of the disease manifestations is consistent with this explanation, as any hemolytic anemia usually appears rather suddenly in the second week of *Mycoplasma* infection and is self-remitting, usually within 4–6 weeks (2, 63).

TREATMENT OF CAD

General Considerations

Non-pharmacological management consists of thermal protection, in particular of exposed parts of the body (3, 7, 11, 118). Some patients even have to avoid cold food and beverages and should not take food from the fridge or freezer without wearing gloves. In my experience, many patients have discovered these precautions before they see the specialist. However, they often need to be explained that these are measures against the hemolytic anemia, not only against the ischemic symptoms. It is equally important for hematologists to provide health care personnel with relevant instructions. In the ward or outpatient department, patients with CAD should keep warm and avoid cold infusions (10, 11, 119). Any bacterial infection should be treated (10, 14, 101). Transfusion, when indicated, can be considered safe. As opposed to wAIHA, in which it is impossible to find compatible donor blood in most cases, compatibility problems are usually not encountered in CAD (2, 118). The patient, including the extremity used for transfusion should be kept warm, however, and most literature recommends the use of an in-line blood warmer (3, 7, 119). Disregarding these precautions has resulted in acute exacerbation, and fatal outcome has been reported (120). Because low complement protein levels are rate-limiting for hemolysis, transfusion of blood products with a high plasma content should probably be avoided (101).

In critical situations where it is not feasible to wait for the effect of specific therapy (see below), plasmapheresis is an option for "first-aid" (121–124). The theoretical rationale for this procedure is strong because virtually all IgM is located intravascularly (124), but no prospective study has been published and some conflicting data do exist (122, 125). Recommendations have been to exchange 1–1.5 times the plasma volume with albumin, not plasma, daily or every second day (7, 123). The effect is short-lived and drug therapy should be initiated concomitantly (7, 10).

According to small retrospective series and case reports, splenectomy has failed to induce remission of CAD (11, 18, 118). This is not surprising, as the extravascular hemolysis mainly takes place in the liver (91). Even though exceptions may exist among the rare patients with CA of the IgG class or with a TA approaching 37°C (57, 118), splenectomy should not be used to treat CAD.

The occurrence of CA in subjects who undergo surgery in hypothermia and/or cardiopulmonary bypass remains a challenge. Diverging recommendations exist regarding routine screening for CA in all patients scheduled for such surgery. The frequency of positive findings is low and the consequences of incidentally detected CA not associated with clinical disease have not been clarified (72, 126). Therefore, the cost-effectiveness of such screening is probably low. In patients with CAD, however, a TA measurement and an assessment by a hematologist should be obtained before cardiac surgery, which should be performed under normothermia (116, 126).

Pharmacological therapy for CAD is not indicated in patients with mild anemia or compensated hemolysis in the absence of troublesome clinical symptoms (3, 7, 10). Still, "real life" studies have found that 70–80% of patients have been treated (16, 18). Unlike in wAIHA, therapy with corticosteroids and other unspecific immunosuppression is generally ineffective in CAD (3, 10). Already 30–60 years ago, Schubothe (11) and Nydegger et al. (119) reported the poor efficacy of corticosteroids. Dacie followed 38 patients with "idiopathic" CAD and noticed that only occasional patients had responded to steroids (118). We found a response rate <20% in a retrospective series of 86 patients

(18), although some retrospective studies have found a slightly higher percentage of responders (4, 16). Furthermore, in the few patients who do respond, unacceptably high maintenance doses are often required for sustained response (3, 18, 118). Therapy directed against the pathogenic B-cell clone, or, more recently, complement modulation is more likely to succeed (3, 7, 10).

B-Cell Directed Therapies

Not all B-cell directed treatments have been successful. A small study of chlorambucil therapy found some effect on IgM concentrations and markers of hemolysis, but no significant increase in Hb levels (127). Although IFN-α is not a specific B-cell targeting agent, it has demonstrated favorable activity in a variety of indolent B-cell LPDs (128, 129). However, two small series of IFN-α therapy in CAD showed conflicting results (130, 131). Cladribine monotherapy was found to be ineffective (132). Approximately 25% of patients seem to respond to cyclophosphamide monotherapy.

The first therapy shown to give acceptable response rates was rituximab monotherapy. Two prospective, nonrandomized studies using rituximab 375 mg/m^2 for four cycles at 1 week interval found partial response (PR) in ∼50% of the patients, but complete response (CR) was rare (133, 134). Median response duration was 11 months (range, 2-42 months), and six of 10 retreated patients achieved a second response (133). The treatment was well tolerated. Other authors have reported responses in up to 100% of the patients, but the highest response rates estimated in the literature have been shown to reflect selection and publication bias as well as non-defined or heterogeneous response criteria (135). Although not approved for this indication by EMA or FDA and not available in all countries, rituximab monotherapy has become the most accepted first-line therapy for CAD (3, 7).

Addition of fludarabine was studied in a prospective, nonrandomized trial of 29 patients (136). This regimen (rituximab 375 mg/m^2 day 1 and fludarabine orally, 40 mg/m^2 days 1-4 for four cycles at 28 days interval) yielded an overall response rate of 76% (21% CR and 55% PR). Median estimated response duration was 66 months. Grade 4 neutropenia occurred in 14% of the patients, but as much as 59% experienced infection grade 1–3 (136). Based on the use of fludarabine in other indications, there are also some concerns about possible long-term toxicities (137).

Rituximab plus bendamustine combination therapy was prospectively studied in a non-randomized, multicenter trial in which we treated 45 CAD patients with rituximab 375 mg/m^2 day 1 and bendamustine 90 mg/m^2 day 1 and 2 for four cycles at 28 days interval (138). This trial had the same inclusion criteria and response definitions as used in the rituximab-fludarabine trial, and the baseline characteristics were almost identical. Thirty-two participants (71%) achieved a response; CR in 18 patients (40%) and PR in 14 (31%). Among 14 patients who had previously received rituximab or fludarabine plus rituximab, response to bendamustine plus rituximab was observed in 7 (50%). Hb levels increased by median 4.4 g/dL in those who achieved CR and 3.9 g/dL in the partial responders. More than 90% of the responders were still in remission after 32 months. Fifty per cent of the responses occurred within 1.9 months, but up to 7 months' time to response was seen in some patients. Neutropenia grade 4 was observed in 9 patients (20%), but only 5 (11%) experienced infection with or without neutropenia. Most clinical adverse events were mild and could be attributed to known non-hematological toxicity of bendamustine.

In a prospective, non-randomized study, 19 patients received one cycle of bortezomib monotherapy. Six participants responded; three responses were graded as CR and three as PR (139). Although these response rates may seem low, the results constitute a promising "proof of principle," and higher response rates might be achieved by extending the duration of treatment or using bortezomib-based combinations.

In theory, administration of Bruton tyrosine kinase inhibitors or other novel specific B-cell targeted agents would be attractive (140). The rationale for this approach is strong, as studies of WM have showed activity of ibrutinib even in *MYD88* L265P negative cases (141). Our group has successfully treated one CAD patient with ibrutinib, and a systematic study should be done.

We regard four cycles of bendamustine plus rituximab as an efficacious and sufficiently safe regimen that may be considered first-line in relatively fit patients who are severely affected by CAD (3, 10, 138). Safety should be carefully monitored. For other patients who require treatment, rituximab monotherapy should be the first choice (3, 7, 10).

Complement Modulation

A non-randomized prospective trial that included 12 patents with CAD and one with severe CAS showed some effect of therapy with the anti-C5 monoclonal antibody, eculizumab (73). However, although intravascular hemolysis was significantly inhibited and most patients became transfusion independent, anemia and quality of life scores did not improve significantly. As explained above, C3b-opsonization followed by extravascular hemolysis is the main mechanism of RBC breakdown in steady-state CAD, terminal pathway activation is limited, and C5 is not the optimal target of complement modulation. A meaningful effect has been reported, however, in severely affected patients (142, 143) and as prophylaxis against exacerbation following heart surgery (116), consistent with the notion that intravascular hemolysis may be more prominent in these situations.

Inhibition at the C1 or C3 level would be expected to work better. Plasma-derived C1 esterase inhibitor (C1-INH) is approved for the treatment of hereditary angioedema, which is not a complement-mediated disorder. High doses of C1-INH were shown to block the complement classical pathway, abrogate hemolysis and improve anemia in a patient with a severe, IgM-mediated wAIHA (144), and a similar effect has been reported in a patient with acute, severe CAS (145). However, endogenous C1-INH production is not deficient in AIHA, and further C1-INH therapy would require frequently repeated high doses. C1-INH, therefore, does not seem attractive as long-term therapy, and no systematic trial has been published.

Sutimlimab (BIVV009, TNT009) is a humanized monoclonal inhibitory antibody that targets C1s (146). The murine precursor of sutimlimab, TNT003, showed ability to efficiently inhibit complement activation, C3 deposition, and phagocytosis of RBCs

in vitro in the presence of normal human serum as a source of complement and patient sera as a source of CA (87). In a phase 1B trial of 10 patients with CAD, weekly intravenous infusions of sutimlimab increased Hb levels by a median of 1.6 g/dL within the first week of treatment and by 3.9 g/dL within 6 weeks (146). According to the results published, "extravascular hemolysis was abrogated in most patients, bilirubin levels mostly normalized within 24 h, and all of six previously transfusion-dependent patients became transfusion-free. Hemolysis recurred after discontinuation, but re-administration of sutimlimab restored the remission" (146). Recently, similar favorable results have been confirmed in a phase 3 trial in transfusion-dependent patients with CAD (107), and a phase 3 trial in transfusion independent patients is ongoing (ClinicalTrials.gov, NCT03347422). Adverse events related to the study drug have not been observed in these trials. Patients received no antimicrobial prophylaxis, but were vaccinated against *Neisseria meningitidis, Streptococcus pneumonia,* and *Haemophilus influenzae* (107, 146).

No clinical results have been published in CAD regarding ANX005, a humanized monoclonal antibody to C1q (147), and peptide inhibitor of C1 (PIC1), a small molecule that targets C1q and blocks the activation of associated serine proteases (148).

Splitting of C3 by C3 convertase is a point of convergence between all three initial complement pathways and critical for activation of the terminal pathway (84, 89). Therefore, inhibition at this level will have the potential to block the entire complement system and is an attractive option in several complement-mediated disorders (149). The C3 inhibitor, pegcetacoplan (APL-2), is a pegylated peptide designed for subcutaneous administration (150). Clinical phase 2 trials have found efficacy of pegcetacoplan in paroxysmal nocturnal hemoglobinuria as well as AIHA (151), and further studies in CAD are warranted. A high risk of infection with encapsulated bacteria might be suspected as a consequence of C3 inhibition, but thus far, clinical data have not supported this concern (150–152). Trial participants were vaccinated as in the C1 modulation trials.

As discussed above, complement-directed therapies for CAD are promising. However, these options are still investigational and will encounter some limitations. First, ischemic symptoms are not complement-mediated and will not be relieved. Second, in contrast to chemoimmunotherapy, treatment will probably have to continue indefinitely to maintain its effect. Third, such therapies will probably be very expensive. On the other hand, the B-cell directed therapies also have obvious limitations: 20–25% of the patients will not respond, the time to response can be several months or even longer (138), and some patients have contraindications or are reluctant to receive treatment with cytotoxic drugs. In contrast, sutimlimab is rapidly acting and seems to have a favorable toxicity profile (107, 146). Undoubtedly, therefore, the upstream complement inhibitors have the potential to fill an unmet need in patients with CAD. It is to be hoped that in severe cases and acute exacerbations, such therapy will "provide a bridge that will allow rapid achievement of remission and transition to B-cell directed treatment when the situation is under control" (88).

TREATMENT OF CAS

As secondary CAS is even rarer than CAD, no systematic study has been published in this group of disorders, and recommendations have been based on theoretical considerations, case reports, and expert opinion (2, 3, 153). In CAS associated with aggressive lymphoma or other malignancies, no therapy has been established except for treatment of the underlying disease (2, 3, 153).

In infection-associated CAS, optimal antimicrobial therapy should be instituted when relevant (2). Whereas appropriate antibiotic therapy for *Mycoplasma pneumoniae* pneumonia is usually effective for control of the infection, the onset of secondary CAS will often occur after antibiotic therapy has been initiated or even completed (2, 63). This hemolytic anemia is self-remitting but can be profound, and there is an unmet need for therapy in severely affected patients until resolution of hemolysis occurs (63, 154). Corticosteroids have been used in CAS secondary to *Mycoplasma* as well as virus infections (155–157). However, no good evidence of benefit has been published, as all reports are case observations and it is difficult to distinguish between effect of therapy and spontaneous resolution. Transfusions can safely be given provided the same precautions are observed as in CAD.

Temporary use of upstream complement inhibition seems to be an attractive approach based on theoretical considerations, but no clinical evidence has been provided for its effect in secondary CAS. Because of the rarity of this syndrome, prospective trials are unlikely to be performed, but a systematic retrospective study might be feasible on a multinational basis.

AUTHOR CONTRIBUTIONS

SB collected the relevant information and references, and wrote the paper.

REFERENCES

1. Sokol RJ, Hewitt S, Stamps BK. Autoimmune haemolysis: an 18-year study of 865 cases referred to a regional transfusion centre. *Br Med J (Clin Res Ed).* (1981) 282:2023–7. doi: 10.1136/bmj.282.6281.2023
2. Berentsen S, Tjønnfjord GE. Diagnosis and treatment of cold agglutinin mediated autoimmune hemolytic anemia. *Blood Rev.* (2012) 26:107–15. doi: 10.1016/j.blre.2012.01.002
3. Jäger U, Barcellini W, Broome CM, Gertz MA, Hill A, Hill QA, et al. Diagnosis and treatment of autoimmune hemolytic anemia in adults: Recommendations from the First International Consensus Meeting. Blood Rev. 2019:100648. doi: 10.1016/j.blre.2019.100648
4. Barcellini W, Fattizzo B, Zaninoni A, Radice T, Nichele I, Di Bona E, et al. Clinical heterogeneity and predictors of outcome in primary autoimmune hemolytic anemia: a GIMEMA study of 308 patients. *Blood.* (2014) 124:2930–6. doi: 10.1182/blood-2014-06-583021
5. Randen U, Trøen G, Tierens A, Steen C, Warsame A, Beiske K, et al. Primary cold agglutinin-associated lymphoproliferative disease: a B-cell lymphoma of the bone marrow distinct from lymphoplasmacytic lymphoma. *Haematologica.* (2014) 99:497–504. doi: 10.3324/haematol.2013.091702

6. Shanbhag S, Spivak J. Paroxysmal cold hemoglobinuria. *Hematol Oncol Clin North Am.* (2015) 29:473–8. doi: 10.1016/j.hoc.2015.01.004
7. Hill QA, Stamps R, Massey E, Grainger JD, Provan D, Hill A, et al. The diagnosis and management of primary autoimmune haemolytic anaemia. *Br J Haematol.* (2017) 176:395–411. doi: 10.1111/bjh.14478
8. Landsteiner K. Über Beziehungen zwischen dem Blutserum und den Körperzellen. *Münch Med Wschr.* (1903) 50:1812–4.
9. Ulvestad E, Berentsen S, Bø K, Shammas FV. Clinical immunology of chronic cold agglutinin disease. *Eur J Haematol.* (1999) 63:259–66. doi: 10.1111/j.1600-0609.1999.tb01887.x
10. Berentsen S. How I manage patients with cold agglutinin disease. *Br J Haematol.* (2018) 181:320–30. doi: 10.1111/bjh.15109
11. Schubothe H. The cold hemagglutinin disease. *Semin Hematol.* (1966) 3:27–47.
12. Hill QA, Hill A, Berentsen S. Defining autoimmune hemolytic anemia: a systematic review of the terminology used for diagnosis and treatment. *Blood Adv.* (2019) 3:1897–906. doi: 10.1182/bloodadvances.2019000036
13. Dacie J. Auto-immune haemolytic anaemia (AIHA): cold-antibody syndromes I: idiopathic types: clinical presentation and haematological and serological findings. In: Dacie J, editor. *The Haemolytic Anaemias,* Vol 3. London: Churchill Livingstone (1992). p. 210–39.
14. Berentsen S, Röth A, Randen U, Jilma B, Tjønnfjord GE. Cold agglutinin disease: current challenges and further prospects. *J Blood Med.* (2019) 10:93–103. doi: 10.2147/JBM.S177621
15. Chandesris MO, Schleinitz N, Ferrera V, Bernit E, Mazodier K, Gayet S, et al. [Cold agglutinins, clinical presentation and significance; retrospective analysis of 58 patients]. *Rev Med Interne.* (2004) 25:856–65. doi: 10.1016/j.revmed.2004.08.001
16. Swiecicki PL, Hegerova LT, Gertz MA. Cold agglutinin disease. *Blood.* (2013) 122:1114–21. doi: 10.1182/blood-2013-02-474437
17. Arthold C, Skrabs C, Mitterbauer-Hohendanner G, Thalhammer R, Simonitsch-Klupp I, Panzer S, et al. Cold antibody autoimmune hemolytic anemia and lymphoproliferative disorders: a retrospective study of 20 patients including clinical, hematological, and molecular findings. *Wien Klin Wochenschr.* (2014) 126:376–82. doi: 10.1007/s00508-014-0547-z
18. Berentsen S, Ulvestad E, Langholm R, Beiske K, Hjorth-Hansen H, Ghanima W, et al. Primary chronic cold agglutinin disease: a population based clinical study of 86 patients. *Haematologica.* (2006) 91:460–6.
19. Malecka A, Delabie J, Østlie I, Tierens A, Randen U, Berentsen S, et al. Cold agglutinin-associated B-cell lymphoproliferative disease shows highly recurrent gains of chromosome 3 and 12 or 18. *Blood Adv.* (2020) 4:993–6. doi: 10.1182/bloodadvances.2020001608
20. Berentsen S, Randen U, Tjønnfjord GE. Cold agglutinin-mediated autoimmune hemolytic anemia. *Hematol Oncol Clin North Am.* (2015) 29:455–71. doi: 10.1016/j.hoc.2015.01.002
21. Berentsen S, Bø K, Shammas FV, Myking AO, Ulvestad E. Chronic cold agglutinin disease of the "idiopathic" type is a premalignant or low-grade malignant lymphoproliferative disease. *APMIS.* (1997) 105:354–62. doi: 10.1111/j.1699-0463.1997.tb00581.x
22. Berentsen S, Ulvestad E, Tjønnfjord GE. B-lymphocytes as targets for therapy in chronic cold agglutinin disease. *Cardiovasc Hematol Disord Drug Targets.* (2007) 7:219–27. doi: 10.2174/187152907781745279
23. Berentsen S. Cold agglutinin disease. *Hematology Am Soc Hematol Educ Program.* (2016) 2016:226–31. doi: 10.1182/asheducation-2016.1.226
24. Ginsberg HS. Acute hemolytic anemia in primary atypical pneumonia associated with high titer of cold agglutinins; report of a case. *N Engl J Med.* (1946) 234:826–9. doi: 10.1056/NEJM194606202342503
25. Jenkins WJ, Koster HG, Marsh WL, Carter RL. Infectious Mononucleosis: An Unsuspected Source on Anti-i. *Br J Haematol.* (1965) 11:480–3. doi: 10.1111/j.1365-2141.1965.tb06611.x
26. El-Ayoubi A, Wang JQ, Hein N, Talaulikar D. Role of plasma cells in Waldenstrom macroglobulinaemia. *Pathology.* (2017) 49:337–45. doi: 10.1016/j.pathol.2017.02.004
27. Winter O, Dame C, Jundt F, Hiepe F. Pathogenic long-lived plasma cells and their survival niches in autoimmunity, malignancy, and allergy. *J Immunol.* (2012) 189:5105–11. doi: 10.4049/jimmunol.1202317
28. Pascual V, Victor K, Spellerberg M, Hamblin TJ, Stevenson FK, Capra JD. VH restriction among human cold agglutinins. The VH4-21 gene segment is required to encode anti-I and anti-i specificities. *J Immunol.* (1992) 149:2337–44.
29. Malecka A, Trøen G, Tierens A, Østlie I, Malecki J, Randen U, et al. Immunoglobulin heavy and light chain gene features are correlated with primary cold agglutinin disease onset and activity. *Haematologica.* (2016) 101:e361–4. doi: 10.3324/haematol.2016.146126
30. Varettoni M, Zibellini S, Capello D, Arcaini L, Rossi D, Pascutto C, et al. Clues to pathogenesis of Waldenstrom macroglobulinemia and immunoglobulin M monoclonal gammopathy of undetermined significance provided by analysis of immunoglobulin heavy chain gene rearrangement and clustering of B-cell receptors. *Leuk Lymphoma.* (2013) 54:2485–9. doi: 10.3109/10428194.2013.779689
31. Bhat NM, Bieber MM, Spellerberg MB, Stevenson FK, Teng NN. Recognition of auto- and exoantigens by V4-34 gene encoded antibodies. *Scand J Immunol.* (2000) 51:134–40. doi: 10.1046/j.1365-3083.2000.00654.x
32. Smith G, Spellerberg M, Boulton F, Roelcke D, Stevenson F. The immunoglobulin VH gene, VH4-21, specifically encodes autoanti-red cell antibodies against the I or i antigens. *Vox Sang.* (1995) 68:231–5. doi: 10.1111/j.1423-0410.1995.tb02578.x
33. Li Y, Spellerberg MB, Stevenson FK, Capra JD, Potter KN. The I binding specificity of human VH 4-34 (VH 4-21) encoded antibodies is determined by both VH framework region 1 and complementarity determining region 3. *J Mol Biol.* (1996) 256:577–89. doi: 10.1006/jmbi.1996.0110
34. Michaux L, Dierlamm J, Wlodarska I, Stul M, Bosly A, Delannoy A, et al. Trisomy 3 is a consistent chromosome change in malignant lymphoproliferative disorders preceded by cold agglutinin disease. *Br J Haematol.* (1995) 91:421–4. doi: 10.1111/j.1365-2141.1995.tb05315.x
35. Malecka A, Trøen G, Tierens A, Østlie I, Randen U, Berentsen S, et al. Highly restricted usage of immunoglobulin light chain IGKV3-20 with stereotyped sequence in primary cold-agglutinin disease (CAD). 57th Annual Meeting of the American Society of Hematology, Orlando, FL, USA: Dec 6 2015. *Blood.* (2015) 126:4137. doi: 10.1182/blood.V126.23.4137.4137
36. Malecka A, Trøen G, Tierens A, Østlie I, Malecki J, Randen U, et al. Frequent somatic mutations of KMT2D (MLL2) and CARD11 genes in primary cold agglutinin disease. *Br J Haematol.* (2018) 183:838–42. doi: 10.1111/bjh.15063
37. Fattizzo B, Barcellini W. Autoimmune Cytopenias in Chronic Lymphocytic Leukemia: Focus on Molecular Aspects. *Front Oncol.* (2019) 9:1435. doi: 10.3389/fonc.2019.01435
38. Lenz G, Davis RE, Ngo VN, Lam L, George TC, Wright GW, et al. Oncogenic CARD11 mutations in human diffuse large B cell lymphoma. *Science.* (2008) 319:1676–9. doi: 10.1126/science.1153629
39. Swerdlow SH, Cook JR, Sohani AR, Pileri SA, Harris NL, Jaffe ES, et al. Lymphoplasmacytic lymphoma. In: Swerdlow SH, Campo E, Harris NL, Jaffe ES, Pileri SA, Stein H, editors. *WHO Classification of Tumours of Haematopoietic and Lymphoid Tissues, 4th Ed*. Lyon: International Agency for Research on Cancer (2017). p. 232–5.
40. de Tute R, Rawstron A, Evans P, Owen R. Cold agglutinin disease is a phenotypically distinct clonal B-cell disorder. 15 International Myeloma Workshop, Rome, Italy: Sept 23-26, 2015. *Clin Lymphoma Myeloma Leuk.* (2015). 15:e184. doi: 10.1016/j.clml.2015.07.410
41. Berentsen S, Malecka A, Randen U, Tjonnfjord GE. Cold agglutinin disease: Where do we stand, and where are we going? *Clin Adv Hematol Oncol.* (2020) 18:35–44.
42. Clough MC, Richter IM. A study of an auto-agglutinin occurring in human serum. *Johns Hopkins Hospital Bulletin.* (1918) 29:86–93.
43. Litman GW. Sharks and the origins of vertebrate immunity. *Sci Am.* (1996) 275:67–71. doi: 10.1038/scientificamerican1196-67
44. Bartl S, Baltimore D, Weissman IL. Molecular evolution of the vertebrate immune system. *Proc Natl Acad Sci USA.* (1994) 91:10769–70. doi: 10.1073/pnas.91.23.10769
45. Litman GW, Rast JP, Shamblott MJ, Haire RN, Hulst M, Roess W, et al. Phylogenetic diversification of immunoglobulin genes and the antibody repertoire. *Mol Biol Evol.* (1993) 10:60–72.
46. Ota T, Sitnikova T, Nei M. Evolution of vertebrate immunoglobulin variable gene segments. In: Pasquiere LD, Litman GW, editors. *Origin and Evolution of the Vertebrate Immune System*. Berlin: Springer Verlag (2000). p. 221-41. doi: 10.1007/978-3-642-59674-2_10

47. Schwartz RS. Jumping genes and the immunoglobulin V gene system. *N Engl J Med.* (1995) 333:42–4. doi: 10.1056/NEJM199507063330108
48. Colling RG, Pearson TC, Brown JC. Association of bacterial carbohydrate-specific cold agglutinin antibody production with immunization by group C, group B type III, and Streptococcus pneumoniae type XIV streptococcal vaccines. *Infect Immun.* (1983) 41:205–13. doi: 10.1128/IAI.41.1.205-213.1983
49. Potter KN. Molecular characterization of cold agglutinins. *Transfus Sci.* (2000) 22:113–9. doi: 10.1016/S0955-3886(00)00031-X
50. Ulvestad E. The "lucky split" hypothesis and the evolution of antigen binding receptors. In: Ulvestad E, editor. *Defending Life: The Nature of Host-Parasite Relations*. Dordrecht: Springer (2007). p. 162–72.
51. Marsh WL. Anti-i: a cold antibody defining the Ii relationship in human red cells. *Br J Haematol.* (1961) 7:200–9. doi: 10.1111/j.1365-2141.1961.tb00329.x
52. Issitt PD. I blood group system and its relationship to disease. *J Med Lab Technol.* (1968) 25:1–6.
53. Dacie J. Auto-immune haemolytic anaemia (AIHA): cold-antibody syndromes II: immunochemistry and specificity of the antibodies; serum complement in autoimmune haemolytic anaemia. In: Dacie J, editor. *The Haemolytic Anaemias, Vol 3*. London: Churchill Livingstone (1992). p. 240–95.
54. Roelcke D. Cold agglutination. *Transfus Med Rev.* (1989) 3:140–66. doi: 10.1016/S0887-7963(89)70075-4
55. Brain MC, Ruether B, Valentine K, Brown C, ter Keurs H. Life-threatening hemolytic anemia due to an autoanti-Pr cold agglutinin: evidence that glycophorin A antibodies may induce lipid bilayer exposure and cation permeability independent of agglutination. *Transfusion.* (2010) 50:292–301. doi: 10.1111/j.1537-2995.2009.02445.x
56. Harboe M, van Furth R, Schubothe H, Lind K, Evans RS. Exclusive occurrence of K chains in isolated cold haemagglutinins. *Scand J Haematol.* (1965) 2:259–66. doi: 10.1111/j.1600-0609.1965.tb01303.x
57. Silberstein LE, Berkman EM, Schreiber AD. Cold hemagglutinin disease associated with IgG cold-reactive antibody. *Ann Intern Med.* (1987) 106:238–42. doi: 10.7326/0003-4819-106-2-238
58. Sefland Ø, Randen U, Berentsen S. Development of Multiple Myeloma of the IgA Type in a Patient with Cold Agglutinin Disease: Transformation or Coincidence? *Case Rep Hematol.* (2019) 2019:1610632. doi: 10.1155/2019/1610632
59. Romer W, Rother U, Roelcke D. Failure of IgA cold agglutinin to activate C. *Immunobiology.* (1980) 157:41–6. doi: 10.1016/S0171-2985(80)80060-X
60. Chadebech P, Michel M, Janvier D, Yamada K, Copie-Bergman C, Bodivit G, et al. IgA-mediated human autoimmune hemolytic anemia as a result of hemagglutination in the spleen, but independent of complement activation and FcalphaRI. *Blood.* (2010) 116:4141–7. doi: 10.1182/blood-2010-03-276162
61. Crisp D, Pruzanski W. B-cell neoplasms with homogeneous cold-reacting antibodies (cold agglutinins). *Am J Med.* (1982) 72:915–22. doi: 10.1016/0002-9343(82)90852-X
62. Linz DH, Tolle SW, Elliot DL. Mycoplasma pneumoniae pneumonia. Experience at a referral center. *West J Med.* (1984) 140:895–900.
63. Dacie J. Auto-immune haemolytic anaemia (AIHA): cold-antibody syndromes III: haemolytic anaemia following mycoplasma pneumonia. In: Dacie J, editor. *The Haemolytic Anaemias, Vol 3*. London: Churchill Livingstone (1992). p. 296–312.
64. Berlin BS, Chandler R, Green D. Anti-"i" antibody and hemolytic anemia associated with spontaneous cytomegalovirus mononucleosis. *Am J Clin Pathol.* (1977) 67:459–61. doi: 10.1093/ajcp/67.5.459
65. Luzuriaga K, Sullivan JL. Infectious mononucleosis. *N Engl J Med.* (2010) 362:1993–2000. doi: 10.1056/NEJMcp1001116
66. Dacie J. Auto-immune haemolytic anaemia (AIHA): cold-antibody syndromes IV: haemolytic anaemia following infectious mononucleosis and other viral infections. In: Dacie J, editor. *The Haemolytic Anaemias, Vol 3*. London: Churchill Livingstone (1992) p. 313-28.
67. Bendix BJ, Tauscher CD, Bryant SC, Stubbs JR, Jacob EK. Defining a reference range for cold agglutinin titers. *Transfusion.* (2014) 54:1294–7. doi: 10.1111/trf.12453
68. Rørvik K. The syndrome of high-titre cold haemagglutination; a survey and a case report. *Acta Med Scand.* (1954) 148:299–308. doi: 10.1111/j.0954-6820.1954.tb01722.x
69. Stone MJ, McElroy YG, Pestronk A, Reynolds JL, Newman JT, Tong AW. Human monoclonal macroglobulins with antibody activity. *Semin Oncol.* (2003) 30:318–24. doi: 10.1053/sonc.2003.50077
70. Garratty G, Petz LD, Hoops JK. The correlation of cold agglutinin titrations in saline and albumin with haemolytic anaemia. *Br J Haematol.* (1977) 35:587–95. doi: 10.1111/j.1365-2141.1977.tb00623.x
71. Rosse WF, Adams JP. The variability of hemolysis in the cold agglutinin syndrome. *Blood.* (1980) 56:409–16. doi: 10.1182/blood.V56.3.409.409
72. Jain MD, Cabrerizo-Sanchez R, Karkouti K, Yau T, Pendergrast JM, Cserti-Gazdewich CM. Seek and you shall find–but then what do you do? Cold agglutinins in cardiopulmonary bypass and a single-center experience with cold agglutinin screening before cardiac surgery. *Transfus Med Rev.* (2013) 27:65–73. doi: 10.1016/j.tmrv.2012.12.001
73. Röth A, Bommer M, Hüttmann A, Herich-Terhurne D, Kuklik N, Rekowski J, et al. Eculizumab in cold agglutinin disease (DECADE): an open-label, prospective, bicentric, nonrandomized phase 2 trial. *Blood Adv.* (2018) 2:2543–9. doi: 10.1182/bloodadvances.2018024190
74. Poldre P, Pruzanski W, Chiu HM, Dotten DA. Fulminant gangrene in transient cold agglutinemia associated with Escherichia coli infection. *Can Med Assoc J.* (1985) 132:261–3.
75. Shiiya C, Ota M. Cold agglutinin disease presenting as livedo racemosa. *CMAJ.* (2017) 189:E781. doi: 10.1503/cmaj.161407
76. Stone MJ, Berentsen S. Hyperviscosity syndrome, cold agglutinin hemolytic anemia, and cryoglobulinemia. In: Leblond V, Treon SP, Dimopoulos M, editors. *Waldenström's Macroglobulinemia*. Switzerland: Springer International Publishing (2017). p. 171–83. doi: 10.1007/978-3-319-22584-5_12
77. Bhattacharyya J, Mihara K, Takihara Y, Kimura A. Successful treatment of IgM-monoclonal gammopathy of undetermined significance associated with cryoglobulinemia and cold agglutinin disease with immunochemotherapy with rituximab, fludarabine, and cyclophosphamide. *Ann Hematol.* (2012) 91:797–9. doi: 10.1007/s00277-011-1322-0
78. Pruzanski W, Faird N, Keystone E, Armstrong M. The influence of homogeneous cold agglutinins on polymorphonuclear and mononuclear phagocytes. *Clin Immunol Immunopathol.* (1975) 4:277–85. doi: 10.1016/0090-1229(75)90063-X
79. Pruzanski W, Farid N, Keystone E, Armstrong M, Greaves MF. The influence of homogeneous cold agglutinins on human B and T lymphocytes. *Clin Immunol Immunopathol.* (1975) 4:248–57. doi: 10.1016/0090-1229(75)90060-4
80. Dunstan RA, Simpson MB, Rosse WF. The presence of the Ii blood group system on human platelets. *Am J Clin Pathol.* (1984) 82:74–7. doi: 10.1093/ajcp/82.1.74
81. Berentsen S. Neutrophil aggregation on the peripheral blood smear in a patient with cold agglutinin disease. *Ann Hematol.* (2017) 96:1767–8. doi: 10.1007/s00277-017-3077-8
82. Meulenbroek EM, de Haas M, Brouwer C, Folman C, Zeerleder SS, Wouters D. Complement deposition in autoimmune hemolytic anemia is a footprint for difficult-to-detect IgM autoantibodies. *Haematologica.* (2015) 100:1407–14. doi: 10.3324/haematol.2015.128991
83. Arndt PA, Leger RM, Garratty G. Serologic findings in autoimmune hemolytic anemia associated with immunoglobulin M warm autoantibodies. *Transfusion.* (2009) 49:235–42. doi: 10.1111/j.1537-2995.2008.01957.x
84. Berentsen S, Hill A, Hill QA, Tvedt THA, Michel M. Novel insights into the treatment of complement-mediated hemolytic anemias. *Ther Adv Hematol.* (2019) 10:2040620719873321. doi: 10.1177/2040620719873321
85. Jonsen J, Kåss E, Harboe M. Complement and complement components in acquired hemolytic anemia with high titer cold antibodies. *Acta Med Scand.* (1961) 170:725–9. doi: 10.1111/j.0954-6820.1961.tb00291.x
86. Zilow G, Kirschfink M, Roelcke D. Red cell destruction in cold agglutinin disease. *Infusionsther Transfusionsmed.* (1994) 21:410–5. doi: 10.1159/000223021
87. Shi J, Rose EL, Singh A, Hussain S, Stagliano NE, Parry GC, et al. TNT003, an inhibitor of the serine protease C1s, prevents

complement activation induced by cold agglutinins. *Blood.* (2014) 123:4015–22. doi: 10.1182/blood-2014-02-556027
88. Berentsen S. Cold agglutinins: fending off the attack. *Blood.* (2019) 133:885–6. doi: 10.1182/blood-2019-01-894303
89. Varela JC, Tomlinson S. Complement: an overview for the clinician. *Hematol Oncol Clin North Am.* (2015) 29:409–27. doi: 10.1016/j.hoc.2015.02.001
90. Lewis SM, Szur L, Dacie JV. The pattern of erythrocyte destruction in haemolytic anaemia, as studied with radioactive chromium. *Br J Haematol.* (1960) 6:122–39. doi: 10.1111/j.1365-2141.1960.tb06224.x
91. Jaffe CJ, Atkinson JP, Frank MM. The role of complement in the clearance of cold agglutinin-sensitized erythrocytes in man. *J Clin Invest.* (1976) 58:942–9. doi: 10.1172/JCI108547
92. Merrill SA, Brodsky RA. Complement-driven anemia: more than just paroxysmal nocturnal hemoglobinuria. *Hematology Am Soc Hematol Educ Program.* (2018) 2018:371–6. doi: 10.1182/asheducation-2018.1.371
93. Berentsen S. Complement activation and inhibition in autoimmune hemolytic anemia: focus on cold agglutinin disease. *Semin Hematol.* (2018) 55:141–9. doi: 10.1053/j.seminhematol.2018.04.002
94. Abramson N, Gelfand EW, Jandl JH, Rosen FS. The interaction between human monocytes and red cells. Specificity for IgG subclasses and IgG fragments. *J Exp Med.* (1970) 132:1207–15. doi: 10.1084/jem.132.6.1207
95. Barcellini W, Revelli N, Imperiali FG, Villa MA, Manera MC, Paccapelo C, et al. Comparison of traditional methods and mitogen-stimulated direct antiglobulin test for detection of anti-red blood cell autoimmunity. *Int J Hematol.* (2010) 91:762–9. doi: 10.1007/s12185-010-0578-9
96. Cofiell R, Kukreja A, Bedard K, Yan Y, Mickle AP, Ogawa M, et al. Eculizumab reduces complement activation, inflammation, endothelial damage, thrombosis, and renal injury markers in aHUS. *Blood.* (2015) 125:3253–62. doi: 10.1182/blood-2014-09-600411
97. Morgan BP, Harris CL. Complement, a target for therapy in inflammatory and degenerative diseases. *Nat Rev Drug Discov.* (2015) 14:857–77. doi: 10.1038/nrd4657
98. Ricklin D, Mastellos DC, Reis ES, Lambris JD. The renaissance of complement therapeutics. *Nat Rev Nephrol.* (2018) 14:26–47. doi: 10.1038/nrneph.2017.156
99. Murphy K. *Janeway's Immunobiology, 8. ed*. New York, NY: Garland Publishing Inc (2011).
100. Landsem A, Nielsen EW, Fure H, Christiansen D, Ludviksen JK, Lambris JD, et al. C1-inhibitor efficiently inhibits *Escherichia coli*-induced tissue factor mRNA up-regulation, monocyte tissue factor expression and coagulation activation in human whole blood. *Clin Exp Immunol.* (2013) 173:217–29. doi: 10.1111/cei.12098
101. Ulvestad E, Berentsen S, Mollnes TE. Acute phase haemolysis in chronic cold agglutinin disease. *Scand J Immunol.* (2001) 54:239–42. doi: 10.1046/j.1365-3083.2001.00960.x
102. Hoyer KK, Kuswanto WF, Gallo E, Abbas AK. Distinct roles of helper T-cell subsets in a systemic autoimmune disease. *Blood.* (2009) 113:389–95. doi: 10.1182/blood-2008-04-153346
103. Toriani-Terenzi C, Fagiolo E. IL-10 and the cytokine network in the pathogenesis of human autoimmune hemolytic anemia. *Ann N Y Acad Sci.* (2005) 1051:29–44. doi: 10.1196/annals.1361.044
104. Xu L, Zhang T, Liu Z, Li Q, Xu Z, Ren T. Critical role of Th17 cells in development of autoimmune hemolytic anemia. *Exp Hematol.* (2012) 40:994–1004 e4. doi: 10.1016/j.exphem.2012.08.008
105. Barcellini W. New insights in the pathogenesis of autoimmune hemolytic anemia. *Transfus Med Hemother.* (2015) 42:287–93. doi: 10.1159/000439002
106. Akcali A, Zengin F, Aksoy SN, Zengin O. Fatigue in multiple sclerosis: is it related to cytokines and hypothalamic-pituitary-adrenal axis? *Mult Scler Relat Disord.* (2017) 15:37–41. doi: 10.1016/j.msard.2017.03.004
107. Röth A, Barcellini W, D'Sa S, Miyakawa Y, Broome CM, Michel M, et al. Inhibition of complement C1s with sutimlimab in patients with cold agglutinin disease (CAD): results from the phase 3 cardinal study. *Blood.* (2019) 134 (Suppl. 2):LBA-2. doi: 10.1182/blood-2019-132490
108. Amara U, Flierl MA, Rittirsch D, Klos A, Chen H, Acker B, et al. Molecular intercommunication between the complement and coagulation systems. *J Immunol.* (2010) 185:5628–36. doi: 10.4049/jimmunol.0903678
109. Hill A, Kelly RJ, Hillmen P. Thrombosis in paroxysmal nocturnal hemoglobinuria. *Blood.* (2013) 121:4985–96; quiz 5105. doi: 10.1182/blood-2012-09-311381
110. Yusuf HR, Hooper WC, Grosse SD, Parker CS, Boulet SL, Ortel TL. Risk of venous thromboembolism occurrence among adults with selected autoimmune diseases: a study among a US cohort of commercial insurance enrollees. *Thromb Res.* (2015) 135:50–7. doi: 10.1016/j.thromres.2014.10.012
111. Audia S, Bach B, Samson M, Lakomy D, Bour JB, Burlet B, et al. Venous thromboembolic events during warm autoimmune hemolytic anemia. *PLoS ONE.* (2018) 13:e0207218. doi: 10.1371/journal.pone.0207218
112. Broome C, Cunningham JM, Mullins M, Jiang X, Bylsma L, Fryzek J, et al. Incidence of thromboembolic events is increased in a retrospective analysis of a large cold agglutinin disease (CAD) cohort. 59th Annual Meeting of the American Society of Hematology, Atlanta, GA. *Blood*. (2017). 130:928. doi: 10.1182/blood.V130.Suppl_1.928.928
113. Bylsma LC, Gulbech Ording A, Rosenthal A, Özturk B, Fryzek JP, Arias JM, et al. Occurrence, thromboembolic risk, and mortality in Danish patients with cold agglutinin disease. *Blood Adv.* (2019) 3:2980–5. doi: 10.1182/bloodadvances.2019000476
114. Maugeri N, Manfredi AA. Tissue factor expressed by neutrophils: another piece in the vascular inflammation puzzle. *Semin Thromb Hemost.* (2015) 41:728–36. doi: 10.1055/s-0035-1564043
115. Ulvestad E. Paradoxical haemolysis in a patient with cold agglutinin disease. *Eur J Haematol.* (1998) 60:93–100. doi: 10.1111/j.1600-0609.1998.tb01004.x
116. Tjønnfjord E, Vengen OA, Berentsen S, Tjønnfjord GE. Prophylactic use of eculizumab during surgery in chronic cold agglutinin disease. *BMJ Case Rep.* (2017) 2017. doi: 10.1136/bcr-2016-219066
117. Peterson OL, Ham TH, Finland M. Cold agglutinins (Autohemagglutinins) in primary atypical pneumonias. *Science.* (1943) 97:167. doi: 10.1126/science.97.2511.167
118. Dacie J. Treatment and prognosis of cold-antibody AIHA. In: Dacie J, editor. *The Haemolytic Anaemias, Vol 3*. London: Churchill Livingstone (1992). p. 502–20.
119. Nydegger UE, Kazatchkine MD, Miescher PA. Immunopathologic and clinical features of hemolytic anemia due to cold agglutinins. *Semin Hematol.* (1991) 28:66–77.
120. Lodi G, Resca D, Reverberi R. Fatal cold agglutinin-induced haemolytic anaemia: a case report. *J Med Case Rep.* (2010) 4:252. doi: 10.1186/1752-1947-4-252
121. Zoppi M, Oppliger R, Althaus U, Nydegger U. Reduction of plasma cold agglutinin titers by means of plasmapheresis to prepare a patient for coronary bypass surgery. *Infusionsther Transfusionsmed.* (1993) 20:19–22. doi: 10.1159/000222800
122. von Baeyer H. Plasmapheresis in immune hematology: review of clinical outcome data with respect to evidence-based medicine and clinical experience. *Ther Apher Dial.* (2003) 7:127–40. doi: 10.1046/j.1526-0968.2003.00004.x
123. Szczepiorkowski ZM, Winters JL, Bandarenko N, Kim HC, Linenberger ML, Marques MB, et al. Guidelines on the use of therapeutic apheresis in clinical practice–evidence-based approach from the Apheresis Applications Committee of the American Society for Apheresis. *J Clin Apher.* (2010) 25:83–177. doi: 10.1002/jca.20240
124. Schwartz J, Padmanabhan A, Aqui N, Balogun RA, Connelly-Smith L, Delaney M, et al. Guidelines on the use of therapeutic apheresis in clinical practice-evidence-based approach from the writing committee of the american society for apheresis: the seventh special issue. *J Clin Apher.* (2016) 31:149–62. doi: 10.1002/jca.21470
125. Rosenfield RE, Jagathambal. Transfusion therapy for autoimmune hemolytic anemia. *Semin Hematol.* (1976) 13:311–21.
126. Barbara DW, Mauermann WJ, Neal JR, Abel MD, Schaff HV, Winters JL. Cold agglutinins in patients undergoing cardiac surgery requiring cardiopulmonary bypass. *J Thorac Cardiovasc Surg.* (2013) 146:668–80. doi: 10.1016/j.jtcvs.2013.03.009
127. Hippe E, Jensen KB, Olesen H, Lind K, Thomsen PE. Chlorambucil treatment of patients with cold agglutinin syndrome. *Blood.* (1970) 35:68–72. doi: 10.1182/blood.V35.1.68.68

128. Quesada JR, Reuben J, Manning JT, Hersh EM, Gutterman JU. Alpha interferon for induction of remission in hairy-cell leukemia. *N Engl J Med.* (1984) 310:15–8. doi: 10.1056/NEJM198401053100104
129. Foon KA, Roth MS, Bunn PA, Jr. Interferon therapy of non-Hodgkin's lymphoma. *Cancer*. (1987) 59(3 Suppl):601–4. doi: 10.1002/1097-0142(19870201)59:3+<601:AID-CNCR2820591304>3.0.CO;2-J
130. O'Connor BM, Clifford JS, Lawrence WD, Logue GL. Alpha-interferon for severe cold agglutinin disease. *Ann Intern Med.* (1989) 111:255–6. doi: 10.7326/0003-4819-111-3-255
131. Hillen HF, Bakker SJ. Failure of interferon-alpha-2b therapy in chronic cold agglutinin disease. *Eur J Haematol.* (1994) 53:242–3. doi: 10.1111/j.1600-0609.1994.tb00197.x
132. Berentsen S, Tjønnfjord GE, Shammas FV, Bergheim J, Hammerstrøm J, Langholm R, et al. No response to cladribine in five patients with chronic cold agglutinin disease. *Eur J Haematol.* (2000) 65:88–90. doi: 10.1034/j.1600-0609.2000.9l201.x
133. Berentsen S, Ulvestad E, Gjertsen BT, Hjorth-Hansen H, Langholm R, Knutsen H, et al. Rituximab for primary chronic cold agglutinin disease: a prospective study of 37 courses of therapy in 27 patients. *Blood.* (2004) 103:2925–8. doi: 10.1182/blood-2003-10-3597
134. Schöllkopf C, Kjeldsen L, Bjerrum OW, Mourits-Andersen HT, Nielsen JL, Christensen BE, et al. Rituximab in chronic cold agglutinin disease: a prospective study of 20 patients. *Leuk Lymphoma.* (2006) 47:253–60. doi: 10.1080/10428190500286481
135. Berentsen S. Rituximab for the treatment of autoimmune cytopenias. *Haematologica.* (2007) 92:1589–96. doi: 10.3324/haematol.11312
136. Berentsen S, Randen U, Vågan AM, Hjorth-Hansen H, Vik A, Dalgaard J, et al. High response rate and durable remissions following fludarabine and rituximab combination therapy for chronic cold agglutinin disease. *Blood.* (2010) 116:3180–4. doi: 10.1182/blood-2010-06-288647
137. Leleu X, Tamburini J, Roccaro A, Morel P, Soumerai J, Levy V, et al. Balancing risk versus benefit in the treatment of Waldenstrom's Macroglobulinemia patients with nucleoside analogue-based therapy. *Clin Lymphoma Myeloma.* (2009) 9:71–3. doi: 10.3816/CLM.2009.n.018
138. Berentsen S, Randen U, Oksman M, Birgens H, Tvedt THA, Dalgaard J, et al. Bendamustine plus rituximab for chronic cold agglutinin disease: results of a Nordic prospective multicenter trial. *Blood.* (2017) 130:537–41. doi: 10.1182/blood-2017-04-778175
139. Rossi G, Gramegna D, Paoloni F, Fattizzo B, Binda F, D'Adda M, et al. Short course of bortezomib in anemic patients with relapsed cold agglutinin disease: a phase 2 prospective GIMEMA study. *Blood.* (2018) 132:547–50. doi: 10.1182/blood-2018-03-835413
140. Treon SP, Tripsas CK, Meid K, Warren D, Varma G, Green R, et al. Ibrutinib in previously treated Waldenstrom's macroglobulinemia. *N Engl J Med.* (2015) 372:1430–40. doi: 10.1056/NEJMoa1501548
141. Abeykoon JP, Paludo J, King RL, Ansell SM, Gertz MA, LaPlant BR, et al. MYD88 mutation status does not impact overall survival in Waldenstrom macroglobulinemia. *Am J Hematol.* (2018) 93:187–94. doi: 10.1002/ajh.24955
142. Röth A, Hüttmann A, Rother RP, Dührsen U, Philipp T. Long-term efficacy of the complement inhibitor eculizumab in cold agglutinin disease. *Blood.* (2009) 113:3885–6. doi: 10.1182/blood-2009-01-196329
143. Makishima K, Obara N, Ishitsuka K, Sukegawa S, Suma S, Kiyoki Y, et al. High efficacy of eculizumab treatment for fulminant hemolytic anemia in primary cold agglutinin disease. *Ann Hematol.* (2018) 98:1031–2. doi: 10.1007/s00277-018-3521-4
144. Wouters D, Stephan F, Strengers P, de Haas M, Brouwer C, Hagenbeek A, et al. C1-esterase inhibitor concentrate rescues erythrocytes from complement-mediated destruction in autoimmune hemolytic anemia. *Blood.* (2013) 121:1242–4. doi: 10.1182/blood-2012-11-467209
145. Tesfaye A, Broome C. A novel approach for treatment of cold agglutinin syndrome-related severe hemolysis. *J Hematol.* (2016) 5:30–3. doi: 10.14740/jh242w
146. Jäger U, D'Sa S, Schorgenhofer C, Bartko J, Derhaschnig U, Sillaber C, et al. Inhibition of complement C1s improves severe hemolytic anemia in cold agglutinin disease: a first-in-human trial. *Blood.* (2019) 133:893–901. doi: 10.1182/blood-2018-06-856930
147. Gertz MA, Qiu H, Kendall L, Saltarelli M, Yednock T, Sankaranarayanan S. ANX005, an inhibitory antibody against c1q, blocks complement activation triggered by cold agglutinins in human disease. 58th Meeting of the American Society of Hematology, San Diego, CA, USA. *Blood*. (2016) 128:1265. doi: 10.1182/blood.V128.22.1265.1265
148. Cunnion KM, Feagin LM, Chicella MF, Kaszowski CL, Hair PS, Price J, et al. Ceftriaxone-induced immune hemolytic anemia: in vitro reversal with peptide inhibitor of complement C1 (PIC1). *Case Rep Hematol.* (2019) 2019:4105653. doi: 10.1155/2019/4105653
149. Risitano AM, Ricklin D, Huang Y, Reis ES, Chen H, Ricci P, et al. Peptide inhibitors of C3 activation as a novel strategy of complement inhibition for the treatment of paroxysmal nocturnal hemoglobinuria. *Blood.* (2014) 123:2094–101. doi: 10.1182/blood-2013-11-536573
150. Grossi FV, Bedwell P, Deschatelets P, Edis L, Francois CG, Johnson PJ, et al. APL-2, a complement C3 inhibitor for the potential treatment of paroxysmal nocturnal hemoglobinuria (PNH): phase I data from two completed studies in healthy volunteers. 58th Annual Meeting of the American Society of Hematology, San Diego, CA. *Blood*. (2016). 128:1251. doi: 10.1182/blood.V128.22.1251.1251
151. Grossi F, Shum MK, Gertz MA, Roman E, Deschatelets P, Hamdani M, et al. Inhibition of C3 with APL-2 results in normalisation of markers of intravascular and extravascular hemolysis in patients with autoimmune hemolytic anemia (AIHA). 60th Annual Meeting of the American Society of Hematology, San Diego, CA. *Blood*. (2018). 132(Suppl 1):3623. doi: 10.1182/blood-2018-99-119468
152. Wong RSM, Pullon RWH, Deschatelets P, Francois CG, Hamdani M, Issaragrisil S, et al. Inhibition of C3 with APL-2 results in normalisation of markers of intravascular and extravascular hemolysis in patients with paroxysmal nocturnal hemoglobinuria (PNH). 60th Annual Meeting of the American Society of Hematology, San Diego, CA. *Blood*. (2018). 132(Suppl 1):2314. doi: 10.1182/blood-2018-99-110827
153. Hill QA, Stamps R, Massey E, Grainger JD, Provan D, Hill A, et al. Guidelines on the management of drug-induced immune and secondary autoimmune, haemolytic anaemia. *Br J Haematol.* (2017) 177:208–20. doi: 10.1111/bjh.14654
154. Nordtveit S, Lerum TV, Ghanima W, Berentsen S. En mann i 50-årene med feber og anemi [A man in his 50s with fever and anemia]. Article in Norwegian. *Tidsskr Nor Laegeforen.* (2018) 138:148–52. doi: 10.4045/tidsskr.17.0460
155. Chu CS, Braun SR, Yarbro JW, Hayden MR. Corticosteroid treatment of hemolytic anemia associated with Mycoplasma pneumoniae pneumonia. *South Med J.* (1990) 83:1106–8. doi: 10.1097/00007611-199009000-00032
156. Tsuruta R, Kawamura Y, Inoue T, Kasaoka S, Sadamitsu D, Maekawa T. Corticosteroid therapy for hemolytic anemia and respiratory failure due to Mycoplasma pneumoniae pneumonia. *Intern Med.* (2002) 41:229–32. doi: 10.2169/internalmedicine.41.229
157. Walia H, Jain R, Bansal RK, Gupta GN. Cold agglutinin disease with erythrophagocytosis by neutrophils occurring during recovery phase of chickenpox. *J Lab Physicians.* (2013) 5:146–7. doi: 10.4103/0974-2727.119873

Conflict of Interest: Outside this work, the author has received research funding from Mundipharma, lecture honoraria from Apellis, Bioverativ (a Sanofi company), Janssen-Cilag, and True North Therapeutics, and advisory board and consultancy honoraria from Apellis, Bioverativ (a Sanofi company), and Momenta Pharmaceuticals.

The reviewer GT declared a past co-authorship with the author to the handling editor

frontiers in Immunology

REVIEW
published: 03 June 2020
doi: 10.3389/fimmu.2020.00946

The Changing Landscape of Autoimmune Hemolytic Anemia

Wilma Barcellini[1]* *and Bruno Fattizzo*[1,2]

[1] UO Ematologia, Fondazione IRCCS Ca' Granda Ospedale Maggiore Policlinico, Milan, Italy, [2] Università degli Studi di Milano, Milan, Italy

Autoimmune hemolytic anemia (AIHA) is a greatly heterogeneous disease due to autoantibodies directed against erythrocytes, with or without complement activation. The clinical picture ranges from mild/compensated to life-threatening anemia, depending on the antibody's thermal amplitude, isotype and ability to fix complement, as well as on bone marrow compensation. Since few years ago, steroids, immunesuppressants and splenectomy have been the mainstay of treatment. More recently, several target therapies are increasingly used in the clinical practice or are under development in clinical trials. This has led to the accumulation of refractory/relapsed cases that often represent a clinical challenge. Moreover, the availability of several drugs acting on the different pathophysiologic mechanisms of the disease pinpoints the need to harness therapy. In particular, it is advisable to define the best choice, sequence and/or combination of drugs during the different phases of the disease. In particular relapsed/refractory cases may resemble pre-myelodysplastic or bone marrow failure syndromes, suggesting a careful use of immunosuppressants, and vice versa advising bone marrow immunomodulating/stimulating agents. A peculiar setting is AIHA after autologous and allogeneic hematopoietic stem cell transplantation, which is increasingly reported. These cases are generally severe and refractory to standard therapy, and have high mortality. AIHAs may be primary/idiopathic or secondary to infections, autoimmune diseases, malignancies, particularly lymphoproliferative disorders, and drugs, further complicating their clinical picture and management. Regarding new drugs, the false positivity of the Coombs test (direct antiglobulin test, DAT) following daratumumab adds to the list of difficult diagnosis, together with the passenger lymphocyte syndrome after solid organ transplants. Diagnosis of DAT-negative AIHAs and evaluation of disease-related risk factors for relapse and mortality, notwithstanding improvement in diagnostic approach, are still an unmet need. Finally, AIHA is increasingly described following therapy of solid cancers with inhibitors of immune checkpoint molecules. On the whole, the double-edged sword of new pathogenetic insights and therapies has changed the landscape of AIHA, both providing enthusiastic knowledge and complicating the clinical management of this disease.

Keywords: warm autoimmune hemolytic anemia, cold agglutinin disease, bone marrow transplant, checkpoint inhibitors, complement inhibitors, target therapy

OPEN ACCESS

Edited by:
Emira Ayroldi,
University of Perugia, Italy

Reviewed by:
Ursula Grohmann,
University of Perugia, Italy
Anne Cooke,
University of Cambridge, United Kingdom

***Correspondence:**
Wilma Barcellini
wilma.barcellini@policlinico.mi.it

Specialty section:
This article was submitted to Inflammation, a section of the journal Frontiers in Immunology

Received: *13 February 2020*
Accepted: *22 April 2020*
Published: *03 June 2020*

Citation:
Barcellini W and Fattizzo B (2020) The Changing Landscape of Autoimmune Hemolytic Anemia. Front. Immunol. 11:946. doi: 10.3389/fimmu.2020.00946

INTRODUCTION

Autoimmune hemolytic anemia (AIHA) has always been considered the simplest and most scholastic example of antibody-mediated autoimmune disease. As a matter of fact, autoantibodies (Ab) directed against erythrocytes, with or without complement (C) activation, are the main pathogenic mechanism of the disease (1). Clinically, it has long been considered a trouble-free disease, easy to treat, and with low clinical impact, compared with malignant hematologic conditions. This approach is quite similar to that of immune thrombocytopenia, which has been defined the "hematology's Cosette from Les Misérables." More recently, AIHA has been identified as a greatly heterogeneous disease, due to several immunological mechanisms involved beyond antibodies, complement and antibody-dependent cell-mediated cytotoxicity (ADCC). Accumulating evidence demonstrates reduced CD4+ T-regs, imbalance of T-helper 1/2 cytokines, increased activity of cytotoxic CD8+ T lymphocytes, natural killer cells, and activated macrophages. More importantly, attention has grown on the pivotal role of bone marrow compensation, and on bone marrow characteristics that may reveal dyserythropoiesis, fibrosis, and clonal lymphoproliferation (1–4). Previously, steroids, immunesuppressants, and splenectomy were the mainstay of AIHA treatment (5–8). More recently, several new targeted therapies are increasingly used in the clinical practice or under development in clinical trials (7, 9). Along with new therapeutic options for patients, this growing armamentarium has complicated the clinical management of AIHA and increased the number of relapsed/refractory cases. Therefore, harnessing treatment and defining a risk-adapted therapy is an emerging unmet need. A peculiar setting is AIHA after autologous and allogeneic hematopoietic stem cell transplantation (HSCT), as well as cases described during therapy with immune checkpoint inhibitors for solid cancers (10). Finally, AIHAs may be associated with several conditions (lymphoproliferative, autoimmune and infectious diseases, immunodeficiencies, solid tumors, transplants, and drugs) where the several immunologic mechanisms are unpredictably involved (7, 11). The recent availability of next generation sequencing has improved the diagnosis of the several associated conditions, but at the same time has extended the proportion of "secondary" vs. "primary" AIHAs (4, 12). All these new insights in the pathogenesis of the disease and treatment opportunities have undoubtedly changed the landscape of AIHA.

In this review we will describe new diagnostic tools, clinical characteristics and therapeutic options of AIHA, focusing on relapsed/refractory cases, secondary forms, and AIHAs associated with HSCT or therapy with immune checkpoint inhibitors (CPIs). Moreover, we will approach the identification of risk factors for the development, clinical severity, response to therapy, and outcome of AIHA in order to start the basis for a risk-adapted therapy.

CLINICAL CHARACTERISTICS AND CLASSIFICATION OF AIHA

The gold standard for the diagnosis of AIHA is the Coombs test or direct antiglobulin test (DAT) that enables the classification of the disease according to the isotype and thermal characteristics of the autoantibody. Warm AIHA (wAIHA), the most common type (60–70% of cases) is typically DAT positive for anti-IgG, or IgG plus C, while cold forms (cold agglutinin disease, CAD, 20–25%), are due to IgM, and the DAT is positive for C3d. Among cold AIHAs it is worth considering paroxysmal cold hemoglobinuria (PCH), usually observed in children and; this very rare type of AIHA (1–5% of cases) is caused by the Donath-Landsteiner autoantibody, a bithermic hemolysin able to fix complement at cold temperatures and to determine RBCs lysis at 37°C. Mixed forms show both characteristics of wAIHA and CAD, with a DAT positive for both IgG and C and high titer cold agglutinins. Finally, there is a heterogeneous group of atypical AIHAs that include DAT negative, IgA driven, and warm IgM types (7, 8, 13). All these forms have a variable degree of anemia, hemolysis and bone marrow compensation, as shown in **Table 1** for Hb and LDH levels, and reticulocyte counts.

Risk Factors for Relapse and Mortality

Given the great clinical heterogeneity of the various AIHA forms, an effort has been made to identify predictors of outcome, including complications, response to therapy and death. The severity of anemia at onset has been identified as the strongest predictor of relapse, with hazard ratios of 1.61, 1.74, and 1.98, for Hb levels of 8.1–10, 6.1–8, <6 g/dL, respectively (5, 8). Complement involvement and thermal characteristics of the autoantibody were also important, with warm IgG+C, mixed, CAD, and atypical forms more frequently needing second or further therapy lines. Moreover, the concomitant presence of immune thrombocytopenia (Evans syndrome) is associated with a higher risk of relapse and refractoriness to treatment. Overall, AIHAs other than warm forms, plus Evans syndrome and Hb<8 g/dL at onset had a 4-fold increased risk of multiple relapses (8). Moreover, bone marrow features impact on disease severity since the presence of reticular fibrosis, dyserithropoiesis, and hypercellularity correlated with shorter relapse-free survival and lower response rate to immunosuppressive therapies (3). Regarding fatal outcome, Hb <6 g/dL at onset, Evans' syndrome, multi-treatment, acute renal failure, and infections have been associated with 5-8 fold risk of increased mortality (8). A case series of 13 very severe relapsed/refractory primary AIHA reported a mortality of 57%, despite intensive treatment, including transfusions, steroid boli, intravenous immunoglobulins, rituximab, erythropoietin, and plasma-exchange (13). More recently, mortality was 30% in a series of 44 AIHA admitted to intensive care unit for severe anemia (14). It is worth remembering that about 15–20% of AIHAs display thrombotic events, including severe episodes (pulmonary embolism, stroke, cardiac infarction), which are generally proportional to active hemolysis (5, 7). Risk factors for these severe, although not fatal, complications are Hb

TABLE 1 | Clinical and laboratory characteristics of patients at onset divided according to AIHA serological type.

	wAIHA ($n = 225$) IgG ($n = 158$); IgG +C ($n = 67$)	CAD ($n = 107$)	Mixed AIHA ($n = 24$)	Atypical AIHA ($n = 22$)
Hematologic features of primary AIHA patients				
Median Age at diagnosis (years, range)	67 (5–94); 65 (21–92)	70 (28–94)	61 (20-86)	45 (25-78)
Hb (g/dL), median (range)	7.3 (2.1–14.1); 6.5 (2.0–11.5)	8.2 (4.0–13.5)	6.4 (4.3–10.7)	6.6 (3.0–10.9)
LDH (ULN), median (range)	1.7 (0.6–26.7); 1.8 (0.8–7.2)	1.4 (0.3–12.2)	1.7 (0.6–9.8)	2 (0.7–18.1)
Ret ($\times 10^9$/L), median (range)	180 (22–644); 143 (53–641)	123 (13–644)	181 (45–576)	195 (29–780)
Inadequate reticulocytosis, *n* of pts (%)	86 (54); 35 (52)	69 (64)	15 (62)	14 (64)
Hazard risks for AIHA relapse				
Hb at onset	<6 g/dl	HR 1.98	95% CI 1.2–3.2	
AIHA type	Non wAIHA	HR 1.21	95% CI 0.9–1.5	
Evans Syndrome	Co-presence of ITP	HR 1.84	95% CI 1.2–2.7	
Hazard risks for AIHA related death				
Evans Syndrome	Co-presence of ITP	HR 8	95% CI 2.5–26	
AIHA related complications	Acute renal failure	HR 6.3	95% CI 1.4–29	
Multi-treatment (>4 lines)	Infections	HR 4.8	95% CI 1.5–15	

wAIHA, warm autoimmune hemolytic anemia; CAD, cold agglutinin disease; IgG, DAT positive for IgG; IgG + C, DAT positive IgG + C; LDH (ULN), LDH is expressed as folds of upper limit of normal.

levels <6 g/dL at onset, increased LDH levels, and previous splenectomy (8).

Secondary AIHAs

Several conditions represent a risk factor for the development of AIHA, including lymphoproliferative and autoimmune diseases, immunodeficiencies, infections, and solid tumors (**Table 2**). Concerning lymphoproliferative disorders, CLL patients show the highest risk with up to 5–10% developing AIHA, with an onset that may precede the diagnosis of lymphoproliferative disease (11, 15). The presence of unmutated IGHV status, sterotyped IGHV frames, and unfavorable cytogenetics (chromosome 17p and/or 11q deletions) represent a risk factor for the development of AIHA (4, 15–17). Other recently identified risk factors were several down-regulated miRNAs, some of them known to be involved in autoimmune phenomena (4). Of note, a positive DAT without hemolysis is frequent in CLL. AIHA prevalence in NHL is 2–3%, with higher frequencies in some subtypes (13–19% in angioimmunoblastic T-cell lymphoma and 50% in marginal zone lymphoma) (7, 11). A particular setting is CAD, which is associated with an indolent clonal lymphoid infiltrate distinct from other NHL (2, 6). In this disease recurrent mutations of KMT2D and CARD11 have been identified in 69 and 31% of cases, respectively (18). Similar mutations have also been reported in Kabuki syndrome, a congenital disorder characterized by malformations, immune-deficiency, and development of autoimmune diseases (4, 18).

Regarding AIHA in the context of immune dysregulation, patients with systemic lupus erythematosus develop AIHA in 14% of pediatric cases and 3% of adults (7, 11). A close association has also been reported with thyroid autoimmune disorders, such as Hashimoto thyroiditis and Graves' disease. Several case reports exist for AIHA association with systemic sclerosis, Sjögren syndrome (SS), autoimmune liver disorders, and inflammatory bowel diseases (7, 11). Moreover, various immunodeficiencies have been identified as predisposing conditions for AIHA, including common variable immunedeficiency (19), IgA deficiency, and autoimmune lymphoproliferative syndromes (ALPS) (20). Interestingly, mutations in genes implicated in primary immunodeficiencies (*TNFRSF6, CTLA4, STAT3, PIK3CD, CBL, ADAR1, LRBA, RAG1, and KRAS*) have been detected in about half of pediatric patients with AIHA and ITP (Evans Syndrome, ES); mutated patients showed more severe disease with higher treatment requirement and fatal outcome (12). These findings underline the close link between autoimmunity and immunodeficiency, i.e., a shared condition of dysregulated immune system.

Genetic Background and Exogenous Triggers for AIHA Development

Although not specifically involved in the changing landscape of AIHA, it is worth considering genetic factors and historically recognized exogenous triggers (4). Several old and recent studies demonstrated a strong association of AIHA with HLA-B locus, particularly HLA-B8 and BW6 (21), or a reduced frequency of the disease in subjects harboring the HLA-DQ6 locus (22) (**Table 2**). As regards humoral immune response, various variable regions of the immunoglobulin heavy and light chains (IGHV and IGKV) have been associated with AIHA, particularly IGHV4-34, IGHV3, and IGKV3-20 genes, responsible for I antigen binding, and mostly represented in CAD (6). Concerning cellular immunity, autoreactive clonal T- CD8+cells have been reported in about 50% of AIHA cases; moreover, polymorphism of the cytotoxic T-lymphocyte antigen-4 (CTLA-4) gene and of lymphotoxin-α

TABLE 2 | Secondary conditions associated with autoimmune hemolytic anemia (AIHA).

	Frequency	Results
Lymphoproliferative disorders		
Chronic lymphoid leukemia and NHL	5–20%	Autoimmune cytopenias may frequently complicate chronic lymphoproliferative disorders and usually correlate with advanced disease and high biologic risk
KMT2D and CARD11	69 and 31% of cAIHA tested	Autoreactive B-cells display somatic mutations favoring proliferation
Congenital syndromes and immunodeficiencies		
Kabuki syndrome and Hemoglobinopathies	4–6%	AIHA and ITP are the most frequent autoimmune complications of Kabuki Syndrome; DAT positivity is frequent, but clinically overt AIHA is rarer in thalassemia (particularly beta intermedia, alloimmunized, and transfused pts)
ALPS; CVID; IgA deficiency	2–70%	AIHA is the most frequent autoimmune complication together with ITP and ES
Genes involved in PIDs TNFRSF6, CTLA4, STAT3, PIK3CD, CBL, ADAR1, LRBA, RAG1, and KRAS	40% of pediatric ES	Majority of pediatric ES display somatic mutations found in immunodeficiencies
Autoimmune diseases		
SLE, Systemic sclerosis; autoimmune thyroiditis; Sjogren Syndrome; IBDs; Autoimmune hepatitis/Primary biliary cirrhosis	1.4–14%	AIHA frequency is higher in pediatric than in adult patients with SLE. AIHA may be rarely associated to systemic sclerosis or Sjogren syndrome, Hashimoto thyroiditis and Graves' disease, ulcerative colitis, and autoimmune hepatitis.
Genetic findings		
HLA I and II	Case series	HLA-B8 and BW6 are strongly associated to wAIHA.
IGHV and IGKV region	>60% cAIHA	Specific IGVH and IGKV regions are related to AIHA development
TCRG and TCRB	50%	Pathogenic T-cells are clonally restricted in AIHA
CTLA-4 exon 1	73%	CTLA-4 signaling is defective in AIHA, particularly in CLL cases
Cytokine polymorphisms	41%	AIHA shows higher frequency of LT-α (+252) AG phenotype
Infections		
Parvovirus B19; HCV; HAV; HBV; HIV Mycoplasma spp.; Tubercolosis; Babesiosis; Brucellosis; Syphilis; EBV; Respiratory Syncytial Virus	0.02–20%	ParvoB19 infection and HCV and its treatment correlate with AIHA development; case reports of association with AIHA are available for the other infectious agents.
Drugs		
Antibiotics (penicillins, cephalosporins, etc.), cytotoxic drugs (oxaliplatin, etc.), antidiabetics (metformin), anti-inflammatory drugs (diclofenac, etc.), neurologic drugs (α-methyldopa, L-dopa, chlorpromazine, etc.), cardiologic drugs (procainamide, etc.)	Case reports and reviews	Various mechanisms are demonstrated: hapten and drug absorption mechanisms; Immune/ternary complex mechanisms; autoantibody mechanism; non-immunologic protein formation; unknown mechanisms.
CLL therapy: fludarabine and Tyrosin kinase inhibitors	6–21%	Fludarabine induced AIHA may be avoided by rituximab association. Ibrutinib was associated to low risk of AIHA development in registrative trials in CLL
Vaccines		
Vaccines	0.8/100.000 person-years	AIHA was the rarest autoimmune complication in a population study
Solid cancers		
Thymoma;Ovarian/Prostate	1.29–30% autoimmune phenomena	Thymoma, prostate and ovarian carcinomas have the highest association with autoimmunity

AIHA, autoimmune hemolytic anemia; wAIHA, warm; cAIHA, cold; ES, Evans syndrome; ITP, immune thrombocytopenia; DAT, direct antiglobulin test; CLL, chronic lymphocytic leukemia; ALPS, autoimmune lymphoproliferative syndrome; CVID, common variable immunodeficiency; SLE, Systemic lupus erythematosus; IBDs, inflammatory bowel syndromes.

(LT-α) may represent a risk factor for primary or secondary AIHA development (4).

Various infections have been associated with an increased incidence of AIHA, particularly Parvovirus B19 (associated with DAT positive hemolysis in up to 20% of cases and hepatotropic virus, mostly HCV and possibly related to interferon therapy (11). Moreover, cold agglutinin AIHA occurs in up to 3% of patients with infectious mononucleosis and Mycoplasma pneumoniae infection (7, 11). Finally, paroxysmal cold hemoglobinuria is almost invariably preceded by an infection, including syphilis and virus, particularly in children (7, 11). In addition there is a long list of drugs that have been proven or highly suspected to induce AIHA, including historical ones (α-methyldopa, procainamide, penicillins, cephalosporins, diclofenac, ibuprofen, thiazides, quinine, quinidine, metformin) and more recent molecules (cladribine, fludarabine, lenalidomide, oxaliplatin, teniposide, pentostatin) (7, 11). Concerning new small molecules (ibrutinib, venetoclax, and idelalisib) few case reports of treatment-emergent AIHAs have been published (4).

COMPREHENSIVE DIAGNOSTIC APPROACH AND NEW DIAGNOSTIC TOOLS

Given the several associated conditions, an accurate diagnostic approach to AIHA is fundamental for a

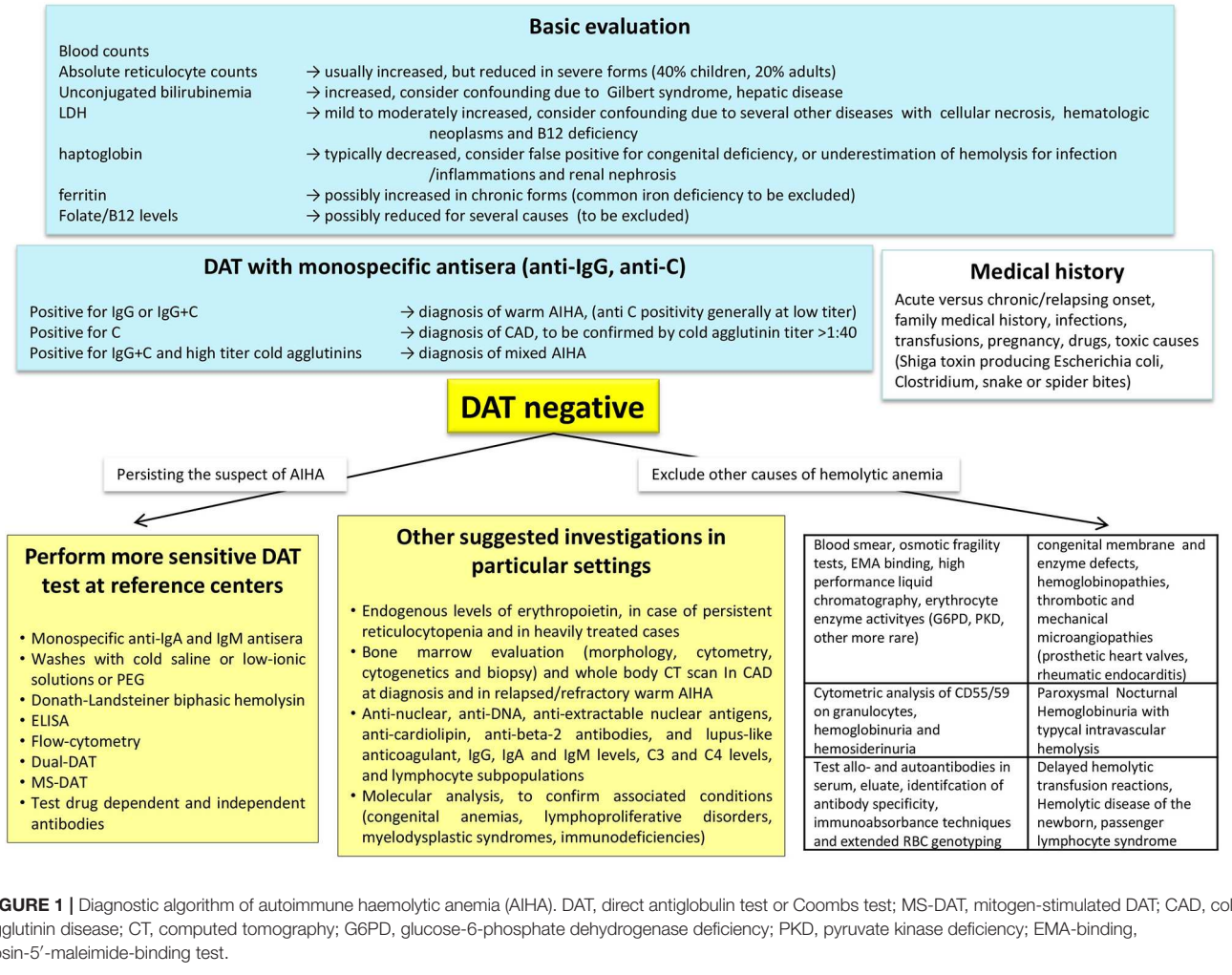

FIGURE 1 | Diagnostic algorithm of autoimmune haemolytic anemia (AIHA). DAT, direct antiglobulin test or Coombs test; MS-DAT, mitogen-stimulated DAT; CAD, cold agglutinin disease; CT, computed tomography; G6PD, glucose-6-phosphate dehydrogenase deficiency; PKD, pyruvate kinase deficiency; EMA-binding, eosin-5′-maleimide-binding test.

comprehensive risk assessment and a proper therapy (**Figure 1**). Medical history and baseline evaluation is still fundamental to assess drug assumption, infections, signs of acute or chronic hemolysis, and bone marrow compensation (reticulocytes).

The Standard DAT and More Sensitive Techniques

As mentioned earlier, the DAT with monospecific antisera (anti-IgG, anti- IgA, anti-IgM, anti C) is the cornerstone of diagnosis, and allows a proper distinction of the various AIHA forms, that have different responses to therapy and prognosis (23). A diagnostic challenge that may take advantage of new diagnostic tools is represented by DAT-negative AIHA, usually 5–10% of all forms. In these cases, excluding other common causes of hemolysis and pursuing the clinical suspicion of AIHA, it is recommended to ask for second-level tests in a reference center. The DAT negativity due to low-affinity antibodies may be overcome by low ionic strength solutions (LISS) or cold washings. The small amounts of RBC-bound antibodies (below the threshold of the test) may take advantage of more sensitive techniques, such as microcolumn and solid-phase antiglobulin tests. In fact, DAT tube effectively diagnoses AIHA when at least 500 molecules of autoantibodies are bound to RBCs, whereas microcolumn and solid phase require ∼200–300 molecules per single RBC to yield a positive result. Consistently, DAT tube is the most specific but least sensitive test, whereas microcolumn and solid phase methods show reduced specificity but increased sensitivity (7, 24, 25). Smaller amounts of autoantibodies can be detected by new, even more sensitive techniques, such as flow cytometry (able to detect about 30–40 antibody molecules per RBC), the enzyme-linked and radiolabeled tests, or the mitogen-stimulated-DAT (able to amplify the autoimmune reaction in culture) (23, 24). Of particular importance is the identification of atypical AIHAs due to warm IgM that are potent activators of complement and often detach from the RBC during washing procedures, causing detrimental delay in diagnosis and therapy. In these cases the DDAT (Dual Direct Antiglobulin Test) may allow the diagnosis of these rare forms, usually severe and potentially lethal (26). In addition, as complement activation is

recognized as negative prognostic factor, evaluation of baseline values of C3 and C4 fractions, would help completing the diagnostic workup. Notwithstanding extensive evaluation, a fraction of AIHA remains DAT-negative: in these cases the diagnosis is made after the exclusion of the many hemolytic disorders (congenital hemolytic anemias, paroxysmal nocturnal hemoglobinuria, thrombotic microangiopathies, mechanical and toxic noxae) and on the basis of an ex-adiuvantibus therapy with steroids.

Causes of Falsely Positive DAT

The DAT may be positive due to the presence of alloantibodies in recently transfused patients, in delayed hemolytic transfusion reactions, and in the hemolytic disease of the newborn (23). The coexistence of auto- and alloantibodies has been reported in about 30% of AIHA patients, and their presence is often masked by autoantibodies, possibly causing severe hemolytic reactions in case of RBC transfusion. In complex cases the distinction between allo- and autoantibody is advisable by immunoabsorbance techniques and by extended RBC genotyping (7, 24). It is worth reminding that daratumumab, the anti-CD38 antibody for the treatment of multiple myeloma, may give false DAT positivity. CD38 is also expressed on red-cell membranes, resulting in panreactive agglutination in the test used for antibody screening and cross-matching. Several methods have been proposed to overcome this interference, including pretreatment of red cells with dithiothreitol, use of antiidiotypic antibodies against daratumumab, supplementation of soluble CD38 to bind daratumumab in patient serum, use of red cells from newborns as test cells, and use of F(ab′)2 fragments of daratumumab by digestion with pepsin (27).

Bone Marrow Evaluation and Exclusion of Secondary AIHA Forms

Among "new" diagnostic approaches to AIHA there is the increasingly recommended (and performed) bone marrow evaluation (morphology, cytometry, cytogenetics and biopsy). Bone marrow evaluation may in fact give important information on adequate erythroid compensation, underlying lymphoproliferative disorder, and evidence of

TABLE 3 | Target therapies in autoimmune hemolytic anemia (AIHA).

Drug	Mechanism	Setting	Route of administration	Efficacy
B-cell directed monoclonal antibodies				
Rituximab	Anti-CD20	wAIHA/CAD	IV	70–80%/50–60%
Rituximab	Anti-CD20	wAIHA/CAD	SC	100%
R-Fludarabine	Anti-CD20 + purine analog	CAD	IV	76%
R-CTX-Dex	Anti-CD20 + alkylator	WAIHA	IV	97%
R-Bendamustine	Anti -CD20 + alkylator	CAD	IV	71%
Ofatumumab	Anti-CD20	Secondary AIHA	IV	Case report
Alemtuzumab	Anti-CD52	Secondary AIHA	SC	Case reports
Daratumumab	Anti-CD38	Secondary AIHA	IV	Case reports
B-cell receptor inhibitors				
Ibrutinib	BTKi	Secondary AIHA	Oral	Case reports
Parsaclisib	PI3Ki	Primary wAIHA/CAD	Oral	Not available
Venetoclax	Bcl2	Secondary AIHA	Oral	Case reports
Proteasome inhibitor				
Bortezomib	Proteasome inhibitor	CAD/Secondary AIHA	IV	Case reports
Bortezomib	Proteasome inhibitor	CAD	IV	31.6%
Complement inhibitors				
Eculizumab	C5i	CAD/Mixed AIHA	IV	Case reports
Sutimlimab	Anti-C1s MoAb	CAD	IV	50%
APL-2	C3/C3bi	CAD/wAIHA	SC	50/40%
T-cell directed therapies				
Soluble IL-2	T-reg stimulation	wAIHA	SC	Not available
Sirolimus	mTORi	Evans'/Secondary AIHA	Oral	80%
Mycophenolate Mofetil	Purine synthesis inhibitor	wAIHA/CAD/Secondary AIHA/Evans'	Oral	81–100%
IgG mediated phagocytosis inhibitors				
Fostamatinib	Syki	wAIHA	Oral	44%
SYNT001	FcRn MoAb	wAIHA	IV	Not available
M281	FcRn MoAb	wAIHA	IV	Not available

CTX, cyclophosphamide; BTKi, Bruton tyrosine kinase inhibitor; Bcl2, B-cell lymphoma 2; δPI3Ki, phosphatidylinositol-4,5-bisphosphate 3-kinase delta type inhibitor; MoAb, monoclonal antibody; mTORi, mammalian Target Of Rapamycin inhibitor; Syki, Spleen tyrosine kinase; FcRn, neonatal crystallizable fragment receptor.

an early/subclinical or therapy-related myelodysplasia or bone marrow failure. These features may help in harnessing therapy, avoiding further detrimental immunesuppression, or selecting immunosupprors among the new targeted therapies, based on the type of bone marrow lymphocyte infiltrate (T or B). Moreover, the determination of endogenous EPO levels may indicate this treatment, which has recently shown effective particularly in relapsed/refractory and heavily treated subjects (7, 28). To properly identify secondary forms imaging and serologic investigation is fundamental (**Figure 1**). It is advised to test for anti-phospholipid antibodies (cardiolipin, beta-2, and lupus-like anticoagulant), given the known thrombotic diathesis of acute/severe AIHAs, and thus advising thromboprophylaxis. Finally, molecular analysis and next generation sequencing would help confirming associated conditions (primary immunodeficiencies, lymphoproliferative disorders, myelodysplastic syndromes, other coexisting congenital anemias) again harnessing therapy.

NEW TREATMENTS FOR AIHA

The availability of several new treatments has undoubtedly boosted the therapeutic possibilities for patients, but at the same time has increased the number of heavily treated, relapsed/refractory cases. The immune-mediated pathogenic mechanisms in AIHA are different and may differently act at various degrees during the various phases of the disease. Therefore, the challenge for the future will be the selection and timing of administration of the several drugs available or under development. Firstly, distinction between wAIHA and CAD is pivotal, as therapy in quite different: the former usually respond to steroids, whereas the latter requires high and unacceptable doses. Splenectomy, although progressively abandoned and moved to third or further lines, is still a valid option for wAIHA; on the contrary it is ineffective and contraindicated in CAD, where RBC destruction occurs mainly in the liver and lymphoid organs. Likewise, it is poorly effective and discouraged in AIHA

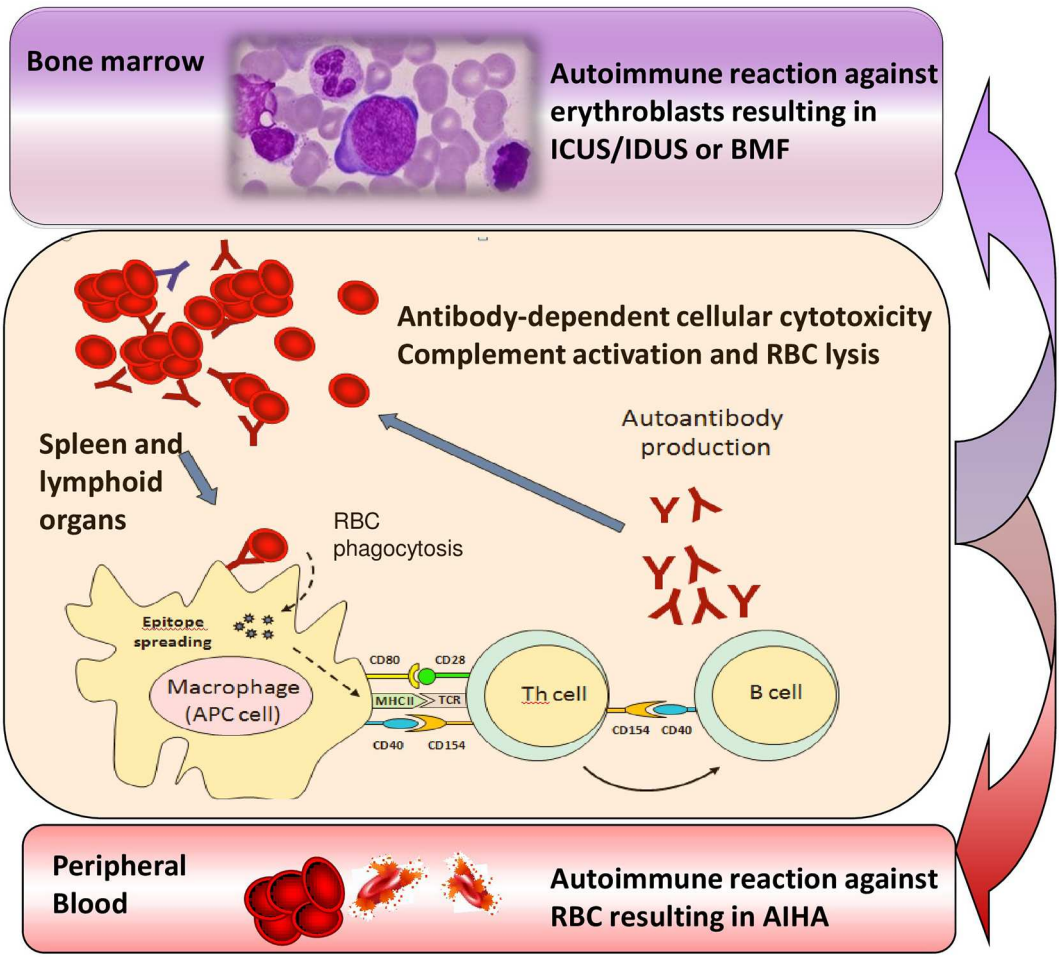

FIGURE 2 | Transition from chronic/relapsing autoimmune hemolytic anemia (AIHA) to idiopathic cytopenias/dysplasias of uncertain significance (ICUS/IDUS) and bone marrow failure (BMF). Various immune effectors such as macrophages, antigen presenting cells (APC), T helper cells and B lymphocytes are involved into the immune attack, which is firstly directed against peripheral erythrocytes, but may persist and involve bone marrow precursors, possibly leading to ICUS/IDUS or BMF syndromes over time.

secondary to immunodeficiencies, autoimmune diseases, and lymphoproliferative disorders. Several target therapies are now in the clinical use or under development in AIHA (**Table 3**) (7, 9). Rituximab is becoming the preferred second-line for wAIHA and is recommended as first line in CAD. In the former, low-doses may be equally effective as standard ones, whereas in CAD the standard schedule is more effective. The drug is successfully administered in primary and secondary cases, alone or associated with chemotherapy (bendamustine, fludarabine, or other) in AIHAs secondary to lymphoproliferative diseases (6, 29, 30). The clinical challenges are wAIHAs relapsed after rituximab and unfit/refusing splenectomy, and CAD relapsed after rituximab monotherapy and unfit for rituximab-combined chemotherapy. In this setting, treatment selection would be ideally driven by disease-related risk factors, and/or associated conditions, as well as patient general comorbidities. Among monoclonal antibodies, ofatumumab (anti-CD20), alemtuzumab (anti-CD52), and daratumumab (anti-CD38) have shown promising results in case reports, mainly secondary AIHAs. Likewise, the orally administered B-cell receptor inhibitors ibrutinib and venetoclax seem particularly effective in secondary AIHAs, and the proteasome inhibitor bortezomib in 1/3 of refractory CADs (9). A further B-cell receptor target therapy is the PI3K inhibitor parsaclisib, which is under investigation in both wAIHA and CAD with very promising results. An interesting new approach for CAD is blocking complement activation, either at the C5 level (eculizumab) or more efficiently at the C3 (APL-2) or C1s level (sutimlimab), the latter with about 50% responses (31). Other drugs are directed at cellular immunity and cytokines, such as subcutaneous low-dose IL-2 and sirolimus (inhibitor of the serine treonine kinase mTOR). Targeting IgG driven extravascular hemolysis by inhibiting the spleen tyrosine kinase (Syk) is also an attractive approach in wAIHA (for example fostamatinib). Finally, inhibition of the neonatal crystallizable fragment receptor (FcRn) is a new interesting approach: these drugs avoid protection of circulating IgG, including pathogenic autoantibodies, from catabolism and thus regulate innate and adaptive responses initiated by IgG immune complexes (9).

It is worth commenting that several trials with these new drugs are ongoing or being planned. In order to achieve meaningful endpoints it will be essential to properly select patients, bringing into consideration the number of previous treatments and related complications, associated conditions, intrinsic AIHA-risk factors, and type and degree of the immunologic dysregulation. This would provide the basis of a risk-adapted therapy in AIHA, as it is now advised for malignant hematologic conditions.

THE TRANSITION FROM CHRONIC/RELAPSING AIHA TO IDIOPATHIC CYTOPENIAS/DYSPLASIAS OF UNCERTAIN SIGNIFICANCE (ICUS/IDUS)

Several lines of evidence support the existence of a relationship between MDS and autoimmunity, including their epidemiologic association, the existence of common immune-mediated physiopathologic mechanisms, and the response to similar immunosuppressive therapies. This relationship may be hypothesized also with the recently-identified conditions ICUS and IDUS, which are defined by unexplained cytopenia (hemoglobin <10 g/dL; platelet count $<100 \times 10^9$/L; absolute neutrophil count$<1.8 \times 10^9$/L) and/or dysplasia in $<10\%$ of bone marrow lineages (32, 33). More recently another category has been proposed, the clonal cytopenias of undetermined significance (CCUS), where both unexplained cytopenias and clonal mutation are found, without fulfilling WHO criteria for MDS (34). Of note, about 10% of the general population aged over 70 years carries mutations in genes associated with myeloid neoplasms, usually single mutations at a low variant allele frequency, whose pathophysiologic role is still unknown. These cytopenias may be considered milder MDS forms that may evolve, after a variable period, in overt MDS or other bone marrow failure syndromes. In this view, we described the presence of anti-erythroblast antibodies in a case of erythroblastic synartesis, a rare disease with an autoimmune pathogenesis against erythroid precursors (35). Moreover, we also described two cases of AIHA and Evan's syndrome with anti-erythroblast antibodies, which showed a clear-cut bone marrow erythrocyte precursor hyperplasia at diagnosis, but evolved into IDUS and AA after several years (33). In this setting it is tempting to speculate that refractory/relapsing AIHAs lose their predominant "peripheral" pattern over time, and shift toward a "central" autoimmunity (**Figure 2**), leading to a refractory anemia. Additional factors, like accumulating somatic mutations, increased apoptosis, overinflammatory response (inflammaging), unfavorable bone marrow cytokine microenvironment, and breakdown of DNA-repairing tools (telomere shortening) are likely to play a role and need to be addressed in large prospective studies. The increasing availability of NGS panels will also help in defining the genetic background of the immunologic dysregulation, both in terms of inability to clear pathogens/external triggers (chronic infection), or failure to tolerate autoantiges (chronic autoimmune stimulation). This would be of great importance to selectively modulate (potentiate, down-regulate, or re-direct) the innate and adaptive immune response and to avoid an excessively toxic approach to autoimmunity.

AIHAs ASSOCIATED WITH TRANSPLANT

Organs and tissues transplants represent a challenging event for the recipient immune system and may evoke an "immunologic storm" resulting in either transplant rejection and/or devastating immune reactions. A particular mild picture is the passenger lymphocyte syndrome due to donor viable, immunocompetent lymphocytes present within the graft that can produce antibodies against donor RBCs. The syndrome involves mainly group O donors, though few cases have been described in AB recipients with non-AB donors. The risk of hemolysis is proportional to the burden of transplanted lymphocytes and ranges from 9 to 70% (kidney $<$ liver $<$ heart-lung transplants) (11, 36).

Onset is between 3 and 24 days post-transplant and hemolysis is generally transient, since the lymphocytes transferred with the donor organ do not engraft. An emerging and more severe clinical entity is AIHA after hematopoietic stem cells transplant (HSCT). In this setting, autoantibodies are produced by the donor immune system against antigens on erythrocytes produced by the graft itself, and the clinical picture is generally severe (10). Several factors are implicated: the disease itself, the conditioning therapy preceding transplant, the subsequent immunosuppressive treatments, and the occurrence of HSCT complications such as viral infections reactivation. Moreover, the unfavorable immunologic microenvironment may lead to graft failure (as observed in transplanted patients with aplastic anemia), and graft immunocompetence may in turn induce graft vs. host disease (GVHD), further complicating the clinical course. Data from the literature report that immune hemolysis may complicate up to 2–4% of HSCTs after a median of 3–10 months. Both warm and cold forms are described, the former developing between 6 and 18 months, vs. 2–8 months for the latter. Risk factors for AIHA post HSCT are summarized in **Table 4** and include use of unrelated donor and HLA-mismatch, occurrence of GVHD, use of cord blood, age < 15 years, CMV reactivation, alemtuzumab use, and non-malignant condition pre-HSCT (10). Mortality may be quite high and increases with infections (37).

Therapy of Post-Transplant AIHA

Table 4 recapitulates current and novel therapies that have been used in AIHA post-HSCT. It is evident that the total number of patients reported in the various studies is small, and case reports and series carry the bias of describing good outcomes only. However, first-line steroids seem to work less than in primary AIHA, being effective in about 20% of cases only. Moreover, frontline rituximab appears much more effective than in second line (89 vs. 52% responses), and most Authors suggest its early use, particularly in severe cases. Splenectomy is effective but its use is limited to selected cases given the high surgical, infectious, and thrombotic risk. Regarding novel targeted therapies, alemtuzumab, bortezomib, sirolimus, eculizumab, daratumumab, and abatacept have all been used in selected cases, as 3rd or further line, with heterogeneous outcomes. Finally, the passenger lymphocyte syndrome may occur also in this setting and is favored by: use of cyclosporine alone for GVHD prophylaxis, use of peripheral blood rather than bone marrow as source

TABLE 4 | Risk factors and therapies for post-allogenic hematopoietic stem cell transplant (allo-HSCT) AIHA.

	Risk factor	Estimated risk	95% confidence interval	*P*-value
Risk factors associated with AIHA development post-allo-HSCT				
Recipient	Age < 15 years	n.a.	n.a.	0.005
Disease features	Nonmalignant diagnosis pre-HSCT	3.5 (Hazard risk)*	1.1–10.9	0.031
Donor	Unrelated donor	1.45 (Relative risk)	1.05–1.99	0.02
	Unrelated donor	5.28 (Hazard risk)	1.22–22.9	0.026
	HLA mismatch donor	n.a.	n.a.	0.005
Source of stem cells	Cord blood use	n.a.	n.a.	0.005
Conditioning	Alemtuzumab use	2.5 (Hazard risk)*	1.1–5.7	0.028
Allo-HSCT complications	Chronic GVHD	12.17 (Relative risk)	96–1.54	0.018
	CMV reactivation	3.4 (Hazard risk)*	1.2–9.6	0.02

Drug	Dose	N of patients	ORR (range)	N of line
Therapy of AIHA post-allo-HSCT				
Wait & See	–	6	83%	–
Steroids	1–2 mg/Kg day	125	20% (10–50)	1st line
IVIG	2 g/Kg × 2 days	51	12% (10–50)	1st line
Splenectomy	–	18	38% (0–100)	2nd line
PEX	–	10	10 (0–14)	>2nd line
Rituximab	375 mg/sm/week × 4 weeks	18	89% (75–100%)	1st line
		125	52% (36–100)	2nd line
Alemtuzumab	15 mg/day × 3/wk	2	50% (0–100)	>2nd line
Bortezomib	1,3 mg/mq	19	63% (25–100)	>2nd line
Sirolimus	3 mg/sm D1–1 mg/sm day	6	100%	>2nd line
Eculizumab	900 mg	3	33% (0–50)	>2nd line
Daratumumab	16 mg/Kg/week	3	100%	>2nd line
Abatacept	10 mg/Kg day	3	100%	>2nd line

*n.a. not available. *refers to all the autoimmune complications; PEX, plasma exchange.*

of the graft, use of reduced-intensity conditioning, use of a non-genotypically HLA-matched donor, and use of a female donor. Umbilical cord blood as source for stem cells appears protective. Careful transfusion procedures are warranted in transplanted patients, particularly in mismatched cases (10, 36, 38).

AIHAS ASSOCIATED WITH NEW BIOLOGICAL ANTI-CANCER THERAPIES

A fascinating field is that of anti-tumor immunotherapy, based on the understanding that tumor cells activate immune checkpoints such as molecular programmed death receptor-1 (PD-1) and cytotoxic T lymphocyte-associated antigen 4 (CTLA-4) signaling pathways to inhibit T lymphocyte activation and thus escape from immune surveillance, known as "immune brake." Checkpoint inhibitors (CPIs) reactivate T lymphocytes to recognize cancer cells by blocking CTLA-4 or PD-1, and are therefore effective in numerous types of cancer. However, immune-related adverse effects have also been reported (39, 40) and hematologic ones are rare but potentially fatal. Most of them are monolineage cytopenia, or bilineage cytopenia, whilst acquired hemophilia A, eosinophilia, large granular lymphocytosis, and hemophagocytic lymphohistiocytosis are rare (41). A meta-analysis of 9,324 patients indicated that the incidence of anemia, neutropenia, and thrombocytopenia was 9.8, 0.94, and 2.8%, respectively (41). AIHA is the most commonly reported hematologic adverse event, with many case reports of fulminant course (40). A recent revision of the database of the Food and Drug Administration revealed a total of 68 cases: men to women ratio was similar, and the underlying diseases were mainly melanoma (41%), non-small cell lung cancer (NSCLC, 26%), and others including kidney cancer, Hodgkin's lymphoma or skin cancers. The reported cases were mostly from North America (49%) and Europe (34%), with a few from Asia (10%) and Australia (7%). Forty-three cases developed after nivolumab, 13 with pembrolizumab, 7 with ipilimumab, and 5 with atezolizumab, and 16% of cases had received two CPIs. The median time to AIHA onset was 50 days, four patients had concurrent thrombocytopenia, other four endocrine abnormalities (thyroiditis, adrenal insufficiency or hypophysitis), and three gastrointestinal adverse events (colitis or hepatitis). Most cases were IgG positive warm AIHA, whilst CADs were rarer. All episodes were severe, with 80% of cases developing grade 3–4 transfusion-dependent anemia, and the risk appeared higher with PD-1 or PD-L1 targeting agents (0.15–0.25%) than with CTLA-4 inhibitors (0.06%). Mortality was as high as 17%, mainly due to multi-organ failure and delayed diagnosis (42). In another recent analysis of 14 cases who developed AIHA after CPIs, median time to AIHA was 55 days (IQR 22–110 days). Compared to primary AIHA, these cases showed a higher proportion of DAT negativity (38%) and of severe anemia (median Hb 6.3 g/dL (IQR, 6.1–8.0 g/dL). Finally, 50% of cases relapsed after first line and 14% became chronic (43). Regarding therapy, prednisone 1.5 mg−2 mg/kg per day along with CPIs discontinuation is recommended, and evidences for the need of early rituximab or further immunosuppressive agents are lacking. The rechallenge of CPIs after AIHA has improved or is stable remains inconclusive. A patient with Hodgkin's lymphoma who developed nivolumab associated AIHA, that recovered after steroids and was later re-challenged with nivolumab without AIHA recurrence, has been described (44).

CONCLUSIONS

Nowadays the pathogenic and therapeutic landscape of AIHA is rapidly changing for several reasons. First, numerous AIHA-associated conditions have been identified, such as autoimmune diseases, immunodeficiencies, and tumors, which may have additional immune-mediated pathogenic mechanisms compared to primary disease, and deserve a specific therapeutic approach. In this view, the increasing use of molecular testing has disclosed several underlying conditions, questioning the distinction between primary and secondary forms. Second, the development of new drugs has offered additional therapeutic opportunities to "cure" the disease, but at the same time has increased the number of relapsed/refractory cases. Moreover, the future availability of even more target therapies will further puzzle the treatment algorithm of the disease. Third, there is increasing awareness of various pathogenic mechanisms that may differently act during the disease course, ranging from a predominant "peripheral" autoimmunity against erythrocytes to a "central" attack against erythroid precursors, possibly preceding a myelodysplastic or aplastic evolution. These findings have further therapeutic implications, suggesting to avoid heavy immunosuppression in favor of immunomodulating/stimulating agents. Finally, there is increasing emergence of complex and severe entities, particularly AIHA developing after HSCT and AIHA associated with novel anti-cancer drugs such as checkpoint inhibitors, which represent a clinical challenge for complications and fatal outcome. Diagnosis of DAT-negative AIHAs and evaluation of disease-related risk factors for relapse and mortality have improved, but are still an unmet need. The assessment of disease-related risk factor would be pivotal to design good clinical trials and to give hints for a risk-adapted therapy of AIHAs.

AUTHOR CONTRIBUTIONS

WB designed the study, searched the literature, analyzed data, wrote the manuscript, and participated in the final revision. BF searched the literature, analyzed data, wrote the manuscript, and participated in the final revision.

ACKNOWLEDGMENTS

All authors participated in the design of the review, literature revision, manuscript writing, and final revision for important intellectual content.

REFERENCES

1. Barcellini W. New insights in the pathogenesis of autoimmune hemolytic anemia. *Transfus Med Hemother*. (2015) 42:287–93. doi: 10.1159/000439002
2. Berentsen S, Bø K, Shammas FV, Myking AO, Ulvestad E. Chronic cold agglutinin disease of the "idiopathic" type is a premalignant or low-grade malignant lymphoproliferative disease. *APMIS*. (1997) 105:354–62. doi: 10.1111/j.1699-0463.1997.tb00581.x
3. Fattizzo B, Zaninoni A, Gianelli U, Zanella A, Cortelezzi A, Kulasekararaj AG, et al. Prognostic impact of bone marrow fibrosis and dyserythropoiesis in autoimmune hemolytic anemia. *Am J Hematol*. (2018) 93:E88–91. doi: 10.1002/ajh.25020
4. Fattizzo B, Barcellini W. Autoimmune cytopenias in chronic lymphocytic leukemia: focus on molecular aspects. *Front Oncol*. (2020) 9:1435. doi: 10.3389/fonc.2019.01435
5. Barcellini W, Fattizzo B, Zaninoni A, Radice T, Nichele I, Di Bona E, et al. Clinical heterogeneity and predictors of outcome in primary autoimmune hemolytic anemia: a GIMEMA study of 308 patients. *Blood*. (2014) 124:2930–6. doi: 10.1182/blood-2014-06-583021
6. Berentsen S. How I manage patients with cold agglutinin disease. *Br J Haematol*. (2018) 181:320–30. doi: 10.1111/bjh.15109
7. Jäger U, Barcellini W, Broome CM, Gertz MA, Hill A, Hill QA, et al. Diagnosis and treatment of autoimmune hemolytic anemia in adults: recommendations from the First International Consensus Meeting. *Blood Rev*. (2019) 5:100648. doi: 10.1016/j.blre.2019.100648
8. Barcellini W, Zaninoni A, Fattizzo B, Giannotta JA, Lunghi M, Ferrari A, et al. Predictors of refractoriness to therapy and healthcare resource utilization in 378 patients with primary autoimmune hemolytic anemia from eight Italian reference centers. *Am J Hematol*. (2018) 93:E243–6. doi: 10.1002/ajh.25212
9. Barcellini W, Fattizzo B, Zaninoni A. Current and emerging treatment options for autoimmune hemolytic anemia. *Expert Rev Clin Immunol*. (2018) 14:857–72. doi: 10.1080/1744666X.2018.1521722
10. Barcellini W, Fattizzo B, Zaninoni A. Management of refractory autoimmune hemolytic anemia after allogeneic hematopoietic stem cell transplantation: current perspectives. *J Blood Med*. (2019) 10:265–78. doi: 10.2147/JBM.S190327
11. Hill QA, Stamps R, Massey E, Grainger JD, Provan D, Hill A. Guidelines on the management of drug-induced immune and secondary autoimmune, haemolytic anaemia. *Br J Haematol*. (2017) 177:208–20. doi: 10.1111/bjh.14654
12. Hadjadj J, Aladjidi N, Fernandes H, Leverger G, Magérus-Chatinet A, Mazerolles F. Pediatric Evans syndrome is associated with a high frequency of potentially damaging variants in immune genes. *Blood*. (2019) 134:9–21 doi: 10.1182/blood-2018-11-887141
13. Fattizzo B, Zaninoni A, Nesa F, Sciumbata VM, Zanella A, Cortelezzi A, et al. Lessons from very severe, refractory, and fatal primary autoimmune hemolytic anemias. *Am J Hematol*. (2015) 90:E149–51. doi: 10.1002/ajh.24047
14. Lafarge A, Bertinchamp R, Pichereau C, Valade S, Chermak A, Theodose I, et al. Prognosis of autoimmune hemolytic anemia in critically ill patients. *Ann Hematol*. (2019) 98:589–94. doi: 10.1007/s00277-018-3553-9
15. Visco C, Barcellini W, Maura F, Neri A, Cortelezzi A, Rodeghiero F. Autoimmune cytopenias in chronic lymphocytic leukemia. *Am J Hematol*. (2014) 89:1055–62. doi: 10.1002/ajh.23785
16. Maura F, Cutrona G, Fabris S, Colombo M, Tuana G, Agnelli L, et al. Relevance of stereotyped B-cell receptors in the context of the molecular, cytogenetic and clinical features of chronic lymphocytic leukemia. *PLoS ONE*. (2011) 6:e24313. doi: 10.1371/journal.pone.0024313
17. Maura F, Visco C, Falisi E, Reda G, Fabris S, Agnelli L, et al. B-cell receptor configuration and adverse cytogenetics are associated with autoimmune hemolytic anemia in chronic lymphocytic leukemia. *Am J Hematol*. (2013) 88:32–6. doi: 10.1002/ajh.23342
18. Malecka A, Troen G, Tierens A, Østlie I, Małecki J, Randen U, et al. Frequent somatic mutations of KMT2D (MLL2) and CARD11 genes in primary cold agglutinin disease. *Br J Haematol*. (2018) 183:838–42. doi: 10.1111/bjh.15063
19. Feuille EJ, Anooshiravani N, Sullivan KE, Fuleihan RL, Cunningham-Rundles C. Autoimmune cytopenias and associated conditions in CVID: a report from the USIDNET Registry. *J Clin Immunol*. (2018) 38:28–34. doi: 10.1007/s10875-017-0456-9
20. Bariş HE, Kiykim A, Nain E, Özen AO, Karakoç-Aydiner E, Bariş S. The plethora, clinical manifestations and treatment options of autoimmunity in patients with primary immunodeficiency. *Turk Pediatri Ars*. (2016) 51:186–92. doi: 10.5152/TurkPediatriArs.2016.3928
21. Abdel-Khalik A, Paton L, White AG, Urbaniak SJ. Human leucocyte antigens A, B, C, and DRW in idiopathic "warm" autoimmune haemolytic anaemia. *Br Med J*. (1980) 280:760–1. doi: 10.1136/bmj.280.6216.760
22. Wang-Rodriguez J, Rearden A. Reduced frequency of HLA-DQ6 in individuals with a positive direct antiglobulin test. *Transfusion*. (1996) 36:979–84. doi: 10.1046/j.1537-2995.1996.36111297091742.x
23. Petz LD, Garratty G. *Immune Hemolytic Anemias*. 2nd ed. Philadelphia: Churchill Livingstone (2004).
24. Barcellini W. Immune hemolysis: diagnosis and treatment recommendations. *Semin Hematol*. (2015) 52:304–12. doi: 10.1053/j.seminhematol.2015.05.001
25. Barcellini W, Fattizzo B. Clinical applications of hemolytic markers in the differential diagnosis and management of hemolytic anemia. *Dis Markers*. (2015) 2015:635670. doi: 10.1155/2015/635670
26. Bartolmäs T, Salama A. A dual antiglobulin test for the detection of weak or nonagglutinating immunoglobulin M warm autoantibodies. *Transfusion*. (2010) 50:1131–4. doi: 10.1111/j.1537-2995.2009.02533.x
27. Lancman G, Arinsburg S, Jhang J, Cho HJ, Jagannath S, Madduri D, et al. Blood transfusion management for patients treated with anti-CD38 monoclonal antibodies. *Front Immunol*. (2018) 9:2616. doi: 10.3389/fimmu.2018.02616
28. Fattizzo B, Michel M, Giannotta J, Guillet S, Frederiksen H, et al. Efficacy of recombinant erythropoietin in autoimmune hemolytic anemia: a multicenter international study. *Haematologica*. (2020). doi: 10.3324/haematol.2020.250522. [Epub ahead of print].
29. Berentsen S, Randen U, Vågan AM, Hjorth-Hansen H, Vik A, Dalgaard J, et al. High response rate and durable remissions following fludarabine and rituximab combination therapy for chronic cold agglutinin disease. *Blood*. (2010) 116:3180–4. doi: 10.1182/blood-2010-06-288647
30. Berentsen S, Randen U, Oksman M, Birgens H, Tvedt THA, Dalgaard J, et al. Bendamustine plus rituximab for chronic cold agglutinin disease: results of a Nordic prospective multicenter trial. *Blood*. (2017) 130:537–41. doi: 10.1182/blood-2017-04-778175
31. Röth A, Barcellini W, D'Sa S, Miyakawa Y, Broome CM, Michel M, et al. Inhibition of complement C1s with sutimlimab in patients with cold agglutinin disease (CAD): results from the Phase 3 Cardinal Study. *Blood*. (2019) 134 (Suppl_2). doi: 10.1182/blood-2019-132490
32. Barcellini W. The relationship between idiopathic cytopenias/dysplasias of uncertain significance(ICUS/IDUS) and autoimmunity. *Expert Rev Hematol*. (2017) 10:649–57. doi: 10.1080/17474086.2017.1339597
33. Barcellini W, Fattizzo B, Zaninoni A, Valli V, Ferri V, Gianelli U, et al. Clinical evolution of autoimmune cytopenias to idiopathic cytopenias/dysplasias of uncertain significance (ICUS/IDUS) and bone marrow failure syndromes. *Am J Hematol*. (2017) 92:E26–9. doi: 10.1002/ajh.24618
34. Bejar R. CHIP, ICUS, CCUS and other four-letter words. *Leukemia*. (2017) 31:1869–71. doi: 10.1038/leu.2017.181
35. Zaninoni A, Imperiali FG, Pomati M, Colombi M, Boschetti C, Barcellini W. Bone marrow mitogen-stimulated direct antiglobulin test in a case of erythroblastic synartesis. *Clin Lab*. (2010) 56:459–62.
36. Skeate R, Singh C, Cooley S, Geller M, Northouse J, Welbig J, et al. Hemolytic anemia due to passenger lymphocyte syndrome in solid malignancy patients treated with allogeneic natural killer cell products. *Transfusion*. (2013) 53:419–23. doi: 10.1111/j.1537-2995.2012.03942.x
37. González-Vicent M, Sanz J, Fuster JL, Cid J, de Heredia CD, Morillo D, et al. Autoimmune hemolytic anemia (AIHA) following allogeneic hematopoietic stem cell transplantation (HSCT): a retrospective analysis and a proposal of treatment on behalf of the Grupo Español De Trasplante de Medula Osea en Niños (GETMON) and the Grupo Español de Trasplante Hematopoyetico (GETH). *Transfus Med Rev*. (2018). doi: 10.1016/j.tmrv.2018.02.005. [Epub ahead of print].

38. Kruizinga MD, van Tol MJD, Bekker V, Netelenbos T, Smiers FJ, Bresters D, et al. Risk Factors, Treatment, and immune dysregulation in autoimmune cytopenia after allogeneic hematopoietic stem cell transplantation in pediatric patients. *Biol Blood Marrow Transplant*. (2018) 24:772–8. doi: 10.1016/j.bbmt.2017.12.782
39. Postow MA, Sidlow R, Hellmann MD. Immune-related adverse events associated with immune checkpoint blockade. *N Engl J Med*. (2018) 378:158–68. doi: 10.1056/NEJMra1703481
40. Zhuang J, Du J, Guo X, Zhou J, Duan L, Qiu W, et al. Clinical diagnosis and treatment recommendations for immune checkpoint inhibitor-related hematological adverse events. *Thorac Cancer*. (2020) 11:799–804. doi: 10.1111/1759-7714.13405
41. Petrelli F, Ardito R, Borgonovo K, Lonati V, Cabiddu M, Ghilardi M, et al. Haematological toxicities with immunotherapy in patients with cancer: a systematic review and meta-analysis. *Eur J Cancer*. (2018) 103:7–16. doi: 10.1016/j.ejca.2018.07.129
42. Tanios GE, Doley PB, Munker R. Autoimmune hemolytic anemia associated with the use of immune checkpoint inhibitors for cancer: 68 cases from the Food and Drug Administration database and review. *Eur J Haematol*. (2019) 102:157–62. doi: 10.1111/ejh.13187
43. Leaf RK, Ferreri C, Rangachari D, Mier J, Witteles W, Ansstas G, et al. Clinical and laboratory features of autoimmune hemolytic anemia associated with immune checkpoint inhibitors. *Am J Hematol*. (2019) 94:563–74. doi: 10.1002/ajh.25448
44. Tardy MP, Gastaud L, Boscagli A, Peyrade F, Gallamini A, Thyss A. Autoimmune hemolytic anemia after nivolumab treatment in Hodgkin lymphoma responsive to immunosuppressive treatment. A case report. *Hematol Oncol*. (2017) 35:875–7. doi: 10.1002/hon.2338

Conflict of Interest: The authors declare that the research was conducted in the absence of any commercial or financial relationships that could be construed as a potential conflict of interest.

frontiers in Immunology

ORIGINAL RESEARCH
published: 04 June 2020
doi: 10.3389/fimmu.2020.01006

Small Paroxysmal Nocturnal Hemoglobinuria Clones in Autoimmune Hemolytic Anemia: Clinical Implications and Different Cytokine Patterns in Positive and Negative Patients

Bruno Fattizzo[1], Juri Giannotta[1], Anna Zaninoni[1], Austin Kulasekararaj[2], Lilla Cro[3,4] and Wilma Barcellini[1]*

[1] UO Ematologia, Fondazione IRCCS Ca' Granda Ospedale Maggiore Policlinico, Milan, Italy, [2] Hematology Unit, King's College Hospital, London, United Kingdom, [3] Servizio di Citofluorometria, Laboratorio Centrale, Fondazione IRCCS Ca' Granda Ospedale Maggiore Policlinico, Milan, Italy, [4] Facoltà di Medicina e Chirurgia, Università degli Studi di Milan, Milan, Italy

OPEN ACCESS

Edited by:
Mark Slevin,
Manchester Metropolitan University,
United Kingdom

Reviewed by:
Giuseppina Ruggiero,
University of Naples Federico II, Italy
Jeffrey J. Pu,
Upstate Medical University,
United States

***Correspondence:**
Bruno Fattizzo
bruno.fattizzo@unimi.it

Specialty section:
This article was submitted to Inflammation, a section of the journal Frontiers in Immunology

Received: *11 February 2020*
Accepted: *28 April 2020*
Published: *04 June 2020*

Citation:
Fattizzo B, Giannotta J, Zaninoni A, Kulasekararaj A, Cro L and Barcellini W (2020) Small Paroxysmal Nocturnal Hemoglobinuria Clones in Autoimmune Hemolytic Anemia: Clinical Implications and Different Cytokine Patterns in Positive and Negative Patients. Front. Immunol. 11:1006. doi: 10.3389/fimmu.2020.01006

Autoimmune hemolytic anemia (AIHA) is characterized by immune mediated erythrocytes destruction by autoantibodies with or without complement activation. Additional pathologic mechanisms include cellular cytotoxicity, cytokline dysregulation, and inadequate bone marrow compensation with fibrosis/dyserythropoiesis. The latter resembles that of bone marrow failures, namely aplastic anemia and myelodysplastic syndromes. Paroxysmal nocturnal hemoglobinuria (PNH) clones are increasingly recognized in bone marrow failure syndromes, and their selection and expansion are thought to be mediated by immune mechanisms. In this study, we aimed to evaluate the prevalence of PNH clones in 99 patients with primary AIHA, and their correlations with disease features and outcomes. Moreover, in the attempt to disclose the physiopathology of PNH positivity in AIHA, serum levels of several immunomodulatory cytokines were tested. A PNH clone was found in 37 AIHA patients (37,4%), with a median size of 0.2% on granulocytes (range 0.03–85). Two patients showed a large clone (16 and 85%) and were therefore considered as AIHA/PNH association and not included in further analysis. Compared to PNH negative, PNH positive cases displayed a higher hemolytic pattern with adequate bone marrow compensation. AIHA type, response to therapy, complications and outcome were comparable between the two groups. Regarding cytokine levels, IFN-γ and IL-17 were lower in PNH positive vs. PNH negative AIHAs (0.3 ± 0.2 vs. 1.33 ± 2.5; 0.15 ± 0.3 vs. $3,7 \pm 9.1$, respectively, $p = 0.07$ for both). In PNH positive AIHAs, IFN-γ positively correlated with reticulocytes ($r = 0.52$, $p = 0.01$) and with the bone marrow responsiveness index ($r = 0.69$, $p = 0.002$). Conversely, IL-6 and IL-10 showed the same pattern in PNH positive and PNH negative AIHAs. IL-6 levels and TGF-β positively correlated with clone size ($r = 0.35$, $p = 0.007$, and $r = 0.38$, $p = 0.05$, respectively), as well as with LDH values ($r = 0.69$, $p = 0.0003$, and $r = 0.34$, $p = 0.07$, respectively). These data suggest testing PNH clones in AIHA since

their prevalence is not negligible, and may correlate with a prominent hemolytic pattern, a higher thrombotic risk, and a different therapy indication. PNH testing is particularly advisable in complex cases with inadequate response to AIHA-specific therapy. Cytokine patterns of PNH positive and negative AIHAs may give hints about the pathogenesis of highly hemolytic AIHA.

Keywords: warm autoimmune hemolytic anemia, cold agglutinin disease, paroxysmal nocturnal hemoglobinuria, rituximab, cytokines

INTRODUCTION

Autoimmune hemolytic anemia (AIHA) is a clinically heterogeneous disease ranging from mild/ compensated to very severe life-threatening hemolysis (1, 2). Several pathogenic mechanisms are involved, mainly encompassing autoantibodies of different classes, thermal amplitude, and affinity/efficiency in activating complement. Other factors include abnormalities of antigen-presenting cells, increased antibody-dependent cellular cytotoxicity (ADCC) and cytotoxic CD8+T cells, aberrant cytokine production and inflammation, and alterations of immunoregulatory T cells. While direct complement-mediated lysis takes place mainly in the circulations and liver, ADCC and phagocytosis occur preferentially in the spleen and lymphoid organs (3). Finally, the efficacy of the erythroblastic compensatory response can greatly influence the clinical picture of AIHA (4–6). Intravascular hemolysis has been shown to correlate with the rate of complement activation and with the risk of AIHA related thrombosis. Bone marrow compensation has been demonstated to contribute to anemia severity at onset, the major predictor of disease relapse and outcome. Paroxysmal nocturnal hemoglobinuria (PNH) is a rare (incidence of 2–6 per million) clonal acquired disease, whose clinical spectrum includes both overt intravascular hemolysis and bone marrow failure, namely aplastic anemia (AA) and hypocellular myelodysplastic syndromes (MDS). PNH is due to a somatic mutation of the hematopoietic stem cell involving the PIG-A gene and resulting in deficiency of the complement inhibitory GPI-anchored proteins CD55 and CD59 (7–9). PNH has been classified by the International PNH Interest Group (IPIG) (8, 10) in three clinical subgroups: classic, PNH in the setting of another bone marrow disorder, and subclinical. The classic form is dominated by intravascular hemolysis, with markedly elevated LDH and a clone size >50%. The second group, mainly AA or MDS associated, is clinically dominated by the underlying bone marrow features and displays a clone size 10–50%. The third category is defined as subclinical, since there is no clinical or biochemical evidence of intravascular hemolysis and the PNH clone is <10%. Since the last 10 years, the increased sensitivity of the cytofluorimetric techniques (up to ≥0.01% clone size) enabled the detection of small PNH clones in up to 60% of AA and 30% of MDS (7–9, 11). The significance of these clones is still unclear, with some evidences for better response to immunosuppressive therapy in PNH positive cases. These tests allowed the detection of small PNH populations even in diseases not commonly associated to PNH such as hypomegakaryocytic thrombocytopenia (12) and chronic benign neutropenia (13). These forms are characterized by both immune mediated peripheral cytopenia and bone marrow failure, similarly to what demonstrated for AA and AIHA itself. We therefore analyzed the presence of small PNH clones in primary AIHA in order to evaluate their clinical significance in this acquired hemolytic disease. Furthermore, given that PNH typically arises in the context of autoimmune activation, we investigated immunoregolatory and inflammatory cytokines to address the role of PNH clones in the pathogenesis of AIHA.

METHODS

Ninety-nine patients with primary AIHA tested at Fondazione IRCCS Ca' Granda Ospedale Policlinico of Milan from March 2001 until October 2019 were included in the analysis. Demographic and clinical phenotypes were retrospectively evaluated from August 2017 until January 2020.

Clinical history, blood counts, hemolytic markers, AIHA type, bone marrow features, number and type of therapeutic interventions and their response rates, occurrence of complications (particularly thrombosis), and death were collected.

Primary AIHA was defined by hemolytic anemia and positive direct antiglobulin test (DAT), in the absence of associated overt lymphoproliferative, infectious, autoimmune, or neoplastic diseases. Patients were classified as wAIHA (DAT positive for IgG or IgG+C), CAD (DAT positive for C only, with high titer cold agglutinins), mixed (DAT positive for IgG+C with high titer cold agglutinins) and atypical (DAT negative, DAT positive for IgA only, warm IgM).

Reticulocytosis was evaluated and expressed as bone marrow responsiveness index (BMRI: absolute reticulocyte count x patient' Hb/normal Hb) (1).

PNH Clone Testing

PNH testing had been performed by classical cytometry technique until 2010 and, thereafter, using high sensitivity (≥0.01%) fluorescent aerolysin (FLAER)-based assay according to 2010 International Clinical Cytometry Society (ICCS) PNH Consensus Guidelines and 2012 Practical PNH Guidelines (14, 15). FLAER/CD33/CD15/CD45 and FLAER/CD59 panels had been used for white blood cell (WBC) and red blood cell (RBC) testing, respectively.

Evaluation of Immunomodulatory and Inflammatory Cytokines

In a fraction of patients ($N = 11$) the following cytokines were evaluated in serum using commercial ELISA kits (High Sensitivity Elisa kits, Invitrogen by Thermo Fisher Scientific, MA, USA, human TGF-β elisa kit, Immunological Sciences, Rome, Italy): interleukin (IL)6, IL10, IL17, tumor necrosis factor (TNF)-α, interferon (IFN)-γ, and transforming growth factor (TGF)-β. Cytokine levels were compared with 40 age and sex matched healthy controls.

Statistical Analysis

Student *t*–test was used for continuous variables and chi-square test for categorical ones. Analysis of variance was performed by using mean, median, ranges and standard errors. Cumulative incidence of relapse, as well as overall survival, was evaluated by Kaplan Meyer method.

RESULTS

Demographics and Hematologic Parameters

Clinical and hematologic features are shown in **Table 1**: 46% of patients were older than 60 years of age, male to female ratio was 0.98, and all AIHA types were represented (wAIHA, cAIHA, wAIHA+C, mixed and atypical cases). One third of cases presented severe anemia and hemoglobin levels positively correlated with LDH > 1.5 x ULN ($r = 0.21$ $p = 0.03$), indicating active intravascular hemolysis, as well as with inadequate reticulocytosis (i.e., BMRI<121, $N = 22$, $r = 0.19$, $p = 0.05$). Bone marrow evaluation had been performed in 74 cases and showed hypercellularity and diserythropoiesis in about half of cases (52 and 57%, respectively), and reticulin fibrosis (MF-1) in 42%; the latter displayed reduced BMRI compared with MF-0 patients (107 vs. 137, $p = 0.05$). Moreover, 63% of patients had a lymphoid infiltrate, with mainly T or mixed phenotype, not diagnostic for overt lymphoproliferative syndromes.

TABLE 1 | Clinical and hematologic characteristics of AIHA patients, altogether and according to PNH positivity.

Clinical characteristics	All patients *N* = 99	PNH neg *N* = 62	PNH pos *N* = 37
Median Age y(range)	57 (5–89)	57 (20–85)	63 (5–89)
M/F	49/50	30/32	20/17
Median follow up m(range)	20 (0–262)	26 (0–205)	24 (2–262)
WAIHA N(%)	37 (38)	27 (43.5)	10 (28.6)
WAIHA IgG+C N(%)	15 (16)	9 (14.5)	6 (17)
CAD N(%)	33 (34)	19 (31)	14 (40)
Mixed N(%)	5 (5)	3 (5)	2 (6)
Atypical N(%)	7(7)	4 (6.5)	3 (8.6)
Median Hb g/dL (range)	7.9 (1.4–13.7)	7.8 (3.5–13.1)	7.9 (1.4–13.7)
Median LDH U/L(range)	451 (150–3,200)	392 (150–1,867)	606 (191–3,200)*
Median LDH ULN (range)	2 (0–14)	2 (0–7)	2 (1–14)**
Median Ret x10^3/mmc (range)	156 (5–574)	151 (5–478)	195 (38–574)
Median BMRI (range)	103 (2–378)	95 (2–305)	128 (18–378)
BMRI<121 N(%)	52 (52)	38 (61)	14 (38)$^{£}$
Bone marrow evaluation	***N* = 74**	***N* = 47**	***N* = 26**
Median Cellularity % (range)	55 (15–100)	55 (20–100)	55 (15–95)
Hypercellularity (%)	38 (51)	24 (51)	14 (54)
Fibrosis MF1 (%)	31 (42)	22 (46)	9 (35)
Dyserythropoiesis (%)	42 (57)	28 (58)	14 (52)
Median lymphoid infiltrate%(range)	5 (0–75)	5 (0–75)	5 (0–30)
Type of infiltrate B(%)	10 (10)	8 (13)	2 (6)
T(%)	28 (29)	16 (26)	12 (34)
Mixed (%)	23 (24)	16 (26)	7 (20)

*PNH paroxysmal nocturnal hemoglobinuria; CAD cold agglutinin disease; WAIHA warm autoimmune haemolytic anemia; Hb hemoglobin; Ret reticulocytes; LDH lactate dehydrogenase; ULN upper limit of normality; BMRI bone marrow responsiveness index. *P = 0.005; **P = 0.03; £P = 0.01.*

AIHA Treatment, Complication and Outcome

Thirty-nine (39%) of patients required at least one transfusion during the follow up, and 94% received AIHA treatment (**Table 2**). Specifically, 89% were treated with steroids, 71% responded, and 55% relapsed and required further treatment. Second line therapy included rituximab (57% with an overall response rate of 81.5%), splenectomy (7.2% with 75% responsive cases), and cytotoxic immunosuppressants (20.8%, with a response in 65% of patients). On the whole, patients received a median of 2 (range 0–5) therapy lines. Regarding AIHA related complications, 7% of cases developed acute renal failure, 31% an infectious episode, 12% experienced a thrombosis (2 pulmonary embolisms and 10 lower limbs deep venous thrombosis), and 8% died (3 patients for AIHA-related complications).

PNH Clone Analysis and Description of Two Peculiar Cases

Thirty-seven cases (37%) showed a PNH clone on granulocytes. Five patients had been tested before FLAER era (2 showed a PNH clone size of 0.2% on granulocytes) and 3 of them were re-evaluated thereafter (all PNH negative). PNH positive AIHA showed increased LDH levels as compared to negative ones ($p = 0.005$) and mostly adequate reticulocytosis (BMRI>121 in 62% vs. 39% in PNH negative, $p = 0.01$). Other hematologic features, including AIHA type, were comparable among the two groups (**Table 1**). Notably, relapse free survival (RFS) after steroids was slightly shorter in PNH positive than in negative cases, whilst no other differences in treatment choice or response rate were noted. In PNH positive patients, median clone size on granulocytes was 0.2% (0.03–85). Only two patients displayed

TABLE 2 | Treatments and outcome of AIHA patients, altogether and according to PNH positivity.

Treatment and outcome	All patients *N* = 99	PNH neg *N* = 62	PNH pos *N* = 37
First therapy line *N*(%)	96 (96)	61(98)	35 (94)
Second therapy line *N*(%)	57 (57)	35 (56)	20 (54)
Third therapy line or > *N*(%)	31 (31)	19 (31)	12 (32)
Median RFS days (range)	539 (25–6,014)	700 (25–6,014)	338 (42–3,483)
Evans (%)	14 (14)	6 (10)	7 (19)
Acute renal failure (%)	7 (7)	6 (10)	1 (3)
Infections (%)	31 (31)	19 (31)	10 (29)
Thrombosis (%)	12 (12)	7 (11)	5 (14)
Death (%)	8 (8)	3(5)	5(14)
Median OS m(%)	25 (0–262)	26 (0–205)	24 (2–62)

OS, overall survival; RFS, relapse free survival.

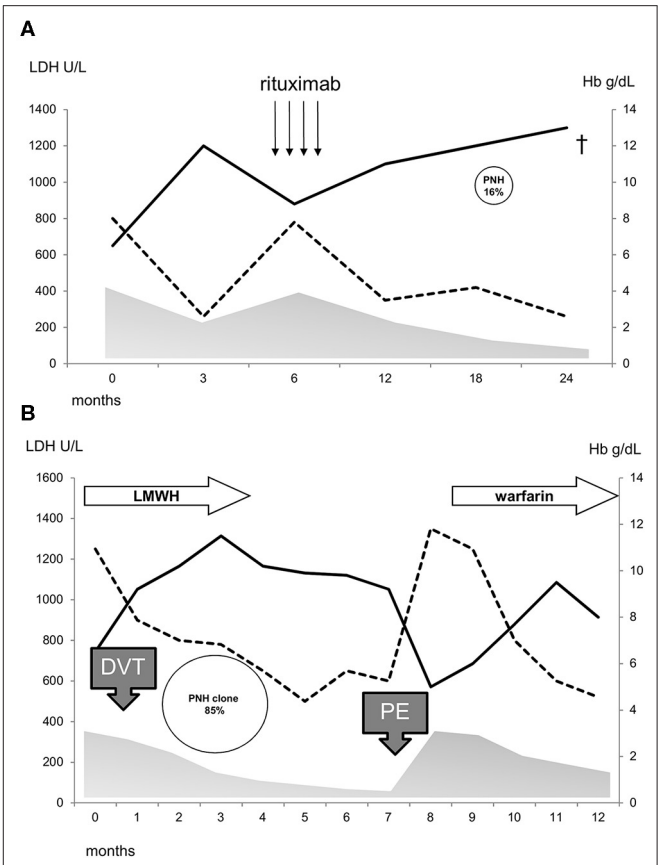

FIGURE 1 | Clinical course of two patients **(A,B)** with PNH/AIHA association and a clone size>10%. Hb, continuous line; LDH, dotted line; gray area, prednisone therapy; arrows, rituximab 375 mg/sm/week for 4 weeks; LMWH, low molecular weight heparin; thrombosis, DVT, deep venous thrombosis; PE, pulmonary embolism; cross indicates death.

a PNH clone >10% and both showed LDH levels >1.5xULN. The first patient was a 40-year-old man, initially diagnosed with primary wAIHA that was effectively treated with steroids and rituximab; subsequently a PNH clone 16% was detected and he developed a severe and fatal *Pneumocystis jerovecii* pneumonia (**Figure 1A**). The second patient was a 65-year-old lady diagnosed with very severe wAIHA responsive to steroids with amelioration of anemia. However, LDH levels were persistently high, and a lower limb venous thrombosis occurred. Re-evaluation of other causes of hemolysis, including congenital, toxic, mechanical, and infective forms, demonstrated a PNH clone 85% on granulocytes (**Figure 1B**). The patient started low molecular weight heparin, but after discharge discontinued treatment. She presented 2 months later with a massive pulmonary embolism and very severe haemolytic anemia (Hb 4.2 g/dL and LDH 5.7xULN). DAT tube was still positive and PNH clone unchanged. She restarted anticoagulation, was transfused, and commenced eculizumab. Since these two cases resemble PNH (subclinical and haemolytic type, respectively), were not included in further correlations.

Cytokine Studies

Figure 2 shows cytokine levels in PNH positive and PNH negative AIHA patients, in age and sex matched controls ($N = 40$), and in a cohort of classic hemolytic PNH cases ($N = 28$). IFN-γ and IL-17 levels were lower in PNH positive vs. PNH negative AIHA (0.3 ± 0.2 vs. 1.33 ± 2.5; 0.15 ± 0.3 vs. $3{,}7 \pm 9.1$, respectively, $p = 0.07$ for both), whilst IL-6 and IL-10 were not significantly different in the two groups.

As compared to healthy controls, IFN-γ and IL-17 levels were reduced in PNH positive AIHA, similarly to what observed in patients with classical PNH. Conversely, IL-6 and IL-10 were greater compared to healthy volunteers. Concerning TNF-α and TGF-β levels, no clear differences emerged among groups. Focusing on PNH positive AIHA patients, IFN-γ positively correlated with reticulocytes ($r = 0.52$, $p = 0.01$) whilst IL-17 showed a negative correlation ($r = -0.4$, $p = 0.04$). Similar results were observed for the bone marrow responsiveness index ($r = 0.69$ for IFN-γ, $p = 0.002$ and $r = -0.40$ for IL-17, $p = 0.04$). IL-6 levels and TGF-β positively correlated with clone size ($r = 0.35$, $p = 0.007$, and $r = 0.38$, $p = 0.05$, respectively), as well as with LDH values ($r = 0.69$, $p = 0.0003$, and $r = 0.34$, $p = 0.07$, respectively). Finally, TNFα levels showed a negative correlation with clone size ($r = -0.4$, $p = 0.03$).

DISCUSSION

In this study we showed for the first time the presence of a PNH clone in about one third of 99 consecutive AIHA patients. Almost all cases displayed a small clone (<10%) considered the hallmark of subclinical PNH according to IPIG classification (8, 10). Two patients showed a greater clone size and were therefore diagnosed as PNH associated with AIHA. This association has not been previously described and should be considered when the patient is referred for hemolytic anemia. In fact, thrombotic events are known to occur in about 10% of active AIHA, whilst the frequency is far higher (about 40%) in classic hemolytic PNH (8, 16). Of note, in one of the two AIHA/PNH patients, a severe

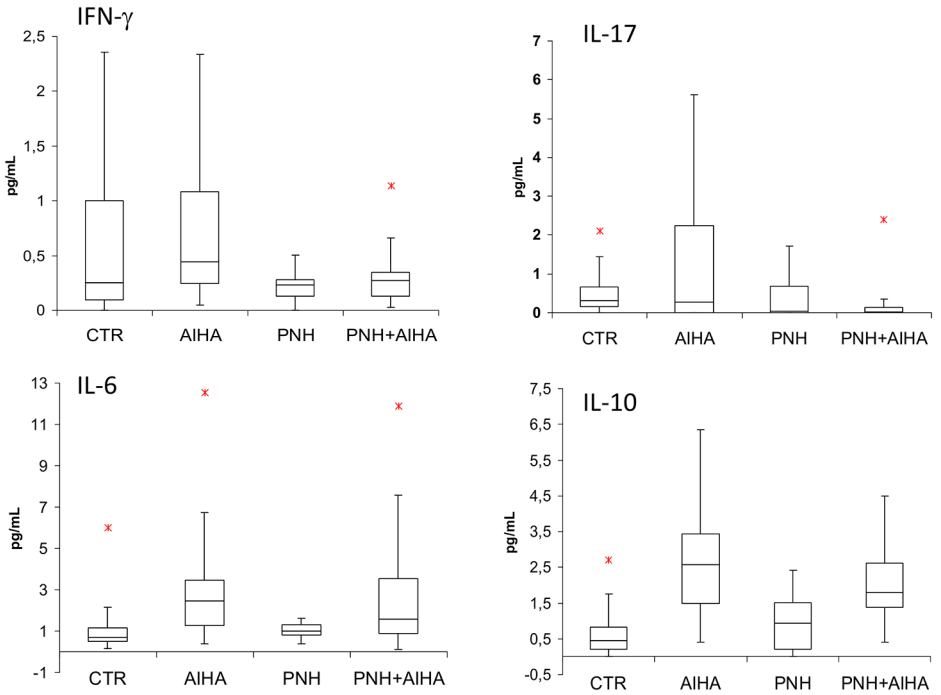

FIGURE 2 | cytokine levels in PNH positive and PNH negative AIHA patients, in age and sex matched controls ($N = 40$), and in a cohort of classic hemolytic PNH cases ($N = 28$). IFN-γ and IL-17 levels were lower in PNH positive versus PNH negative AIHA ($p = 0.07$ for both). No significant p values were obtained. TNF-α and TGF-β levels are not shown into the figure; their values were (mean ± SD): TNF-α 0.2 ± 0.2 pg/mL in PNH+AIHA, 0.2 ± 0.1 pg/mL in PNH-AIHA, 0.23 ± 0.29 pg/mL in classic PNH, and 1.3 ± 0.9 pg/mL in healthy controls. TGF-β 3,249 ± 1,570 pg/mL in PNH+AIHA, 3,295 ± 1,697 pg/mL in PNH-AIHA, 21,010 ± 602 pg/mL in classic PNH, and 3,160 ± 1,884 pg/mL in healthy controls. *represent outlier values.

thrombotic event occurred soon after the discontinuation of anticoagulant prophylaxis.

An interesting point is the clinical significance of small PNH clones in the remaining AIHA studied patients. It is known that small PNH clones are present in more than 50 and 20% of patients with aplastic anemia or hypoplastic MDS, respectively (8, 11, 16). Their clinical significance is still a matter of debate, although in various series an association with a deeper cytopenia, increased LDH levels, and thrombotic tendency have been demonstrated in PNH positive cases (11). Moreover, a better response to immunosuppressive treatment was reported in this group, stressing the link between PNH clone emergence and immune mediated bone marrow failure. Among the hypothesis of PNH clone selection in the context of bone marrow failure, it has been reported that GPI molecules may be the target of the autoimmune attack; therefore, GPI negative stem cells are spared and may further expand through still unknown mechanisms, including additional mutations and environmental factors (8, 9, 16). Our results showed that PNH positive AIHA cases had greater LDH levels, suggesting a higher hemolytic pattern and possibly an increased thrombotic risk, although the number of cases and the follow up may be insufficient to draw definitive conclusions. As regards therapy outcome, no clear associations have been demonstrated with PNH positivity in this AIHA cohort. Another feature of PNH positive AIHAs is their better bone marrow compensatory response compared with PNH negative cases. Consistently, hemoglobin values were comparable between the two groups, in spite of the more marked hemolytic pattern observed in the former.

On the whole, despite the few clinical correlations found possibly due to the small sample size and relative short follow-up, PNH clone testing may be included in the initial work up of AIHA to either assess the presence of the two diseases requiring different and specific therapy. Moreover, PNH clone testing is advisable in complex cases with inadequate response to AIHA-specific therapy and with persistent hemolytic activity.

In the attempt to investigate the physiopathology underlying the emergence of PNH clones in AIHA, we tested several immunomodulatory and inflammatory cytokines. PNH positive AIHA patients showed an immunological signature distinct from negative cases, with reduced levels of IFN-γ and IL-17. The former is a classic T-helper 1 cytokine involved in the autoimmune attack against bone marrow precursors typical of aplastic anemia (3) and reported elevated also in AIHA. Likewise, IL-17, a cytokine known to amplify the pro-inflammatory and autoimmune response, has been reported elevated in the same settings (17–19). In our study, PNH positive AIHA showed a Th1 profile more similar to hemolytic PNH than to "classic" (PNH negative) AIHA, suggesting that

these small clones might mitigate Th1 response. On the contrary, Th2 cytokines levels, i.e., IL-6 and IL-10, were not different in PNH positive and negative AIHA cases. This finding suggests that Th2 signature, the hallmark of humoral autoimmunity, is particularly strong in AIHA and is not influenced by the presence of a small PNH clone. Although these data are preliminary and would need further *ad-hoc* studies, it is tempting to speculate that the detection of a small PNH clone in AIHA reveals the presence of a wider spectrum of immunologic mechanisms involved in pathogenesis of the disease compared with PNH-negative AIHAs. In fact, in the PNH-positive AIHAs the immunologic signature ranges from overt antibody mediated autoimmunity against peripheral erythrocytes to a "central" autoimmune attack to bone marrow precursors. As a matter of fact, PNH clones, in the context of AA, are thought to be "surviving clones" spared after autoimmune attack against hematopoietic stem cells (8, 9); similarly, autoimmunity against erythroid precursors has been demonstrated in AIHA (3). Whether the emergence of PNH clones in AIHA is related to coexisting immune-mediated bone marrow failure and/or represents a favorable response to bone marrow stress related to acute hemolysis would require further investigation.

In conclusion, our data suggest testing PNH clones in AIHA since their prevalence is not negligible. Moreover, PNH positivity correlates with a prominent hemolytic pattern and may confer a higher thrombotic risk. Finally, cytokine patterns of PNH positive and negative AIHAs may give hints about the pathogenesis of highly hemolytic AIHA.

DATA AVAILABILITY STATEMENT

The datasets generated for this study are available on request to the corresponding author.

ETHICS STATEMENT

The studies involving human participants were reviewed and approved by Ethical Committee of the Fondazione IRCCS Ca' Granda Ospedale Maggiore Policlinico. The patients/participants provided their written informed consent to participate in this study.

AUTHOR CONTRIBUTIONS

BF and WB designed the study, followed patients, collected and analyzed data, wrote the manuscript, and participated to the final revision. JG and AK followed patients, collected data, wrote the manuscript, and participated to the final revision. AZ performed the cytokine studies, wrote the manuscript, and participated to the final revision. LC performed the PNH clone testing. All authors participated to the design of the review, literature revision, manuscript writing, and final revision for important intellectual content.

FUNDING

The study was supported by Fondazione IRCCS Ca' Granda Policlinico Milano, Project number RC 175/04, 2019.

REFERENCES

1. Barcellini W, Fattizzo B, Zaninoni A, Radice T, Nichele I, Di Bona E, et al. Clinical heterogeneity and predictors of outcome in primary autoimmune hemolytic anemia: a GIMEMA study of 308 patients. *Blood*. (2014) 124:2930–6. doi: 10.1182/blood-2014-06-583021
2. Fattizzo B, Zaninoni A, Nesa F, Sciumbata VM, Zanella A, Cortelezzi A, et al. Lessons from very severe, refractory, and fatal primary autoimmune hemolytic anemias. *Am J Hematol*. (2015) 90:E149–51. doi: 10.1002/ajh.24047
3. Barcellini W. New insights in the pathogenesis of autoimmune hemolytic anemia. *Transfus Med Hemother*. (2015) 42:287–93. doi: 10.1159/000439002
4. Barcellini W, Zaninoni A, Fattizzo B, Giannotta JA, Lunghi M, Ferrari A, et al. Predictors of refractoriness to therapy and healthcare resource utilization in 378 patients with primary autoimmune hemolytic anemia from eight Italian reference centers. *Am J Hematol*. (2018) 93:E243–6. doi: 10.1002/ajh.25212
5. Fattizzo B, Zaninoni A, Gianelli U, Zanella A, Cortelezzi A, Kulasekararaj AG, et al. Prognostic impact of bone marrow fibrosis and dyserythropoiesis in autoimmune hemolytic anemia. *Am J Hematol*. (2018) 93:E88–91. doi: 10.1002/ajh.25020
6. Fattizzo B, Barcellini W. Autoimmune cytopenias in chronic lymphocytic leukemia: focus on molecular aspects. *Front Oncol*. (2020) 9:1435. doi: 10.3389/fonc.2019.01435
7. Hillmen P, Lewis SM, Bessler M, Luzzatto L, Dacie JV. Natural history of paroxysmal nocturnal hemoglobinuria. *N Engl J Med*. (1995) 333:1253–8. doi: 10.1056/NEJM199511093331904
8. Parker CJ. Update on the diagnosis and management of paroxysmal nocturnal hemoglobinuria. *Hematol Am Soc Hematol Educ Program*. (2016) 2016:208–16. doi: 10.1182/asheducation-2016.1.208
9. Luzzatto L, Risitano AM. Advances in understanding the pathogenesis of acquired aplastic anaemia. *Br. J. Haematol*. (2018) 182:758–76. doi: 10.1111/bjh.15443
10. Parker C, Omine M, Richards S. International PNH Interest Group. Diagnosis and management of paroxysmal nocturnal hemoglobinuria. *Blood*. (2005) 106:3699–709. doi: 10.1182/blood-2005-04-1717
11. Fattizzo B, Dunlop A, Ireland RM, Kassam S, Consonni D, Yallop D, et al. Prognostic and predictive impact of small pnh clones in a large cohort of patients with myelodysplastic syndromes and aplastic anemia: a single-center experience. *Blood*. (2018) 132:3870. doi: 10.1182/blood-2018-99-116772
12. Rafferty M, Leach M. Hypomegakaryocytic thrombocytopenia and increased number of PNH-phenotype cells - an emerging subgroup of myelodysplastic syndrome showing frequent response to immunosuppression. *Br J Haematol*. (2018) 182:152–4. doi: 10.1111/bjh.14760
13. Damianaki A, Stagakis E, Mavroudi I, Spanoudakis M, Koutala H, Papadogiannis F, et al. Minor populations of paroxysmal nocturnal hemoglobinuria-type cells in patients with chronic idiopathic neutropenia. *Eur J Haematol*. (2016) 97:538–46. doi: 10.1111/ejh.12766
14. Dezern AE, Borowitz MJ. ICCS/ESCCA consensus guidelines to detect GPI-deficient cells in paroxysmal nocturnal hemoglobinuria (PNH) and related disorders part 1 - clinical utility. *Cytometry B Clin Cytom*. (2018) 94:16–22. doi: 10.1002/cyto.b.21608
15. Illingworth A, Marinov I, Sutherland DR, Wagner-Ballon O, DelVecchio L. ICCS/ESCCA consensus guidelines to detect GPI-deficient cells in paroxysmal nocturnal hemoglobinuria (PNH) and related disorders part 3 - data analysis, reporting and case studies. *Cytometry B Clin Cytom*. (2018) 94:49–66. doi: 10.1002/cyto.b.21609
16. de Latour RP, Mary JY, Salanoubat C, Terriou L, Etienne G, Mohty M, et al. Paroxysmal nocturnal hemoglobinuria: natural history of disease. *Blood*. (2008) 112:3099–106. doi: 10.1182/blood-2008-01-133918

17. Du HZ, Wang Q, Ji J, Shen BM, Wei SC, Liu LJ, et al. Expression of IL-27, Th1 and Th17 in patients with aplastic anemia. *J Clin Immunol*. (2013) 33:436–45. doi: 10.1007/s10875-012-9810-0
18. Elmahdi S, Hama A, Manabe A, Hasegawa D, Muramatsu H, Narita A, et al. A cytokine-based diagnostic program in pediatric aplastic anemia and hypocellular refractory cytopenia of childhood. *Pediatr Blood Cancer*. (2016) 63:652–8. doi: 10.1002/pbc.25799
19. Niu Q, Zhou Q, Liu Y, Jiang H. Expression of CXCR4 on T-cell subsets and plasma IL-17 concentrations in patients with aplastic anaemia. *Sci Rep*. (2017) 7:9075. doi: 10.1038/s41598-017-08699-z

Conflict of Interest: The authors declare that the research was conducted in the absence of any commercial or financial relationships that could be construed as a potential conflict of interest.

frontiers in Immunology

REVIEW
published: 23 June 2020
doi: 10.3389/fimmu.2020.01309

Congenital Hemolytic Anemias: Is There a Role for the Immune System?

*Anna Zaninoni, Elisa Fermo, Cristina Vercellati, Anna Paola Marcello, Wilma Barcellini and Paola Bianchi**

UOS Fisiopatologia delle Anemie, UOC Ematologia, Fondazione IRCCS Ca' Granda Ospedale Maggiore Policlinico, Milan, Italy

Congenital hemolytic anemias (CHAs) are a heterogeneous group of rare hereditary conditions including defects of erythrocyte membrane proteins, red cell enzymes, and disorders due to defective erythropoiesis. They are characterized by variable degree of anemia, chronic extravascular hemolysis, reduced erythrocyte life span, splenomegaly, jaundice, biliary lithiasis, and iron overload. Although few data are reported on the role of the immune system in CHAs, several immune-mediated mechanisms may be involved in the pathogenesis of these rare diseases. We reported in ∼60% of patients with hereditary spherocytosis (HS), the presence of naturally-occurring autoantibodies (NAbs) directed against different membrane proteins (α- and β-spectrin, band 3, and dematin). Positive HS subjects showed a more hemolytic pattern and NAbs were more evident in aged erythrocytes. The latter is in line with the function of NAbs in the opsonization of damaged/senescent erythrocytes and their consequent removal in the spleen. Splenectomy, usually performed to reduce erythrocyte catheresis and improve Hb levels, has different efficacy in various CHAs. Median Hb increase is 3 g/dL in HS, 1.6–1.8 g/dL in pyruvate kinase deficiency (PKD), and 1 g/dL in congenital dyserythropoietic anemias (CDA) type II. Consistently with clinical severity, splenectomy is performed in 20% of HS, 45% of CDAII, and in 60% of PKD patients. Importantly, sepsis and thrombotic events have been registered, particularly in PKD with a frequency of ∼7% for both. Furthermore, we analyzed the role of pro-inflammatory cytokines and found that interleukin 10 and interferon γ, and to a lesser extent interleukin 6, were increased in all CHAs compared with controls. Moreover, CDAII and enzymatic defects showed increased tumor necrosis factor-α and reduced interleukin 17. Finally, we reported that iron overload occurred in 31% of patients with membrane defects, in ∼60% of CDAII cases, and in up to 82% of PKD patients (defined by MRI liver iron concentration >4 mg Fe/gdw). Hepcidin was slightly increased in CHAs compared with controls and positively correlated with ferritin and with the inflammatory cytokines interleukin 6 and interferon γ. Overall the results suggest the existence of a vicious circle between chronic hemolysis, inflammatory response, bone marrow dyserythropoiesis, and iron overload.

Keywords: congenital hemolytic anemias, splenectomy, inflammation, cytokines, iron overload, naturally occurring antibodies

OPEN ACCESS

Edited by:
Mark Slevin,
Manchester Metropolitan University,
United Kingdom

Reviewed by:
Immacolata Andolfo,
University of Naples Federico II, Italy
Shelley Crary,
University of Arkansas for Medical Sciences, United States

****Correspondence:***
Paola Bianchi
paola.bianchi@policlinico.mi.it

Specialty section:
This article was submitted to Inflammation, a section of the journal Frontiers in Immunology

Received: *17 February 2020*
Accepted: *22 May 2020*
Published: *23 June 2020*

Citation:
Zaninoni A, Fermo E, Vercellati C, Marcello AP, Barcellini W and Bianchi P (2020) Congenital Hemolytic Anemias: Is There a Role for the Immune System? Front. Immunol. 11:1309. doi: 10.3389/fimmu.2020.01309

INTRODUCTION

Congenital hemolytic anemias (CHAs) are a heterogeneous group of rare hereditary conditions characterized by reduced life span and premature removal of the erythrocytes from the circulation. They comprise defects of the erythrocyte membrane proteins and of red cell enzymes metabolism, as well as alterations at the level of erythrocyte precursors, resulting in defective bone marrow erythropoiesis. The typical examples of membrane defects are hereditary spherocytosis (HS), hereditary elliptocytosis (HE), and the group of hereditary stomatocytosis (HSt). Glucose-6-phosphate dehydrogenase (G6PD) and pyruvate kinase (PK), are the most common enzyme deficiencies, and congenital dyserythropoietic anemia (CDA) type II is the best studied form among defective erythropoiesis. The role of the immune system has been poorly investigated in these conditions, at variance with the several reports in hemoglobinopathies such as sickle cell disease and thalassemia, which are beyond the scope of this review.

In this review the role of naturally-occurring autoantibodies will be discussed focusing on their ability to opsonize damaged/senescent erythrocytes that are consequently removed in the spleen. Furthermore, as splenectomy is one of the therapeutic options in these conditions, we will describe the immunological abnormalities following this procedure, with particular reference to increased infectious and thrombotic risk. Finally, given the increasing interest in the occurrence of iron overload in CHAs and consequent relevant clinical complications, we will review available literature on this topic. We will focus on the pathophysiology of iron overload which is closely linked to inflammatory cytokines and to the hepcidin pathway, which in turn is straightly linked to the immune system.

CLINICAL AND MOLECULAR FINDINGS IN CHAs

Although some hemolytic features are present also in hemoglobinopathies, the classic CHAs are characterized by chronic extravascular hemolysis, splenomegaly, jaundice, biliary lithiasis, and a variable degree of anemia and iron overload. The most relevant genetic basis of CHAs are shown in **Table 1** and more detailed description of the different forms is given in the following sections.

Red Cell Membrane Disorders

Inherited RBC membrane disorders are caused by quantitative or qualitative defects in transmembrane or cytoskeletal proteins of erythrocytes (1–3). HS is the most frequent congenital hemolytic anemia in Caucasians, with reported prevalence ranging from 1:2,000 to 1:5,000, and is characterized by a highly heterogeneous molecular defect, involving the genes coding for RBC membrane proteins *SPTA1* (α-spectrin), *SPTB* (β-spectrin), *SLC4A1* (band 3), *ANK1* (ankyrin), *EPB42* (protein 4.2). In general, these abnormalities affect the vertical interactions between phospholipid bilayer and the cytoskeleton of RBC membrane, resulting in a progressive change of the discocytes into osmotically fragile spherocytes that are recognized and sequestered by the spleen (4). HE, characterized by the presence of elliptocytes in peripheral blood smear, is more prevalent in malaria endemic regions in West Africa; it is usually an asymptomatic condition, but moderate to severe anemia may be present in ∼10% of cases (5). The severe recessive variant is hereditary pyropoikilocytosis, in which the significant membrane fragmentation and reduced surface area is mostly caused by a pathogenic mutation in *SPTA1* gene inherited *in trans* to the hypomorphic variant αLELY (Low Expression LYon) (6). In HSt the inability to regulate the cation homeostasis lead to inappropriate shrinkage (dehydrated HSt) or swelling (overhydrated HSt) of the RBCs (7–13). Finally, "Gardos cahnnelopathy" is a recently described form of HSt with some differences in the clinical phenotype and hematological features, caused by mutations in *KCNN4* gene (14–18).

Defects of Red Cell Metabolism

CHAs also occur as a consequence of RBC metabolism defects, affecting one of the three main metabolic pathways: the Embden-Myerhof pathway (glycolysis), the nucleotide metabolism, and the exose-monophosphate shunt. G6PD deficiency is the most common erythroenzymopathy, usually causing acute hemolysis during oxidative stress, with the exception of the class-I variants, which also result in chronic hemolysis (19, 20). Among the abnormalities of glycolytic enzymes, the most common is PK deficiency (PKD) (21–25), followed by glucosephosphate isomerase and hexokinase deficiency (26–29). Pyrimidine 5′-nucleotidase is the most frequent defect of nucleotide metabolism (30), whereas adenylate kinase deficicency has been reported in 12 families only (31). When the involved gene is ubiquitously expressed, the enzymopathy may be associated to extra-hematological signs such neuromuscular abnormalities, myopathy and mental retardation, as in the case of triosephosphate isomerase (32, 33), phosphoglycerate kinase deficiency (34) and phosphofructokinase deficiency (35).

Congenital Dyserythropoietic Anemias

Congenital dyserythropoietic anemias (CDA) comprise a group of rare/very rare diseases characterized by ineffective erythropoiesis and morphological abnormalities of bone marrow erythroblasts (36, 37), caused by different molecular mechanisms affecting cell maturation and division. Three major types and other more rare or sporadic variants can be classified, on the basis of the typical morphology and on the affected genes (38–40). CDA type I, caused by biallelic mutations in *CDAN1* (CDAIa) or *c15orf41* (CDAIb) genes, is characterized by the presence of 2-5% binucleated erythroblasts of different size and shape in bone marrow, chromatin bridges between nuclei, and dense heterochromatin with a "Swiss cheese" appearance when observed at electron microscopy (41). CDA type II (CDAII) is a recessive disease caused by mutations in the *SEC23B* gene (42, 43), characterized by 10–35% binucleated and multinucleated erythroblasts which present with a peripheral double membrane, and hypoglycosylation of band 3 as a biochemical hallmark. CDAIII is caused by the dominant P916R mutation of *KIF23* gene with large multinucleated erythroblasts (44), whereas E325K mutation of *KLF1* gene is responsible for

TABLE 1 | Genetic basis of congenital hemolytic anemias.

	Gene	Gene location	Function	Trasmission
RBC membrane defects				
Hereditary spherocytosis	*SPTA1*	1q23.1	Membrane skeletal network	AR
	SPTB	14q23.3	Membrane skeletal network	AD
	SLC4A1	17q21.31	Anion exchange channel Link to glycoltytic enzymes Vertical interactions	AD
	ANK1	8p11.21	Vertical interactions	AD, *de novo*
	EPB42	15q15.2	Stabilize band3/ankyrin complex	AR
Hereditary elliptocyosis	*SPTA1*	1q23.1	Membrane skeletal network	AD
	SPTB	14q23.3	Membrane skeletal network	AD
	EPB41	1p35.3	Stabilize spectrin-ankyrin contact	AD
Hereditary pyropoikylocytosis	*SPTA1/ SPTA1^{LELY}* *SPTA1/ SPTB* *SPTB/SPTB*	1q23.1	Membrane skeletal network	AR
Hereditary stomatocytosis				
Dehydrated	*PIEZO1*	16q24.3	Mechanosensitive ion channel	AD
Overhydrated	*RHAG*	6p12.3	Rh -blood group	AD
Gardos Channelopathy	*KCNN4*	19q13.31	Potassium Ca2+-Activated Channel	AD, *de novo*
RBC enzyme defects				
Glucose-6-phosphate dehydrogenase deficiency	*G6PD*	Xq28	Hexose-monophosphate shunt	X-linked
Pyruvate kinase deficiency	*PK-LR*	1q22	Glycolysis	AR
Glucosephosphate isomerase deficiency	*GPI*	19q13.11	Glycolysis	AR
Triosephosphate isomerase deficiency	*TPI1*	12p13.31	Glycolysis	AR
Hexokinase deficiency	*HK1*	10q22.1	Glycolysis	AR
Phosphofructokinase deficiency	*PFK-M* *PFK-L*	12q13.31 21q22.3	Glycolysis	AR
Phosphoglycerate kinase deficiency	*PGK1*	Xq21.1	Glycolysis	X-linked
Pyrimidine-5′-nucleotidase deficiency	*NT5C3A*	7p14.3	Nucleotide metabolism	AR
Adenylate kinase deficiency	*AK1*	9q34.11	Nucleotide metabolism	AR
Congenital dyserythropoietic anemias				
CDAI	*CDAN1* *C15ORF41*	15q15.2 15q14	Microtubule attachments Restriction endonuclease	AR
CDAII	*SEC23B*	20p11.23	Vescicle trafficking	AR
CDAIII	*KIF23*	15q23	Cytokinesis	AD
CDA variants	*GATA1*	Xp11.23	Transcription factor	X-linked
	KLF1	19p13.13	Transcriptional activator	AD

AR, Autosomic recessive; AD, Autosomic dominant.

CDAIV (45) and mutations in *GATA1* gene cause an X-linked sporadic form (46).

THE ROLE OF NATURALLY OCCURRING ANTIBODIES IN CHAs

Natural antibodies (Nabs) are circulating antibodies that, in healthy subjects, occur without known immune exposure or vaccination. They are mainly moderate affinity polyreactive IgM and are secreted by B1 cells, a subset of B cells that have been identified as $CD20^+CD27^+CD43^+$ memory B cells without activation markers (47, 48). NAbs play different roles in health and disease (49). They contribute as a first line of defense from infection of bacterial, viruses, protozoa, and fungi (50, 51). This activity is mediated by opsonisation and neutralization of the pathogens, by activation of T cell and B cell responses, and by the induction of long-term immune memory cells (52, 53). NAbs play also a crucial role in the maintenance of the immune homeostasis by recognizing apoptotic cells membrane markers and promoting the process of their phagocytic clearance (54). Moreover, there is evidence that NAbs binding to inflammatory cytokines protect

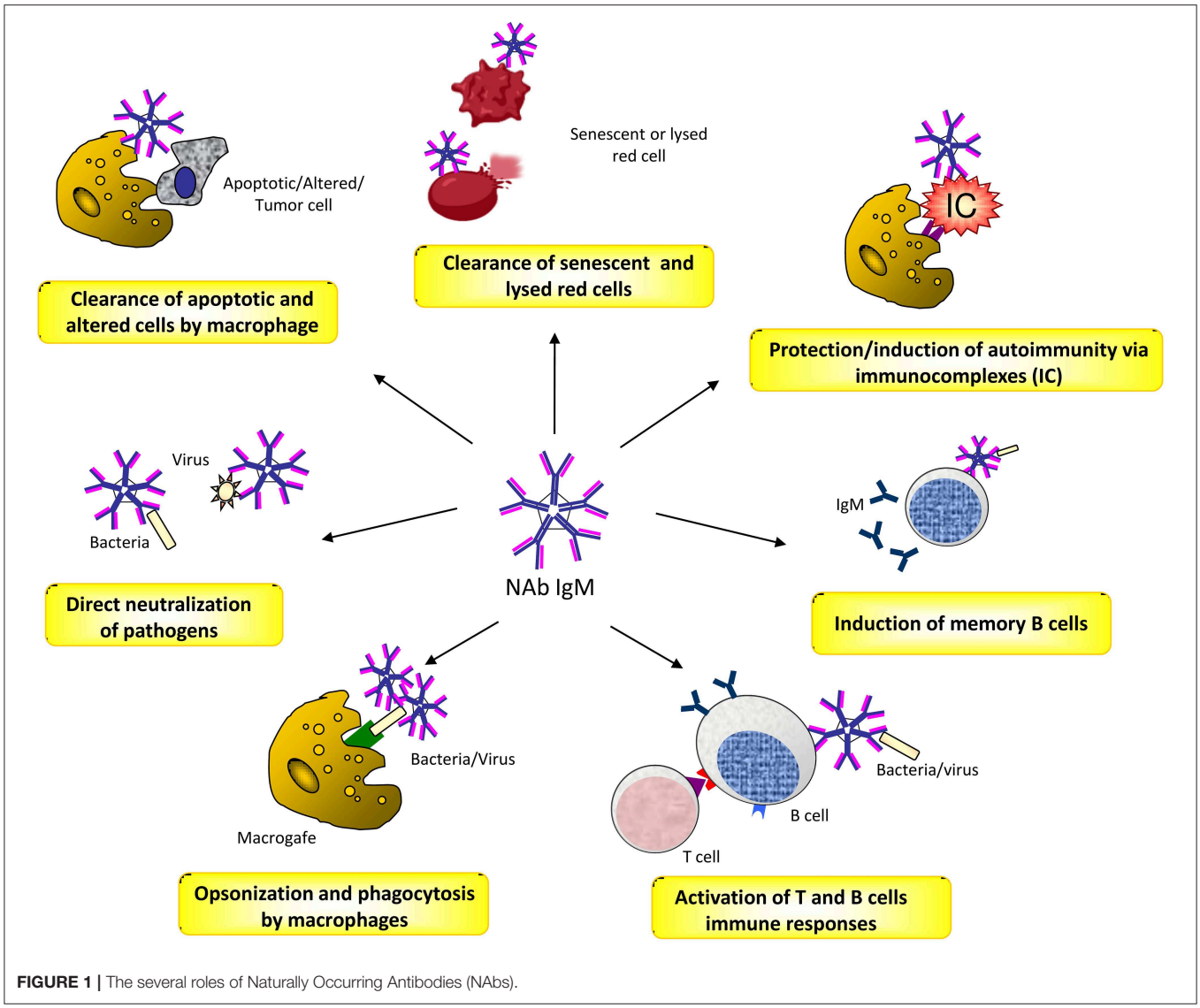

FIGURE 1 | The several roles of Naturally Occurring Antibodies (NAbs).

against improper inflammation (55). In addition, they concur to the opsonisation and removal of potentially harmful elements, thus exerting a physiologic antitumor surveillance (56). Finally, NAbs are closely related to autoimmunity, acting in a dual manner. On one hand, they prevent autoimmune disease by binding to immune-complexes and promoting their removal, or to self-antigens by increasing their exposure to immature B cells, and thus inducing tolerance (57, 58). On the other hand, in systemic autoimmune diseases, NAbs can bind to different self-molecules, such as nucleic acids, phospholipids, erythrocytes, serum proteins and cellular components, and cause disease through the formation of immune complexes (49, 59, 60) (**Figure 1**).

Regarding CHAs, NAbs anti-spectrin and anti-band 3 had been described long ago in sera from healthy subjects and in β-thalassemia patients, hypothesizing a physiologic role in the clearance of debris of lysed cells (61, 62). In particular, Reliene et al. (63) demonstrated the presence of high-affinity NAbs directed against RBCs (up to 140 molecules per cell) in band 3-deficient HS patients. Moreover, their number increased in with cell age, suggesting a possible role in removal of senescent cells. In line with these results, Zaninoni et al. (56) found that 61% of HS cases showed RBC-bound IgG positive values (up to 330 ng/mL), detected by mitogen-stimulated direct antiglobulin test (MS-DAT). The latter, is a sensitive test that may amplify autoantibody secretion, including NAbs production, through mitogen stimulation *in vitro* (64, 65). RBC-bound IgG were directed against different membrane proteins (α- and β-spectrin, band 3, and dematin) and were more evident in aged samples obtained after several days of storage at 4°C (56). As shown in **Table 2**, positive HS cases, mainly spectrin-deficient cases, had an increased number of spherocytes and showed a more hemolytic pattern (increased number of reticulocytes, unconjugated bilirubin and LDH values), suggesting that these

TABLE 2 | Hematological characteristics of HS patients divided according to MS-DAT positivity.

	MSDAT negative	MSDAT positive
Non-splenectomized		
N° patients	30	48
Hemoglobin (g/dL)	12.5 ± 2.2	12.3 ± 1.8
Spherocytes (%)	5 (2–24)	7 (1–68)
Reticulocytes $\times 10^3$/mmc	147 ± 98	278 ± 133
Unconjugated bilirubin	2.7 ± 2.3	3.0 ± 2.1
LDH (U/L)	396 ± 158	473 ± 163
Haptoglobin <20 mg/dL (N)	22/30 (73%)	43/48 (89%)
IgG bound to RBC (ng/mL)	105 ± 31	331 ± 217
Splenectomized		
N° patients	6	3
Hemoglobin (g/dL)	15 ± 0.65	13.9 ± 1.6
Spherocytes (%)	8 (5–11)	4 (3–20)
Reticulocytes $\times 10^3$/mmc	85 ± 29	95 ± 77
Unconjugated bilirubin	0.5 ± 0.17	1.5 ± 1.8
LDH (U/L)	342 ± 54	322 ± 93
Haptoglobin <20 mg/dL (N)	0/6 (0%)	2/7 (35%)
IgG bound to RBC (ng/mL)	100 ± 44	277 ± 131

Values are expressed as median (range) or mean±DS. Normal values are Hb: 13.6–16.7 g/dL; MCV 78-99 fL; reticulocytes: 16–84 × 10^3/mmc; unconjugated bilirubin <0.75 mg/dL, aptoglobin: 30–200 mg/dL; LDH: 135–214 U/L. Data obtained from Zaninoni et al. (56).

antibodies may have a pathogenic role, participating in the loss of membrane area and reduction of surface-to-volume ratio (66). This phenomenon is less evident in splenectomised patients who lack the main organ in which RBC clearance occurs. In fact, the amount of RBC-bound IgG is slightly lower in these patients compared to non-splenectomised ones. Although there is no direct evidence that RBC antibodies induced by mitogen stimulation are NAbs, their increase with RBC age, and their greater amount in more hemolytic HS subjects are in favor of this hypothesis. Altogether these findings suggest that a humoral immune response has a role in removing senescent and damaged HS cells, thus participating in the clinical picture, and severity of the disease.

THE ROLE OF THE SPLEEN AND EFFECTS OF SPLENECTOMY IN CHAs

It is well-established that the spleen is the main catheretic organ involved in the removal of damaged or abnormal red blood cells, mainly via the macrophage system. In fact, splenectomy has been suggested as a possible therapeutic approach for various hemolytic diseases including CHAs. Its efficacy greatly varies among different pathologies, being maximal in HS, moderate in red cell enzyme defects, and minimal in dyserythropoietic anemias. Autoimmune hemolytic anemia (AIHA) and immune thrombocytopenia (ITP) are two acquired autoimmune disorders were splenectomy has been the only second line therapy for many years (67, 68). In recent years, the percentage of patients with CHAs or autoimmune cytopenias subjected to this therapeutic option has progressively declined due to the availability of new drugs and to the increasing awareness of possible complications. They include short- and long-term infections by encapsulated microorganisms (*Streptococcus pneumonie, Neisseria meningitides, and Hemophilus influenza)* (69), thrombotic events and pulmonary hypertension (70, 71). The mechanism underlying thrombotic complications are poorly understood. Early thrombotic events have been related to stasis in the splenic vein remnant, increased numbers of platelets, and to large spleen size previous surgery. Additional mechanisms, under investigation, are endothelial alterations, presence of activated platelets, and increased amounts of circulating procoagulant microvescicles. Moreover, there is an interplay between the coagulation and the immune system, particularly with the complement cascade as highlighted in paroxysmal nocturnal hemoglobinuria (72).

Concerning CHAs, a large retrospective analysis reported that splenectomy has been performed in 21% of HS patients and induced a median Hb increase of 3 g/dL (from 10.8 g/dL to 13.9 g/dL) (73). After splenectomy no infectious complications have been reported in a recent meta-analysis (74). On the contrary, episodes of stroke, pulmonary emboli or pulmonary arterial hypertension have been described with an overall risk 5.6-fold higher than in non-splenectomised (71, 75–77).

Regarding PKD, Zanella et al. (21, 22) reported that 18/61 (30%) patients had been splenectomised with an amelioration of the hemoglobin levels (median Hb increase of 1.8 g/dL, range 0.4–3.4). In the more recent and larger international series of splenectomised PKD cases, Grace et al. (23) showed that 59% of patients have been splenectomised at a median age of 6.5 years (range 0.4–37.8) with a median Hb increase of 1.6 g/dL. Sepsis and thrombotic events have been registered in 7 and 8%, respectively.

Regarding HSt, splenectomy is contraindicated in both dehydrated and overhydrated types, due to the highly increased risk of thromboembolic complications. In old case reports, severe thrombotic complications after surgery have been documented in 100% of cases, of which 3 were fatal (78–80). More recently, Andolfo et al. (81) reported that Hb levels did not improve and severe thrombotic episodes occurred in 5 *PIEZO1*-mutated splenectomized cases. Moreover, Picard et al. (82) described 12 cases in which splenectomy has been performed at a median age of 24 years (range, 4–41) and before the diagnosis of DHSt. Surgery didn't ameliorate hemolysis (mean Hb level 11.2±1.9 g/dL and reticulocytes count 280 ± 134 × 10^9/L after splenectomy). Thrombotic complications occurred in all the 8 splenectomised patients with *PIEZO1* mutation, while in none of the 4 subjects with *KCNN4* mutation.

Finally, splenectomy has been described in 13/53 (25%) CDAI patients with severe anemia and mainly transfusion-dependent. Surgery has been performed mainly in adulthood (range 27–42 yrs) and 6/13 patients became transfusions-independent. However, the long follow-up performed revealed that 3 patients died, 1 of pulmonary arterial hypertension and 2 of overwhelming sepsis (83, 84). Concerning CDAII, Heimpel et al. (85) described that splenectomy has been performed in

22/48 (46%) patients at a median age of 19.9 years (range 1–50) with a median Hb improvement of about 1 g/dL, remaining below the reference values. The analysis of a larger series of 101 CDAII patients from 91 families, with a median follow-up of 23 years (range 0–65), is in line with these results (86): 40/101 cases underwent splenectomy, 16 of whom before diagnosis of CDAII, and at median age of 19 years (range 3–56). The rate of splenectomy dropped from 40 to 24% by considering only patients splenectomised after the diagnosis of CDAII, and further decreased to 7.5% by considering only the patients splenectomised in the past 15 years. The median Hb increase was 1.7 g/dL (range 1–6,7 g/dL, and splenectomy abrogated transfusion requirement in all patients but three. Information on splenectomy complications was available in 12 patients: one child had a thromboembolic event soon after surgery, and two patients had sepsis after 3 and 15 years. **Table 3** summarizes available studies on splenectomy in CHAs with the relative efficacy and safety data.

In conclusion, the efficacy of splenectomy in CHAs mainly resides in the removal of the catheretic organ. However, as the spleen plays an important role in the immune system, this therapeutic option may be accompanied by a reduction of the immune competence with possible serious consequences. To reduce their development, patient education and immediate interventions in case of febrile episodes are pivotal. Additional important prophylaxis includes continuous antimicrobial therapy and periodical re-vaccination.

CYTOKINE AND ERYTHROPOIETIN LEVELS IN CHAs

It is well-known that there is a complex interplay between hemolysis, inflammation, and erythropoiesis (87). Although intravascular hemolysis is not the main pathogenic mechanism in CHAs, it may occur in acute and severe hemolytic crisis, and results in the release of cell-free hemoglobin that has pro-inflammatory properties (88). Moreover, it is clearly demonstrated that anemia of chronic inflammatory disease is driven by alterations of several immune-regulatory cytokines. In particular, overproduction of pro-inflammatory mediators, such as interleukin (IL)1-β, tumor necrosis factor (TNF)-α, IL-6, and interferon (INF)-γ, have been reported in several conditions including autoimmune diseases, chronic kidney and pulmonary disease, cancer, and chronic infections (89). In particular, in autoimmune hemolytic anemia several abnormalities of immune regulatory cytokines have been reported: high serum levels of IL-10 and IL-12 (90) and increased IL-1α, IL-2/IL-2R, IL-6, and IL-21. In cell supernatants, the T helper (Th)-1 cytokines IL-2 and IL-12 were reported elevated, whereas IFN-γ was found reduced, and the Th-2 cytokines IL-4 and IL-13 were increased, together with elevated production of IL-6, IL-10, and IL-17 (64, 91). Moreover, AIHA patients with active hemolysis showed further reduction of IFN-γ and increased secretion of transforming growth factor (TGF)-β that favor the differentiation of a Th-17 subset, which amplifies the pro-inflammatory and autoimmune response (92). It is known that inflammatory cytokines down-regulate erythropoietin (EPO) production, thus compromising erythropoiesis, and can activate erythrophagocytosis, especially in acute inflammation (89, 93).

Regarding CHAs, little is known about cytokine levels. Barcellini et al. (94) described cytokine status and EPO levels in 52 patients with membrane or enzymatic defects and CDAII. As shown in **Figure 2**, IL-10 and IFN-γ were increased in all groups compared to age and sex matched controls, being particularly evident in membrane defects. IL-6 was increased as well, although to a lesser extent. Interestingly, CDAII and enzymatic defects showed a similar pattern regarding TNF-α and IL-17 with increased values of TNF-α and reduced levels of IL-17. Finally, EPO levels were increased in CHAs compared with controls, particularly in CDAII, possibly reflecting an attempt to compensate anemia. These alterations showed no relationship with severity of the clinical phenotype, i.e., degree of anemia and hemolysis. This was the first evaluation of cytokines in these diseases and results should be interpreted with caution due to the limited sample size and to the high inter-individual variation of the cytokine signature. However, it can be speculated that a chronic inflammation exists also in CHAs and may affect proper bone marrow compensatory erythropoiesis. Moreover, it may play a role in the complex interplay between hemolysis and iron overload.

THE VICIOUS CIRCLE OF IRON AND THE IMMUNE SYSTEM IN CHAs

It is well-recognized that iron overload (IO) occurs in hemoglobinopathies, also because of transfusion support. Complication of IO are well-described in these diseases, and include cardiac dysfunction (arrhythmia, cardiomyopathy, hemosiderosis), liver cirrhosis, liver cancer and hepatitis, metabolism dysfunction (diabetes, hypogonadism, thyroid disorders, parathyroid, and less level of adrenal glands), and delays in sexual maturity, impotence and infertility (95–97).

Occurrence of iron overload is well-documented in dyserythropoietic anemias, PKD and HSt. Russo et al. (98) reviewed data of 205 CDAII showing that 57% patients had a serum ferritin level of >500 μg/ml, of whom 15% never transfused, and a transferrin saturation (TfSat) value of about 60%. More recently, IO was reported in 45% of PKD patients, as defined by ferritin levels >1,000 μg/L or chelation. A liver iron concentration (LIC) > 4 mg Fe/gdw was observed in 82% of patients by magnetic resonance imaging (MRI), even in absence of regular transfusions (23, 99). Moreover, van Strateen et al. (100), showed that LIC ≥ 3 mg Fe/gdw was present in 71% (31/44) of patients with CHAs and LIC ≥ 7 mg Fe/gdw was present in 36% (16/44), regardless of transfusion dependency and ferritin levels >1,000 μg/L. None of the patients had cardiac iron overload. Iron overload has been also described in HSt, particularly in the DHSt form and Gardos chanellopathy, where hyperferritinemia, high transferrin saturation or clinical iron overload are very frequent (81, 82, 101). In these cases hyperferritinemia is not related to transfusions since usually

TABLE 3 | Effect of splenectomy in congenital hemolytic anemias.

	Main hematological findings	Complications	References
Hereditary Spherocytosis	Median Hb increase of 3 g/dL Normalization of reticulocytosis Decrease of unconjugated bilirubin and LDH levels	No infectious complications Thrombotic events (risk 5.6-fold higher)	(75) (76) (73) (77) (71) (74)
Dehidrated Hereditary Stomatoytosis (*PIEZO1*)	Hb amelioration in few reported cases No amelioration of Hb levels	Severe/fatal thrombotic complications (PHT, PE; priapism) Severe thrombotic events	(78) (79) (80) (81) (82)
Gardos Chanellopathy (*KCNN4*)	Amelioration of Hb levels	No thrombotic events	(81) (82)
Piryuvate Kinase deficiency	Median Hb increase of 1.6–1.8 g/dL Decrease of unconjugated bilirubin Reduction in the number of patients receiving regular transfusions	Sepsis in 7% of cases Thrombotic events in 8% of cases	(21) (22) (23)
Congenital Dyserythropoietic anemia type I	Amelioration of Hb levels Transfusion-independency in some cases	Fatal complications: 1 pulmonary arterial hypertension and 2 overwhelming sepsis	(83) (84)
Congenital Dyserythropoietic anemia type II	Hemoglobin concentration improved in all patients but remaining below reference values Decrease of bilirubin levels Median Hb increase of 1.7 g/dL Transfusion-independency in almost all cases	No infectious or thrombotic episodes Sepsis: 2 episodes Thrombotic event: 1 episode	(85) (86)

PE, pulmonary embolism; PHT, pulmonary hypertension.

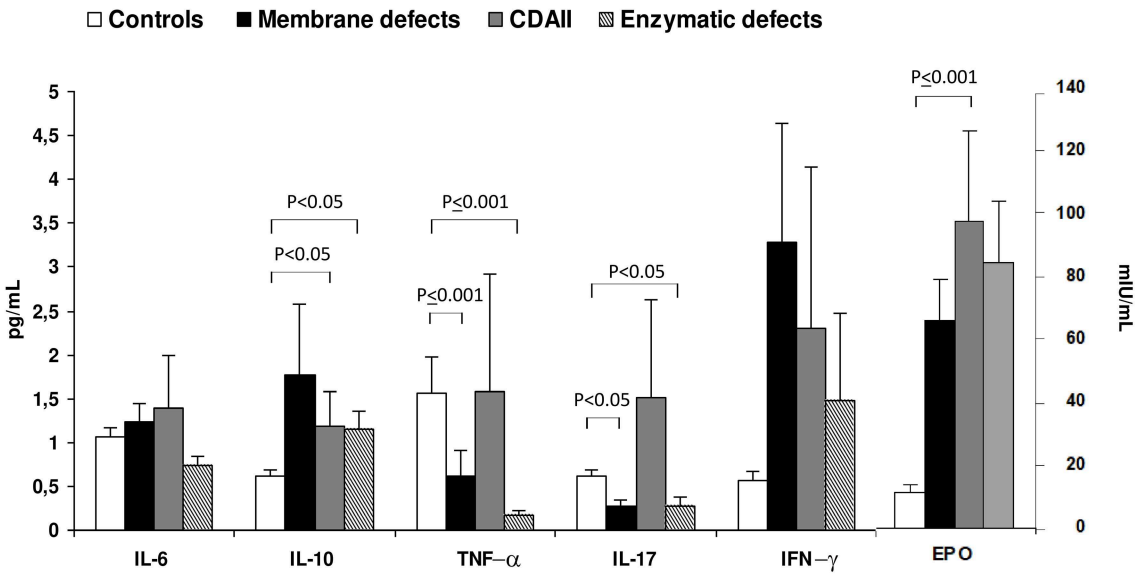

FIGURE 2 | Cytokine and erythropoietin serum levels in congenital hemolytic anemias. Values are expressed as mean±SD. Data obtained from Barcellini et al. (94).

patients are not transfused on a regular basis. Serum ferritin level up to ∼1,000 μg/L, TfSat value of about 60–70%, LIC ≥ 4 mg Fe/gdw, and cardiac T2* < 10 ms, have been described in case reports (102–105). Similar results have been reported in a large series of 126 patients were the mean±SD ferritin level at diagnosis was 764±480 μg/L (1,702 ± 1,048 μg/L in 5 *KCNN4* gene mutated cases, and 656 ± 428 μg/L in 40 *PIEZO1* mutated patients); mean liver iron content, evaluated by MRI, was 200 ± 103 μmol/g at diagnosis (82). Finally, Barcellini et al. (94) studied 52 patients with different CHAs showing that 60% of subjects had

TABLE 4 | Iron overload in congenital haemolytic anemias.

	Main hematological findings	Complications	Reference
Hereditary Spherocytosis	Median ferritin value 634 μg/L (192–1,171) ($n = 26$) Median TfSat value 36 % (23–67) Median NTBI value −0.08 μmol/L (−1.1 to 4.05) Mean ± SD hepcidin value 29.7 ± 4 ng/mL	LIC > 4 mg Fe/gdw in 8/26 cases 1 patient showed moderate cardiac IO (T2* 13 ms)	(94)
Dehidrated Hereditary Stomatoytosis (*PIEZO1*)	Ferritin value up to ∼1,000 μg/L TfSat value of ∼60–70%	LIC ≥ 4 mg Fe/gdw Cardiac IO with T2* < 10 ms	(102) (103) (105) (104)
	Mean ± SD ferritin value 656 ± 428 μg/L ($n = 40$)	Mean liver iron content, evaluated by MRI, was 200±103 μmol/g	(82)
	Median ferritin value 425 μg/L ($n = 20$)	Not reported	(81) (106)
Gardos Chanellopathy (*KCNN4*)	Mean ± SD ferritin value 1,702 ± 1,048 μg/L ($n = 5$)	Mean liver iron content, evaluated by MRI, was 200±103 μmol/g	(82)
Piruvate Kinase Deficiency	Median ferritin value 425 μg/L (182–1,605) ($n = 17$) Median TfSat value 52% (22–89) Median NTBI value 0.26 μmol/L (−0.48 to 2.37), Mean ± SD hepcidin value 15.15 ± 3 ng/mL.	LIC > 4 mg Fe/gdw in 6/17 cases. Overall prevalence of IO was 45% (82/181) as defined by ferritin or chelation; 82% (67/82) as define by LIC > 4 mg Fe/gdw	(94)
	Median ferritin value 583 ng/mL (17–5,630).	7% (5/75) of cases had cardiac IO	(99) (23)
Congenital Dyserythropoietic Anemia type II	Median ferritin value 441 μg/L (206–1,605) ($n = 9$) Median TfSat value 85% (13–92) Median NTBI value 1.07 μmol/L (0.9–2.15) Mean ± SD hepcidin value 17.6 ± 6.5 ng/mL.	LIC > 4 mg Fe/gdw in 7/9 cases 1 patient showed moderate cardiac IO (T2* 12.7 ms)	(94)
	Median ferritin value 464.8 ± 55.9 μg/L ($n = 109$) Median TfSat value of ∼60%	Not reported	(98)
	Median max ferritin value 668 μg/L (27–5,267) ($n = 98$) Median max TfSat value of 81% /20–157) ($n = 79$)	Not reported	(86)

n, number of patients; TfSat, Transferrin saturation; NTBI, Non-transferrin-bound serum iron; LIC, liver iron concentration.

ferritin values> 500 μg/L. TfSat was > 50% in 31% of patients with membrane defects, in 66% with CDAII, and in 53% with enzymopathies. Moreover, non-transferrin-bound serum iron (NTBI) serum levels were increased in CDAII and moderately augmented in enzymatic defects. By MRI, median LIC value was 3.4 mg Fe/gdw (range 1.4–16.1) and 40% of patients, almost all CDAII, had a LIC ≥4 mg Fe/gdw (**Table 4**).

Among factors possibly involved in IO, low hepcidin levels, ineffective erythropoiesis and an altered pro-inflammatory cytokine profile have been suggested to play different roles in CHAs (107–109). Ineffective erythropoiesis is probably the leading mechanism, since the greater frequency of IO is observed in CDAII, and dehydrated stomatocytosis (13, 110). In line with this hypothesis a correlation was observed between LIC and EPO levels (94). In the same series, hepcidin, the main hormone involved in the regulation of iron homeostasis, was slightly increased in CHAs compared with controls, and positively correlated with ferritin. Moreover, hepcidn positively correlated with the inflammatory cytokines IL-6 and IFN-γ, and has a direct pro-inflammatory activity (89, 93). Further evidence for the interplay between iron and inflammation comes from studies in DHSt, where hepcidin levels were decreased and erythroferrone (ERFE), the negative regulator of hepcidin, slightly increased. In patients with gain-of-function mutations in *PIEZO1*, inhibition of the bone morphogenetic proteins (BMP)/small mother against decapentaplegic (SMADs) pathway was involved in hepatic iron metabolism impairment (106). In addition, another important factor for iron balance is emojuvelin (HJV), a co-receptor of BMP that is degraded in juvenile hemochromatosis, causing severe hepcidin deficiency and iron overload. Fillebeen et al. (111) showed that HJV knocked-out mice failed to mount an

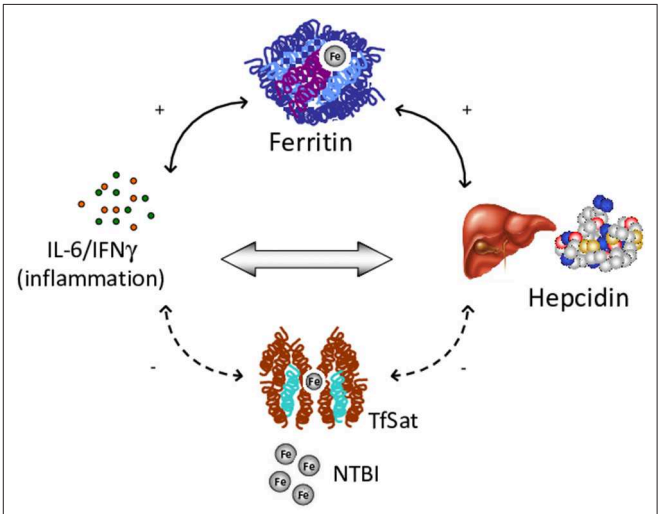

FIGURE 3 | Vicious circle among chronic hemolysis, inflammatory response and iron overload. IL, Interleukin; IFN, Interferon; TfSat, Transferrin saturation; NTBI, Non-transferrin-bound serum iron.

appropriate hypoferremic response to acute inflammation caused by lipopolysaccharide. Finally, it is well-known that hemolytic crisis in CHAs may be triggered by infectious episodes that may therefore fuel the inflammatory loop. Overall the results suggest the existence of a vicious circle between chronic hemolysis, inflammatory response and IO (**Figure 3**).

CONCLUSION

Although few data are reported on the role of the immune system in CHAs, several immune-mediated mechanisms are certainly involved in the pathogenesis of these rare diseases, namely naturally-occurring autoantibodies, spleen catheresis, overexpression of inflammatory cytokines, and iron overload. Regarding the first, naturally-occurring autoantibodies have a function in the opsonization of damaged/senescent erythrocytes and consequently further increase of their removal in the spleen, participating in the clinical picture and severity of the disease. Furthermore, splenectomy is performed in CHAs with variable degree of efficacy related to reduction of erythrocyte catheresis. However, it is important to remind that spleen is part of the immune system and its removal is associated with a variable immune deficiency, infections, and a higher thrombotic risk. Regarding the third mechanism, there is undoubtedly a role for pro-inflammatory cytokines in perpetuating chronic inflammation, which in turn may affect proper bone marrow compensatory erythropoiesis. This may account for a vicious circle among low-grade chronic inflammation, chronic hemolysis, and increased production of hepcidin, resulting in iron overload in a considerable and underestimated proportion of CHAs.

AUTHOR CONTRIBUTIONS

AZ, EF, WB, and PB prepared the manuscript. CV and AM critically revised the manuscript. All authors contributed to the article and approved the submitted version.

FUNDING

This study was supported by Fondazione IRCCS Ca' Granda Policlinico Milano, Project number RC 175/04, 2019.

REFERENCES

1. Perrotta S, Gallagher PG, Mohandas N. Hereditary spherocytosis. *Lancet*. (2008) 372:1411–26. doi: 10.1016/S0140-6736(08)61588-3
2. Narla J, Mohandas N. Red cell membrane disorders. *Int J Lab Hematol*. (2017) 39:47–52. doi: 10.1111/ijlh.12657
3. Iolascon A, Andolfo I, Russo R. Advances in understanding the pathogenesis of red cell membrane disorders. *Br J Haematol*. (2019) 187:13–24. doi: 10.1111/bjh.16126
4. Mohandas N, Gallagher PG. Red cell membrane: Past, present, and future. *Blood*. (2008) 112:3939–48. doi: 10.1182/blood-2008-07-161166
5. Niss O, Chonat S, Dagaonkar N, Almansoori MO, Kerr K, Rogers ZR, et al. Genotype-phenotype correlations in hereditary elliptocytosis and hereditary pyropoikilocytosis. *Blood Cells Mol Dis*. (2016) 61:4–9. doi: 10.1016/j.bcmd.2016.07.003
6. Al-Riyami AZ, Iolascon A, Al-Zadjali S, Andolfo I, Al-Mammari S, Manna F, et al. Targeted next generation sequencing identifies a novel β-spectrin gene mutation A2059P in two Omani children with hereditary pyropoikilocytosis. *Am J Hematol*. (2017) 92:E607–9. doi: 10.1002/ajh.24853
7. Iolascon A, Stewart GW, Ajetunmobi JF, Perrotta S, Delaunay J, Carella M, et al. Familial pseudohyperkalemia maps to the same locus as dehydrated hereditary stomatocytosis (hereditary xerocytosis). *Blood*. (1999) 93:3120–23.
8. Grootenboer S, Schischmanoff PO, Laurendeau I, Cynober T, Tchernia G, Dommergues JP, et al. Pleiotropic syndrome of dehydrated hereditary stomatocytosis, pseudohyperkalemia, and perinatal edema maps to 16q23-q24. *Blood*. (2000) 96:2599–605.
9. Bruce LJ, Guizouarn H, Burton NM, Gabillat N, Poole J, Flatt JF, et al. The monovalent cation leak in overhydrated stomatocytic red blood cells results from amino acid substitutions in the Rh-associated glycoprotein. *Blood*. (2009) 113:1350–7. doi: 10.1182/blood-2008-07-171140
10. Zarychanski R, Schulz VP, Houston BL, Maksimova Y, Houston DS, Smith B, et al. Mutations in the mechanotransduction protein PIEZO1 are associated with hereditary xerocytosis. *Blood*. (2012) 120:1908–15. doi: 10.1182/blood-2012-04-422253
11. Andolfo I, Alper SL, De Franceschi L, Auriemma C, Russo R, De Falco L, et al. Multiple clinical forms of dehydrated hereditary stomatocytosis arise from mutations in PIEZO1. *Blood*. (2013) 121:3925–35. doi: 10.1182/blood-2013-02-482489
12. Albuisson J, Murthy SE, Bandell M, Coste B, Louis-Dit-Picard H, Mathur J, et al. Dehydrated hereditary stomatocytosis linked to gain-of-function mutations in mechanically activated PIEZO1 ion channels. *Nat Commun*. (2013) 4:1884. doi: 10.1038/ncomms2899 Erratum in: Nat. Commun. 2013; 4, 2440.
13. Moura PL, Hawley BR, Dobbe JGG, Streekstra GJ, Rab MAE, Bianchi P. PIEZO1 gain-of-function mutations delay reticulocyte maturation in hereditary xerocytosis. *Haematologica*. (2020) 105:e268–71. doi: 10.3324/haematol.2019.231159
14. Andolfo I, Russo R, Manna F, Shmukler BE, Gambale A, Vitiello G, et al. Novel Gardos channel mutations linked to dehydrated hereditary stomatocytosis (xerocytosis). *Am J Hematol*. (2015) 90:921–916. doi: 10.1002/ajh.24117
15. Rapetti-Mauss R, Lacoste C, Picard V, Guitton C, Lombard E, Loosveld M, et al. A mutation in the Gardos channel is associated with hereditary xerocytosis. *Blood*. (2015) 126:1273–80. doi: 10.1182/blood-2015-04-642496
16. Glogowska E, Lezon-Geyda K, Maksimova Y, Schulz VP, Gallagher PG. Mutations in the Gardos channel (KCNN4) are associated with hereditary xerocytosis. *Blood*. (2015) 126:1281–4. doi: 10.1182/blood-2015-07-657957
17. Rivera A, Vandorpe DH, Shmukler BE, Andolfo I, Iolascon A, Archer NM, et al. Erythrocyte ion content and dehydration modulate maximal Gardos channel activity in KCNN4 V282M/+ Hereditary Xerocytosis (HX) red cells. *Am J Physiol Cell Physiol*. (2019) 317:C287–302. doi: 10.1152/ajpcell.00074.2019
18. Fermo E, Bogdanova A, Petkova-Kirova P, Zaninoni A, Marcello AP, Makhro A, et al. 'Gardos Channelopathy': a variant of hereditary Stomatocytosis with complex molecular regulation. *Sci Rep*. (2017) 7:1744. doi: 10.1038/s41598-017-01591-w
19. Beutler E. (2001). Glucose-6-phosphate dehydrogenase deficiency and other red cell enzyme abnormalities. In: Beutler E, Lichtman MA, Coller BS, et al., editors. *Williams Hematology*, 6th ed. New York, NY: McGraw-Hill, Ed. 2001. p. 527–547.
20. Mason PJ, Bautista JM, Gilsanz F. G6PD deficiency: the genotype-phenotype association. *Blood Rev*. (2007) 21:267–83. doi: 10.1016/j.blre.2007.05.002

21. Zanella A, Fermo E, Bianchi P, Valentini G. Red cell pyruvate kinase deficiency: molecular and clinical aspects. *Br J Hematol.* (2005) 130:11–25. doi: 10.1111/j.1365-2141.2005.05527.x
22. Zanella A, Fermo E, Bianchi P, Chiarelli LR, Valentini G. Pyruvate kinase deficiency: the genotype-phenotype association. *Blood Rev.* (2007) 21:217–31. doi: 10.1016/j.blre.2007.01.001
23. Grace RF, Bianchi P, van Beers EJ, Eber SW, Glader B, Yaish HM, et al. Clinical spectrum of pyruvate kinase deficiency: data from the Pyruvate Kinase Deficiency Natural History Study. *Blood.* (2018) 131:2183–92. doi: 10.1182/blood-2017-10-810796
24. Grace RF, Glader B. Red blood cell enzyme disorders. *Pediatr Clin North Am.* (2018) 65:579–95. doi: 10.1016/j.pcl.2018.02.005
25. Bianchi P, Fermo E, Lezon-Geyda K, van Beers E, Morton DH, Barcellini W, et al. Genotype-phenotype correlation molecular heterogeneity in pyruvate kinase deficiency. *Am J Hematol.* (2020) 95:472–82. doi: 10.1002/ajh.25753
26. Prchal JT, and Gregg XT. Red cell enzymes. *Am Soc Hematol Educ Program.* (2005) 2005:19–23. doi: 10.1182/asheducation-2005.1.19
27. van Wijk R, van Solinge WW. The energy-less red blood cell is lost: erythrocyte enzyme abnormalities of glycolysis. *Blood.* (2005) 106:4034–42. doi: 10.1182/blood-2005-04-1622
28. Koralkova P, van Solinge WW, van Wijk R. Rare hereditary red blood cell enzymopathies associated with hemolytic anemia - pathophysiology, clinical aspects, and laboratory diagnosis. *Int J Lab Hematol.* (2014) 36:388–97. doi: 10.1111/ijlh.12223
29. Fermo E, Vercellati C, Marcello AP, Zaninoni A, Aytac S, Cetin M, et al. Clinical and molecular spectrum of glucose-6-phosphate isomerase deficiency. report of 12 new cases. *Front Physiol.* (2019) 10:467. doi: 10.3389/fphys.2019.00467
30. Zanella A, Bianchi P, Fermo E, Valentini G. Hereditary pyrimidine 5′-nucleotidase deficiency: from genetics to clinical manifestations. *Br J Hematol.* (2006) 133:113–23. doi: 10.1111/j.1365-2141.2006.05992.x
31. Abrusci P, Chiarelli LR, Galizzi A, Fermo E, Bianchi P, Zanella A, et al. Erythrocyte adenylate kinase deficiency: characterization of recombinant mutant forms and relationship with nonspherocytic hemolytic anemia. *Exp Hematol.* (2007) 35:1182–9. doi: 10.1016/j.exphem.2007.05.004
32. Orosz F, Oláh J, Ovádi J. Triosephosphate isomerase deficiency: new insights into an enigmatic disease. *Biochim Biophys Acta.* (2009) 1792:1168–74. doi: 10.1016/j.bbadis.2009.09.012
33. Fermo E, Bianchi P, Vercellati C, Rees DC, Marcello AP, Barcellini W, et al. Triose phosphate isomerase deficiency associated with two novel mutations in TPI gene. *Eur J Hematol.* (2010) 85:170–3. doi: 10.1111/j.1600-0609.2010.01451.x
34. Beutler E. PGK deficiency. *Br J Hematol.* (2007) 136:3–11. doi: 10.1111/j.1365-2141.2006.06351.x
35. Nakajima H, Raben N, Hamaguchi T, Yamasaki T. Phosphofructokinase deficiency: past, present and future. *Curr Mol Med.* (2002) 2:197–212. doi: 10.2174/1566524024605734
36. Iolascon A, Russo R, Delaunay J. Congenital dyserythropoietic anemias. *Curr Opin Hematol.* (2011) 18:146–51. doi: 10.1097/MOH.0b013e32834521b0
37. Gambale A, Iolascon A, Andolfo I, Russo R. Diagnosis and management of congenital dyserythropoietic anemias. *Expert Rev Hematol.* (2016) 9:283–96. doi: 10.1586/17474086.2016.1131608
38. Heimpel H, Kellermann K, Neuschwander N, Hogel J, Schwarz K. The morphological diagnosis of congenital dyserythropoietic anemia: results of a quantitative analysis of peripheral blood and bone marrow cells. *Hematologica.* (2010) 95:1034–6. doi: 10.3324/haematol.2009.014563
39. Iolascon A, Esposito MR, Russo R. Clinical aspects and pathogenesis of congenital dyserythropoietic anemias: from morphology to molecular approach. *Hematologica.* (2012) 97:1786–94. doi: 10.3324/haematol.2012.072207
40. Heimpel H. Congenital dyserythropoietic anemias: epidemiology, clinical significance, and progress in understanding their pathogenesis. *Ann Hematol.* (2004) 83:613–21. doi: 10.1007/s00277-004-0892-5
41. Tamary H, Dgany O, Proust A, Krasnov T, Avidan N, Eidelitz-Markus T, et al. Clinical molecular variability in congenital dyserythropoietic anemia type I. *Br J Hematol.* (2005) 130:628–34. doi: 10.1111/j.1365-2141.2005.05642.x
42. Bianchi P, Fermo E, Vercellati C, Boschetti C, Barcellini W, Iurlo A, et al. Congenital dyserythropoietic anemia type II (CDAII) is caused by mutations in the SEC23B gene. *Hum Mutat.* (2009) 30:1292–8. doi: 10.1002/humu.21077
43. Schwarz K, Iolascon A, Verissimo F, Trede NS, Horsley W, Chen W, et al. Mutations affecting the secretory COPII coat component SEC23B cause congenital dyserythropoietic anemia type II. *Nat Genet.* (2009) 41:936–40. doi: 10.1038/ng.405
44. Liljeholm M, Irvine AF, Vikberg *AL, Norberg A, Month S, Sandström H, et al.* Congenital dyserythropoietic anemia type III (CDA III) is caused by a mutation in kinesin family member, KIF23. *Blood.* (2013) 121:4791–9. doi: 10.1182/blood-2012-10-461392
45. Arnaud L, Saison C, Helias V, Lucien N, Steschenko D, Giarratana MC, et al. A dominant mutation in the gene encoding the erythroid transcription factor KLF1 causes a congenital dyserythropoietic anemia. *Am J Hum Genet.* (2010) 87:721–7. doi: 10.1016/j.ajhg.2010.10.010
46. Nichols KE, Crispino JD, Poncz M, White JG, Orkin SH, Maris JM, et al. Familial dyserythropoietic anemia and thrombocytopenia due to an inherited mutation in GATA1. *Nat Genet.* (2000) 24:266–70. doi: 10.1038/73480
47. Griffin DO, Holodick NE, Rothstein TL. Human B1 cells in umbilical cord and adult peripheral blood express the novel phenotype CD20+ CD27+ CD43+ CD70. *J Exp Med.* (2011) 208:67–80. doi: 10.1084/jem.20101499
48. Yoshimoto M. The ontogeny of murine B-1a cells. *Int. J. Hematol.* (2020) 111:622–7. doi: 10.1007/s12185-019-02787-8
49. Ehrenstein MR, Notley CA. The importance of natural IgM: scavenger, protector and regulator. *Nat Rev Immunol.* (2010) 10:778–86. doi: 10.1038/nri2849
50. Ochsenbein AF, Fehr T, Lutz C, Suter M, Brombacher F, Hengartner H, et al. Control of early viral and bacterial distribution and disease by natural antibodies. *Science.* (1999) 286:2156–9. doi: 10.1126/science.286.5447.2156
51. Zhou ZH, Zhang Y, Hu YF, Wahl LM, Cisar JO, Notkins AL. The broad antibacterial activity of the natural antibody repertoire is due to polyreactive antibodies. *Cell Host Microbe.* (2007) 1:51–61. doi: 10.1016/j.chom.2007.01.002
52. Fernandez Gonzalez S, Jayasekera JP, Carroll MC. Complement and natural antibody are required in the long-term memory response to influenza virus. *Vaccine.* (2008) 26:I86–93. doi: 10.1016/j.vaccine.2008.11.057
53. Rapaka RR, Ricks DM, Alcorn JF, Chen K, Khader SA, Zheng M, et al. Conserved natural IgM antibodies mediate innate and adaptive immunity against the opportunistic fungus Pneumocystis murina. *J Exp Med.* (2010) 207:2907–19. doi: 10.1084/jem.20100034
54. Chen Y, Park YB, Patel E, Silverman GJ. IgM antibodies to apoptosis-associated determinants recruit C1q and enhance dendritic cell phagocytosis of apoptotic cells. *J Immunol.* (2009) 182:6031–43. doi: 10.4049/jimmunol.0804191
55. Wildbaum G, Nahir MA, Karin N. Beneficial autoimmunity to proinflammatory mediators restrains the consequences of self-destructive immunity. *Immunity.* (2003) 19:679–88. doi: 10.1016/s1074-7613(03)00291-7
56. Zaninoni A, Vercellati C, Imperiali FG, Marcello AP, Fattizzo B, Fermo E, et al. Detection of red blood cell antibodies in mitogen-stimulated cultures from patients with hereditary spherocytosis. *Transfusion.* (2015) 55:2930–8. doi: 10.1111/trf.13257
57. Anania C, Gustafsson T, Hua X, Su J, Vikstrom M, de Faire U, et al. Increased prevalence of vulnerable atherosclerotic plaques and low levels of naturalIgM antibodies against phosphorylcholine in patients with systemic lupus erythematosus. *Arthritis Res Ther.* (2010) 12:R214. doi: 10.1186/ar3193
58. Mehrani T, Petri M. IgM Anti-β2 glycoprotein i is protective against lupus nephritis and renal damage in systemic lupus erythematosus. *J Rheumatol.* (2011) 38:450–3. doi: 10.3899/jrheum.100650
59. Boes M, Schmidt T, Linkemann K, Beaudette BC, Marshak-Rothstein A, Chen J. Accelerated development of IgG autoantibodies and autoimmune disease in the absence of secreted IgM. *Proc Natl Acad Sci USA.* (2000) 97:1184–9. doi: 10.1073/pnas.97.3.1184
60. Ehrenstein MR, Cook HT, Neuberger MS. Deficiency in serum immunoglobulin (Ig)M predisposes to development of IgG autoantibodies. *J Exp Med.* (2000) 191:1253–8. doi: 10.1084/jem.191.7.1253

61. Lutz HU, Wipf G. Naturally occurring autoantibodies to skeletal proteins from human red blood cells. *J Immunol.* (1982) 128:1695–9.
62. Lutz HU, Flepp R, Stammler P, Baccalà R. Red cell associated, naturally occurring anti-spectrin antibodies. *Clin Exp Immunol*. (1987) 67:674–6.
63. Reliene R, Mariani M, Zanella A, Reinhart WH, Ribeiro ML, del Giudice EM, et al. Splenectomy prolongs *in vivo* survival of erythrocytes differently in spectrin/ankyrin- and band 3-deficient hereditary spherocytosis. *Blood*. (2002) 100:2208–15.
64. Barcellini W, Clerici G, Montesano R, Taioli E, Morelati F, Rebulla P, et al. *In vitro* quantification of anti-red blood cell antibody production in idiopathic autoimmune hemolytic anemia: effect of mitogen and cytokine stimulation. *Br J Hematol.* (2000) 111:452–60. doi: 10.1046/j.1365-2141.2000.02380.x
65. Barcellini W, Revelli N, Imperiali FG, Villa MA, Manera MC, Paccapelo C, et al. Comparison of traditional methods mitogen-stimulated direct antiglobulin test for detection of anti-red blood cell autoimmunity. *Int J Hematol*. (2010) 91:762–9. doi: 10.1007/s12185-010-0578-9
66. Da Costa L, Mohandas N, Sorette M, Grange MJ, Tchernia G, Cynober T. Temporal differences in membrane loss lead to distinct reticulocyte features in hereditary spherocytosis and in immune hemolytic anemia. *Blood*. (2001) 98:2894–9. doi: 10.1182/blood.v98.10.2894
67. Jäger U, Barcellini W, Broome CM, Gertz MA, Hill A, Hill QA, et al. Diagnosis and treatment of autoimmune hemolytic anemia in adults: recommendations from the first International Consensus Meeting. *Blood Rev*. (2020) 41:100648. doi: 10.1016/j.blre.2019.100648
68. Chaturvedi S, Arnold DM, McCrae KR. Splenectomy for immune thrombocytopenia: down but not out. *Blood.* (2018) 131:1172–82. doi: 10.1182/blood-2017-09-742353
69. Bisharat N, Omari H, Lavi I, Raz R. Risk of infection death among post-splenectomy patients. *J Infect*. (2001) 43:182–6. doi: 10.1053/jinf.2001.0904
70. Crary SE, Buchanan GR. Vascular complications after splenectomy for hematologic disorders. *Blood.* (2009) 114:2861–8. doi: 10.1182/blood-2009-10-251439
71. Crary SE, Ramaciotti C, Buchanan GR. Prevalence of pulmonary hypertension in hereditary spherocytosis. *Am J Hematol.* (2011) 86:E73–E76. doi: 10.1002/ajh.22182
72. Hill A, Kelly RJ, Hillmen P. Thrombosis in paroxysmal nocturnal hemoglobinuria. *Blood.* (2013) 121:4985–96. doi: 10.1182/blood-2012-09-311381
73. Mariani M, Barcellini W, Vercellati C, Marcello AP, Fermo E, Pedotti P, et al. Clinical and hematologic features of 300 patients affected by hereditary spherocytosis grouped according to the type of the membrane protein defect. *Hematologica*. (2008) 93:1310–7. doi: 10.3324/haematol.12546
74. Guizzetti L. Total versus partial splenectomy in pediatric hereditary spherocytosis: a systematic review and meta-analysis. *Pediatr Blood Cancer*. (2016) 63:1713–22. doi: 10.1002/pbc.26106
75. Schilling RF. Spherocytosis, splenectomy, strokes, and heat attacks. *Lancet*. (1997) 350:1677–8. doi: 10.1016/s0140-6736(05)64276-6
76. Jardine DL, Laing AD. Delayed pulmonary hypertension following splenectomy for congenital spherocytosis. *Intern Med J.* (2004) 34:214–6. doi: 10.1111/j.1444-0903.2004.00580.x
77. Schilling RF, Gangnon RE, Traver MI. Delayed adverse vascular events after splenectomy in hereditary spherocytosis. *J Thromb Hemost.* (2008) 6:1289–95. doi: 10.1111/j.1538-7836.2008.03024.x
78. Stewart GW, Amess JA, Eber SW, Kingswood C, Lane PA, Smith BD, et al. Thrombo-embolic disease after splenectomy for hereditary stomatocytosis. *Br J Haematol.* (1996) 93:303–10.
79. Perel Y, Dhermy D, Carrere A, Chateil JF, Bondonny JM, Micheau M, et al. Portal vein thrombosis after splenectomy for hereditary stomatocytosis in childhood. *Eur J Pediatr*. (1999) 158:628–30. doi: 10.1007/s004310051165
80. Jaïs X, Till SJ, Cynober T, Ioos V, Garcia G, Tchernia G, et al. An extreme consequence of splenectomy in dehydrated hereditary stomatocytosis: gradual thromboembolic pulmonary hypertension and lungheart transplantation. *Hemoglobin.* (2003) 27:139–47. doi: 10.1081/hem-120023377
81. Andolfo I, Russo R, Gambale A, Iolascon A. Hereditary stomatocytosis: an underdiagnosed condition. *Am J Hematol.* (2018) 93:107–21. doi: 10.1002/ajh.24929
82. Picard V, Guitton C, Thuret I, Rose C, Bendelac L, Ghazal KL, et al. Clinical and biological features in PIEZO1-hereditary xerocytosis and gardos channelopathy: a retrospective series of 126 patients. *Haematologica.* (2019) 104:1554–64; doi: 10.3324/haematol.2018.205328
83. Heimpel H, Schwarz K, Ebnöther M, Goede JS, Heydrich D, Kamp T, et al. Congenital dyserythropoietic anemia type I (CDA I): molecular genetics, clinical appearance, and prognosis based on long-term observation. *Blood.* (2006) 107:334–40. doi: 10.1182/blood-2005-01-0421
84. Shalev H, Al-Athamen K, Levi I, Levitas A, Tamary H. Morbidity and mortality of adult patients with congenital dyserythropoietic anemia type I. *Eur J Hematol.* (2017) 98:13–8. doi: 10.1111/ejh.12778
85. Heimpel H, Anselstetter V, Chrobak L, Denecke J, Einsiedler B, Gallmeier K, et al. Congenital dyserythropoietic anemia type II: epidemiology, clinical appearance, and prognosis based on long-term observation. *Blood.* (2003) 102:4576–81. doi: 10.1182/blood-2003-02-0613
86. Bianchi P, Schwarz K, Högel J, Fermo E, Vercellati C, Grosse R, et al. Analysis of a cohort of 101 CDAII patients: description of 24 new molecular variants and genotype-phenotype correlations. *Br J Haematol.* (2016) 175:696–704. doi: 10.1111/bjh.14271
87. Pradhan P, Vijayan V, Gueler F, Immenschuh S. Interplay of heme with macrophages in homeostasis and inflammation. *Int J Mol Sci.* (2020) 21:740. doi: 10.3390/ijms21030740
88. Silva JAF, Gotardo ÉMF, Chweih H, Miguel LI, Ferreira WA Jr, Hedlund B, et al. Didox (3,4-dihydroxybenzohydroxamic acid) reduces the vascular inflammation induced by acute intravascular hemolysis. *Blood Cells Mol Dis.* (2020) 81:102404. doi: 10.1016/j.bcmd.2020.102404
89. Ganz T. Anemia of inflammation. *N Engl J Med.* (2019) 381:1148–57. doi: 10.1056/NEJMra1804281
90. Ahmad E, Elgohary T, Ibrahim H. Naturally occurring regulatory T cells interleukins 10 12 in the pathogenesis of idiopathic warm autoimmune hemolytic anemia. *J Investig Allergol Clin Immunol*. (2011) 21:297–304.
91. Toriani-Terenzi C, Fagiolo E. IL-10 and the cytokine network in the pathogenesis of human autoimmune hemolytic anemia. *Ann N Y Acad Sci.* (2005) 1051:29–44. doi: 10.1196/annals.1361.044
92. Xu L, Zhang T, Liu Z, Li Q, Xu Z, Ren T. Critical role of Th17 cells in development of autoimmune hemolytic anemia. *Exp Hematol.* (2012) 40:994–1004. doi: 10.1016/j.exphem.2012.08.008
93. Weiss G, Goodnough LT. Anemia of chronic disease. *N Engl J Med.* (2005) 352:1011–23. doi: 10.1056/NEJMra041809
94. Barcellini W, Zaninoni A, Gregorini AI, Soverini G, Duca L, Fattizzo B, et al. Iron overload in congenital haemolytic anaemias: role of hepcidin and cytokines and predictive value of ferritin and transferrin saturation. *Br J Haematol.* (2019) 185:523–31. doi: 10.1111/bjh.15811
95. Shander A, Cappellini. M. D., and Goodnough LT. Iron overload and toxicity: the hidden risk of multiple blood transfusions. *Vox Sang.* (2009) 97:185–97. doi: 10.1111/j.1423-0410.2009.01207.x
96. Rifkind JM, Mohanty JG, Nagababu E. The pathophysiology of extracellular hemoglobin associated with enhanced oxidative reactions. *Front Physiol.* (2015) 5:500. doi: 10.3389/fphys.2014.00500
97. Pilo F, Angelucci EA. Storm in the niche: iron, oxidative stress and hemopoiesis. *Blood Rev*. (2018) 32:29–35. doi: 10.1016/j.blre.2017.08.005
98. Russo R, Gambale A, Langella C, Andolfo I, Unal S, Iolascon A. Retrospective cohort study of 205 cases with congenital dyserythropoietic anemia type II: definition of clinical and molecular spectrum and identification of new diagnostic scores. *Am J Hematol.* (2014) 89:E169–75. doi: 10.1002/ajh.23800
99. van Beers EJ, van Straaten S, Morton DH, Barcellini W, Eber SW, Glader B, et al. Prevalence and management of iron overload in pyruvate kinase deficiency: report from the Pyruvate Kinase Deficiency Natural History Study. *Hematologica.* (2018) 104:e51–e53. doi: 10.3324/haematol.2018.196295
100. van Straaten S, Biemond BJ, Kerkhoffs JL, Gitz-Francois J, van Wijk R, van Beers EJ. Iron overload in patients with rare hereditary hemolytic anemia: evidence-based suggestion on whom and how to screen. *Am J of Hematol.* (2018) 93:E374–6. doi: 10.1002/ajh.25251
101. Andolfo I, Russo R, Rosato BE, Manna F, Gambale A, Brugnara C, et al. Genotype-phenotype correlation and risk stratification in a cohort

of 123 hereditary stomatocytosis patients. *Am J Hematol.* (2018) 93:1509–17. doi: 10.1002/ajh.25276
102. Syfuss PY, Ciupea A, Brahimi S, Cynober T, Stewart GW, Grandchamp B, et al. Mild dehydrated hereditary stomatocytosis revealed by marked hepatosiderosis. *Clin Lab Haematol.* (2006) 28:270–4. doi: 10.1111/j.1365-2257.2006.00774.x
103. Assis RA, Kassab C, Seguro FS, Costa FF, Silveira PA, Wood J, et al. Iron overload in a teenager with xerocytosis: the importance of nuclear magnetic resonance imaging. *Einstein (São Pãulo).* (2013) 11:528–32. doi: 10.1590/s1679-45082013000400022
104. Orvain C, Da Costa L, Van Wijk R, Pissard S, Picard V, Mansour-Hendili L, et al. Inherited or acquired modifiers of iron status may dramatically affect the phenotype in dehydrated hereditary stomatocytosis. *Eur J Haematol.* (2018) 101:566–9. doi: 10.1111/ejh.13135
105. Fermo E, Vercellati C, Marcello AP, Zaninoni A, van Wijk R, Mirra N, et al. Hereditary xerocytosis due to mutations in PIEZO1 gene associated with heterozygous pyruvate kinase deficiency and beta-thalassemia trait in two unrelated families. *Case Rep Hematol.* (2017) 2017:2769570. doi: 10.1155/2017/2769570
106. Andolfo I, Rosato BE, Manna F, De Rosa G, Marra R, Gambale A, et al. Gain-of-function mutations in PIEZO1 directly impair hepatic iron metabolism via the inhibition of the BMP/SMADs pathway. *Am J Hematol.* (2020) 95:188–97. doi: 10.1002/ajh.25683
107. Chuncharunee S, Archararit N, Hathirat P, Udomsubpayakul U, Atichartakarn V. Levels of serum interleukin-6 and tumor necrosis factor in postsplenectomized thalassemic patients. *J Med Assoc Thai.* (1997) 80:S86–S91.
108. Baharlou R, Davami MH, Ahmadi Vasmehjani A, Ebrahimi M. Increased IL-17 and TGF-b serum levels in peripheral blood of patients with b-thalassemia major: implication for continual transfusions role in T helper17-mediated proinflammatory responses. *Turk J Med Sci.* (2016) 46:749–55. doi: 10.3906/sag-1409-57
109. Camaschella C, Nai A. Ineffective erythropoiesis and regulation of iron status in iron loading anemias. *Br J Hematol.* (2016) 172:512–23. doi: 10.1111/bjh.13820
110. Caulier A, Jankovsky N, Demont Y, Ouled-Haddou H, Demagny J, Guitton C, et al. PIEZO1 activation delays erythroid differentiation of normal and Hereditary Xerocytosis-derived human progenitors. *Haematologica.* (2020) 105:610–22. doi: 10.3324/haematol.2019.218503
111. Fillebeen C, Wilkinson N, Charlebois E, Katsarou A, Wagner J, Pantopoulos K. Hepcidin-mediated hypoferremic response to acute inflammation requires a threshold of Bmp6/Hjv/Smad signaling. *Blood.* (2018) 132:1829–41. doi: 10.1182/blood-2018-03-841197

Conflict of Interest: The authors declare that the research was conducted in the absence of any commercial or financial relationships that could be construed as a potential conflict of interest.

frontiers in Immunology

ORIGINAL RESEARCH
published: 30 June 2020
doi: 10.3389/fimmu.2020.01370

Identification of a Heme Activation Site on the MD-2/TLR4 Complex

John D. Belcher[1], Ping Zhang[1], Julia Nguyen[1], Zachary M. Kiser[1], Karl A. Nath[2], Jianjun Hu[3], John O. Trent[4] and Gregory M. Vercellotti[1]*

[1] Division of Hematology, Oncology and Transplantation, Department of Medicine, University of Minnesota, Minneapolis, MN, United States, [2] Division of Nephrology and Hypertension, Mayo Clinic, Rochester, MN, United States, [3] College of Engineering and Computing, University of South Carolina, Columbia, SC, United States, [4] Departments of Medicine, and Biochemistry and Molecular Genetics, James Graham Brown Cancer Center, University of Louisville, Louisville, KY, United States

Myeloid differentiation factor-2 (MD-2) binds lipopolysaccharide (LPS) and initiates toll-like receptor-4 (TLR4) pro-inflammatory signaling. Heme also activates TLR4 signaling, but it is unknown if heme interacts with MD-2. Therefore, we examined MD-2 for a potential heme activation site. Heme-agarose and biotin-heme/streptavidin-agarose pulled down recombinant MD-2, which was inhibited by excess free heme. UV/visible spectroscopy confirmed MD-2-heme binding. To determine whether MD-2 was required for heme-mediated TLR4 signaling, HEK293 cells were transfected with MD-2, TLR4, CD14, and an NF-κB luciferase reporter, and then stimulated with heme or LPS. Heme or LPS treatment elicited robust reporter activity. Absence of MD-2, TLR4 or CD14 plasmid abolished NF-κB reporter responses to heme or LPS. *In silico* analysis identified two potential heme docking sites on MD-2 near conserved amino acids W23/S33/Y34 and Y36/C37/I44. Heme-induced NF-κB activity was reduced by 39 and 78% in HEK293 cells transfected with MD-2 mutants W23A and Y34A, respectively, compared to WT-MD-2. NF-κB activation by LPS was not affected by the same mutants. Biotinyl-heme/streptavidin-agarose pulled down 68% less W23A and 80% less W23A/S33A/Y34A mutant MD-2 than WT-MD-2. In contrast, at the Y36/C37/I44 MD-2 site, heme-induced NF-κB activity was significantly increased by mutants Y36A (191% of WT-MD-2) and unchanged by mutants C37A and I44A (95 and 92%, respectively, of WT-MD-2). In conclusion, these data suggest that heme binds and activates TLR4 signaling at amino acids W23 and Y34 on MD-2.

Keywords: MD-2, TLR4, heme, LPS, NF-κB

OPEN ACCESS

Edited by:
Caroline Le Van Kim, Université Paris Diderot, France

Reviewed by:
Anna Maria Piccinini, University of Nottingham, United Kingdom
Vineesh Vimala Raveendran, King Faisal Specialist Hospital & Research Centre, Saudi Arabia

****Correspondence:***
John D. Belcher
belcher@umn.edu

Specialty section:
This article was submitted to Inflammation, a section of the journal Frontiers in Immunology

Received: *06 February 2020*
Accepted: *28 May 2020*
Published: *30 June 2020*

Citation:
Belcher JD, Zhang P, Nguyen J, Kiser ZM, Nath KA, Hu J, Trent JO and Vercellotti GM (2020) Identification of a Heme Activation Site on the MD-2/TLR4 Complex. Front. Immunol. 11:1370. doi: 10.3389/fimmu.2020.01370

INTRODUCTION

Toll-like receptors are central to vertebrate innate immune responses (1, 2). They recognize broad but highly conserved structural patterns on bacteria, fungi and viruses called pathogen-associated molecular patterns or PAMPs as well as non-pathogenic chemicals and non-patterned molecules. Unique among toll-like receptors, TLR4 activity depends on a molecular interaction with the extracellular adaptor protein MD-2 (3, 4). TLR4 and MD-2 form a heterodimer that recognizes LPS molecules delivered to MD-2/TLR4 by CD14 (5). LPS binds to a large hydrophobic pocket in MD-2 and directly bridges the MD-2/TLR4 heterodimer (6). Binding of LPS to MD-2 triggers homodimerization of MD-2/TLR4 complexes and recruitment of specific adaptor proteins to

TLR4 cytoplasmic domains that initiates a signaling cascade leading to the activation of NF-κB, inflammasome formation, and production of pro-inflammatory cytokines such as TNF-α, IL-1β, IL-8, and IL-18 by macrophages, and the expression of adhesion molecules such as P-selectin and von Willebrand factor on endothelium (7–11).

The MD-2/TLR4 complex also recognizes a diverse number of endogenous molecules released from injured cells called damage-associated molecular patterns or DAMPs. One such DAMP is heme (7, 9, 12). The activation of MD-2/TLR4 by heme is distinct from the activation of MD-2/TLR4 by LPS (7). An anti-TLR4/MD2 antibody or a lipid A antagonist inhibits LPS-induced, but not heme-induced MD-2/TLR4 signaling and conversely, protoporphyrin IX inhibits heme-induced, but not LPS-induced MD-2/TLR4 signaling (7, 9).

Large amounts of heme can be released intravascularly by trauma, sepsis, malaria and red blood cell disorders such as sickle cell disease (SCD). Recent studies underscore the importance of heme-mediated MD-2/TLR4 activation in inflammation, vaso-occlusion, lethality and pulmonary injury in SCD (9, 13). In monocyte/macrophages, heme promotes a pro-inflammatory M1 phenotype, induces tissue factor, and activates coagulation in a TLR4-dependent fashion (9, 14, 15). We previously demonstrated that TLR4 signaling is required for vaso-occlusion induced by heme in SCD mice (9). In endothelial cells, heme mobilizes Weibel-Palade body P-selectin and von Willebrand factor onto the cell surface within minutes, activates the pro-inflammatory transcription factor NF-κB, and induces microvascular stasis in SCD mice in a TLR4-dependent manner. All of these heme-mediated effects can be blocked by adding back the high-affinity heme scavenger hemopexin that is depleted in the plasma of SCD mice and patients (9, 16). Disrupting heme-mediated MD-2/TLR4 signaling might provide a potential therapeutic opportunity to interrupt heme-mediated inflammation and vaso-occlusion in SCD and other hemolytic conditions. Because of heme and MD-2's mutual hydrophobicity and the precedence for LPS binding to MD-2, we explored potential heme activation sites on MD-2.

MATERIALS AND METHODS

Site-Directed Mutagenesis of Human MD-2

Plasmid pFlag-CMV1–hMD2 was a gift from Doug Golenbock (Addgene plasmid #13028). Site-directed mutagenesis was performed using a QuickChange II XL site-directed mutagenesis kit (Agilent Technologies). Mutagenic primers were designed using web-based QuickChange primer design program, and synthesized by Integrated DNA Technologies (IDT) with polyacrylamide gel electrophoresis (PAGE) purification. Mutant strands were synthesized and transformed into XL10-gold ultracompetent cells (Agilent), the DNA from the colonies were checked with restriction digestion and confirmed with DNA sequencing.

Expression and Purification of N-Flag Tagged Recombinant MD-2 and Its Mutants

WT and mutant N-Flag-hMD-2 fragments from pFlag-CMV1–hMD-2 plasmids were subcloned into expression plasmids with a CAG promoter (pT2/Caggs-Flag-hMD2) that were used to produce WT and mutant MD-2 recombinant proteins in Chinese Hamster Ovary Cells (CHO) as described previously (16) with modifications. CHO cells were maintained in T225 flasks in RPMI-1640 with L-glutamine (Gibco) supplemented with 10% fetal bovine serum (FBS) in a 5% CO_2 incubator at 37°C. Cells in T225 cm^2 culture flasks were transiently transfected with polyethylenimine (PEI, linear, MW 2500) (Polysciences) using a 4:1 ratio of PEI to DNA (w/w). After 18 h at 37°C, the cells were changed to ProCHO-AT protein-free media (Lonza). After 4 days in ProCHO-AT media, the conditioned media was collected, and cleared by centrifugation at 600 × g for 30 min at 4°C and filtered using a 0.22 μm Stericup Vacuum Filtration System (EMD Millipore). In the UV/Vis heme-MD-2 binding assays described below, the recombinant proteins in the filtered media were purified using anti-Flag M2 affinity gel (Sigma-Aldrich) column chromatography following the manufacturer's instructions. The bound Flag fusion proteins were eluted by competition with Flag peptide, and further concentrated using 10k centrifugal filter units (Amicon). The purity and concentration of the protein was determined by a 4–15% SDS-PAGE and Coomassie R-250 stain (Bio-Rad) with BSA standards (0.2–5 μg) loaded on the same gel to estimate the Flag-MD-2 concentration by comparing the band intensities with BSA. The recombinant WT and mutant MD-2 proteins were confirmed by Western blots with a primary MD-2 antibody (Abcam).

Heme-Agarose and Biotin-Heme/Streptavidin-Agarose Pull-Down Assays

Pull-down assays were used to determine if there was a physical interaction between MD-2 and heme. Conditioned ProCHO-AT culture media (30 ml) from T225 tissue culture flasks containing CHO cells overexpressing recombinant wild-type (WT) Flag-MD2, mutants or recombinant Flag-hemopexin (Hpx) as a positive control as previously described (16) were concentrated to 3 ml using a 10k centrifugal filter units (Amicon). For the heme-agarose pull-down assays, 1 ml of the concentrated ProCHO-AT media was incubated overnight at 4°C with 35 μl heme-agarose, or control agarose beads (Sigma, pre-washed with PBS). For the biotin-heme/streptavidin-agarose pull-down assays, 1 ml of concentrated ProCHO-AT media was incubated with 15 μM biotin-heme (Frontier Scientific) overnight at 4°C in the dark, then 40 μl of 50% streptavidin-agarose (Sigma-Aldrich) was added to the mixture and incubated an additional 2 h at 4°C. To test the binding specificity of biotin-heme and recombinant MD-2 proteins, 1 ml of concentrated ProCHO-AT media was pre-incubated with a 6.7-fold excess of unlabeled free heme (100 μM) for 2 h at 4°C before the incubation with 15 μM biotin-heme. The resulting beads from both heme-agarose and streptavidin-agarose pull-down assays were washed with PBS 6 times and run

on an SDS-PAGE Western bot using an anti-Flag monoclonal antibody (Sigma-Aldrich) for detection. Hematin, herein referred to as heme, was prepared immediately before use by mixing 10 mg hemin chloride (Frontier Scientific), 10 mg D-sorbitol (Sigma-Aldrich), and 6.9 mg sodium carbonate (Sigma-Aldrich) in 5.7 ml of sterile saline (Baxter) for 30 min in the dark. All heme preparations, appropriately diluted in saline, were filtered at 0.22 μm before use. Endotoxin levels were monitored using a Limulus amebocyte lysate test (GenScript). Heme preparations contained <0.01 endotoxin units/ml at 10 mM heme; all assays used 10 μM heme.

UV/Vis Heme-MD-2 Binding Assays

The UV/Vis absorption spectra (250–600 nm) of heme, MD-2 and heme + MD-2 were measured using a Nanophotometer P330 (Implen) with an optical path length of 1 cm. Human recombinant Flag-Hpx was used as a positive heme-binding control.

In situ Identification of Potential Heme-Binding Sites on MD-2

Potential heme-binding amino acid (AA) residues on human and mouse MD-2 were identified using the HemeBind web server that is freely accessible online (http://mleg.cse.sc.edu/hemeBIND/). HemeBind is a specialized algorithm that combines both structure- and sequence-based methods to identify potential heme-binding sites on heme proteins (17).

NF-κB Reporter Assays

Human embryonic kidney 293 (HEK293) cells were seeded in 96-well plates at 2×10^4 cells per well and incubated overnight in a 5% CO_2 incubator at 37°C. In the morning, cells were transiently transfected with 50 ng TLR4 expression vector (pcDNA3.1-hTLR4, a gift from Ruslan Medzhitov, Addgene plasmid #13086) or empty vector, along with 15 ng of *Firefly* luciferase NF-κB reporter vector (pNifty-Luc, InvivoGen), 15 ng of *Renilla* luciferase control vector (pRL-TK, Promega), 10 ng of wt or mutant MD-2 expression vector (pFlag-CMV1-hMD2), and 10 ng of CD14 expression vector (pCDNA3.1-hCD14, a gift from Doug Golenbock, Addgene plasmid #13645) per well using Lipofectamine Plus reagent (LifeTechnology). Four h after transfection, cells were incubated 24 h in media containing 10% fetal bovine serum (FBS). Twenty-four hours after transfection, cells were incubated with media with 1% FBS (control), or media with 1% FBS supplemented with heme (10 μM), LPS (10 ng/ml, Escherichia coli, serotype O111:B4; Sigma-Aldrich) or heme + LPS for 6 h, then cells were lysed and luciferase activity was measured.

Statistical Analysis

Results are presented as means ± standard deviation unless otherwise indicated. Analyses were performed with SigmaStat 3.5 for Windows (Systat Software, San Jose, CA). Comparisons of multiple treatment groups were made using One Way ANOVA with Holm-Sidac correction, Kruskal-Wallis One Way Analysis of Variance on Ranks, or a student's unpaired *t*-test. Statistical significance was considered to be $p < 0.05$.

RESULTS

Heme Binding to MD-2

To determine if heme binds to MD-2, recombinant MD-2 was expressed by transfecting CHO cells with a plasmid encoding human MD-2 with a Flag tag at the N-terminus. After transfection, cells were washed and incubated for 3 or 4 days in protein-free ProCHO medium. Transfected, but not untransfected CHO cells secrete soluble recombinant human MD-2 into the media (**Supplemental Figure 1**). Flag-MD-2 had an apparent molecular weight of ∼25 kDa, which is close to the predicted mass of 19.2 kDa.

The recombinant human flag-MD-2 (rhMD-2) was highly purified as seen on an SDS PAGE gel stained with Coomassie Brilliant Blue R-250 (**Supplemental Figure 2**). After 4 days, Flag-MD-2 was present in the conditioned medium of transfected CHO cells as demonstrated by a Western blot of the medium with an anti-Flag primary antibody (**Figure 1A**, lane 3). The conditioned CHO medium containing Flag-MD-2 was incubated with heme-agarose beads in a pull-down assay. Flag-MD-2 in the medium was pulled down with heme-agarose as demonstrated on a Western blot of the pull-down proteins with anti-Flag IgG (**Figure 1A**, lane 2). Flag-MD-2 was not pulled down from conditioned medium by control agarose without heme (**Figure 1A**, lane 1). As a positive control, recombinant human hemopexin (Hpx), which binds heme with high affinity, was expressed by transfecting CHO cells with a plasmid encoding Flag-labeled Hpx. After 4 days, Flag-Hpx was present in the conditioned medium of transfected CHO cells as demonstrated by a Western blot with anti-Flag IgG (**Figure 1B**, lane 6). Flag-Hpx had an apparent molecular weight of ∼59 kd, which is the predicted mass. The medium containing Flag-Hpx was incubated with heme-agarose beads in a pull-down assay. Flag-Hpx in the medium was pulled down with heme-agarose as demonstrated on a Western blot of the pull-down proteins with anti-Flag IgG detection (**Figure 1B**, lane 5). Flag-Hpx was not pulled down from conditioned medium by control agarose without heme (**Figure 1B**, lane 4).

To confirm heme binding to MD-2, additional pull-down assays were run using recombinant MD-2, biotin-heme and streptavidin-agarose (**Figure 1C**). Flag-MD-2 was present in the conditioned CHO medium as demonstrated by a Western blot of the medium with an anti-Flag primary antibody (**Figure 1C**, lane 4). Conditioned CHO medium containing Flag-MD-2 was incubated with biotin-heme followed by streptavidin-agarose. Flag-MD-2 in the medium of conditioned CHO cells was pulled down with biotin-heme + streptavidin-agarose as demonstrated by a Western blot of the pull-down proteins with anti-Flag IgG (**Figure 1C**, lane 2). Biotin-heme binding to MD-2 was markedly diminished in the presence of a 6.7-fold excess of unlabeled free heme in the assay, demonstrating specific heme binding to MD-2 (**Figure 1C**, lane 3). Flag-MD-2 was not pulled down from conditioned medium by control agarose without streptavidin (**Figure 1C**, lane 1). As a positive control, CHO medium containing Flag-Hpx was incubated with biotin-heme + streptavidin-agarose. Flag-Hpx was present in the conditioned CHO medium as demonstrated by a Western blot with anti-Flag

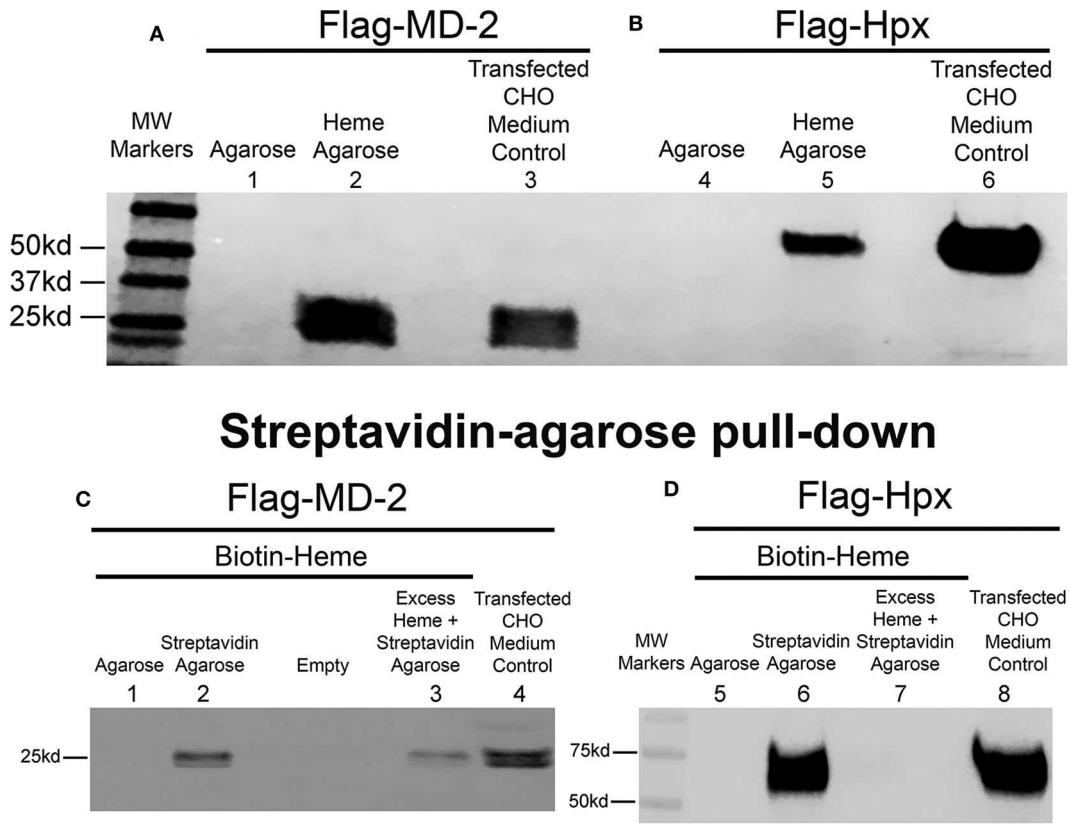

FIGURE 1 | Heme binds to MD-2 in pull-down assays. Recombinant MD-2 and hemopexin (Hpx) were expressed by transfecting Chinese hamster ovary (CHO) cells with plasmids encoding human Flag-MD-2 or Flag-Hpx. Flag-Hpx served as a positive control for heme binding. After transfection, cells were washed and incubated for 72 h in protein-free CHO medium to allow the recombinant proteins to be transcribed, translated, and secreted into the CHO media. After 72 h, Flag-MD-2 (**A**, lane 3 and **C**, lane 4) and Flag-Hpx (**B**, lane 6 and **D**, lane 8) were present in the conditioned media of transfected CHO cells as demonstrated by a Western blot of the concentrated media with an anti-Flag primary antibody. **(A,B)** Heme-agarose pull-down assays. Conditioned CHO media containing **(A)** Flag-MD-2 or **(B)** Flag-Hpx were incubated overnight at 4°C with heme-agarose (lanes 2 and 5) or control agarose beads (lanes 1 and 4) and then pelleted, washed, and run on a Western blot with anti-Flag detection. **(C,D)** Streptavidin-agarose pull-down assays. Conditioned CHO media containing **(C)** Flag-MD-2 or **(D)** Flag-Hpx were incubated with 15 μM biotin-heme overnight at 4°C in the dark, then streptavidin-agarose (lanes 2, 3, 6, and 7) or control agarose (lanes 1 and 5) was added to the mixture for an additional 2 h at 4°C. After incubation, the agarose pellets were washed and run on Western blots with anti-Flag detection. To test the binding specificity of biotin-heme and recombinant Flag-MD-2 (**C**, lane 3) and Flag-Hpx (**D**, lane 7), conditioned CHO media were pre-incubated with an excess of unlabeled free heme (100 μM) for 2 h at 4°C before the incubation with 15 μM biotin-heme. The results shown are representative of four (**A** and **B**) and two (**C** and **D**) independent experiments, respectively.

IgG (**Figure 1D**, lane 8). Flag-Hpx in the medium was pulled down with biotin-heme + streptavidin-agarose as demonstrated by a Western blot of the pull-down proteins with anti-Flag IgG (**Figure 1D**, lane 6). Biotin-heme binding to Hpx was eliminated in the presence of a 6.7-fold excess of unlabeled free heme in the assay, demonstrating specific heme binding to Hpx (**Figure 1D**, lane 7). Flag-Hpx was not pulled down from conditioned medium by agarose without streptavidin (**Figure 1D**, lane 5).

To further confirm heme-MD-2 binding, UV/visible spectroscopy was used to detect heme binding to MD-2. Proteins such as Hpx when bound to heme have an increase in absorbance at ∼414 nm (18). Recombinant Flag-MD-2 and Flag-Hpx were purified from conditioned CHO media using anti-Flag-IgG-agarose affinity chromatography. A UV/visible absorbance scan of heme, Flag-MD-2, and Flag-MD-2 + heme demonstrated an increase in absorbance at 414 nm when heme was added to Flag-MD-2 (**Figure 2A**), consistent with heme binding to MD-2 that was similar to, but less than, Flag-Hpx + heme (**Figure 2B**).

Heme Activation Sites on MD-2

Potential heme-binding amino acid residues on human and mouse MD-2 were identified using the HemeBind web server that is freely accessible online. HemeBind is a specialized algorithm that combines both structure- and sequence-based methods to identify potential heme-binding sites on heme proteins (17). These *in silico* analyses identified two potential heme docking sites on both human and murine MD-2 near conserved amino

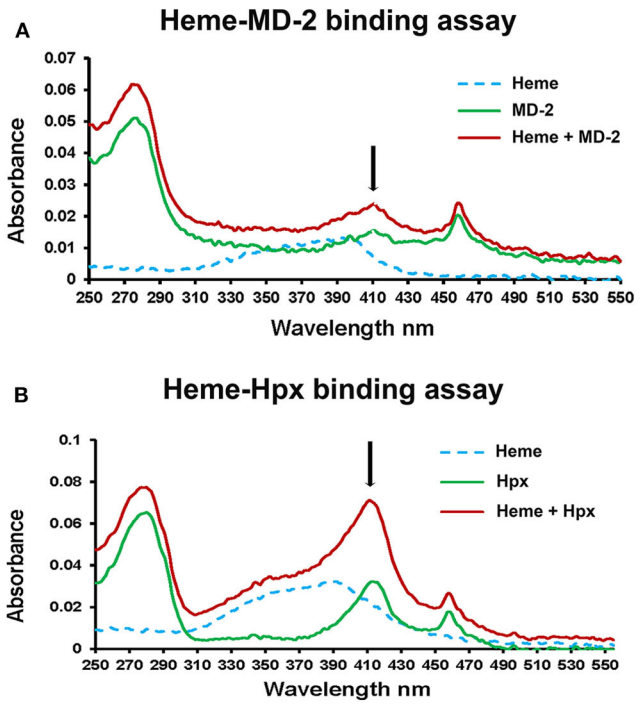

FIGURE 2 | Heme binds to MD-2 in absorbance spectroscopy assay. **(A)** The UV/Vis absorption spectra (250–550 nm) of heme (10 μM, dashed blue line), recombinant MD-2 (green line), and heme + MD-2 (red line) were measured. **(B)** As a positive heme-binding control, the experiment was repeated using recombinant human Hpx instead of MD-2. The black arrows show the location of a characteristic Soret peak at ~414 nm seen in heme proteins. The results shown in **(A,B)** are representative of three independent experiments. Each spectrum was blanked against the buffer vehicle.

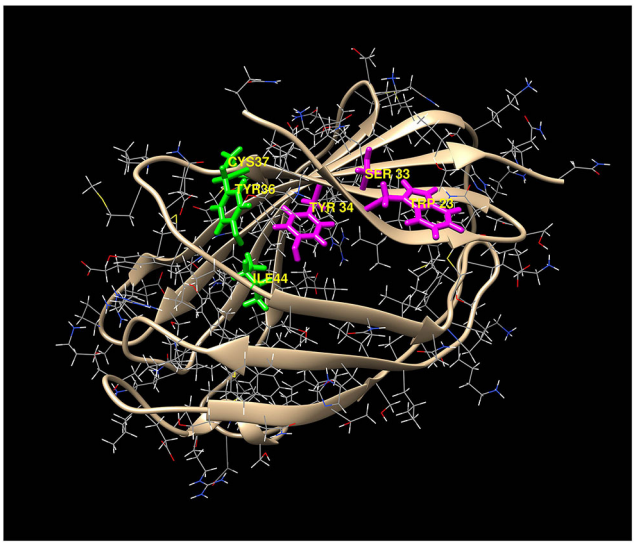

FIGURE 3 | Two potential heme-docking sites on MD-2. Potential heme-binding amino acid residues on human and mouse MD-2 were identified using the online HemeBind algorithm that combines both structure- and sequence-based methods to identify potential heme-binding sites on heme proteins (17). These *in silico* analyses identified six potential heme binding amino acids located in two separate clusters on the surface of MD-2. The amino acids in the 2 clusters, W23/S33/Y34 (magenta) and Y36/C37/I44 (green), are highlighted on the 3-dimentional structure of human MD-2.

acids W23/S33/Y34 and Y36/C37/I44 highlighted in magenta and green, respectively (**Figure 3**).

NF-κB Reporter Assays With CD14, MD-2, and TLR4

LPS activation of TLR4 signaling requires CD14, MD-2 and TLR4, which leads to the activation of the pro-inflammatory transcription factor NF-κB. Previously, heme activation of TLR4 signaling in macrophages was shown to require TLR4 and CD14 (7), but it is unknown if heme activation of TLR4 requires MD-2. To determine whether heme-mediated TLR4 signaling requires MD-2, an NF-κB reporter assay was developed using HEK293 cells transfected with a *Firefly* luciferase NF-κB reporter with or without plasmids encoding MD-2, TLR4, and CD14. Twenty-four hours after transfection, HEK293 cells were incubated with media (control), heme (10 μM), LPS (10 ng/ml), or heme + LPS for 6 h, followed by measurement of NF-κB luciferase reporter activity. Heme, LPS and heme + LPS treatment elicited robust luciferase activity in the presence of CD14, MD-2, and TLR4 (**Figure 4**, gray bars). The absence of a CD14 (orange bars), MD-2 (blue bars) or TLR4 (green bars) inhibited NF-κB luciferase reporter responses to heme, LPS, and heme + LPS similar to control cells. TLR4, MD-2 and CD14 replete cells (gray bars) stimulated with heme + LPS had more activity than replete cells treated with heme or LPS alone.

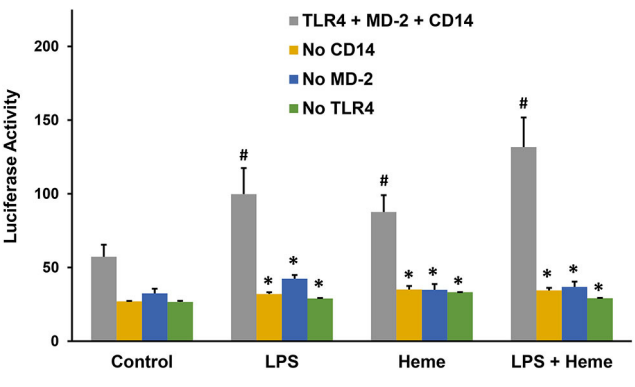

FIGURE 4 | NF-κB Reporter Assays with TLR4, MD-2, and CD14. Human embryonic kidney 293 (HEK293) cells were transfected with plasmid expression vectors for *Firefly* NF-κB and *Renilla* luciferase reporters, plus CD14, MD-2, and TLR4 (gray bar); MD-2 and TLR4 (no CD14, orange bar); CD14 and TLR4 (no MD-2, blue bar); or CD14 and MD-2 (no TLR4, green bar). Twenty-four hours after transfection, cells were incubated with media (Control), 10 μM heme, 10 ng/ml LPS, or heme + LPS for 6 h in media containing 1% serum. After 6 h, cells were lysed and luciferase activity was measured and expressed as the ratio of *Firefly* luciferase NF-κB reporter to *Renilla* luciferase control. Results are representative of 3 independent experiments run in triplicate. Bars are means + SD. $^{\#}P < 0.01$ control vs. heme, LPS, and heme + LPS. $^{*}P < 0.01$ TLR4 + MD-2 + CD14 (gray bar) vs. no CD14 (purple bar), no MD-2 (orange bar), and no TLR4 (green bar) for each stimulant, using One Way ANOVA with Holm-Sidac correction.

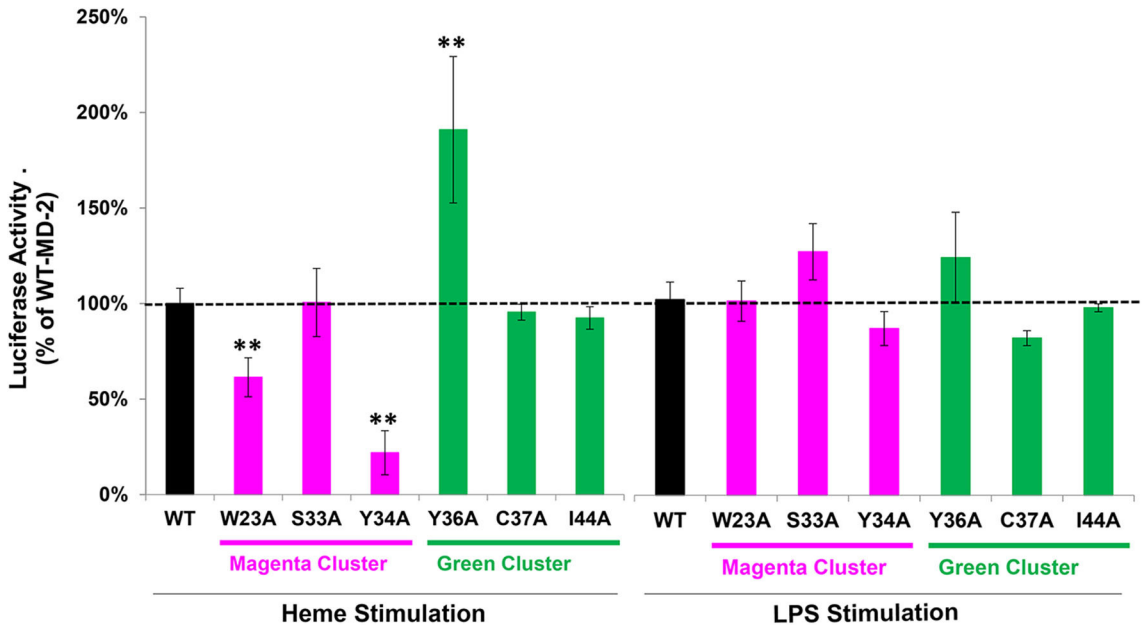

FIGURE 5 | NF-κB reporter assays with WT and mutant MD-2. HEK293 cells were transfected with plasmid expression vectors for WT or mutant MD-2, TLR4, CD14, *Firefly* luciferase NF-κB reporter, and *Renilla* luciferase control. Twenty-four hours after transfection, cells were treated with 10 μM heme or 10 ng/ml LPS for 6 h in media containing 0.1% serum. After 6 h, cells were lysed and luciferase activity was measured and expressed as the ratio of *Firefly* luciferase NF-κB reporter to *Renilla* luciferase control. Luciferase activity is expressed as a percent of cells transfected with WT MD-2 stimulated with heme or LPS (100% activity, black bars and horizontal dashed black line). Magenta cluster and green cluster refer to the 2 clusters of potential heme binding amino acids in **Figure 3**. Results are representative of 3 independent experiments run in triplicate. Bar values are means ± SD. $^{**}P < 0.01$ vs. WT MD-2 using Kruskal-Wallis One Way Analysis of Variance on Ranks.

NF-κB Reporter Assays With WT or Mutant MD-2

We next examined the effect of MD-2 point mutations on heme and LPS stimulation in the NF-κB reporter assay. MD-2 amino acids located at the potential heme binding sites on MD-2 identified in the magenta and green amino acid clusters in **Figure 3** were each mutated individually to alanine. HEK293 cells were transfected with wild-type (WT) or mutant MD-2, WT CD14, WT TLR4, and the NF-κB luciferase reporter. NF-κB reporter activity was then expressed as a percent of WT MD-2 (100%) with heme or LPS stimulation (**Figure 5**). MD-2 point mutants W23A or Y34A in the magenta cluster significantly reduced heme-mediated NF-κB luciferase activity to 61 and 22%, respectively, relative to WT MD-2 (**Figure 5**, left). The S33A MD-2 mutation in the magenta cluster was similar to WT MD-2 NF-κB luciferase activity with heme stimulation. In contrast, MD-2 mutations in the green cluster, Y36A markedly stimulated heme-induced NF-κB luciferase activity to 191% compared to WT MD-2 (**Figure 5**, left). The C37A and I44A MD-2 mutations in the green cluster were not significantly different from WT MD-2. When the transfected HEK293 cells were stimulated with LPS (**Figure 5**, right), MD-2 mutations in the magenta and green cluster had no significant effects on NF-κB reporter activity relative to WT MD-2.

Heme Binding to Mutant MD-2

To determine if MD-2 mutations at the W23/S33/Y34 site affect heme binding to MD-2, WT MD-2, W23A MD-2, and W23A/S33A/Y34A MD-2 with Flag tags were expressed in CHO cells and the MD-2-containing media were used in heme-agarose and biotin-heme/streptavidin-agarose pull-down assays. Four days after transfection, the conditioned CHO media contained similar amounts of WT, W23A, and W23A-S33A-Y34A MD-2 on Western blots using Flag detection (**Figure 6A**, lanes 5, 6, and 7 and **Figure 6B**, lanes 6, 7, and 8). Heme-agarose pulled down 47% of the W23A and 36% of the W23A/S33A/Y34A MD-2 mutants compared to WT MD-2 (**Figure 6A**, lanes 2, 3, and 4 and **Figure 6C**). WT MD-2 was not pulled down from conditioned medium by control agarose without heme (**Figure 6A**, lane 1).

Similarly, the biotin-heme/streptavidin-agarose pulled down 32% of the W23A and 20% of the W23A/S33A/Y34A MD-2 mutants compared to WT MD-2 (**Figure 6B**, lanes 2, 3, and 4 and **Figure 6D**). WT MD-2 incubated with biotin-heme was not pulled down from conditioned medium by agarose without streptavidin (**Figure 6B**, lane 1). As previously shown, the addition of excess unlabeled heme markedly reduced the amount of WT MD-2 pulled down by biotin-heme/streptavidin-agarose (**Figure 6B**, lane 5).

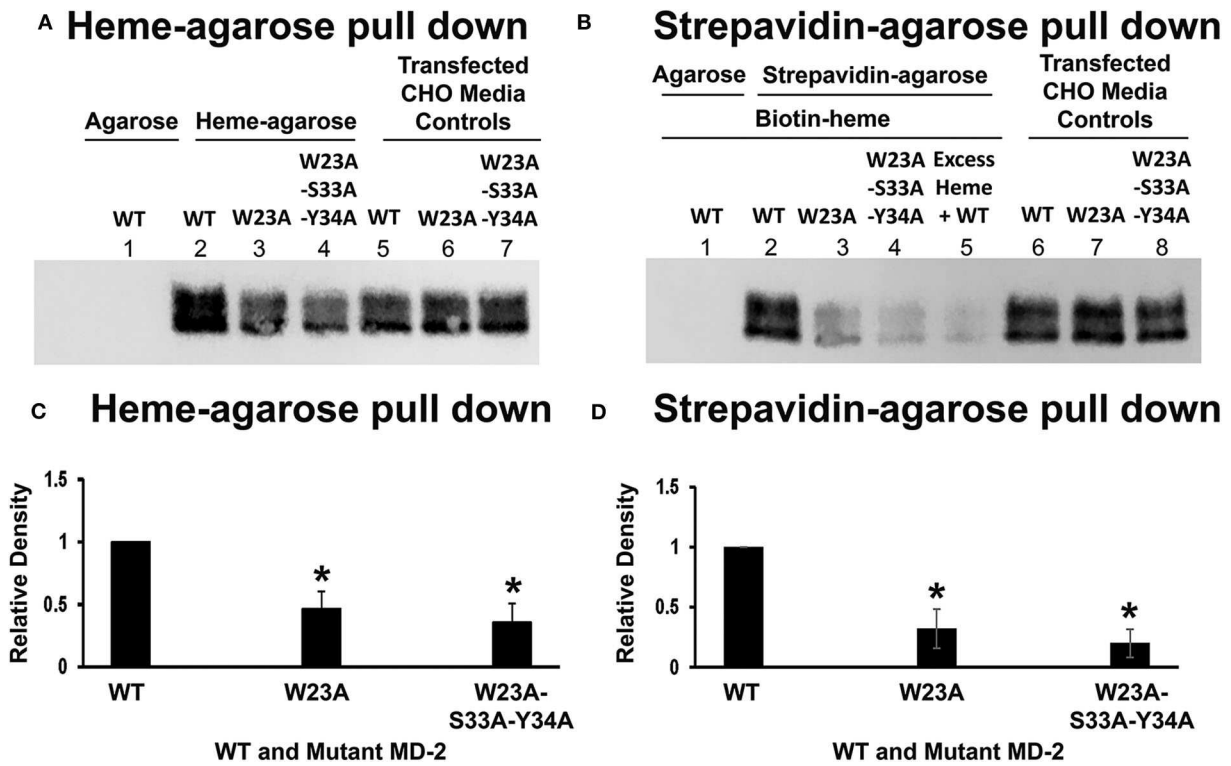

FIGURE 6 | Heme binds poorly to W23A and W23A-S33A-Y34A mutant MD-2. WT MD-2, W23A MD-2, and W23A/S33A/Y34A MD-2 with Flag tags were expressed in CHO cells and the MD-2-containing media were used in heme-agarose and biotin-heme/streptavidin-agarose pull-down assays. Three days after transfection, the conditioned CHO media contained similar amounts of WT, W23A, and W23A/S33A/Y34A MD-2 on Western blots using Flag detection (**A**, lanes 5, 6, and 7 and **B**, lanes 6, 7, and 8). Heme-agarose pulled down only 47% of the W23A and 36% of the W23A/S33A/Y34A MD-2 mutants compared to WT MD-2 (**A**, lanes 2, 3, and 4 and **C**). WT MD-2 incubated with control agarose without heme was not pulled down (**A**, lane 1). Similarly, the biotin-heme/streptavidin-agarose pulled down only 32% of the W23A and 20% of the W23A/S33A/Y34A MD-2 mutants compared to WT MD-2 (**B**, lanes 2, 3, and 4 and **D**). WT MD-2 incubated with biotin-heme was not pulled down by agarose without streptavidin (**B**, lane 1). As previously shown, the addition of excess unlabeled heme markedly reduced the amount of WT MD-2 pulled down by biotin-heme/streptavidin-agarose (**B**, lane 5). The results shown in **(A,B)** are representative of four independent experiments. **(C,D)** show the results of quantitation of the Western blots. Bars are means + SD. $^*P < 0.05$ compared to WT MD-2 using a student's unpaired *T*-test.

DISCUSSION

Heme is essential for life, but when released from damaged cells it can act as a DAMP that promotes activation of MD-2/TLR4 signaling (7, 9, 12). Sickle cell disease (SCD), sepsis, malaria, viral hemorrhagic fevers, trauma, and hemorrhagic stroke can release large amounts of heme into the vasculature thereby promoting pro-inflammatory responses and tissue damage. We used pull-down assays and UV-VIS absorbance spectroscopy to demonstrate that recombinant MD-2 can bind heme. *In silico* analyses identified two potential heme docking sites on both human and murine MD-2 near conserved amino acids W23/S33/Y34 and Y36/C37/I44. HEK293 cells transfected with plasmids encoding WT MD-2, TLR4, and CD14 produced robust NF-κB reporter activity when stimulated with heme, LPS, or heme + LPS. NF-κB reporter activity was lost when MD-2, TLR4 or CD14 was omitted. MD-2 point mutations W23A and Y34A markedly inhibited the reporter responses to heme, but not LPS compared to WT MD-2. These data suggest that heme initiates MD-2/TLR4 signaling upon docking with MD-2 amino acids W23 and Y34. Y34 is a tyrosine residue; we speculate that the OH group on Y34 interacts with the iron moiety of heme as the heme iron is required for MD-2/TLR4 signaling (7, 9). W23 is a tryptophan which may provide a hydrophobic docking site for the vinyl groups on heme as the vinyl groups on heme are also required for MD-2/TLR4 signaling (7). The role of CD14 in heme-mediated MD-2/TLR4 signaling is unclear, but CD14 might be involved in the transfer of heme to MD-2 as has been reported for LPS (5, 19–21).

The function of sMD-2 has been extensively studied in LPS-TLR4 signaling. This LPS-sMD-2-TLR4 activation model is different from the classic LPS-TLR4 activation model in which MD-2 is co-localized with TLR4 on the cell surface, indispensable for LPS recognition and signaling (6). Heme-mediated MD-2/TLR4 signaling by macrophages does require MyD88 (7), suggesting dimerization of TLR4. However, it is possible that the model of a circulating sMD-2-heme complex to activate TLR4 is different from the model in which heme binds to the MD-2 co-localized with TLR4 on cell surface.

The activation of TLR4 signaling is unlikely to have been caused by LPS contamination of our hemin preparations. Endotoxin levels were monitored using a Limulus amebocyte lysate test. Heme preparations (10 mM) contained <0.01 endotoxin units/ml. Our NF-κB reporter assays used 10 uM hemin. We have previously shown that anti-LPS IgG directed against the LPS core does not inhibit heme-induced TLR4 signaling (9), but significantly inhibits LPS-induced MD-2/TLR4 signaling. The original paper describing the activation of TLR4 signaling by heme (7), showed that signaling of heme through TLR4 depended on an interaction distinct from the one established between TLR4 and lipopolysaccharide (LPS) since anti-TLR4/MD2 antibody or a lipid A antagonist inhibited LPS-induced TNF-alpha secretion but not heme activity. These data indicate that heme activates TLR4 signaling independently of LPS. In addition, the specificity of heme activation of MD-2/TLR4 signaling is supported in several published papers by our lab and others showing that the high affinity heme-binding protein, hemopexin, blocks the activation of MD-2/TLR4 signaling by heme (9, 14, 16, 22–24).

Some of our MD-2 Western blots appear to have 2 bands. Ohnishi et al. (25) reported that MD-2 has N-linked glycosylations at Asn (25) and Asn(114), which give up to 3 molecular weight bands on SDS PAGE gels. When cellular extracts are treated with N-glycosidase, only a single band with the fastest mobility was detected. It is likely the two bands seen on our MD-2 Western blots represent different glycosylation states of MD-2. Glycosylation of MD-2 appears to be important for TLR4-mediated signal transduction of LPS (25, 26). The impact on signal transduction of heme is unknown, but should be explored further.

There could potentially be other heme-activation sites on MD-2 or TLR4 that were not identified. We used a specialized algorithm that combines both structure- and sequence-based methods to identify potential heme-binding sites on heme proteins (17). This algorithm identified the same two distinct clusters of potential heme-binding amino acids at W23/S33/Y34 and Y36/C37/I44 on the surface of both human and mouse MD-2. Point mutations at W23A and Y34A inhibited heme activation of TLR4 signaling and a point mutation at W23A and a triple mutation at W23A-S33A-Y34A inhibited heme binding to MD-2. In contrast, point mutations S33A, Y36A, C37A, and I44A either stimulated or had little effect on heme-mediated MD-2/TLR4 signaling. Thus, it seems likely that the pocket located at W23 and Y34 on MD-2 is the most likely site for heme docking and activation of TLR4 signaling. However, a limitation of this study is the incomplete heme-binding data with the other MD-2 site mutations at S33A, Y34A, Y36A, C37A, and I44A. Confirmation of the NF-kB activation data in **Figure 5** and the heme binding site on MD-2 awaits additional studies to confirm the W23/Y34 activation site.

Another possibility is that mutations of MD-2 at the proposed activation site might affect the folding and 3-dimensional structure of MD-2 and thereby indirectly affect MD-2 binding to heme and TLR4 signaling. However, nearby mutations Y36A, C37A, and I44A on MD-2 did not inhibit heme-mediated MD-2/TLR4 signaling. An important caveat of our data interpretation assumes the mutants were properly folded.

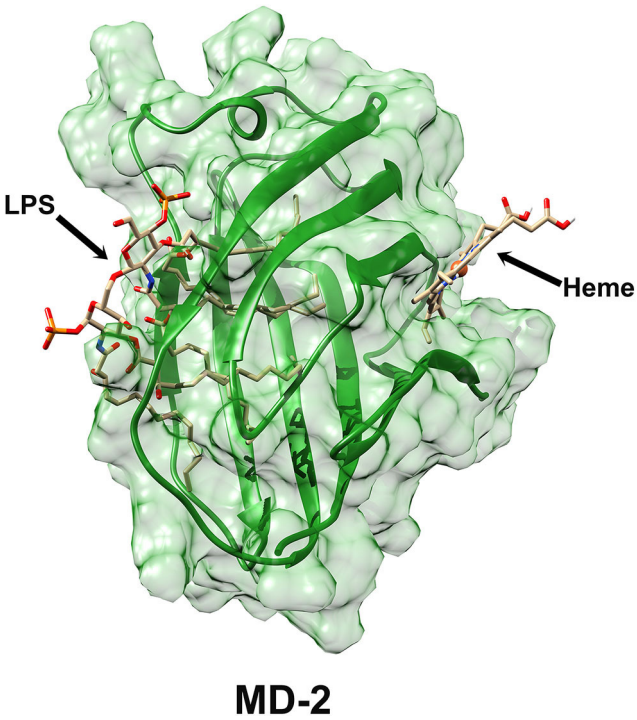

FIGURE 7 | Surface representation of MD-2 structure derived from Protein Data Bank 3VQ2 (29) showing the LPS-binding site and the putative heme-binding site on MD-2.

Another limitation is the limited characterization of heme-MD-2 interactions. Future experiments will further characterize the interactions of heme with MD-2 using differential scanning fluorimetry to detect heme's binding affinity to MD-2 (27). Heme binding to MD-2 will be confirmed using secondary screens of melting by circular dichroism (non-fluorescent confirmation of ligand-binding stabilizing MD-2) and analytical centrifugation (non-fluorescent confirmation of heme-binding to MD-2 and stoichiometry). Heme-binding will also be analyzed by isothermal titration calorimetry. Our laboratory was unable to obtain reproducible data on heme binding to recombinant MD-2 using surface plasmon resonance. Verification of the heme docking site on MD-2 awaits confirmation of the crystal structure as was done with TLR4-MD-2 complexes with LPS and LPS analogs (6, 28–30). The interaction with LPS is mediated by a hydrophobic internal pocket in MD-2. However, there appears to be no overlap of MD-2 residues involved in the binding of LPS and the MD-2 heme-binding site at W23 and Y34 near the N-terminus. In fact, the heme and LPS binding sites are located on opposite sides of the MD-2 protein (**Figure 7**), which might partially explain why mutations at the heme binding site had no significant effects on the LPS-stimulated NF-κB reporter assays.

Future studies will use virtual screening to identify small molecules that might interact at the W23/Y34 site and inhibit heme-mediated MD-2/TLR4 signaling. Their interaction with

MD-2 will be characterized by differential scanning fluorimetry, circular dichroism, and analytical centrifugation as described above for heme-MD-2 interactions. Candidate molecules will be screened for their ability to inhibit heme-mediated chemokine production in human monocyte/macrophages. Follow-up screens will include inhibition of heme activation of P-selectin and von Willebrand factor expression on the membrane of endothelial cells, vaso-occlusion in SCD mice, and heme binding to MD-2.

We conclude that heme activates TLR4 signaling at residues W23 and Y34 on MD-2. This site on MD-2 appears to be a possible target for inhibition of heme-mediated TLR4 signaling. We speculate that targeted inhibition of heme-mediated TLR4 signaling would be beneficial in hemolytic diseases such as SCD without affecting innate immunity to gram negative bacteria expressing LPS.

DATA AVAILABILITY STATEMENT

All datasets generated for this study are included in the article/**Supplementary Material**.

AUTHOR CONTRIBUTIONS

JB and GV designed the research. JT and JH contributed computational tools. JB, PZ, KN, JT, and GV wrote and edited the manuscript. JB, PZ, and JT prepared the figures. PZ, JN, and ZK performed the biochemical analyses. All authors contributed to the article and approved the submitted version.

FUNDING

This work was supported by a grant from the National Institute of Health grant numbers NIH R01 HL114567, T32 HL007062, and R01 DK119167.

SUPPLEMENTARY MATERIAL

The Supplementary Material for this article can be found online at: https://www.frontiersin.org/articles/10.3389/fimmu.2020.01370/full#supplementary-material

REFERENCES

1. Medzhitov R, Preston-Hurlburt P, Janeway CA Jr. A human homologue of the drosophila Toll protein signals activation of adaptive immunity. *Nature*. (1997) 388:394–7. doi: 10.1038/41131
2. Gay NJ, Gangloff M. Structure and function of Toll receptors and their ligands. *Annu Rev Biochem.* (2007) 76:141–65. doi: 10.1146/annurev.biochem.76.060305.151318
3. Miyake K. Endotoxin recognition molecules, Toll-like receptor 4-MD-2. *Semin Immunol.* (2004) 16:11–6. doi: 10.1016/j.smim.2003.10.007
4. Visintin A, Iliev DB, Monks BG, Halmen KA, Golenbock DT. MD-2. *Immunobiology*. (2006) 211:437–47. doi: 10.1016/j.imbio.2006.05.010
5. Da Silva Correia J, Soldau K, Christen U, Tobias PS, Ulevitch RJ. Lipopolysaccharide is in close proximity to each of the proteins in its membrane receptor complex. transfer from CD14 to TLR4 and MD-2. *J Biol Chem.* (2001) 276:21129–35. doi: 10.1074/jbc.M009164200
6. Park BS, Song DH, Kim HM, Choi BS, Lee H, Lee JO. The structural basis of lipopolysaccharide recognition by the TLR4-MD-2 complex. *Nature*. (2009) 458:1191–5. doi: 10.1038/nature07830
7. Figueiredo RT, Fernandez PL, Mourao-Sa DS, Porto BN, Dutra FF, Alves LS, et al. Characterization of heme as activator of Toll-like receptor 4. *J Biol Chem.* (2007) 282:20221–9. doi: 10.1074/jbc.M610737200
8. Thompson MR, Kaminski JJ, Kurt-Jones EA, Fitzgerald KA. Pattern recognition receptors and the innate immune response to viral infection. *Viruses*. (2011) 3:920–40. doi: 10.3390/v3060920
9. Belcher JD, Chen C, Nguyen J, Milbauer L, Abdulla F, Alayash AI, et al. Heme triggers TLR4 signaling leading to endothelial cell activation and vaso-occlusion in murine sickle cell disease. *Blood*. (2014) 123:377–90. doi: 10.1182/blood-2013-04-495887
10. Kawasaki T, Kawai T. Toll-like receptor signaling pathways. *Front Immunol.* (2014) 5:461. doi: 10.3389/fimmu.2014.00461
11. Burm SM, Zuiderwijk-Sick EAT, Jong AE, Van Der Putten C, Veth J, et al. Inflammasome-induced IL-1beta secretion in microglia is characterized by delayed kinetics and is only partially dependent on inflammatory caspases. *J Neurosci.* (2015) 35:678–87. doi: 10.1523/JNEUROSCI.2510-14.2015
12. Wegiel B, Hauser CJ, Otterbein LE. Heme as a danger molecule in pathogen recognition. *Free Radic Biol Med.* (2015) 89:651–61. doi: 10.1016/j.freeradbiomed.2015.08.020
13. Ghosh S, Adisa O, Yang Y, Tan F, Ofori-Acquah SF. Toll-like receptor 4 mediates heme induced acute lung injury: preclinical study of resatorvid in sickle cell disease. *ASH Ann Meet Abst.* (2011) 118:2113. doi: 10.1182/blood.V118.21.2113.2113
14. Ghosh S, Adisa OA, Chappa P, Tan F, Jackson KA, Archer DR, et al. Extracellular hemin crisis triggers acute chest syndrome in sickle mice. *J Clin Invest.* (2013) 123:4809–20. doi: 10.1172/JCI64578
15. Camus SM, De Moraes JA, Bonnin P, Abbyad P, Le Jeune S, Lionnet F, et al. Circulating cell membrane microparticles transfer heme to endothelial cells and trigger vasoocclusions in sickle cell disease. *Blood*. (2015) 125:3805–14. doi: 10.1182/blood-2014-07-589283
16. Vercellotti GM, Zhang P, Nguyen J, Abdulla F, Chen C, Nguyen P, et al. Hepatic overexpression of hemopexin inhibits inflammation and vascular stasis in murine models of sickle cell disease. *Mol Med*. (2016) 22:437–51. doi: 10.2119/molmed.2016.00063
17. Liu R, Hu J. HemeBIND: a novel method for heme binding residue prediction by combining structural and sequence information. *BMC Bioinformatics*. (2011) 12:207. doi: 10.1186/1471-2105-12-207
18. Morgan WT, Muster P, Tatum FM, Mcconnell J, Conway TP, Hensley P, et al. Use of hemopexin domains and monoclonal antibodies to hemopexin to probe the molecular determinants of hemopexin-mediated heme transport. *J Biol Chem.* (1988) 263:8220–5.
19. Gioannini TL, Teghanemt A, Zhang D, Coussens NP, Dockstader W, Ramaswamy S, et al. Isolation of an endotoxin-MD-2 complex that produces Toll-like receptor 4-dependent cell activation at picomolar concentrations. *Proc Natl Acad Sci USA*. (2004) 101:4186–91. doi: 10.1073/pnas.0306906101
20. Jerala R. Structural biology of the LPS recognition. *Int J Med Microbiol.* (2007) 297:353–63. doi: 10.1016/j.ijmm.2007.04.001
21. Vasl J, Oblak A, Peternelj TT, Klett J, Martin-Santamaria S, Gioannini TL, et al. Molecular basis of the functional differences between soluble human versus murine MD-2: role of Val135 in transfer of lipopolysaccharide from CD14 to MD-2. *J Immunol.* (2016) 196:2309–18. doi: 10.4049/jimmunol.1502074
22. Lin T, Kwak YH, Sammy F, He P, Thundivalappil S, Sun G, et al. Synergistic inflammation is induced by blood degradation products with microbial Toll-like receptor agonists and is blocked by hemopexin. *J Infect Dis.* (2010) 202:624–32. doi: 10.1086/654929
23. Stapley R, Rodriguez C, Oh JY, Honavar J, Brandon A, Wagener BM, et al. Red blood cell washing, nitrite therapy, and antiheme therapies prevent stored

red blood cell toxicity after trauma-hemorrhage. *Free Radic Biol Med.* (2015) 85:207–18. doi: 10.1016/j.freeradbiomed.2015.04.025
24. Belcher JD, Chen C, Nguyen J, Abdulla F, Zhang P, Nguyen H, et al. Haptoglobin and hemopexin inhibit vaso-occlusion and inflammation in murine sickle cell disease: role of heme oxygenase-1 induction. *PLoS ONE.* (2018) 13:e0196455. doi: 10.1371/journal.pone.0196455
25. Ohnishi T, Muroi M, Tanamoto K. N-linked glycosylations at Asn(26) and Asn(114) of human MD-2 are required for Toll-like receptor 4-mediated activation of NF-kappaB by lipopolysaccharide. *J Immunol.* (2001) 167:3354–9. doi: 10.4049/jimmunol.167.6.3354
26. Da Silva Correia J, Ulevitch RJ. MD-2 and TLR4 N-linked glycosylations are important for a functional lipopolysaccharide receptor. *J Biol Chem.* (2002) 277:1845–54. doi: 10.1074/jbc.M109910200
27. Niesen FH, Berglund H, Vedadi M. The use of differential scanning fluorimetry to detect ligand interactions that promote protein stability. *Nat Protoc.* (2007) 2:2212–21. doi: 10.1038/nprot.2007.321
28. Kim HM, Park BS, Kim JI, Kim SE, Lee J, Oh SC, et al. Crystal structure of the TLR4-MD-2 complex with bound endotoxin antagonist Eritoran. *Cell.* (2007) 130:906–17. doi: 10.1016/j.cell.2007.08.002
29. Ohto U, Fukase K, Miyake K, Shimizu T. Structural basis of species-specific endotoxin sensing by innate immune receptor TLR4/MD-2. *Proc Natl Acad Sci USA.* (2012) 109:7421–6. doi: 10.1073/pnas.1201193109
30. Klett J, Reeves J, Oberhauser N, Perez-Regidor L, Martin-Santamaria S. Modulation of Toll-like receptor 4. Insights from x-ray crystallography and molecular modeling. *Curr Top Med Chem.* (2014) 14:2672–83. doi: 10.2174/1568026614666141215144831

Conflict of Interest: The authors declare that the research was conducted in the absence of any commercial or financial relationships that could be construed as a potential conflict of interest.

frontiers in Immunology

REVIEW
published: 30 June 2020
doi: 10.3389/fimmu.2020.01323

Pro-inflammatory Actions of Heme and Other Hemoglobin-Derived DAMPs

Marcelo T. Bozza[1] *and Viktória Jeney*[2]*

[1] *Laboratório de Inflamação e Imunidade, Departamento de Imunologia, Universidade Federal Do Rio de Janeiro, Rio de Janeiro, Brazil,* [2] *MTA-DE Lendület Vascular Pathophysiology Research Group, Research Centre for Molecular Medicine, Faculty of Medicine, University of Debrecen, Debrecen, Hungary*

Damage associated molecular patterns (DAMPs) are endogenous molecules originate from damaged cells and tissues with the ability to trigger and/or modify innate immune responses. Upon hemolysis hemoglobin (Hb) is released from red blood cells (RBCs) to the circulation and give a rise to the production of different Hb redox states and heme which can act as DAMPs. Heme is the best characterized Hb-derived DAMP that targets different immune and non-immune cells. Heme is a chemoattractant, activates the complement system, modulates host defense mechanisms through the activation of innate immune receptors and the heme oxygenase-1/ferritin system, and induces innate immune memory. The contribution of oxidized Hb forms is much less studied, but some evidence show that these species might play distinct roles in intravascular hemolysis-associated pathologies independently of heme release. This review aims to summarize our current knowledge about the formation and pro-inflammatory actions of heme and other Hb-derived DAMPs.

Keywords: hemoglobin, heme, TLR4 (toll-like receptor 4), NLRP3, DAMP, hemolysis (red blood cells)

OPEN ACCESS

Edited by:
Nicola Conran,
Campinas State University, Brazil

Reviewed by:
Lubka T. Roumenina,
INSERM U1138 Centre de Recherche des Cordeliers, France
Swee Lay Thein,
National Institutes of Health (NIH), United States

***Correspondence:**
Viktória Jeney
jeney.viktoria@med.unideb.hu

Specialty section:
This article was submitted to Inflammation, a section of the journal Frontiers in Immunology

Received: *01 April 2020*
Accepted: *26 May 2020*
Published: *30 June 2020*

Citation:
Bozza MT and Jeney V (2020) Pro-inflammatory Actions of Heme and Other Hemoglobin-Derived DAMPs. Front. Immunol. 11:1323. doi: 10.3389/fimmu.2020.01323

INTRODUCTION

Red blood cells (RBCs)—the most abundant cell type of the human body—deliver oxygen to the tissues during their lifespan of about 120 days. Under homeostasis, destruction of aged RBCs is usually an unrecognized event that takes place in macrophages of splenic and hepatic sinusoids (1). After RBC phagocytosis macrophages efficiently handle the high hemoglobin (Hb) load, break down heme, and redistribute iron for further use, or store it in a catalytically inactive form in ferritin (FT) (1). Some RBCs lyse intravascularly even under physiological conditions releasing Hb and heme to the circulation. To prevent the deleterious effects of extracellular Hb and heme they are scavenged by the acute phase plasma proteins haptoglobin (Hp) and hemopexin (Hx), respectively, and removed from the circulation rapidly (2). On the other hand, oversaturation of this defense system leads to the accumulation of different redox forms of Hb and heme in the circulation.

Heme is a well-known pro-oxidant that feature relies—at least in part—on the ability of heme iron to catalize the generation of hydroxyl-radicals in the Fenton reaction, due to its capability of acting as both an electron donor and an acceptor (3). Another important source of radical species that could mediate heme-induced toxicity is the conversion of organic hydroperoxides (ROOH) into highly reactive alkoxyl (RO•) and peroxyl (ROO•) radicals (4, 5). These radicals trigger lipid peroxidation forming alkyl radicals that in the presence of O_2 will generate more peroxyl radicals, thus amplifying free radical reactions (6). Finally, heme can also promote reactive oxygen species

(ROS) generation through enzymatic reactions mediated by NADPH oxidases (7–11) and by the mitochondria (11).

Besides being a pro-oxidant, three lines of evidence indicated that heme is an inflammatory molecule with unique properties: (i) sterile intra or extra vascular hemolysis cause inflammation, that is controlled by Hx and heme oxygenase-1 (HO-1) (12); (ii) injection of heme in experimental animals triggers local and systemic inflammation (11–14); (iii) heme activates innate immune cells *in vitro* acting as a chemoatractant, inducing cytokine production, ROS generation, and cell death (7, 8, 11, 15, 16). The observations that heme causes macrophage activation dependently of the innate immune receptors TLR4 and NLRP3 were important to a paradigm shift, defining heme as a prototipical damage-associated molecular pattern (DAMP) (11, 16–18). The requirement of TLR4 or NLRP3 to the pathological consequences of experimental sterile hemolysis suggest that heme-induced activation of these pathways contributes to the pathology (11, 12, 19, 20). Importantly, the tissue damage triggered by the actions of labile heme also critically contributes to the pathogenesis of severe infections such as malaria (21–24) and sepsis (14, 25). Growing evidence shows that the complement system can be activated by heme which mechanism play a role in the pathomechanism of certain hemolytic diseases (20, 26–28). On the other hand heme can activate defense mechanisms to establish tolerance and to foster survival of the host in diverse pathological conditions via the induction of the HO-1/FT system (17, 23, 29, 30). Recent investigation showed that heme can induce innate immune memory as well (31).

Growing evidence suggest that besides labile heme other Hb-related DAMPs e.g., metHb, ferrylHb as well as covalently crosslinked Hb multimers can be considered as alarmins (32–34). These species might play distinct, heme-independent roles in intravascular hemolysis-associated pathologies. The multiple mechanisms by which Hb-derived DAMPs modulate cell activation and inflammation, contributing to pathology, are object of intense research. In this review we aim to give an overview of the most recent development of this dynamically evolving field.

Abbreviations: ALIS, aggresome-like induced structures; AP: alternative pathway; ATP, adenosine triphosphate; CNS, central nervous system; CO, carbon monoxide; DAMPs, damage-associated molecular patterns; EC, endothelial cell; ferrylHb, ferryl hemoglobin; FT, ferritin; FTH, ferritin heavy chain; GPXs, glutathione peroxidases; Hb, hemoglobin; HO, heme oxygenase; H_2O_2, hydrogen-peroxide; Hp, haptoglobin; Hsp, heat shock protein; Hx, hemopexin; H3K9ac, histone 3 acetylation at lysine-9; H3K27ac, histone 3 acetylation at lysine-27; ICAM-1, intracellular adhesion molecule-1; ICH, intracerebral hemorrhage; IgG, immunoglobulin G; IL, interleukin; LPS, lipopolysaccharide; MAC, membrane attack complex; metHb, met(ferric) hemoglobin; MyD88, myeloid differentiation primary response gene 88; NADPH, nicotinamide adenine dinucleotide phosphate; NET, neutrophil extracellular trap; NLR, NOD-like receptor; NLRP3, NLR family pyrin domain containing 3; NO, nitric oxide; NOD, nucleotide-binding oligomerization domain; NOX, NADPH oxidase; PAMPs, pathogen-associated molecular patterns; PMNs, polymorphonuclear cells; PPARγ, Peroxisome proliferator-activated receptor γ; PRR, pattern recognition receptor; PRXs, peroxiredoxins; RBC, red blood cell; ROS, reactive oxygen species; SAH, subarachnoid hemorrhage; SOD, superoxide dismutase; Syk, spleen tyrosine kinase; TLR, toll-like receptor; TNF-α, tumor necrosis factor-alpha; TRIF, TIR-domain-containing adapter-inducing interferon-β; VCAM-1, vascular cell adhesion molecule-1.

Hb INSIDE OF THE RBCs

Hb, the major oxygen-transport protein consist of 2 different subunits, α and β, that compose a α2β2 tetrahedron. Each of the four subunits contains a heme prosthetic group with a central Fe^{2+} (ferrous) ion. Heme iron is critically involved in O_2 binding. Each ml of human blood contains ∼0.3 g of Hb, most of it is compartmentalized within RBCs.

Circulating RBCs are continuously exposed to high levels of ROS of both endogenous and exogenous origin [reviewed in (35)]. When Hb binds O_2, Hb auto-oxidation frequently occurs in which the central heme Fe^{2+} is oxidized into Fe^{3+} (ferric, metHb) with the concomitant reduction of O_2 into superoxide anion ($O_2^{\bullet -}$) (**Figure 1**). This reaction is a major source of endogenous ROS inside the RBCs. Cytochrome-b5 reductase, an NADH-dependent enzyme present in RBCs convert metHb to Hb, therefore metHb content in intact RBC generally stays below 1%.

A highly effective antioxidant defense system protects RBCs from the continuously produced ROS. This system consists of enzymes, such as Cu/Zn superoxide dismutase that converts superoxide anion to hydrogen-peroxide (H_2O_2), catalase, glutathione peroxidase, and peroxiredoxins which decompose H_2O_2 to H_2O [reviewed in (35–37)] and non-enzymatic low molecular weight scavengers, such as glutathione, ascorbic acid, and vitamin E (**Figure 1**). When ROS production exceeds the capability of ROS neutralization, RBC membrane damage occurs which impairs oxygen delivery.

During their lifespan in the circulation RBCs lose about 20% of their initial Hb content via vesiculation (38). This process is considered an efficient mechanism to remove damaged membrane patches, senescent cell antigens and intracellular inclusion bodies (Heinz bodies) from the otherwise healthy RBCs, therefore they can stay longer in the circulation (39). Approximately after 120 days in the circulation RBCs are completely worn out, and they are cleaned from the circulation by hemophagocytic macrophages, mainly in the spleen, via a non-inflammatory process which allows efficient and safe recycling of the RBC components, particularly the heme iron (40–42).

Hb OUTSIDE OF THE RBCs

Diverse inherited or acquired conditions can trigger uncontrolled destruction of RBCs in the vasculature or in the extravascular space. Upon RBC lysis a large amounts of Hb is released into the circulation, or into the surrounding tissues.

Elimination of Cell Free Hb and Limitations of the Clearance System

Following RBC lysis extracellular Hb is promptly removed from the circulation. Hp, an acute phase plasma protein is in the first line of defense [reviewed in (43)]. Hp binds extracellular Hb avidly, protects Hb from oxidation (44–48), and facilitates its clearance from the circulation through endocytosis via the CD163 macrophage scavenger receptor (49). Although abundant in the plasma (0.41–1.65 mg/ml), the amount of Hp allows the clearance of ∼3 g of Hb, <1% of the Hb amount in the

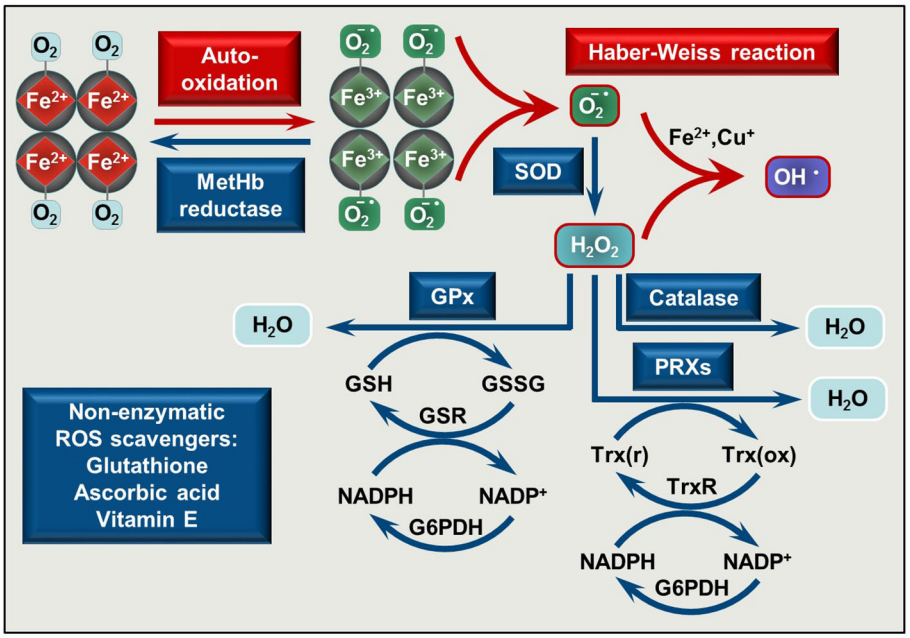

FIGURE 1 | Pro-oxidant and antioxidant mechanisms is RBCs. O_2 binding to Hb initiates Hb auto-oxidation in which process metHb (Fe^{3+}) and superoxide anion ($O_2^{\bullet-}$) are formed. MetHb is reduced by metHb reductase, while $O_2^{\bullet-}$ is converted to H_2O_2 by superoxide dismutase (SOD). In the presence of transition metals such as Fe^{2+} or Cu^+ a reaction between $O_2^{\bullet-}$ and H_2O_2 occurs yielding hydroxyl radical ($OH^{\bullet}$) (Haber Weiss reaction). Catalase, glutathione peroxidases (GPx), and peroxiredoxins (PRXs) decompose H_2O_2. The antioxidant system is completed with non-enzymatic low molecular weight scavengers, such as glutathione, ascorbic acid, and vitamin E. SOD, superoxide dismutase; GPx, glutathione peroxidase; PRXs, peroxiredoxins; GSH, reduced glutathione; GSSG, glutathione disulfide; GSR, glutathione-disulfide reductase; $NADP^+$, nicotinamide adenine dinucleotide phosphate; NADPH, reduced NADP; G6PDH, glucose-6-phosphate dehydrogenase; Trx(r), reduced thioredoxin; Trx(ox), oxidized thioredoxin; TrxR, thioredoxin reductase.

circulation. Therefore, massive hemolysis with more than 1% of RBC lysis, Hp is depleted from the plasma and cell-free Hb is eliminated from the circulation via alternative mechanisms. These include (i) a low-affinity pathway through CD163 by macrophages (50) and (ii) renal excretion which is accompanied by profound oxidative stress and organ damage (51, 52).

Failure of Hb Clearance: Nitric Oxide Depletion, Hb Oxidation, and Heme Release

Once the capacity of the Hp/CD163 system is overwhelmed, cell free Hb accumulates in the plasma. Hb exhibits a high affinity for nitric oxide (NO), the important endogenously produced gas that plays a major role in the regulation of vascular tone [reviewed in (53, 54)]. Scavenging of NO by Hb triggers vasoconstriction that contributes to clinical complications in diverse forms of hereditary or acquired hemolytic anemias (55). Furthermore, non-compartmentalized Hb cannot benefit from the highly efficient antioxidant defense system present in intact RBCs, and Hb tends to oxidize. One-electron oxidation of Hb occurs when Hb reacts with NO resulting metHb. Also auto-oxidation of oxyHb triggers metHb generation with the concomitant production of superoxide anions (**Figure 2A**). Two-electron oxidation of Hb occurs when Hb reacts with peroxides, such as H_2O_2 or lipid hydroperoxides leading to the formation of ferryl ($Fe^{4+} = O^{2-}$) Hb (**Figure 2B**). When metHb reacts with peroxides ferrylHb radical is formed [$Hb^{\bullet+}(Fe^{4+} = O^{2-})$] in which the unpaired electron is located at either the globin chain or at the porphyrin ring (56–59). The ferryl oxidation state of iron is very unstable, therefore these high-valence Hb forms are short-lived intermediates that decay quickly (60).

Ferryl iron can oxidize the neighboring oxidation-prone amino acid residues of the globin chains (i.e., αTyr-24, αTyr-42, αHis-20, βTyr-35, βTyr-130, and βCys-93) with the concomitant reduction of Fe^{4+} into Fe^{3+} (37, 61, 62). This intramolecular electron transfer between the ferryl iron and the amino acids yields metHb globin radicals in which the unpaired electrons are located on the oxidized amino acid residues (37, 61, 62). Reactions between globin radicals or between globin and porphyrin-centered radicals lead to the formation of globin-globin and porphyrin-globin adducts, respectively (**Figure 2C**). These structurally altered Hb forms are less efficiently removed from the circulation because both high-affinity (Hb-Hp/CD163) and low-affinity (Hb/CD163) endocytosis pathways are compromised (50, 63).

The prosthetic heme group is tightly bound in Hb, while this bound is weakened in oxidized Hb forms. Both metHb and ferrylHb releases heme moiety (**Figure 2**) which is captured by the acute phase plasma protein Hx (64). Hx-heme complexes are taken up mainly by macrophages and hepatocytes through the scavenger receptor LDL receptor-related protein 1/CD91 (65,

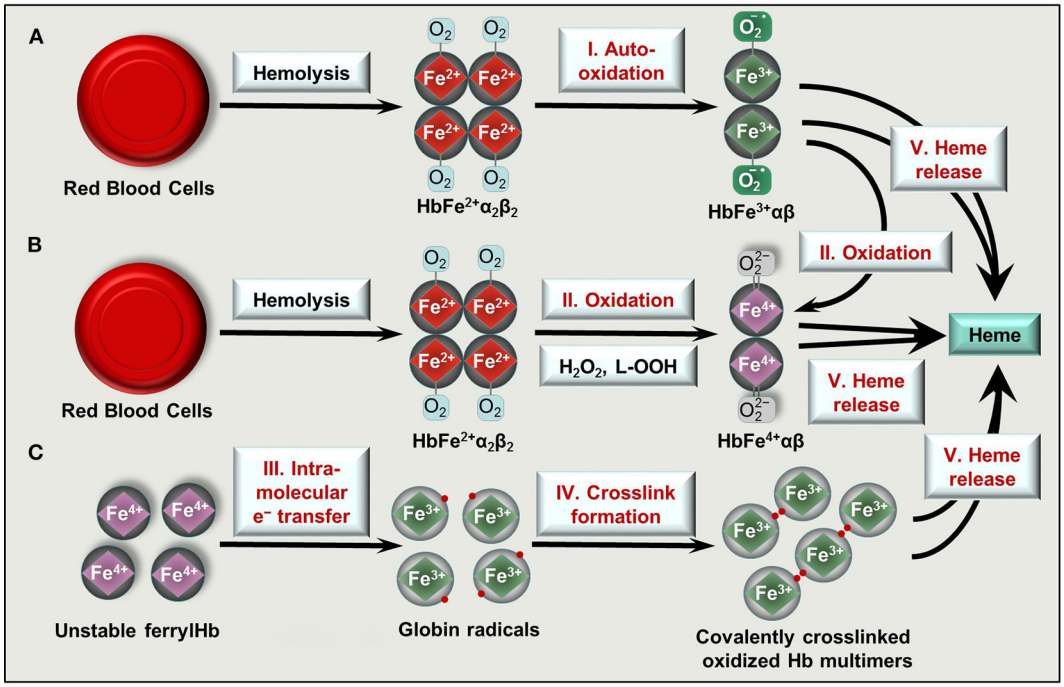

FIGURE 2 | Formation of oxidized Hb forms and labile heme upon hemolysis. Hb tetramers ($HbFe^{2+}\alpha_2\beta_2$) is released from RBCs following intra- or extravascular hemolysis. **(A)** Hb outside of RBCs dimerize and can undergo spontaneous auto-oxidation (reaction I) to metHb ($HbFe^{3+}\alpha\beta$). **(B)** Two-electron oxidation (reactions II) of Hb and metHb by H_2O_2 or lipid hydroperoxides (L-OOH) lead to the formation of ferrylHb ($HbFe^{4+}\alpha\beta$) or ferrylHb radicals, respectively. **(C)** FerrylHb get stabilized via intramolecular electron transfer (reaction III) between iron and the globin chain forming globin radicals. Globin radicals get stabilized via covalent crosslinking (reaction IV) producing covalently crosslinked Hb multimers. Oxidized Hb forms (metHb, ferrylHb, covalently crosslinked Hb) release their heme prosthetic group (reactions V).

66). Similarly to Hp, Hx is also depleted from the plasma upon massive intravascular hemolysis, leading to the appearance of labile heme, that is, a redox active form of heme which is loosely bound to molecules, other than hemoproteins including albumin, α_1-microglobulin and lipoproteins such as LDL and HDL.

Recycling of heme iron is a critical component of systemic iron metabolism. Iron is released from the heme molecule via the action of heme oxygenases (HOs), mainly HO-1, the inducible isoenzyme that catabolizes free heme into equimolar amounts of Fe^{2+}, carbon monoxide (CO), and biliverdin (67). HO-1 induction and heme degradation products exhibit various cytoprotective mechanisms (29). Heme-mediated HO-1 induction and iron release is associated with the upregulation of ferritin, the major intracellular iron storage protein, assuring that iron is stored in a catalytically inactive still bioavailable form inside the cells (68).

ACTIVATION OF THE INNATE IMMUNE SYSTEM BY LABILE HEME AND OXIDIZED Hb FORMS

Hemolytic and hemorrhagic episodes are often accompanied by inflammation even in the absence of pathogens (17, 69). Accumulating evidence suggest that upon hemolysis RBCs release large amounts of DAMPs including RBC microvesicles, heme, ATP, heat shock protein 70, interleukin-33 that induce pro-inflammatory responses in different cells (70, 71). Here we will focus on the contribution of Hb-derived DAMPs to the hemolysis-induced sterile inflammatory responses (**Figure 3**).

Endothelial Cells (ECs) as First Line Targets of Hb-Derived DAMPs

A monolayer of ECs cover the entire vasculature and the lymphatic system providing a semi-permeable barrier between blood and tissue, and lymph and tissue, respectively. Under physiological conditions, ECs are involved in many processes including the regulation of metabolic homeostasis, vascular hemodynamics, vascular permeability, coagulation, and cell trafficking [reviewed in (72)]. Besides of these numerous functions, ECs are one of the first cell types to detect pathogen-associated molecular patterns (PAMPs) and DAMPs in the bloodstream, therefore ECs have important immunological functions in the early innate immune system activation as danger signal sensors [reviewed in (72)]. ECs are equipped with a series of pathogen-associated pattern recognition receptors (PRRs) including toll-like receptors (TLRs) and nucleotide-binding oligomerization domain (NOD)-like receptors (NLRs), as well as diverse chemokine receptors [reviewed in (73)]. Growing evidence shows that ECs respond to various Hb-derived DAMPs.

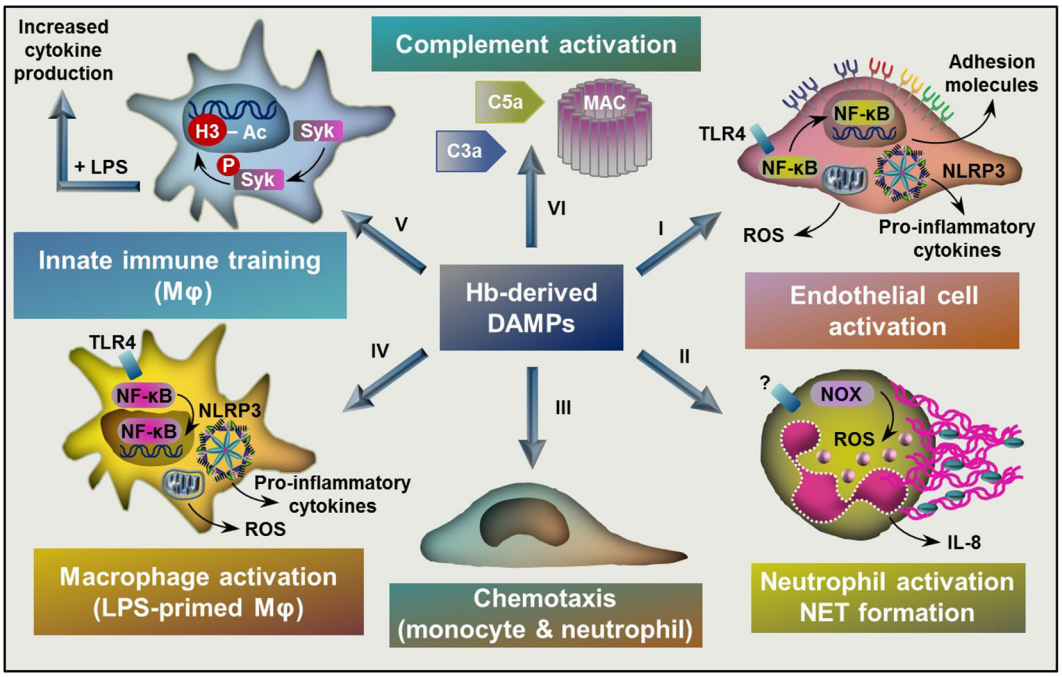

FIGURE 3 | Targets of Hb-derived DAMPs. (I) Labile heme and ferrylHb induces endothelial cell activation characterized by NF-κB activation, elevated ROS production, and increased expression of adhesion molecules and pro-inflammatory cytokines. (II) Heme activates neutrophils characterized by elevated ROS production through the activation of NOX, increased production of IL-8 and NET formation. (III) Heme and ferrylHb induces monocyte and neutrophil chemotaxis. (IV) Labile heme and ferrylHb induces ROS production, NLRP3 activation, and pro-inflammatory cytokine production in LPS-primed macrophages. (V) Heme induces innate immune training through triggering epigenetic changes, such as acetylation of H3 at lysine-27 in monocytes and macrophages in a Syk-dependent manner. (VI) Heme induces complement activation leading to the formation of C3a and C5a activation fragments and the assembly of MAC. NF-κB, nuclear factor kappa B; ROS, reactive oxygen species; NOX, NADPH oxidase; NET, neutrophil extracellular trap; TLR4, toll-like receptor 4, NLRP3, NLR family pyrin domain containing 3; LPS, lipopolysaccharide; Syk, Spleen tyrosine kinase; H3, histone 3, MAC, membrane attack complex.

Heme-Mediated TLR4-Dependent EC Activation (Adhesion Molecules and Barrier Function)

ECs respond to a variety of inflammatory stimuli e.g., IL-1, tumor necrosis factor α (TNF-α), lipopolysacharid (LPS) by upregulating the expression of cellular adhesion molecules including intracellular adhesion molecule-1 (ICAM-1), vascular cell adhesion molecule-1 (VCAM-1), and E selectin (74, 75). These adhesion molecules anchor leukocytes to the endothelial surface and facilitate their transmigration into the inflamed tissue. Interestingly heme, similarly to that of IL-1, TNF-α, or LPS upregulates the expressions of adhesion molecules (76) in a TLR4-dependent manner (19, 20).

This heme-mediated TLR4-dependent mechanism has been connected to vaso-occlusive crisis in sickle cell disease (**Figure 3**) (19). Recent evidence shows that TLR4-dependent upregulation of endothelial P-selectin triggers an unconventional route of complement activation by non-covalent binding of C3 activation fragments on the surface of ECs, which mechanism contributes to liver injury in hemolytic diseases such as sickle cell disease (20).

Besides increased expression of cell surface adhesion molecules, increased endothelial permeability contributes to inflammatory cell extravasation upon hemolysis. Many attempts were made to identify the molecular mechanism of this phenomenon which revealed that ferrylHb and free heme trigger the loss of endothelial integrity (33, 77–80). Heme-induced loss of endothelial barrier function is dependent on the activation of the p38/heat shock protein 27 pathway (79) and associated with TLR4-dependent production of ROS and necroptosis (77).

FerrylHb-Mediated TLR4-Independent EC Activation (Adhesion Molecules and Barrier Function)

Besides heme, ferrylHb but not Hb or metHb induces up-regulation of adhesion molecules ICAM-1, VCAM-1, and E-selectin, and increase endothelial cell monolayer permeability in human ECs (**Figure 3**) (33). Interestingly, ferrylHb-mediated responses are dependent on the activation of nuclear factor kappaB (NF-κB), requires actin polymerization, involves the activation of the c-Jun N-terminal kinase and the p38 mitogen-activated protein kinase signal transduction pathways but not dependent on TLR4 activation (33). The facts that (i) ferrylHb and heme trigger endothelial activation with the use different signaling mechanisms and that (ii) metHb – that can release heme more avidly than ferrylHb – does not induce EC activation suggest that ferrylHb-mediated EC activation cannot be simply considered as a consequence of heme release from ferrylHb. The putative receptors associated with ferrylHb-induced EC activation are currently unknown.

Induction of Cytokine Production by Hb-Derived DAMPs in ECs

Growing evidence suggest that endothelial cells are not only sentinels of the activation of the innate immune system but actively participate in cytokine production upon hemolysis. Recently heme and ferrylHb were identified as activators of the NLRP3 inflammasome leading to processing and secretion of active IL-1β in LPS-primed macrophages (11, 34). Previously it has been shown that ECs respond to classical DAMPs such as extracellular ATP and high mobility group box 1 protein (HMGB1) by the activation of NLRP3 inflammasome and the subsequent production of IL-1β (81, 82). Based on these information we investigated whether heme and the different Hb redox forms induce NLRP3 inflammasome activation in ECs (32). We showed that heme but not the different Hb redox forms induced NLRP3 inflammasome activation and IL-1β production ECs (**Figure 3**). Heme-induced inflammasome activation in ECs requires LPS priming, structural integrity of the heme molecule, and ROS production (32). Recent data suggest that globin-derived peptides formed during Hb oxidation are also capable to induce NLRP3 inflammasome activation and IL-1β production in ECs (83). Besides IL-1β production, Hb-derived DAMPs, namely metHb but not Hb has been implicated in IL-6 and IL-8 production in ECs (84). In the same experimental setting heme did not induce IL-6 and IL-8 production in ECs, so we can assume that metHb-induced EC response was independent of heme release.

Hb-Derived Molecules as Chemoattractants

Heme is chemoatractant *in vivo*, which notion is supported by the finding that peritoneal injection of heme causes the recruitment of neutrophils and intravenous administration of heme causes leukocyte infiltration in various organs (7, 11, 15, 85). Heme-induced neutrophil recruitment is independent of TLR4 activation (16), but depends on the endogenous production of leukotriene B4 by macrophages (86) and the activation of the NLRP3 inflammasome (11).

Recent studies showed that besides heme, ferrylHb, but not Hb and metHb triggers peritoneal infiltration of monocytes and neutrophils (33, 34). The chemotactic effect of ferrylHb is less likely to be dependent on heme release exclusively, which is supported by two facts; first, ferrylHb is a more powerful inducer of leukocyte infiltration than heme and second, metHb that has the ability to release heme at the same or even higher rate as ferrylHb (87) fails to trigger leukocyte recruitment (34).

Actions on Neutrophils

Neutrophil granulocytes play a fundamental role in innate and adaptive immunity. Upon infection or inflammation, neutrophils are the first leukocytes migrating from the blood into the affected tissues. Neutrophils are equipped with sensors of PAMPs and DAMPs, they kill and phagocytose pathogens and clear cellular debris (88). In the recent years, it has become evident that neutrophils not only sense PAMPs but can recognize and respond to endogenous DAMPs as well. As it was mentioned before, heme and ferrylHb are potent triggers of neutrophil infiltration (7, 15, 33, 85). Moreover, heme has been shown to activate neutrophils characterized by elevated ROS production and increased expression of the pro-inflammatory cytokine IL-8 (**Figure 3**) (7, 15). Heme is a potent chemoattractant of neutrophils *in vitro* in a mechanism characteristic of a G protein-coupled receptor activation (7, 15). Heme-induced neutrophil chemotaxis and ROS production are independent of the coordinated iron present in heme, while requires the vinyl groups in the porphyrin ring (15, 89).

Upon activation neutrophils release extracellular traps—meshes composed of chromatin and neutrophil granular proteins—which plays a critical role in immobilization of invading pathogens (90). Recently heme has been identified as a potent inducer of neutrophil extracellular trap (NET) formation in TNF-α-primed neutrophils *in vitro* and *in vivo* (91). Accumulating evidence show that heme-mediated NET formation plays a pathogenic role in vaso-occlusion crises in sickle cell disease, in transfusion-related acute lung injury, in systemic inflammation in paroxysmal nocturnal hemoglobinuria as well as in malaria (91–94). Interestingly, heme-induced NET formation requires the coordinated heme iron, is dependent on NADPH oxidase and ROS formation but occurs independently of TLR4 (95). These results suggest that at least two different signaling pathways are activated by heme on neutrophils. One that triggers chemotaxis and is independent of the heme iron while requires the vinyl groups, and one that triggers the NET release, requires the iron but not the vinyl groups of the porphyrin ring. The putative receptors associated with these activities are currently unknown.

Activation of Macrophages by Hb-Derived DAMPs

Macrophages are effector cells of the innate immune system, which respond to a variety of PAMPs and DAMPs. Macrophages are present in all vertebrate tissues and have highly heterogeneous phenotypes depending on the environmental cues encountered.

TLR4 Activation by Heme in Macrophages

Heme profoundly affect macrophage physiology through multiple pathways (17, 18). The requirement of TLR4 to the induction of TNF production by heme on macrophages was the first demonstration of a receptor-mediated effect of heme (16). The coordinated iron and the vinyl groups are essential for heme to induce TLR4-dependent TNF production. The effect of heme on macrophages through TLR4 is exquisitely different from the effect of LPS, the canonical agonist of TLR4. While LPS triggers the activation of the Myeloid differentiation primary response 88 (MyD88) and the TIR-domain-containing adapter-inducing interferon-β (TRIF) pathways (96) on macrophages and DCs, heme activates only the MYD-88 pathway and is unable to induce the expression of type I interferon or co-stimulatory molecules (16).

Heme-Induced Macrophage Necroptosis

High amounts of free heme due to hemolysis is involved with the loss of macrophages, specially in the absence of HO-1 (97). Heme induces macrophage necroptotic cell death in a

mechanism that requires TNF, ROS, and the kinases RIPK1 and RIPK3 (98). Although required to heme-induced TNF production, TLR4 is not essential for the necroptosis induced by heme in the presence of exogenous TNF. An important study demonstrated that heme triggers tissue macrophage differentiation by inducing the transcriptional factor Spic in monocytes through a mechanism dependent on the degradation of the transcriptional repressor Bach1 (99). During pathological hemolysis, the axis formed by heme, Bach1, and Spic is critically involved in the homeostatic response to the macrophage loss. Another compensatory response to hemolysis and heme is the formation of aggresome-like induced structures (ALIS) on macrophages, p62/SQTM1 aggregates containing ubiquitinated proteins (100, 101). The heme-induced ALIS formation on macrophages requires mitochondrial ROS, NRF2 and HO-1, while is independent of TLR4. Moreover, iron from heme is necessary, while both Fe^{2+} and Fe^{3+} are sufficient to trigger ALIS formation (100). The physiopathological role of heme-iduced ALIS formation is currently unknown.

NLRP3 Activation by Heme in Macrophages

Heme has a synergistic effect with microbial molecules on macrophages, increasing the production of inflammatory cytokines in a mechanism dependent of ROS and spleen tyrosine kinase (Syk) (13). Moreover, heme induces NLRP3 inflammasome activation leading to processing and secretion of active IL-1β in LPS-primed macrophages (11). Heme-mediated NLRP3 inflammasome activation is found to be dependent on the coordinated heme iron, and also involves activation of Syk, elevated ROS production by NOX2 and the mitochondria and K(+) efflux, contributing to intravascular hemolysis-induced lethality (11). An interesting study demonstrated that heme reduces the host resistance to bacterial infection (102). Treatment of macrophages with heme, but not with Hb, free iron, or the heme analogs protoporphyrin IX and tin-protoporphyrin IX, causes a dose-dependent inhibition of *E. coli* phagocytosis by macrophages (102). This inhibitory effect of heme on macrophage phagocytosis and chemotaxis occurs through the activation of the GTP-binding Rho family protein Cdc42 by DOCK8, a guanine nucleotide exchange factor, disrupting actin cytoskeletal dynamics (102). Together, these results indicate possible signaling pathways for therapeutic intervention during hemolytic infectious conditions.

NLRP3 Activation by ferrylHb in Macrophages

Besides heme, the involvement of different Hb redox forms was investigated in hemolysis-associated NLRP3 inflammasome activation in macrophages. That study revealed that ferrylHb but not Hb or metHb induce active IL-1β production in LPS-primed macrophages in an NLRP3-dependent manner (34). Based on the fact that metHb cannot induce IL-1β production in LPS-primed macrophages it is unlikely that heme release plays a critical role in the ferrylHb-triggered response. FerrylHb-induced NLRP3 activation is associated with elevated ROS production but the detailed molecular mechanism needs to be further explored (34).

Hemorrhage-Associated Macrophage Subsets

Besides the two extreme canonical macrophage phenotypes, the pro-inflammatory M1 and the anti-inflammatory M2, many other specific and distinct macrophage subsets exist (103). Both extracellular Hb and heme are implicated in macrophage polarization triggering the formation of hemorrhage-associated M(Hb) and M(heme) subsets, respectively (103–106). These hemorrhage-associated macrophage subsets were first identified in advanced human atherosclerotic lesions with intraplaque hemorrhage (103–106). M(Hb) macrophages represent a subpopulation of CD68+ macrophages and their characteristic markers are the macrophage mannose receptor 1 and the CD163 receptor through which macrophages recognize and endocytose Hp-Hb complexes (103–105). Additionally, due to their role in Hb clearance, M(Hb) macrophages exhibit increased HO-1 and ferroportin expressions thereby facilitating heme catabolism and cellular efflux of excess iron (105). Reduced labile iron content in M(Hb) macrophages is associated with less ROS production which is linked to increased activity of the transcription factor liver X receptor-α and the induction of cholesterol efflux (105). Because of this, M(Hb) macrophages are protected from lipid accumulation and produce anti-inflammatory factors, such as IL-10 (105). M(heme) macrophage polarization is driven by extracellular heme, and similarly to that of M(Hb) this subset is protected from oxidative stress and lipid accumulation (107).

Activation of Microglia by Hb-Derived DAMPs

Microglia are the primary innate immune effector cells of the central nervous system (CNS) with a similar function to macrophages. Intracerebral and subarachnoid hemorrhages (ICH and SAH, respectively) are associated with activation of microglia and growing evidence suggest that inflammation is the key contributor of secondary brain injury induced by ICH or SAH (108, 109). Microglia have an important function in hematoma resolution by phagocytosing RBCs which process is mediated by the class B scavenger receptor CD36 (110, 111). CD36 expression is regulated by peroxisome proliferator-activated receptor γ (PPARγ), and activation of PPARγ has been shown to promote hematoma resolution and decrease neuronal damage following ICH (111). Incomplete removal of RBCs leads to hemolysis and the production of oxidized Hb forms and free heme (112, 113). Microglia plays a critical role in removing these toxic Hb derivatives from the central nervous system through CD163-Hp-Hb and CD91-Hx-heme scavenging mechanisms and heme degradation by HO enzymes (114–117). These mechanisms can attenuate bleeding-associated neuronal damage, though we have to note that upon significant intrathecal hemolysis the Hb-heme elimination system is largely overwhelmed leading to the accumulation of oxidized Hb forms and free heme in the CNS (112–114).

These Hb-derived DAMPs trigger neuroinflammation following ICH and SAH. In line of this notion it has been shown that heme induces TLR4-mediated inflammatory injury via the

activation of MyD88/TRIF pathways in microglia following ICH (118). Importantly, mice deficient of *Tlr4* or anti-TLR4 treatment reduce heme-induced neurologic deficit, brain edema, and inflammation. Not only heme, but also metHb has been identified as a TLR4 agonist that triggers the secretion of TNF-α by the microglia (119). A number of studies support the notion that TLR4 contributes to the brain injury due to ICH (120–123). Additionally, heme induces the release of IL-1α but not IL-1β in primary mixed glia (124). Targeting these inflammatory pathways with anti-TLR4 antibody or with IL-1 receptor antagonist attenuate intrathecal hemorrhage-associated inflammatory injury (118, 124). A recent study showed that besides heme and metHb, large amounts of covalently crosslinked Hb multimers (dimers and tetramers) accumulate in the cerebrospinal fluid of preterm infants following IVH (112). Further work needed to address whether these Hb multimers are implicated in the inflammatory microglia activation following IVH.

Induction of Innate Immune Memory by Heme

Trained immunity or innate immune memory is the ability of the innate immune system to adapt its function after previous encounters with pathogens or their products (125). This mechanism not only provides protection against reinfection but also contributes cross-protection between infections with different pathogens (125, 126). The major cell types in which trained immunity occurs are myeloid cells, natural killer cells, and innate lymphoid cells. Trained immunity is activated by PAMPs such as LPS or β-glucan via PRR signaling, resulting changes in transcription programs through epigenetic regulation that can persist for up to several weeks (125, 126). Epigenetic reprogramming – driven by histone acetylation, for example at lysine-9 (H3K9ac) and lysine-27 (H3K27ac) of H3 histones that almost exclusively determines transcriptional capability – is a critical determinant of trained immunity (127).

Recently it was reported that heme is a potent inducer of trained immunity in monocytes and macrophages both *in vitro* and *in vivo* (31). Heme pretreatment increased pro-inflammatory cytokine (TNF-α, IL-6, IL-8) release from macrophages upon secondary challenge by LPS (**Figure 3**) (31). Such effect of heme was independent on the pro-oxidant nature of heme, which notion is supported by the fact that (i) trained immunity is induced by protoporphyrin IX, lacking iron and (ii) it is not prevented by the glutathione precursor N-acetyl cysteine (31). Heme pretreatment triggered epigenetic changes, such as acetylation of H3k27. Comparing heme and β-glucan-induced training in monocytes revealed overlapping as well as distinct epigenetic and transcriptional responses between the two triggers (31). Common pathways, regulated by both heme and β-glucan included lysosome maturation and metabolism. Genes only induced by heme are mainly involved in inflammatory pathways, and as expected heme/iron related metabolism (31). Another remarkable difference between heme- and β-glucan-induced training is that heme-mediated training relies on the activation of Syk and c-Jun n-terminal kinase, but independent on the activation of the Mammalian Target of Rapamycin which is largely involved in β-glucan training (31). This finding reinforces the critical role of Syk signaling on heme-induced macrophage activation (11, 13). At present, the mechanism by which heme triggers Syk phosphorylation is unknown (17). Interestingly, heme seems to be a Janus-faced training molecule *in vivo* resulting that the outcome of heme pretreatment largely depends on the experimental conditions (31).

Complement Activation and the Thromboinflammatory Loop

Originally the complement system has been considered as a simple mechanism to induce bacterial lysis. Recently it became evident that complement has diverse functions in both physiologic and pathologic conditions (128). The complement system senses PAMPs and DAMPs and translate the danger information into an adequate cellular innate or adaptive immune response (129). The complement system is a cascade of more than 40 proteins, which can be initiated by different ways. There are three known distinct ways for complement activation: the classical, the lectin-mediated, and the alternative pathway (AP) (130). Activation of each of the three pathways leads to a common terminal pathway in which the inactive C3 protein is cleaved into the functional fragments C3a and C3b, and the membrane attack complex (MAC) is formed (130). These products of complement activation mediate a diverse inflammatory response that includes opsonization and phagocytosis, bacterial killing, immune cell recruitment, endothelial and epithelial cell activation, platelet activation and interaction with the adaptive immune system (128).

It has long been known that hemolytic disorders, such as sickle-cell disease, beta-thalassemia major, thrombotic thrombocytopenic purpura, and paroxysmal nocturnal hemoglobinuria are associated with complement over-activation (131–136). Recent evidence suggest that heme has a direct role in hemolysis-associated complement activation (**Figure 3**). In line of this notion heme has been shown to activate the complement AP and trigger the deposition of C3 activation fragments on the surface of RBCs (28). A detailed work showed that C3a, C5a, and sC5b9 activation fragments are formed during heme-mediated activation of the complement AP in normal human serum (**Figure 3**) (26). Additionally, heme-exposed ECs also activate the AP resulting in cell-bound C3 and MAC, which mechanism contributes to endothelial damage and thrombosis in atypical hemolytic uremic syndrome (26). Drug-induced intravascular hemolysis or injection of heme trigger C3 deposition in the kidneys and subsequent renal damage which can be attenuated by the heme scavenger Hx. Also, deficiency of C3 attenuates hemolysis-induced kidney injury in mice, suggesting that heme-mediated complement activation and C3 deposition play a fundamental role in renal damage upon intravascular hemolysis (27).

Clinical and epidemiological studies revealed that RBC abnormalities such as abnormal hematocrit, sickle cell disease, thalassemia, hemolytic anemias, and malaria are associated with

increased incidence of both arterial and venous thrombosis (137). Recently it has been shown that heme activates the tissue factor (TF)-dependent extrinsic coagulation pathway both *in vitro* and *in vivo* which can be attenuated by an anti-TF antibody (138, 139). Importantly, inhibition of TF-induced coagulation activation reduces microvascular stasis and lung vaso-occlusion in sickle mice (140). By activating both inflammatory and hemostatic pathways extracellular heme can trigger a thromboinflammatory vicious cycle that can contribute to the pathogenesis of hemolytic diseases. Recently the heme-induced thrombogenecity was studied in an *ex vivo* human whole blood model. Heme-induced thromboinflammation was attenuated by the inhibition of the complement component C5 and the TLR coreceptor CD14 (141). Inhibition of the thromboinflammatory loop can be a meaningful therapeutic target in hemolytic diseases (141).

Modulation of Host Defense Mechanism by Labile Heme

High concentrations of labile heme are observed in infectious conditions, such as malaria and sepsis, both in humans and experimental animals (14, 17, 21, 29). As in sterile hemolytic conditions, the axis Hp/Hx and HO-1/FT heavy chain (FTH) also provides critical host protection against free heme on infectious disease with increased hemolysis (14, 21–25, 29). Two complementary mechanisms comprise the host response to infection. Resistance, a primarily attribute of the immune system, is associated with the reduction or elimination of infectious agents, while tolerance is the capacity of limiting the pathological consequences of an infection (142, 143). Heme can affect the host responses in multiple ways, modulating both the disease tolerance and the resistance to infection. In a series of important studies, it has been demonstrated that heme contributes to the pathogenesis of malaria by increasing tissue damage, while HO-1 and FTH contributes to disease tolerance irrespective of changes on pathogen loads (21–24). A recent study indicates that sickle cell trait with low grade hemolysis is beneficial in malaria infection due to an increased in disease tolerance associated with higher HO-1 expression (23). CO, generated by the catabolism of heme by HO-1, binds to heme inhibiting its release from the Hb during malaria, thus preventing pathology (21). Moreover, the antioxidant effects of HO-1 inhibits the hepatocyte apoptosis induced by the synergistic effects of heme and TNF, preventing hepatic failure, and death in a mouse model of malaria (144).

In a mouse model of endotoxemia heme enhances the plasma concentrations of TNF and IL-6, drastically increasing the lethality induced by LPS (13). This increased lethality in mice is observed even when the challenge with LPS occurs after 6 days of treatment with heme and correlates with increased numbers of tissue macrophages (31). Heme reduces blood glucose levels dependently of TLR4, contributing to the severity of sepsis, while FTH reverts this effect contributing to glucose and tissue homeostasis (25). In mouse models of severe bacterial infection, heme increases multi organ failure, and lethality irrespective to a change on pathogen load (14). An interesting study has shown that heme reduces resistance to Gram-negative infection in mice predisposing to pathogen dissemination through the suppression of phagocytic function and independently of bacterial growth due to nutritional advantage (102). These results suggest that upon acute bacterial infection heme can be deleterious due to an increase on tissue damage and bacterial loads.

Heme can also modify immunoglobulin-mediated immune responses. This activity relies on the ability of heme to bind to immunoglobulins of different isotypes (IgG, IgA and IgM) leading to the formation of heme-immunoglobulin complexes that exhibit increased reactivities toward various self and bacterial antigens (145). Besides that, it has been shown that heme-IgG complex can interact with previously unrecognized bacterial antigens and intact bacteria through binding to an enlarged panel of structurally unrelated epitopes (146). Heme-induced expansion of the antibody repertoire may represent an inducible innate-type host defense mechanism against infections (146).

CONCLUSIONS

Upon hemolysis a large amount of Hb is released from RBCs that is oxidized in the extracellular milieu. Cell free Hb, its oxidation products and heme that is released from oxidized Hb forms are potential DAMPs. Among these numerous Hb oxidation products heme is the most widely studied molecule, and its contribution as a DAMP in hemolysis-associated pathologies has been confirmed. Because of structural alterations oxidized Hb forms (metHb and ferrylHb) bind heme less avidly than Hb, therefore pro-inflammatory actions of oxidized Hb forms was thought to be attributed to their ability to release the heme prosthetic group. This idea is challenged by recent studies suggesting that oxidized Hb forms, in particular ferrylHb exhibit pro-inflammatory actions independently of heme release. A lot of work needs to be done to further explore the colorful picture of Hb-derived DAMPs, their targeted cells and the mechanisms of their actions. Comprehensive understanding of hemolysis/hemorrhage-associated inflammation could contribute to the development of novel therapeutics intended to interrupt these pathological events.

AUTHOR CONTRIBUTIONS

MB and VJ planned and wrote the manuscript. VJ draw the figures. All authors contributed to the article and approved the submitted version.

FUNDING

This research was funded by the Hungarian National Research, Development and Innovation Office (NKFIH), Grant No. K131535 and by the Hungarian Academy of Sciences, MTA-DE Lendület Vascular Pathophysiology Research Group, Grant No. 96050. MB received support from the Brazilian agencies FAPERJ, CNPq, and CAPES.

REFERENCES

1. Ganz T. Macrophages and systemic iron homeostasis. *J Innate Immun*. (2012) 4:446–53. doi: 10.1159/000336423
2. Schaer DJ, Vinchi F, Ingoglia G, Tolosano E, Buehler PW. Haptoglobin, hemopexin, and related defense pathways-basic science, clinical perspectives, and drug development. *Front Physiol*. (2014) 5:415. doi: 10.3389/fphys.2014.00415
3. Sadrzadeh SM, Graf E, Panter SS, Hallaway PE, Eaton JW. Hemoglobin. A biologic fenton reagent. *J Biol Chem*. (1984) 259:14354–6.
4. Tappel AL. Unsaturated lipide oxidation catalyzed by hematin compounds. *J Biol Chem*. (1955) 217:721–33.
5. VanderZee J, Barr DP, Mason RP. ESR spin trapping investigation of radical formation from the reaction between hematin and tert-butyl hydroperoxide. *Free Radical Bio Med*. (1996) 20:199–206. doi: 10.1016/0891-5849(95)02031-4
6. Ryter SW, Tyrrell RM. The Heme synthesis and degradation pathways: role in oxidant sensitivity - heme oxygenase has both pro- and antioxidant properties. *Free Radical Bio Med*. (2000) 28:289–309. doi: 10.1016/S0891-5849(99)00223-3
7. Graca-Souza AV, Arruda MA, de Freitas MS, Barja-Fidalgo C, Oliveira PL. Neutrophil activation by heme: implications for inflammatory processes. *Blood*. (2002) 99:4160–5. doi: 10.1182/blood.V99.11.4160
8. Arruda MA, Barcellos-de-Souza P, Sampaio AL, Rossi AG, Graca-Souza AV, Barja-Fidalgo C. NADPH oxidase-derived ROS: key modulators of heme-induced mitochondrial stability in human neutrophils. *Exp Cell Res*. (2006) 312:3939–48. doi: 10.1016/j.yexcr.2006.08.022
9. Moraes JA, Barcellos-de-Souza P, Rodrigues G, Nascimento-Silva V, Silva SV, Assreuy J, et al. Heme modulates smooth muscle cell proliferation and migration via NADPH oxidase: a counter-regulatory role for heme oxygenase system. *Atherosclerosis*. (2012) 224:394–400. doi: 10.1016/j.atherosclerosis.2012.07.043
10. Barcellos-de-Souza P, Moraes JA, de-Freitas-Junior JC, Morgado-Diaz JA, Barja-Fidalgo C, Arruda MA. Heme modulates intestinal epithelial cell activation: involvement of NADPHox-derived ROS signaling. *Am J Physiol Cell Physiol*. (2013) 304:C170–9. doi: 10.1152/ajpcell.00078.2012
11. Dutra FF, Alves LS, Rodrigues D, Fernandez PL, de Oliveira RB, Golenbock DT, et al. Hemolysis-induced lethality involves inflammasome activation by heme. *Proc Natl Acad Sci USA*. (2014) 111:E4110–8. doi: 10.1073/pnas.1405023111
12. Ghosh S, Adisa OA, Chappa P, Tan F, Jackson KA, Archer DR, et al. Extracellular hemin crisis triggers acute chest syndrome in sickle mice. *J Clin Invest*. (2013) 123:4809–20. doi: 10.1172/JCI64578
13. Fernandez PL, Dutra FF, Alves L, Figueiredo RT, Mourao-Sa D, Fortes GB, et al. Heme amplifies the innate immune response to microbial molecules through spleen tyrosine kinase (Syk)-dependent reactive oxygen species generation. *J Biol Chem*. (2010) 285:32844–51. doi: 10.1074/jbc.M110.146076
14. Larsen R, Gozzelino R, Jeney V, Tokaji L, Bozza FA, Japiassu AM, et al. A central role for free heme in the pathogenesis of severe sepsis. *Sci Transl Med*. (2010) 2:51ra71. doi: 10.1126/scitranslmed.3001118
15. Porto BN, Alves LS, Fernandez PL, Dutra TP, Figueiredo RT, Graca-Souza A et al. Heme induces neutrophil migration and reactive oxygen species generation through signaling pathways characteristic of chemotactic receptors. *J Biol Chem*. (2007) 282:24430–6. doi: 10.1074/jbc.M703570200
16. Figueiredo RT, Fernandez PL, Mourao-Sa DS, Porto BN, Dutra FF, Alves LS, et al. Characterization of heme as activator of toll-like receptor 4. *J Biol Chem*. (2007) 282:20221–9. doi: 10.1074/jbc.M610737200
17. Dutra FF, Bozza MT. Heme on innate immunity and inflammation. *Front Pharmacol*. (2014) 5:115. doi: 10.3389/fphar.2014.00115
18. Soares MP, Bozza MT. Red alert: labile heme is an alarmin. *Curr Opin Immunol*. (2016) 38:94–100. doi: 10.1016/j.coi.2015.11.006
19. Belcher JD, Chen C, Nguyen J, Milbauer L, Abdulla F, Alayash AI, et al. Heme triggers TLR4 signaling leading to endothelial cell activation and vaso-occlusion in murine sickle cell disease. *Blood*. (2014) 123:377–90. doi: 10.1182/blood-2013-04-495887
20. Merle NS, Paule R, Leon J, Daugan M, Robe-Rybkine T, Poillerat V, et al. P-selectin drives complement attack on endothelium during intravascular hemolysis in TLR-4/heme-dependent manner. *Proc Natl Acad Sci USA*. (2019) 116:6280–5. doi: 10.1073/pnas.1814797116
21. Pamplona A, Ferreira A, Balla J, Jeney V, Balla G, Epiphanio S, et al. Heme oxygenase-1 and carbon monoxide suppress the pathogenesis of experimental cerebral malaria. *Nat Med*. (2007) 13:703–10. doi: 10.1038/nm1586
22. Ferreira A, Balla J, Jeney V, Balla G, Soares MP. A central role for free heme in the pathogenesis of severe malaria: the missing link? *J Mol Med*. (2008) 86:1097–111. doi: 10.1007/s00109-008-0368-5
23. Ferreira A, Marguti I, Bechmann I, Jeney V, Chora A, Palha NR, et al. Sickle hemoglobin confers tolerance to *Plasmodium* infection. *Cell*. (2011) 145:398–409. doi: 10.1016/j.cell.2011.03.049
24. Gozzelino R, Andrade BB, Larsen R, Luz NF, Vanoaica L, Seixas E, Coutinho A, et al. Metabolic adaptation to tissue iron overload confers tolerance to malaria. *Cell Host Microbe*. (2012) 12:693–704. doi: 10.1016/j.chom.2012.10.011
25. Weis S, Carlos AR, Moita MR, Singh S, Blankenhaus B, Cardoso S, et al. Metabolic adaptation establishes disease tolerance to sepsis. *Cell*. (2017) 169:1263–75 e14. doi: 10.1016/j.cell.2017.05.031
26. Frimat M, Tabarin F, Dimitrov JD, Poitou C, Halbwachs-Mecarelli L, Fremeaux-Bacchi Vet al. Complement activation by heme as a secondary hit for atypical hemolytic uremic syndrome. *Blood*. (2013) 122:282–92. doi: 10.1182/blood-2013-03-489245
27. Merle NS, Grunenwald A, Rajaratnam H, Gnemmi V, Frimat M, Figueres ML, et al. Intravascular hemolysis activates complement via cell-free heme and heme-loaded microvesicles. *JCI Insight*. (2018) 3:e96910. doi: 10.1172/jci.insight.96910
28. Pawluczkowycz AW, Lindorfer MA, Waitumbi JN, Taylor RP. Hematin promotes complement alternative pathway-mediated deposition of C3 activation fragments on human erythrocytes: potential implications for the pathogenesis of anemia in malaria. *J Immunol*. (2007) 179:5543–52. doi: 10.4049/jimmunol.179.8.5543
29. Gozzelino R, Jeney V, Soares MP. Mechanisms of cell protection by heme oxygenase-1. *Annu Rev Pharmacol*. (2010) 50:323–54. doi: 10.1146/annurev.pharmtox.010909.105600
30. Ramos S, Carlos AR, Sundaram B, Jeney V, Ribeiro A, Gozzelino R, et al. Renal control of disease tolerance to malaria. *Proc Natl Acad Sci USA*. (2019) 116:5681–6. doi: 10.1073/pnas.1822024116
31. Jentho E, Novakovic B, Ruiz-Moreno C, Kourtzelis I, Martins R, Chavakis T, et al. Heme induces innate immune memory. *bioRxiv. [Preprint]*. (2019). doi: 10.1101/2019.12.12.874578
32. Erdei J, Toth A, Balogh E, Nyakundi BB, Banyai E, Ryffel B, et al. Induction of NLRP3 inflammasome activation by heme in human endothelial cells. *Oxid Med Cell Longev*. (2018) 2018:4310816. doi: 10.1155/2018/4310816
33. Silva G, Jeney V, Chora A, Larsen R, Balla J, Soares MP. Oxidized hemoglobin is an endogenous proinflammatory agonist that targets vascular endothelial cells. *J Biol Chem*. (2009) 284:29582–95. doi: 10.1074/jbc.M109.045344
34. Nyakundi BB, Toth A, Balogh E, Nagy B, Erdei J, Ryffel B, et al. Oxidized hemoglobin forms contribute to NLRP3 inflammasome-driven IL-1beta production upon intravascular hemolysis. *Biochim Biophys Acta Mol Basis Dis*. (2019) 1865:464–75. doi: 10.1016/j.bbadis.2018.10.030
35. Mohanty JG, Nagababu E, Rifkind JM. Red blood cell oxidative stress impairs oxygen delivery and induces red blood cell aging. *Front Physiol*. (2014) 5:84. doi: 10.3389/fphys.2014.00084
36. Siems WG, Sommerburg O, Grune T. Erythrocyte free radical and energy metabolism. *Clin Nephrol*. (2000) 53:S9–17.
37. Jeney V, Eaton JW, Balla G, Balla J. Natural history of the bruise: formation, elimination, and biological effects of oxidized hemoglobin. *Oxid Med Cell Longev*. (2013) 2013:703571. doi: 10.1155/2013/703571
38. Willekens FL, Roerdinkholder-Stoelwinder B, Groenen-Dopp YA, Bos HJ, Bosman GJ, van den Bos AG, et al. Hemoglobin loss from erythrocytes *in vivo* results from spleen-facilitated vesiculation. *Blood*. (2003) 101:747–51. doi: 10.1182/blood-2002-02-0500
39. Willekens FL, Werre JM, Groenen-Dopp YA, Roerdinkholder-Stoelwinder B, de Pauw B, Bosman GJ. Erythrocyte vesiculation: a self-protective mechanism? *Br J Haematol*. (2008) 141:549–56. doi: 10.1111/j.1365-2141.2008.07055.x

40. Muckenthaler MU, Rivella S, Hentze MW, Galy B. A red carpet for iron metabolism. *Cell*. (2017) 168:344–61. doi: 10.1016/j.cell.2016.12.034
41. Bratosin D, Mazurier J, Tissier JP, Estaquier J, Huart JJ, Ameisen JC, et al. Cellular and molecular mechanisms of senescent erythrocyte phagocytosis by macrophages. A review. *Biochimie*. (1998) 80:173–95. doi: 10.1016/S0300-9084(98)80024-2
42. de Back DZ, Kostova EB, van Kraaij M, van den Berg TK, van Bruggen R. Of macrophages and red blood cells; a complex love story. *Fronti Physiol*. (2014) 5:9. doi: 10.3389/fphys.2014.00009
43. Alayash AI. Haptoglobin: old protein with new functions. *Clin Chim Acta*. (2011) 412:493–8. doi: 10.1016/j.cca.2010.12.011
44. Miller YI, Altamentova SM, Shaklai N. Oxidation of low-density lipoprotein by hemoglobin stems from a heme-initiated globin radical: antioxidant role of haptoglobin. *Biochemistry*. (1997) 36:12189–98. doi: 10.1021/bi970258a
45. Buehler PW, Abraham B, Vallelian F, Linnemayr C, Pereira CP, Cipollo JF, et al. Haptoglobin preserves the CD163 hemoglobin scavenger pathway by shielding hemoglobin from peroxidative modification. *Blood*. (2009) 113:2578–86. doi: 10.1182/blood-2008-08-174466
46. Pimenova T, Pereira CP, Gehrig P, Buehler PW, Schaer DJ, Zenobi R. Quantitative mass spectrometry defines an oxidative hotspot in hemoglobin that is specifically protected by haptoglobin. *J Proteome Res*. (2010) 9:4061–70. doi: 10.1021/pr100252e
47. Banerjee S, Jia Y, Siburt CJ, Abraham B, Wood F, Bonaventura C, et al. Haptoglobin alters oxygenation and oxidation of hemoglobin and decreases propagation of peroxide-induced oxidative reactions. *Free Radic Biol Med*. (2012) 53:1317–26. doi: 10.1016/j.freeradbiomed.2012.07.023
48. Andersen CB, Torvund-Jensen M, Nielsen MJ, de Oliveira CL, Hersleth HP, Andersen NH, et al. Structure of the haptoglobin-haemoglobin complex. *Nature*. (2012) 489:456–9. doi: 10.1038/nature11369
49. Kristiansen M, Graversen JH, Jacobsen C, Sonne O, Hoffman HJ, Law SK, et al. Identification of the haemoglobin scavenger receptor. *Nature*. (2001) 409:198–201. doi: 10.1038/35051594
50. Schaer DJ, Schaer CA, Buehler PW, Boykins RA, Schoedon G, Alayash AI, et al. CD163 is the macrophage scavenger receptor for native and chemically modified hemoglobins in the absence of haptoglobin. *Blood*. (2006) 107:373–80. doi: 10.1182/blood-2005-03-1014
51. Schaer DJ, Buehler PW, Alayash AI, Belcher JD, Vercellotti GM. Hemolysis and free hemoglobin revisited: exploring hemoglobin and hemin scavengers as a novel class of therapeutic proteins. *Blood*. (2013) 121:1276–84. doi: 10.1182/blood-2012-11-451229
52. Murray RK, Connell GE, Pert JH. The role of haptoglobin in the clearance and distribution of extracorpuscular hemoglobin. *Blood*. (1961) 17:45–53. doi: 10.1182/blood.V17.1.45.45
53. Rother RP, Bell L, Hillmen P, Gladwin MT. The clinical sequelae of intravascular hemolysis and extracellular plasma hemoglobin: a novel mechanism of human disease. *JAMA*. (2005) 293:1653–62. doi: 10.1001/jama.293.13.1653
54. Helms CC, Gladwin MT, Kim-Shapiro DB. Erythrocytes and vascular function: oxygen and nitric oxide. *Front Physiol*. (2018) 9:125. doi: 10.3389/fphys.2018.00125
55. Kato GJ, Steinberg MH, Gladwin MT. Intravascular hemolysis and the pathophysiology of sickle cell disease. *J Clin Invest*. (2017) 127:750–60. doi: 10.1172/JCI89741
56. Harel S, Kanner J. The generation of ferryl or hydroxyl radicals during interaction of haemproteins with hydrogen peroxide. *Free Radic Res Commun*. (1988) 5:21–33. doi: 10.3109/10715768809068555
57. Patel RP, Svistunenko DA, Darley-Usmar VM, Symons MC, Wilson MT. Redox cycling of human methaemoglobin by H2O2 yields persistent ferryl iron and protein based radicals. *Free Radic Res*. (1996) 25:117–23. doi: 10.3109/10715769609149916
58. Jia Y, Buehler PW, Boykins RA, Venable RM, Alayash AI. Structural basis of peroxide-mediated changes in human hemoglobin: a novel oxidative pathway. *J Biol Chem*. (2007) 282:4894–907. doi: 10.1074/jbc.M609955200
59. Alayash AI, Patel RP, Cashon RE. Redox reactions of hemoglobin and myoglobin: biological and toxicological implications. *Antioxid Redox Signal*. (2001) 3:313–27. doi: 10.1089/152308601300185250
60. Reeder BJ, Cutruzzola F, Bigotti MG, Hider RC, Wilson MT. Tyrosine as a redox-active center in electron transfer to ferryl heme in globins. *Free Radic Biol Med*. (2008) 44:274–83. doi: 10.1016/j.freeradbiomed.2007.06.030
61. Deterding LJ, Ramirez DC, Dubin JR, Mason RP, Tomer KB. Identification of free radicals on hemoglobin from its self-peroxidation using mass spectrometry and immuno-spin trapping: observation of a histidinyl radical. *J Biol Chem*. (2004) 279:11600–7. doi: 10.1074/jbc.M310704200
62. Ramirez DC, Chen YR, Mason RP. Immunochemical detection of hemoglobin-derived radicals formed by reaction with hydrogen peroxide: involvement of a protein-tyrosyl radical. *Free Radic Biol Med*. (2003) 34:830–9. doi: 10.1016/S0891-5849(02)01437-5
63. Vallelian F, Pimenova T, Pereira CP, Abraham B, Mikolajczyk MG, Schoedon G, et al. The reaction of hydrogen peroxide with hemoglobin induces extensive alpha-globin crosslinking and impairs the interaction of hemoglobin with endogenous scavenger pathways. *Free Radic Biol Med*. (2008) 45:1150–8. doi: 10.1016/j.freeradbiomed.2008.07.013
64. Hrkal Z, Vodrazka Z and Kalousek I. Transfer of heme from ferrihemoglobin and ferrihemoglobin isolated chains to hemopexin. *Eur J Biochem*. (1974) 43:73–8. doi: 10.1111/j.1432-1033.1974.tb03386.x
65. Hvidberg V, Maniecki MB, Jacobsen C, Hojrup P, Moller HJ, Moestrup SK. Identification of the receptor scavenging hemopexin-heme complexes. *Blood*. (2005) 106:2572–9. doi: 10.1182/blood-2005-03-1185
66. Herz J, Strickland DK. LRP: a multifunctional scavenger and signaling receptor. *J Clin Invest*. (2001) 108:779–84. doi: 10.1172/JCI200113992
67. Tenhunen R, Marver HS, Schmid R. The enzymatic conversion of heme to bilirubin by microsomal heme oxygenase. *Proc Natl Acad Sci USA*. (1968) 61:748–55. doi: 10.1073/pnas.61.2.748
68. Eisenstein RS, Garcia-Mayol D, Pettingell W, Munro HN. Regulation of ferritin and heme oxygenase synthesis in rat fibroblasts by different forms of iron. *Proc Natl Acad Sci USA*. (1991) 88:688–92. doi: 10.1073/pnas.88.3.688
69. Arruda MA, Graca-Souza AV, Barja-Fidalgo C. Heme and innate immunity: new insights for an old molecule. *Mem Inst Oswaldo Cruz*. (2005) 100:799–803. doi: 10.1590/S0074-02762005000700022
70. Mendonca R, Silveira AA, Conran N. Red cell DAMPs and inflammation. *Inflamm Res*. (2016) 65:665–78. doi: 10.1007/s00011-016-0955-9
71. Jeney V. Pro-inflammatory actions of red blood cell-derived DAMPs. *Exp Suppl*. (2018) 108:211–33. doi: 10.1007/978-3-319-89390-7_9
72. Mai J, Virtue A, Shen J, Wang H, Yang XF. An evolving new paradigm: endothelial cells–conditional innate immune cells. *J Hematol Oncol*. (2013) 6:61. doi: 10.1186/1756-8722-6-61
73. Opitz B, Eitel J, Meixenberger K, Suttorp N. Role of toll-like receptors, NOD-like receptors and RIG-I-like receptors in endothelial cells and systemic infections. *Thromb Haemost*. (2009) 102:1103–9. doi: 10.1160/TH09-05-0323
74. Bevilacqua MP, Pober JS, Wheeler ME, Cotran RS, Gimbrone MA Jr. Interleukin 1 acts on cultured human vascular endothelium to increase the adhesion of polymorphonuclear leukocytes, monocytes, and related leukocyte cell lines. *J Clin Invest*. (1985) 76:2003–11. doi: 10.1172/JCI112200
75. Pohlman TH, Stanness KA, Beatty PG, Ochs HD, Harlan JM. An endothelial cell surface factor(s) induced *in vitro* by lipopolysaccharide, interleukin 1, and tumor necrosis factor-alpha increases neutrophil adherence by a CDw18-dependent mechanism. *J Immunol*. (1986) 136:4548–53.
76. Wagener FA, Feldman E, de Witte T, Abraham NG. Heme induces the expression of adhesion molecules ICAM-1, VCAM-1, and E selectin in vascular endothelial cells. *Proc Soc Exp Biol Med*. (1997) 216:456–63. doi: 10.3181/00379727-216-44197
77. Singla S, Sysol JR, Dille B, Jones N, Chen J, Machado RF. Hemin causes lung microvascular endothelial barrier dysfunction by necroptotic cell death. *Am J Respir Cell Mol Biol*. (2017) 57:307–14. doi: 10.1165/rcmb.2016-0287OC
78. Kuck JL, Bastarache JA, Shaver CM, Fessel JP, Dikalov SI, May JM et al. Ascorbic acid attenuates endothelial permeability triggered by cell-free hemoglobin. *Biochem Biophys Res Commun*. (2018) 495:433–7. doi: 10.1016/j.bbrc.2017.11.058
79. Rafikova O, Williams ER, McBride ML, Zemskova M, Srivastava A, Nair V, et al. Hemolysis-induced lung vascular leakage contributes to the development of pulmonary hypertension. *Am J Respir Cell Mol Biol*. (2018) 59:334–45. doi: 10.1165/rcmb.2017-0308OC

80. Wagener BM, Hu PJ, Oh JY, Evans CA, Richter JR, Honavar J, et al. Role of heme in lung bacterial infection after trauma hemorrhage and stored red blood cell transfusion: a preclinical experimental study. *PLoS Med*. (2018) 15:e1002522. doi: 10.1371/journal.pmed.1002522
81. Li YX, Wang P, Yang XF, Wang WR, Zhang JY, He YH, et al. SIRT1 inhibits inflammatory response partly through regulation of NLRP3 inflammasome in vascular endothelial cells. *Mol Immunol*. (2016) 77:148–56. doi: 10.1016/j.molimm.2016.07.018
82. Chen Y, Pitzer AL, Li X, Li PL, Wang L, Zhang Y. Instigation of endothelial Nlrp3 inflammasome by adipokine visfatin promotes inter-endothelial junction disruption: role of HMGB1. *J Cell Mol Med*. (2015) 19:2715–27. doi: 10.1111/jcmm.12657
83. Posta N, Csosz E, Oros M, Petho D, Potor L, Kallo G, et al. Hemoglobin oxidation generates globin-derived peptides in atherosclerotic lesions and intraventricular hemorrhage of the brain, provoking endothelial dysfunction. *Lab Invest*. (2020) 1–17. doi: 10.1038/s41374-020-0403-x
84. Liu XY, Spolarics Z. Methemoglobin is a potent activator of endothelial cells by stimulating IL-6 and IL-8 production and E-selectin membrane expression. *Am J Physiol Cell Physiol*. (2003) 285:C1036–46. doi: 10.1152/ajpcell.00164.2003
85. Wagener FADTG, Eggert A, Boerman OC, Oyen WJG, Verhofstad A, Abraham NG, et al. Heme is a potent inducer of inflammation in mice and is counteracted by heme oxygenase. *Blood*. (2001) 98:1802–11. doi: 10.1182/blood.V98.6.1802
86. Monteiro AP, Pinheiro CS, Luna-Gomes T, Alves LR, Maya-Monteiro CM, Porto BN, et al. Leukotriene B4 mediates neutrophil migration induced by heme. *J Immunol*. (2011) 186:6562–7. doi: 10.4049/jimmunol.1002400
87. Kassa T, Jana S, Meng F, Alayash AI. Differential heme release from various hemoglobin redox states and the upregulation of cellular heme oxygenase-1. *Febs Open Bio*. (2016) 6:876–84. doi: 10.1002/2211-5463.12103
88. Rosales C, Demaurex N, Lowell CA, Uribe-Querol E. Neutrophils: their role in innate and adaptive immunity. *J Immunol Res*. (2016) 2016:1469780. doi: 10.1155/2016/1469780
89. Kono M, Saigo K, Takagi Y, Kawauchi S, Wada A, Hashimoto M, et al. Morphological and flow-cytometric analysis of haemin-induced human neutrophil activation: implications for transfusion-related acute lung injury. *Blood Transfus*. (2013) 11:53–60. doi: 10.2450/2012.0141-11
90. Brinkmann V, Reichard U, Goosmann C, Fauler B, Uhlemann Y, Weiss DS, et al. Neutrophil extracellular traps kill bacteria. *Science*. (2004) 303:1532–5. doi: 10.1126/science.1092385
91. Chen G, Zhang D, Fuchs TA, Manwani D, Wagner DD, Frenette PS. Heme-induced neutrophil extracellular traps contribute to the pathogenesis of sickle cell disease. *Blood*. (2014) 123:3818–27. doi: 10.1182/blood-2013-10-529982
92. Kono M, Saigo K, Takagi Y, Takahashi T, Kawauchi S, Wada A, et al. Heme-related molecules induce rapid production of neutrophil extracellular traps. *Transfusion*. (2014) 54:2811–9. doi: 10.1111/trf.12700
93. van Bijnen STA, Wouters D, van Mierlo GJ, Muus P, Zeerleder S. Neutrophil activation and nucleosomes as markers of systemic inflammation in paroxysmal nocturnal hemoglobinuria: effects of eculizumab. *J Thromb Haemost*. (2015) 13:2004–11. doi: 10.1111/jth.13125
94. Knackstedt SL, Georgiadou A, Apel F, Abu-Abed U, Moxon CA, Cunnington AJ, et al. Neutrophil extracellular traps drive inflammatory pathogenesis in malaria. *Sci Immunol*. (2019) 4:eaaw0336. doi: 10.1126/sciimmunol.aaw0336
95. Ohbuchi A, Kono M, Kitagawa K, Takenokuchi M, Imoto S, Saigo K. Quantitative analysis of hemin-induced neutrophil extracellular trap formation and effects of hydrogen peroxide on this phenomenon. *Biochem Biophys Rep*. (2017) 11:147–53. doi: 10.1016/j.bbrep.2017.07.009
96. Takeuchi O, Akira S. Pattern recognition receptors and inflammation. *Cell*. (2010) 140:805–20. doi: 10.1016/j.cell.2010.01.022
97. Kovtunovych G, Eckhaus MA, Ghosh MC, Ollivierre-Wilson H, Rouault TA. Dysfunction of the heme recycling system in heme oxygenase 1-deficient mice: effects on macrophage viability and tissue iron distribution. *Blood*. (2010) 116:6054–62. doi: 10.1182/blood-2010-03-272138
98. Fortes GB, Alves LS, de Oliveira R, Dutra FF, Rodrigues D, Fernandez PL, et al. Heme induces programmed necrosis on macrophages through autocrine TNF and ROS production. *Blood*. (2012) 119:2368–75. doi: 10.1182/blood-2011-08-375303
99. Haldar M, Kohyama M, So AYL, Wumesh KC, Wu XD, Briseno CG, et al. Heme-mediated SPI-C induction promotes monocyte differentiation into iron-recycling macrophages. *Cell*. (2014) 156:1223–34. doi: 10.1016/j.cell.2014.01.069
100. Vasconcellos LRC, Dutra FF, Siqueira MS, Paula-Neto HA, Dahan J, Kiarely E, et al. Protein aggregation as a cellular response to oxidative stress induced by heme and iron. *Proc Natl Acad Sci USA*. (2016) 113:E7474–82. doi: 10.1073/pnas.1608928113
101. Travassos LH, Vasconcellos LRC, Bozza MT, Carneiro LAM. Heme and iron induce protein aggregation. *Autophagy*. (2017) 13:625–6. doi: 10.1080/15548627.2016.1271515
102. Martins R, Maier J, Gorki AD, Huber KV, Sharif O, Starkl P, et al. Heme drives hemolysis-induced susceptibility to infection via disruption of phagocyte functions. *Nat Immunol*. (2016) 17:1361–72. doi: 10.1038/ni.3590
103. Chinetti-Gbaguidi G, Colin S, Staels B. Macrophage subsets in atherosclerosis. *Nat Rev Cardiol*. (2015) 12:10–7. doi: 10.1038/nrcardio.2014.173
104. Vinchi F, Muckenthaler MU, Da Silva MC, Balla G, Balla J, Jeney V. Atherogenesis and iron: from epidemiology to cellular level. *Front Pharmacol*. (2014) 5:94. doi: 10.3389/fphar.2014.00094
105. Finn A, Nakano M, Polavarapu R, Karmali V, Saeed O, Zhao XQ, et al. Hemoglobin directs macrophage differentiation and prevents foam cell formation in human atherosclerotic plaques. *Circulation*. (2011) 124:166–177. doi: 10.1016/j.jacc.2011.10.852
106. Boyle JJ, Harrington HA, Piper E, Elderfield K, Stark J, Landis RC, et al. Coronary intraplaque hemorrhage evokes a novel atheroprotective macrophage phenotype. *Am J Pathol*. (2009) 174:1097–108. doi: 10.2353/ajpath.2009.080431
107. Boyle JJ, Johns M, Kampfer T, Nguyen AT, Game L, Schaer DJ, et al. Activating transcription factor 1 directs Mhem atheroprotective macrophages through coordinated iron handling and foam cell protection. *Circ Res*. (2012) 110:20–33. doi: 10.1161/CIRCRESAHA.111.247577
108. Zhou Y, Wang Y, Wang J, Anne Stetler R, Yang QW. Inflammation in intracerebral hemorrhage: from mechanisms to clinical translation. *Prog Neurobiol*. (2014) 115:25–44. doi: 10.1016/j.pneurobio.2013.11.003
109. Schneider UC, Xu R, Vajkoczy P. Inflammatory events following subarachnoid hemorrhage (SAH). *Curr Neuropharmacol*. (2018) 16:1385–95. doi: 10.2174/1570159X16666180412110919
110. Connor J, Pak CC, Schroit AJ. Exposure of phosphatidylserine in the outer leaflet of human red-blood-cells - relationship to cell-density, cell age, and clearance by mononuclear-cells. *J Biol Chem*. (1994) 269:2399–404.
111. Zhao XR, Sun GH, Zhang J, Strong R, Song WT, Gonzales N, et al. Hematoma resolution as a target for intracerebral hemorrhage treatment: role for peroxisome proliferator-activated receptor gamma in microglia/macrophages. *Ann Neurol*. (2007) 61:352–62. doi: 10.1002/ana.21097
112. Erdei J, Toth A, Nagy A, Nyakundi BB, Fejes Z, Nagy B, et al. The role of hemoglobin oxidation products in triggering inflammatory response upon intraventricular hemorrhage in premature infants. *Front Immunol*. (2020) 11:228. doi: 10.3389/fimmu.2020.00228
113. Nyakundi BB, Erdei J, Toth A, Balogh E, Nagy A, Nagy B Jr, et al. Formation and detection of highly oxidized hemoglobin forms in biological fluids during hemolytic conditions. *Oxid Med Cell Longev*. (2020) 2020:8929020. doi: 10.1155/2020/8929020
114. Bulters D, Gaastra B, Zolnourian A, Alexander S, Ren DX, Blackburn SL, et al. Haemoglobin scavenging in intracranial bleeding: biology and clinical implications. *Nat Rev Neurol*. (2018) 14:416–32. doi: 10.1038/s41582-018-0020-0
115. Galea J, Cruickshank G, Teeling JL, Boche D, Garland P, Perry VH, et al. The intrathecal CD163-haptoglobin-hemoglobin scavenging system in subarachnoid hemorrhage. *J Neurochem*. (2012) 121:785–92. doi: 10.1111/j.1471-4159.2012.07716.x
116. Schallner N, Pandit R, LeBlanc R, Thomas AJ, Ogilvy CS, Zuckerbraun BS, et al. Microglia regulate blood clearance in subarachnoid hemorrhage by heme oxygenase-1. *J. Clin. Investigat*. (2015) 125:2609–25. doi: 10.1172/JCI78443
117. Ma B, Day JP, Phillips H, Slootsky B, Tolosano E, Dore S. Deletion of the hemopexin or heme oxygenase-2 gene aggravates brain injury

following stroma-free hemoglobin-induced intracerebral hemorrhage. *J Neuroinflammation*. (2016) 13:26. doi: 10.1186/s12974-016-0490-1
118. Lin S, Yin Q, Zhong Q, Lv FL, Zhou Y, Li JQ, et al. Heme activates TLR4-mediated inflammatory injury via MyD88/TRIF signaling pathway in intracerebral hemorrhage. *J Neuroinflammation*. (2012) 9:46. doi: 10.1186/1742-2094-9-46
119. Kwon MS, Woo SK, Kurland DB, Yoon SH, Palmer AF, Banerjee U, et al. Methemoglobin is an endogenous toll-like receptor 4 ligand-relevance to subarachnoid hemorrhage. *Int J Mol Sci*. (2015) 16:5028–46. doi: 10.3390/ijms16035028
120. Teng W, Wang L, Xue W, Guan C. Activation of TLR4-mediated NfκB signaling in hemorrhagic brain in rats. *Mediat Inflamm*. (2009) 2009:473276. doi: 10.1155/2009/473276
121. Sansing LH, Harris TH, Welsh FA, Kasner SE, Hunter CA, Kariko K. Toll-like receptor 4 contributes to poor outcome after intracerebral hemorrhage. *Ann Neurol*. (2011) 70:646–56. doi: 10.1002/ana.22528
122. Fang H, Wang PF, Zhou Y, Wang YC, Yang QW. Toll-like receptor 4 signaling in intracerebral hemorrhage-induced inflammation and injury. *J Neuroinflammation*. (2013) 10:27. doi: 10.1186/1742-2094-10-27
123. Wang YC, Wang PF, Fang H, Chen J, Xiong XY, Yang QW. Toll-like receptor 4 antagonist attenuates intracerebral hemorrhage-induced brain injury. *Stroke*. (2013) 44:2545–52. doi: 10.1161/STROKEAHA.113.001038
124. Greenhalgh AD, Brough D, Robinson EM, Girard S, Rothwell NJ, Allan SM. Interleukin-1 receptor antagonist is beneficial after subarachnoid haemorrhage in rat by blocking haem-driven inflammatory pathology. *Dis Model Mech*. (2012) 5:823–33. doi: 10.1242/dmm.008557
125. Netea MG, Joosten LA, Latz E, Mills KH, Natoli G, Stunnenberg HG, et al. Trained immunity: a program of innate immune memory in health and disease. *Science*. (2016) 352:aaf1098. doi: 10.1126/science.aaf1098
126. Quintin J, Cheng SC, van der Meer JW, Netea MG. Innate immune memory: towards a better understanding of host defense mechanisms. *Curr Opin Immunol*. (2014) 29:1–7. doi: 10.1016/j.coi.2014.02.006
127. van der Heijden C, Noz MP, Joosten LAB, Netea MG, Riksen NP, Keating ST. Epigenetics and trained immunity. *Antioxid Redox Signal*. (2018) 29:1023–40. doi: 10.1089/ars.2017.7310
128. Merle NS, Noe R, Halbwachs-Mecarelli L, Fremeaux-Bacchi V, Roumenina LT. Complement system part II: role in immunity. *Front Immunol*. (2015) 6:257. doi: 10.3389/fimmu.2015.00257
129. Kohl J. Self, non-self, and danger: a complementary view. *Adv Exp Med Biol*. (2006) 586:71–94. doi: 10.1007/0-387-34134-X_6
130. Merle NS, Church SE, Fremeaux-Bacchi V, Roumenina LT. Complement system part I - molecular mechanisms of activation and regulation. *Front Immunol*. (2015) 6:262. doi: 10.3389/fimmu.2015.00262
131. Mold C, Tamerius JD, Phillips G Jr. Complement activation during painful crisis in sickle cell anemia. *Clin Immunol Immunopathol*. (1995) 76:314–20. doi: 10.1006/clin.1995.1131
132. deCiutiis AC, Peterson CM, Polley MJ, Metakis LJ. Alternative pathway activation in sickle cell disease and beta-thalassemia major. *J Natl Med Assoc*. (1978) 70:503–6.
133. Ruiz-Torres MP, Casiraghi F, Galbusera M, Macconi D, Gastoldi S, Todeschini M, et al. Complement activation: the missing link between ADAMTS-13 deficiency and microvascular thrombosis of thrombotic microangiopathies. *Thromb Haemostasis*. (2005) 93:443–52. doi: 10.1160/TH04-07-0450
134. Hochsmann B, Murakami Y, Osato M, Knaus A, Kawamoto M, Inoue N, et al. Complement and inflammasome overactivation mediates paroxysmal nocturnal hemoglobinuria with autoinflammation. *J Clin Invest*. (2019) 129:5123–36. doi: 10.1101/635573
135. Logue GL, Rosse WF, Adams JP. Mechanisms of immune lysis of red blood cells *in vitro*. I. Paroxysmal nocturnal hemoglobinuria cells. *J Clin Invest*. (1973) 52:1129–37. doi: 10.1172/JCI107279
136. Roumenina LT, Chadebech P, Bodivit G, Vieira-Martins P, Grunenwald A, Boudhabhay I, et al. Complement activation in sickle cell disease: Dependence on cell density, hemolysis and modulation by hydroxyurea therapy. *Am J Hematol*. (2020) 95:456–64. doi: 10.1002/ajh.25742
137. Byrnes JR, Wolberg AS. Red blood cells in thrombosis. *Blood*. (2017) 130:1795–9. doi: 10.1182/blood-2017-03-745349
138. Sparkenbaugh EM, Chantrathammachart P, Wang S, Jonas W, Kirchhofer D, Gailani D, et al. Excess of heme induces tissue factor-dependent activation of coagulation in mice. *Haematologica*. (2015) 100:308–14. doi: 10.3324/haematol.2014.114728
139. de Souza GR, Hounkpe BW, Fiusa MML, Colella MP, Annichino-Bizzacchi JM, Traina F, et al. Tissue factor-dependent coagulation activation by heme: a thromboelastometry study. *PLoS ONE*. (2017) 12:e0176505. doi: 10.1371/journal.pone.0176505
140. Sparkenbaugh EM, Chen C, Brzoska T, Nguyen J, Wang S, Vercellotti GM, et al. Thrombin activation of PAR-1 contributes to microvascular stasis in mouse models of sickle cell disease. *Blood*. (2020) 135:1783–7. doi: 10.1182/blood.2019003543
141. Thomas AM, Gerogianni A, McAdam MB, Floisand Y, Lau C, Espevik T, et al. Complement component C5 and TLR molecule CD14 mediate heme-induced thromboinflammation in human blood. *J Immunol*. (2019) 203:1571–8. doi: 10.4049/jimmunol.1900047
142. Schneider DS, Ayres JS. Two ways to survive infection: what resistance and tolerance can teach us about treating infectious diseases. *Nat Rev Immunol*. (2008) 8:889–95. doi: 10.1038/nri2432
143. Medzhitov R, Schneider DS, Soares MP. Disease tolerance as a defense strategy. *Science*. (2012) 335:936–41. doi: 10.1126/science.1214935
144. Seixas E, Gozzelino R, Chora A, Ferreira A, Silva G, Larsen R, et al. Heme oxygenase-1 affords protection against noncerebral forms of severe malaria. *Proc Natl Acad Sci USA*. (2009) 106:15837–42. doi: 10.1073/pnas.0903419106
145. Dimitrov JD, Vassilev TL, Andre S, Kaveri SV, Lacroix-Desmazes S. Functional variability of antibodies upon oxidative processes. *Autoimmun Rev*. (2008) 7:574–8. doi: 10.1016/j.autrev.2008.04.009
146. Dimitrov JD, Roumenina LT, Doltchinkova VR, Mihaylova NM, Lacroix-Desmazes S, Kaveri Svet al. Antibodies use heme as a cofactor to extend their pathogen elimination activity and to acquire new effector functions. *J Biol Chem*. (2007) 282:26696–706. doi: 10.1074/jbc.M702751200

Conflict of Interest: The authors declare that the research was conducted in the absence of any commercial or financial relationships that could be construed as a potential conflict of interest.

frontiers in Immunology

ORIGINAL RESEARCH
published: 17 July 2020
doi: 10.3389/fimmu.2020.01488

Hydroxyurea Scavenges Free Radicals and Induces the Expression of Antioxidant Genes in Human Cell Cultures Treated With Hemin

Sânzio Silva Santana[1,2], *Thassila Nogueira Pitanga*[1,2], *Jeanne Machado de Santana*[1], *Dalila Lucíola Zanette*[1], *Jamile de Jesus Vieira*[1], *Sètondji Cocou Modeste Alexandre Yahouédéhou*[1], *Corynne Stéphanie Ahouefa Adanho*[1], *Sayonara de Melo Viana*[1], *Nivea Farias Luz*[1], *Valeria Matos Borges*[1] and *Marilda Souza Goncalves*[1,3]*

[1] Instituto Gonçalo Moniz, Fundação Oswaldo Cruz (IGM/FIOCRUZ-BA), Salvador, Brazil, [2] Faculdade de Biomedicina, Universidade Católica do Salvador (UCSal), Salvador, Brazil, [3] Faculdade de Farmácia, Universidade Federal da Bahia (UFBA), Salvador, Brazil

OPEN ACCESS

Edited by:
Caroline Le Van Kim,
Université Paris Diderot, France

Reviewed by:
Nicola Conran,
Campinas State University, Brazil
Marc Romana,
INSERM U1134 Biologie Intégrée du Globule Rouge, France

***Correspondence:**
Marilda Souza Goncalves
mari@bahia.fiocruz.br

Specialty section:
This article was submitted to Inflammation, a section of the journal Frontiers in Immunology

Received: 16 February 2020
Accepted: 08 June 2020
Published: 17 July 2020

Citation:
Santana SS, Pitanga TN, de Santana JM, Zanette DL, Vieira JJ, Yahouédéhou SCMA, Adanho CSA, Viana SM, Luz NF, Borges VM and Goncalves MS (2020) Hydroxyurea Scavenges Free Radicals and Induces the Expression of Antioxidant Genes in Human Cell Cultures Treated With Hemin. Front. Immunol. 11:1488. doi: 10.3389/fimmu.2020.01488

The excessive release of heme during hemolysis contributes to the severity of sickle cell anemia (SCA) by exacerbating hemoglobin S (HbS) autoxidation, inflammation and systemic tissue damage. The present study investigated the effect of hydroxyurea (HU) on free radical neutralization and its stimulation of antioxidant genes in human peripheral blood mononuclear cells (PBMC) and human umbilical vein endothelial cells (HUVEC) in the presence or absence of hemin. HU (100 and 200 μM) significantly reduced the production of intracellular reactive oxygen species (ROS) induced by hemin at 70 μM in HUVEC. HUVECs treated with HU+hemin presented significant increases in nitric oxide (NO) production in culture supernatants. HU alone or in combination with hemin promoted the induction of superoxide dismutase-1 (*SOD1*) and glutathione disulfide-reductase (*GSR*) in HUVECs and PBMCs, and glutathione peroxidase (*GPX1*) in PBMCs. Microarray analysis performed in HUVECs indicated that HU induces increased expression of genes involved in the antioxidant response system: *SOD2*, *GSR*, microsomal glutathione S-transferase (*MGST1*), glutathione S-transferase mu 2 (*GSTM2*), carbonyl reductase 1 (*CBR1*) and klotho B (*KLB*). Significant increases in expression were observed in genes with kinase activity: protein kinase C beta (*PRKCB*), zeta (*PRKCZ*) and phosphatidylinositol-4-phosphate 3-kinase catalytic subunit type 2 beta (*PIK3C2B*). HU also induced a significant increase in expression of the gene p62/sequestosome (*p62/SQSTM1*) and a significant decrease in the expression of the transcriptional factor *BACH1* in HUVECs. Upstream analysis predicted the activation of Jun, miR-155-5p and mir-141-3p. These results suggest that HU directly scavenges free radicals and induces the expression of antioxidant genes via induction of the Nrf2 signaling pathway.

Keywords: sickle cell anemia, hydroxyurea, hemin, antioxidant response, Nrf2

INTRODUCTION

Hydroxyurea (HU) is a hydroxylated analog of urea, which was initially identified as a myelosuppressive drug that acts by inhibiting ribonucleotide reductase. After determining its antisickling effect, HU was approved in 1998 by the U.S. Food and Drug Administration (FDA) for the treatment of sickle cell anemia (SCA). SCA is a hereditary autosomal recessive disease, characterized by the homozygosity of the beta S (β^S) allele (HbSS), which is derived from the GAG>GTG mutation in the sixth position of the β globin gene (*HBB*) (1). The pathophysiological condition of SCA is recurrent and characterized by a large production of reactive oxygen species (ROS) and reactive nitrogen species (RNS), which play a crucial role in the maintenance of inflammation (2–6).

The imbalance caused by increased oxidation-reduction (redox) reactions in the vascular microenvironment in SCA provokes important deleterious effects (4). Indeed, patients with SCA can present (i) intravascular and extravascular hemolysis with free heme release; (ii) autoxidation of HbS (3, 7); (iii) nitric oxide (NO) depletion and endothelial dysfunction (8, 9); (iv) ischemia-reperfusion events (10); (v) marked leukocyte dysfunction, conferring a non-effector response against pathogens, and the dysregulation of inflammatory equilibrium that increases susceptibility to secondary infections (11–13).

Despite the recent approval of L-arginine by the FDA, HU remains the drug most indicated for SCA patients who present a severe clinical profile (14, 15). Experimental studies have demonstrated that after oral administration, HU is absorbed, converted into a nitroxide radical and transported to the active site of the M2 subunit of the ribonucleotide reductase protein, inactivating the enzyme and generating cytotoxic suppression, most likely via the induction of an antioxidant response (16). Ware (17) pointed out the main benefits of HU therapy in patients with SCA: HU induces fetal hemoglobin (HbF) production through the activation of guanylate cyclase and reduces neutrophil and reticulocyte counts by inhibiting ribonucleotide reductase activity and bone marrow toxicity. Moreover, it decreases adhesiveness and improves the rheology of circulating neutrophils and reticulocytes, reduces hemolysis and improves erythrocyte hydration, promotes macrocytosis, reduces intracellular sickling and stimulates the release of NO as a potential local vasodilator. Despite these benefits, relatively few studies have specifically focused on the action of HU in alternative mechanisms that broaden the field of knowledge regarding its action and systemic effects.

We hypothesized that HU can act by decreasing ROS/RNS and stimulating antioxidant defense systems in endothelial cells and leukocytes. To this end, we investigated the effects of HU in human peripheral blood mononuclear cells (PBMC) and umbilical cord vein endothelial cells (HUVEC) pre-treated or not with hemin, an important pro-oxidant molecule released during hemolysis (3, 18, 19). We then specifically investigated the antioxidant effect of HU, as well as the expression of antioxidant genes, such as heme oxygenase-1 (*HMOX1*), superoxide dismutase-1 (*SOD1*), glutathione disulfide-reductase (*GSR*) and glutathione peroxidase (*GPX1*).

Abbreviations: BACH1, BTB (Broad-Complex, Tramtrack and Bric-a-brac) Domain and CNC Homolog 1, Basic Leucine Zipper Transcription Factor 1; CBR1, Carbonyl reductase 1; DPPH, 2,2-Diphenyl-1-picrylhydrazyl; GPX, Glutathione peroxidase; GSH, Reduced glutathione; GSR, Glutathione-disulfide reductase; GST, Glutathione S-transferase; GSTM2, Glutathione S-transferase mu 2; H_2O_2, Hydrogen peroxide; HbF, Fetal hemoglobin; HbS, Hemoglobin S; *HMOX1*, Heme oxigenase-1 gene; HU, Hydroxyurea; HUVEC, Human umbilical vein endothelial cells; Keap1, Kelch-like ECH-associated protein1; KLB, Klotho beta; MAPK, Mitogen-activated protein kinase; MGST1, Microsomal glutathione S-transferase; NO_3^-, Nitrate; Nrf2, Nuclear factor erythroid 2 (NF-E2) p45-related factor 2; NO, Nitric oxide; PBMC, Peripheral blood mononuclear cells; p62/SQSTM1, Sequestosome1; RNS, Reactive nitrogen species; ROS, Reactive oxygen stress; SCA, Sickle cell anemia; SOD-1, Superoxide dismutase-1.

METHODS

Drugs

HU, butylated hydroxytoluene (BHT) and L-ascorbate were purchased from Sigma Aldrich (St. Louis, MO, USA) and prepared following the manufacturer's instructions. After complete solubilization, drugs were sterilized by filtration using a 0.22 μm polyethersulfone membrane (PES) (Jet Biofil, Guangzhou, China) for use in culturing assays.

Preparation of Hemin

Hemin (Sigma Aldrich, St. Louis, MO, USA), a ferric chloride hemin, was prepared from a 5 mM stock solution solubilized in 0.1 M NaOH using non-pyrogenic water under dark conditions. The hemin solution was then diluted in RPMI 1640 medium (Gibco, New York, NY, USA) to obtain optimal concentrations. Finally, a non-pyrogenic hemin solution was obtained following 0.22 μm PES-membrane filtration (Jet Biofil, Guangzhou, China) for use in cell culture assays.

Scavenging Activity Assay of 2,2-Diphenyl-1-Picrylhydrazyl (DPPH)

DPPH free scavenging activity was assessed by a modified microplate assay method previously described by Li et al. (20). Initially, 200 μM of DPPH stock solution (Sigma Aldrich, St. Louis, MO, USA) was prepared in methanol p.a. (Synth, Diadema, SP, Brazil) 10–15 min before experimentation, stored in a sealed bottle, and kept away from light. For this assay, stock drug solutions were prepared, using methanol, at concentrations ranging from 3.13 to 800 μM/well. HU, as well as the antioxidant external controls BHT and L-ascorbate, were incubated for 30 or 60 min at a volume of 0.1 mL on 96-well flat-bottom microtiter plates (Greiner Bio-one, Monroe, North Carolina, USA) at a ratio of 1:1 (v/v), with the addition of DPPH (100 μM/well). All plates were covered and kept in the dark to minimize evaporation and to avoid the photosensitization of DPPH radicals. Finally, the plated solutions were homogenized for 5 sec, and absorbance was measured on a microplate reader (SpectraMax 190, Molecular Devices Corporation, Sunnyvale, CA) using Softmax software v. 5.0 (Molecular Devices, Sunnyvale, CA, USA) at a wavelength of 517 nm. DPPH radical scavenging activity was determined

using the following equation: *Scavenging activity of DPPH (%)* = $[(Abs_{dpph}\text{-}Abs_{drug}) \times 100]/Abs_{dpph}$.

Cell Cultures

HUVECs were cultured in 25 cm^2 cell culture flasks (Costar, Corning, NY, USA) containing 5 mL RPMI 1640 medium (Gibco, New York, NY, USA) supplemented with 10% heat-inactivated fetal bovine serum (FBS) (Gibco, New York, NY, USA), 20 mM glutamine (Sigma Aldrich, St. Louis, MO, USA), 10 mM HEPES, 5 mM NaOH and the following antibiotics: 100 U/mL penicillin and 10 mg/mL streptomycin (Sigma Aldrich, St. Louis, MO, USA). For all assays, HUVECs were used in passages 1–5 and phenotypically characterized by the evaluation of typical cobblestone morphology and surface tissue factor (CD142) (**Supplementary Figure 1**).

Human peripheral venous blood samples were collected from healthy volunteers (HbAA genotype) to obtain PBMCs. Written informed consent was obtained from all study participants, and the present protocol was conducted in compliance with the 1975 Helsinki Declaration and its amendments, as well as the Brazilian ethical guidelines (466-CNS-2012). PBMCs were obtained by Ficoll-Paque Plus (GE Healthcare, Uppsala, Sweden) density gradient centrifugation following the manufacturer's instructions. Both HUVEC and PBMC were cultivated in a humidified atmosphere at 37°C under 5% CO_2.

Cytotoxicity Assays

The cytotoxic effects of the drugs and hemin on HUVEC were assessed using a resazurin sodium salt reduction colorimetric assay. For this, 2×10^4 cells/well (0.2 mL) were plated on 96-well plates (Costar, Corning, NY, USA) and cultivated for 20–24 h under the culture conditions described above, until reaching a confluency of 70–80%. Cells were then treated with HU in combination or not with hemin for 24 h. After incubation, the medium was collected and the wells were gently washed once with preheated (37°C) 0.85% saline solution to avoid cell damage and detachment. Finally, 0.1 mL of 12.5 μM resazurin sodium salt solution (Sigma Aldrich, St. Louis, MO, USA) diluted in RPMI 1640 with 10% FBS was added to each well, followed by incubation at 37°C under 5% CO_2 in a humidified atmosphere for 3 h according to standardization protocols (**Supplementary Figure 2A**). Absorbance was simultaneously read at wavelengths of 570 and 600 nm on a microplate reader. Cell viability was determined by measuring the percentage of sodium salt (deep blue fluorescent compound) that was reduced to resorufin (pink fluorescent product). For PBMC cytotoxicity assays, 3×10^5 cells were incubated for 24 h with HU in combination or not with hemin. Cytotoxicity was assessed using propidium iodide (BD, Pharmigen, USA) following the manufacturer's specifications. For each sample, 20,000 events were acquired on a BD LSRFortessa™ cytometer (Biosciences, San Jose, CA, USA).

Determination of Intracellular ROS

The detection of reactive oxygen species was determined in HUVECs using a 2′, 7′-dichlorodihydrofluorescein diacetate (DCFH-DA) probe (Sigma Aldrich, St. Louis, MO, USA). Initially, 3.3×10^5 cells (0.5 mL) were seeded on 24-well plates for 20 h in the presence of 70 μM hemin to induce the intracellular production of ROS. Cells were then subjected to different concentrations of HU (100 and 200 μM) in the presence or absence of 70 μM hemin for 2 h. Next, the supernatants were discarded, the cell monolayers were gently washed twice with pre-heated (37°C) sterile saline (0.85% NaCl), followed by reincubation for 30 min with 10 μM of DCFH-DA probe in SFB-depleted medium without phenol red (Gibco, New York, NY, USA) to avoid probe degradation. Finally, the monolayers were washed twice with saline and trypsinized with 0.3 mL of trypsin-EDTA (0.25%) for 4 min at 37°C. Trypsin was neutralized with RPMI medium without phenol red supplemented with 10% SFB, and cells were transferred to sterile 1.5 mL microtubes, washed twice with saline solution and then placed in specific tubes for flow cytometry acquisition using Ex/Em: ∼492–495/517–527 nm on a BD LSRFortessa™ cytometer (Biosciences, San Jose, CA, USA). ROS measurements are expressed by mean fluorescence intensity (MFI) and replicate values are expressed as means (10,000 events for each condition).

Nitrite Accumulation in Supernatants

NO production was indirectly quantified in PBMC and HUVEC supernatants using the Griess method (21) after treatment with HU (100 and 200 μM) alone or in combination with 70 μM hemin for 24 h. First, 1.2×10^6 PBMC/well (0.3 mL) and 8×10^4 HUVEC/well (0.5 mL) were seeded on 48-well and 24 well-plates, respectively, in the presence of stimuli. Next, 50 μL (1:1, v/v) of the supernatant was added to Griess reagent [1% sulfanilamide and 0.1% naphthyl ethylenediamine dihydrochloride (Sigma Aldrich, St. Louis, MO, USA) in 2.5% H_3PO_4 solution] for 5 min. Absorbance was measured on a microplate reader at a wavelength of 550 nm. The conversion of absorbance into micromolar concentrations of NO was deduced from a standard curve using a known concentration of $NaNO_2$ diluted in RPMI medium. The standard curves used to determine molar concentrations assumed a coefficient of determination (R^2) value $\geq$ 0.999.

Gene Expression and RNA Extraction Assays

HUVEC and PBMC were challenged with different HU concentrations in the presence and absence of 70 μM hemin for 4 h. Gene expression assays were performed by real-time quantitative reverse-transcription polymerase chain reaction (RT-qPCR). Total RNA was extracted from HUVEC and PBMC samples using TRIzol Reagent (Invitrogen, Carlsbad, CA, USA) according to the manufacturer's specifications. The concentration and purity of the extracted RNA were determined at the optical densities of 260 and 280 nm using a NanoDrop 2000 spectrophotometer (ThermoFisher Scientific, Rockford, IL, USA) at an absorbance ratio $A_{260/280}$ of 1.90–2.02. Reverse cDNA synthesis by reverse transcription of RNA (RT-PCR) was performed using 250 ng of the RNA transcript in a High-Capacity cDNA Reverse Transcription Kit (ThermoFisher Scientific, Rockford, IL, USA) following the manufacturer's specifications. Real-time PCR was performed on an ABI PRISM 7500 Fast Real-Time PCR System (Applied Biosystems, Foster City, CA, USA)

TABLE 1 | Scavenging activity (corresponding to 50% of 100 μM DPPH) of hydroxyurea, L-ascorbate and butylated hydroxytoluene.

Drugs	IC_{50} (μM) ± SD	One-way ANOVA	Tukey's *post-hoc* test		
			HU vs. BHT	HU vs. L-Asc	L-Asc vs. BHT
Hydroxyurea	38.68 ± 0.47	$p<0.0001$	$p<0.0001$	$p<0.0001$	$p<0.05$
Butylated hydroxytoluene	23.07 ± 2.64				
L-Ascorbate	18.22 ± 5.93				

IC_{50} values correspond to the mean inhibitory concentration of three independent experiments. SD, Standard deviation; HU, Hydroxyurea; BHT, Butylated hydroxytoluene; L-Asc, L-Ascorbate.

under the following cycling conditions: 95°C for 20 s, 95°C for 1 s, 60°C for 20 s for 40 cycles. For the RT-qPCR reactions, mixtures containing SYBR® Green PCR Master Mix (SYBR® Green I dye, AmpliTaq Gold® DNA Polymerase, dNTPs with dUTP, passive reference 1–ROX) (Applied Biosystems, Foster City, CA, USA), the primers specific to the target genes and 2 μL of the cDNA sample product were added to the optical plates. The primers used for quantitative PCR were as follows: [*HMOX1*: 5′-ATG GCC TCC CTG TAC CAC ATC-3′ (forward); 5′-TGT TGC GCT CAA TCT CCT CCT-3′ (reverse); *SOD1*: 5′-TGG CCG ATG TGT CTA TTG AA-3′ (forward); 5′-CAC CTT TGC CCA AGT CAT CT-3′ (reverse); *GSR*: 5′-ACT TGC CCA TCG ACT TTT TG-3′ (forward); 5′-GGT GGC TGA AGA CCA CAG TT-3′ (reverse); *GPX1*: 5′-CCA AGC TCA TCA CCT GGT CT-3′ (forward); 5′-TCG ATG TCA ATG GTC TGG AA-3′ (reverse); β-actin: 5′-CCT GGC ACC CAG CAC AAT-3′ (forward); 5′-GCC GAT CCA CAC GGA GTA CT-3′ (reverse); tubulin isotype a1C: 5′-TCA ACA CCT TCT TCA GTG AAA GG-3′ (forward); 5′-AGT GCC AGT GCG AAC TTC ATC (reverse). After determining the threshold cycle (CT), gene expression was measured by relative quantification using the following expression: fold-change $= 2^{-\Delta(\Delta CT)}$, where $\Delta CT = CT_{target} - CT_{housekeeping}$ and $\Delta(\Delta CT) = \Delta CT_{treated} - \Delta CT_{control(medium)}$. Beta-actin and tubulin isotype a1C were used as housekeeping genes.

Microarray Assays with HUVEC

Microarray analyses were performed using a HumanHT-12 v.4 Expression BeadChip Kit (Illumina Inc., San Diego, CA, USA) and a TargetAmp™ Nano Labeling Kit for Illumina® Expression BeadChip® (Epicenter Technologies, Madison, Wisconsin, USA), in accordance with the manufacturers' specifications. Fluorescence values were acquired on an Illumina HiScan system using iScan Control software (Illumina Inc., San Diego, CA, USA). After quality control assessments, the generated data were exported for analysis using Genome Studio software (Illumina Inc., San Diego, CA, USA). Results with a detected $p > 0.05$ and a differential score < 0.05 were discarded. After validation, the transcripts were selected and analyzed using Ingenuity Pathway Analysis (IPA) software (QIAGEN). Experiments were performed in triplicate and results reflect relative expression (log fold-change > 1.5), determined by comparing HUVECs treated with 200 μM HU to untreated cells.

Statistical Analysis

Data are expressed as means ± standard deviation of at least one representative experiment. All experiments were performed in triplicate. One-way ANOVA followed by Tukey's *post-hoc* test was applied to test variance between multiple groups. Significance was considered when $p < 0.05$. GraphPad Prism software version v.6.0 was used for statistical analyses (GraphPad, San Diego, CA, USA).

RESULTS

HU Scavenges Free Radicals

To investigate the possible antioxidant effects of HU, we performed assays evaluating radical scavenging activity using 100 μM DPPH, a stable free radical. Initially, we found that HU presents significantly superior scavenging activity at 60 min of incubation after standardization (**Supplementary Figure 3**). Next, radical scavenging assays involving DPPH demonstrated a concentration-dependent activity for HU. Our global analysis found that HU ($IC_{50} = 38.68 \pm 0.47$ μM) presents lower DPPH radical scavenging activity than the reference antioxidant compounds BHT ($IC_{50} = 23.07 \pm 2.64$ μM, $p < 0.05$) and L-ascorbate ($IC_{50} = 18.22 \pm 5.93$ μM, $p < 0.001$) (**Table 1**). However, scavenging activity equivalent or superior to BHT was observed at concentrations ≥200 μM (**Figure 1**). Based on these findings, HU was used in all further assays at concentrations of 100 and 200 μM.

HU and Hemin Present Non-Toxic Effects in HUVEC and PBMC

Cytotoxicity evaluations in HUVECs and PBMCs were carried out using resazurin sodium salt and propidium iodide methods, respectively. For toxicity testing in HUVECs, we initially standardized the time required to reduce resazurin sodium salt to a level equivalent to the same percentage of cell viability found in unstimulated cell cultures (**Supplementary Figure 2A**). No decreases in HUVEC viability were seen at the concentrations evaluated, ranging from 6.25 to 100 μM of hemin (**Supplementary Figure 2B**). Considering these findings, all following assays employed a hemin concentration of 70 μM, which corresponds to the plasmatic concentrations of free hemin observed in a previous study by our group involving steady-state SCA patients. No toxicity was observed in the HUVEC and PBMC samples at any of the HU or hemin concentrations evaluated (**Supplementary Figures 2C,D**).

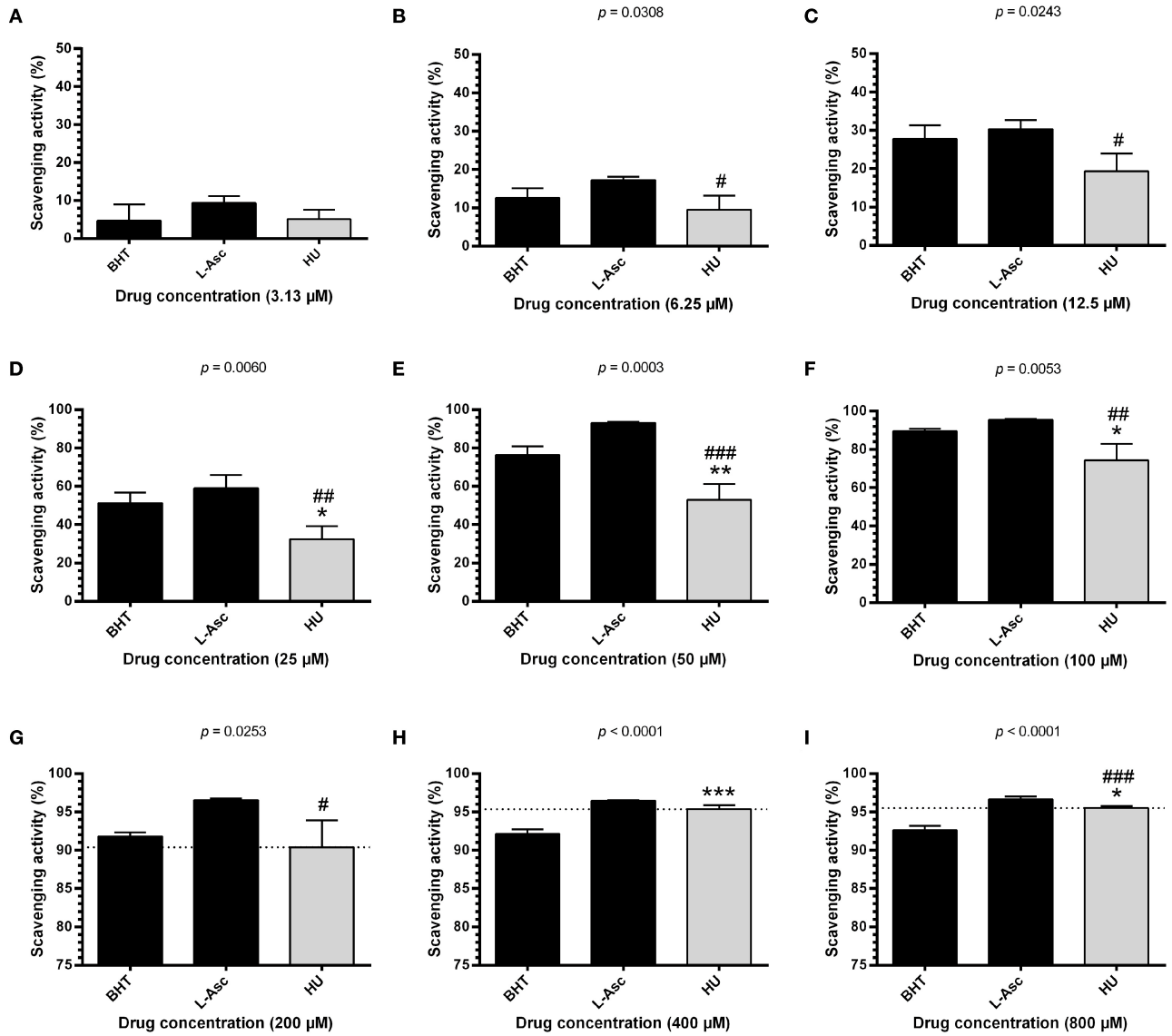

FIGURE 1 | DPPH scavenging activity of different concentrations of hydroxyurea after 60 min of incubation. Antioxidant activity was measured by scavenging of the DPPH free radical using the HU concentrations 3.13 μM **(A)**, 6.25 μM **(B)**, 12.5 μM **(C)**, 25 μM **(D)**, 50 μM **(E)**, 100 μM **(F)**, 200 μM **(G)**, 400 μM **(H)** and 800 μM **(I)**. Results correspond to the mean ± standard deviation of four independent experiments. BHT and L-ascorbate were used as reference antioxidant compounds. HU, hydroxyurea; L-Asc, L-ascorbate; BHT, butylated hydroxytoluene. Statistical significance determined by one-way ANOVA, $p < 0.0001$, followed by Tukey's *post-hoc* test: HU vs. BHT: $^{*}p < 0.05$, $^{**}p < 0.01$, $^{***}p < 0.001$; HU vs. L-Asc, $^{\#}p < 0.05$, $^{\#\#}p < 0.01$, $^{\#\#\#}p < 0.001$.

HU Increases NO Production and Decreases the Formation of Cytosolic ROS in HUVEC Treated with HU plus Hemin

Hemin alone was shown to induce NO production in PBMCs and HUVECs. PBMCs and HUVECs treated with HU at 100 μM and 200 μM did not show any significant increases in NO (**Figures 2A,B**). However, when we evaluated the combined treatment of HU plus hemin vs. negative controls or hemin alone, significantly increased NO production was seen only in HUVECs. HU plus 70 μM hemin was found to markedly reduce ROS in HUVECs in a concentration dependent-manner (**Figure 2C**).

Treatments with HU Alone or Combined with Hemin Induce Antioxidant Enzyme Gene Expression in HUVEC and PBMC

Treatment with 200 μM HU increased the expression of *SOD1* in PBMCs and HUVECs by 2.57 ± 0.86-fold ($p < 0.05$) and 1.84 ± 0.36-fold, ($p < 0.01$), respectively, compared to negative controls (**Figure 3A**). Combined treatments using 100 and 200 μM of HU

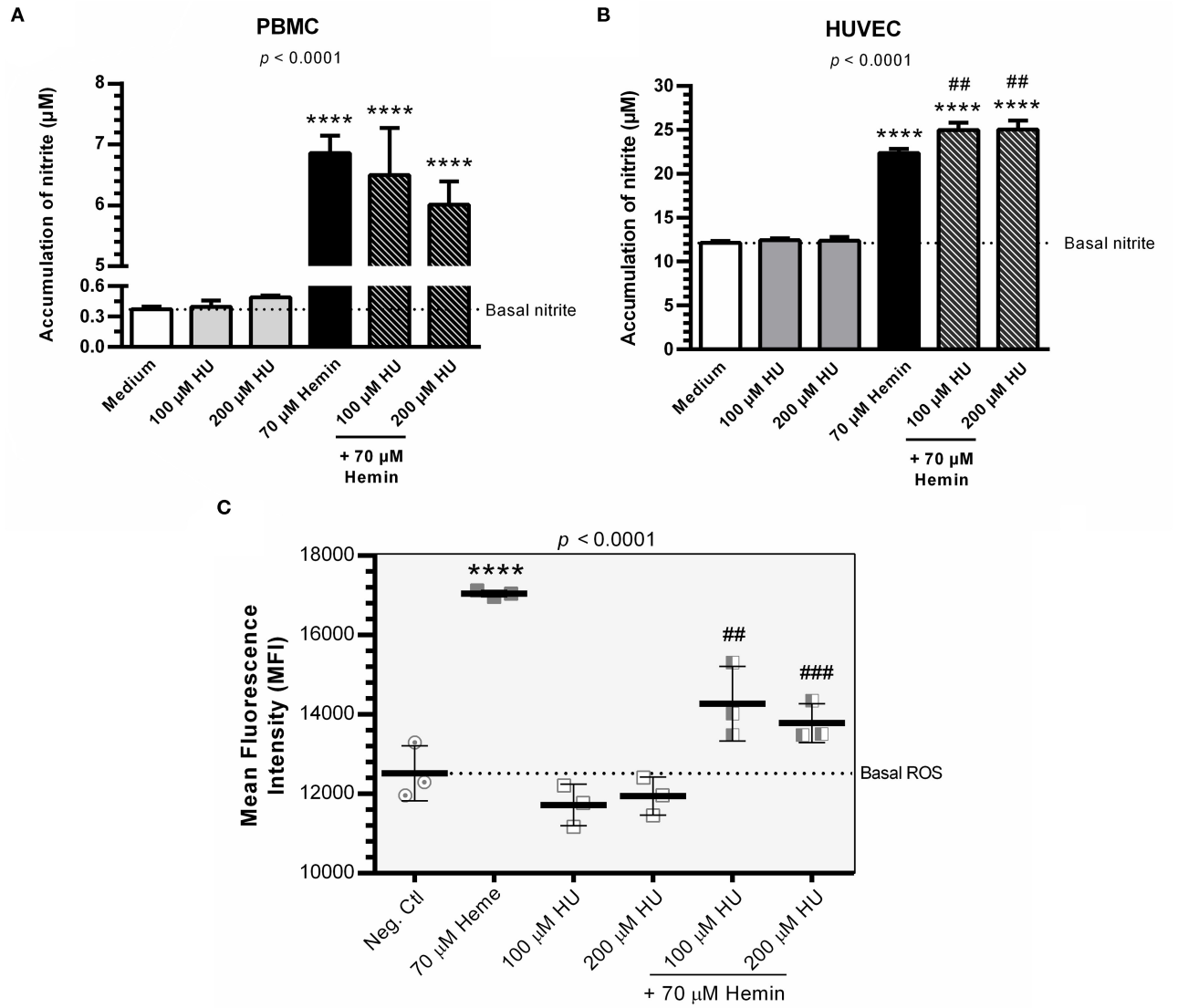

FIGURE 2 | NO production and formation of intracellular ROS in the presence of Hydroxyurea and/or hemin. **(A)** Production of NO in supernatants of PBMCs in response to various treatment protocols. Results correspond to means ± SD of three independent experiments. Statistical significance determined by one-way ANOVA, $p < 0.0004$, followed by Tukey's *post-hoc* test: HU alone or in combination with hemin vs medium, or hemin vs medium, $^{**}p < 0.01$; HU + hemin vs hemin, $^{\#\#}p < 0.01$. **(B)** Production of NO in supernatants of HUVECs in response to various treatment protocols. Results correspond to the mean ± SD of three independent experiments. Statistical significance determined by one-way ANOVA, $p < 0.0001$, followed Tukey's *post-hoc* test: HU alone or HU + hemin vs. medium, or hemin vs. medium, $^{****}p < 0.0001$; HU + hemin vs. hemin, $^{\#\#}p < 0.01$. **(C)** Decreased ROS formation in HUVECs using the oxidant-sensing fluorescent probe 10 μM 2', 7'-dichlorodihydrofluorescein diacetate (DCFH-DA). Statistical significance determined by mean fluorescence intensity (MFI) values representative of the mean ± SD of three experimental replicates. One-way ANOVA, $p < 0.0001$, followed by Tukey's *post-hoc* test: HU alone or associated with hemin vs. medium, or hemin vs. medium, $^{****}p < 0.0001$; HU + hemin vs. hemin, $^{\#\#}p < 0.01$; $^{\#\#\#}p < 0.001$.

plus 70 μM hemin promoted a statistically significant increase of 3.37 ± 0.42-fold ($p < 0.01$) and 3.39 ± 0.37-fold ($p < 0.01$) in *SOD1* expression in PMBCs, vs. 1.53 ± 0.07-fold ($p < 0.05$) in HUVECs (100 μM HU plus hemin).

Considerable *GPX* expression was observed in PBMCs treated with 100 μM (2.27 ± 0.14-fold, $p < 0.0001$) and 200 μM HU (2.40 ± 0.12-fold; $p < 0.0001$) (**Figure 3B**). Similar expression values were observed in hemin-treated PBMCs at both HU concentrations (2.25 ± 0.05-fold, $p < 0.001$ and 2.11 ± 0.11-fold, respectively). In contrast, *GPX* expression levels in HUVECS did not vary in response to the treatments.

Treatment with HU alone did not provoke increased *GSR* expression at any of the concentrations evaluated in either cell type evaluated (**Figure 3C**). However, an increase in *GSR* expression was observed in PBMCs and HUVECs submitted to combined HU plus hemin treatment. PBMCs treated with 100 μM or 200 μM of HU and 70 μM of hemin presented 1.79 ± 0.22-fold ($p < 0.05$) and 1.42 ± 0.43-fold increases in *GSR*

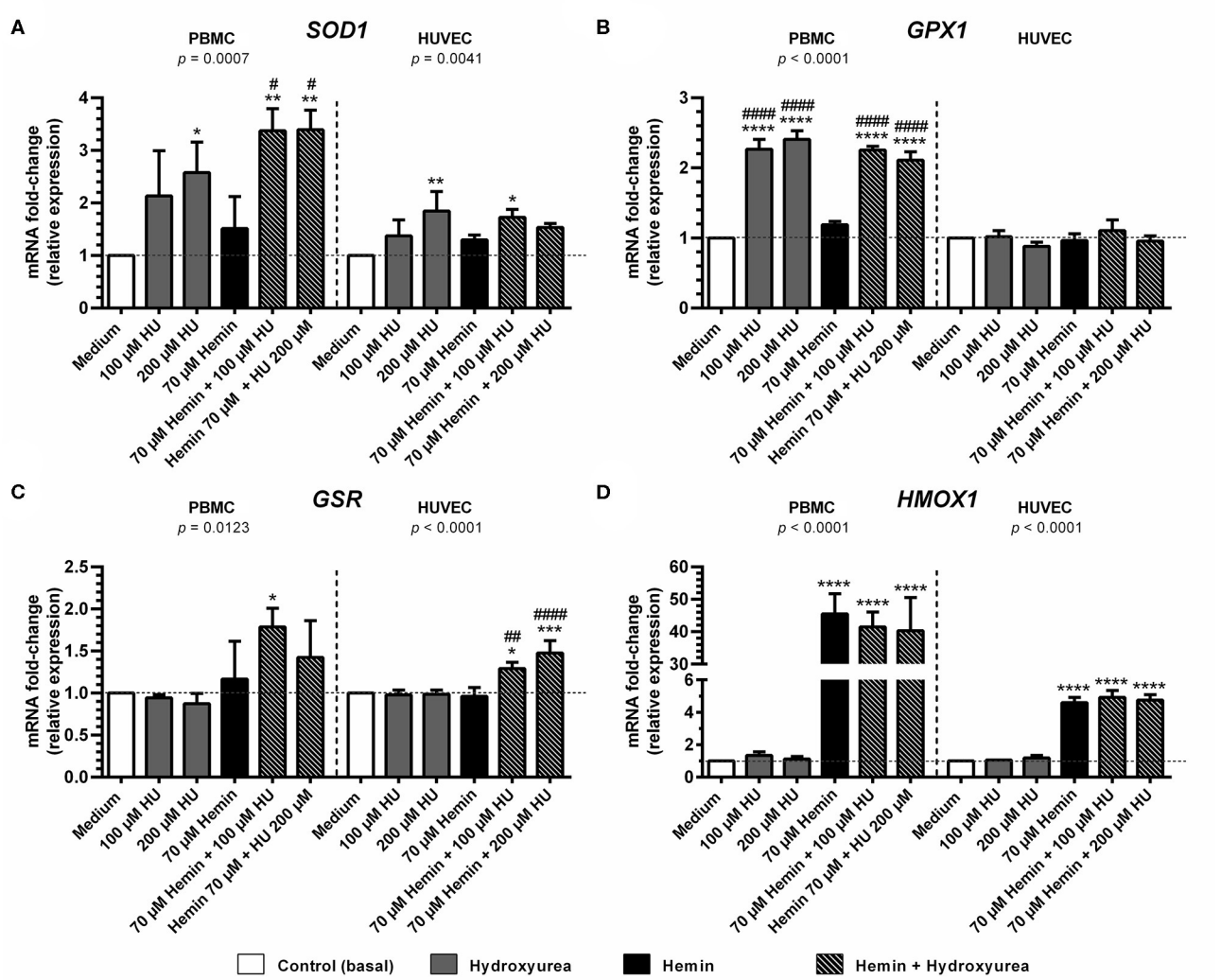

FIGURE 3 | Effect of Hydroxyurea on induction of antioxidant response gene expression in PBMC and HUVEC treated with different concentrations of hydroxyurea (100 and 200 µM) in the presence or absence of 70 µM hemin for 4 h. **(A)** superoxide dismutase-1 (*SOD1*); **(B)** glutathione peroxidase (*GPX1*); **(C)** glutathione-disulfide reductase (*GSR*); **(D)** Heme-oxygenase 1 (*HMOX1*). Results correspond to the mean ± standard deviation of three independent experiments. Expression values determined by relative quantification using the following expression: fold-change = $2^{-\Delta(\Delta CT)}$, where $\Delta CT = CT_{target}\text{-}CT_{housekeeping}$ and $\Delta(\Delta CT) = \Delta CT_{treated} - \Delta CT_{control}$ (medium). Data were normalized to represent fold expression above controls for each gene. Statistical significance determined by one-way ANOVA, $p < 0.05$, followed by Tukey's *post-hoc* test: HU alone or HU + hemin vs. medium, or hemin vs. medium, $^{*}p < 0.05$; $^{**}p < 0.01$, $^{***}p < 0.001$, $^{****}p < 0.0001$; hemin + HU vs. hemin, $^{\#}p < 0.05$; $^{\#\#}p < 0.01$; $^{\#\#\#\#}p < 0.0001$.

expression, respectively, while HUVECs presented 1.30 ± 0.07 ($p < 0.05$) and 1.48 ± 0.15-fold ($p < 0.001$) higher expression in comparison to the negative control.

Significantly higher levels of *HMOX1* were observed in hemin-treated PBMCs and HUVECs, regardless of HU concentration (**Figure 3D**). In PBMCs, increased *HMOX1* expression was 45.5 ± 6.2-fold ($p < 0.0001$) vs. controls. HUVECs exhibited modest increases in *HMOX1* expression (4.6 ± 0.32-fold; $p < 0.0001$) compared to PBMCs, despite high statistical significance. Despite a slight decrease in *HMOX1* expression in PBMCs treated with 100 µM (41.5 ± 4.6-fold) and 200 µM HU (40.31 ± 10.2-fold) compared to hemin alone, combined HU plus hemin treatment did not significantly reduce this expression.

Microarray Analysis in HUVEC Suggests that HU Induces the Nrf2-Antioxidant Response Element/Electrophile Signaling Pathway Regulated by p62/SQSTM1

Preliminary canonical pathway analysis identified 39 genes related to Nrf2-mediated oxidative stress response in HUVECs (**Table 2**). HU treatment induced increased expression levels of *SOD2* (1.852 Expr Log Ratio), *GSR* (2.882 Expr Log Ratio),

TABLE 2 | Differential expression of genes involved in Nrf2-antioxidant/electrophile response element signaling pathway, identified through microarray analysis of HUVEC treated with hydroxyurea.

Symbol	Gene name	Expr log ratio‡	Location	Type
ENZYMES				
GSR	Glutathione-disulfide reductase	2.882	Cytoplasm	Enzyme
GSTM2	Glutathione S-transferase mu 2	2.210	Cytoplasm	Enzyme
KLB	Klotho beta	1.974	Plasma membrane	Enzyme
SOD2	Superoxide dismutase 2	1.852	Cytoplasm	Enzyme
HACD3	3-hydroxyacyl-CoA dehydratase 3	1.807	Cytoplasm	Enzyme
MGST1	Microsomal glutathione S-transferase	1.733	Cytoplasm	Enzyme
CBR1	Carbonyl reductase 1	1.727	Cytoplasm	Enzyme
RRAS	RAS related	1.517	Cytoplasm	Enzyme
NRAS	NRAS proto-oncogene, GTPase	−1.521	Plasma Membrane	Enzyme
AOX1	Aldehyde oxidase 1	−2.188	Cytoplasm	Enzyme
PEPTIDASES				
CLPP	Caseinolytic mitochondrial matrix peptidase proteolytic subunit	1.551	Cytoplasm	Peptidase
ENC1	Ectodermal-neural cortex 1	−1.996	Nucleus	Peptidase
EPHX1	Epoxide hydrolase 1	−3.291	Cytoplasm	Peptidase
TRANSCRIPTION REGULATOR				
SQSTM1	Sequestosome 1	1.639	Cytoplasm	Transcription regulator
ATF4	Activating transcription factor 4	−1.639	Nucleus	Transcription regulator
BACH1	BTB domain and CNC homolog 1	−1.721	Nucleus	Transcription regulator
PMF1/PMF1-BGLAP	Polyamine modulated factor 1	−1.740	Nucleus	Transcription regulator
CREBBP	CREB binding protein	−1.743	Nucleus	Transcription regulator
MAFG	MAF bZIP transcription factor G	−1.823	Nucleus	Transcription regulator
UBE2K	Ubiquitin conjugating enzyme E2 K	−1.830	Cytoplasm	Transcription regulator
FOS	Fos proto-oncogene, AP-1 Transcription factor subunit	−3.950	Nucleus	Transcription regulator
KINASE/OTHERS				
PRKCB	Protein kinase C beta	4.026	Cytoplasm	Kinase
PRKCZ	Protein kinase C zeta	1.902	Cytoplasm	Kinase
PIK3C2B	Phosphatidylinositol-4-phosphate 3-kinase catalytic subunit type 2 beta	1.892	Cytoplasm	Kinase
DNAJB12	DnaJ heat shock protein family (Hsp40) member B12	1.794	Cytoplasm	Other
FGFR3	Fibroblast growth factor receptor 3	1.685	Plasma Membrane	Kinase
GSK3B	Glycogen synthase kinase 3 beta	1.607	Nucleus	Kinase
PIK3R3	Phosphoinositide-3-kinase regulatory subunit 3	1.597	Cytoplasm	Kinase
PIK3C2A	Phosphatidylinositol-4-phosphate 3-kinase catalytic subunit type 2 alpha	−1.716	Cytoplasm	Kinase
PIK3CB	Phosphatidylinositol-4,5-bisphosphate 3-kinase catalytic subunit beta	−1.761	Cytoplasm	Kinase
DNAJB14	DnaJ heat shock protein family (Hsp40) member B14	−1.532	Cytoplasm	Enzyme
DNAJC21	DnaJ heat shock protein family (Hsp40) member C21	−1.649	Other	Other
FRS2	Fibroblast growth factor receptor substrate 2	−1.665	Plasma Membrane	Kinase
PIK3R1	Phosphoinositide-3-kinase regulatory subunit 1	−1.690	Cytoplasm	Kinase
PRKCE	Protein kinase C epsilon	−1.679	Cytoplasm	Kinase
DNAJB4	DnaJ heat shock protein family (Hsp40) member B4	−1.843	Nucleus	Other
DNAJC18	DnaJ heat shock protein family (Hsp40) member C18	−1.897	Other	Enzyme
GAB1	GRB2 associated binding protein 1	−2.156	Cytoplasm	Kinase
MAPK14	Mitogen-activated protein kinase 14	−2.418	Cytoplasm	Kinase

‡*Based on relative expression (log fold-change > 1.5).*

GSTM2 (2.210 Expr Log Ratio), microsomal glutathione S-transferase 1 (*MGST1*) (1.733 Expr Log Ratio) and carbonyl reductase 1 (*CR1*) (1.727 Expr Log Ratio). We also found increased expression of phosphatidylinositol-4-phosphate 3-kinase catalytic subunit type 2 beta (*PIK3C2B*) (1.892 Expr Log Ratio), phosphoinositide-3-kinase regulatory subunit 3 (*PIK3R*) (1.597 Expr Log Ratio), protein kinases C beta (*PRKCB*) (4.026 Expr Log Ratio) and zeta (*PRKCZ*) (1.902 Expr Log Ratio), and glycogen synthase kinase 3 beta (*GSK3B*) (1.607 Expr Log Ratio). Moreover, HU induced

TABLE 3 | Upstream analysis of genes identified through microarray analysis of HUVEC treated with hydroxyurea.

Upstream regulator	Molecule type	Predicted activation state	Activation z-sore	*p*-value of overlap
15-deoxy-delta-12,14 -PGJ 2	Chemical–endogenous non-mammalian	Inhibited	−2.125	1.00E00
Pkc(s)	Group	Inhibited	−3.043	1.00E00
Vegf	Group	Inhibited	−2.126	1.41E−02
PRKAA2	Kinase	Inhibited	−2.101	4.06E−03
CD24	Other	Inhibited	−4.459	5.89E−04
GJA1	Transporter	Inhibited	−2.190	2.56E−02
FOXM1	Transcription regulator	Inhibited	−2.242	1.40E−06
FOXO1	Transcription regulator	Inhibited	−2.628	2.12E−01
S100A6	Transporter	Inhibited	−2.345	1.42E−02
YAP1	Transcription regulator	Inhibited	−2.449	1.23E−02
TCF4	Transcription regulator	Inhibited	−2.252	2.59E−02
OSM	Cytokine	Inhibited	−2.123	4.56E−01
ESR1	Ligand-dependent nuclear receptor	Inhibited	−2.662	3.28E−07
Ellagic acid	Chemical–endogenous non-mammalian	Inhibited	−2.000	4.71E−02
Imatinib	Chemical drug	Inhibited	−2.097	3.11E−01
GW9662	Chemical reagent	Inhibited	−2.055	2.31E−01
Isoproterenol	Chemical drug	Inhibited	−2.789	3.52E−01
Cholecalciferol	Chemical–endogenous mammalian	Inhibited	−2.331	1.00E00
R-WIN 55,212	Chemical reagent	Inhibited	−2.063	3.88E-04
zVAD-FMK	Chemical–protease inhibitor	Inhibited	−2.000	1.36E-01
Cocaine	Chemical drug	Inhibited	−2.193	1.00E00
25-hydroxycholesterol	Chemical reagent	Inhibited	−2.190	1.00E00
Hyaluronic acid	Chemical–endogenous mammalian	Activated	2.000	1.00E00
E2f	Group	Activated	2.725	8.25E−06
SPDEF	Transcription regulator	Activated	2.158	2.85E−01
EPAS1	Transcription regulator	Activated	2.059	1.00E00
SPI1	Transcription regulator	Activated	2.565	1.00E00
miR-155-5p (miRNAs w/seed UAAUGCU)	Mature microRNA	Activated	2.840	2.12E−01
mir-15	MicroRNA	Activated	2.277	9.16E−02
miR-29b-3p (and other miRNAs w/seed AGCACCA)	Mature microRNA	Activated	2.255	4.19E−01
miR-141-3p (and other miRNAs w/seed AACACUG)	Mature microRNA	Activated	2.801	2.69E−02
mir-145	MicroRNA	Activated	2.236	4.67E−01
NUPR1	Transcription regulator	Activated	4.357	1.63E−05
JUN	Transcription regulator	Activated	2.560	1.00E00
SRSF3	Other	Activated	2.229	1.78E−02
KLF4	transcription regulator	Activated	2.020	1.00E00
SYK	Kinase	Activated	2.695	1.78E−01
TBX5	Transcription regulator	Activated	2.000	1.00E00
MEOX2	Transcription regulator	Activated	2.200	4.96E−01
IFNB1	Cytokine	Activated	2.183	1.00E00
IL15	Cytokine	Activated	2.280	1.00E00
Sulindac sulfide	Chemical drug	Activated	2.192	2.65E−01
GW3965	Chemical reagent	Activated	2.204	1.00E00
Mifepristone	Chemical drug	Activated	2.201	3.74E−01

increased p62/sequestosome (*p62/SQSTM1*) (1.639 Expr Log Ratio) expression and decreased expression of BTB domain and CNC homolog 1 (*BACH1*) (-1.721 Expr Log Ratio), as well as ubiquitin-conjugating enzyme E2 K (*UBE2K*) (−1.830 Expr Log Ratio). **Table 3** presents the results of our upstream analyses, which predicted the activation of mature microRNAs, such as miR-155-5p (activation z-score = 2.840) and miR-141-3p (activation z-score = 2.801), as well as the activation of the Jun transcription regulator (activation z-score = 2.560).

DISCUSSION

The present study aimed to confirm the antioxidant potential of HU and investigate its effects on the modulation of the antioxidant cellular response. DPPH scavenging activity assays revealed that, despite higher IC_{50} values determined for HU at 100 and 200 μM, HU demonstrated considerable scavenging activity compared to controls. This finding suggests that HU may be able to directly neutralize free radicals in the extracellular microenvironment, which could be explained by its ability to donate a hydrogen atom electron in the neutralization of the radical compound DPPH (22). Moreover, our results also indicate that HU may scavenge ROS/RNS by inducing the antioxidant enzyme system. This finding is of great importance, as HU could potentially confer an important protective effect against direct oxidative attacks on membrane phospholipids, as well as prevent/minimize the triggering of activation responses involved in the initiation of the oxidative cascade and establishment of inflammation (23–26).

Both concentrations mentioned above are consistent with the plasma levels of HU generally observed in patients with SCA, which have been extensively used in *in vitro* studies (27–30). Accordingly, we chose these concentrations for our additional assays, in addition to combined therapy with hemin at 70 μM based on the findings from Carvalho et al. (31). Cytotoxicity assays involving hemin did not reveal any significant effects on cell viability in either PBMCs or HUVECs. This may be explained by the degree of resilience both cell types present in the pro-oxidative microenvironment promoted by hemin. It was previously shown that hemin can induce HO-1 production in monocytes, which promotes a cytoprotective effect through the inhibition of apoptosis (32). Our results corroborate this finding, as we observed higher levels of *HMOX1* expression in PBMCs and HUVECs following treatment with hemin. HUVECs treated with HUs plus hemin presented significant increases in NO production, which corroborates previously published results. Other studies have suggested that treatment with HU in the presence of heme resulted in the production of iron nitrosyl-heme (Fe^{2+}-NO), nitrite, and nitrate in SCA individuals (33–37).

Our investigation of antioxidant gene expression indicated differential expression profiles for each cell type after 4 h of incubation with HU in combination or not with hemin. Higher gene expression was seen in PBMCs than in HUVECs, which can be explained by the substantial capacity of recognition and effector responses in leukocytes, especially monocytes, present in PBMCs (38, 39). Our results show that treatment with HU in combination or not with hemin significantly provoked increases in *SOD1* and *GSR* expression in both cell types, similarly to the higher *GPX* expression found in PBMCs. Previous studies have demonstrated that HU activates the *GPX*-mediated NO-cGMP pathway in patients with SCA (40, 41). This activation may be due to the induction of transcriptional factors and/or H_2O_2 production controlled by the production of GPX, which is dependent on the reduced glutathione (GSH) synthesized by GSR (33, 42–45). This would seem to corroborate the higher levels of *SOD1*, *GPX* and *GSR* expression found herein in response to HU treatment. Interestingly, no association between HU and *HMOX1* expression was found, suggesting that the mechanism by which the antioxidant response system becomes activated does not involve the activation of *HMOX1*.

Microarray analyses were performed in HUVECs treated with HU to investigate the possible pathways involved in the antioxidant response system. HU induced significant increases in the expression of genes encoding antioxidant enzymes, such as *SOD2*, *GSR*, *GSTM2*, *CBR1*, *MGST1*, and *KLB,* as well as *p62/SQSTM1*. This antisickling agent was also associated with decreases in *BACH1* and *UBE2K* expression. Studies have demonstrated a positive correlation between *p62/SQSTM1* expression and Nrf2 induction (46–48), leading to the activation of antioxidant systems (49–51). BACH1 acts as a negative regulator of Nrf2, preventing the induction of an antioxidant response, while UBE2K is involved in Nrf2 degradation via the ubiquitin-proteasome system (49, 52, 53). Accordingly, the negative correlations observed between *p62/SQSTM1* and *BACH1,* as well as between *p62/SQSTM1* and *UBE2K,* suggest that HU may be capable of inducing an antioxidant response via the Nrf2 signaling pathway.

HUVECs treated with HU also presented increased expression of genes encoding *PIK3C2B*, *PIK3R3*, *PRKCB*, *PRKCZ* and *GSK3B*. Previous results have demonstrated that the activation of these genes is associated with the induction of the antioxidant response, mediated by the Nrf2 signaling pathway (54–57).

In addition, our upstream analyses performed in HUVECs treated with HU indicate the activation of miR-155-5p and miR-141-3p, which are involved in the inhibition of *BACH1* and *Keap1*, respectively, in addition to the activation of Jun, which is involved in the activation of the Nrf2-mediated antioxidant pathway (55, 58–60).

Our results suggest that HU directly scavenges free radicals and can induce the expression of antioxidant genes via induction of the Nrf2 signaling pathway. In addition, the findings herein preliminarily expand on the previously described primary mechanisms of HU, i.e., the induction of HbF production and NO release. However, further *in vitro* and *in vivo* studies will be necessary to validate the role of the Nrf2-mediated antioxidant pathway proposed by the present study.

DATA AVAILABILITY STATEMENT

All datasets generated for this study are included in the article/**Supplementary Material**.

ETHICS STATEMENT

The present study received approval from the Institutional Review Board of the Gonçalo Moniz Institute of the Oswaldo Cruz Foundation (IGM-FIOCRUZ). The patients/participants provided their written informed consent to participate in this study.

AUTHOR CONTRIBUTIONS

SS, TP, and MG conceived and designed the study, performed statistical analyses, and wrote the manuscript. SS performed all experiments. JS, DZ, JV, SY, CA, SV, NL, and VB assisted in some experimentation and provided technical support and discussed the results and participated in manuscript elaboration. MG, TP, and SY critically revised the manuscript. All authors revised and approved the final version of the manuscript.

FUNDING

This work was supported by grants from the Brazilian National Council of Research (CNPq) (311888/2013-5) (MG); MCD/CNPq/MS-SCTIE-DECIT (409800/2006-6) (MG); the Foundation for the Support of Research in the State of Bahia (FAPESB) (3626/2013, 1431040053063, and 9073/2007) (MG); PPSUS/FAPESB (020/2013 EFP00007295) (MG); and the Coordination for the Improvement of Higher Education Personnel (CAPES) agency–Finance Code 001 (SY). The sponsors of this study are public or nonprofit organizations that support science in general.

ACKNOWLEDGMENTS

The authors would like to thank Dr. Ana Moretti, Ph.D. and Dr. Heraldo Possolo de Souza, M.D., both from the São Paulo State University Medical School (FMUSP-Brazil), for generously donating the HUVEC cells used in this study. We would also like to thank Andris K. Walter for his critical analysis and English revision of the final manuscript.

SUPPLEMENTARY MATERIAL

The Supplementary Material for this article can be found online at: https://www.frontiersin.org/articles/10.3389/fimmu.2020.01488/full#supplementary-material

REFERENCES

1. Steinberg MH, Rodgers GP. Pathophysiology of sickle cell disease: role of cellular and genetic modifiers. *Semin Hematol*. (2001) 38:299–306. doi: 10.1016/S0037-1963(01)90023-X
2. Steinberg MH. Sickle cell anemia, the first molecular disease: overview of molecular etiology, pathophysiology, and therapeutic approaches. *TheScientificWorldJournal*. (2008) 8:1295–324. doi: 10.1100/tsw.2008.157
3. Belcher JD, Beckman JD, Balla G, Balla J, Vercellotti G. Heme degradation and vascular injury. *Antioxid Redox Signal*. (2010) 12:233–48. doi: 10.1089/ars.2009.2822
4. Nur E, Biemond BJ, Otten HM, Brandjes DP, Schnog JJ. Oxidative stress in sickle cell disease; pathophysiology and potential implications for disease management. *Am J Hematol*. (2011) 86:484–9. doi: 10.1002/ajh.22012
5. Chirico EN, Pialoux V. Role of oxidative stress in the pathogenesis of sickle cell disease. *IUBMB Life*. (2012) 64:72–80. doi: 10.1002/iub.584
6. Kato GJ, Piel FB, Reid CD, Gaston MH, Ohene-Frempong K, Krishnamurti L, et al. Sickle cell disease. *Nat Rev Dis Primers*. (2018) 4:18010. doi: 10.1038/nrdp.2018.10
7. Hebbel RP, Morgan WT, Eaton JW, Hedlund BE. Accelerated autoxidation and heme loss due to instability of sickle hemoglobin. *Proc Natl Acad Sci USA*. (1988) 85:237–41. doi: 10.1073/pnas.85.1.237
8. Bonaventura C, Taboy CH, Low PS, Stevens RD, Lafon C, Crumbliss AL. Heme redox properties of S-nitrosated hemoglobin A0 and hemoglobin S: implications for interactions of nitric oxide with normal and sickle red blood cells. *J Biol Chem*. (2002) 277:14557–63. doi: 10.1074/jbc.M107658200
9. Reiter CD, Wang X, Tanus-Santos JE, Hogg N, Cannon RO III, Schechter AN, et al. Cell-free hemoglobin limits nitric oxide bioavailability in sickle-cell disease. *Nat Med*. (2002) 8:1383–9. doi: 10.1038/nm1202-799
10. Kaul DK, Hebbel RP. Hypoxia/reoxygenation causes inflammatory response in transgenic sickle mice but not in normal mice. *J Clin Invest*. (2000) 106:411–20. doi: 10.1172/JCI9225
11. Schimmel M, Nur E, Biemond BJ, van Mierlo GJ, Solati S, Brandjes DP, et al. Nucleosomes and neutrophil activation in sickle cell disease painful crisis. *Haematologica*. (2013) 98:1797–803. doi: 10.3324/haematol.2013.088021
12. Chen G, Zhang D, Fuchs TA, Manwani D, Wagner DD, Frenette PS. Heme-induced neutrophil extracellular traps contribute to the pathogenesis of sickle cell disease. *Blood*. (2014) 123:3818–27. doi: 10.1182/blood-2013-10-529982
13. Balandya E, Reynolds T, Obaro S, Makani J. Alteration of lymphocyte phenotype and function in sickle cell anemia: implications for vaccine responses. *Am J Hematol*. (2016) 91:938–46. doi: 10.1002/ajh.24438
14. Charache S. Mechanism of action of hydroxyurea in the management of sickle cell anemia in adults. *Semin Hematol*. (1997) 34(3 Suppl. 3):15–21.
15. Agrawal RK, Patel RK, Shah V, Nainiwal L, Trivedi B. Hydroxyurea in sickle cell disease: drug review. *Indian J Hematol Blood Transfusion*. (2014) 30:91–6. doi: 10.1007/s12288-013-0261-4
16. Zhou B, Mo X, Liu X, Qiu W, Yen Y. Human ribonucleotide reductase M2 subunit gene amplification and transcriptional regulation in a homogeneous staining chromosome region responsible for the mechanism of drug resistance. *Cytogenet Cell Genet*. (2001) 95:34–42. doi: 10.1159/000057014
17. Ware RE. How i use hydroxyurea to treat young patients with sickle cell anemia. *Blood*. (2010) 115:5300–11. doi: 10.1182/blood-2009-04-146852
18. Martin D, Rojo AI, Salinas M, Diaz R, Gallardo G, Alam J, et al. Regulation of heme oxygenase-1 expression through the phosphatidylinositol 3-kinase/Akt pathway and the Nrf2 transcription factor in response to the antioxidant phytochemical carnosol. *J Biol Chem*. (2004) 279:8919–29. doi: 10.1074/jbc.M309660200
19. Bean CJ, Boulet SL, Ellingsen D, Pyle ME, Barron-Casella EA, Casella JF, et al. Heme oxygenase-1 gene promoter polymorphism is associated with reduced incidence of acute chest syndrome among children with sickle cell disease. *Blood*. (2012) 120:3822–8. doi: 10.1182/blood-2011-06-361642
20. Li WJ, Cheng XL, Liu J, Lin RC, Wang GL, Du SS, et al. Phenolic compounds and antioxidant activities of *Liriope muscari*. *Molecules*. (2012) 17:1797–808. doi: 10.3390/molecules17021797
21. Bryan NS, Grisham MB. Methods to detect nitric oxide and its metabolites in biological samples. *Free Radic Biol Med*. (2007) 43:645–57. doi: 10.1016/j.freeradbiomed.2007.04.026
22. Blois MS. Antioxidant determinations by the use of a stable free radical. *Nature*. (1958) 181:1199–200. doi: 10.1038/1811199a0
23. Halliwell B, Gutteridge JM. Lipid peroxidation, oxygen radicals, cell damage, and antioxidant therapy. *Lancet*. (1984) 1:1396–7. doi: 10.1016/S0140-6736(84)91886-5
24. Grijalba MT, Andrade PB, Meinicke AR, Castilho RF, Vercesi AE, Schreier S. Inhibition of membrane lipid peroxidation by a radical scavenging mechanism: a novel function for hydroxyl-containing ionophores. *Free Radic Res*. (1998) 28:301–18. doi: 10.3109/10715769809069282
25. Noor JI, Ikeda T, Ueda Y, Ikenoue T. A free radical scavenger, edaravone, inhibits lipid peroxidation and the production of nitric oxide in hypoxic-ischemic brain damage of neonatal rats. *Am J Obstet Gynecol*. (2005) 193:1703–8. doi: 10.1016/j.ajog.2005.03.069
26. Mittal M, Siddiqui MR, Tran K, Reddy SP, Malik AB. Reactive oxygen species in inflammation and tissue injury. *Antioxid Redox Signal*. (2014) 20:1126–67. doi: 10.1089/ars.2012.5149

27. Elias DBD, Carvalho TMDJP, Soares JEDS, Gonçalves RP. Standardization method for measurement of hydroxyurea by ultra high efficiency liquid chromatography in plasma of patients with sickle cell disease. *Braz J Pharm Sci.* (2014) 50:621–8. doi: 10.1590/S1984-82502014000300022
28. Lopes FCM, Ferreira R, Albuquerque DM, Silveira AAA, Costa R, Soares R, et al. *In vitro* and *in vivo* anti-angiogenic effects of hydroxyurea. *Microvasc Res*. (2014) 94:106–13. doi: 10.1016/j.mvr.2014.05.009
29. Almeida CB, Souza LE. Acute hemolytic vascular inflammatory processes are prevented by nitric oxide replacement or a single dose of hydroxyurea. *Blood*. (2015) 126:711–20. doi: 10.1182/blood-2014-12-616250
30. da Guarda CC, Santiago RP, Pitanga TN, Santana SS, Zanette DL, Borges VM, et al. Heme changes HIF-alpha, eNOS and nitrite production in HUVECs after simvastatin, HU, and ascorbic acid therapies. *Microvasc Res*. (2016) 106:128–36. doi: 10.1016/j.mvr.2016.04.002
31. Carvalho MOS, Araujo-Santos T, Reis JHO, Rocha LC, Cerqueira BAV, Luz NF, et al. Inflammatory mediators in sickle cell anaemia highlight the difference between steady state and crisis in paediatric patients. *Br J Hametol.* (2017) 182:933–6. doi: 10.1111/bjh.14896
32. Lang D, Reuter S, Buzescu T, August C, Heidenreich S. Heme-induced heme oxygenase-1 (HO-1) in human monocytes inhibits apoptosis despite caspase-3 up-regulation. *Int Immunol*. (2005) 17:155–65. doi: 10.1093/intimm/dxh196
33. Huang J, Kim-Shapiro DB, King SB. Catalase-mediated nitric oxide formation from hydroxyurea. *J Med Chem*. (2004) 47:3495–501. doi: 10.1021/jm030547z
34. King SB. Nitric oxide production from hydroxyurea. *Free Radic Biol Med*. (2004) 37:737–44. doi: 10.1016/j.freeradbiomed.2004.02.073
35. Lockamy VL, Shields H, Kim-Shapiro DB, King SB. Iron nitrosyl hemoglobin formation from the reaction of hydroxylamine and hemoglobin under physiological conditions. *Biochim Biophys Acta*. (2004) 1674:260–7. doi: 10.1016/j.bbagen.2004.07.003
36. King SB. N-hydroxyurea and acyl nitroso compounds as nitroxyl (HNO) and nitric oxide (NO) donors. *Curr Top Med Chem*. (2005) 5:665–73. doi: 10.2174/1568026054679362
37. Fotiou S, Fotiou D, Deliconstantinos G. Formation of heme-iron complexes with nitric oxide (NO) and peroxynitrite (ONOO-) after ultraviolet radiation as a protective mechanism in rat skin. *In Vivo*. (2009) 23:281–6.
38. Chaplin DD. Overview of the immune response. *J Allergy Clin Immunol.* (2010) 125(2 Suppl. 2):S3–23. doi: 10.1016/j.jaci.2009.12.980
39. Gladwin MT, Ofori-Acquah SF. Erythroid DAMPs drive inflammation in SCD. *Blood*. (2014) 123:3689–90. doi: 10.1182/blood-2014-03-563874
40. Cho C-S, Kato GJ, Yang SH, Bae SW, Lee JS, Gladwin MT, et al. Hydroxyurea-induced expression of glutathione peroxidase 1 in red blood cells of individuals with sickle cell anemia. *Antioxid Redox Signal.* (2010) 13:1–11. doi: 10.1089/ars.2009.2978
41. Itokua EK, Ngiyulu R, Makulo JR, Lepira FB, Aloni M, Sadiki H. GPx and Cu-Zn SOD activities in homozygous sickle cell anemia: the primary role of hydroxyurea. *J. innov. res. health sci. biotechnol.* (2016) 1:85–91. doi: 10.18644/jiresh-biotech.0000014
42. Malec J, Przybyszewski WM, Grabarczyk M, Sitarska E. Hydroxyurea has the capacity to induce damage to human erythrocytes which can be modified by radical scavengers. *Biochem Biophys Res Commun*. (1984) 120:566–73. doi: 10.1016/0006-291X(84)91292-0
43. Iyamu EW, Fasold H, Roa D, del Pilar Aguinaga M, Asakura T, Turner EA. Hydroxyurea-induced oxidative damage of normal and sickle cell hemoglobins *in vitro*: amelioration by radical scavengers. *J Clin Lab Anal*. (2001) 15:1–7. doi: 10.1002/1098-2825(2001)15:1<1::AID-JCLA1>3.0.CO;2-I
44. Sakano K, Oikawa S, Hasegawa K, Kawanishi S. Hydroxyurea induces site-specific DNA damage via formation of hydrogen peroxide and nitric oxide. *Jpn J Cancer Res*. (2001) 92:1166–74. doi: 10.1111/j.1349-7006.2001.tb02136.x
45. Nagai T, Tarumoto T, Miyoshi T, Ohmine K, Muroi K, Komatsu N, et al. Oxidative stress is involved in hydroxyurea-induced erythroid differentiation. *Br J Haematol.* (2003) 121:657–61. doi: 10.1046/j.1365-2141.2003.04309.x
46. Ishii T, Itoh K, Takahashi S, Sato H, Yanagawa T, Katoh Y, et al. Transcription factor Nrf2 coordinately regulates a group of oxidative stress-inducible genes in macrophages. *J Biol Chem*. (2000) 275:16023–9. doi: 10.1074/jbc.275.21.16023
47. Warabi E, Takabe W, Minami T, Inoue K, Itoh K, Yamamoto M, et al. Shear stress stabilizes NF-E2-related factor 2 and induces antioxidant genes in endothelial cells: role of reactive oxygen/nitrogen species. *Free Radic Biol Med*. (2007) 42:260–9. doi: 10.1016/j.freeradbiomed.2006.10.043
48. Maltese G, Psefteli P-M, Rizzo B, Srivastava S, Gnudi L, Mann GE, et al. The anti-ageing hormone klotho induces Nrf2-mediated antioxidant defences in human aortic smooth muscle cells. *J Cell Mol Med*. (2017) 21:621–7. doi: 10.1111/jcmm.12996
49. Copple IM, Lister A, Obeng AD, Kitteringham NR, Jenkins RE, Layfield R, et al. Physical and functional interaction of sequestosome 1 with Keap1 regulates the Keap1-Nrf2 cell defense pathway. *J Biol Chem*. (2010) 285:16782–8. doi: 10.1074/jbc.M109.096545
50. Furfaro AL, Traverso N, Domenicotti C, Piras S, Moretta L, Marinari UM, et al. The Nrf2/HO-1 axis in cancer cell growth and chemoresistance. *Oxid Med Cell Longev*. (2016) 2016:14. doi: 10.1155/2016/1958174
51. Taniguchi K, Yamachika S, He F, Karin M. p62/SQSTM1-Dr. Jekyll and Mr Hyde that prevents oxidative stress but promotes liver cancer. *FEBS Lett*. (2016) 590:2375–97. doi: 10.1002/1873-3468.12301
52. Cullinan SB, Gordan JD, Jin J, Harper JW, Diehl JA. The Keap1-BTB protein is an adaptor that bridges Nrf2 to a Cul3-based E3 ligase: oxidative stress sensing by a Cul3-Keap1 ligase. *Mol Cell Biol*. (2004) 24:8477–86. doi: 10.1128/MCB.24.19.8477-8486.2004
53. He X, Chen MG, Lin GX, Ma Q. Arsenic induces NAD(P)H-quinone oxidoreductase I by disrupting the Nrf2 x Keap1 x Cul3 complex and recruiting Nrf2 x Maf to the antioxidant response element enhancer. *J Biol Chem*. (2006) 281:23620–31. doi: 10.1074/jbc.M604120200
54. Nakaso K, Yano H, Fukuhara Y, Takeshima T, Wada-Isoe K, Nakashima K. PI3K is a key molecule in the Nrf2-mediated regulation of antioxidative proteins by hemin in human neuroblastoma cells. *FEBS Lett*. (2003) 546:181–4. doi: 10.1016/S0014-5793(03)00517-9
55. Niture SK, Khatri R, Jaiswal AK. Regulation of Nrf2-an update. *Free Radic Biol Med*. (2014) 66:36–44. doi: 10.1016/j.freeradbiomed.2013.02.008
56. Jain AK, Jaiswal AK. Phosphorylation of tyrosine 568 controls nuclear export of Nrf2. *J Biol Chem*. (2006) 281:12132–42. doi: 10.1074/jbc.M511198200
57. Niture SK, Jain AK, Shelton PM, Jaiswal AK. Src subfamily kinases regulate nuclear export and degradation of transcription factor Nrf2 to switch off Nrf2-mediated antioxidant activation of cytoprotective gene expression. *J Biol Chem*. (2017) 292:2048. doi: 10.1074/jbc.A117.255042
58. Pullarkat V, Meng Z, Tahara SM, Johnson CS, Kalra VK. Proteasome inhibition induces both antioxidant and hb f responses in sickle cell disease via the nrf2 pathway. *Hemoglobin*. (2014) 38:188–95. doi: 10.3109/03630269.2014.898651
59. Cheng LB, Li KR, Yi N, Li XM, Wang F, Xue B, et al. miRNA-141 attenuates UV-induced oxidative stress via activating Keap1-Nrf2 signaling in human retinal pigment epithelium cells and retinal ganglion cells. *Oncotarget*. (2017) 8:13186–94. doi: 10.18632/oncotarget.14489
60. Gu SY, Chen HY, Dai HM, Li XY, Zhang ZZ. [miR-155/BACH1 signaling pathway in human lung adenocarcinoma cell death induced by arsenic trioxide]. *Sichuan Da Xue Xue Bao Yi Xue Ban.* (2017) 48:828–33.

Conflict of Interest: The authors declare that the research was conducted in the absence of any commercial or financial relationships that could be construed as a potential conflict of interest.

frontiers in Immunology

ORIGINAL RESEARCH
published: 31 July 2020
doi: 10.3389/fimmu.2020.01684

Hemopexin as an Inhibitor of Hemolysis-Induced Complement Activation

*Victoria Poillerat[1], Thomas Gentinetta[2], Juliette Leon[1], Andreas Wassmer[2], Monika Edler[2], Carine Torset[1], Dandan Luo[3], Gerald Tuffin[2] and Lubka T. Roumenina[1]**

[1] Centre de Recherche des Cordeliers, INSERM, Sorbonne Université, Université de Paris, Paris, France, [2] CSL Behring AG, Bern, Switzerland, [3] CSL Behring, King of Prussia, PA, United States

Hemopexin is the main plasmatic scavenger of cell-free heme, released in the context of intravascular hemolysis or major cell injury. Heme is indispensable for the oxygen transport by hemoglobin but when released outside of the erythrocytes it becomes a danger-associated molecular pattern, contributing to tissue injury. One of the mechanisms of pro-inflammatory action of heme is to activate the innate immune complement cascade. Therefore, we hypothesized that injection of hemopexin will prevent hemolysis-induced complement activation. Human plasma-derived hemopexin is compatible with the heme clearance machinery of the mice. 100 or 500 mg/kg of hemopexin was injected in C57Bl/6 mice before treatment with phenylhydrazine (inducer of erythrocytes lysis) or with PBS as a control. Blood was taken at different timepoints to determine the pharmacokinetic of injected hemopexin in presence and absence of hemolysis. Complement activation was determined in plasma, by the C3 cleavage (western blot) and in the kidneys (immunofluorescence). Kidney injury was evaluated by urea and creatinine in plasma and renal NGAL and HO-1 gene expression were measured. The pharmacokinetic properties of hemopexin (mass spectrometry) in the hemolytic mice were affected by the target-mediated drug disposition phenomenon due to the high affinity of binding of hemopexin to heme. Hemolysis induced complement overactivation and signs of mild renal dysfunction at 6 h, which were prevented by hemopexin, except for the NGAL upregulation. The heme-degrading capacity of the kidney, measured by the HO-1 expression, was not affected by the treatment. These results encourage further studies of hemopexin as a therapeutic agent in models of diseases with heme overload.

Keywords: hemopexin, heme, hemolysis, complement, kidney injury, C3

OPEN ACCESS

Edited by:
Nicola Conran, Campinas State University, Brazil

Reviewed by:
Erich Vinicius De Paula, Campinas State University, Brazil
Viktória Jeney, University of Debrecen, Hungary
Marcelo Torres Bozza, Federal University of Rio de Janeiro, Brazil

***Correspondence:**
Lubka T. Roumenina
lubka.roumenina@sorbonne-universite.fr

Specialty section:
This article was submitted to Inflammation, a section of the journal Frontiers in Immunology

Received: *05 May 2020*
Accepted: *24 June 2020*
Published: *31 July 2020*

Citation:
Poillerat V, Gentinetta T, Leon J, Wassmer A, Edler M, Torset C, Luo D, Tuffin G and Roumenina LT (2020) Hemopexin as an Inhibitor of Hemolysis-Induced Complement Activation. Front. Immunol. 11:1684. doi: 10.3389/fimmu.2020.01684

INTRODUCTION

In physiological conditions heme is compartmentalized inside the cells and serves as an indispensable cofactor for aerobic life, by its interaction with conventional heme-binding proteins, such as hemoglobin, myoglobin and cytochromes. Nevertheless, it becomes a danger associated molecular pattern, when released in the circulation or in tissues during intravascular hemolysis [red blood cells (RBC) lysis during sickle cell disease (SCD), hemolytic uremic syndrome (HUS), malaria, transfusion reactions, etc.] or rhabdomyolysis (crush syndrome, muscle damage as

in car accidents, natural cataclysms, or military trauma) (1). Heme triggers inflammation by activating immune and endothelial cells (EC) or plasma systems, such as the complement cascade, coagulation, or inducing antibody polyreactivity (2–4). In physiological conditions excess of cell-free heme is scavenged by its natural binding protein hemopexin (Hpx).

Hpx is a liver-produced plasma glycoprotein (0.5–1.15 g/l) of 60 kDa. Hpx binds free heme with a very high affinity (Kd $< 10^{-13}$ M) (5, 6), which makes it virtually irreversible. The heme:Hpx complex binds to CD91/LRP1 and is endocytosed (7). Part of Hpx may be recycled, but the majority is degraded, creating acquired Hpx deficiency in case of massive hemolysis (6). Hpx-knockout mice presented severe renal injury upon phenylhydrazine (PHZ triggered hemolysis), contrary to the WT mice (8). Moreover, Hpx deficiency promoted acute kidney injury in sickle mice under hemolytic stress, which was blocked by pre-treatment with purified Hpx (9). Injection of heme in SCD mice induce stasis (10, 11), cardiovascular injury and cardiomyocytes alteration (12–14), all of which have been prevented by pre-treatment with Hpx. Heme-carrying erythrocyte microparticles from SCD patients, injected in a SCD mice, induced kidney vaso-occlusion and endothelium injury, which was also prevented by Hpx administration (15, 16). Hpx also prevents the activation of the pro-inflammatory complement system in the kidneys of hemolytic mice (PHZ model) and *in vitro*, in serum and on endothelial cells. Moreover, it prevented the complement deposition on endothelial cells, incubated with serum from SCD patients (17). This complement activation plays a key role in the organ injury in SCD and in hemolytic mice, since C3 deficiency or complement blockade alleviate the vaso-occlusion and the kidney and liver damage, respectively (18, 19).

Taken together, these examples demonstrate that replenishing the Hpx pool is a potential promising therapeutic strategy to avoid the heme-mediated toxicity. In order to be tested as a therapeutic agent in pre-clinical models, the pharmacokinetic, and the active concentrations of Hpx have to be evaluated in the context of an intravascular hemolysis. Here we demonstrate that the pharmacokinetic properties of Hpx in the hemolytic mice were affected by the target-mediated drug disposition phenomenon. The dose of 100 mg/kg is well tolerated and sufficient to prevent the hemolysis-induced complement activation.

METHOD

Animal Experimentation

Experimental protocols were approved by Charles Darwin ethical committee (Paris, France) and of French Ministry of Agriculture (Paris, France) number #3764 201601121739330 v3. All experiments were conducted in accordance with the recommendations for the care and use laboratory animal.

A first experiment was performed to determine the pharmacokinetic properties of Hpx in hemolytic mice (**Figure 1A**). Three groups of mice were injected in i.v. with 100 mg/kg of human plasma derived Hpx (CSL Behring) and three other groups with 500 mg/kg of Hpx. An i.p. PHZ injection (0.125 mg/g body weight) was performed immediately after Hpx administration. The mice from each Group 1 were bled at 15 min, 1 and 6 h. They were sacrificed at 6 h. Each Group 2 was bled at 30 min, 10 and 24 h and sacrificed at 24 h. Each Group 3 was bled at 3, 48, and 72 h followed by a sacrifice at 72 h. The bleeding schema is given in **Supplementary Table 1**.

A second experiment aimed to evaluate the complement inhibition capacity of Hpx and its impact on complement activation and renal function. Three groups of 8-week-old C56BL/6 male mice ($n = 10$) were pretreated with human Hpx (CSL Behring) in i.v. with 100 or 500 mg/kg or equivalent volume of PBS (0 mg/kg) immediately before i.p. PHZ injection (0.125 mg/g body weight) (**Figure 2A**). A control group of 8 mice received two injections of PBS, corresponding to the volume of Hpx and PHZ. All mice were sacrificed by cervical dislocation, 6 or 72 h after Hpx administration. Whole blood was collected 3 days before experimentation and at day 1 into microtubes filled with 2 μL of heparin (Heparine Choay® 5000 ui/ L Sanofi) by venipuncture in the cheek. Microtubes were centrifuged at 604 g for 10 min at room temperature to separate plasma. Kidneys were harvested for immunofluorescence (IF) and gene expression analyses. Plasma and organs were directly frozen in liquid nitrogen and stored at −80°C.

Quantification of Human Hpx in Animal Plasma by LC/MS

Ten microliters of plasma sample were placed into a clean Eppendorf tube followed by the addition of 80 μL MeOH to precipitate the protein. The methanol was removed after centrifugation and the pellet was air-dried and afterwards re-suspended in 50 mM NH_4HCO_3/0.16% ProteaseMAX containing a heavy-isotope labeled peptide, which is specific for human Hpx and is used as internal standard. After incubation at 56°C/550 rpm for 45 min the samples were reduced by adding 0.5 M DTT (56°C/550 rpm for 20 min). The samples were then alkylated by addition of 0.5 M IAA and incubation for 20 min at RT protected from light. Tryptic digestion was carried out at 37°C/550 rpm and stopped after 3 h by addition of formic acid. After centrifugation the samples were separated immediately on a C18 column (AdvanceBio Peptide Mapping, 2.1 × 150 mm). The measurements were conducted using an Agilent 1290 Infinity II – 6550 iFunnel QTOF LC-MS system.

Data was analyzed by calculating the peak area of the analyte and the internal standard using Agilent MassHunter Quant software. A standard curve was created in Agilent MassHunter Quant by plotting the average response ratio of analyte to internal standard against concentration for each standard sample. The analyte concentration in the plasma samples was backcalculated using the standard curve equation.

Preparation of Heme

Hemin (Frontier Scientific) was dissolved in 10 mL NaOH (100 mmol/L) at 37°C. The pH of the solution was adjusted to pH 7.8 using phosphoric acid. The solution was sterile-filtered (0.22 μm) and used immediately.

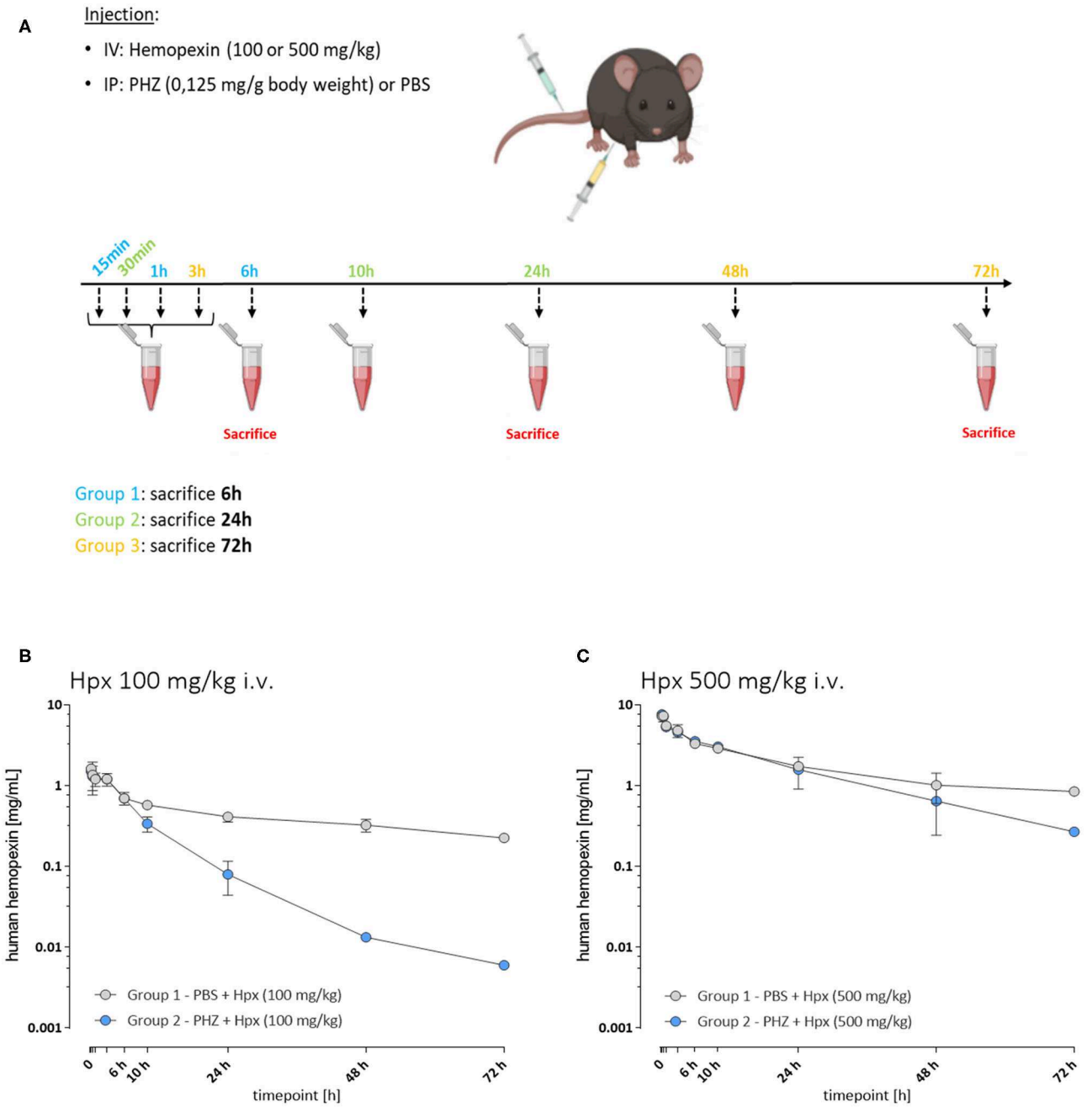

FIGURE 1 | The pharmacokinetic of hemopexin in hemolytic mice is affected by target-mediated drug disposition phenomenon. **(A)** Protocol to study pharmacokinetic of Hpx. Three groups of mice were injected with PHZ and Hpx and bled as follows: Group 1 (15 min, 1 and 6 h), Group 2 (30 min, 10 and 24 h), and Group 3 (3, 48, and 72 h). **(B,C)** *In vivo* Hpx exposure in presence and absence of induced hemolysis. **(B)** Mean ± SD plasma concentration vs. time plotted for human hemopexin administered to mice (100 mg/kg i.v.; $n = 3$/timepoint). In presence of PHZ (0.125 mg/g weight, blue circles) or control (PBS, gray circles). Pharmacokinetic parameter estimates are shown in **Table 1**. **(C)** Mean ± SD plasma concentration vs. time plotted for human hemopexin administered to mice (500 mg/kg; $n = 3$/timepoint). In presence of PHZ (0.125 mg/g weight, blue circles) or control (PBS, gray circles). Pharmacokinetic parameter estimates are shown in **Table 1**.

Total Heme in Mouse Plasma

Total plasma heme concentration in mouse plasma was determined according manufacturer's protocols using the QuantiChrom™ Heme Assay Kit (BioAssay Systems). Briefly, 50 µL of sample (diluted in water 1:2) was placed into a 96-well plate. Assay reagent (200 µl per well) was added and incubated for 5 min at room temperature. Absorbance at λ_{400} nm was measured using a microplate reader (Synergy BioTek). Heme concentration was determined by comparison to a hemin standard curve (hemin preparation see above).

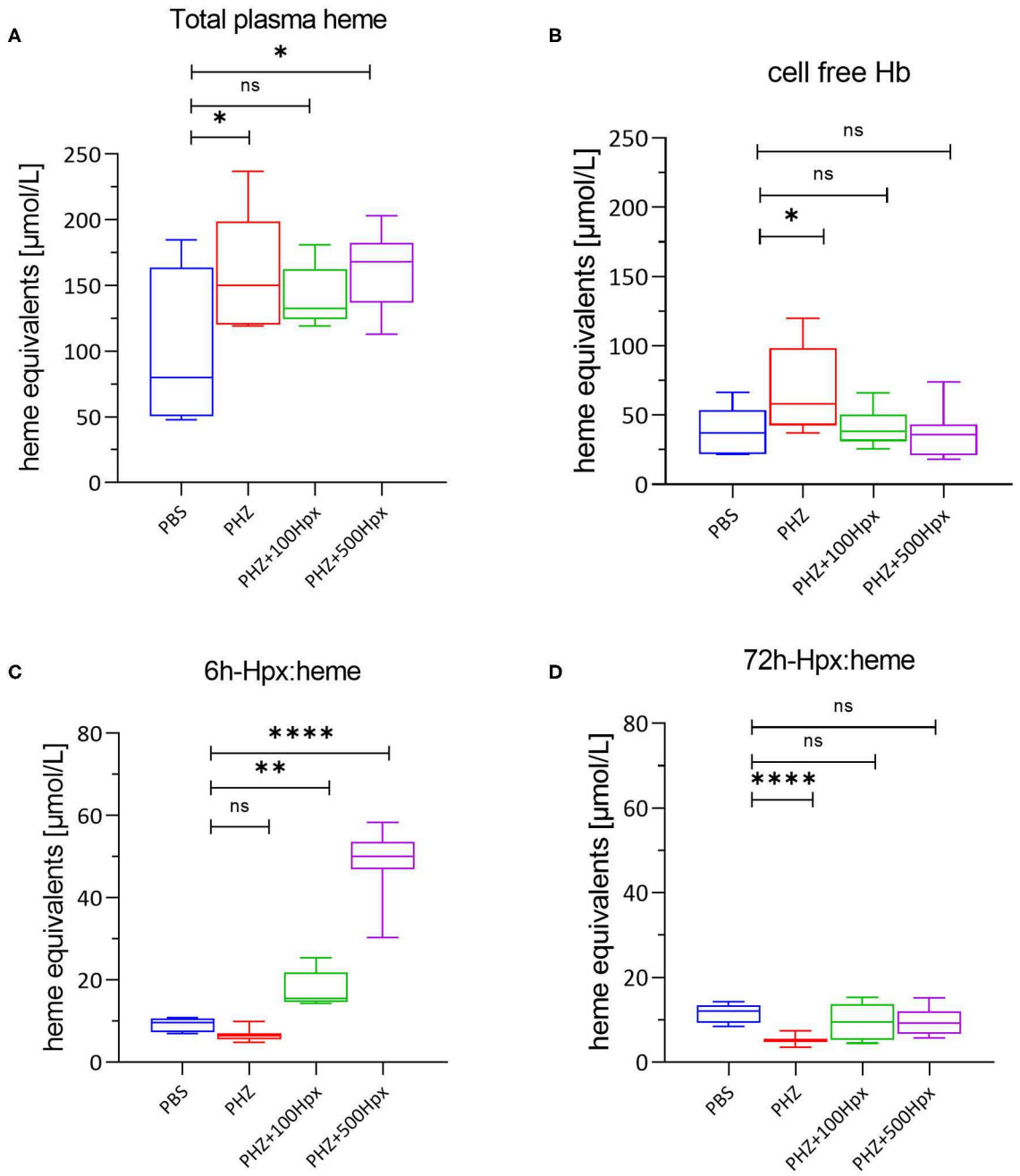

FIGURE 2 | Heme scavenging upon PHZ induced hemolysis by hemopexin. **(A)** Mean total heme plasma concentration at 6 h, **(B)** mean cell free hemoglobin at 6 h and **(C)** hemopexin:heme complexes at 6 h, and **(D)** 72 h shown for each group [(1) PBS; $n = 7$, (2) PHZ, (3) PHZ + 100 mg/kg, and (4) PHZ + 500 mg/kg; $n = 10$]. Box and whiskers plots represent means ± Min to Max. ****$p < 0.0001$, **$p < 0.01$, and *$p < 0.05$ comparisons to PBS treated, Two-way ANOVA Kruskal Wallis test, ns, not significant.

Detection of Heme:Hpx Complexes in Mouse Plasma

Fifty microliters of plasma sample were placed into a clean Eppendorf tube followed by the addition of 150 µL Buffer A (Multiple Affinity Removal Systems, Agilent). In a first chromatography step high abundant mouse proteins were depleted and carried out according to the manufacturer's protocol on an Ultimate 3000SD HPLC attached to two LPG-3400SD quaternary pumps and a photodiode array detector (DAD) (ThermoFisher). Briefly, the diluted plasma sample was injected onto a multi affinity removal column depleting mouse albumin, IgG, and Transferrin (Mouse-3, 4.6 × 50 mm, Agilent)

and separated with Buffer A (Multiple Affinity Removal Systems, Agilent) as the mobile phase at a flow rate of 0.25 mL/min. Depleted plasma was collected into a fresh HPLC vial and re-injected and separated on a Diol-300 (3 µm, 300 × 8.0 mm) column (YMC Co., Ltd.) with PBS, pH 7.4 (Bichsel) as the mobile phase at a flow rate of 1 mL/min. For all samples two wavelengths were recorded ($\lambda = 280$ nm and $\lambda = 414$ nm). The amount of Heme:Hpx complexes was determined by calculating the peak area of the complex (9 min retention time). Values from depleted plasma samples were interpolated by generating a standard curve based on peak area and plotted against the concentrations.

Plasma Hb Measurements

Hp-bound and unbound fractions of Hb (cell free Hb) were determined by SEC–high-performance liquid chromatography (SEC-HPLC) using an Ultimate 3000SD HPLC attached to a LPG-3400SD quaternary pump and a photodiode array detector (DAD) (ThermoFisher). Plasma samples and Hb standards were separated on a Diol-120 (3 µm, 300 × 8.0 mm) column (YMC Co., Ltd.) with PBS, pH 7.4 (Bichsel) as the mobile phase at a flow rate of 1 mL/min. For all samples two wavelengths were recorded ($\lambda = 280$ nm and $\lambda = 414$ nm). Bound and unbound Hb in plasma was determined by calculating the peak area of both peaks (6 min retention time for Hb:Hp, 8 min retention time for cell free Hb). Values from plasma samples were interpolated by generating a standard curve based on peak area and plotted against the concentrations.

Pharmacokinetic (PK) Analysis

Four groups were evaluated: (I) PBS + Hpx (100 mg/kg i.v.), (II) PHZ + Hpx (100 mg/kg i.v.), (III) PBS + Hpx (500 mg/kg i.v.), and PHZ + Hpx (500 mg/kg i.v.) (group size $n = 3$/timepoint).

Hpx PK in PBS vs. PHZ treated mice were conducted via non-compartmental analysis (NCA) using Phoenix WinNonlin version 7.4 (Certara, St. Louis, MO, USA). Linear up-log down method was used for area under the concentration curve (AUC) calculation. Besides directly observed maximum concentration (C_{max}) and AUC_{0-72h}, other derived PK parameters including area under the concentration curve till infinity (AUC_{inf}), clearance (CL), volume at steady state (Vss), and half-life (T1/2) were reported.

Evaluation of the Kidney and Liver Function

Kidney function was evaluated by blood urea nitrogen (urea) and creatinine, measured by a colorimetric analysis using Konelab Clinical Chemistry Analyzers in the Renal Function Exploration platform of the Cordeliers Research Center. ALT was measured using Olympus AU400 multiparameter equipment on the biochemistry platform in Hospital Bichat (Centre Recherche sur l'Inflammation-Paris).

Immunofluorescence

Six micrometer thick frozen kidney sections were cut with Cryostat at −20°C (Leica AS-LMD, Leica Biosystem) and fixed in acetone on ice for 10 min. The primary antibody was C3b/iC3b (rat anti-mouse, Hycult biotech, HM1065, 1 µg/ml) and CD31 (rat anti-mouse, Abcam Ab7388, 2 µg/mL). Staining was revealed by Donkey anti-rabbit AF647 (Thermoscientific, A21447, 5 µg/mL) and chicken anti-rat AF488 (Thermoscientific, A21470, 5 µg/mL). Slides were scanned by Axio Scan™ Z1 (Zeiss, Oberkochen, Germany). Images were analyzed using Zen lite software (Zeiss). C3 and CD31 staining were quantified using HALO® (Indica Labs) software.

Gene Expression Analysis

Frozen kidneys were sectioned at 30 µm with Cryostat at −20°C (Leica AS-LMD, Leica Biosystem). Twenty sections were recovered and homogenized in the tubes with 200 µL of 1-Thioglycerol/Homogenization Solution (Maxwell® 16 LEV simplyRNA Tissue Kit Promega AS1280). The quality and quantity of mRNA were evaluated with the Agilent 2100 bioanalyzer using the Agilent TNA 6000 NanoKit, followed by retro-transcription to cDNA. All RNA Integrity Numbers superior to 7 were retained for reverse transcription in cDNA. Gene markers of early kidney injury [LCN2 (Lcn2-Mm01324470_m1)], and for cytoprotection [HO-1 (Hmox1-Mm00516005_m1)] was analyzed with SDS 2.1® software (ThermoFisher), after normalization on actin (Actb_Mm02613580_g1) housekeeping gene expression. The gene expression for the PHZ-treated mice was expressed as fold change compared to the gene expression from the pool of the PBS treated mice.

Detection of C3 Cleavage in the Plasma of Mice by Western Blot (WB)

Plasma was diluted 1/100 in H_2O. Two volumes of this sample were mixed with one volume of NuPAGE® LDS sample buffer (4X) (Thermofisher) containing reducing agent (DTT 0.33 M) and then denatured at 90°C for 10 min. Proteins were separated in NuPAGE 10% Bis-Tris gel (Thermofisher). The proteins were transferred onto a nitrocellulose membrane using iBlot (Invitrogen). The membranes were incubated overnight with primary antibody (Goat IgG fraction anti-mouse complement C3, MP BIOMEDICALS, #55463), followed by a secondary antibody (rabbit anti-goat HRP, Thermofisher, #31402). Revelation was done by chemiluminescence using a substrate for HRP (SuperSignal® WestDuraLuminol Thermofisher, #1856145), detected by iBright Western Blot Imaging System (iBright FL1500 Thermofisher).

Statistics

Analyses were performed with GraphPad Prism 8.0. Comparisons of multiple treatment groups were made using one-way analysis of variance (ANOVA) (Dunnett's multiple comparisons test) or Two-way ANOVA Kruskal Wallis test, as indicated in the figure legends. Statistical significance was defined as $p < 0.05$.

RESULTS

Pharmacokinetics of Human Hpx in Mice in Presence of Induced Hemolysis

To characterize potential differences in the pharmacokinetics (PK) and the exposure time of Hpx in a mouse model of

TABLE 1 | Pharmacokinetic parameters of human Hpx in mice (± induced hemolysis).

Group	Dose (mg/kg)	CL (mL/h/kg)	Vss (mL/kg)	C_{max} (mg/mL)	$T_{1/2}$ (h)	$AUC_{0-72\,h}$ (h*mg/mL)	AUC_{inf} (h*mg/mL)
PBS + Hpx	100	2.11	140	1.62	49.2	31.4	47.3
PHZ + Hpx	100	8.13	78.7	1.52	13.6	12.2	12.3
PBS + Hpx	500	2.79	154	7.35	41.4	128	179
PHZ + Hpx	500	4.30	107	7.63	19.1	109	116

CL, clearance; Vss, volume at steady state; C, concentration; AUC, area under the curve.

intravascular hemolysis, induced by phenylhydrazine (PHZ; 0.125 mg/g) two different Hpx doses were administered by bolus intravenous administration through the tail vein (**Figure 1A**). That allowed the investigation of the PK profile in presence and absence of circulating plasma heme. Blood sampling was performed to cover the range of plasma concentrations from Cmax and to monitor clearance over 72 h in plasma. **Figure 1B** shows the mean ± SD of human Hpx analyzed at the given timepoint. Pharmacokinetic parameter estimates for human Hpx in absence and presence of hemolysis were calculated via non-compartmental analysis (NCA) and are summarized in **Table 1**. Upon injection of a lower Hpx dose (100 mg/kg), clearance seemed to be facilitated in presence of circulating plasma heme demonstrated by the decreased half-life (T1/2) of 13.6 h compared to 49.2 h under non-hemolytic conditions. Similar finding, although less pronounced, was observed upon injection of a high Hpx dose (500 mg/kg) with determined half-life of 19.1 h under hemolytic conditions and 41.4 h in absence of plasma heme. Hpx clearance at 100 mg/kg was around 4-fold higher and 2-fold higher at 500 mg/kg in PHZ treated groups compared to PBS groups (**Figure 1C**).

The difference of Hpx pharmacokinetic profiles at the 100 mg/Kg dose, between the PHZ mice pre-treated vs. the non-PHZ pre-treated mice, demonstrated that the Heme:Hpx complexes distribution and elimination were strongly influenced by the complexes affinity to their receptors. This phenomenon was observed as well in the groups of mice treated with a 500 mg/Kg dose of Hpx. However, the difference of Hpx clearance between the non-hemolytic and the PHZ induced hemolytic condition was less important for the 500 vs. the 100 mg/kg Hpx treated mice. This results in a non-linear elimination phase of Hpx in the hemolytic condition, while Hpx terminal elimination phase appears to be linear in the non-hemolytic mice. This demonstrates that in presence of accessible heme in the blood compartment, Hpx pharmacokinetic profile is strongly influence by its affinity to its receptors which is characteristic of a target-mediated drug disposition (TMDD) phenomenon.

PHZ Induced Hemolysis Increases Total Plasma Heme, Which Is Scavenged by Hpx

In a next study we characterized the different heme binding proteins, especially the presence of Heme:Hpx complexes upon PHZ induced hemolysis. In a similar experimental setup as before, we performed an intravenous injection of human Hpx at two different doses (100 and 500 mg/kg) followed by administration of phenylhydrazine (PHZ; 0.125 mg/g) to induce intravascular hemolysis. Mice were sacrificed at 6 or 72 h after infusion. All mice in the PBS and PHZ-injected group survived (as usual). In the Hpx-injected groups, all mice survived but the dose of 100 mg/kg seems to be well-tolerated at the background of PHZ injection, contrary to 500 mg/kg, for which some mice showed adverse effects. At 6 h 2/10 mice of the 500 mg/kg + PHZ showed weakness, their body temperature was decreased as sensed by the manipulator in comparison to the other mice and had paler paws, nose and ears. At 72 h 2/10 mice showed moderate neurological symptoms (abnormal movement), decreased body temperature and paler paws, nose and ears.

The plasma was analyzed for the presence of total plasma heme, cell free hemoglobin, and Hpx heme complexes. As expected and previously shown (20), total plasma heme increased significantly upon PHZ induced hemolysis assessed after 6 h in all groups in a similar fashion compared to the control group (**Figure 2A**). In addition, we could demonstrate a significant increase of cell-free Hb, but only in absence of human Hpx (**Figure 2B**). Dose dependent lower levels of cell free hemoglobin with concurrent dose dependent increase of complexes Hpx (Hpx:heme) at 6 h, as shown in **Figure 2C**, demonstrates that Hpx scavenges heme from oxidized hemoglobin (metHb). In alignment with the pharmacokinetic behavior of human Hpx in presence of intravascular hemolysis almost no Heme:Hpx complexes were detected after 72 h of infusion (**Figure 2D**).

Hpx Partially Prevents Renal Suffering

The kidney function was evaluated at 6 and 72 h after induction of hemolysis, in presence or absence of Hpx (**Figure 3A**). We detected signs of kidney injury in PHZ-treated mice by measuring plasma urea and creatinine levels at 6 h, which were significantly decreased in mice pretreated with Hpx (**Figures 3B,C**). Further, we studied hypoxic cellular stress response protein Lcn2 (NGAL), a sensitive marker for acute kidney injury. The expression of NGAL in PHZ-treated mice increased compared to PBS controls, but remained unchanged after injection of Hpx (**Figure 4A**). The upregulation of the cytoprotective enzyme HO-1 by the hemolytic event was also unaffected by the Hpx injection, since injection of Hpx at 100 or 500 mg/kg did not modify expression of HO-1 in PHZ-treated mice (**Figure 4B**). At 72 h NGAL and

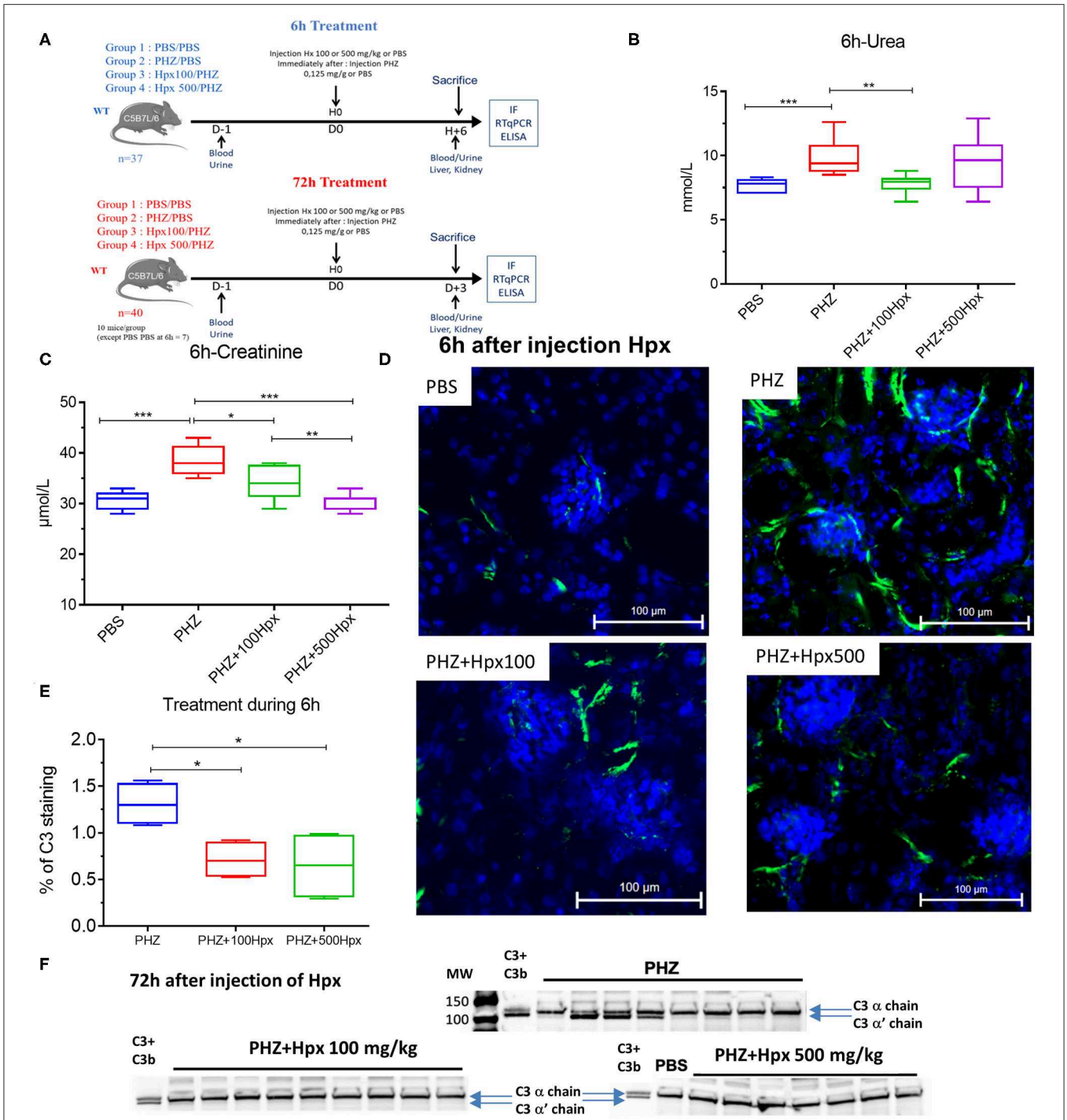

FIGURE 3 | Hemopexin prevents hemolysis-induced complement activation. **(A)** Protocol of mice with or without pretreatment to Hpx in PHZ-treated mice and control **(B)** urea and **(C)** creatinine concentrations in blood 6 h after pretreatment with Hpx or PBS of the PHZ-treated mice, compared to control mice without PHZ treatment measured by KONELAB equipment. **(D)** C3b/iC3b (green) deposition in kidney after 6 h treatment with Hpx to 100 and 500 mg/kg in kidney section **(E)** quantification of C3b/iC3b staining in glomeruli after 6 h treatment with Hpx C3 and CD31 staining were quantified using HALO® (Indica Labs) software. **(F)** Western blot analysis of C3 cleavage in plasma from mice treated with PHZ, PHZ + Hpx 100 and 500 mg/kg and PBS only. Statistical analyses: $^{*}p < 0.05$, $^{**}p < 0.005$, and $^{***}p < 0.001$, Two-way ANOVA Kruskal Wallis test.

HO-1 were still elevated, without effect of the treatment (**Figures 4C,D**), while urea and creatinine were back to normal (not shown).

No liver injury was detected at the selected time points, since ALAT remained at basal level in presence and in absence of PHZ and Hpx at 6 h (**Figure 4E**) and at 72 h (not shown).

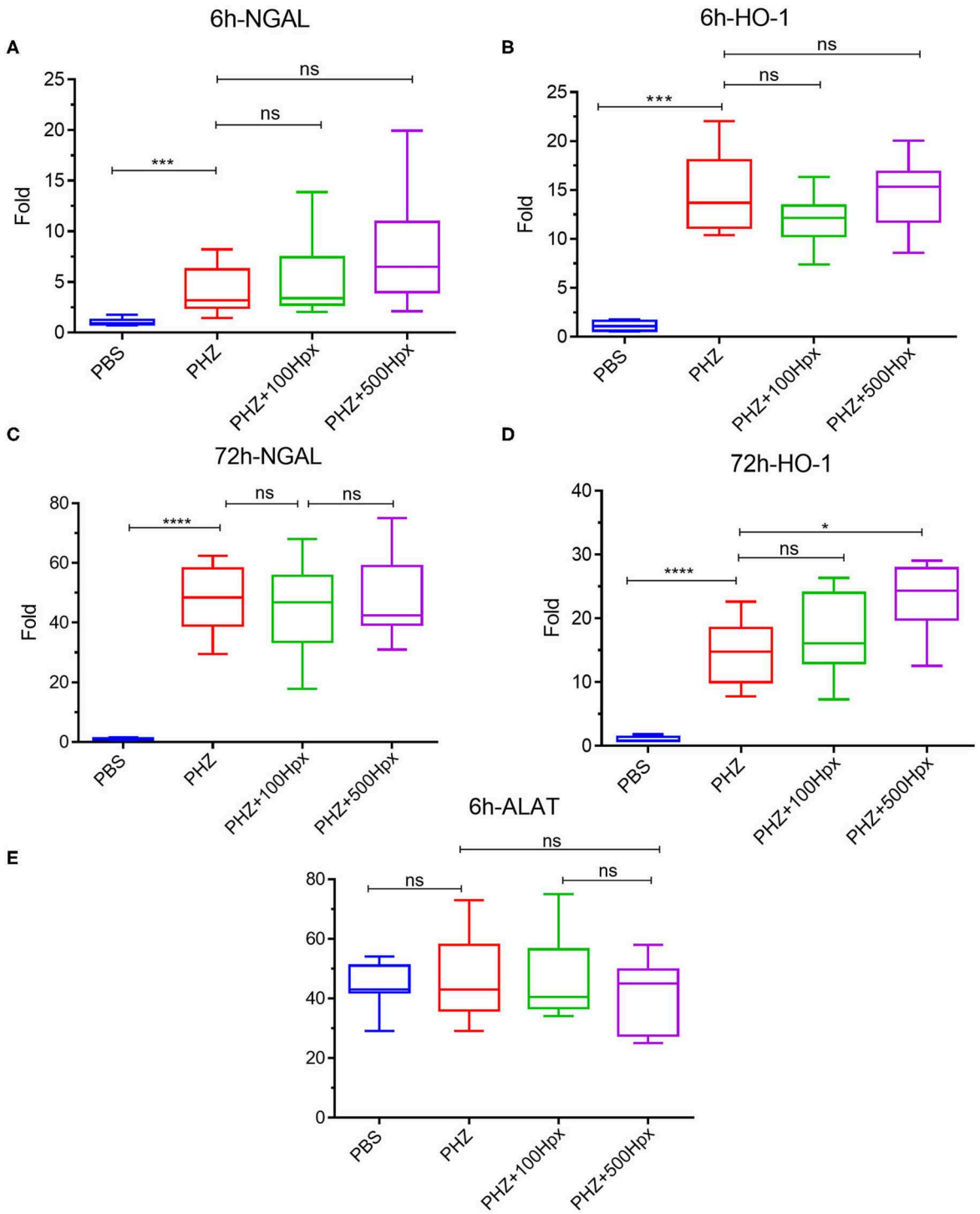

FIGURE 4 | Impact of hemopexin pre-treatment on the kidney parameters (6 and 72 h). Kidney mRNA expression of tubular aggression markers **(A)** LCN2 (NGAL) and **(B)** cytoprotective markers HO-1 statistical analyst 6 h after treatment with Hpx and after 72 h **(C)** LCN2 (NGAL) and **(D)** HO-1. **(E)** ALAT levels in blood 6 h after pretreatment with Hpx on PHZ-treated mice and control. Statistical analyses: $^{*}p < 0.05$, $^{****}p < 0.0001$, Two-way ANOVA Kruskal Wallis test. ns, non significant.

Hpx Inhibits the Deposits of C3b/iC3b in the Kidneys of Mice With Intravascular Hemolysis

Since intravascular hemolysis was already evident 6 h after injection of PHZ, we evaluated complement deposits at 6 h in presence and absence of Hpx. We detected a significant increase in C3b/iC3b staining in renal glomeruli within 6 h after inducing intravascular hemolysis with PHZ, which was attenuated by 100 and 500 mg/kg of Hpx (**Figures 3D,E**). At 72 h the staining was indistinguishable between PBS and PHZ injected mice (data not shown).

Hpx Inhibits the C3 Activation in Plasma of Hemolytic Mice

Intravascular hemolysis induced by PHZ was associated with C3 activation in the circulation, 72 h after injection. This was evident by the appearance of the α' band on the WB, attesting for appearance of C3b (**Figure 3F**). The cleavage was heterogeneous. In the PHZ group, among 9 tested plasma samples, the intensity of the α' band was strong in 4; weaker but detectable in 4 and undetectable in 1. Very weak intensity of the α' band was detected in 2/10 tested plasma samples of mice injected with 100 mg/kg Hpx (**Figure 3F**) and for the remaining 8/10 it was undetectable. In all 8 tested plasma samples of mice injected with 500 mg/kg (**Figure 3F**), the α' band was absent.

DISCUSSION

Here we show that during intravascular hemolysis injected Hpx is rapidly complexed with heme and cleared from the circulation, contrary to the context of non-hemolytic mice. The pharmacokinetic characteristics of Hpx were affected by the target-mediated drug disposition phenomenon. Nevertheless, even the lower dose of 100 mg/kg was sufficient to prevent the heme-mediated complement activation in the plasma and in the kidney.

The target mediated drug disposition is a phenomenon in which a drug binds with high affinity to its pharmacological target to such an extent that this affects its pharmacokinetic characteristics (21). The target binding and subsequent elimination of the drug-target complexes could affect both drug distribution and elimination and result in non-linearity of PK in a dose-dependent manner. Our results show formation of Hpx-heme complexes which are rapidly eliminated in the hemolytic mice. This can explain the rapid disappearing of the injected Hpx from the circulation of the PHZ-injected mice, contrary to the control animals. This results in an increase of the effective exposure time to the drug. The target mediated drug disposition and the effective exposure time to the drug, needed to achieve the biological effect are key parameters to be evaluated during the design of therapeutic pre-clinical protocols. Our results provide a rational about the selection of doses to be tested in future experiments.

Increased extracellular concentration of heme is an important driver of the disease state associated with hemolysis. In normal condition the excess of heme is complexed with Hpx and transported to the liver and detoxified. Interestingly, the amount of detected cell-free Hb decreased and the Hpx:heme complexes increased simultaneously when Hpx was injected. This suggests that heme may be taken out from oxidized forms of cell free Hb (MetHb or hemichromes) by Hpx, thus preventing heme to be present in the circulation.

The kidney is one of the most affected organs during intravascular hemolysis (22). In SCD a consumption of Hpx occurs, heme binds to alpha-1-microglobulin, is directed to the kidney and contributes to an acute kidney injury (9). Intravascular hemolysis induces intrarenal complement activation, contributing to the kidney injury (20). Our results show that this complement activation is an early event, detectable at 6 h post-hemolysis but disappearing at 72 h. Moreover, the pre-treatment with Hpx prevented the C3 fragments deposition at the early timepoint, complexing the excess of heme. Even though the concentration of injected Hpx decreased rapidly afterwards, new complement activation did not occur, suggesting that the majority of the cell-free heme was already scavenged. Moreover, new hemolysis did not occur in this model after the initial burst (23). The prevention of complement activation could be attributed to a direct effect of Hpx, preventing the access of heme to C3 (19, 24) and to an indirect, cytoprotective effect, especially on macrophages and endothelial cells (10, 14, 19, 20, 24–27). Glomerular endothelial cells are particularly vulnerable to heme-mediated complement activation in part because they are unable to overexpress HO-1 in hemolytic conditions (23, 28). Therefore, it is likely that Hpx protects glomerular endothelial cells from heme toxicity and they, in turn, do not express complement-activating phenotype. The inflammatory cytokines, released by heme-activated macrophages could also contribute to the endothelial activation and complement deposits, process which also will be indirectly prevented by Hpx. Interestingly, C3 cleavage in plasma was not detected at the early but at the late timepoint. Therefore, the intrarenal C3b/iC3b deposits and the plasma C3 cleavage are separated phenomena occurring consecutively. Although at 72 h there was no more heme release, the tissue injury persisted, as evidenced by the upregulation of the NGAL and HO-1. It is, therefore, tempting to speculate that cell debris released in the circulation from the injured tissues at later timepoints could serve as complement activators in the fluid phase. The cell/tissue protective effect of the heme scavenging even with the lower dose of 100 mg/kg at the early phase of the hemolytic process could explain the fact that Hpx-treated hemolytic mice had no fluid phase C3 cleavage even at a moment, when most of the injected Hpx was already eliminated.

The kidney injury marker NGAL was elevated in hemolytic conditions, which was not prevented by Hpx in agreement with previous studies (23, 29). This result suggests that other factors, such as released Hb and its different oxidation forms or covalently crosslinked Hb multimers or the oxidative stress, hallmarks of intravascular hemolysis (30–33) could be responsible for NGAL upregulation. HO-1 was also up-regulated, but independently of the presence of Hpx, as reported previously (23, 29) and contrary to mice with SCD, where Hpx resulted in further enhancement of the HO-1 expression (11). We

hypothesized that in the previous studies the dose of injected Hpx was not high enough to downregulate NGAL and to further enhance the expression of HO-1. Nevertheless, this was not the case, since these makers remained unaltered in our model even at 500 mg/kg Hpx, dose at which Hpx remained in the circulation for the duration of the experiment. Therefore, Hpx could prevent some but not all adverse effects of the hemolytic conditions. Nevertheless, the creatinine and urea were decreased suggesting overall beneficial effect of Hpx on the hemolysis-induced kidney injury. Attention should be made, though, to not

TABLE 2 | Use of Hpx as a therapeutic molecule in different disease model.

Disease model	Animals	Used to dose of Hpx	Effect of Hpx	References
Rat liver model of cold storage and reperfusion and tested the potential anti-oxidant effects of Hpx	Rat Sprague-Dawley	Reperfused with 5 μM Hpx	Decreasing oxyradical production in a model of cold storage/reperfusion	(35)
Implanted intracranially with 50,000 U87 glioma cells	Nude and BALB/C mice	Intra cerebral delivery to PEX (recombinant Hpx) 0.25–1 with minipumps mg/kg/day (29 days)	Local intracerebral delivery of endogenous inhibitors decreased of tumors growth	(36)
Mesenchymal stem cells-PEX (hMSC-Hpx) injected adjacent to glioblastoma tumors	Nude mice	No dose reported	Mice treated with hMSC-PEX reduction tumor volume and weight measurements decrease 22 days	(37)
SCD and B-thalassemic model	HbS SCD mice and B-thalassemic mice	I.P. To 700 μg injection purified human Hpx	Hpx to treat vasculopathy in hemolytic disorders Decrease cardiac output, aortic valve peak pressure in different mice model	(13)
SCD mouse models	NYDD and Townes SCD mice	I.V. 0.4 or 1.6 μmol/kg	Hemoglobin-induced vaso-occlusion was blocked by the heme-binding protein Hpx	(10)
Hemorrhagic shock (HS) and resuscitated with either FRBCs or SRBCs	C57BL/6 mice	HS and resuscitated with FRBCs/SRBCs to simultaneous infusion of 7.5 mg Hpx	Increase the survival rate and reduced the early proinflammatory response after HS resuscitation with stored blood	(29)
Atherosclerosis	Hpx and Hpx/ApoE KO mice	I.P. human Hpx to HpxApoE KO during 24 h	hHpx significantly reduced serum heme levels Increase in the expression of LXR-α and ABCA1 genes Reduction in expression of CCR-2, and a significant increase in expression of Arg-1	(38)
SCD model	Townes SCD model	I.P. human Hpx (4 mg)	Administration of Hpx is beneficial to counteract heme-driven macrophage-mediated inflammation and its pathophysiologic consequences in sickle cell disease	(14)
Hpx KO and B-thalassemic model	C57BL/6 $Hpx^{-/-}$ and $Hbb^{th3/+}$ mice	160 mg/kg Hpx	Hpx rescued contraction defects of heme-treated cardiomyocytes and preserved cardiac function in hemolytic mice	(33)
Spinal Cord Injury (SCI)	Hpx KO mice	I.P. 0.5–50 ng/mL Hpx	Acute-phase plasma glycoprotein, in the regulation of microglia polarization Hpx in alleviating the secondary injury and improving functional repair after SCI	(39)
Intravascular hemolysis induced by PHZ and heme injection	C57BL/6 and $C3^{-/-}$ mice	I.P. injection of 40 μmol/kg of human Hpx 1 h before heme or PHZ injection	Decreased kidney complement deposition	(20)
Intravascular hemolysis induced by PHZ and heme injection	C57BL/6 mice	I.P. injection of 40 μmol/kg of human Hpx 1 h before heme or PHZ injection	No effect on renal NGAL, Kim1, and HO-1 genes expression	(23)
Cerebral Ischemia reperfusion Injury (CIRI)	Rat Sprague-Dawley	Insert beneath the dural surface to inject rat Hpx (10 μL, 1.86 g/L Hpx)	HPX can alleviate cognitive dysfunction after focal CIRI through HO-1 pathway and preventing the impairment of the blood-brain barrier in rats	(40)
SCD model	Hpx KO and littermate SCD mice Hpx KO (SS $Hpx^{-/-}$ and SS $Hpx^{+/+}$)		Hpx deficiency promotes AKI development in SCD, and we provide proof-of-principle for Hpx replacement therapy to treat AKI in SCD	(41)
Intravascular hemolysis induced by PHZ and heme injection	C57BL/6, $C3^{-/-}$, and $TLR4^{-/-}$ mice	I.P. injection of 40 μmol/kg of human Hpx 1 h before heme or PHZ injection	Decreased NGAL gene expression, decreased liver complement deposition	(19)

exceed the dose of 500 mg/kg for mice with hemolytic conditions. Even though this concentration is very well-tolerated by the control animals, some hemolytic mice showed signs of suffering at this dose.

Based on our data, administration of Hpx could be a possible approach to counteract heme driven toxicity under hemolytic conditions. Therefore, Hpx could potentially be applied as a human blood-derived product similar to other plasma proteins, such as albumin, α1-antitrypsin or immunoglobulins, which are well-established therapies (34). Hpx has already been tested in numerous animal models and showed beneficial effect in most of the tested parameters [(10, 13, 14, 19, 20, 23, 29, 33, 35–41); **Table 2**].

In conclusion, hemolysis-induced complement activation is prevented by injection of heme scavenger Hpx. These results encourage further studies of Hpx as a potential therapeutic agent in models of diseases with heme overload, such as SCD, transfusion reactions, etc., taking into account its pharmacokinetic properties.

DATA AVAILABILITY STATEMENT

The original contributions presented in the study are included in the article/**Supplementary Material**, further inquiries can be directed to the corresponding author/s.

ETHICS STATEMENT

Experimental protocols were approved by Charles Darwin ethical committee (Paris, France) and of French Ministry of Agriculture (Paris, France) number #3764 201601121739330 v3. All experiments were conducted in accordance with the recommendations for the care and use laboratory animal.

AUTHOR CONTRIBUTIONS

LR and GT designed the research. VP, TG, JL, AW, ME, CT, and DL performed research and analyzed data. LR, VP, and TG wrote the manuscript. All authors discussed the data and approved the manuscript. All authors contributed to the article and approved the submitted version.

FUNDING

This study was supported by CSL Behring.

SUPPLEMENTARY MATERIAL

The Supplementary Material for this article can be found online at: https://www.frontiersin.org/articles/10.3389/fimmu.2020.01684/full#supplementary-material

REFERENCES

1. Soares MP, Bozza MT. Red alert: labile heme is an alarmin. *Curr Opin Immunol.* (2016) 38:94–100. doi: 10.1016/j.coi.2015.11.006
2. Roumenina LT, Rayes J, Lacroix-Desmazes S, Dimitrov JD. Heme: modulator of plasma systems in hemolytic diseases. *Trends Mol Med.* (2016) 22:200–13. doi: 10.1016/j.molmed.2016.01.004
3. Kanyavuz A, Marey-Jarossay A, Lacroix-Desmazes S, Dimitrov JD. Breaking the law: unconventional strategies for antibody diversification. *Nat Rev Immunol.* (2019) 19:355–68. doi: 10.1038/s41577-019-0126-7
4. Frimat M, Boudhabhay I, Roumenina LT. Hemolysis derived products toxicity and endothelium: model of the second hit. *Toxins.* (2019) 11:660. doi: 10.3390/toxins11110660
5. Lin T, Maita D, Thundivalappil SR, Riley FE, Hambsch J, Van Marter LJ, et al. Hemopexin in severe inflammation and infection: mouse models and human diseases. *Crit Care.* (2015) 19:166. doi: 10.1186/s13054-015-0885-x
6. Schaer DJ, Vinchi F, Ingoglia G, Tolosano E, Buehler PW. Haptoglobin, hemopexin, and related defense pathways—basic science, clinical perspectives, and drug development. *Front Physiol.* (2014) 5:415. doi: 10.3389/fphys.2014.00415
7. Hvidberg V, Maniecki MB, Jacobsen C, Højrup P, Møller HJ, Moestrup SK. Identification of the receptor scavenging hemopexin-heme complexes. *Blood.* (2005) 106:2572–9. doi: 10.1182/blood-2005-03-1185
8. Tolosano E, Hirsch E, Patrucco E, Camaschella C, Navone R, Silengo L, et al. Defective recovery and severe renal damage after acute hemolysis in hemopexin-deficient mice. *Blood.* (1999) 94:3906–14.
9. Ofori-Acquah S, Hazra R, Orikogbo OO, Crosby D, Flage B, Ackah EB, et al. Hemopexin deficiency promotes acute kidney injury in sickle cell disease. *Blood.* (2020) 135:1044–8. doi: 10.1182/blood.2019002653
10. Belcher JD, Chen C, Nguyen J, Milbauer L, Abdulla F, Alayash AI, et al. Heme triggers TLR4 signaling leading to endothelial cell activation and vaso-occlusion in murine sickle cell disease. *Blood.* (2014) 123:377–90. doi: 10.1182/blood-2013-04-495887
11. Belcher JD, Chen C, Nguyen J, Abdulla F, Zhang P, Nguyen H, et al. Haptoglobin and hemopexin inhibit vaso-occlusion and inflammation in murine sickle cell disease: role of heme oxygenase-1 induction. *PLoS ONE.* (2018) 13:e0196455. doi: 10.1371/journal.pone.0196455
12. Ingoglia G, Sag CM, Rex N, De Franceschi L, Vinchi F, Cimino J, et al. Data demonstrating the anti-oxidant role of hemopexin in the heart. *Data Brief.* (2017) 13:69–76. doi: 10.1016/j.dib.2017.05.026
13. Vinchi F, De Franceschi L, Ghigo A, Townes T, Cimino J, Silengo L, et al. Hemopexin therapy improves cardiovascular function by preventing heme-induced endothelial toxicity in mouse models of hemolytic diseases. *Circulation.* (2013) 127:1317–29. doi: 10.1161/CIRCULATIONAHA.112.130179
14. Vinchi F, Costa da Silva M, Ingoglia G, Petrillo S, Brinkman N, Zuercher A, et al. Hemopexin therapy reverts heme-induced proinflammatory phenotypic switching of macrophages in a mouse model of sickle cell disease. *Blood.* (2016) 127:473–86. doi: 10.1182/blood-2015-08-663245
15. Camus SM, De Moraes JA, Bonnin P, Abbyad P, Le Jeune S, Lionnet F, et al. Circulating cell membrane microparticles transfer heme to endothelial cells and trigger vasoocclusions in sickle cell disease. *Blood.* (2015) 125:3805–14. doi: 10.1182/blood-2014-07-589283
16. Camus SM, Gausserès B, Bonnin P, Loufrani L, Grimaud L, Charue D, et al. Erythrocyte microparticles can induce kidney vaso-occlusions in a murine model of sickle cell disease. *Blood.* (2012) 120:5050–8. doi: 10.1182/blood-2012-02-413138
17. Roumenina LT, Chadebech P, Bodivit G, Vieira-Martins P, Grunenwald A, Boudhabhay I, et al. Complement activation in sickle cell disease: dependence on cell density, hemolysis and modulation by hydroxyurea therapy. *Am J Hematol.* (2020) 95:456–64. doi: 10.1002/ajh.25742
18. Vercellotti GM, Belcher JD. Not simply misshapen red cells: multimolecular and cellular events in sickle vaso-occlusion. *J Clin Invest.* (2014) 124:1462–5. doi: 10.1172/JCI75238
19. Merle NS, Paule R, Leon J, Daugan M, Robe-Rybkine T, Poillerat V, et al. P-selectin drives complement attack on endothelium during intravascular

hemolysis in TLR-4/heme-dependent manner. *Proc Natl Acad Sci USA*. (2019) 116:6280–5. doi: 10.1073/pnas.1814797116
20. Merle NS, Grunenwald A, Rajaratnam H, Gnemmi V, Frimat M, Figueres M-L, et al. Intravascular hemolysis activates complement via cell-free heme and heme-loaded microvesicles. *JCI Insight*. (2018) 3:e96910. doi: 10.1172/jci.insight.96910
21. Dua P, Hawkins E, van der Graaf P. A tutorial on target-mediated drug disposition (TMDD) models: a tutorial on target-mediated drug disposition (TMDD) models. *CPT Pharmacomet Syst Pharmacol.* (2015) 4:324–37. doi: 10.1002/psp4.41
22. Van Avondt K, Nur E, Zeerleder S. Mechanisms of haemolysis-induced kidney injury. *Nat Rev Nephrol.* (2019) 15:671–92. doi: 10.1038/s41581-019-0181-0
23. Merle NS, Grunenwald A, Figueres M-L, Chauvet S, Daugan M, Knockaert S, et al. Characterization of renal injury and inflammation in an experimental model of intravascular hemolysis. *Front Immunol.* (2018) 9:179. doi: 10.3389/fimmu.2018.00179
24. Frimat M, Tabarin F, Dimitrov JD, Poitou C, Halbwachs-Mecarelli L, Fremeaux-Bacchi V, et al. Complement activation by heme as a secondary hit for atypical hemolytic uremic syndrome. *Blood.* (2013) 122:282–92. doi: 10.1182/blood-2013-03-489245
25. Lin T, Sammy F, Yang H, Thundivalappil S, Hellman J, Tracey KJ, et al. Identification of hemopexin as an anti-inflammatory factor that inhibits synergy of hemoglobin with HMGB1 in sterile and infectious inflammation. *J Immunol.* (2012) 189:2017–22. doi: 10.4049/jimmunol.1103623
26. Pradhan P, Vijayan V, Gueler F, Immenschuh S. Interplay of heme with macrophages in homeostasis and inflammation. *Int J Mol Sci.* (2020) 21:740. doi: 10.3390/ijms21030740
27. Vinchi F, Gastaldi S, Silengo L, Altruda F, Tolosano E. Hemopexin prevents endothelial damage and liver congestion in a mouse model of heme overload. *Am J Pathol.* (2008) 173:289–99. doi: 10.2353/ajpath.2008.071130
28. May O, Merle NS, Grunenwald A, Gnemmi V, Leon J, Payet C, et al. Heme drives susceptibility of glomerular endothelium to complement overactivation due to inefficient upregulation of heme oxygenase-1. *Front Immunol.* (2018) 9:3008. doi: 10.3389/fimmu.2018.03008
29. Graw JA, Mayeur C, Rosales I, Liu Y, Sabbisetti VS, Riley FE, et al. Haptoglobin or hemopexin therapy prevents acute adverse effects of resuscitation after prolonged storage of red cells. *Circulation.* (2016) 134:945–60. doi: 10.1161/CIRCULATIONAHA.115.019955
30. Nyakundi BB, Erdei J, Tóth A, Balogh E, Nagy A, Nagy B, et al. Formation and detection of highly oxidized hemoglobin forms in biological fluids during hemolytic conditions. *Oxid Med Cell Longev.* (2020) 2020:8929020. doi: 10.1155/2020/8929020
31. Rifkind JM, Mohanty JG, Nagababu E. The pathophysiology of extracellular hemoglobin associated with enhanced oxidative reactions. *Front Physiol.* (2015) 5:500. doi: 10.3389/fphys.2014.00500
32. Baek JH, D'Agnillo F, Vallelian F, Pereira CP, Williams MC, Jia Y, et al. Hemoglobin-driven pathophysiology is an *in vivo* consequence of the red blood cell storage lesion that can be attenuated in guinea pigs by haptoglobin therapy. *J Clin Invest.* (2012) 122:1444–58. doi: 10.1172/JCI59770
33. Ingoglia G, Sag CM, Rex N, De Franceschi L, Vinchi F, Cimino J, et al. Hemopexin counteracts systolic dysfunction induced by heme-driven oxidative stress. *Free Radic Biol Med.* (2017) 108:452–64. doi: 10.1016/j.freeradbiomed.2017.04.003
34. Immenschuh S, Vijayan V, Janciauskiene S, Gueler F. Heme as a target for therapeutic interventions. *Front Pharmacol.* (2017) 8:146. doi: 10.3389/fphar.2017.00146
35. Brass CA, Immenschuh S, Song D-X, Liem HH, Eberhard UM. Hemopexin decreases spontaneous chemiluminescence of cold preserved liver after reperfusion. *Biochem Biophys Res Commun.* (1998) 248:574–7. doi: 10.1006/bbrc.1998.9023
36. Giussani C, Carrabba G, Pluderi M, Lucini V, Pannacci M, Caronzolo D, et al. Local intracerebral delivery of endogenous inhibitors by osmotic minipumps effectively suppresses glioma growth *in vivo*. *Cancer Res.* (2003) 63:2499–505. Available online at: https://cancerres.aacrjournals.org/content/63/10/2499.long
37. Goren A, Dahan N, Goren E, Baruch L, Machluf M. Encapsulated human mesenchymal stem cells: a unique hypoimmunogenic platform for long-term cellular therapy. *FASEB J.* (2010) 24:22–31. doi: 10.1096/fj.09-131888
38. Mehta NU, Grijalva V, Hama S, Wagner A, Navab M, Fogelman AM, et al. Apolipoprotein E $^{-/-}$ mice lacking hemopexin develop increased atherosclerosis via mechanisms that include oxidative stress and altered macrophage function. *Arterioscler Thromb Vasc Biol.* (2016) 36:1152–63. doi: 10.1161/ATVBAHA.115.306991
39. Han D, Yu Z, Liu W, Yin D, Pu Y, Feng J, et al. Plasma hemopexin ameliorates murine spinal cord injury by switching microglia from the M1 state to the M2 state. *Cell Death Dis.* (2018) 9:181. doi: 10.1038/s41419-017-0236-8
40. Dong B, Yang Y, Zhang Z, Xie K, Su L, Yu Y. Hemopexin alleviates cognitive dysfunction after focal cerebral ischemia-reperfusion injury in rats. *BMC Anesthesiol.* (2019) 19:13. doi: 10.1186/s12871-019-0681-2
41. Ghosh S, Orikogbo O, Hazra R, Flage B, Crosby D, Ofori-Acquah S. Hemopexin replacement therapy protects sickle cell disease mice from acute kidney injury. *Blood.* (2019) 134(Suppl. 1):78. doi: 10.1182/blood-2019-127161

Conflict of Interest: TG, AW, ME, DL, and GT are employees of CSL Behring. LR has received research funding from CSL Behring.

The remaining authors declare that the research was conducted in the absence of any commercial or financial relationships that could be construed as a potential conflict of interest.

frontiers in Immunology

ORIGINAL RESEARCH
published: 21 August 2020
doi: 10.3389/fimmu.2020.01910

Heme Induces IL-6 and Cardiac Hypertrophy Genes Transcripts in Sickle Cell Mice

Oluwabukola T. Gbotosho[1,2], *Maria G. Kapetanaki*[2,3], *Samit Ghosh*[1,4], *Flordeliza S. Villanueva*[5], *Solomon F. Ofori-Acquah*[1,2,4,6] *and Gregory J. Kato*[1,2]*

[1] *Division of Hematology-Oncology, Department of Medicine, University of Pittsburgh School of Medicine, Pittsburgh, PA, United States,* [2] *Department of Medicine, Pittsburgh Heart, Lung, Blood, and Vascular Medicine Institute, University of Pittsburgh School of Medicine, Pittsburgh, PA, United States,* [3] *Division of Pulmonary, Allergy and Critical Care Medicine, Department of Medicine, University of Pittsburgh School of Medicine, Pittsburgh, PA, United States,* [4] *Department of Medicine, Center for Translational and International Hematology, School of Medicine, University of Pittsburgh, Pittsburgh, PA, United States,* [5] *Center for Ultrasound Molecular Imaging and Therapeutics, Heart and Vascular Institute, Pittsburgh Heart, Lung, Blood and Vascular Medicine Institute, University of Pittsburgh, Pittsburgh, PA, United States,* [6] *School of Biomedical and Allied Health Sciences, University of Ghana, Accra, Ghana*

OPEN ACCESS

Edited by:
Renata Sesti-Costa, Campinas State University, Brazil

Reviewed by:
John D. Belcher, University of Minnesota Twin Cities, United States
Ann Smith, University of Missouri–Kansas City, United States

***Correspondence:**
Gregory J. Kato
gregorykatomd@gmail.com

Specialty section:
This article was submitted to Inflammation, a section of the journal Frontiers in Immunology

Received: *03 March 2020*
Accepted: *16 July 2020*
Published: *21 August 2020*

Citation:
Gbotosho OT, Kapetanaki MG, Ghosh S, Villanueva FS, Ofori-Acquah SF and Kato GJ (2020) Heme Induces IL-6 and Cardiac Hypertrophy Genes Transcripts in Sickle Cell Mice. Front. Immunol. 11:1910. doi: 10.3389/fimmu.2020.01910

Emerging data indicate that free heme promotes inflammation in many different disease settings, including in sickle cell disease (SCD). Although free heme, proinflammatory cytokines, and cardiac hypertrophy are co-existing features of SCD, no mechanistic links between these features have been demonstrated. We now report significantly higher levels of IL-6 mRNA and protein in hearts of the Townes sickle cell disease (SS) mice (2.9-fold, $p \leq 0.05$) than control mice expressing normal human hemoglobin (AA). We find that experimental administration of heme 50 μmoles/kg body weight induces IL-6 expression directly *in vivo* and induces gene expression markers of cardiac hypertrophy in SS mice. We administered heme intravenously and found that within three hours plasma IL-6 protein significantly increased in SS mice compared to AA mice (3248 ± 275 vs. 2384 ± 255 pg/ml, $p \leq 0.05$). In the heart, heme induced a 15-fold increase in IL-6 transcript in SS mice heart compared to controls. Heme simultaneously induced other markers of cardiac stress and hypertrophy, including atrial natriuretic factor (Nppa; 14-fold, $p \leq 0.05$) and beta myosin heavy chain (Myh7; 8-fold, $p \leq 0.05$) in SS mice. Our experiments in Nrf2-deficient mice indicate that the cardiac IL-6 response to heme does not require Nrf2, the usual mediator of transcriptional response to heme for heme detoxification by heme oxygenase-1. These data are the first to show heme-induced IL-6 expression *in vivo*, suggesting that hemolysis may play a role in the elevated IL-6 and cardiac hypertrophy seen in patients and mice with SCD. Our results align with published evidence from rodents and humans without SCD that suggest a causal relationship between IL-6 and cardiac hypertrophy.

Keywords: heme, hemolysis, sickle cell disease, IL-6, inflammation, cardiac hypertrophy genes

INTRODUCTION

Sickle cell disease (SCD) is a complex hematological disorder that affects ∼100,000 Americans and millions of people worldwide, especially in sub-Saharan Africa and India (1). Hemolysis and chronic inflammation are major components of the pathophysiology of SCD. Hemolysis is caused by erythrocyte injury due to secondary defects in erythrocyte fragility, deformability and increased endothelial adhesion resulting in release of hemoglobin and heme (2, 3). Chronic inflammation in SCD is partly due to leukocytosis with the abnormally high leukocytes and monocytes that secrete proinflammatory cytokines. In addition, products of hemolysis act as damage-associated molecular patterns (DAMPs) potentiating activation of many inflammatory mechanisms (4). Additionally, products of intravascular hemolysis such as free hemoglobin and arginase-1 impair nitric oxide bioavailability, endothelial function and organ function in SCD (2). Limited data indicate that heme can induce production of proinflammatory cytokines such as interleukin-6 (IL-6) by stimulating immune responses and inflammatory reactions (5). Hemolysis and inflammation are components of a wide spectrum of other clinical conditions including sepsis (6, 7), malaria (8, 9), and preeclampsia (10, 11). Common to patients with all these syndromes is an increased risk of cardiac dysfunction (12–15). Notable among proinflammatory cytokines elevated in SCD is IL-6. Serum levels of IL-6 are elevated both at steady state and during vaso occlusive crisis in both children and adults with SCD (16–20), concurrently with severe anemia and increased markers of hemolysis. Furthermore, IL-6 is associated with cardiomyopathies such as cardiac hypertrophy and fibrosis in experimental animals (21, 22) and in the general human population (23, 24). Importantly, cardiopulmonary complications are one of the leading causes of death in SCD (25, 26). This accounts for about 26% of deaths in adults with SCD (27), with left ventricular hypertrophy (LVH) found in over 60% of children and 37% in adults with SCD (28, 29). No prior publications have investigated any potential linkage between IL-6 and hemolysis in mice and patients with SCD, particularly in cardiac disease. In this study, we assess direct heme induction *in vivo* of IL-6 and genes relevant to cardiac hypertrophy in the heart of sickle cell mice. Our study shows that IL-6 is highly expressed in the circulation and in the heart of sickle cell mice at steady state. Furthermore, administration of extracellular heme further increased IL-6 and cardiac hypertrophy genes expression. To gain insight of the mechanism by which heme induces IL-6, we investigated the role of nuclear factor (erythroid derived 2)-like 2 (Nfe2L2 or Nrf2). Nrf2 is the master regulator of the cellular oxidative defense system and plays a significant role in the regulation of multiple heme-induced genes (30, 31).

MATERIALS AND METHODS

Mouse Strains and Treatment

Male and female Townes' knocked-in transgenic sickle mouse (SS) and strain controls expressing normal human Hb (AA mice), C57BL/6J ($Nrf2^{+/+}$) and $Nrf2^{-/-}$ mice were used. C57BL/6 mice were obtained from the Jackson Laboratory (stock #000664) while SS, AA and $Nrf2^{-/-}$ mice were obtained from a colony maintained by Dr. Solomon Ofori-Acquah's laboratory in our institution. Mouse genotypes were confirmed by PCR. Hemin [Fe(III)PPIX, Sigma-Aldrich, St. Louis, MO] was prepared as described elsewhere (32, 33). Freshly prepared hemin solution was protected from light and injected into 12–16 week old mice. A range of doses and times were tested and 3 h after injection produced consistent survival with no adverse effects on all strains of mice in this study. The mice were injected in the tail vein with a hemin dose of 50 μmoles/kg body weight for SS and AA mice, and 120 μmoles/kg body weight for $Nrf2^{+/+}$ and $Nrf2^{-/-}$ mice. Higher doses were needed for $Nrf2^{+/+}$ and $Nrf2^{-/-}$ mice to be able to neutralize the endogenous hemopexin and other heme-binding proteins and mimic the increase in circulating heme in chronic hemolysis. This allows comparable assessment of the transcriptional response. Control mice received sterile vehicle containing 0.25M NaOH adjusted to pH 7.5 with HCl used in preparation of hemin.

Plasma Analysis

Freshly collected blood samples were centrifuged at 1,200 × g for 15 min to separate blood plasma. Plasma IL-6 concentration was measured using the mouse IL-6 ELISA kit (Sigma-Aldrich) following the manufacturer's instructions.

Real-Time PCR

Whole organs were harvested from mice 3 h after hemin injection. Freshly isolated organs (300 mg) were snap-frozen and kept at −80°C until use. Organs were homogenized in Qiazol lysis reagent using the Next Advance Bullet Blender (Next Advance, Inc. Troy, NY). Clear lysates were obtained by centrifuging homogenized samples at 18,800 × g for 10 min. All tissue processing was carried out at 4°C. Total RNA was extracted from the tissue lysates using the miRNeasy Mini Kit (#217004, QIAGEN, Germantown, MD) and quantified using the Nanodrop 8000 microvolume spectrophotometer (ThermoFisher Scientific). Real-time PCR reactions were set-up in duplicates using 50 ng of RNA. Genes of interest were evaluated using the TaqMan® Gene expression assay (ThermoFisher) and the TaqMan® RNA-to-Ct™ 1-Step Kit (ThermoFisher) according to the manufacturer's instructions. Relative quantification was calculated with the standard ΔΔCt method; amplification signals from target gene transcripts were normalized to those from beta-glucuronidase (*Gusb*) transcripts. Relative fold induction was calculated by further normalization to gene transcripts from vehicle treated animals. *Gusb* gene expressions were similar across all mouse strains used and across all organs within a given mouse strain. *Gusb* gene expression in organs from control mice was similar to that from the corresponding organs from hemin-injected mice. We have previously published this in different organs from SS mice here (32) and in the heart of AA control mice in **Supplementary Figure 1** in this study.

IL-6 Protein Quantification

Mice were perfused with phosphate-buffered saline under anesthesia. Harvested organs (300 mg) were homogenized

in RIPA buffer using the Next Advance Bullet Blender (Next Advance, Inc. Troy, NY). Homogenized samples were centrifuged at 18,800 x g for 10 min to obtain clear lysates. All tissue processing was carried out at 4°C. Heart IL-6 concentration was measured using the mouse IL-6 ELISA kit (Sigma-Aldrich) following the manufacturer's instructions. Total protein was quantified in the lysates using the BCA assay kit (ThermoFisher Scientific, #23225).

Statistical Analysis

GraphPad Prism 7 software was used for all statistical analyses. Results are reported as mean ± SEM. Group means were compared using parametric tests, such as *t*-test (for 2 groups) and One-way ANOVA for more than two conditions. Statistical significance was set at p values of < 0.05.

RESULTS

High Basal Expression and Heme-Induced Cardiac IL-6 in Sickle Cell Mice

We investigated the basal expression of IL-6 transcripts in the heart of Townes SS mice and AA control mice. IL-6 expression was 2.9-fold higher in the heart of Townes SS mice compared to AA controls (**Figure 1A**, $p \leq 0.05$). Hmox1 expression was significantly elevated in the heart (2.1-fold) of untreated Townes SS mice compared to AA controls (**Figure 1B**, $p \leq 0.01$). We tested the hypothesis that products of hemolysis, specifically heme, would promote IL-6 expression in the AA heart to mimic the SS steady state expression. Injection of heme as previously described (32, 34) increased cardiac IL-6 transcript expression to levels comparable to vehicle-treated SS mice (**Figure 1C**, $p < 0.05$). This suggests that heme release in SS mice may be the critical factor that stimulates high SS basal IL-6 expression. SS mice were even more responsive to heme injection, with cardiac IL-6 transcripts rising 15.4-fold higher in heme-treated SS mice compared to vehicle controls (**Figure 1D**, $p \leq 0.05$) and by about 53% in SS mice compared to AA mice controls (**Figure 1C**, $p \leq 0.001$). We confirmed these mRNA results with analysis of IL-6 protein, which documented a 34% increase in IL-6 protein in the heart of SS mice injected with heme compared to vehicle controls (**Figure 2A**, $p \leq 0.05$). These data support a role of heme in cardiac IL-6 regulation at steady-state and during acute heme increase in sickle cell disease.

Increased Levels of Circulating IL-6 in Heme-Treated Sickle Mice

Elevated heme (3, 35) and IL-6 (16, 18) have been individually reported in the serum of SCD patients. We hypothesized that increase in extracellular heme rapidly upregulates IL-6 in the plasma of SS and AA mice. Heme treatment significantly increased plasma IL-6 protein levels about 25-fold in both AA and SS mice 3 h after heme injections. The heme-induced IL-6 level was significantly higher in SS mice than AA mice (3249 ± 276 vs. 2385 ± 256 pg/ml, $p \leq 0.05$, **Figure 2B**). These data indicate a role for free heme in systemic regulation of IL-6.

Heme-Induced Cardiac IL-6 Expression Is Negatively Regulated via Nrf2 Pathway

Our recent studies confirmed that the Nrf2 pathway mediates heme induction of cardiac Hmox-1 expression in SS mice (32), human monocytes (36), and keratinocytes (37). This led us to investigate whether the same pathway regulates cardiac IL-6 expression and its response to heme. We find no significant differences in cardiac IL-6 mRNA expression in vehicle-treated $Nrf2^{+/+}$ and $Nrf2^{-/-}$ mice (**Figure 3A**). Treatment with heme significantly augmented cardiac IL-6 mRNA levels in both strains (**Figure 3A**, $p \leq 0.001$). Unexpectedly, IL-6 mRNA rose significantly higher in the hearts of the heme-treated Nrf2-deficient mice compared to the heme-treated $Nrf2^{+/+}$ control mice. Confirming this mRNA finding, cardiac IL-6 protein was about 51% higher in heme-treated $Nrf2^{-/-}$ mice compared to heme-treated $Nrf2^{+/+}$ mice ($p < 0.01$, **Figure 3B**). The result shows that Nrf2 is not required for heme induction of cardiac IL-6 expression.

Heme Upregulates Markers of Cardiac Hypertrophy in Sickle Mice

Our results above showed elevated basal expression of cardiac IL-6 in SS mice, which was further elevated by increase in extracellular heme. Elevated IL-6 is associated with higher risk of left ventricular dysfunction and progression to heart failure in humans (38), and hypertrophy in rodents (39). Furthermore, in SCD patients LV dysfunction was an independent risk factor for death (40, 41), while diastolic dysfunction and myocardial fibrosis were reported in sickle cell mouse model (42). Therefore, we hypothesized that heme might induce cardiac hypertrophy genes in sickle cell mice. We evaluated expression of atrial natriuretic factor (Nppa) and β-Myosin heavy chain 7 (Myh7), known to be associated with cardiac hypertrophy (43). Baseline expression of both Nppa and myh7 were similar in the hearts of AA and SS mice (**Supplementary Figure 2**). Heme treatment resulted in a 14.8-fold increase in Nppa transcripts and 8.1-fold increase in Myh7 transcripts in the heart of SS mice 3 h after injection of heme (**Figures 4A–C**), but not AA control mice (**Figure 4C**). The heart in SCD appears to be more sensitive to heme induction of these two cardiac hypertrophy genes.

DISCUSSION

Intravascular hemolysis is an important modifier of outcome and pathogenesis of SCD (2). The plasma cell-free hemoglobin and heme are elevated at steady state in SCD and are associated with disease severity and end organ damage (2, 44). Cardiac-related complications represent a leading cause of death in SCD (26). In SCD patients, there is also a dysregulated expression of IL-6 and other inflammatory cytokines linked to vaso-occlusive crisis and other complications (18, 20). In this study, we report for the first time elevated basal cardiac IL-6 mRNA and protein levels in SS mice compared to AA controls. We also showed that experimental increase in circulating heme further elevates cardiac and plasma IL-6 expression in control mice and even more so in SS mice. Our result is consistent with earlier studies that reported

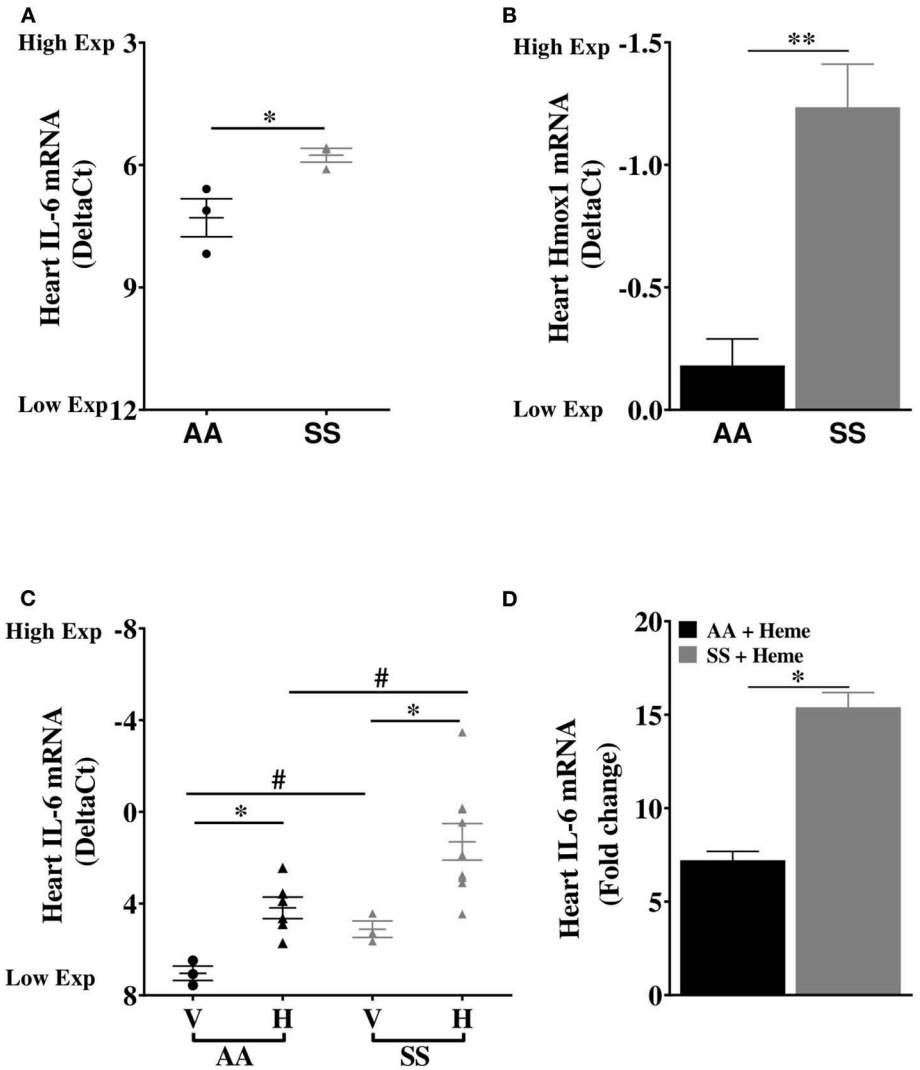

FIGURE 1 | Cardiac expression of IL-6 and Hmox1 in SS mice. Heart mRNA expression of **(A)** IL-6 and **(B)** Hmox1 in naïve in 14 week old SS mice compared to age-matched AA mice ($n = 3$). The SS mice Hmox1 data was published here (32). **(C)** Heme induced cardiac IL-6 mRNA in SS and AA mice ($n = 3$–10). **(D)** Relative fold change in heme-induced cardiac IL-6 mRNA expression in heme treated AA and SS mice ($n = 6$–10). For $DeltaC_t$, lowest value = highest expression and highest value = lowest expression. Target gene transcripts were normalized to Gusb for all mRNA expression levels. Gusb expression was similar in all mice strains used and in all of these organs in animals injected with either vehicle or hemin. For relative fold change, samples were further normalized to vehicle control gene transcripts. Unpaired Student's *t*-test or one-way ANOVA. Error bars indicate SEM. $^*p \leq 0.05$; $^{**}p \leq 0.01$. $\#p < 0.05$ AA vs. SS. V, Vehicle and H, Heme.

elevated serum IL-6 in SCD patients (16, 18), but those studies did not investigate the heart. It is possible that cardiomyocytes and non-cardiomyocytes including fibroblasts and macrophages in the heart as well as cells in other organs may be contributing to the elevated plasma IL-6 after heme injection.

Hemopexin, the endogenous scavenger of free heme, is depleted from the serum of both human (45, 46) and mice (34, 47) with SCD, making them more susceptible to acute increases in heme concentration. This promotes the elevated circulating heme levels reported in human (35) and mice with SCD (34). Once the plasma heme scavenging system is saturated, circulating heme can generate reactive oxygen species, resulting in tissue injury. Our results indicate that heme also upregulates inflammatory cytokine IL-6. Our finding of heme induction of cardiac IL-6 complements a recent report of higher cardiac IL-6 transcripts in hemopexin deficient mice compared to wildtype control (48). The protective effect of hemopexin in heme injection experiments in sickle cell and hemopexin deficient mice has previously been published by our group (34, 49) and other authors (47, 50).

Our findings show that Nrf2 is dispensable for heme induction of IL-6 expression. Further investigation of this pathway was beyond the scope of this current investigation, with several possible mechanisms that might be involved in this heme response. Multiple regulatory elements in the promoter region of the IL-6 gene may contribute to its regulation in a cell

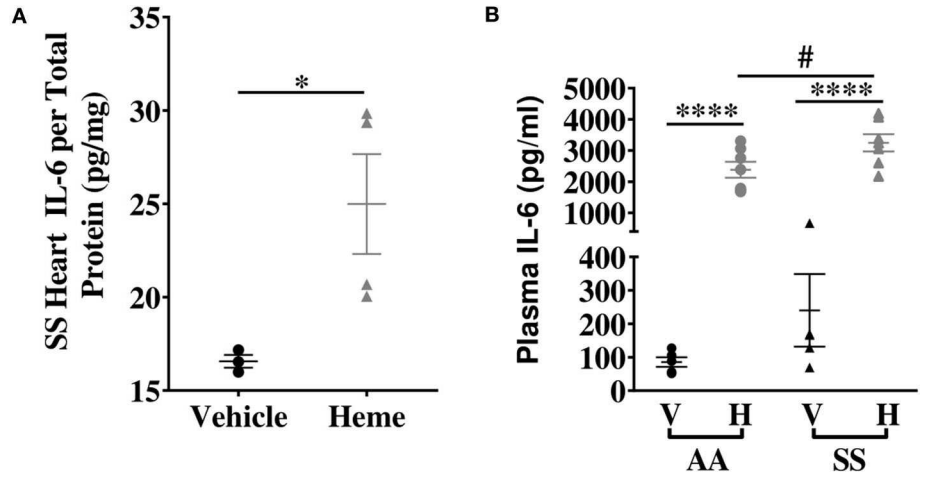

FIGURE 2 | Heme induces IL-6 protein with a more pronounced effect in SS mice compared to AA controls. **(A)** Heme induced cardiac IL-6 protein in SS mice ($n = 3$–4). **(B)** Plasma IL-6 in SS and AA mice injected (IV) with 50 μmoles/kg body weight heme or vehicle ($n = 5$–7). Unpaired Student's *t*-test or one-way ANOVA. Error bars indicate SEM. *$p < 0.05$, ****$p < 0.0001$. #$p < 0.05$ AA vs. SS. V, Vehicle and H, Heme.

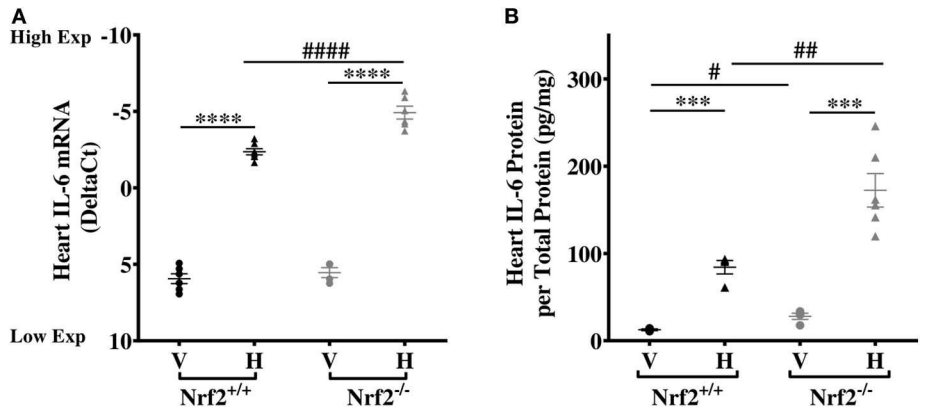

FIGURE 3 | Nrf2 is not required for heme-induced cardiac IL-6. Heme-induced cardiac IL-6 in $Nrf2^{+/+}$ and $Nrf2^{-/-}$ mice. **(A)** RNA **(B)** Protein. $Nrf2^{+/+}$ and $Nrf2^{-/-}$ mice were injected with vehicle or heme (120 μmoles/Kg body weight). For $DeltaC_t$, lowest value = highest expression and highest value = lowest expression. Target gene transcripts were normalized to Gusb for all mRNA expression level. Gusb expression was similar in all mice strains used and in all of these organs in animals injected with either vehicle or hemin. This dose was selected after standardization for producing consistent survival with no adverse effects on both strains of mice. One-way ANOVA. Error bars are SEM. ***$p \leq 0.001$; ****$p \leq 0.0001$, vehicle vs. heme within strain. #$p \leq 0.05$ ##$p \leq 0.01$ $Nrf2^{+/+}$ vs. $Nrf2^{-/-}$ ($n = 3$–7; 14–16 weeks old). V, Vehicle and H, Heme.

type-specific manner (51). Nrf2 might act as a transcriptional repressor or it might regulate another transcriptional inhibitor of IL-6 expression (52). Additionally, reduced inducibility in $Nrf2^{-/-}$ mice of cardiac Hmox1, the principal enzyme in heme catabolism (32), could result in slower degradation of heme leading to prolonged heme-induced activation of IL-6 through an Nrf2-independent pathway. Chronic long-term signaling of IL-6 induces inflammation and promotes cardiac hypertrophy in other models (53). Both features are risk factors for morbidity and mortality in SCD (29, 40, 54), although their relationship to each other has not been investigated in SCD.

Our pilot analysis of other cardiac mRNAs shows a concurrent induction of transcripts of cardiac hypertrophy genes Nppa and MyH7 by heme in the heart of SS mice. Additional inflammatory cytokines such as PlGF contributes to cardiac hypertrophy through IL-6 signaling (55) and it is a predictor of increased left ventricular mass in non-hemolytic diseases such as chronic kidney disease (56). We recently published evidence of elevated basal cardiac expression of PlGF in SS mice with further inducibility by heme (32). These results support a hypothetical model that chronic hemolysis induces expression of both PlGF and IL-6, and this elevation of inflammatory cytokines might contribute to the development of LVH in SCD through a yet to be experimentally identified mechanism. The association of hemolysis, IL-6 induction and organ damage in SCD is supported by previous published research. A recent report showed an association between a polymorphism in the IL-6 gene and development of leg ulcer in SCD patients (57),

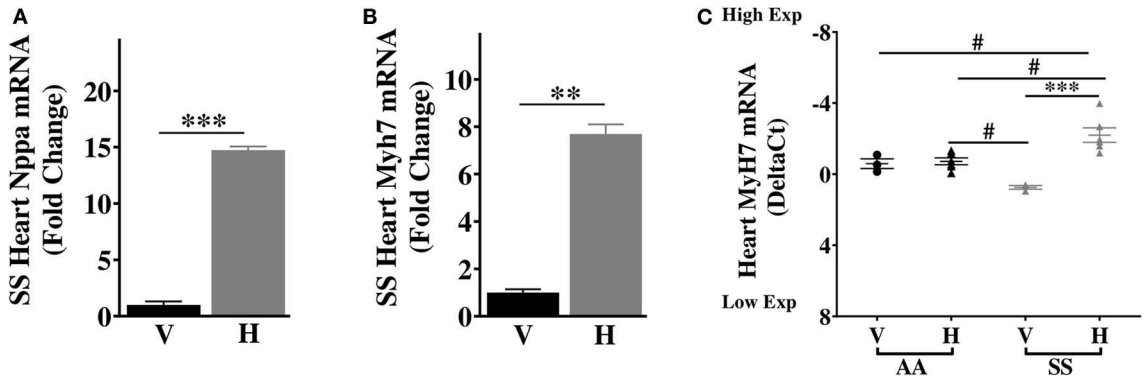

FIGURE 4 | Heme induces high expression of transcripts of cardiac hypertrophy markers in SS mice. Heme induced the expression of **(A)** Nppa **(B)** Myh7 in the heart of SS mice 3 h after heme or vehicle injection **(C)** Myh7 in the heart of SS and AA mice 3 h after heme (50 μmoles/kg body weight) or vehicle injection. For DeltaC_t, lowest value = highest expression and highest value = lowest expression. Target gene transcripts were normalized to Gusb for all mRNA expression level. Gusb expression was similar in all mice strains used and in all of these organs in animals injected with either vehicle or hemin. For relative fold change, samples were further normalized to vehicle control gene transcripts. Unpaired student's *t*-test and one-way ANOVA. Error bars indicate SEM. ***$p \leq 0.001$; **$p \leq 0.001$, vehicle vs. heme within strain. #$p \leq 0.05$ AA vs. SS ($n = 3$–8; 14–16 weeks old). V, Vehicle and H, Heme.

while previous publications showed hemolysis as a risk factor for leg ulcer in these patients (2, 58). Taken together, these suggest that increased hemolysis and inflammatory cytokines including IL-6 may play an important role in organ injury and pathophysiology of SCD.

Our study has several limitations. We did not evaluate the hemopexin levels in plasma or the heart and we did not test whether hemopexin would be protective against heme induction of IL-6. We did not determine a specific cell type in the heart in which heme activates IL-6 expression, and this is a future goal. The mechanism of heme-induced IL-6 expression remains to be determined, although our present evidence unequivocally demonstrates that Nrf2 is not required. An alternative mechanism might involve the activation of the Toll-like receptor 4 (TLR4) induction of MyD88, activator protein-1 (AP-1) and nuclear factor–κB (NF-κB) pathways (59–61). The specific mechanisms by which hemolysis-induced IL-6 contributes to the development of cardiac hypertrophy in SCD warrants future investigation. Despite these limitations, the findings of this study are novel and set the stage for detailed mechanistic studies of heme induction of cardiac IL-6 in SCD. This may lead to the development of novel therapeutic targets for ameliorating or preventing heme-induced IL-6 and cardiac dysfunction in SCD.

In conclusion, we show for the first time direct induction of IL-6 by heme in the plasma and heart of SS mice, in a mechanism that does not require Nrf2. We also show for the first time that heme induces cardiac expression of genes associated with cardiac hypertrophy, a clinically significant complication found in SCD patients with especially severe chronic hemolysis. These new observations provide the basis for a previously unknown heme/IL-6 axis in the development of cardiac disease in patients with SCD. This new model provides potential therapeutic targets for intervention in the heme response and IL-6 pathways to prevent cardiac disease in SCD that merit additional investigation.

DATA AVAILABILITY STATEMENT

The datasets generated for this study are available on request to the corresponding author.

ETHICS STATEMENT

The animal study was reviewed and approved by University of Pittsburgh Institutional Animal Care and Use Committee (IACUC).

AUTHOR CONTRIBUTIONS

OG and GK designed the research project, analyzed, interpreted data, and drafted the manuscript. OG performed the experiments. MK and SG assisted with the experiments. FV and SO-A supervised experiments, and interpreted data. All authors critically reviewed and approved the final version.

FUNDING

GK received support from NIH grants HL133864, MD009162 and from the Institute for Transfusion Medicine Hemostasis and Vascular Biology Research Institute at the University of Pittsburgh School of Medicine. SO-A is supported by NIH grants R01HL106192, U01HL117721, and U54HL141011. FV is supported by NIH grants R01EB026966, R01HL146465, UG3HL143192, and R01HL125777.

ACKNOWLEDGMENTS

We thank Diane Lenhart, Bethany Flage, and Danielle Crosby for technical assistance.

SUPPLEMENTARY MATERIAL

The Supplementary Material for this article can be found online at: https://www.frontiersin.org/articles/10.3389/fimmu.2020.01910/full#supplementary-material

Supplementary Figure 1 | GUSB expression in vehicle and haem-injected mice. Endogenous GUSB expression in vehicle and hemin-treated AA mice (n = 3–6). For C_t, lowest value = highest expression and highest value = lowest expression. All values are mean ± SEM. Exp, Expression. There were no significant differences between vehicle control and hemin treated values.

Supplementary Figure 2 | Similarity in baseline transcripts of markers of cardiac hypertrophy in AA and SS mice. Baseline expression of Nppa and Myh7 in the heart of AA and SS mice. For DeltaC_t, lowest value = highest expression and highest value = lowest expression. Target gene transcripts were normalized to Gusb for all mRNA expression level. All values are mean ± SEM. Exp, Expression.

REFERENCES

1. Piel FB, Hay SI, Gupta S, Weatherall DJ, Williams TN. Global burden of sickle cell anaemia in children under five, 2010-2050: modelling based on demographics, excess mortality, and interventions. *PLoS Med.* (2013) 10:e1001484. doi: 10.1371/journal.pmed.1001484
2. Kato GJ, Gladwin MT, Steinberg MH. Deconstructing sickle cell disease: reappraisal of the role of hemolysis in the development of clinical subphenotypes. *Blood Rev.* (2007) 21:37–47. doi: 10.1016/j.blre.2006.07.001
3. Kato GJ, Steinberg MH, Gladwin MT. Intravascular hemolysis and the pathophysiology of sickle cell disease. *J Clin Invest.* (2017) 127:750–60. doi: 10.1172/JCI89741
4. Gladwin MT, Ofori-Acquah SF. Erythroid DAMPs drive inflammation in SCD. *Blood.* (2014) 123:3689–90. doi: 10.1182/blood-2014-03-563874
5. Simoes RL, Arruda MA, Canetti C, Serezani CH, Fierro IM, Barja-Fidalgo C. Proinflammatory responses of heme in alveolar macrophages: repercussion in lung hemorrhagic episodes. *Mediators Inflamm.* (2013) 2013:946878. doi: 10.1155/2013/946878
6. Adamzik M, Hamburger T, Petrat F, Peters J, De Groot H, Hartmann M. Free hemoglobin concentration in severe sepsis: methods of measurement and prediction of outcome. *Crit Care.* (2012) 16:R125. doi: 10.1186/cc11425
7. Ekregbesi P, Shankar-Hari M, Bottomley C, Riley EM, Mooney JP. Relationship between anaemia, haemolysis, inflammation and haem oxygenase-1 at admission with sepsis: a pilot study. *Sci Rep.* (2018) 8:11198. doi: 10.1038/s41598-018-29558-5
8. Soares MP, Bach FH. Heme oxygenase-1: from biology to therapeutic potential. *Trends Mol Med.* (2009) 15:50–58. doi: 10.1016/j.molmed.2008.12.004
9. Yeo TW, Lampah DA, Tjitra E, Gitawati R, Kenangalem E, Piera K, et al. Relationship of cell-free hemoglobin to impaired endothelial nitric oxide bioavailability and perfusion in severe falciparum malaria. *J Infect Dis.* (2009) 200:1522–29. doi: 10.1086/644641
10. Abildgaard U, Heimdal K. Pathogenesis of the syndrome of hemolysis, elevated liver enzymes, and low platelet count (HELLP): a review. *Eur J Obstet Gynecol Reprod Biol.* (2013) 166:117–23. doi: 10.1016/j.ejogrb.2012.09.026
11. Burwick RM, Rincon M, Beeraka SS, Gupta M, Feinberg BB. Evaluation of hemolysis as a severe feature of preeclampsia. *Hypertension.* (2018) 72:460–5. doi: 10.1161/HYPERTENSIONAHA.118.11211
12. Pathan N, Hemingway CA, Alizadeh AA, Stephens AC, Boldrick JC, Oragui EE, et al. Role of interleukin 6 in myocardial dysfunction of meningococcal septic shock. *Lancet.* (2004) 363:203–9. doi: 10.1016/S0140-6736(03)15326-3
13. Nayak KC, Meena SL, Gupta BK, Kumar S, Pareek V. Cardiovascular involvement in severe vivax and falciparum malaria. *J Vector Borne Dis.* (2013) 50:285–91.
14. Melchiorre K, Sharma R, Thilaganathan B. Cardiovascular implications in preeclampsia: an overview. *Circulation.* (2014) 130:703–14. doi: 10.1161/CIRCULATIONAHA.113.003664
15. Greer J. Pathophysiology of cardiovascular dysfunction in sepsis. *British Journal of Anaesthesia Education.* (2015) 15:316–21. doi: 10.1093/bjaceaccp/mkv003
16. Taylor SC, Shacks SJ, Mitchell RA, Banks A. Serum interleukin-6 levels in the steady state of sickle cell disease. *J Interferon Cytokine Res.* (1995) 15:1061–4. doi: 10.1089/jir.1995.15.1061
17. Duits AJ, Rodriguez T, Schnog JJ. Serum levels of angiogenic factors indicate a pro-angiogenic state in adults with sickle cell disease. *Br J Haematol.* (2006) 134:116–9. doi: 10.1111/j.1365-2141.2006.06103.x
18. Sarray S, Saleh LR, Lisa Saldanha F, Al-Habboubi HH, Mahdi N, Almawi WY. Serum IL-6, IL-10, and TNFalpha levels in pediatric sickle cell disease patients during vasoocclusive crisis and steady state condition. *Cytokine.* (2015) 72:43–7. doi: 10.1016/j.cyto.2014.11.030
19. Kelaidi C, Kattamis A, Apostolakou F, Poziopoulos C, Lazaropoulou C, Delaporta P, et al. PlGF and sFlt-1 levels in patients with non-transfusion-dependent thalassemia: correlations with markers of iron burden and endothelial dysfunction. *Eur J Haematol.* (2018) 100:630–5. doi: 10.1111/ejh.13061
20. Barbu EA, Mendelsohn L, Samsel L, Thein SL. Pro-inflammatory cytokines associate with NETosis during sickle cell vaso-occlusive crises. *Cytokine.* (2019) 127:154933. doi: 10.1016/j.cyto.2019.154933
21. Dinh W, Futh R, Nickl W, Krahn T, Ellinghaus P, Scheffold T, et al. Elevated plasma levels of TNF-alpha and interleukin-6 in patients with diastolic dysfunction and glucose metabolism disorders. *Cardiovasc Diabetol.* (2009) 8:58. doi: 10.1186/1475-2840-8-58
22. Melendez GC, Mclarty JL, Levick SP, Du Y, Janicki JS, Brower GL. Interleukin 6 mediates myocardial fibrosis, concentric hypertrophy, and diastolic dysfunction in rats. *Hypertension.* (2010) 56:225–231. doi: 10.1161/HYPERTENSIONAHA.109.148635
23. Fredj S, Bescond J, Louault C, Delwail A, Lecron JC, Potreau D. Role of interleukin-6 in cardiomyocyte/cardiac fibroblast interactions during myocyte hypertrophy and fibroblast proliferation. *J Cell Physiol.* (2005) 204:428–36. doi: 10.1002/jcp.20307
24. Kumar S, Wang G, Zheng N, Cheng W, Ouyang K, Lin H, et al. HIMF (Hypoxia-Induced mitogenic factor)-IL (interleukin)-6 signaling mediates cardiomyocyte-fibroblast crosstalk to promote cardiac hypertrophy and fibrosis. *Hypertension.* (2019) 73:1058–70. doi: 10.1161/HYPERTENSIONAHA.118.12267
25. Gladwin MT, Barst RJ, Gibbs JS, Hildesheim M, Sachdev V, Nouraie M, et al. Patients risk factors for death in 632 patients with sickle cell disease in the United States and United Kingdom. *PLoS ONE.* (2014) 9:e99489. doi: 10.1371/journal.pone.0099489
26. Gladwin MT. Cardiovascular complications and risk of death in sickle-cell disease. *Lancet.* (2016) 387:2565–74. doi: 10.1016/S0140-6736(16)00647-4
27. Crocker P, Werb Z, Gordon S, Bainton D. Ultrastructural localization of a macrophage-restricted sialic acid binding hemagglutinin, SER. in macrophage-hematopoietic cell clusters. *Blood.* (1990) 76:1131–8. doi: 10.1182/blood.V76.6.1131.1131
28. Lester LA, Sodt PC, Hutcheon N, Arcilla RA. Cardiac abnormalities in children with sickle cell anemia. *Chest.* (1990) 98:1169–74. doi: 10.1378/chest.98.5.1169
29. Faro GB, Menezes-Neto OA, Batista GS, Silva-Neto AP, Cipolotti R. Left ventricular hypertrophy in children, adolescents and young adults with sickle cell anemia. *Rev Bras Hematol Hemoter.* (2015) 37:324–8. doi: 10.1016/j.bjhh.2015.07.001
30. Alam J, Cook JL. Transcriptional regulation of the heme oxygenase-1 gene via the stress response element pathway. *Curr Pharm Des.* (2003) 9:2499–511. doi: 10.2174/1381612033453730
31. Motohashi H, Yamamoto M. Nrf2-Keap1 defines a physiologically important stress response mechanism. *Trends Mol Med.* (2004) 10:549–57. doi: 10.1016/j.molmed.2004.09.003
32. Gbotosho OT, Ghosh S, Kapetanaki MG, Lin Y, Weidert F, Bullock GC, et al. Cardiac expression of HMOX1 and PGF in sickle cell mice and haem-treated wild type mice dominates organ expression profiles via Nrf2 (Nfe2l2). *Br J Haematol.* (2019) 187:666–75. doi: 10.1111/bjh.16129

33. Kapetanaki MG, Gbotosho OT, Sharma D, Weidert F, Ofori-Acquah SF, Kato GJ. Free heme regulates placenta growth factor through NRF2-antioxidant response signaling. *Free Radic Biol Med.* (2019) 143:300–8. doi: 10.1016/j.freeradbiomed.2019.08.009
34. Ghosh S, Adisa OA, Chappa P, Tan F, Jackson KA, Archer DR, et al. Extracellular hemin crisis triggers acute chest syndrome in sickle mice. *J Clin Invest.* (2013) 123:4809–20. doi: 10.1172/JCI64578
35. Oh JY, Hamm J, Xu X, Genschmer K, Zhong M, Lebensburger J, et al. Absorbance and redox based approaches for measuring free heme and free hemoglobin in biological matrices. *Redox Biol.* (2016) 9:167–77. doi: 10.1016/j.redox.2016.08.003
36. Boyle JJ, Johns M, Lo J, Chiodini A, Ambrose N, Evans PC, et al. Heme induces heme oxygenase 1 via Nrf2: role in the homeostatic macrophage response to intraplaque hemorrhage. *Arterioscler Thromb Vasc Biol.* (2011) 31:2685–91. doi: 10.1161/ATVBAHA.111.225813
37. Reichard JF, Motz GT, Puga A. Heme oxygenase-1 induction by NRF2 requires inactivation of the transcriptional repressor BACH1. *Nucleic Acids Res.* (2007) 35:7074–86. doi: 10.1093/nar/gkm638
38. Yan AT, Yan RT, Cushman M, Redheuil A, Tracy RP, Arnett DK, et al. Relationship of interleukin-6 with regional and global left-ventricular function in asymptomatic individuals without clinical cardiovascular disease: insights from the multi-ethnic study of atherosclerosis. *Eur Heart J.* (2010) 31:875–82. doi: 10.1093/eurheartj/ehp454
39. Sano M, Fukuda K, Kodama H, Pan J, Saito M, Matsuzaki J, et al. Interleukin-6 family of cytokines mediate angiotensin II-induced cardiac hypertrophy in rodent cardiomyocytes. *J Biol Chem.* (2000) 275:29717–23. doi: 10.1074/jbc.M003128200
40. Sachdev V, Machado RF, Shizukuda Y, Rao YN, Sidenko S, Ernst I, et al. Diastolic dysfunction is an independent risk factor for death in patients with sickle cell disease. *J Am Coll Cardiol.* (2007) 49:472–9. doi: 10.1016/j.jacc.2006.09.038
41. Niss O, Fleck R, Makue F, Alsaied T, Desai P, Towbin JA, et al. Association between diffuse myocardial fibrosis and diastolic dysfunction in sickle cell anemia. *Blood.* (2017) 130:205–13. doi: 10.1182/blood-2017-02-767624
42. Bakeer N, James J, Roy S, Wansapura J, Shanmukhappa SK, Lorenz JN, et al. Sickle cell anemia mice develop a unique cardiomyopathy with restrictive physiology. *Proc Natl Acad Sci USA.* (2016) 113:E5182–91. doi: 10.1073/pnas.1600311113
43. Marian AJ. Genetic determinants of cardiac hypertrophy. *Curr Opin Cardiol.* (2008) 23:199–205. doi: 10.1097/HCO.0b013e3282fc27d9
44. Vichinsky E. Chronic organ failure in adult sickle cell disease. *Hematology Am Soc Hematol Educ Program.* (2017) 2017:435–9. doi: 10.1182/asheducation-2017.1.435
45. Santiago RP, Guarda CC, Figueiredo CVB, Fiuza LM, Aleluia MM, Adanho CSA, et al. Serum haptoglobin and hemopexin levels are depleted in pediatric sickle cell disease patients. *Blood Cells Mol Dis.* (2018) 72:34–6. doi: 10.1016/j.bcmd.2018.07.002
46. Yalamanoglu A, Deuel JW, Hunt RC, Baek JH, Hassell K, Redinius K, et al. Depletion of haptoglobin and hemopexin promote hemoglobin-mediated lipoprotein oxidation in sickle cell disease. *Am J Physiol Lung Cell Mol Physiol.* (2018) 315:L765–L74. doi: 10.1152/ajplung.00269.2018
47. Vercellotti GM, Zhang P, Nguyen J, Abdulla F, Chen C, Nguyen P, et al. Hepatic overexpression of hemopexin inhibits inflammation and vascular stasis in murine models of sickle cell disease. *Mol Med.* (2016) 22:63. doi: 10.2119/molmed.2016.00063
48. Ingoglia G, Sag CM, Rex N, De Franceschi L, Vinchi F, Cimino J, et al. Data demonstrating the anti-oxidant role of hemopexin in the heart. *Data Brief.* (2017) 13:69–76. doi: 10.1016/j.dib.2017.05.026
49. Ofori-Acquah SF, Hazra R, Orikogbo OO, Crosby D, Flage B, Ackah EB, et al. Hemopexin deficiency promotes acute kidney injury in sickle cell disease. *Blood.* (2020) 135:1044–8. doi: 10.1182/blood.2019002653
50. Belcher JD, Chen C, Nguyen J, Abdulla F, Zhang P, Nguyen H, et al. Haptoglobin and hemopexin inhibit vaso-occlusion and inflammation in murine sickle cell disease: Role of heme oxygenase-1 induction. *PLoS ONE.* (2018) 13:e0196455. doi: 10.1371/journal.pone.0196455
51. Wruck CJ, Streetz K, Pavic G, Gotz ME, Tohidnezhad M, Brandenburg LO, et al. Nrf2 induces interleukin-6 (IL-6) expression via an antioxidant response element within the IL-6 promoter. *J Biol Chem.* (2011) 286:4493–9. doi: 10.1074/jbc.M110.162008
52. Kobayashi EH, Suzuki T, Funayama R, Nagashima T, Hayashi M, Sekine H, et al. Nrf2 suppresses macrophage inflammatory response by blocking proinflammatory cytokine transcription. *Nat Commun.* (2016) 7:11624. doi: 10.1038/ncomms11624
53. Fontes JA, Rose NR, Cihakova D. The varying faces of IL-6: from cardiac protection to cardiac failure. *Cytokine.* (2015) 74:62–68. doi: 10.1016/j.cyto.2014.12.024
54. Bandeira IC, Rocha LB, Barbosa MC, Elias DB, Querioz JA, Freitas MV, et al. Chronic inflammatory state in sickle cell anemia patients is associated with HBB(*)S haplotype. *Cytokine.* (2014) 65:217–21. doi: 10.1016/j.cyto.2013.10.009
55. Jaba IM, Zhuang ZW, Li N, Jiang Y, Martin KA, Sinusas AJ, et al. NO triggers RGS4 degradation to coordinate angiogenesis and cardiomyocyte growth. *J Clin Invest.* (2013) 123:1718–31. doi: 10.1172/JCI65112
56. Peiskerova M, Kalousova M, Danzig V, Mikova B, Hodkova M, Nemecek E, et al. Placental growth factor may predict increased left ventricular mass index in patients with mild to moderate chronic kidney disease–a prospective observational study. *BMC Nephrol.* (2013) 14:142. doi: 10.1186/1471-2369-14-142
57. Vicari P, Adegoke SA, Mazzotti DR, Cancado RD, Nogutti MA, Figueiredo MS. Interleukin-1beta and interleukin-6 gene polymorphisms are associated with manifestations of sickle cell anemia. *Blood Cells Mol Dis.* (2015) 54:244–9. doi: 10.1016/j.bcmd.2014.12.004
58. Nolan VG, Adewoye A, Baldwin C, Wang L, Ma Q, Wyszynski DF, et al. Sickle cell leg ulcers: associations with haemolysis and SNPs in Klotho, TEK and genes of the TGF-beta/BMP pathway. *Br J Haematol.* (2006) 133:570–8. doi: 10.1111/j.1365-2141.2006.06074.x
59. Lavrovsky Y, Schwartzman ML, Levere RD, Kappas A, Abraham NG. Identification of binding sites for transcription factors NF-kappa B and AP-2 in the promoter region of the human heme oxygenase 1 gene. *Proc Natl Acad Sci USA.* (1994) 91:5987–91. doi: 10.1073/pnas.91.13.5987
60. Figueiredo RT, Fernandez PL, Mourao-Sa DS, Porto BN, Dutra FF, Alves LS, et al. Characterization of heme as activator of Toll-like receptor 4. *J Biol Chem.* (2007) 282:20221–9. doi: 10.1074/jbc.M610737200
61. Belcher JD, Chen C, Nguyen J, Milbauer L, Abdulla F, Alayash AI, et al. Heme triggers TLR4 signaling leading to endothelial cell activation and vaso-occlusion in murine sickle cell disease. *Blood.* (2014) 123:377–90. doi: 10.1182/blood-2013-04-495887

Conflict of Interest: The authors declare that the research was conducted in the absence of any commercial or financial relationships that could be construed as a potential conflict of interest.

frontiers in Immunology

MINI REVIEW
published: 25 August 2020
doi: 10.3389/fimmu.2020.01835

Heme on Pulmonary Malaria: Friend or Foe?

*Tatiana Almeida Pádua and Mariana Conceição Souza**

Laboratory of Applied Pharmacology, Institute of Drug Technology (Farmanguinhos), Oswaldo Cruz Foundation, Rio de Janeiro, Brazil

Malaria is a hemolytic disease that, in severe cases, can compromise multiple organs. Pulmonary distress is a common symptom observed in severe malaria caused by *Plasmodium vivax* or *Plasmodium falciparum*. However, biological components involved in the development of lung malaria are poorly studied. In experimental models of pulmonary malaria, it was observed that parasitized red blood cell-congested pulmonary capillaries are related to intra-alveolar hemorrhages and inflammatory cell infiltration. Thus, it is very likely that hemolysis participates in malaria-induced acute lung injury. During malaria, heme assumes different biochemical structures such as hemin and hemozoin (biocrystallized structure of heme inside *Plasmodium* sp.). Each heme-derived structure triggers a different biological effect: on the one hand, hemozoin found in lung tissue is responsible for the infiltration of inflammatory cells and consequent tissue injury; on the other hand, heme stimulates heme oxygenase-1 (HO-1) expression and CO production, which protect mice from severe malaria. In this review, we discuss the biological mechanism involved in the dual role of heme response in experimental malaria-induced acute lung injury.

Keywords: hemolysis, MA-RD, *Plasmodium*, heme, severe malaria, HO-1

OPEN ACCESS

Edited by:
Nicola Conran,
Campinas State University, Brazil

Reviewed by:
Padmanaban Govindarajan,
Indian Institute of Science (IISc), India
Claudio Romero Farias Marinho,
University of São Paulo, Brazil

****Correspondence:***
Mariana Conceição Souza
mariana.souza@fiocruz.br

Specialty section:
This article was submitted to Inflammation, a section of the journal Frontiers in Immunology

Received: *17 February 2020*
Accepted: *08 July 2020*
Published: *25 August 2020*

Citation:
Pádua TA and Souza MC (2020) Heme on Pulmonary Malaria: Friend or Foe? Front. Immunol. 11:1835. doi: 10.3389/fimmu.2020.01835

INTRODUCTION

Malaria remains one of the major public health problems. In 2018, 228 million cases and 405,000 deaths from malaria were estimated worldwide (1). Malaria is particularly prevalent in tropical and subtropical low-income regions of the world such as the African region, which accounts for 93% of the cases, followed by the Southeast Asia region with 3.4% and the Eastern Mediterranean region with 2.1% (1). The World Health Organization's (WHO) mission is to reduce global malaria mortality rates by 90% by 2030 (2). Malaria is caused by at least six known species of *Plasmodium* infecting humans: *Plasmodium falciparum*, *Plasmodium vivax*, *Plasmodium malariae*, *Plasmodium ovale*, *Plasmodium knowlesi* (3), and the more recently described *Plasmodium simium* (4). Its transmission occurs by female anopheles mosquito bites, transfusion of infected blood, or transplacentally, from infected mother to fetus [reviewed in (5)]. The vast majority of human malaria worldwide is uncomplicated resulting in fever, and factors involved in disease complications are unknown.

Severe malaria is a complication that affects multiple organs, including lungs (6). (7) reviewed the incidence of lung dysfunction in malaria patients and showed data ranging from 2 to 29%. The wide range is related to different methods to diagnose dysfunction severity. Considering the classification of pulmonary complications, it is worth mentioning that malaria is most prevalent in poor countries where methods of diagnoses, documentation, and

reporting are weak. Furthermore, a large proportion of severe malaria illnesses and deaths occur in people's homes without coming to the attention of a formal health service. In accordance, although the Berlin definition is a robust and reproducible tool for identifying acute respiratory distress syndrome (ARDS), it could not be applied in low-income countries because of inaccessibility of mechanical ventilators, arterial blood gas diagnostics, and chest radiography. For instance, none of the patients with malaria in the studies of Leopold et al. (8) could be diagnosed with ARDS using the conventional Berlin definition because the requirements for positive end-expiratory pressure criteria were not known since patients were managed outside of the intensive care unit (ICU). This limitation could have the unintended consequence of underestimating and undertreating the burden of malaria-induced ARDS in many countries (9). Thus, available data concerning malaria induced-ARDS incidence worldwide may be underestimated. Herein, we use the term malaria-induced respiratory distress (MA-RD) to present studies in which ARDS has not been formally diagnosed.

Almost all *Plasmodium* species that infect humans can induce MA-RD [reviewed in (10)], including *P. malariae* (11), *P. ovale* (12), and *P. knowlesi* (13); however, this syndrome is more common in *P. falciparum* and *P. vivax* malaria (14–17). MA-RD can be observed at early time points after diagnosis or even when the parasitemia decreases or disappears [reviewed in (7)]. Besides, antimalarial treatment can also lead to lung dysfunction. For instance, during quinine therapy, it is possible to observe pulmonary exacerbated inflammatory response and reduced alveolar-capillary gas exchange (18). Primaquine treatment also leads to hemolysis and consequent ARDS in malaria patients that present G6PD deficiency (19).

The most common pathologies associated with MA-RD are pulmonary edema, dyspnea, reduction in the capacity of gas exchange, and increased levels of inflammatory mediators (7). Autopsies in patients who have died of severe malaria and ARDS symptoms showed pleural and pulmonary hemorrhages, sequestered parasitized red blood cells (PRBC), neutrophils, and monocytes containing malarial pigment in lung tissue (20). Nevertheless, the biological process that triggers MA-RD is not clear. In this way, animal models have been an indispensable tool to understand lung dysfunction during malaria. However, since most experimental studies did not evaluate all factors that characterize ARDS, it is more appropriate to use the term malaria-induced acute lung injury (MA-ALI) to depict experimental results. Unlike cerebral malaria, which is mainly studied in *P. berghei*-infected C57BL/6 mice (21), lung malaria can be observed in *P. berghei* ANKA-infected C57BL/6 (22, 23), *P. berghei* NK65-infected C57BL/6 (24, 25), *P. berghei* ANKA-infected DBA mice (26), *P. berghei* ANKA-infected CBA mice (27), among others (28). These models show that malaria-induced experimental lung dysfunction is characterized by vascular dysfunction induced by $CD8^+$ T cells, presence of PRBC, hemorrhages, neutrophils, and monocytes containing malarial pigment. On the other hand, it has been shown that, at 24 h after infection, a time point at which inflammatory mediators are not yet detected, it is possible to observe PRBC, neutrophils, and mononuclear cells in the lung tissue (29, 30). Thus, it is unclear whether inflammatory cells, PRBC, blood, and pigment from malaria are a consequence or trigger the pulmonary pathology seen during malaria.

THE ROLE OF HEME DERIVATIVES IN LUNG PATHOLOGY DURING MALARIA

The study of heme and its derivatives in MA-RD is not elementary. The complex named heme (protoporphyrin IX + Fe II) is an important cofactor in several biological processes such as oxygen transfer, storage and activation, and electron transfer (31). During the respiratory process, the hemoglobin (Hb) containing heme captures and releases the oxygen without modifying iron oxidative state (32). However, 1–3% of Hb undergoes auto-oxidation, and oxygen is reduced to superoxide anion ($O_2^{\bullet -}$) and generates methemoglobin [Hb plus hemin (Fe III)] (32).

Heme and its analogs localize differently on erythrocyte membranes and exhibit distinct roles in its partitioning, leakage, and fusion (33). Under physiological conditions, when intravascular hemolysis occurs during the destruction of senescent erythrocytes and/or enucleation of erythroblasts, some hemoglobin, free heme, or hemin can be released into the plasma where they bind to soluble haptoglobin (Hp) or hemopexin (Hx) (reviewed by 27; 28). In the liver, the complexes are recognized by specific receptors on Kupffer cells such as CD163 and CD91/LRP-1, respectively, and metabolized by heme oxygenase-1 (HO-1) to iron, carbon monoxide, and biliverdin that will be stored or act as antioxidant molecules (34–36) (**Figure 1A**).

However, in hemolytic diseases, intravascular hemolysis increases, becoming a serious pathological complication (37). During the intraerythrocytic stage, parasites lyse the erythrocyte to release merozoites that rapidly invade new host cells (38). This lytic process also releases the infected red blood cell contents into the host bloodstream, including undigested hemoglobin, free heme, and hemozoin. The augment of extracellular levels of hemoglobin may reduce levels of available free Hp, making this pathway ineffective (39), while the large content of heme and hemin circulating in plasma can exhaust the binding capacity of Hx and their metabolism by HO-1. These events result in the increase in oxidation from heme to hemin and consequently methemoglobin (hemoglobin plus hemin) formation (40). It is important to note that the binding affinity of globin to hemin is weak and can lead to free heme release (32). The free heme leads to oxidative damage by the generation of reactive oxygen species (ROS) [e.g., superoxide ($O_2^{\bullet -}$), hydrogen peroxide (H_2O_2), and hydroxyl radical ($HO\bullet$)], reactive nitrogen species (RNS) (e.g., nitric oxide ($\bullet NO$), nitrogen dioxide ($\bullet NO_2$)], and peroxynitrite ($ONOO^-$) (41). These reactive species mediate the activation of inflammatory pathways and tissue damage, in addition to the loss of erythrocyte deformation ability and the endothelial barrier integrity by inducing lipid peroxidation of the membrane (42–44). Therefore, the consequences of heme derivative release might depend on their concentration and the environment in which they are found (38, 40).

As mentioned above, malaria is a hemolytic disease; thus, free heme and hemin released during hemolysis due

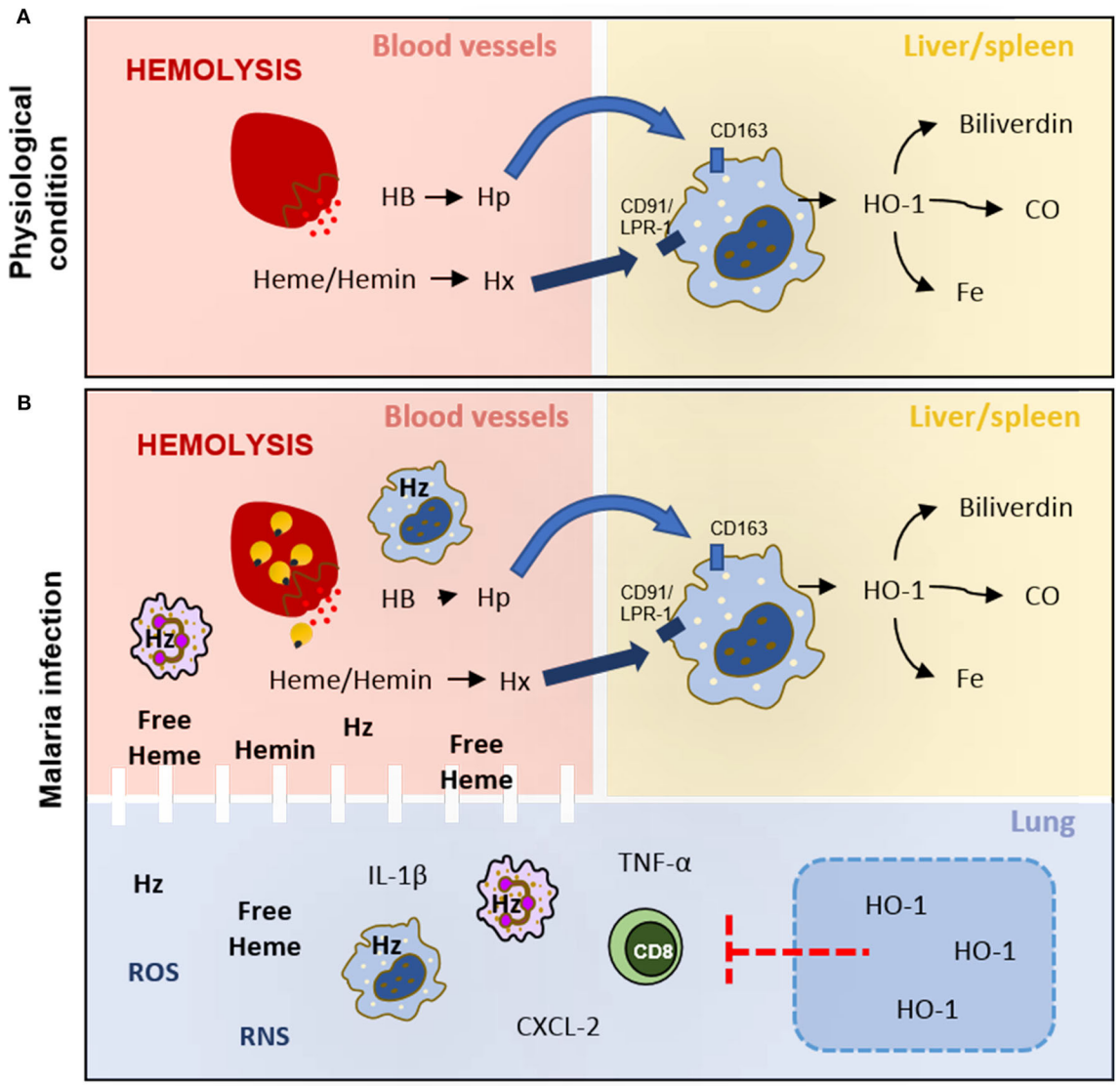

FIGURE 1 | Hemolysis under physiological conditions and malaria infection. **(A)** During hemolysis, hemoglobin (HB) and free heme/hemin are captured by haptoglobin (Hp) and hemopexin (Hx), respectively, in blood vessels. These complexes (HB-Hp and Heme-Hx) target macrophages CD163^{+} and CD91/LRP-1^{+} in the liver and spleen to be metabolized by heme oxygenase 1 (HO-1) to biliverdin, carbon monoxide (CO), and iron (Fe). **(B)** The hemolysis increases during the release of merozoites saturates the activity of haptoglobin (Hp) and hemopexin (Hx), leading to heme, hemin, and hemozoin (Hz) circulating in plasma. These heme derivatives increase ROS and RNS production and activate leukocytes to produce cytokines and chemokines that damage lung tissue and endothelial barriers. HO-1 induction would decrease leukocyte activation and migration, reduce inflammatory mediators production, and restore the integrity of the endothelial cell barrier in lung tissue.

to erythrocyte rupture during the plasmodium life cycle exert effects that contribute to malaria pathology. Beyond the free heme and hemin, heme can also be found in a biocrystallized structure named hemozoin in the *Plasmodium* sp. *Plasmodium* digest ~65% of total erythrocyte hemoglobin during intraerythrocytic development. Part of the hemoglobin's amino acids is incorporated in parasite proteins; however, since free heme released during hemoglobin digestion is a toxic by-product, *Plasmodium* biocrystallizes heme to hemozoin to store it as a nontoxic molecule in the digestive vacuole (45, 46).

The erythrocyte content (cytoplasm, parasite components, hemozoin, and free heme) released during hemolysis is engulfed by phagocytes such as macrophages, neutrophils, and dendritic cells (47). The accumulation of hemozoin in these immune phagocytic cells reflects the parasite burden and coincides with periodic fevers and high circulating levels of proinflammatory cytokines. In this way, this pigment is used to measure malaria severity and identify parasite developmental stages (6). Adult patients who died of severe *P. falciparum* malaria had significantly higher proportions of neutrophils and monocytes containing hemozoin than surviving patients (48). In addition,

patients with MA-RD demonstrated high lung deposition of hemozoin and internal alveolar hemorrhage compared with those with non-MA-RD lungs (49). The same group also showed that hemozoin leads to loss of alveolar integrity by increasing the production of interleukin (IL)-1β by monocytes, which induces pneumocytes type II apoptosis (50). These observations are also seen in mouse lungs. The C57BL/6 mice infected with *P. berghei* NK65 showed a grayish-brown discoloration due to hemorrhages and hemozoin deposition, in addition to tissue edema and a marked inflammatory cells influx (24, 51).

The use of purified hemozoin has already been proposed to access its pathological role *in vitro* and *in vivo* (52). However, the method used to extract hemozoin is not effective in purifying it, since biological effects observed were attributed to a DNA contamination in hemozoin extract (53). In this context, some authors resort to the use of β-hematin, a compound produced *in vitro* using parasite lysate to provide necessary enzymes to biocrystallization. However, the artificial process to produce β-hematin results in substances different in shape and size from the natural ones, which could mask the results [reviewed in (46)]. Despite the immunological activity of synthetic hemozoin being controversial, several studies have demonstrated that both parasite-derived hemozoin and synthetically produced hemozoin, once phagocytized, activates both mouse and human leukocytes to produce proinflammatory cytokines such as tumor necrosis factor alpha (TNF-α) and IL-1β (54) and macrophage inflammatory protein (MIP)-1α/CCL3, MIP-1β/CCL4, MIP-2/C-X-C Motif Chemokine Ligand 2 (CXCL2), and MCP-1/CCL2 chemokines through oxidative stress-dependent and stress-independent mechanisms (55). Besides, Huy and coworkers showed that the treatment with β-hematin increased myeloperoxidase activity of peritoneal cells *in vivo* and neutrophil chemotaxis *in vitro* (56).

Despite the compelling data showing the deleterious effects of heme during malaria, in the last decade, several studies have shown that heme pathway could be beneficial to host outcomes. Balb/c mice, a resistant strain to multiorgan dysfunction (MOD) triggered by *P. berghei*-ANKA infection, expressed HO-1 in brain tissue during *P. berghei* infection. In addition, HO-1 knockout Balb/c mice succumb to *P. berghei* infection, through a mechanism that can be reversed by $CD8^+$ T cell depletion, which suggests that heme metabolism is involved in malaria resistance by modulating immunological response. Interestingly, studies with C57BL/6 mice, a susceptible strain to MOD triggered by *P. berghei*-ANKA infection, also produced HO-1 in brain tissue, however, correlated with parasite inoculum. It is well established that parasite inoculum modulates disease outcome (57). Additionally, the 10^5 *P. berghei* pRBC inoculum did not induce HO-1 expression in the brain tissue (58), while the 10^6 *P. berghei* pRBC inoculum induces HO-1 expression in the brain 4 days postinfection (59). It is noteworthy that parasite inoculum did not interfere in increased levels of free heme in plasma, which suggests that heme in malaria-susceptible hosts is not enough to induce HO-1; HO-1 is insufficiently produced/activated to induce free heme clearance, or the produced HO-1 is saturated. For instance, C57BL/6 *P. berghei*-infected mice treated with cobalt protoporphyrin, a pharmacological intervention that stimulates HO-1 production and activity, reduced brain edema and microvascular congestion (58). The authors also gave CO, a downstream metabolite in the heme clearance pathway, and further observed a reduction in $CD8^+$ T cells in the brain tissue, showing that the appropriate amounts of HO-1 are effective to protect susceptible mice from MOD. In accordance, the balance between free heme and HO-1 production is important to improve the outcome of *P. berghei*-infected mice that carry hemoglobin beta-chain mutation, named sickle Hb (HbS). The authors observed that mice with HbS phenotype did not develop cerebral malaria by two different mechanisms, and both pathways depend on low levels of free heme on the bloodstream. The first mechanism involves the stimulation of HO-1 production, and the second one involves heme-induced immunoregulatory roles. The authors suggest that there is a pathogenic and a protective concentration of circulating free heme during malaria (60).

In recent reviews by Frimat et al. (61) and Immenschuh et al. (40), the heme clearance pathway has been proposed as targets to treat hemolytic diseases. Frimat suggests that two different approaches should be considered to treat hemolytic disease: first, by modulating molecules from the heme clearance pathway as by administering hemopexin or inducing HO-1, and second, by treating oxidative stress and inflammation induced by heme (61). In addition, Immenschuh and colleagues state that heme exerts different effects depending on the target cell. Endothelial cells rapidly respond to heme by means of HO-1 production, which suggests that the lung, as a highly vascularized organ, is an important organ to study therapeutic interventions aiming at heme clearance. Compounds such as desoxyrhapontigenin, statins, curcumin, hemin, quercetin, and cobalt protoporphyrin have already been used to attenuate experimental lung dysfunction by inducing HO-1 expression (40). However, few studies have been dedicated to assessing whether HO-1 induction would attenuate malaria-induced ALI. Pereira et al. (62), using the *P. berghei*-infected DBA/2 mice model of MA-ALI, gave hemin to infected mice and observed an increase in HO-1 production correlated with attenuation of lung dysfunction and inflammatory response associated to alteration in lung histoarchitecture. As well, Liu et al. (59) showed that HO-1 expression in the lung tissue during experimental malaria depends on CXCL10 and signal transducer and activator of transcription 3 (STAT3). The authors further show that free heme is detectable in plasma since the second day of infection. At the same time point, they also observed HO-1 expression in the lung tissue but not in the brain tissue, supporting the idea that the lung is one of the most important organs for the heme clearance pathway (**Figure 1B**).

Thus, considering the biological mechanism by which HO-1 induction attenuates brain dysfunction during experimental cerebral malaria, we can speculate that during experimental MA-ALI, the induction of HO-1 downmodulates $CD8^+$ T cell activation and migration to lung tissue, reduces the production of inflammatory mediators, and restores endothelial cell barrier integrity.

CONCLUSION

Free heme and heme derivatives have been widely recognized as pathological molecules in several hemolytic conditions. The participation of heme in malaria is very peculiar because it exerts its effects through different molecular structures as free heme, hemin, and hemozoin. Several studies concerning malaria-induced lung dysfunction show that heme derivatives affect alveolar integrity, induce the production of inflammatory mediators, and accumulate the inflammatory cells in the lung tissue. On the other hand, more recent studies propose that heme exerts a beneficial role during malaria infection by inducing cytoprotective pathways such as HO-1 production. Indeed, more studies are necessary to define the role of heme during malaria-induced lung dysfunction. Overall, we can conclude that the imbalance between free concentration, production/saturation of HO-1, and the activation of coexisting anti-inflammatory pathways dictate if heme is a friend or foe to malaria patients.

AUTHOR CONTRIBUTIONS

TP and MS wrote the manuscript. All authors contributed to the article and approved the submitted version.

FUNDING

This work was supported by Conselho Nacional de Desenvolvimento Científico e Tecnológico, grant 407835/2017-2.

REFERENCES

1. World Health Organization (WHO). *World Malaria Report 2019*. Geneva (2019).
2. World Health Organization (WHO). *World Malaria Report 2018*. Guinea (2018).
3. Phillips MA, Burrows JN, Manyando C, van Huijsduijnen RH, Van Voorhis WC, Wells TNC. Malaria. *Nat Rev Dis Prim.* (2017) 3:17050. doi: 10.1038/nrdp.2017.50
4. Brasil P, Zalis MG, de Pina-Costa A, Siqueira AM, Júnior CB, Silva S, et al. Outbreak of human malaria caused by *Plasmodium simium* in the atlantic forest in rio de janeiro: a molecular epidemiological investigation. *Lancet Glob Health.* (2017) 5:e1038–e1046. doi: 10.1016/S2214-109X(17)30333-9
5. Basu S, Sahi PK. Malaria: an update. *Ind J Pedi.* (2017) 84:521–8. doi: 10.1007/s12098-017-2332-2
6. World Health Organization (WHO). WHO severe malaria 2014. *Trop Med Int Health.* (2014) 19 Suppl 1:7–131. doi: 10.1111/tmi.12313_2
7. Alladi M, Surendra MK, Srinivas B. Acute lung injury and acute respiratory distress syndrome in malaria. *J Vector Borne Dis.* (2008) 45:179–93.
8. Leopold SJ, Ghose A, Plewes KA, Mazumder S, Pisani L, Kingston HWF, et al. Point-of-care lung ultrasound for the detection of pulmonary manifestations of malaria and sepsis: an observational study. *PLoS ONE.* (2018) 13:e0204832. doi: 10.1371/journal.pone.0204832
9. Riviello ED, Kiviri W, Twagirumugabe T, Mueller A, Banner-Goodspeed VM, Officer L, et al. Hospital incidence and outcomes of the acute respiratory distress syndrome using the kigali modification of the berlin definition. *Am J Resp Crit Care Med.* (2016) 193:52–9. doi: 10.1164/rccm.201503-0584OC
10. Souza MC, Tatiana PA, Maria das Graças H. Multiple organ dysfunction during severe malaria: the role of the inflammatory response world's largest science, technology & medicine. In: *Current Topics in Malaria*. Rijeka: InTech. (2015). p. 85–104.
11. Hwang J, Cullen KA, Kachur SP, Arguin PM, Baird JK. Severe morbidity and mortality risk from malaria in the United States, 1985 – 2011. *Open Forum Infect Dis.* (2014) 1:ofu034. doi: 10.1093/ofid/ofu034
12. Haydoura S, Mazboudi O, Charafeddine K, Bouakl I, Baban TA, Taher AT. Transfusion-related plasmodium ovale malaria complicated by acute respiratory distress syndrome (ARDS) in a non-endemic country. *Parasitol Int.* (2011) 60:114–6. doi: 10.1016/j.parint.2010.10.005
13. Seilmaier M, Hartmann W, Beissner M, Fenzl T, Haller C, Guggemos W, et al. Severe *Plasmodium knowlesi* infection with multi-organ failure imported to Germany from Thailand/Myanmar. *Malaria J.* (2014) 13:422. doi: 10.1186/1475-2875-13-422
14. Mohapatra BN, Jangid SK, Mohanty R. GCRBS score: a new scoring system for predicting outcome in severe *Falciparum malaria*. *J Assoc Phys India.* (2014) 62:14–7.
15. Sulaiman H, Ismail MD, Jalalonmuhali M, Atiya N, Ponnampalavanar S. Severe *Plasmodium falciparum* infection mimicking acute myocardial infarction. *Malaria J.* (2014) 13:341. doi: 10.1186/1475-2875-13-341
16. Lacerda MV, Fragoso SC, Alecrim MG, Alexandre MA, Magalhães BM, Siqueira AM, et al. Postmortem characterization of patients with clinical diagnosis of plasmodium vivax malaria: to what extent does this parasite kill? *Clin Infect Dis.* (2012) 55:67–74. doi: 10.1093/cid/cis615
17. Londhe C, Ganeriwal A, deSouza R. Study of clinical profile of acute respiratory distress syndrome and acute lung injury in *Plasmodium vivax* malaria. *J Vector Borne Dis.* (2014) 51:339–42.
18. Maguire GP, Handojo T, Pain MC, Kenangalem E, Price RN, Tjitra E, et al. Lung injury in uncomplicated and severe falciparum malaria: a longitudinal study in Papua, Indonesia. *J Infect Dis.* (2005) 192:1966–74. doi: 10.1086/497697
19. Ramos Júnior WM, Sardinha JF, Costa MR, Santana MS, Alecrim MG, Lacerda MV. Clinical aspects of hemolysis in patients with *P. vivax* malaria treated with primaquine, in the Brazilian Amazon. *Brazil J Infect Dis.* (2010) 14:410–2. doi: 10.1016/S1413-8670(10)70084-2
20. Taylor WRJ, Hanson J, Turner GDH, White NJ, Dondorp AM. Respiratory manifestations of malaria. *Chest*. (2012) 142:492–505. doi: 10.1378/chest.11-2655
21. de Souza JB, Hafalla JC, Riley EM, Couper KN. Cerebral malaria: why experimental murine models are required to understand the pathogenesis of disease. *Parasitology.* (2009) 137:755–72. doi: 10.1017/S0031182009991715
22. Pádua TA, Torres ND, Candéa ALP, Costa MFS, Silva JD, Silva-Filho JL, et al. Therapeutic effect of lipoxin a4 in malaria-induced acute lung injury. *J Leukoc Biol.* (2018) 103:657–70. doi: 10.1002/JLB.3A1016-435RRR
23. Carla C, Samantha N, Teng Y, Akhila B, Howland W, Becht S, et al. Lung endothelial cell antigen cross-presentation to CD8+T cells drives malaria-associated lung injury. *Nat Commun.* (2019) 10:4241. doi: 10.1038/s41467-019-12017-8
24. Van den Steen PE, Geurts N, Deroost K, Van Aelst I, Verhenne S, Heremans H, et al. Immunopathology and dexamethasone therapy in a new model for malaria-associated acute respiratory distress syndrome. *Am J Resp Crit Care Med.* (2010) 181:957–68. doi: 10.1164/rccm.200905-0786OC
25. Pham TT, Verheijen M, Vandermosten L, Deroost K, Knoops S, Van den Eynde K, et al. Pathogenic CD8+ T cells cause increased levels of VEGF-A in experimental malaria-associated acute respiratory distress syndrome, but therapeutic VEGFR inhibition is not effective. *Front Cell Infect Microbiol.* (2017) 7:416. doi: 10.3389/fcimb.2017.00416
26. Epiphanio S, Campos MG, Pamplona A, Carapau D, Pena AC, Ataíde R, et al. VEGF promotes malaria-associated acute lung injury in mice. *PLoS Pathog.* (2010) 6:1–10. doi: 10.1371/journal.ppat.1000916
27. Carvalho LJM, Lenzi HL, Pelajo-Machado M, Oliveira DN, Daniel-Ribeiro CT, Ferreira-da-Cruz MF. *Plasmodium berghei*: cerebral malaria in CBA mice is not clearly related to plasma TNF levels or intensity of histopathological changes. *Exp Parasitol.* (2000) 95:1–7. doi: 10.1006/expr.2000.4508

28. Pereira MLM, Marinho CRF, Epiphanio S. Could heme oxygenase-1 be a new target for therapeutic intervention in malaria-associated acute lung injury/acute respiratory distress syndrome? *Front Cell Infect Microbiol.* (2018) 8:161. doi: 10.3389/fcimb.2018.00161
29. Souza MC, Silva JD, Pádua TA, Capelozzi VL, Rocco PR, da Henriques M. Early and late acute lung injury and their association with distal organ damage in murine malaria. *Resp Physiol Neurobiol.* (2013) 186:65–72. doi: 10.1016/j.resp.2012.12.008
30. Franke-Fayard B, Janse CJ, Cunha-Rodrigues M, Ramesar J, Büscher P, Que I, et al. Murine malaria parasite sequestration: CD36 is the major receptor, but cerebral pathology is unlinked to sequestration. *Proc Natl Acad Sci USA.* (2005) 102:11468–73. doi: 10.1073/pnas.0503386102
31. Tohru F, Hideo H. Biology of heme in mammalian erythroid cells and related disorders. *BioMed Research Int.* (2015) 2015:278536. doi: 10.1155/2015/278536
32. Quaye IK. Extracellular hemoglobin: the case of a friend turned foe. *Front Physiol.* (2015) 6:96. doi: 10.3389/fphys.2015.00096
33. Das D, Tarafdar PK, Chakrabarti A. Structure-activity relationship of heme and its analogues in membrane damage and inhibition of fusion. *FEBS Lett.* (2018) 592:2458–65. doi: 10.1002/1873-3468.13165
34. Umbreit J. Methemoglobin—it's not just blue: a concise review. *Am J Hematol.* (2007) 82:807–11. doi: 10.1002/ajh.20738
35. Gianrico F, Joseph SH. Carbon monoxide, hydrogen sulfide, and nitric oxide as signaling molecules in the gastrointestinal tract. *Gastroenterology.* (2014) 147:303–13. doi: 10.1053/j.gastro.2014.04.041
36. Schmidt HM, Kelley EE, Straub AC. The impact of xanthine oxidase (XO) on hemolytic diseases. *Redox Biol.* (2019) 21:101072. doi: 10.1016/j.redox.2018.101072
37. Ascenzi P, Bocedi A, Visca P, Altruda F, Tolosano E, Beringhelli T, et al. Hemoglobin and heme scavenging. *IUBMB Life.* (2005) 57:749–59. doi: 10.1080/15216540500380871
38. Sigala PA, Goldberg DE. The peculiarities and paradoxes of Plasmodium heme metabolism. *Ann Rev Microbiol.* (2014) 68:259–78. doi: 10.1146/annurev-micro-091313-103537
39. Schaer DJ, Vinchi F, Ingoglia G, Tolosano E, Buehler PW. Haptoglobin, hemopexin and related defense pathways-basic science, clinical perspectives and drug development. *Front Physiol.* (2014) 5:415. doi: 10.3389/fphys.2014.00415
40. Immenschuh S, Vijayan V, Janciauskiene S, Gueler F. Heme as a target for therapeutic interventions. *Front Pharmacol.* (2017) 8:146. doi: 10.3389/fphar.2017.00146
41. Man SS. Reactive oxygen and nitrogen species in pathogenesis of vascular complications of diabetes. *Diab Metab J.* (2012) 36:190–8. doi: 10.4093/dmj.2012.36.3.190
42. Aslan M, Ryan TM, Adler B, Townes TM, Parks DA, Thompson JA, et al. Oxygen radical inhibition of nitric oxide-dependent vascular function in sickle cell disease. *Proc Natl Acad Sci USA.* (2001) 98:15215–20. doi: 10.1073/pnas.221292098
43. Vinchi F, Costa da Silva M, Ingoglia G, Petrillo S, Brinkman N, Zuercher A, et al. Hemopexin therapy reverts heme-induced proinflammatory phenotypic switching of macrophages in a mouse model of sickle cell disease. *Blood.* (2016) 127:473–86. doi: 10.1182/blood-2015-08-663245
44. Matthews K, Duffy SP, Myrand-Lapierre ME, Ang RR, Li L, Scott MD, et al. Microfluidic analysis of red blood cell deformability as a means to assess hemin-induced oxidative stress resulting from *Plasmodium falciparum* intraerythrocytic parasitism. *Integr Biol.* (2017) 9:519–28. doi: 10.1039/c7ib00039a
45. Krugliak M, Zhang J, Ginsburg H. Intraerythrocytic *Plasmodium falciparum* utilizes only a fraction of the amino acids derived from the digestion of host cell cytosol for the biosynthesis of its proteins. *Mol Biochem Parasitol.* (2002) 119:249–56. doi: 10.1016/S0166-6851(01)00427-3
46. Timothy EJ. Haemozoin formation. *Mol Biochem Parasitol.* (2008) 157:127–36. doi: 10.1016/j.molbiopara.2007.11.005
47. Olivier M, Van Den Ham K, Shio MT, Kassa FA, Fougeray S. Malarial pigment hemozoin and the innate inflammatory response. *Front Immunol.* (2014) 5:25. doi: 10.3389/fimmu.2014.00025
48. Nguyen PH, Day N, Pram TD, Ferguson DJ, White NJ. Intraleucocytic malaria pigment and prognosis in severe malaria. *Trans R Soc Trop Med Hyg.* (1995) 89:200–4. doi: 10.1016/0035-9203(95)90496-4
49. Maknitikul S, Luplertlop N, Grau GER, Ampawong S. Dysregulation of pulmonary endothelial protein C receptor and thrombomodulin in severe falciparum malaria-associated ARDS relevant to hemozoin. *PLoS ONE.* (2017) 12:e0181674. doi: 10.1371/journal.pone.0181674
50. Maknitikul S, Luplertlop N, Chaisri U, Maneerat Y, Ampawong S. Featured article: immunomodulatory effect of hemozoin on pneumocyte apoptosis via CARD9 pathway, a possibly retarding pulmonary resolution. *Exp Biol Med.* (2018) 243:395–407. doi: 10.1177/1535370218757458
51. Deroost K, Tyberghein A, Lays N, Noppen S, Schwarzer E, Vanstreels E, et al. Hemozoin induces lung inflammation and correlates with malaria-associated acute respiratory distress syndrome. *Am J Resp Cell Mol Biol.* (2013) 48:589–600. doi: 10.1165/rcmb.2012-0450OC
52. Coban C, Ishii KJ, Kawai T, Hemmi H, Sato S, Uematsu S, et al. Toll-like receptor 9 mediates innate immune activation by the malaria pigment hemozoin. *J Exp Med.* (2005) 201:19–25. doi: 10.1084/jem.20041836
53. Parroche P, Lauw FN, Goutagny N, Latz E, Monks BG, Visintin A, et al. Malaria hemozoin is immunologically inert but radically enhances innate responses by presenting malaria DNA to toll-like receptor 9. *Proc Natl Acad Sci USA.* (2007) 104:1919–24. doi: 10.1073/pnas.0608745104
54. Giribaldi G, Prato M, Ulliers D, Gallo V, Schwarzer E, Akide-Ndunge OB, et al. Involvement of inflammatory chemokines in survival of human monocytes fed with malarial pigment. *Infect Immun.* (2010) 78:4912–21. doi: 10.1128/IAI.00455-10
55. Jaramillo M, Godbout M, Olivier M. Hemozoin induces macrophage chemokine expression through oxidative stress-dependent and -independent mechanisms. *J Immunol.* (2005) 174:475–84. doi: 10.4049/jimmunol.174.1.475
56. Nguyen Tien H, Xuan TDT, Tohru K, Motohiro S, Katsuya S, Shigeharu H, et al. Leukocyte activation by malarial pigment. *Parasitol Int.* (2006) 55:75–81. doi: 10.1016/j.parint.2005.10.003
57. Amani V, Boubou MI, Pied S, Marussig M, Walliker D, Mazier D, et al. Cloned lines of *Plasmodium berghei* ANKA differ in their abilities to induce experimental cerebral malaria. *Infect Immun.* (1998) 66:4093–9. doi: 10.1128/.66.9.4093-4099.1998
58. Pamplona A, Ferreira A, Balla J, Jeney V, Balla G, Epiphanio S. Heme oxygenase-1 and carbon monoxide suppress the pathogenesis of experimental cerebral malaria. *Nat Med.* (2007) 13:703–10. doi: 10.1038/nm1586
59. Liu M, Amodu AS, Pitts S, Patrickson J, Hibbert JM, Battle M, et al. Heme mediated STAT3 activation in severe malaria. *PLoS ONE.* (2012) 7:e34280. doi: 10.1371/journal.pone.0034280
60. Ferreira A, Marguti I, Bechmann I, Jeney V, Chora A, Palha NR. Sickle hemoglobin confers tolerance to plasmodium infection. *Cell.* (2011) 145:398–409. doi: 10.1016/j.cell.2011.03.049
61. Frimat M, Boudhabhay I, Roumenina LT. Hemolysis derived products toxicity and endothelium: model of the second hit. *Toxins.* (2019) 11:660. doi: 10.3390/toxins11110660
62. Pereira ML, Ortolan LS, Sercundes MK, Debone D, Murillo O, Lima FA. Association of heme oxygenase 1 with lung protection in malaria-associated ALI/ARDS. *Med Inflam.* (2016) 2016:4158698. doi: 10.1155/2016/4158698

Conflict of Interest: The authors declare that the research was conducted in the absence of any commercial or financial relationships that could be construed as a potential conflict of interest.

frontiers in Immunology

ORIGINAL RESEARCH
published: 15 October 2020
doi: 10.3389/fimmu.2020.561947

Spatiotemporal Alterations in Gait in Humanized Transgenic Sickle Mice

*Stacy Kiven[1,2], Ying Wang[3], Anupam Aich[1], Donovan A. Argueta[1], Jianxun Lei[2], Varun Sagi[2], Madhushan Tennakoon[2], Saad J. Bedros[4], Nils Lambrecht[5] and Kalpna Gupta[1,2,6]**

[1] Hematology/Oncology, Department of Medicine, University of California, Irvine, Irvine, CA, United States, [2] Division of Hematology, Oncology and Transplantation, Department of Medicine, Vascular Biology Center, University of Minnesota, Minneapolis, MN, United States, [3] Department of Anesthesia, Stark Neuroscience Research Institute, Indiana University School of Medicine, Indianapolis, IN, United States, [4] College of Science & Engineering, University of Minnesota, Minneapolis, MN, United States, [5] Pathology and Laboratory Medicine, Long Beach VA Healthcare System, Long Beach, CA, United States, [6] Southern California Institute for Research and Education, Long Beach VA Healthcare System, Long Beach, CA, United States

Sickle cell disease (SCD) is a hemoglobinopathy affecting multiple organs and featuring acute and chronic pain. Purkinje cell damage and hyperalgesia have been demonstrated in transgenic sickle mice. Purkinje cells are associated with movement and neural function which may influence pain. We hypothesized that Purkinje cell damage and/or chronic pain burden provoke compensatory gait changes in sickle mice. We found that Purkinje cells undergoe increased apoptosis as shown by caspase-3 activation. Using an automated gait measurement system, MouseWalker, we characterized spatiotemporal gait characteristics of humanized transgenic BERK sickle mice in comparison to control mice. Sickle mice showed alteration in stance instability and dynamic gait parameters (walking speed, stance duration, swing duration and specific swing indices). Differences in stance instability may reflect motor dysfunction due to damaged Purkinje cells. Alterations in diagonal and all stance indices indicative of hesitation during walking may originate from motor dysfunction and/or arise from fear and/or anticipation of movement-evoked pain. We also demonstrate that stance duration, diagonal swing indices and all stance indices correlate with both mechanical and deep tissue hyperalgesia, while stance instability correlates with only deep tissue hyperalgesia. Therefore, objective analysis of gait in SCD may provide insights into neurological impairment and pain states.

Keywords: purkinje cell, sickle cell disease, gait, hyperalgesia, histopathology

OPEN ACCESS

Edited by:
Renata Sesti-Costa, Campinas State University, Brazil

Reviewed by:
Robert Campbell, The University of Utah, United States
Kempuraj Duraisamy, University of Missouri, United States
Manu Platt, Georgia Institute of Technology, United States

***Correspondence:**
Kalpna Gupta
kalpnag@hs.uci.edu

Specialty section:
This article was submitted to Inflammation, a section of the journal Frontiers in Immunology

Received: *14 May 2020*
Accepted: *07 September 2020*
Published: *15 October 2020*

Citation:
Kiven S, Wang Y, Aich A, Argueta DA, Lei J, Sagi V, Tennakoon M, Bedros SJ, Lambrecht N and Gupta K (2020) Spatiotemporal Alterations in Gait in Humanized Transgenic Sickle Mice. Front. Immunol. 11:561947. doi: 10.3389/fimmu.2020.561947

INTRODUCTION

Chronic pain and organ damage are major comorbidities of sickle cell disease (SCD) (1–5). Organ pathology has been observed in humanized sickle mice, which show several clinical features of SCD including chronic pain and multi-organ pathology (6, 7). Interestingly, Purkinje cell damage in the brain of the HbSS-BERK mice has been previously observed (6). Purkinje cells are the principal output neurons of the cerebellar cortical microcircuit, and thus play a fundamental role in coordinating cerebellar function by integrating massive excitatory synaptic input, as well as firing high–frequency and highly regular action potentials in the absence of synaptic drive (8). Purkinje cell malfunction has been observed in mouse models of several forms of ataxia, which exhibit

alterations in gait (9, 10). Since Purkinje cells regulate the sensory-motor functions, it is likely that the pathological changes in Purkinje cells of sickle mice may contribute to alterations in gait.

The Pain in Sickle Cell Epidemiology Study (PiSCES) cohort demonstrated that the adult sickle population suffers from knee-skin, lower back, and hip pain for about one-third of the chronic pain days (11). Additionally, bone complications-associated joint pain is common in SCD with about 50% adults developing avascular osteonecrosis due to loss of blood supply to the femoral head in addition to osteoporosis and osteopenia (12–14). Femurs from transgenic sickle mice exhibit altered microstructure with 40% reduced mechanical strength compared to control mice (15). In addition to sudden and intractable acute pain, chronic joint and back pain in combination with reduced bone strength could contribute to difficulty in mobility and subsequent postural adjustment to compensate for the pain, i.e., change in gait (16). Therefore, gait patterns in SCD can be a result of compensatory adaptation to avoid movement-evoked pain in addition to alterations in gait due to Purkinje cell damage.

Analysis of dynamic gait parameters such as walking speed, stand/swing duration, and step length are of interest for assessing locomotion function in many motion-affected human conditions (17). Automated gait measurement has also been used as an objective measure of pain in inflammatory and neuropathic pain models in mice (18). In the present study, we evaluated the Purkinje cell pathology and gait changes in transgenic HbSS-BERK sickle mice compared to HbAA-BERK control mice. We utilized the novel video-based automated "MouseWalker" system to analyze gait and simultaneously examine the correlation of hyperalgesia with gait in sickle mice.

MATERIALS AND METHODS

Animals

We used a total of 24 mice consisting of control (HbAA-BERK) and sickle (HbSS-BERK), hereafter referred to as control and sickle mice, respectively. All mice were bred and raised in-house with *ad libitum* access to food and water on a 12-h light/dark cycle in conventional housing and used at ∼3.5 months of age (7). Control and sickle mice are homozygous for knockout of both murine α and β globins. Control mice express normal human hemoglobin A and sickle mice express human α and β^S globin chains with >99% human hemoglobin S, but no murine α or β globin (19). Sickle mice show similarities with human SCD including erythrocytic sickling, intravascular hemolysis, reticulocytosis, severe anemia (hematocrit, 10–30%), leukocytosis, elevation of inflammatory cytokines, pulmonary congestion, and shortened life-span (6, 20, 21). Interestingly, increased multiorgan infarcts and pyknotic Purkinje cells have been observed in sickle mice compared to non-sickle control mice (6, 22). Sickle pain is characteristically complex in nature with nociceptive, neuropathic, and inflammatory components in its etiology (1, 2). Humanized HbSS-BERK sickle mice exhibit enhanced mechanical, thermal and deep tissue hyperalgesia compared to control mice (23, 24). All mice were validated by phenotyping for sickle and normal human hemoglobin by isoelectric focusing as previously described (7).

Assessment of Hyperalgesia

Mice were acclimatized to each test protocol in a quiet room at constant temperature, and tested for mechanical (von Frey) and spontaneous musculoskeletal/deep (grip force) as previously described (7, 23). Behavioral tests were performed consecutively at a 5-min interval between tests, in a double-blind manner.

Mechanical hyperalgesia was measured by applying a 1.0 g (4.08 mN) von Frey (Semmes-Weinstein) monofilament (Stoelting Co, Wood Dale, IL) to the mid-plantar surface of each hindpaw for a total of 10 trials per hindpaw with a 5-s inter-stimulus interval, and paw withdrawal frequency (PWF) was recorded. Deep tissue/musculoskeletal hyperalgesia was assessed by placing mice on a wire-mesh gauge by their forepaws, and the peak grip force exerted in grams was recorded by a computerized grip-force meter (SA Maier Co, Milwaukee, WI).

Histopathological Analysis

Whole brains were collected immediately following euthanasia and fixed in 10% formalin (575A-14 43 mm; Medical Chemical Corporation, Torrance, CA, USA). Using routine histology methods, fixed tissues were processed, embedded in paraffin, and sections were stained with hematoxylin and eosin (H&E) or with routine immunohistochemical methods. H&E stained sections were analyzed using a Nikon eclipse 50i light microscope equipped with a 10× ocular with an edged-in 1 mm scale with 0.01 mm divisions calibrated to the 10× objective. Images were acquired by an attached Nikon DS-Fi1 camera.

Immunohistochemistry

Slides with 5 μm sections of brain were deparaffinized and rehydrated with Histo-Clear (National Diagnostics, Atlanta, GA, USA) and ethanol gradient, respectively. Sections were processed for cleaved caspase-3 (an activated form) detection to assess Purkinje cell apoptosis. Antigen retrieval was performed with Target Retrieval Solution (Agilent, Santa Clara, CA, USA), and subsequently processed with ABC detection kit (ab64261; Abcam, Cambridge, MA, USA). Endogenous peroxidase was inactivated by incubating with manufacturer-provided hydrogen peroxide solution (Abcam) for 10 min. Non-specific binding was blocked with blocking solution (Abcam) for additional 10 min. Sections were incubated for 1 h at room temperature in 1:500 rabbit anti-mouse cleaved caspase-3 primary antibody (ab2302; Abcam), then in prediluted biotinylated goat-anti rabbit secondary antibody (Abcam). Slides were then incubated for 10 min with streptavidin peroxidase and stained with DAB chromagen (Abcam), after which samples were counterstained with hematoxylin. Slides were dehydrated with ethanol gradient and Histo-Clear before cover slipping. Stained sections were examined and analyzed by a board-certified surgical pathologist with expertise in mouse histopathology, in a double-blind manner.

Assessment of Gait

The MouseWalker system was assembled in our laboratory following the design described for gait measurement of mice (25). Each mouse was individually placed in a transparent corridor (8 × 80 cm^2) with acrylic glass floor panel mounted with LED lights, which produced a detectable touch sensor. Total internal reflection (TIR) of the LEDs in the acrylic surface was measured with embedded light sensors. During mouse natural walking gait, foot contact disrupted TIR causing frustrated total internal reflection (fTIR) within the transparent material. The fTIR-illuminated points of contact were detected by a high-speed CMOS camera (Lumenera Lt425C, Lumenera Corporation, Ottawa, Ontario) with a 16 mm lens. Constant background lighting was established with a backlit board placed 40 cm over the corridor, which comprised two colored LEDs and aluminum bar sets (HL-LS5050_RGB300NW44K, HitLights, LA, USA; 9001 K25, MacMaster-Carr, IL, USA). The light color was set by a controller box and remote control. The background light and fTIR light were set to blue (intensity: 60%) and white (intensity: 100%), respectively, for optimum video quality. High-performance digital video recording software was used (StreamPix 7, Norpix, Montreal, Quebec) at a resolution of 2048 × 2048 for data analysis. Mice were habituated in the corridor during the 3 days prior to experiment date. Four videos were acquired of each mouse and 2 videos of uninterrupted walking were selected and analyzed. The MouseWalker program was run in Matlab (The Mathworks, MA, USA). Both the program and manual are available online (biooptics.markalab.org). Matlab software was used to distinguish the footprints from background, and convert the videos to grayscale prior

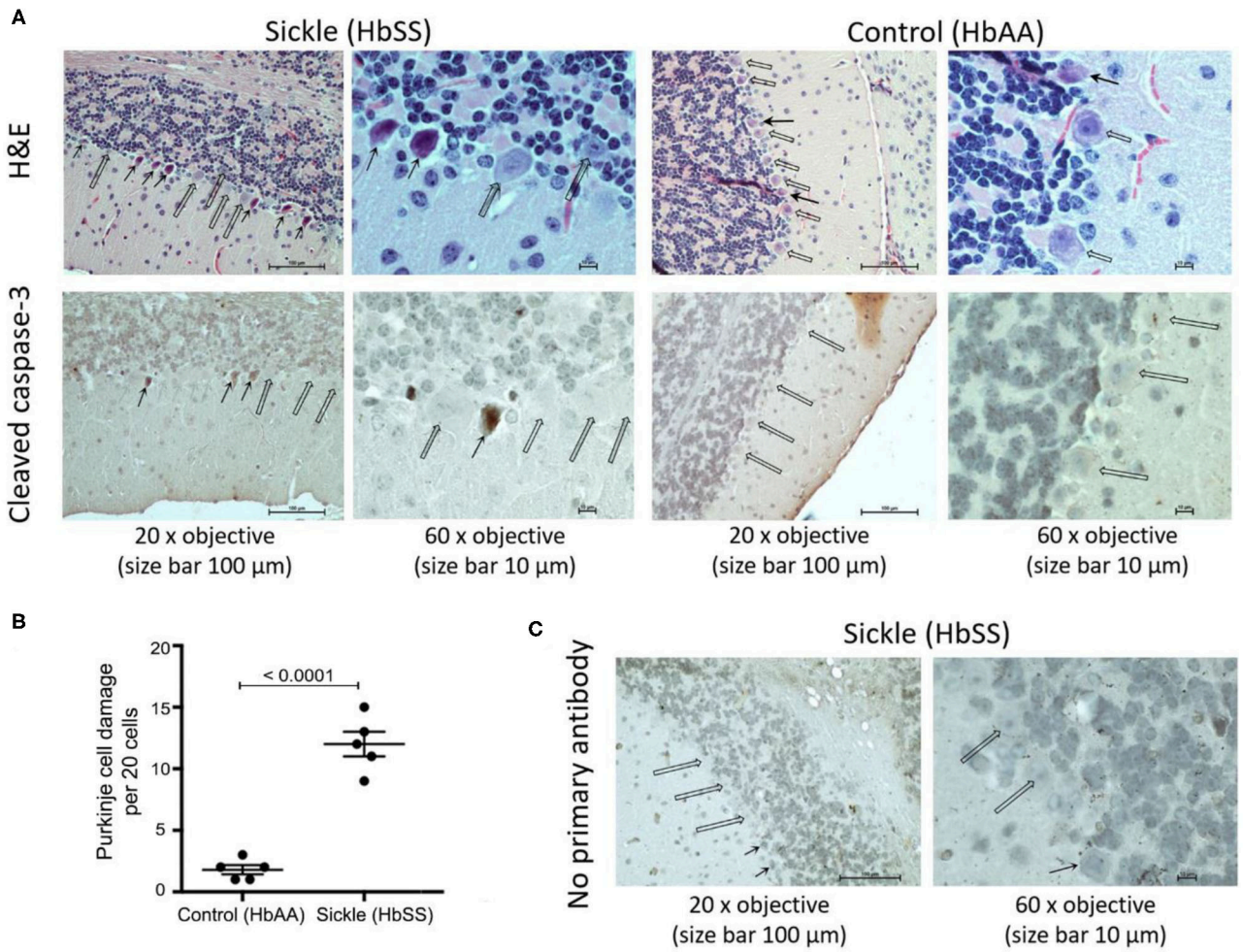

FIGURE 1 | Sickle mice show increased Purkinje cell damage compared to control mice. Cerebellum from ~3.5 month old female HbSS-BERK sickle and HbAA-BERK control mice. **(A)** H&E and capase-3 stained sections of cerebellum at 20x objective, size bar 100 µm and at 60x objective, size bar 10 µm. Open arrows: normal Purkinje cells with well-organized nucleus. Solid arrows: apoptotic Purkinje cells with smudged and irregular nuclei with condensed chromatin. **(B)** Quantification of Purkinje cell apoptosis per 20 cells/mouse brain from 5 control 5 sickle mice (unpaired two-tailed *t*-test). **(C)** Incubation of sickle mice brain sections without primary antibody showed no cross reactivity with secondary antibody as a negative control. Open arrows: normal Purkinje cells. Solid arrows: apoptotic Purkinje cells with smudged irregular nuclei.

to analysis in the MouseWalker software. The mislabeled footprints or body features were manually adjusted following automatic detection with MouseWalker software. Gait-related parameters including walking speed, stance instability, and stance duration were extracted and exported from the MouseWalker software to determine correlation with measures of hyperalgesia.

Statistical Analysis

All data were analyzed using Prism software (v 6.0f, GraphPad Prism Inc., San Diego, CA). Data between groups were analyzed using 1-way analysis of variance (ANOVA) with *post hoc* Bonferroni's multiple comparisons. Data within groups were compared using 2-way repeated measures ANOVA with *post hoc* Bonferroni's/Sidak's multiple comparisons tests. Gait parameters were analyzed using Student's unpaired two-tailed *t*-test, and Pearson correlation analysis was performed to detect associations of gait parameters with hyperalgesia—normality of data for correlation analysis was determined with Anderson-Darling test. A $p < 0.05$ was considered statistically significant. All data are represented as mean ± SEM.

RESULTS

Increased Purkinje Cell Apoptosis in the Cerebellum of Sickle Mice

H&E staining shows that Purkinje cells in control mice have a well-shaped nucleus, finely granular distributed chromatin, and an intact nucleolus (**Figure 1A**, open arrows). In contrast, H&E stained sections from sickle mice brains show morphological features of apoptosis in Purkinje cells with a smudged nucleus with condensed chromatin and lack of a well-formed nucleolus (**Figure 1A**, solid arrows). Cellular apoptosis was further validated by immunostaining the brain section with cleaved caspase-3 (active form), a critical protease in the pro-apoptosis pathway (26–29). Purkinje cells of control mice did not show the expression of cleaved caspase-3, consistent with histopathological observations of intact nucleus and well-shaped cellular morphology. However, Purkinje cells of sickle mice clearly showed cleaved caspase-3 immunoreactivity, consistent with histopathology suggestive of apoptosis (**Figure 1A**, solid arrows). Purkinje cell apoptosis was quantified by counting the number of damaged cells per 20 cells/brain of each mouse. Sickle mice showed significantly more Purkinje cell apoptosis compared to control mice (**Figure 1B**; $p \leq 0.0001$). These

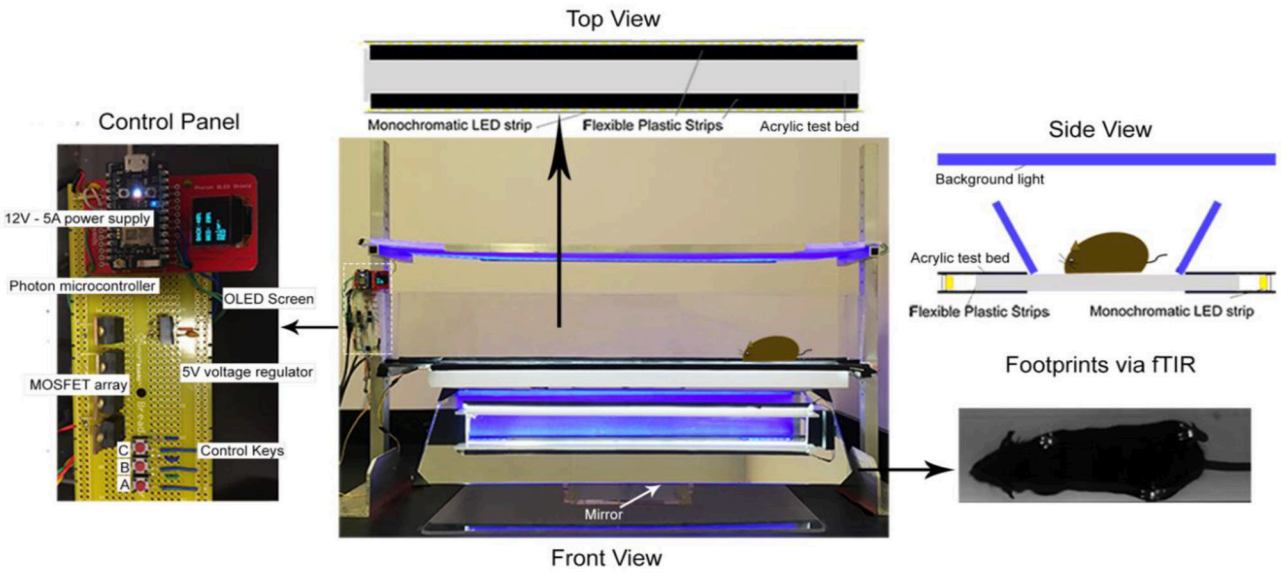

FIGURE 2 | MouseWalker Apparatus. Each mouse was individually placed in a transparent corridor (8 × 80 cm^2) with acrylic glass floor panel mounted with LED lights, which produced a detectable touch sensor. Total internal reflection (TIR) of the LEDs in the acrylic surface was measured with embedded light sensors. During natural walking, foot contact disrupted TIR causing frustrated total internal reflection (fTIR) within the transparent material. The fTIR illuminated points of contact, which were detected by a high-speed CMOS camera (Lumenera Lt425C, Lumenera Corporation, Ottawa, Ontario) with a 16 mm lens. Constant background lighting was established with a backlit board placed 40 cm over the corridor, which comprised two-colored LEDs and aluminum bar sets (HL-LS5050_RGB300NW44K, HitLights, LA, USA; 9001 K25, MacMaster-Carr, IL, USA). The light color was set by a controller box and remote control. The background light and FTIR light were set to blue (intensity: 60%) and white (intensity: 100%), respectively, for optimum video quality. High-performance digital video recording software was used (StreamPix 7, Norpix, Montreal, Quebec) at a resolution of 2048 × 2048 for data assessment. Mice were habituated in the corridor during 3 days before experiment date. Four videos were taken of each mouse and 2 videos of uninterrupted walking were selected and analyzed. The MouseWalker program was developed and compiled in MATLAB (The Mathworks, MA, USA). Matlab software was used to distinguish the footprints from background and convert the videos to grayscale prior to analysis in the MouseWalker software. The mislabeled footprints or body features were manually adjusted following automatic detection with MouseWalker software. Gait-related parameters such as stance instability, walking speed, and swing/stance duration were extracted and exported from the MouseWalker software to determine correlation with measures of hyperalgesia.

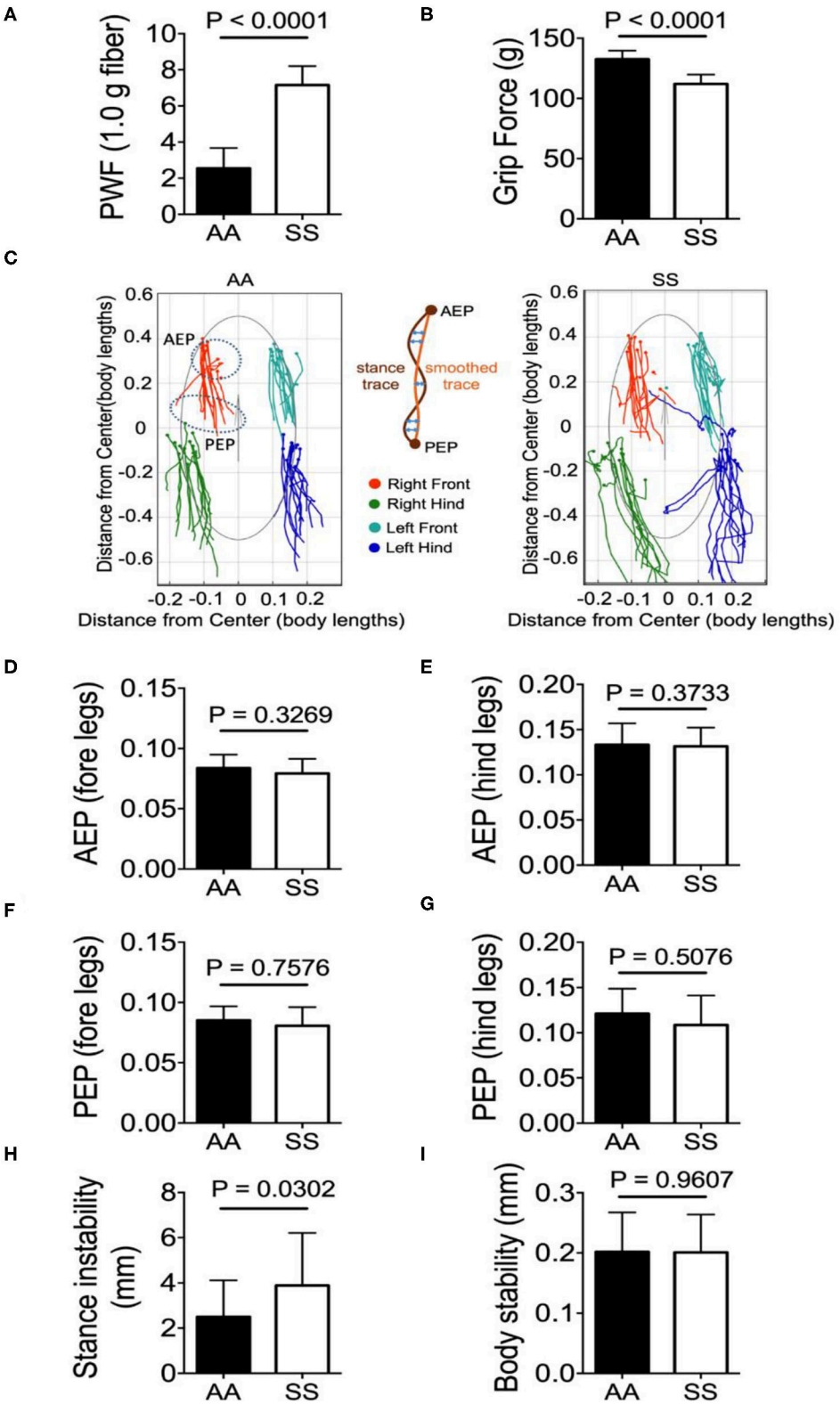

FIGURE 3 | Sickle mice with chronic pain present stance instability. Hyperalagesia and gait parameters were measured in the test groups of untreated HbSS-BERK sickle (SS) and HbAA-BERK control (AA) mice. **(A)** Mechanical hyperalgesia assessed by Paw Withdrawal Frequency (PWF) in response to 1.0-g von Frey filaments.

(Continued)

FIGURE 3 | Mechanical and **(B)** deep tissue hyperalgesia assessed by a computerized grip-force measure. **(C)** shows representative stance trace of one sickle (right) and control mouse (left) walking at 21.59 and 21.20 cm/s, respectively. The traces were determined by measuring the position of the stance phase footprints relative to the body center. The anterior extreme position (AEP) indicates stance onset and the posterior extreme position (PEP) indicates stance offset (positions encircled by a dashed line for the right fore paw). For each stance trace (maroon), a smoothed trace is generated (using data from every five frames; yellow trace), and the average of the difference between these two lines (orange arrows) corresponds to the stance instability. **(D,E)** Perpendicular AEP and **(F,G)** perpendicular PEP plots for both fore and hind legs, respectively. **(H,I)** show stance instability and body instability, respectively. Gait parameters were analyzed using Student's unpaired two-tailed *t*-test. Significance was determined by *t*-test (unpaired, two-tailed). A $p < 0.05$ was considered statistically significant. All data are represented as mean ± SEM. [$n = 7$ per group in **(A,B,D–I)**].

results (along with previous observations) indicate that Purkinje cell apoptosis is a characteristic feature of sickle pathobiology (**Figure 1C**). As Purkinje cell apoptosis is often associated with motor dysfunction, we tested whether sickle mice with chronic pain display altered gait compared to control mice, using our custom-built in-house *MouseWalker* platform (**Figure 2**).

Spatiotemporal Changes in Gait in Sickle Mice

Hyperalgesia and Stance Instability Are Significantly Higher in Sickle Mice

Mechanical hyperalgesia was assessed by quantifying the PWF in response to 10 applications of von Frey monofilaments to the hind paw of mice. Higher PWF is indicative of more pain, which was the case in sickle mice compared to control mice. Deep tissue hyperalgesia was measured by assessing the grip force applied by the fore limbs of the mouse while pulling a wire gauge. Mice with more pain exert lower force and sickle mice showed lower grip force compared to control mice. Together, these data show that sickle mice demonstrate significantly increased mechanical (**Figure 3A**; $p < 0.0001$) and deep tissue/musculoskeletal hyperalgesia (**Figure 3B**; $p < 0.0001$) compared to control mice.

All the gait and body parameters extracted from *MouseWalker* software were compared between sickle and control mice to examine the difference in walking speeds within the range of 10–40 cm/s. A single gait cycle of movement is known as stride that is divided into two major phases: stance phase and swing phase. The phase/duration in which the paw/foot stays in touch with the ground is referred to as stance phase and conversely, in the swing phase the paw/foot is not in contact with the ground. A major gait measure is the stance trace during the stride that is defined as the position of the foot relative to the center of the body from paw touchdown (anterior extreme position, AEP) to the end of the stance phase (posterior extreme position, PEP) and reflects the amount of body wobble during stance phases (25). Representative stance traces from a sickle and control mouse each with similar walking velocity (control: 14.50 cm/s, sickle: 14.56 cm/s) are presented (**Figure 3C**). Compared to the control mice, the stance traces of sickle mice at ∼14.50 cm/s displayed large variations of AEP and PEP for both fore- and hind-limbs with fore-limb traces being less variable than the hind-limb traces, although no statistical difference was observed (**Figures 3D–G**; $p = 0.3269$, $p = 0.3733$, $p = 0.7576$, $p = 0.5076$, respectively). Interestingly, sickle mice with pain showed significantly higher stance instability compared to control mice (**Figure 3H**; $P = 0.0302$) while the body stability remained similar among the two groups (**Figure 3I**; $p = 0.9607$). The stance instability is determined from the stance linearity index, which reflects the linearity of the stance traces by calculating the average difference between the actual stance trace and a smoothed version of the trace (25). Thus, higher stance instability in sickle mice may be indicative of locomotion abnormality either due to hyperalgesia or due to motor dysfunction suggested by Purkinje cell damage.

Stance and Swing Phase Durations Are Significantly Longer and Posit Non-uniform Distribution for Sickle Mice

Mendes et al. demonstrated that the step distances of C57BL/6J mice were exponentially increased with faster velocities (25). However, we have observed that the majority of sickle mice walked at a visibly lower velocity in comparison with control mice (**Figure 4A**; $p = 0.0062$), although the step lengths were similar (**Figure 4B**; $p = 0.5829$). Consistent with Mendes' study (25), we also observed a large variation in the stance duration (**Figure 4C**; $p = 0.0009$) and smaller variation of swing duration (**Figure 4D**; $p = 0.1009$) in both sickle and control mice which exponentially decreased as the speed increased [data not shown]. Lastly, stance phases lasted longer than swing phases at all speeds in both mice (**Figures 4C,D**). These data indicate that sickle mice inherently suffer from altered walking gait patterns that may have resulted from hyperalgesia/motor dysfunction.

Diagonal Swing Indices Are Decreased and All Stance Indices Are Significantly Increased for Sickle Mice

Walking/running gait involves swing modalities depending on how the legs are being moved/lifted during swing phase. We analyzed seven walking modes of leg combinations in sickle and control mice: no swing (stance), single-limb swing (lifting of one limb, four modes), diagonal-limb swing (lifting left/right fore limb with right/left hind limb, two modes), lateral-limb swing (both left or both right limbs, two modes), bound-limb swing (both hind or both fore legs, two modes), three-limb swing (lifting of any three legs, 4 modes), or all-limb swing (lifting of all limbs, one mode) (**Figure 4E**). A walking speed of 52.8 cm/s is the transitional speed from walking to running in which situation swing duration basically surpasses stance duration (25). Since we have only included sickle and control mice with walking speeds (10–40 cm/s) instead of running (>52.8 cm/s) speed, all swing indices turned out to be zero for both control and sickle mice, meaning at no point of time all the limbs were in the air (**Figure 4F**). Three limb swing and lateral swing indices

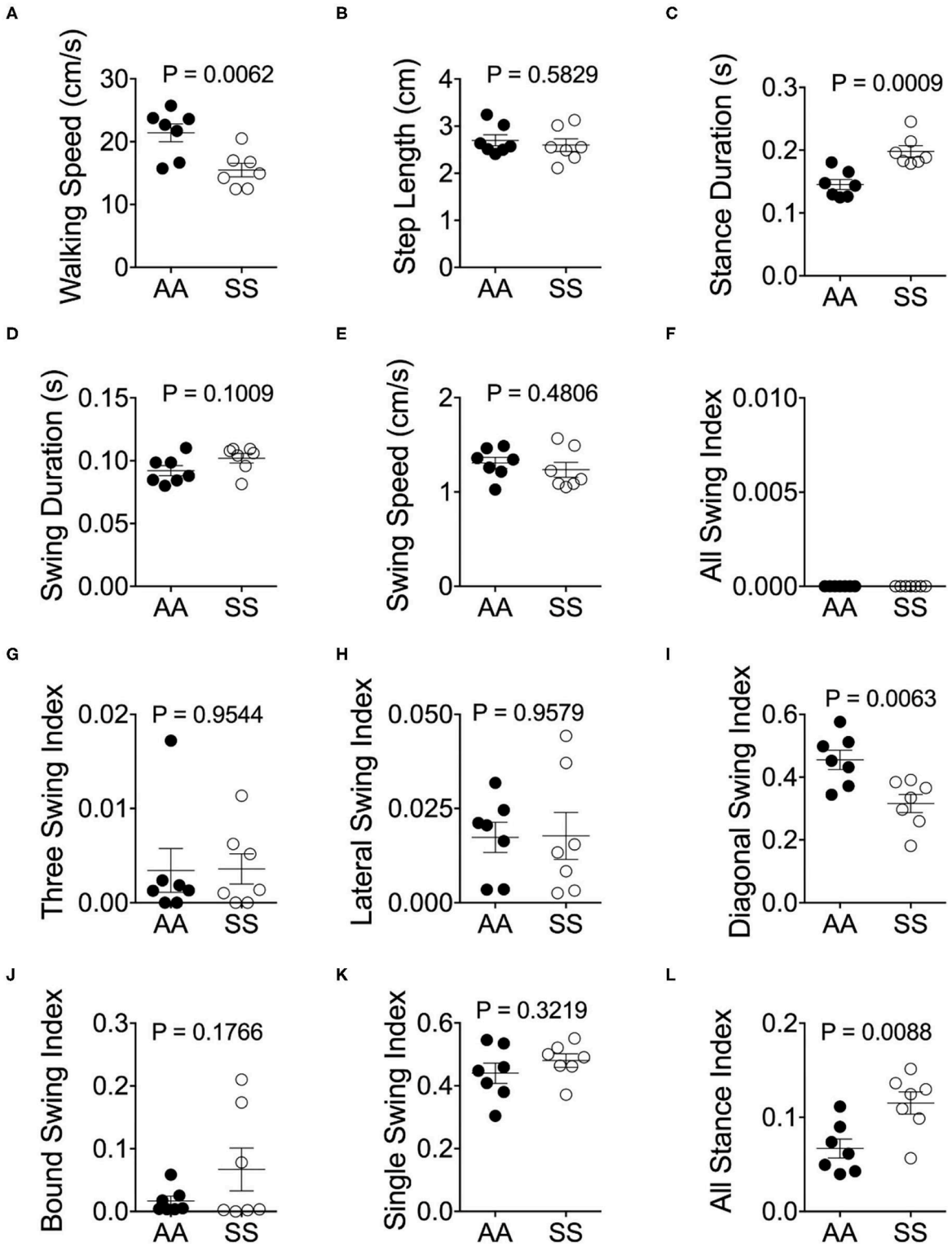

FIGURE 4 | Alterations of gait parameters in sickle mice. Gait parameters were analyzed and compared between HbSS-BERK sickle (SS) and HbAA-BERK control (AA) mice The average walking speed **(A)**, step length **(B)**, stance **(C)**, swing duration **(D)**, and swing speed **(E)**, were compared at walking speed between 10–40 cm/s. The seven stance indices of all-leg swing analyzed were **(F)**, three-leg swing **(G)**, lateral swing **(H)**, diagonal swing **(I)**, bound swing **(J)**, single swing **(K)**, and all stance **(L)**. Gait parameters were analyzed using Student's unpaired two-tailed *t*-test. Significance was determined by *t*-test (unpaired, two-tailed). [$n = 7$ per group in **(A–E)**]. **(F–H)** Individual results of 3 videos per mouse. A $p < 0.05$ was considered statistically significant. All data are represented as mean ± SEM.

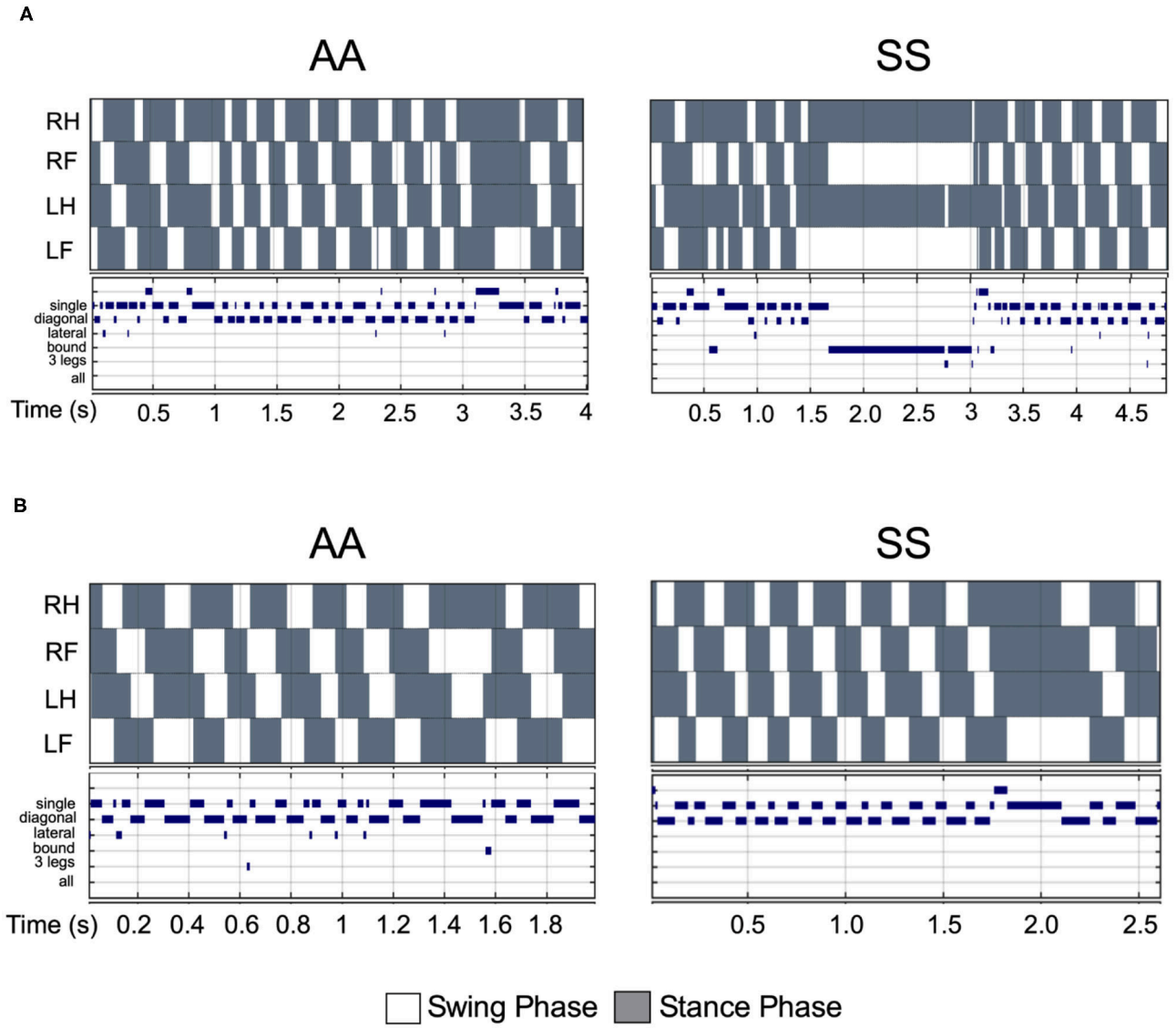

FIGURE 5 | Comparison of step pattern and modalities between sickle and control mice under same walking velocity. **(A)** Representative stance trace and gait parameters of inter-leg coordination of HbSS-BERK sickle (SS) and HbAA-BERK control (AA) mice with walking speeds at 14.50 and 14.56 cm/s, respectively. **(B)** Representative stance trace and gait parameters of inter-leg coordination of SS and AA mice with walking speeds at 21.2 and 21.59 cm/s, respectively. The upper images of all graphs are gait patterns are composed of two phases which are swing phase (white areas) and stance phase (gray areas). The lower panel shows step combinations.

approach "0" in both groups (**Figures 4G,H**; $p = 0.9544$ and $p = 0.9579$, respectively). Diagonal swing conformations were the most representative configuration and constituted more than 50% of the frames in our control mice and significantly reduced to 40% in sickle mice (**Figure 4I**; $p = 0.0063$). Moreover, BERK sickle mice showed increased but insignificant bound (**Figure 4J**; $p = 0.1766$) and single swing (**Figure 4K**; $p = 0.3219$) modality (vs. control mice). Consistent with our observation during the whole course of the experiment, the frequent hesitant stops in sickle mice resulted in significantly increased all stance index (**Figure 4L**; $p = 0.0088$). Moreover, compared to control mice, sickle mice with nearly the same walking speed showed unequally distributed gait patterns with more frequent swing phases (increased appearance of white squares) and extended stance duration (elongated gray square) at certain points, leading to an incoherent walking speed with frequently altered gait patterns (**Figures 5A,B**). Cumulatively, these data indicate an important behavioral aspect of sickle mice—a hesitation in breaking inertia to move on to the next phase, be it swing or stance phase. This hesitation may be a reflection of motor dysfunction due to Purkinje cell damage or may result from fear or anticipation of movement-evoked pain.

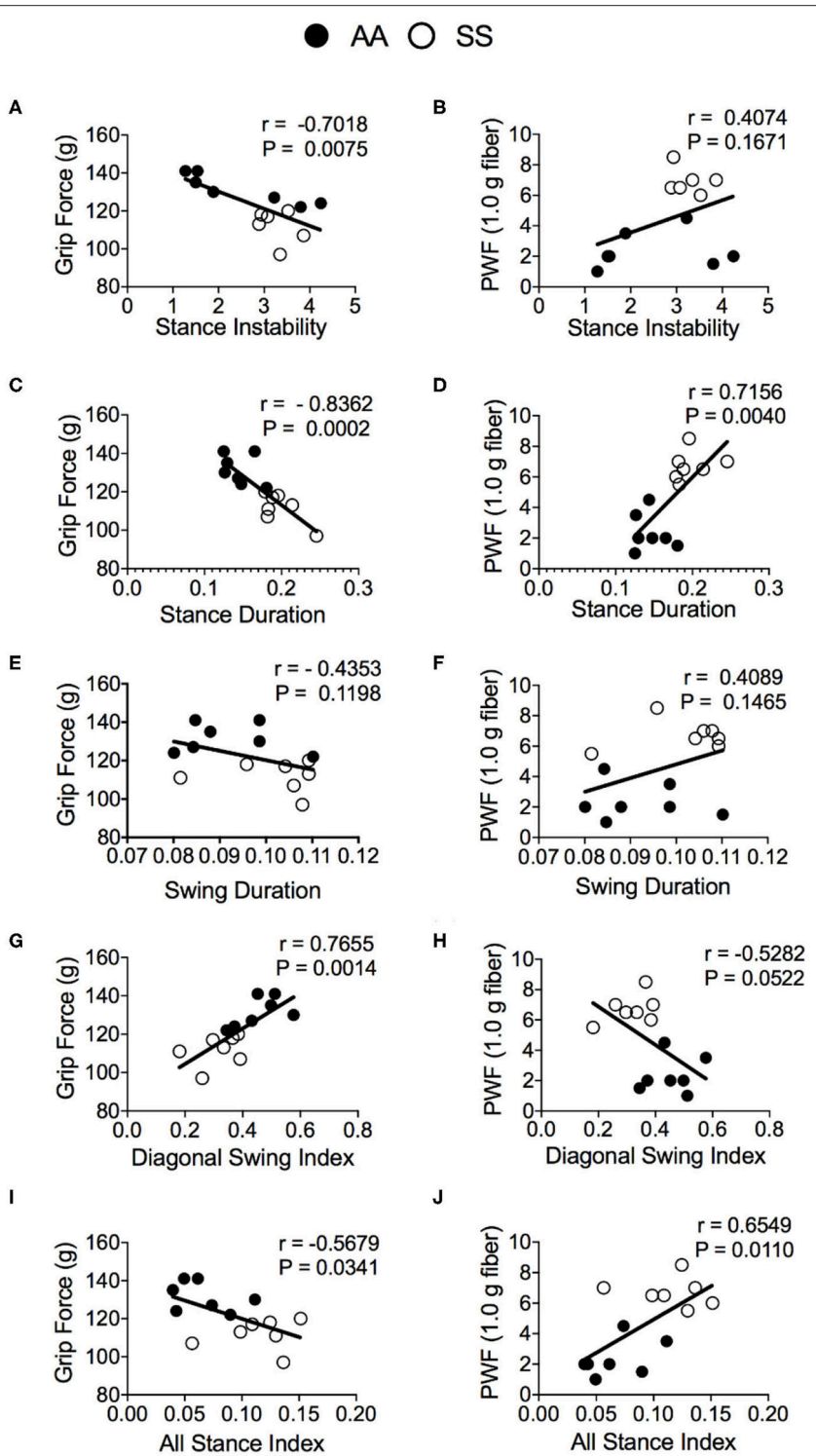

FIGURE 6 | Correlation of gait parameters with deep tissue and mechanical hyperalgesia measures. Pearson correlation analysis was performed to detect associations of gait parameters with hyperalgesia in HbSS-BERK sickle (SS) and HbAA-BERK control (AA) mice. Correlation test results of grip force measures and paw withdrawal frequency (PWF) in response to 1.0-g von Frey filament, respectively, with stance instability **(A,B)**, stance duration **(C,D)**, swing duration **(E,F)**, diagonal swing index **(G,H)**, and all stance index **(I,J)** are shown. [$n = 7$ per group in **(A–J)**] A $p < 0.05$ was considered statistically significant. All data are represented as mean ± SEM.

Selective Spatial and Temporal Gait Parameters Correlate With Hyperalgesia

To evaluate the utility of automated gait measurement as a complementary approach for assessing pain, we conducted a Pearson correlation analysis between conventional mechanical and deep tissue hyperalgesia measurements and gait parameters for combined groups of sickle and control mice. The stance instability demonstrated a strong correlation with deep tissue hyperalgesia (**Figure 6A**; $r = -0.70$, $p = 0.0075$) but no significant correlation with mechanical hyperalgesia (**Figure 6B**). However, the strongest correlation with hyperalgesia are observed for the stance duration with both grip force (**Figure 6C**; $r = -0.84$, $p = 0.0002$) and PWF (**Figure 6D**; $r = 0.72$, $p = 0.004$) indicating that stance duration is affected by existence of deep tissue and mechanical hyperalgesia. There was no correlation for the swing duration with both mechanical and deep tissue hyperalgesia (**Figures 6E,F**), even though there was a significant difference in swing duration between the sickle and control mice as described above. Among the swing indices, the diagonal swing index had strong (**Figure 6G**; $r = 0.77$, $p = 0.0014$) correlation with grip force and moderate (**Figure 6H**; $r = -0.53$, $p = 0.0522$) correlation with PWF, thus indicating a moderate decrease in the trot gait (walking with higher speed) with increasing hyperalgesia. All stance indices moderately correlated with both grip force (**Figure 6I**; $r = -0.56$, $p = 0.034$) and PWF (**Figure 6J**; $r = 0.65$, $p = 0.011$), demonstrating that anticipation of movement-evoked pain may contribute to more frequent hesitant stops with increasing pain.

DISCUSSION

Our results demonstrate increased caspase-3 activation in Purkinje cells of sickle mice compared to control mice, indicative of apoptosis and neurodegenerative changes in the cerebellar cortex. In sickle mice, the nucleolus is missing and the nucleus is smudged with condensed chromatin, clearly morphological signs of apoptosis. These misshapen nucleoli are immunopositive for cleaved caspase-3 (active form), a key protease in the apoptotic pathway and a known marker of cellular apoptosis including Purkinje cell apoptosis in the cerebellum (26–29). Therefore, increased cleaved caspase-3 positive immunostaining in the Purkinje cells of BERK sickle mice compared to control mice validates the histological observations of Purkinje cell apoptosis. It is likely that increased numbers of apoptotic Purkinje cells in the cerebellum of sickle mice contribute to alterations in their motor function leading to changes in gait. Gait characteristics during walking are significantly different in sickle mice compared to control mice perhaps due to increased Purkinje cell apoptosis. Purkinje cells provide primary outputs from the cerebellar cortex and are known to modulate motor functions.

Preclinical studies using transgenic sickle mice to elucidate mechanisms of sickle pain have evolved around traditional methods of stimulus-evoked hyperalgesia assessments (7) that are limited to the subjective nature of observations and an associated potential for bias (30). Most importantly, these methods performed in restraint and with noxious stimuli can generate stress (30). Therefore, objective measure of spontaneous pain without any stimuli are of growing interest. We have previously demonstrated that image analysis of facial expressions using mouse grimace scale (MGS) could detect pain in response to cold stimuli, although the method suffers from observer bias (31). Simultaneously, we tested the utility of static body length and curvature parameters (e.g., eccentricity of a fitted ellipse) extracted from image analysis as objective measures of hyperalgesia, and found that sickle mice had higher percent change in these parameters compared to control mice in response to cold stimuli, which was reversed upon analgesic treatment in sickle mice (31).

Complementary to the static gait changes sickle mice demonstrate alterations in walking gait parameters. Sickle mice displayed more stance instability and body sway from the center of the mass during their movement suggesting loss of balance during movement. Interestingly, human subjects with spinocerebellar ataxia type 6 (SCA6) standing on a flat surface demonstrate global stance instability with body sway that strongly correlates with disease severity (32). Human brain tissue examination and mouse models of SCA6 showed involvement of apoptotic Purkinje cells and their dysfunctional firing in SCA6–a predominantly hereditary neurodegenerative disease (33, 34). Therefore, higher stance instability in sickle mice suggests cerebellar Purkinje cell damage-associated disruption in sensorimotor processing of balance control. Sickle mice evinced significantly decreased walking speed, increased stance and swing duration, and also exhibit avoidance behaviors in hind paw gait parameters (increased hind paw bound swing), compared to control mice. Sickle mice consistently exhibited hesitation during recording for gait measurement, which is also reflected in their significantly increased swing and stance duration. Moreover, diagonal swing indices were significantly reduced in sickle mice in addition to reduced walking speed. Lower speed and increased reluctance to walk in sickle mice may be indicative of compensation for existing hyperalgesia and fear/anticipation of movement-evoked pain, respectively. Stance duration exhibited significantly positive correlation with deep tissue- and mechanical-hyperalgesia; and stance instability demonstrated significant correlation with deep tissue hyperalgesia. Also, diagonal swing indices and all stance indices demonstrate moderate to strong negative and positive correlation, respectively, with both deep tissue and mechanical hyperalgesia—indicating that gait compensation to avoid movement-evoked pain may contribute to reduced speed and increased hesitation during mobility. The evaluation of gait parameters, thus, can provide objective estimates of sickle pain devoid of observer bias and restraint-evoked stress in preclinical studies.

Alongside a large number of studies on experimental osteoarthritis (18), recent preclinical studies have tested the efficacy of automated gait analysis systems in murine models of neuropathic pain by spinal nerve injury (30, 35, 36), chronic constriction injury-induced pain [AU—(37)], CFA-induced pain (35, 36), paclitaxel-induced polyneuropathy (38)

and post-operative pain in bone-reconstruction surgery (39). Commercially available systems such as CatWalk XT (Noldus) and GaitLab (ViewPoint Behavior Technology) rely on imaging paw prints reflected internally across an elevated glass floor where the animal walks (40). Other systems such as DigiGait (Mouse Specifics Inc.) and GaitScan/TreadScan (CleverSys) use video recordings to analyze paw prints of walking animals (41–43). However, these platforms do not offer user-customization according to specific needs as their software source codes are proprietary. On the contrary, *MouseWalker* system (used in this study) is a simpler system with walking apparatus assembled from readily available materials and inexpensive components, and the software is available free of cost (25).

Traditionally human sickle pain studies have relied on patient-reported visual analog scores or pain diaries, or relatively recent objective tools such as quantitative sensory testing (QST) (44–51). However, QST measures hypersensitivity to evoked thermal or mechanical stimuli. A 6-min walk study demonstrated that reduction of walking distance among children on hydroxyurea treatment and without cardiopulmonary complications correlated with history of silent strokes (52). Using 36-item short form (SF-36) survey that assesses quality of life (QoL) in patients, bodily pain that affects activities of daily life (ADL) was found to be significantly associated with chronic pain in thoracic spine and hip/lower limbs in adult sickle patients (53). In a study of children hospitalized for VOC, the rate of improvement of daily physical functions and rate of reduction in pain intensities were significant over the course of hospital stay, with negative effects in mood being associated proportionately with pain intensities and inversely with physical functioning scores (53). Therefore, negative scores of physical functioning or movement-gait changes may be indicative of pain. Peripheral neuropathy leading to acute loss of lower extremity mobility have been reported recently in sickle patients (54, 55). Our murine data indicates that if a similar correlation between pain scores and gait changes is seen in humans, monitoring gait in sickle patients to detect any onset/offset of abnormal or altered patterns may serve as tools to evaluate post-treatment improvement and/or monitoring chronic pain and associated QoL. Automated gait analysis using wearable technology has been used for objective detection of gradual improvement in physical functioning in post-operative period in patients with total hip arthroplasty (53). Thus, early assessment of dynamic gait features and locomotion deficits may help in early diagnosis of avascular necrosis and associated bone disorders prompting preventive measures.

An important characteristic of gait in sickle mice is the existence of longer and frequent hesitant stops reflected by significantly higher all stance indices compared to control mice which were also moderately associated with mechanical and deep tissue hyperalgesia independently–which may represent stalling due to fear or anticipation of movement-evoked pain. Autonomic nervous system (ANS) responses have been shown to be significantly disrupted in sickle patients (56). Vasoconstriction (or decrease in microvascular perfusion) is influenced greatly in response to anticipation of thermal pain in human sickle patients (57), and degree and rate of such neurally mediated-vasoconstriction is correlated with anxiety scores (51). While mental stress causes vasoconstriction in both sickle and healthy individuals (58), such vascular response may increase transit time of sickled RBCs and contribute to entrapment in microvasculature resulting in acute VOC. Additionally, neuroimaging analysis revealed that resting state functional connectivity is intensified in the locus coeruleus of the brain stems of SCD subjects compared to non-SCD anemic controls—indicating possibility of hyperactive sympathetic neurons contributing to modulation in peripheral microvascular blood flow (58). In patients with type1 and type2 diabetes (compared to healthy controls) decreased walking speed, more frequent stops and altered joint gait during movement were observed, while these patients also demonstrated 50% impairment in local tissue blood flow and other autonomic functions (vs. controls) (58). Thus, it is possible that gait alteration in sickle mice is both a function of existing pain and its effect on the sympathetic nervous system. Conversely, anticipation of pain may contribute to VOC. Thus, monitoring of gait characteristics of SCD subjects may provide information regarding prognosis of the disease, onset of acute crises and/or transition to chronic pain.

The role of cerebellar Purkinje cells in peripheral nociception is unclear. However, A-delta and C-fiber signals are relayed to Purkinje cells in the cerebellum (59–61) and nociceptive somatosensory and visceral signals stimulate Purkinje cell firing (62, 63). Interestingly, Purkinje cells in the vermis of the cerebellum project into the fastigial nucleus and these cerebellar structures are connected to cerebral areas controlling autonomic functions (64). Additionally, recent neuroimaging studies demonstrated enhanced cerebellar activity both in anticipation of and violation of expected level of pain (65, 66). Another study demonstrated overlapping cerebellar activity suggestive of pain-evoked motor adaptation (67). Therefore, Purkinje cell damage and altered stance behaviors in sickle mice with chronic pain in relation to sympathetic modulation of anticipated pain and pain-induced gait adaptation warrant further investigation.

CONCLUSION

In conclusion, we provide first evaluation of walking-gait differences in sickle mice compared to control mice. Increased Purkinje cell apoptosis could contribute to altered movement leading to changes in gait. Importantly, several parameters of gait correlate with deep tissue and mechanical hyperalgesia in sickle mice. Thus, gait analysis can be used as a complementary and objective pain assessment tool devoid of stimuli-evoked techniques for assessing sickle pain. Recent advances in wearable technology offer the potential of monitoring gait from remote access in an unbiased and natural environment. Therefore, our observations provide a proof of principle to examine gait in SCD as a predictor of pain and other consequences of the disease.

DATA AVAILABILITY STATEMENT

The raw data supporting the conclusions of this article will be made available by the authors, without undue reservation.

ETHICS STATEMENT

The animal study was reviewed and approved by Institutional Animal Care and Use Committee VA Long Beach Healthcare Center.

AUTHOR CONTRIBUTIONS

SK performed behavioral and histological analysis, wrote the manuscript, and prepared for submission. YW assembled the MouseWalker and performed MouseWalker experiments and collected the data. AA analyzed and interpreted the MouseWalker data, wrote the manuscript, and prepared for submission. DA performed behavioral analysis, preparation of tissues for histological analysis, and edited the manuscript. JL performed experiments and analyzed the data for hyperalgesia. VS analyzed and interpreted the data and prepared the figures. MT and SB extracted the parameters from video recordings for gait analysis. NL analyzed and interpreted pathology data, and prepared the pathology figures. KG developed the concept, designed, planned, and supervised the study, interpreted the data, and edited the manuscript. All authors contributed to the article and approved the submitted version.

FUNDING

This work was supported by NIH Grants Nos. U18 EB029354 and HL147562 and SCIRE Foundation to KG, Diversity Supplement 3R01HL147562-03S to SK, and University of California President's Fellowship to DA. The content is solely the responsibility of the authors and does not necessarily represent the official views of the National Institutes of Health.

ACKNOWLEDGMENTS

The authors thank Ritu Jha for breeding, genotyping, and maintaining mice. Sarah Lam, Ellis Raduenz, Gauri Madhok, Khalid Ishani, and Om Jahagirdar for their assistance in standardization of the mouse walker equipment, and aiding in the mouse walker experiments. Dominic Marticorena for the images of mouse walker equipment. The authors would also like to thank Dr. Joni Ricks-Odie for advise with the biostatistical analysis.

REFERENCES

1. Aich A, Jones MK, Gupta K. Pain and sickle cell disease. *Curr Opin Hematol.* (2019) 26:131–8. doi: 10.1097/MOH.0000000000000491
2. Ballas SK, Gupta K, Adams-Graves P. Sickle cell pain: a critical reappraisal. *Blood*. (2012) 120:3647–56. doi: 10.1182/blood-2012-04-383430
3. Kato GJ, Piel FB, Reid CD, Gaston MH, Ohene-Frempong K, Krishnamurti L, et al. Sickle cell disease. *Nat Rev Dis Primers*. (2018) 4:18010. doi: 10.1038/nrdp.2018.10
4. Telen MJ, Malik P, Vercellotti GM. Therapeutic strategies for sickle cell disease: towards a multi-agent approach. *Nat Rev Drug Discov*. 18:139–58 (2019). doi: 10.1038/s41573-018-0003-2
5. Tran H, Gupta M, Gupta K. Targeting novel mechanisms of pain in sickle cell disease. *Blood*. (2017) 130:2377–85. doi: 10.1182/blood-2017-05-782003
6. Manci EA, Hillery CA, Bodian CA, Zhang ZG, Lutty GA, Coller BS. Pathology of berkeley sickle cell mice: similarities and differences with human sickle cell disease. *Blood*. (2006) 107:1651–8. doi: 10.1182/blood-2005-07-2839
7. Sagi V, Song-Naba WL, Benson BA, Joshi SS, Gupta K. Mouse models of pain in sickle cell disease. *Curr Protoc Neurosci.* (2018) 85:e54. doi: 10.1002/cpns.54
8. Ady V, Toscano-Márquez B, Nath M, Chang PK, Hui J, Cook A, et al. Altered synaptic and firing properties of cerebellar purkinje cells in a mouse model of ARSACS. *J Physiol.* (2018) 596:4253–67. doi: 10.1113/JP275902
9. Hourez R, Servais L, Orduz D, Gall D, Millard I, Kerchove d'Exaerde AK, et al. Aminopyridines correct early dysfunction and delay neurodegeneration in a mouse model of spinocerebellar ataxia type 1. *J Neurosci.* (2011) 31:11795 LP—807 LP. doi: 10.1523/JNEUROSCI.0905-11.2011
10. Walter JT, Alviña K, Womack MD, Chevez C, Khodakhah K. Decreases in the precision of purkinje cell pacemaking cause cerebellar dysfunction and ataxia. *Nat Neurosci*. (2006) 9:389–97. doi: 10.1038/nn1648
11. McClish DK, Smith WR, Dahman BA, Levenson JL, Roberts JD, Penberthy LT, et al. Pain site frequency and location in sickle cell disease: the PiSCES project. *Pain*. (2009) 145:246–51. doi: 10.1016/j.pain.2009.06.029
12. Almeida A, Roberts I. Bone involvement in sickle cell disease. *Br J Haematol*. (2005) 129:482–90. doi: 10.1111/j.1365-2141.2005.05476.x
13. Benenson I, Porter S. Sickle cell disease: bone, joint, muscle, and motor complications. *Orthop Nurs*. (2018) 37:221–7. doi: 10.1097/NOR.0000000000000464
14. Martí-Carvajal AJ, Solà I, Agreda-Pérez LH. Treatment for avascular necrosis of bone in people with sickle cell disease. *Cochrane Database of Syst Rev*. (2016) 8:CD004344. doi: 10.1002/14651858.CD004344.pub6
15. Green M, Akinsami I, Lin A, Banton S, Ghosh S, Chen B, et al. Microarchitectural and mechanical characterization of the sickle bone. *J Mech Behav Biomed Mater*. (2015) 48:220–8. doi: 10.1016/j.jmbbm.2015.04.019
16. Sawyer JR, Kapoor M. The limping child: a systematic approach to diagnosis. *Am Fam Physi.* (2009) 79:215–24.
17. Preisig DF, Kulic L, Krüger M, Wirth F, McAfoose J, Späni C, et al. High-speed video gait analysis reveals early and characteristic locomotor phenotypes in mouse models of neurodegenerative movement disorders. *Behav Brain Res*. (2016) 311:340–53. doi: 10.1016/j.bbr.2016.04.044
18. Lakes EH, Allen KD. Gait analysis methods for rodent models of arthritic disorders: reviews and recommendations. *Osteoarthritis Cartilage*. (2016) 24:1837–49. doi: 10.1016/j.joca.2016.03.008
19. Pászty C, Brion CM, Manci E, Witkowska HE, Stevens ME, Mohandas N, et al. Transgenic knockout mice with exclusively human sickle hemoglobin and sickle cell disease. *Science*. (1997) 278:876–8. doi: 10.1126/science.278.5339.876
20. Hebbel RP, Osarogiagbon R, Kaul D. The endothelial biology of sickle cell disease: inflammation and a chronic vasculopathy. *Microcirculation*. (2004) 11:129–51. doi: 10.1080/mic.11.2.129.151
21. Tran H, Sagi V, Song-Naba WL, Wang Y, Mittal A, Lamarre Y, et al. Effect of chronic opioid therapy on pain and survival in a humanized mouse model of sickle cell disease. *Blood Adv*. (2019) 3:869–73. doi: 10.1182/bloodadvances.2018024299
22. Arumugam PI, Mullins ES, Shanmukhappa SK, Monia BP, Loberg A, Shaw MA, et al. Genetic diminution of circulating prothrombin ameliorates

multiorgan pathologies in sickle cell disease mice. *Blood*. (2015) 126:1844–55. doi: 10.1182/blood-2015-01-625707
23. Kohli DR, Li Y, Khasabov SG, Gupta P, Kehl LJ, Ericson ME, et al. Pain-related behaviors and neurochemical alterations in mice expressing sickle hemoglobin: modulation by cannabinoids. *Blood*. (2010) 116:456–65. doi: 10.1182/blood-2010-01-260372
24. Lei J, Benson B, Tran H, Ofori-Acquah SF, Gupta K. Comparative analysis of pain behaviours in humanized mouse models of sickle cell anemia. *PLoS ONE*. (2016) 11:e0160608. doi: 10.1371/journal.pone.0160608
25. Mendes CS, Bartos I, Márka Z, Akay T, Márka S, Mann RS. Quantification of gait parameters in freely walking rodents. *BMC Biol*. (2015) 13:50. doi: 10.1186/s12915-015-0154-0
26. Gown AM, Willingham MC. Improved detection of apoptotic cells in archival paraffin sections: immunohistochemistry using antibodies to cleaved caspase 3. *J Histochem Cytochem*. (2002) 50:449–54. doi: 10.1177/002215540205000401
27. Haraguchi S, Hara S, Ubuka T, Mita M, Tsutsui K. Possible role of pineal allopregnanolone in Purkinje cell survival. *Proc Natl Acad Sci USA*. (2012) 109:21110–5. doi: 10.1073/pnas.1210804109
28. Matsunaga E, Tauszig-Delamasure S, Monnier PP, Mueller BK, Strittmatter SM, Mehlen P, et al. RGM and its receptor neogenin regulate neuronal survival. *Nat Cell Biol*. (2004) 6:749–55. doi: 10.1038/ncb1157
29. Puig B, Ferrer I. Cell death signaling in the cerebellum in Creutzfeldt-Jakob disease. *Acta Neuropathol*. (2001) 102:207–15. doi: 10.1007/s004010100368
30. Pitzer C, Kuner R, Tappe-Theodor A. Voluntary and evoked behavioral correlates in neuropathic pain states under different social housing conditions. *Mol Pain*. (2016) 12:1744806916656635. doi: 10.1177/1744806916656635
31. Mittal A, Gupta M, Lamarre Y, Jahagirdar B, Gupta K. Quantification of pain in sickle mice using facial expressions and body measurements. *Blood Cells Mol Dis*. (2016) 57:58–66. doi: 10.1016/j.bcmd.2015.12.006
32. Bunn LM, Marsden JF, Giunti P, Day BL. Stance instability in spinocerebellar ataxia type 6. *Move Disord*. (2013) 28:510–6. doi: 10.1002/mds.25163
33. Jayabal S, Chang HHV, Cullen KE, Watt AJ. 4-Aminopyridine reverses ataxia and cerebellar firing deficiency in a mouse model of spinocerebellar ataxia type 6. *Sci Rep*. (2016) 6:29489. doi: 10.1038/srep29489
34. Yang Q, Hashizume Y, Yoshida M, Wang Y, Goto Y, Mitsuma N, et al. Morphological purkinje cell changes in spinocerebellar ataxia type 6. *Acta Neuropathol*. (2000) 100:371–6. doi: 10.1007/s004010000201
35. Shepherd AJ, Mohapatra DP. Pharmacological validation of voluntary gait and mechanical sensitivity assays associated with inflammatory and neuropathic pain in mice. *Neuropharmacology*. (2018) 130:18–29. doi: 10.1016/j.neuropharm.2017.11.036
36. Xu Y, Tian NX, Bai QY, Chen Q, Sun XH, Wang Y. Gait assessment of pain and analgesics: comparison of the digigait^{TM} and catwalk^{TM} gait imaging systems. *Neurosci Bull*. (2019) 35:401–18. doi: 10.1007/s12264-018-00331-y
37. Kang DW, Choi JG, Moon JY, Kang SY, Ryu Y, Park JB, et al. Automated gait analysis in mice with chronic constriction injury. *J Vis Exp*. (2017) 128:56402. doi: 10.3791/56402
38. Huehnchen P, Boehmerle W, Endres M. Assessment of paclitaxel induced sensory polyneuropathy with 'catwalk' automated gait analysis in mice. *PLoS ONE*. (2013) 8:e76772. doi: 10.1371/journal.pone.0076772
39. Dupleichs M, Masson M, Gauthier O, Dutilleul M, Bouler JM, Verron E, et al. Pain management after bone reconstruction surgery using an analgesic bone cement: a functional noninvasive *in vivo* study using gait analysis. *J Pain*. (2018) 19:1169–80. doi: 10.1016/j.jpain.2018.04.014
40. Deuis JR, Dvorakova LS, Vetter I. Methods used to evaluate pain behaviors in rodents. *Front Mol Neurosci*. (2017) 10:284. doi: 10.3389/fnmol.2017.00284
41. Adams BL, Guo W, Gors RT, Knopp KL. Pharmacological interrogation of a rodent forced ambulation model: leveraging gait impairment as a measure of pain behavior pre-clinically. *Osteoarthritis Cartilage*. (2016) 24:1928–39. doi: 10.1016/j.joca.2016.05.022
42. Berryman ER, Harris RL, Moalli M, Bagi CM. Digigait quantitation of gait dynamics in rat rheumatoid arthritis model. *J Musculoskelet Neuronal Interact*. (2009) 9:89–98.
43. Parvathy SS, Masocha W. Gait analysis of C57BL/6 mice with complete freund's adjuvant-induced arthritis using the catwalk system. *BMC Musculoskelet Disord*. (2013) 14:14. doi: 10.1186/1471-2474-14-14
44. Bakshi N, Lukombo I, Shnol H, Belfer I, Krishnamurti L. Psychological characteristics and pain frequency are associated with experimental pain sensitivity in pediatric patients with sickle cell disease. *J Pain*. (2017) 18:1216–28. doi: 10.1016/j.jpain.2017.05.005
45. Brandow AM, Farley RA, Panepinto JA. Early insights into the neurobiology of pain in sickle cell disease: a systematic review of the literature. *Pediatr Blood Cancer*. (2015) 62:1501–11. doi: 10.1002/pbc.25574
46. Brandow AM, Panepinto JA. Clinical interpretation of quantitative sensory testing as a measure of pain sensitivity in patients with sickle cell disease. *J Pediatr Hematol Oncol*. (2016) 38:288–93. doi: 10.1097/MPH.0000000000000532
47. Campbell CM, Carroll CP, Kiley K, Han D, Haywood Jr C, Lanzkron S, et al. Quantitative sensory testing and pain-evoked cytokine reactivity: comparison of patients with sickle cell disease to healthy matched controls. *Pain*. (2016) 157:949–56. doi: 10.1097/j.pain.0000000000000473
48. Ezenwa MO, Molokie RE, Wang ZJ, Yao Y, Suarez ML, Pullum C, et al. Safety and utility of quantitative sensory testing among adults with sickle cell disease: indicators of neuropathic pain? *Pain Pract*. (2016) 16:282–93. doi: 10.1111/papr.12279
49. Jacob E, Chan VW, Hodge C, Zeltzer L, Zurakowski D, Sethna NF. Sensory and thermal quantitative testing in children with sickle cell disease. *J Pediatr Hematol Oncol*. (2015) 37:185–9. doi: 10.1097/MPH.0000000000000214
50. O'leary JD, Crawford MW, Odame I, Shorten GD, McGrath PA. Thermal pain and sensory processing in children with sickle cell disease. *Clin JPain*. (2014) 30:244–50. doi: 10.1097/AJP.0b013e318292a38e
51. Veluswamy S, Shah P, Khaleel M, Puliyel M, Thuptimdang W, Chalacheva P, et al. Sickle cell subjects have a stronger and faster neurally mediated vasoconstriction response to cold pain that correlates with anxiety scores. *Blood*. (2018) 132 (Suppl. 1):854. doi: 10.1182/blood-2018-99-113655
52. Aguilar CM, Neumayr LD, Eggleston BE, Earles AN, Robertson SM, Jergesen HE, et al. Clinical evaluation of avascular necrosis in patients with sickle cell disease: children's hospital oakland hip evaluation scale; a modification of the harris hip score. *Arch Phys Med Rehabil*. (2005) 86:1369–75. doi: 10.1016/j.apmr.2005.01.008
53. Ohara DG, Ruas G, Castro SS, Martins PRJ, Walsh IAP. Musculoskeletal pain, profile and quality of life of individuals with sickle cell disease. *Br J Phys Ther*. (2012) 16:431–8. doi: 10.1590/S1413-35552012005000043
54. Agapidou A, Aiken L, Linpower L, Tsitsikas DA. Ischemic monomeric neuropathy in a woman with sickle cell anaemia. *Case Rep Hematol*. (2016) 2016:8628425. doi: 10.1155/2016/8628425
55. Tsen LC, Cherayil G. Sickle cell–induced peripheral neuropathy following spinal anesthesia for cesarean delivery. *Anesthesiology*. (2001) 95:1298–9. doi: 10.1097/00000542-200111000-00042
56. Coates TD, Chalacheva P, Zeltzer L, Khoo MCK. Autonomic nervous system involvement in sickle cell disease. *Clin Hemorheol Microcircul*. (2018) 68:251–62. doi: 10.3233/CH-189011
57. Khaleel M, Puliyel M, Shah P, Sunwoo J, Kato RM, Chalacheva P, et al. Individuals with sickle cell disease have a significantly greater vasoconstriction response to thermal pain than controls and have significant vasoconstriction in response to anticipation of pain. *Am J Hematol*. (2017) 92:1137–45. doi: 10.1002/ajh.24858
58. Shah P, Khaleel M, Thuptimdang W, Sunwoo J, Veluswamy S, Chalacheva P, et al. Mental stress causes vasoconstriction in sickle cell disease and normal controls. *Haematol April Haematol*. (2019) 2018:211391. doi: 10.3324/haematol.2018.211391
59. Ekerot CF, Garwicz M, Schouenborg J. The postsynaptic dorsal column pathway mediates cutaneous nociceptive information to cerebellar climbing fibres in the cat. *J Physiol*. (1991) 441:275–84. doi: 10.1113/jphysiol.1991.sp018751
60. Ekerot CF, Gustavsson P, Oscarsson O, Schouenborg J. Climbing fibres projecting to cat cerebellar anterior lobe activated by cutaneous A and C fibres. *J Physiol*. (1987) 386:529–38. doi: 10.1113/jphysiol.1987.sp016549
61. Ekerot CF, Oscarsson O, Schouenborg J. Stimulation of cat cutaneous nociceptive c fibres causing tonic and synchronous activity in climbing fibres. *J Physiol*. (1987) 386:539–46. doi: 10.1113/jphysiol.1987.sp016550

62. Jie W, Pei-Xi C. Discharge response of cerebellar purkinje cells to stimulation of C-fiber in cat saphenous nerve. *Brain Res*. (1992) 581:269–72. doi: 10.1016/0006-8993(92)90717-N
63. Saab C, Willis W. Nociceptive visceral stimulation modulates the activity of cerebellar purkinje cells. *Exp Brain Res*. (2001) 140:122–6. doi: 10.1007/s002210100824
64. Baumann O, Borra RJ, Bower JM, Cullen KE, Habas C, Ivry RB, et al. Consensus paper: the role of the cerebellum in perceptual processes. *Cerebellum*. (2015) 14:197–220. doi: 10.1007/s12311-014-0627-7
65. Seifert F, Schuberth N, De Col R, Peltz E, Nickel FT, Maihöfner C. Brain activity during sympathetic response in anticipation and experience of pain. *Hum Brain Mapp*. (2013) 34:1768–82. doi: 10.1002/hbm.22035
66. Zeidan F, Lobanov OV, Kraft RA, Coghill RC. Brain mechanisms supporting violated expectations of pain. *Pain*. (2015) 156:1772–85. doi: 10.1097/j.pain.0000000000000231
67. Coombes SA, Misra G. Pain and motor processing in the human cerebellum. *Pain*. (2016) 157:117–27. doi: 10.1097/j.pain.0000000000000337

Conflict of Interest: KG reports grants from Grifols, 1910 Genetics and Cyclerion and honorarium from Novartis, Tautona Group, and CSL Behring, outside the submitted work.

The remaining authors declare that the research was conducted in the absence of any commercial or financial relationships that could be construed as a potential conflict of interest.

frontiers in Immunology

ORIGINAL RESEARCH
published: 04 November 2020
doi: 10.3389/fimmu.2020.551441

Association Between Nitric Oxide, Oxidative Stress, Eryptosis, Red Blood Cell Microparticles, and Vascular Function in Sickle Cell Anemia

Elie Nader[1,2], Marc Romana[2,3,4†], Nicolas Guillot[5†], Romain Fort[1,2,6], Emeric Stauffer[1,2,7], Nathalie Lemonne[8], Yohann Garnier[2,3,4], Sarah Chambers Skinner[1,2], Maryse Etienne-Julan[8], Mélanie Robert[9], Alexandra Gauthier[1,10], Giovanna Cannas[1,6], Sophie Antoine-Jonville[3], Benoît Tressières[11], Marie-Dominique Hardy-Dessources[2,3,4], Yves Bertrand[10], Cyril Martin[1,2], Céline Renoux[1,2,12], Philippe Joly[1,2,12], Marijke Grau[13‡] and Philippe Connes[1,2,14‡]*

[1] Laboratoire Interuniversitaire de Biologie de la Motricité (LIBM) EA7424, Team « Vascular Biology and Red Blood Cell », Université Claude Bernard Lyon 1, Université de Lyon, Lyon, France, [2] Laboratoire d'Excellence du Globule Rouge (Labex GR-Ex), PRES Sorbonne, Paris, France, [3] Université des Antilles, Pointe-à-Pitre, France, [4] Université de Paris, Paris, France, [5] Laboratoire Carmen Inserm, Université Claude Bernard Lyon 1, Université de Lyon, Villeurbanne, France, [6] Département de Médecine Interne, Hôpital Edouard Herriot, Hospices Civils de Lyon, Lyon, France, [7] Centre de Médecine du Sommeil et des Maladies Respiratoires, Hospices Civils de Lyon, Hôpital de la Croix Rousse, Lyon, France, [8] Unité Transversale de la Drépanocytose, Hôpital de Pointe-á-Pitre, Hôpital Ricou, Guadeloupe, France, [9] Erytech Pharma, Lyon, France, [10] Institut d'Hématologie et d'Oncologie Pédiatrique, Hospices Civils de Lyon, Lyon, France, [11] Centre Investigation Clinique Antilles Guyane, 1424 Inserm, Academic Hospital of Pointe-á-Pitre, Pointe-á-Pitre, Guadeloupe, France, [12] Laboratoire de Biochimie et de Biologie Moléculaire, UF de Biochimie des Pathologies érythrocytaires, Centre de Biologie et de Pathologie Est, Hospices Civils de Lyon, Lyon, France, [13] Molecular and Cellular Sport Medicine, Deutsche Sporthochschule Köln, Köln, Germany, [14] Institut Universitaire de France, Paris, France

Chronic hemolysis, enhanced oxidative stress, and decreased nitric oxide (NO) bioavailability promote vasculopathy in sickle cell anemia (SCA). Oxidative stress and NO are known to modulate eryptosis in healthy red blood cells (RBCs); however, their role in SCA eryptosis and their impact on the genesis of RBC-derived microparticles (RBC-MPs) remains poorly described. RBC-MPs could play a role in vascular dysfunction in SCA. The aims of this study were to evaluate the roles of oxidative stress and NO in eryptosis and RBC-MPs release, and to determine whether RBC-MPs could be involved in vascular dysfunction in SCA. Markers of eryptosis and oxidative stress, plasma RBC-MPs concentration and arterial stiffness were compared between SCA and healthy (AA) individuals. *In-vitro* experiments were performed to test: 1) the effects of oxidative stress (antioxidant: n-acetylcysteine (NAC); pro-oxidant: cumene hydroperoxide) and NO (NO donor: sodium nitroprusside (SNP); NO-synthase inhibitor (L-NIO)) on eryptosis, RBC deformability and RBC-MP genesis; 2) the effects of SCA/AA-RBC-MPs on human aortic endothelial cell (HAEC) inflammatory phenotype and TLR4 pathway. Eryptosis, RBC-MPs, oxidative stress and arterial stiffness were increased in SCA. NAC increased RBC deformability and decreased eryptosis and RBC-MPs release, while cumene did the

OPEN ACCESS

Edited by:
Renata Sesti-Costa, Campinas State University, Brazil

Reviewed by:
Ting Yang, Duke University, United States
Erich Vinicius De Paula, Campinas State University, Brazil

***Correspondence:**
Philippe Connes
pconnes@yahoo.fr;
philippe.connes@univ-lyon.fr

†These authors have contributed equally to this work

‡These authors have contributed equally to this work and share last authorship

Specialty section:
This article was submitted to Inflammation, a section of the journal Frontiers in Immunology

Received: *13 April 2020*
Accepted: *14 October 2020*
Published: *04 November 2020*

Citation:
Nader E, Romana M, Guillot N, Fort R, Stauffer E, Lemonne N, Garnier Y, Skinner SC, Etienne-Julan M, Robert M, Gauthier A, Cannas G, Antoine-Jonville S, Tressières B, Hardy-Dessources M-D, Bertrand Y, Martin C, Renoux C, Joly P, Grau M and Connes P (2020) Association Between Nitric Oxide, Oxidative Stress, Eryptosis, Red Blood Cell Microparticles, and Vascular Function in Sickle Cell Anemia. Front. Immunol. 11:551441. doi: 10.3389/fimmu.2020.551441

opposite. SNP increased RBC deformability and limited eryptosis, but had no effect on RBC-MPs. L-NIO did not affect these parameters. Arterial stiffness was correlated with RBC-MPs concentration in SCA. RBC-MPs isolated directly from SCA blood increased adhesion molecules expression and the production of cytokines by HAEC compared to those isolated from AA blood. TLR4 inhibition alleviated these effects. Our data show that oxidative stress could promote eryptosis and the release of RBC-MPs that are potentially involved in macrovascular dysfunction in SCA.

Keywords: sickle cell anemia, eryptosis, red blood cell microparticles, vascular dysfunction, endothelial cells, TLR4

INTRODUCTION

Sickle cell anemia (SCA) is the most prevalent genetic disease worldwide. SCA is caused by a mutation in the β-globin gene that leads to the substitution of a glutamic acid by a valine at the 7th codon, which results in the production of abnormal hemoglobin called hemoglobin S (HbS). HbS can polymerize in deoxygenated conditions, causing red blood cell (RBC) sickling. Sickled RBCs are poorly deformable and very fragile. Indeed, patients with SCA suffer from chronic hemolytic anemia and repeated vaso-occlusive crises (1). Accumulating evidence suggests that chronic hemolysis, enhanced oxidative stress and decreased bioavailability of nitric oxide (NO) are at the origin of the vascular dysfunction observed in patients with SCA (2–4), which could be involved in the pathogenesis of several acute and chronic complications (3). In addition, heme released by red blood cells into the plasma could play a role in vascular dysfunction by promoting inflammation through the activation of Toll Like Receptor 4 (TLR4) (5).

Furthermore, it has been shown that oxidative stress could promote eryptosis, i.e., RBC suicidal death, in healthy RBCs *in vitro* (6). A previous study has also suggested that NO prevents eryptosis induced by calcium ionophore stimulation (7). Eryptosis is characterized by increased intra-erythrocyte calcium levels, increased phosphatidylserine (PS) exposure, RBC shrinkage (followed by a decrease of RBC deformability), energetic depletion and membrane blebbing (8). Eryptosis has been shown to be increased in SCA (8). Several authors reported alteration in the PS asymmetry of the RBC membrane (9) and high RBC calcium levels in SCA (10–12) but the exact role of oxidative stress and NO in eryptosis in SCA is unknown.

RBC membrane blebbing during eryptosis could lead to the release of microparticles (MPs) into the blood circulation (8, 13). Several studies observed increased levels of MPs in the blood of SCA patients compared to healthy individuals at steady state (14, 15), and a further rise during vaso-occlusive crisis (16, 17), with platelet- and RBC-derived MPs (RBC-MPs) representing the majority of the circulating MPs detected (18). It has been suggested that RBC-MPs may promote vascular dysfunction in SCA. A recent study by Camus et al. (19) showed that SCA RBC-MPs could promote the apoptosis of endothelial cells *in vitro*, and stimulate renal vaso-occlusion in a sickle cell mice model. However, the MPs used in this study were artificially generated *ex vivo*, and were not representative of RBC-MP properties *in vivo*. Furthermore, the mechanisms at the origin of the enhanced RBC-MPs release, and especially the implications of high oxidative stress and decreased NO bioavailability, are still poorly understood in SCA.

The primary aims of our study were to investigate the effects of oxidative stress and NO on eryptosis and the release of MPs by sickle RBCs, and to explore the role of RBC-MPs generated *in vivo*, and thus isolated from SCA patients, in the vascular dysfunction associated with SCA. We compared several markers of eryptosis and RBC-MPs plasma concentrations between healthy individuals and patients with SCA, and then modulated these biological parameters *in vitro* using agents that modify oxidative stress and NO bioavailability. *In vivo* macrovascular function was also evaluated in patients, and activation of endothelial cells from the macrocirculation were evaluated after *in vitro* incubation with RBC-MPs directly isolated from blood of AA individuals and SCA patients, with and without a TLR4 inhibitor.

METHODS

Subjects and Sampling

A total of sixty-two patients with SCA (SS, 25 children, 37 adults) and 22 healthy controls (AA, 10 children, 12 adults) were included in the different experiments (see **Table 1** for subject characteristics). Patients with SCA were recruited from the Edouard Herriot Hospital (Lyon, France), the Institut d'Hématologie et d'Oncologie Pédiatrique (Lyon, France) and the University hospital of Pointe à Pitre (Guadeloupe, France). All subjects were in clinical steady-state at the time of the study;

TABLE 1 | Hematological characteristics of subjects and patients included.

	AA	SCA
N [HU+]	22	62 [55]
Age (yrs)	21.5 ± 2.2	24.5 ± 2.1
Hb (g/dl)	/	8.5 ± 0.4
HbF (%)	/	15.7 ± 8.4
MCV (fl)	/	95 ± 13.1

AA, healthy subjects; SCA, sickle cell anemia patients; N, number; HU+, patients under hydroxyurea treatment; yrs, years; Hb, hemoglobin; HbF, fetal hemoglobin; MCV, Mean Corpuscular Volume.
Data are presented as mean ± SD.

i.e., without any vaso-occlusive crisis or other acute medical complication within the last 2 months, and without any blood transfusions for at least 3 months before inclusion. Patients received common treatment as recommended in sickle cell disease (vitamin B9 and vitamin D). The mean daily dose of hydroxyurea for patients receiving this therapy (n = 55/62) was 18.8 ± 0.9 mg/kg. The study was conducted in accordance with the guidelines set by the Declaration of Helsinki, and all subjects gave informed written consent before their participation. The study was approved by the CPP Sud-Est IV (Lyon, France, L16-47) and the CPP Sud/Ouest Outre Mer III (Bordeaux, France, 2012-A00701-42) Ethics Committees.

Venous blood was taken from the antecubital vein and collected into EDTA tubes for RBC deformability and hematological measurements, and into citrate tubes for eryptosis and microparticle analyses (BD Vacutainer, Plymouth, UK). Serum lactate dehydrogenase (LDH) concentration was determined by standard biochemical methods.

Arterial Stiffness

Arterial stiffness is considered to be a relevant indicator of macrovascular function (20), and is increased in patients with SCA (21). We evaluated arterial stiffness by measuring carotid-radial pulse wave velocity (CR-PWV) with a non-invasive automated device (SphygmoCor System, Actor, Sydney, Australia). A 3-lead electrocardiogram was used and pressure waves were recorded using an arterial tonometer. Pulse wave velocity (PWV) was calculated as the distance between two measuring sites, divided by the transit time (in seconds) of the related pulse waves. Transit time was defined as the difference between the delay of the distal pulse wave to the R wave of the ECG and the delay of the proximal pulse wave to R wave of the ECG. The pulse wave delay was determined by calculating the time elapsed from the peak of the R wave and the foot of the pressure pulse wave. The same experienced operator conducted the measurements throughout the whole study. Measurements were repeated two times at each measurement site, and the mean values were calculated and used for analyses. This technique has been demonstrated to be highly reproducible in both healthy and diseased populations (22, 23), and has been previously been used in individuals with SCA (21, 24).

RBC Deformability

RBC deformability was assessed at 37°C, at 3 and 30 Pa by laser diffraction analysis (ektacytometry), using the Laser-assisted Optical Rotational Cell Analyzer (LORRCA MaxSis, RR Mechatronics, Hoorn, The Netherlands). The system has been described in detail elsewhere (25). Briefly, 10 µl of blood were mixed with 1 ml polyvinylpyrrolidone (PVP; viscosity ≈ 30 cP) and sheared into a Couette system. A laser beam was directed through the samples. The shear stress-induced deformation of RBCs affected the laser beam's diffraction pattern, which was measured by the LORRCA software, and used to calculate an elongation index. A higher elongation index represents greater RBC deformability. The procedure was carried out according to the international methodological recommendations (25, 26).

For pharmacological modulation experiments, whole blood was centrifuged (800*g*, 10 min at 20°C), and plasma and buffy coat were discarded. RBCs were washed in PBS 1× buffer, and the RBC pellets were resuspended at a hematocrit (Hct) of 20% in PBS with either sodium nitroprusside (SNP; 100 µM), a NO donor, L-NIO (10 µM), a nitric oxide synthase (NOS) inhibitor, n-acetylcysteine (NAC; 2,5 mM), an antioxidant agent, or cumene hydroperoxide (100 µM), a pro-oxidant molecule, or vehicle for the control condition, and then incubated for 40 min at 37°C. RBC suspensions were then washed with PBS and resuspended in PBS buffer (Hct = 20%), and RBC deformability was measured as previously described.

Measurement of RBC Nitrite

Previous studies have shown that nitrite levels reflect NO content in both physiological and pathophysiological conditions (27, 28). RBC nitrite content in control condition and after incubation with SNP was measured in order to confirm the effectiveness of the NO donor properties of the molecule within RBCs. Measurements of RBC nitrite content were realized according to previous studies (29, 30).

For nitrite measurement in RBCs, methanol (VWR international, Darmstadt, Germany) was added to the RBC frozen samples in a 1:2-ratio to remove proteins and the suspensions were centrifuged at 21 000 g, at 4°C for 15 min to collect the supernatants.

An ozone-based chemiluminescence NO detector was used to determine Nitrite levels (CLD 88e, EcoPhysics, Switzerland). Samples were injected into an acidified tri-iodide solution that reduces nitrite but also iron-nitrosylheme, and S-nitrosothiols to NO gas. NO is transported by a helium gas stream to a NaOH trap and finally transported to the CLD device where it can be measured by its gas-phase chemiluminescent reaction with ozone. The tri-iodide solution stoichiometrically releases NO from nitrite. Samples were measured in triplicate. A calibration curve with solution containing known concentrations of nitrite was realized to calculate nitrite concentration in the samples.

Nitrite content of methanol was also determined and nitrite concentrations measured in RBC samples were adjusted accordingly. Data analysis was done with the Chart FIA software (Ecophysics, Switzerland) to integrate the area under the curve.

RBC β-Spectrin S-Nitrosylation

NO has been shown to S-nitrosylate cytoskeletal protein β-spectrin (28). S-nitrosylation of the β-spectrin in SCA patients in control and SNP conditions was assessed using the S-Nitrosylated Protein Detection Assay kit (Cayman Chemical, Ann Arbor, MI, USA) according to manufacturer's instructions. The protocol contains three steps: 1) blocking of free SH groups; 2) cleavage of potential S-NO bonds and 3) biotinylation and avidin labeling of the newly formed SH groups. Additionally, the protein concentration of the samples was determined using the DC-Protein Assay Kit (BioRad, Munich, Germany) to ensure that equal amounts of protein were analyzed. A total of 20 µg protein was loaded into each lane of a 3–8% Tris-acetate gel (BioRad) and separated for 1 h under constant 90 mA current in

a 1 × XT Tricine running buffer (BioRad). Proteins were blotted onto a polyvinylidene difluoride (PVDF) membrane (0.45 mm pore size). Background was blocked in 2% bovine serum albumin (in 1× TBS with 0.1% Tween 20) overnight at room temperature. Horseradish peroxidase (dilution 1:2000) was added which binds to the biotin-avidin complex, and the reaction was developed using a chemiluminescence kit containing peroxidase substrate (Thermo Fischer Scientific, Darmstadt, Germany). S-nitrosylated protein band of 220 kDa, previously identified as β-spectrin, was analyzed for differing "Integrated densities" using "Image J" software.

Systemic Oxidative Stress Markers

Plasma Advanced Oxidation Protein Products (AOPP) were determined using the semi-automated method developed by Witko-Sarsat et al. (31), as previously described (32). Concentrations of plasma MDA were determined as previously described (32), using a modified method reported by Ohkawa et al. (33), based on thiobarbituric acid reactions.

Eryptosis Markers

RBC Preparation

Citrate tubes were centrifuged (800 g, 10 min at 20°C) and plasma and buffy coat were discarded. RBCs were washed in PBS 1×, and RBC pellets resuspended at 0.4% Hct in PBS buffer containing 2.5 mM Ca^{2+} (for PS, ROS, and Ca^{2+} analysis) or 5 mM EDTA (for the PS negative control). For pharmacological modulation experiments, suspensions were incubated at 37°C for 40 min with either SNP (100 µM), L-NIO (10 µm), NAC (2.5 mM), cumene hydroperoxide (100 µM) or the vehicle for the control condition. Then, RBC suspensions were washed with PBS 1× and resuspended in PBS buffer as mentioned above.

Phosphatidylserine Exposure

PS exposure on the outer membrane leaflet of the RBCs was evaluated by using Annexin V-FITC, which binds to PS. RBC suspensions were protected from light and incubated for 30 min at room temperature (RT) with Annexin V-FITC (1:200 dilution, Beckman Coulter, California, US). Immediately after incubation, samples were diluted and analyzed by FACS (BD Accuri C6, Franklin Lakes, USA). PS exposure was measured in the FITC channel (with an excitation wavelength of 488 nm and an emission wavelength of 530 nm) according to manufacturer's instructions. Negative controls were obtained by replacing Ca^{2+} by EDTA to prevent Annexin V from binding to PS. For each sample, 50 000 events, gated for the appropriate Forward Scatter (FSC), were counted.

Reactive Oxygen Species (ROS)

Intracellular RBC oxidative stress was determined using 2′,7′–dichlorofluorescin diacetate (DCFDA, Sigma-Aldrich, Saint-Quentin-Fallavier, France). RBC suspensions at 0.4% Hct were incubated for 30 min at RT in the dark with 10 µM of DCFDA (Sigma-Aldrich, Saint-Quentin-Fallavier, France). The samples were then analyzed using FACS, according to manufacturer's instructions. The Median Fluorescence Intensity (MFI) of 50 000 gated events was recorded to quantify ROS levels.

Intracellular Calcium (Ca^{2+})

RBC Ca^{2+} content was measured with a Fluo3/AM (Biotium, Fremont, USA) probe. RBC suspensions were incubated for 30 min at RT with 5 µM of Fluo3/AM, and analyzed using FACS, according to the manufacturer's instructions. MFI of the 50 000 gated events was recorded to quantify Ca^{2+} levels.

Glucose Uptake

RBC glucose uptake was analyzed using the 2-NBD-Glucose (Abcam, Cambridge, USA) probe. RBC suspensions were incubated for 30 min at RT with 200 µM of 2-NBD-Glucose, and analyzed by FACS according to manufacturer's instructions. The MFI of the 50 000 gated events was recorded to quantify levels of glucose uptake.

RBC Microparticles Extraction and Quantification

Microparticles were quantified as previously reported (34). Briefly, citrate tubes were centrifuged at 1 000 g for 10 min at 20°C. Platelet poor plasma was then submitted to ultracentrifugation (20 000 g, 20 min at 20°C) to extract MPs. Supernatant was discarded and the pellet was washed twice in working buffer (10 mM HEPES pH 7.4, 136 mM NaCl, 5 mM KCl, 2 mM $MgCl_2$) containing 5 mM of EDTA for the first washing step and no EDTA for the second one. Working buffer was finally added to the MPs pellet, and the suspensions were stored at −80°C until the day of analysis. MPs quantification was performed with the FC500 Beckman Coulter flow cytometer (Beckman Coulter, Brea, CA, USA) and calibrated fluorescent microbeads (Flowcount; Beckman Coulter). MPs were incubated with Annexin V-FITC and an anti-CD235a-PE antibody to specifically quantify MPs from RBCs. The Megamix kit was used to standardize MPs acquisition gate based on fluorescent microbead size (0.5, 0.9, and 3 µm; Biocytex, Marseille, France) according to the supplier's instructions. MPs were defined as events both smaller or equal in size to the 0.9 µm-large microbeads, and positively labeled with Annexin V-FITC.

For pharmacological modulation experiments, whole blood collected in citrate tube was centrifuged (800*g*, 10 min at 20°C), and plasma and buffy coat were discarded. RBCs were washed in PBS, and RBC pellets were resuspended at 20% Hct in PBS buffer containing 2.5 mM Ca^{2+} with either SNP (100 µM), L-NIO (10 µM), NAC (2.5 mM), cumene hydroperoxyde (100 µM) or vehicle for control condition for 24 h at 37°C and under constant shaking. Then, microparticles were extracted in the supernatant and quantified as previously described.

Red Blood Cell Microparticle Isolation

Red blood cell microparticles were negatively selected from total purified MPs by using a depletion kit composed of anti-PE microbeads and LD columns (130-097-054 and 130-042-901, both from Macs, Miltenyi Biotec, Bergisch Gladbach, Germany) according to the manufacturer's instructions. Briefly, total MPs were incubated with relevant PE conjugated antibodies targeting unwanted MPs (anti-CD15, anti-CD41, anti-CD14, and anti-CD106 antibodies). Then, microbeads coupled with antibody directed against PE were added to bind to these antibodies and allowed subsequent depletion of unwanted MPs by applying a

strong magnetic field. FACs was used to quantify purified RBC-MPs using the method previously described. The depletion procedure allowed to obtain a suspension containing 95% of RBC-MPs (see **Figure 1** in **Supplementary Data**).

Endothelial Cell Incubation With Sickle RBC-Derived Microparticles and Cytokine Supernatant Analysis

Human aortic endothelial cells (HAEC, Promocell Germany) were grown at 90% confluence in 96 well plates with fetal bovine serum (MV2 medium). Cells were pre-activated with TNF-α (0.6 ng/ml), as previously described (35, 36). Then, RBC-MPs that had been directly isolated from the plasma of SCA patients and healthy individuals, were incubated with HAEC cells for 24 h at a concentration of 50 000 MPs/100 µl with or without TAK 242 (2 µM), a TLR4 inhibitor. For negative controls, cells were incubated with TAK 242 vehicle (DMSO). Then, cells were washed twice with PBS containing BSA, detached from wells with Accutase (StemPro Accutase, Thermofisher Scientific) and resuspended in PBS-BSA. Cells were stained for 20 min at RT with anti-CD62E-FITC (0.125 µg/100 µl) and anti-CD54-PE (0.125 µg/100 µl) antibodies to assess E-Selectin and ICAM-1 expression at the surface of the cells. Stained cells were washed and re-suspended in FACS buffer, and analyzed by flow cytometry, according to manufacturer's instructions. MFI or percentage of positive cells were recorded to quantify E-Selectin and I-CAM1 expression.

Cell supernatant in the wells was immediately collected after the 24-h incubation, and stored at −80°C until analysis. Cytokines and stimulating factors in the supernatant were quantified by Bio-Plex Multiplex immunoassay (Biorad, California, USA), using the Bio-Plex Pro™ Human Cytokine 17-plex Assay kit and the BioPlex 3D platform (Biorad, California, USA), according to manufacturer's instructions.

Statistical Analysis

Data are represented as individual points with mean. Comparisons between AA and SCA groups were achieved by using student T-tests or Mann-Whitney tests, when appropriate. The effects of molecules on SCA RBCs were analyzed by using paired t-tests and a Friedman test for RBC-MPs production modulation. Pearson or Spearman correlations were performed to test the associations between the parameters investigated. Multivariate linear regression analysis was performed to test the presence of independent associations. Effects of RBC-MPs on endothelial cells were analyzed using Friedmann test followed by Dunn's *post hoc* test for multiple comparisons. GraphPad Prism 7 (La Jolla, CA, USA) and SPSS 23.0 (IBM, Armonk, NY, USA) softwares were used for statistical analyses. A p-value < 0.05 was considered as significant.

RESULTS

Eryptosis and RBC-MPs Are Increased in SCA

As expected, RBC deformability was lower in SCA patients than in healthy individuals ($p < 0.001$, **Figure 1A**). Analysis of eryptosis markers by FACS revealed that all markers were significantly increased in SCA RBCs compared to healthy RBCs: PS externalization at the surface of SCA RBCs ($p < 0.001$, **Figure 1B**, see **Figures 2A, B** in **Supplementary Data** for representative dot plots), RBC ROS content ($p < 0.001$, **Figure 1C**), intracellular levels of Ca^{2+} ($p < 0.01$, **Figure 1E**) and glucose uptake ($p < 0.05$, **Figure 1F**). ROS levels and the percentage of RBCs with externalized PS were positively correlated ($p < 0.0001$, $r = 0.70$, **Figure 1D**). RBC-MPs concentration was increased in SCA patients compared to healthy individuals ($p < 0.01$, **Figure 1G**). **Figure 1H** represents a flow-cytometric dot-plot image used to specifically identify RBC-MPs.

NO and Oxidative Stress Modulate RBC Deformability, Eryptosis Markers, and MPs Emission by Sickle RBCs

Incubation of SCA RBCs with the anti-oxidant agent NAC caused an increase of RBC deformability ($p < 0.01$, **Figure 2A**) and a decrease of the percentage of PS-exposing RBCs ($p < 0.01$, **Figure 2B**), RBC ROS content ($p < 0.01$, **Figure 2C**), RBC Ca^{2+} content ($p < 0.05$, **Figure 2D**) and RBC glucose uptake ($p < 0.05$, **Figure 2E**). The experiments performed with cumene hydroperoxide showed a decrease of RBC deformability ($p < 0.01$, **Figure 2F**), and an increase of the percentage of PS-exposing RBCs ($p < 0.01$, **Figure 2G**), RBC ROS content ($p < 0.05$, **Figure 2H**), RBC Ca^{2+} content ($p < 0.01$, **Figure 2I**), and RBC glucose uptake ($p < 0.05$, **Figure 2J**).

The use of the NO donor SNP also led to a rise of RBC deformability ($p < 0.01$, **Figure 2K**), a decrease of the percentage of PS-exposing RBCs ($p < 0.05$, **Figure 2L**) and RBC ROS content ($p < 0.05$, **Figure 2M**), but no significant change was observed for RBC Ca^{2+} content (**Figure 2N**) or RBC glucose uptake (**Figure 2O**). SNP also significantly increased RBC nitrite content and RBC β-Spectrin S-nitrosylation (see **Figures 3A, B** in **Supplementary Data**). The NOS inhibitor L-NIO had no significant effect on RBC nitrite content, deformability and eryptosis markers (data not shown).

SCA RBCs were also incubated for 24 h with NAC, cumene, SNP and L-NIO to test the effects of these chemical agents on the release of MPs. The results (**Figure 2P**) demonstrated that NAC decreased the amount of RBC-MPs ($p < 0.05$) while cumene hydroperoxide increased their release ($p < 0.05$). No significant effect of SNP and L-NIO was observed.

Following the quantification of RBC-MPs, AOPP and MDA levels in the blood of a SCA cohort at steady state ($n = 28$), positive correlations between several parameters were observed (RBC-MPs vs AOPP: $r = 0.44$, $p < 0.01$; RBC-MPs vs MDA: $r = 0.66$, $p < 0.001$; **Figures 3A, B**, respectively). These results suggest that the higher the systemic oxidative stress, the higher the amount of circulating RBC-derived MPs.

Arterial Stiffness Is Increased in SCA Patients and Correlates With the Amount of Circulating RBC-MPs

CR-PWV was measured in a cohort of 24 SCA patients, and compared to a group of AA ($n = 16$) of the same ethnic origin. As

previously reported (21), PWV was higher in SCA than in AA (**Figure 3C**, $p < 0.01$), indicating increased arterial stiffness in the former group. Circulating RBC-MPs were also measured in 24 patients of this cohort to test the association with the carotid-radial PWV. Our results showed a positive association between these two parameters (**Figure 3D**, $p < 0.01$, $r = 0.55$). Because chronic anemia may lead to important cardiovascular adaptations in order to compensate for the decrease in hemoglobin concentration (37), and because chronic hemolysis participates in the development of vasculopathy in SCA (38), a multivariate linear analysis was performed between carotid-radial PWV and RBC-MPs, LDH, AOPP, MDA and hemoglobin levels. The model was significant ($R^2 = 0.74$, $p < 0.05$), and only RBC-MPs were independently associated with the carotid-radial PWV ($p < 0.01$).

RBC-MPs Activate Endothelial Cells and Promote Inflammation Through TLR4

To better understand the relationship between RBC-MPs and macrovascular dysfunction, we analyzed the effects of RBC-MPs isolated from SCA and AA blood on the expression of ICAM-1 and E-selectin in HAEC. Incubation of plasma RBC-MPs with HAEC revealed that MPs from SCA patients significantly increased ICAM-1 ($p < 0.01$) and E-selectin ($p < 0.05$) expression compared to AA MPs (**Figures 4A, B**, respectively). The large amount of heme transported by RBC-MPs in SCA has been suspected to play a key role in endothelial dysfunction (19, 39). Because heme is an erythrocytic danger-associated molecular pattern (eDAMP) molecule, we further tested the effects of SCA RBC-MPs on ICAM-1 expression in HAEC in the presence or absence of TAK-242, a TLR4 inhibitor. We observed a decrease in the ICAM-1 expression induced by SCA RBC-MPs when inhibiting TLR4 ($p < 0.05$), although ICAM-1 expression was still higher than in the control condition (**Figure 4C**). Furthermore, the use of TAK-242 decreased the production of IL-1β, IL-6, and GM-CSF by HAEC in comparison to the condition in which HAEC were incubated with RBC-MPs without this inhibitor, but the concentrations of these molecules in the supernatant were still greater than in the control condition (**Figures 4D–F** $p < 0.05$ for all, 18).

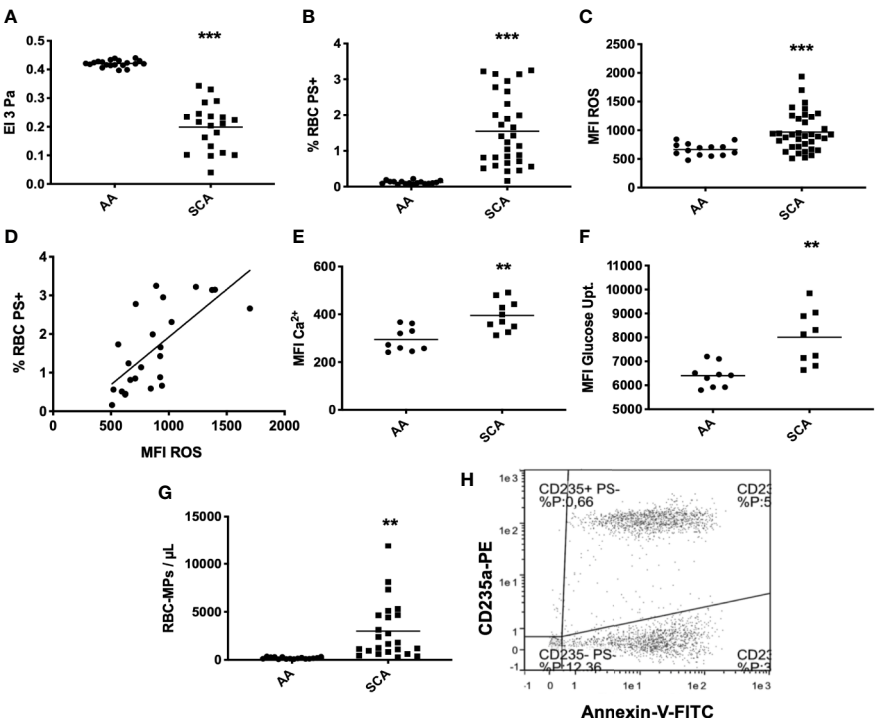

FIGURE 1 | RBC deformability, eryptosis markers, and RBC-MPs in SCA and healthy (AA) individuals. **(A)** RBC deformability in SCA (n = 35) and AA (n = 20) subjects. **(B)** RBC PS exposure in SCA (n = 30) and AA (n = 20) subjects. **(C)** ROS content in SCA (n = 31) and AA (n = 20) subjects. **(D)** Correlation between PS exposure and ROS level in SCA (correlation was made in 23 patients who had both RBC-PS exposure and RBC ROS measurements, using Pearson correlation). **(E)** RBC Ca^{2+} level in SCA (n = 10) and AA (n = 9) subjects. **(F)** Glucose uptake in SCA (n = 9) and AA (n = 9) subjects. **(G)** RBC-MP plasma concentrations in SCA (n = 24) and AA (n = 16) subjects. **(H)** Representative flow-cytometric dot-plot used to quantify RBC-MPs in SCA patient. RBC-MPs were determined as events smaller than 0.9 µm and both positive for annexin-V and CD235a. Significant difference between AA and SCA. **p < 0.01, ***p < 0.001. Statistical comparisons between AA and SCA for RBC deformability, PS exposure, ROS content and MPs concentration were achieved using Student T-test. Statistical comparisons between AA and SCA for Ca^{2+} level and glucose uptake content were achieved using Mann Whitney test. MFI, mean fluorescence intensity; %RBC PS+, percentage of RBCs positive for Annexin-V; ROS, level of reactive oxygen species in RBCs detected with DCFDA; Ca2+, level of calcium in RBCs detected with Fluo3.

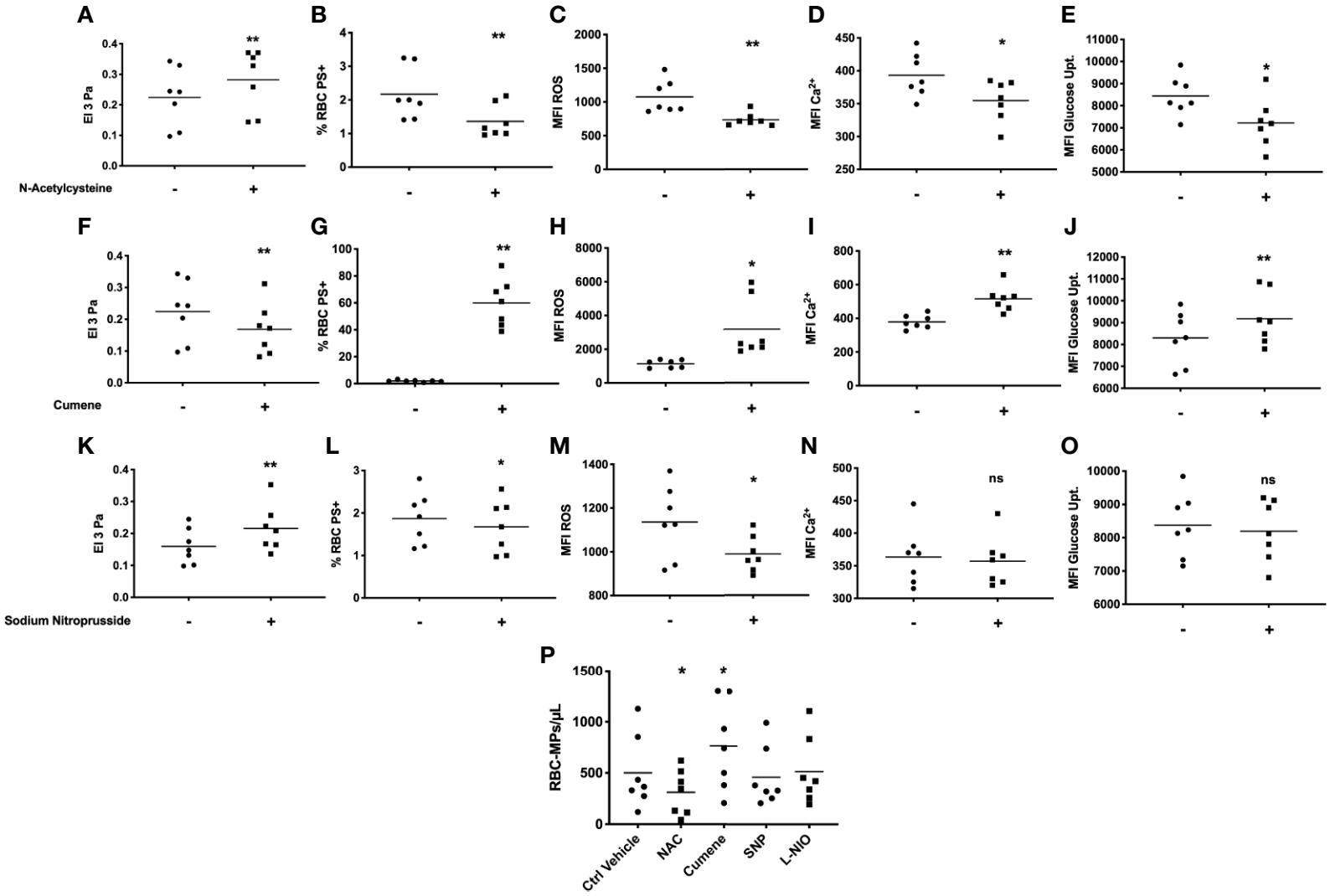

FIGURE 2 | *In vitro* modulation of RBC deformability, eryptosis, and RBC-MPs by oxidative stress and NO related agents on SCA RBCs. Impact of NAC (n = 7) on SCA RBC deformability **(A)**, RBC PS exposure **(B)**, ROS level **(C)**, RBC Ca^{2+} content **(D)** and glucose uptake **(E)**. Effect of cumene hydroperoxide (n = 7) on SCA RBC deformability **(F)**, RBC PS exposure **(G)**, ROS level **(H)**, RBC Ca^{2+} content **(I)** and glucose uptake **(J)**. Effect of SNP (n = 7) on SCA RBC deformability **(K)**, RBC PS exposure **(L)**, ROS level **(M)**, RBC Ca^{2+} content **(N)** and glucose uptake **(O).** Impact of NAC, cumene hydroperoxide, SNP and L-NIO on the release of MPs by RBCs in the supernatant **(P)** (n = 7). Significantly different from the control condition: *p < 0.05, **p < 0.01. ns, not significant. All statistical comparisons were performed using paired T-test except for the MPs modulation where a Friedmann test was used. MFI, mean fluorescence intensity; %RBC PS+, percentage of RBCs positive to Annexin-V; ROS, level of reactive oxygen species in RBCs detected with DCFDA; Ca2+, level of calcium in RBCs detected with Fluo3; NAC: N-Acetylcysteine; SNP, sodium nitroprusside; Cumene, cumene hydroperoxide; –, incubation with ctrl vehicle, +, incubation with pharmacological molecule.

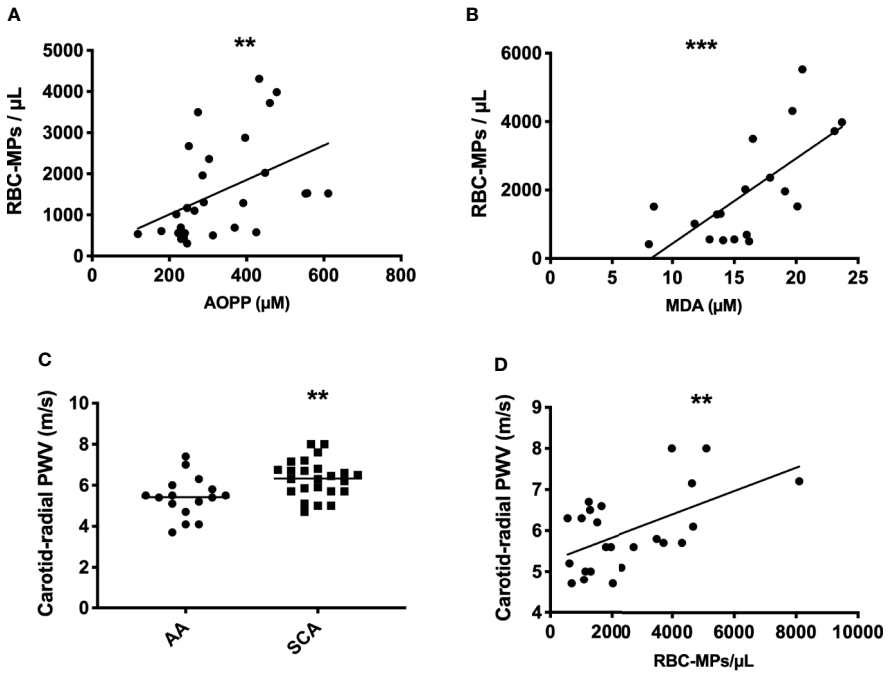

FIGURE 3 | Relationship betweent RBC-MPs, oxidative stress and carotid-radial pulse wave velocity (PWV) in SCA patients, and comparaison of PWV between AA and SCA individuals. Correlation between RBC-MPs plasma concentration and AOPP (n = 28) **(A)** and MDA (n = 19) **(B)** concentration in SCA patients. Carotid-radial PWV measured in 24 SCA and 16 AA subjects **(C)**. Correlation between RBC-MPs plasma concentration and carotid-radial PWV in 24 SCA patients **(D)**. $^{**}p < 0.01$, $^{***}p < 0.001$. Statistical correlations were determined using Pearson correlation test. Comparison between PWV in SCA and AA individuals were performed using Student T-test. PWV, pulse wave velocity.

DISCUSSION

Our study reports for the first time that 1) oxidative stress and NO modulate eryptosis in SCA, 2) oxidative stress increases the release of RBC-MPs in SCA and 3) RBC-MPs directly isolated from SCA blood partly modulate the inflammatory phenotype of endothelial cells through TLR4 activation. In addition, our study confirmed that increased levels of circulating RBC-MPs are associated with increased arterial stiffness in SCA (40).

As previously demonstrated, our results showed higher levels of eryptosis in SCA patients compared to healthy individuals (9, 10, 41, 42). Indeed, we demonstrated that SCA RBCs had higher Ca^{2+} content and increased PS exposure compared to RBC from healthy subjects. Increased PS exposure (1.5% in SCA compared to 0.1% in AA, i.e. a 15-fold increase) could promote RBCs adhesion to the vascular wall and activate coagulation, hence contributing to vaso-occlusive complications (41, 43). *In vitro* studies performed on healthy RBCs have suggested that oxidative stress could trigger eryptosis (6). Several mechanisms contribute to the increased levels of ROS in both plasma and RBCs in SCA (13, 44, 45). We detected higher levels of ROS in RBCs from SCA patients compared to healthy RBCs, and a positive association between RBC ROS level and RBC-PS exposure. We also observed higher glucose uptake in RBCs from patients with SCA compared to healthy RBCs, suggesting an increased metabolic demand and/or an energy depletion; conditions known to trigger eryptosis (46). Several proteins regulate RBC hydration state (47), Ca^{2+} concentration (48) and membrane asymmetry (49) in an energy dependent manner. Therefore, ATP depletion could be involved in eryptosis. Unfortunately, we were not able to assess the impact of hydroxyurea therapy on eryptosis markers as the majority of the cohort was under this treatment. Indeed, hydroxyurea could affect RBC physiology by its effects on oxidative stress and its NO donor properties (50).

Challenging SCA RBCs with antioxidant and pro-oxidant molecules demonstrated that oxidative stress could play an important role in eryptosis. Cumene hydroperoxide promoted eryptosis, while NAC, an antioxidant, limited this phenomenon by improving RBC deformability (+25%), and decreasing ROS (−33.5%), Ca^{2+} (−11.3%) and PS exposure levels (−40%). The increase of RBC deformability observed with NAC could be particularly relevant in the pathophysiological context of SCA, since the loss of deformability is a major contributor of several acute and chronic complications (51, 52). Clinical trials performed in SCA patients showed that NAC limits oxidative stress, hemolysis and RBC dehydration (53, 54). However, the recent study of Sins et al. (55) failed to clearly detect any clinical impact of NAC treatment in SCA. One possible explanation of this disappointing result could be that adherence to NAC treatment was very low in this study. Another explanation for the failure of NAC to provide a significant clinical effect could be its low bioavailability and its hydrophobicity. For this reason it

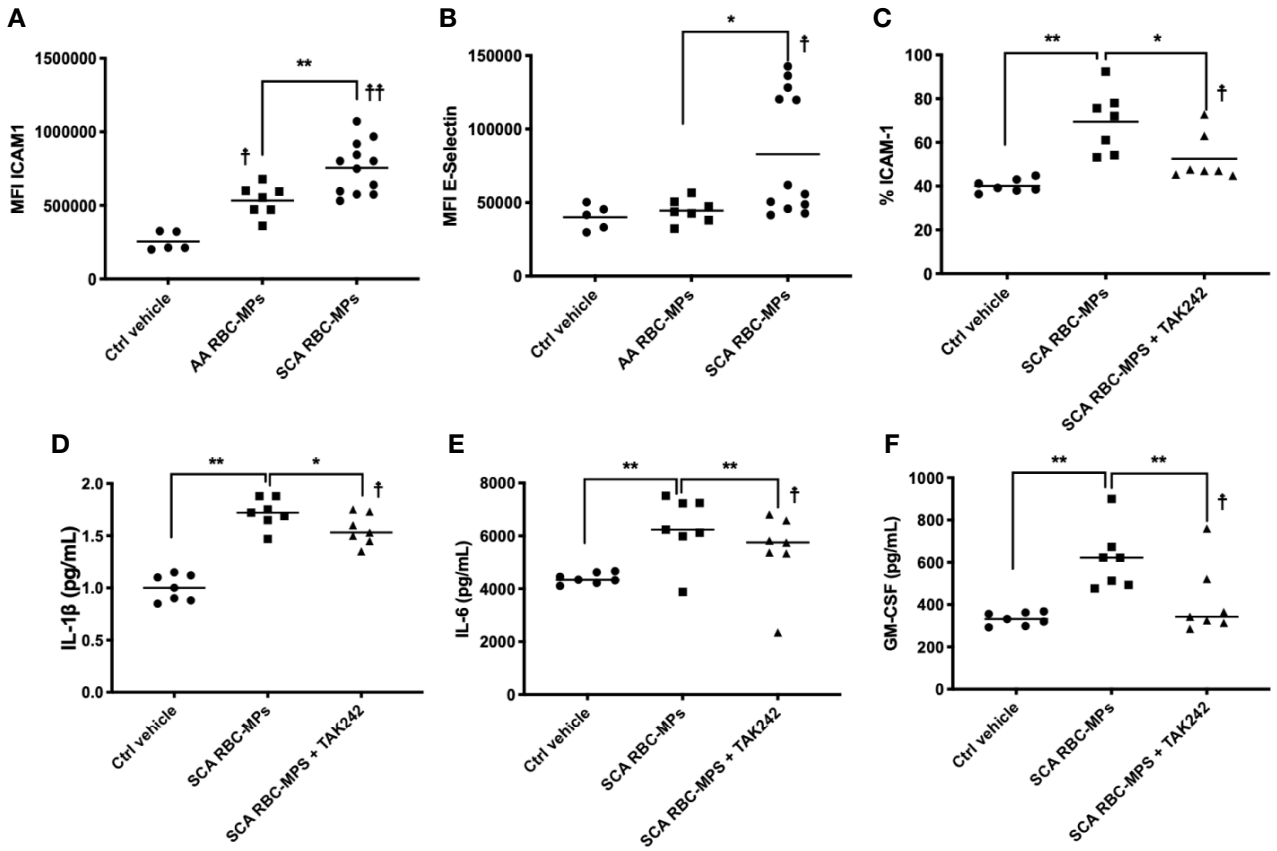

FIGURE 4 | Endothelial cell activation by RBC-MPs and TLR4 inhibition. Impact of RBC-MPs from AA (n = 7) and SCA (n = 12) subjects on ICAM-1 **(A)** and E-Selectin **(B)** expression by HAEC. Impact of TLR4 inhibition (TAK 242) on the effect mediated by SCA RBC-MPs (n = 7) on ICAM-1 expression by HAEC **(C)**. Effects of SCA RBC-MPs incubation on IL-1β **(D)**, IL-6 **(E)** as well as GM-CSF **(F)** production by HAEC, with or without TAK 242. *$p < 0.05$, **$p < 0.01$, †$p < 0.05$ vs ctrl vehicle, ††$p < 0.01$ vs ctrl vehicle. Statistical comparisons were achieved with Friedmann test followed by Dunn's test.

has been suggested that N-Acetylcysteine amides could be more efficient (56). Interestingly, the findings of Sins et al. showed that rates of vaso-occlusive crisis (VOC) were decreased in adherent patients (55). NAC is a precursor of reduced glutathione (GSH), an endogenous antioxidant, and GSH has been shown to be reduced in RBCs of SCA patients (57, 58). Therefore, our results suggest that GSH depletion could be involved in the enhanced eryptosis found in SCA by increasing levels of RBC-ROS. ROS are suspected to activate Ca^{2+} permeable unselective cation channels with subsequent Ca^{2+} entry (6). Increased Ca^{2+} concentration promotes membrane scrambling by inhibiting flippase and activating scramblase and floppase, which disrupt membrane asymmetry, and results in the exposure of PS on the outer leaflet of the membrane (49). Furthermore, the influx of Ca^{2+} into RBCs may activate proteases, like caspase 3 and calpains, that alter membrane and cytoskeleton interactions, leading to membrane blebbing and the release of MPs (59). In the present study, we showed that Cumene hydroperoxide increased Ca^{2+} level in SCA RBCs which could explain the greater RBC-MPs release induced by this oxidative molecule. On the opposite, NAC treatment decreased SCA RBCs Ca^{2+} level which could have contributed to the decrease of RBC-MPs release observed. However, it is unknown whether the MPs production modulation was directly related to oxidative stress process or Ca^{2+} influx.

We also found that the concentrations of RBC-MPs were higher in patients with SCA than in healthy individuals, in accordance with previous studies (14, 15). The positive associations found between AOPP or MDA and the amount of circulating RBC-MPs suggested that oxidative stress would likely play a role in the release of MPs by SCA RBCs. Enhanced oxidative stress during VOC is also suspected to promote RBC-MPs release (16). Indeed, Hierso et al. suggested that exacerbation of oxidative stress during VOC may induce the recruitment of oxidized band 3 in membrane aggregates which could lead to RBC-MPs release (16). It has also been shown in SCD mice model that hemoglobin oxidation and subsequent β-globin posttranslational modifications, including the irreversible oxidation of βCys93 and the ubiquitination of βLys96 and βLys145, were related to band 3 clustering and RBC-MPs emission (60).

NO bioavailability is decreased in SCA (38). It has been suggested that NO modulates eryptosis in healthy RBCs. Nikolay et al. (7) showed that NO could limit PS externalization induced by

Ca^{2+} ionophore in healthy RBCs, but no study has tested whether this is also the case in SCA RBCs. Our results showed that incubation of SCA RBCs with SNP effectively increased intracellular NO metabolites. SNP decreased slightly but significantly PS exposure and ROS level and had no effect on Ca^{2+} content. This latter result suggests that the rupture of membrane asymmetry may not be uniquely driven by Ca^{2+} influx, and could explain why no decrease in the concentration of RBC-MPs was observed in the SNP experiments. It has been observed that ROS may directly activate scramblase activity and promote PS exposure (61). Further studies need to be carried out to better understand the mechanism by which SNP can decrease levels of ROS. However, Ca^{2+} can inhibit thioredoxin, an antioxidant and antiapoptotic enzyme. NO has been shown to protect thioredoxin activity by S-nitrosylation of the protein (62), which could explain the decrease in levels of ROS and PS exposure in samples treated with SNP. The increased RBC deformability after incubation with SNP could be the consequence of the lower levels of RBC-ROS, since increasing RBC oxidative stress impairs RBC rheological properties (28). Moreover, the increased RBC β-Spectrin S-nitrosylation caused by SNP could have participated in the improvement of RBC deformability (28). Besides, inhibition of RBC NOS using L-NIO did not affect RBC nitrite content, deformability and eryptosis markers. These results could indicate that RBC NOS was not activated in basal condition in our cohort. We previously showed that RBC-NOS in SCA patients under HU treatment was less activated compared to AA and SCA patients without HU, because of the NO donor properties of the molecule. In the current study, the majority of the patients was under HU treatment which could explain why no effect of L-NIO and only a slight effect of SNP were observed. Indeed, patients under HU treatment had already high level of NO metabolites in RBC which could have limited the potential effects of SNP (50).

Vascular function has been shown to be altered in SCA in both the micro- (21, 63, 64) and macro-circulation (21, 65). It has been suggested that RBC-MPs could participate in the alterations of vascular function in SCA. Camus et al. showed that RBC-MPs generated *ex vivo* induced renal arterial vaso-occlusion in a murine model of SCA, and compromised vasodilation in isolated micro-vessels (66). These effects were mediated by the PS exposed on MPs, which is a common feature of all sub-cellular types of MPs. In 2015, the same group showed that heme-laden RBC-MPs generated *ex vivo* could transfer heme to the vascular endothelium and mediate *in vitro* oxidative stress and apoptosis of endothelial cells (19). However, the MPs used by Camus et al. were generated *ex vivo* by shearing sickle RBCs in a high viscous buffer (30 cP; i.e., 25-fold the viscosity of plasma) with thrombospondin-1 at 1500 s^{-1} (i.e., a very high shear rate that may occur in arterial stenosis or artificial devices). These conditions clearly do not recapitulate those leading to the *in vivo* release of RBC-MPs, and the characteristics of the *in vitro* produced RBC-MPs could be very different from RBC-MPs isolated directly from sickle patients with various clinical histories. Our study revealed an independent association between the concentration of circulating RBC-MPs and arterial stiffness, a marker of macrovascular dysfunction. Tantawy et al. (40) previously found a correlation between RBC-MPs concentration and aortic stiffness, evaluated by echocardiography, in SCA children. However, the direct impact of SCA RBC-MPs on endothelial cells from the macrocirculation has never been investigated. Compared to AA RBC-MPs, RBC-MPs from SCA patients increased the expression of adhesion molecules (ICAM-1 and E-selectin) in human aortic endothelial cells, indicating higher cell activation. These findings are in agreement with a recent study showing an impact of SCA RBC-MPs on microcirculation endothelial cells phenotype (67). ICAM-1 and E-selectin are implicated in circulating cell interactions with the endothelium, which contribute to vascular dysfunction (68). We further showed that inhibition of TLR4 partially decreased the deleterious consequences of MPs on the endothelial cells by limiting ICAM-1 expression and the production of the pro-inflammatory cytokines IL-1β and IL-6. Indeed, RBC-MPs would be able to activate TLR4 and promote inflammasome activation. This mechanism would lead to endothelial cell activation, cell adhesion, and a pro-inflammatory environment that supports vascular dysfunction. IL-1β and IL-6 can activate platelets and leukocytes, promote their adhesiveness (55), and damage the endothelium itself (68). IL-1β has been associated with stroke in SCA (69), and it has been suggested that IL-6 could be related to the development of pulmonary hypertension in SCA children (70). TLR4 inhibition only partially limited the effects mediated by SCA RBC-MPs, which suggests that other mechanisms could be involved in the detrimental consequences of SCA RBC-MPs on endothelial cells. Garnier et al. recently showed that the deleterious effects of SCA MPs on endothelial cells were mediated by the PS exposure on their surface (67). Evaluating the specific phenotype of RBC-MPs from SCA patients could help in better understanding the mechanisms involved in their deleterious effects on endothelial function.

Limitations

Due to logistical reasons (i.e. limited quantity of collected blood and purified RBC-MPs, and necessity to work on fresh blood sample), *in vivo* modulation experiments have only been performed in a sub-set of the total population recruited. Further studies involving larger cohort are required to fully evaluate the mechanisms at the origin of eryptosis in SCA and the consequences of RBC-MPs on endothelial cells. Besides, in this study, vascular function has been evaluated by pulse wave velocity only. Studies investigating vascular reactivity, and more particularly endothelium-dependent macro- and microvascular reactivity, would help in understanding more deeply the link between vascular dysfunction and RBC-MPs in SCA and could increase the biological relevance of our findings.

CONCLUSION

Together, our results suggest that RBC-MPs, that are released during enhanced eryptosis, could play a crucial role in macrovascular dysfunction in SCA patients, and that oxidative stress would modulate eryptosis and RBC-MPs release. RBC-MPs could exert deleterious properties on endothelial cells of the macrocirculation, partly through the activation of TLR4, promoting the expression of adhesion molecules and cytokine

production, which may contribute to vascular dysfunction. Further investigations are required to identify the specificity of SCA RBC-MPs at the origin of TLR4 activation, but this study opens new perspectives to understand the underlying mechanisms of vascular dysfunction in SCA. It also points toward new therapeutic targets focusing on preventing eryptosis and/or TLR4 activation in SCA.

DATA AVAILABILITY STATEMENT

The raw data supporting the conclusions of this article will be made available by the authors, without undue reservation.

ETHICS STATEMENT

The studies involving human participants were reviewed and approved by The CPP Sud-Est IV (Lyon, France, L16-47) and the CPP Sud/Ouest Outre Mer III (Bordeaux, France, 2012-A00701-42). Written informed consent to participate in this study was provided by the participants' legal guardian/next of kin.

AUTHOR CONTRIBUTIONS

All authors approved the final version of the manuscript. EN, MaR, MG and PC designed the protocol, performed research, analyzed the data, and wrote the manuscript. NG, YG, SS, CM, CR, PJ, ES, and M-DH-D performed research and edited the manuscript. SA-J and BT designed the protocol and performed research. MG designed the protocol and edited the manuscript. MéR performed research. AG, YB, NL, and RF provided help to organize the different protocols and edited the manuscript. GC and ME-J provided help to organize the different protocols. All authors contributed to the article and approved the submitted version.

FUNDING

The study was funded by DFG grant GR4467/3-1.

ACKNOWLEDGMENTS

We sincerely thank the technicians of the Laboratoire de Biochimie et de Biologie Moléculaire (UF de Biochimie des Pathologies érythrocytaires, Centre de Biologie et de Pathologie Est, Hospices Civils de Lyon) for their help in the characterization of sickle blood.

SUPPLEMENTARY MATERIAL

The Supplementary Material for this article can be found online at: https://www.frontiersin.org/articles/10.3389/fimmu.2020.551441/full#supplementary-material

REFERENCES

1. Ballas SK. Sickle cell disease: Classification of clinical complications and approaches to preventive and therapeutic management. *Clin Hemorheol Microcirc* (2018) 68(2-3):105–28. doi: 10.3233/CH-189002
2. Reiter CD, Wang X, Tanus-Santos JE, Hogg N, Cannon RO,3, Schechter AN, et al. Cell-free hemoglobin limits nitric oxide bioavailability in sickle-cell disease. *Nat Med* (2002) 8(12):1383–9. doi: 10.1038/nm1202-799
3. Kato GJ, Steinberg MH, Gladwin MT. Intravascular hemolysis and the pathophysiology of sickle cell disease. *J Clin Invest* (2017) 127(3):750–60. doi: 10.1172/JCI89741
4. Mockesch B, Connes P, Charlot K, Skinner S, Hardy-Dessources MD, Romana M, et al. Association between oxidative stress and vascular reactivity in children with sickle cell anaemia and sickle haemoglobin C disease. *Br J Haematol* (2017) 178(3):468–75. doi: 10.1111/bjh.14693
5. Belcher JD, Chen C, Nguyen J, Milbauer L, Abdulla F, Alayash AI, et al. Heme triggers TLR4 signaling leading to endothelial cell activation and vaso-occlusion in murine sickle cell disease. *Blood.* (2014) 123(3):377–90. doi: 10.1182/blood-2013-04-495887
6. Lang F, Abed M, Lang E, Foller M. Oxidative stress and suicidal erythrocyte death. *Antioxid Redox Signal* (2014) 21(1):138–53. doi: 10.1089/ars.2013.5747
7. Nicolay JP, Liebig G, Niemoeller OM, Koka S, Ghashghaeinia M, Wieder T, et al. Inhibition of suicidal erythrocyte death by nitric oxide. *Pflugers Arch* (2008) 456(2):293–305. doi: 10.1007/s00424-007-0393-1
8. Lang E, Lang F. Mechanisms and pathophysiological significance of eryptosis, the suicidal erythrocyte death. *Semin Cell Dev Biol* (2015) 39:35–42. doi: 10.1016/j.semcdb.2015.01.009
9. Weiss E, Rees DC, Gibson JS. Role of calcium in phosphatidylserine externalisation in red blood cells from sickle cell patients. *Anemia.* (2011) 2011:379894. doi: 10.1155/2011/379894
10. Hertz L, Huisjes R, Llaudet-Planas E, Petkova-Kirova P, Makhro A, Danielczok JG, et al. Is Increased Intracellular Calcium in Red Blood Cells a Common Component in the Molecular Mechanism Causing Anemia? *Front Physiol* (2017) 8:673:673. doi: 10.3389/fphys.2017.00673
11. Yasin Z, Witting S, Palascak MB, Joiner CH, Rucknagel DL, Franco RS. Phosphatidylserine externalization in sickle red blood cells: associations with cell age, density, and hemoglobin F. *Blood.* (2003) 102(1):365–70. doi: 10.1182/blood-2002-11-3416
12. Kato GJ, Piel FB, Reid CD, Gaston MH, Ohene-Frempong K, Krishnamurti L, et al. Sickle cell disease. *Nat Rev Dis Primers* (2018) 4:18010. doi: 10.1038/nrdp.2018.10
13. Voskou S, Aslan M, Fanis P, Phylactides M, Kleanthous M. Oxidative stress in beta-thalassaemia and sickle cell disease. *Redox Biol* (2015) 6:226–39. doi: 10.1016/j.redox.2015.07.018
14. Piccin A, Murphy C, Eakins E, Kunde J, Corvetta D, Di Pierro A, et al. Circulating microparticles, protein C, free protein S and endothelial vascular markers in children with sickle cell anaemia. *J Extracell Vesicles* (2015) 4:28414. doi: 10.3402/jev.v4.28414
15. van Beers EJ, Schaap MC, Berckmans RJ, Nieuwland R, Sturk A, van Doormaal FF, et al. Circulating erythrocyte-derived microparticles are associated with coagulation activation in sickle cell disease. *Haematologica.* (2009) 94(11):1513–9. doi: 10.3324/haematol.2009.008938
16. Hierso R, Lemonne N, Villaescusa R, Lalanne-Mistrih ML, Charlot K, Etienne-Julan M, et al. Exacerbation of oxidative stress during sickle vaso-occlusive crisis is associated with decreased anti-band 3 autoantibodies rate and increased red blood cell-derived microparticle level: a prospective study. *Br J Haematol* (2017) 176(5):805–13. doi: 10.1111/bjh.14476
17. Kasar M, Boga C, Yeral M, Asma S, Kozanoglu I, Ozdogu H. Clinical significance of circulating blood and endothelial cell microparticles in sickle-cell disease. *J Thromb Thrombolysis* (2014) 38(2):167–75. doi: 10.1007/s11239-013-1028-3

18. Romana M, Connes P, Key NS. Microparticles in sickle cell disease. *Clin Hemorheol Microcirc* (2018) 68(2-3):319–29. doi: 10.3233/CH-189014
19. Camus SM, De Moraes JA, Bonnin P, Abbyad P, Le Jeune S, Lionnet F, et al. Circulating cell membrane microparticles transfer heme to endothelial cells and trigger vasoocclusions in sickle cell disease. *Blood.* (2015) 125(24):3805–14. doi: 10.1182/blood-2014-07-589283
20. Tomiyama H, Yamashina A. Non-invasive vascular function tests: their pathophysiological background and clinical application. *Circ J* (2010) 74 (1):24–33. doi: 10.1253/circj.cj-09-0534
21. Mockesch B, Charlot K, Jumet S, Romana M, Divialle-Doumdo L, Hardy-Dessources MD, et al. Micro- and macrovascular function in children with sickle cell anaemia and sickle cell haemoglobin C disease. *Blood Cells Mol Dis* (2017) 64:23–9. doi: 10.1016/j.bcmd.2017.02.001
22. Butlin M, Qasem A. Large Artery Stiffness Assessment Using SphygmoCor Technology. *Pulse (Basel)* (2017) 4(4):180–92. doi: 10.1159/000452448
23. Wilkinson IB, Hall IR, MacCallum H, Mackenzie IS, McEniery CM, van der Arend BJ, et al. Pulse-wave analysis: clinical evaluation of a noninvasive, widely applicable method for assessing endothelial function. *Arterioscler Thromb Vasc Biol* (2002) 22(1):147–52. doi: 10.1161/hq0102.101770
24. Ranque B, Menet A, Boutouyrie P, Diop IB, Kingue S, Diarra M, et al. Arterial Stiffness Impairment in Sickle Cell Disease Associated With Chronic Vascular Complications: The Multinational African CADRE Study. *Circulation.* (2016) 134(13):923–33. doi: 10.1161/CIRCULATIONAHA.115.021015
25. Baskurt OK, Boynard M, Cokelet GC, Connes P, Cooke BM, Forconi S, et al. New guidelines for hemorheological laboratory techniques. *Clin Hemorheol Microcirc* (2009) 42(2):75–97. doi: 10.3233/CH-2009-1202
26. Renoux C, Parrow N, Faes C, Joly P, Hardeman M, Tisdale J, et al. Importance of methodological standardization for the ektacytometric measures of red blood cell deformability in sickle cell anemia. *Clin Hemorheol Microcirc* (2016) 62(2):173–9. doi: 10.3233/CH-151979
27. Kleinbongard P, Dejam A, Lauer T, Rassaf T, Schindler A, Picker O, et al. Plasma nitrite reflects constitutive nitric oxide synthase activity in mammals. *Free Radic Biol Med* (2003) 35(7):790–6. doi: 10.1016/S0891-5849(03)00406-4
28. Grau M, Pauly S, Ali J, Walpurgis K, Thevis M, Bloch W, et al. RBC-NOS-dependent S-nitrosylation of cytoskeletal proteins improves RBC deformability. *PloS One* (2013) 8(2):e56759. doi: 10.1371/journal.pone.0056759
29. Pelletier MM, Kleinbongard P, Ringwood L, Hito R, Hunter CJ, Schechter AN, et al. The measurement of blood and plasma nitrite by chemiluminescence: pitfalls and solutions. *Free Radic Biol Med* (2006) 41(4):541–8. doi: 10.1016/j.freeradbiomed.2006.05.001
30. Hendgen-Cotta U, Grau M, Rassaf T, Gharini P, Kelm M, Kleinbongard P. Reductive gas-phase chemiluminescence and flow injection analysis for measurement of the nitric oxide pool in biological matrices. *Methods Enzymol* (2008) 441:295–315. doi: 10.1016/S0076-6879(08)01216-0
31. Witko-Sarsat V, Gausson V, Descamps-Latscha B. Are advanced oxidation protein products potential uremic toxins? *Kidney Int Suppl* (2003) 84):S11–4. doi: 10.1046/j.1523-1755.63.s84.47.x
32. Diaw M, Pialoux V, Martin C, Samb A, Diop S, Faes C, et al. Sickle Cell Trait Worsens Oxidative Stress, Abnormal Blood Rheology, and Vascular Dysfunction in Type 2 Diabetes. *Diabetes Care* (2015) 38(11):2120–7. doi: 10.2337/dc15-0699
33. Ohkawa H, Ohishi N, Yagi K. Assay for lipid peroxides in animal tissues by thiobarbituric acid reaction. *Anal Biochem* (1979) 95(2):351–8. doi: 10.1016/0003-2697(79)90738-3
34. Nebor D, Romana M, Santiago R, Vachiery N, Picot J, Broquere C, et al. Fetal hemoglobin and hydroxycarbamide moduate both plasma concentration and cellular origin of circulating microparticles in sickle cell anemia children. *Haematologica.* (2013) 98(6):862–7. doi: 10.3324/haematol.2012.073619
35. Chaar V, Laurance S, Lapoumeroulie C, Cochet S, De Grandis M, Colin Y, et al. Hydroxycarbamide decreases sickle reticulocyte adhesion to resting endothelium by inhibiting endothelial lutheran/basal cell adhesion molecule (Lu/BCAM) through phosphodiesterase 4A activation. *J Biol Chem* (2014) 289 (16):11512–21. doi: 10.1074/jbc.M113.506121
36. Verger E, Schoevaert D, Carrivain P, Victor JM, Lapoumeroulie C, Elion J. Prior exposure of endothelial cells to hydroxycarbamide alters the flow dynamics and adhesion of sickle red blood cells. *Clin Hemorheol Microcirc* (2014) 57(1):9–22. doi: 10.3233/CH-131762
37. Kato GJ, Hebbel RP, Steinberg MH, Gladwin MT. Vasculopathy in sickle cell disease: Biology, pathophysiology, genetics, translational medicine, and new research directions. *Am J Hematol* (2009) 84(9):618–25. doi: 10.1002/ajh.21475
38. Kato GJ, Gladwin MT, Steinberg MH. Deconstructing sickle cell disease: reappraisal of the role of hemolysis in the development of clinical subphenotypes. *Blood Rev* (2007) 21(1):37–47. doi: 10.1016/j.blre.2006.07.001
39. Vercellotti GM. Special delivery: microparticles convey heme. *Blood.* (2015) 125(24):3677–8. doi: 10.1182/blood-2015-04-639484
40. Tantawy AA, Adly AA, Ismail EA, Habeeb NM, Farouk A. Circulating platelet and erythrocyte microparticles in young children and adolescents with sickle cell disease: Relation to cardiovascular complications. *Platelets.* (2013) 24 (8):605–14. doi: 10.3109/09537104.2012.749397
41. Setty BN, Kulkarni S, Stuart MJ. Role of erythrocyte phosphatidylserine in sickle red cell-endothelial adhesion. *Blood.* (2002) 99(5):1564–71. doi: 10.1182/blood.v99.5.1564
42. .Tait JF, Gibson D. Measurement of membrane phospholipid asymmetry in normal and sickle-cell erythrocytes by means of annexin V binding. *J Lab Clin Med* (1994) 123(5):741–8
43. Setty BN, Kulkarni S, Rao AK, Stuart MJ. Fetal hemoglobin in sickle cell disease: relationship to erythrocyte phosphatidylserine exposure and coagulation activation. *Blood.* (2000) 96(3):1119–24. doi: 10.1182/blood.V96.3.1119
44. Aslan M, Freeman BA. Oxidant-mediated impairment of nitric oxide signaling in sickle cell disease–mechanisms and consequences. *Cell Mol Biol (Noisy-le-grand)* (2004) 50(1):95–105.
45. George A, Pushkaran S, Konstantinidis DG, Koochaki S, Malik P, Mohandas N, et al. Erythrocyte NADPH oxidase activity modulated by Rac GTPases, PKC, and plasma cytokines contributes to oxidative stress in sickle cell disease. *Blood.* (2013) 121(11):2099–107. doi: 10.1182/blood-2012-07-441188
46. Klarl BA, Lang PA, Kempe DS, Niemoeller OM, Akel A, Sobiesiak M, et al. Protein kinase C mediates erythrocyte "programmed cell death" following glucose depletion. *Am J Physiol Cell Physiol* (2006) 290(1):C244–53. doi: 10.1152/ajpcell.00283.2005
47. Gallagher PG. Disorders of red cell volume regulation. *Curr Opin Hematol* (2013) 20(3):201–7. doi: 10.1097/MOH.0b013e32835f6870
48. Lew VL, Tiffert T. On the Mechanism of Human Red Blood Cell Longevity: Roles of Calcium, the Sodium Pump, PIEZO1, and Gardos Channels. *Front Physiol* (2017) 8:977:977. doi: 10.3389/fphys.2017.00977
49. Barber LA, Palascak MB, Joiner CH, Franco RS. Aminophospholipid translocase and phospholipid scramblase activities in sickle erythrocyte subpopulations. *Br J Haematol* (2009) 146(4):447–55. doi: 10.1111/j.1365-2141.2009.07760.x
50. Nader E, Grau M, Fort R, Collins B, Cannas G, Gauthier A, et al. Hydroxyurea therapy modulates sickle cell anemia red blood cell physiology: Impact on RBC deformability, oxidative stress, nitrite levels and nitric oxide synthase signalling pathway. *Nitric Oxide* (2018) 81:28–35. doi: 10.1016/j.niox.2018.10.003
51. Connes P, Alexy T, Detterich J, Romana M, Hardy-Dessources MD, Ballas SK. The role of blood rheology in sickle cell disease. *Blood Rev* (2016) 30(2):111–8. doi: 10.1016/j.blre.2015.08.005
52. Connes P, Renoux C, Romana M, Abkarian M, Joly P, Martin C, et al. Blood rheological abnormalities in sickle cell anemia. *Clin Hemorheol Microcirc* (2018) 68(2-3):165–72. doi: 10.3233/CH-189005
53. Nur E, Brandjes DP, Teerlink T, Otten HM, Oude Elferink RP, Muskiet F, et al. N-acetylcysteine reduces oxidative stress in sickle cell patients. *Ann Hematol* (2012) 91(7):1097–105. doi: 10.1007/s00277-011-1404-z
54. Al Balushi H, Hannemann A, Rees D, Brewin J, Gibson JS. The Effect of Antioxidants on the Properties of Red Blood Cells From Patients With Sickle Cell Anemia. *Front Physiol* (2019) 10:976:976. doi: 10.3389/fphys.2019.00976
55. Sins JWR, Fijnvandraat K, Rijneveld AW, Boom MB, Kerkhoffs JH, van Meurs AH, et al. Effect of N-acetylcysteine on pain in daily life in patients with sickle cell disease: a randomised clinical trial. *Br J Haematol* (2018) 182(3):444–8. doi: 10.1111/bjh.14809
56. Sunitha K, Hemshekhar M, Thushara RM, Santhosh MS, Yariswamy M, Kemparaju K, et al. N-Acetylcysteine amide: a derivative to fulfill the promises of N-Acetylcysteine. *Free Radic Res* (2013) 47(5):357–67. doi: 10.3109/10715762.2013.781595

57. Zafarullah M, Li WQ, Sylvester J, Ahmad M. Molecular mechanisms of N-acetylcysteine actions. *Cell Mol Life Sci* (2003) 60(1):6–20. doi: 10.1007/s000180300001
58. Gizi A, Papassotiriou I, Apostolakou F, Lazaropoulou C, Papastamataki M, Kanavaki I, et al. Assessment of oxidative stress in patients with sickle cell disease: The glutathione system and the oxidant-antioxidant status. *Blood Cells Mol Dis* (2011) 46(3):220–5. doi: 10.1016/j.bcmd.2011.01.002
59. Westerman M, Porter JB. Red blood cell-derived microparticles: An overview. *Blood Cells Mol Dis* (2016) 59:134–9. doi: 10.1016/j.bcmd.2016.04.003
60. Jana S, Strader MB, Meng F, Hicks W, Kassa T, Tarandovskiy I, et al. Hemoglobin oxidation-dependent reactions promote interactions with band 3 and oxidative changes in sickle cell-derived microparticles. *JCI Insight* (2018) 3(21). doi: 10.1172/jci.insight.120451
61. Kamp D, Sieberg T, Haest CW. Inhibition and stimulation of phospholipid scrambling activity. Consequences for lipid asymmetry, echinocytosis, and microvesiculation of erythrocytes. *Biochemistry.* (2001) 40(31):9438–46. doi: 10.1021/bi0107492
62. Haendeler J, Hoffmann J, Tischler V, Berk BC, Zeiher AM, Dimmeler S. Redox regulatory and anti-apoptotic functions of thioredoxin depend on S-nitrosylation at cysteine 69. *Nat Cell Biol* (2002) 4(10):743–9. doi: 10.1038/ncb851
63. Mohan JS, Lip GY, Blann AD, Bareford D, Marshall JM. Endothelium-dependent and endothelium-independent vasodilatation of the cutaneous circulation in sickle cell disease. *Eur J Clin Invest* (2011) 41(5):546–51. doi: 10.1111/j.1365-2362.2010.02444.x
64. Tharaux PL, Girot R, Kanfer A, Dussaule JC, Gaitz JP, Tribout L, et al. Cutaneous microvascular blood flow and reactivity in patients with homozygous sickle cell anaemia. *Eur J Haematol* (2002) 68(6):327–31. doi: 10.1034/j.1600-0609.2002.02701.x
65. Pikilidou M, Yavropoulou M, Antoniou M, Papakonstantinou E, Pantelidou D, Chalkia P, et al. Arterial Stiffness and Peripheral and Central Blood Pressure in Patients With Sickle Cell Disease. *J Clin Hypertens (Greenwich)* (2015) 17(9):726–31. doi: 10.1111/jch.12572
66. Camus SM, Gausseres B, Bonnin P, Loufrani L, Grimaud L, Charue D, et al. Erythrocyte microparticles can induce kidney vaso-occlusions in a murine model of sickle cell disease. *Blood.* (2012) 120(25):5050–8. doi: 10.1182/blood-2012-02-413138
67. Garnier Y, Ferdinand S, Garnier M, Cita-Baltyde K, Hierso R, Claes A, et al. Plasma microparticles of sickle patients during crisis or taking hydroxyurea modify endothelium inflammatory properties. *Blood* (2020) 136(2):247–56. doi: 10.1182/blood.2020004853
68. Zhang D, Xu C, Manwani D, Frenette PS. Neutrophils, platelets, and inflammatory pathways at the nexus of sickle cell disease pathophysiology. *Blood.* (2016) 127(7):801–9. doi: 10.1182/blood-2015-09-618538
69. Asare K, Gee BE, Stiles JK, Wilson NO, Driss A, Quarshie A, et al. Plasma interleukin-1beta concentration is associated with stroke in sickle cell disease. *Cytokine.* (2010) 49(1):39–44. doi: 10.1016/j.cyto.2009.10.002
70. Niu X, Nouraie M, Campbell A, Rana S, Minniti CP, Sable C, et al. Angiogenic and inflammatory markers of cardiopulmonary changes in children and adolescents with sickle cell disease. *PloS One* (2009) 4(11):e7956. doi: 10.1371/journal.pone.0007956

Conflict of Interest: MéR was employed by the company Erytech Pharma (Lyon, France).

The remaining authors declare that the research was conducted in the absence of any commercial or financial relationships that could be construed as a potential conflict of interest. Part of the study was funded by DFG grant GR4467/3-1.

frontiers in Immunology

ORIGINAL RESEARCH
published: 14 December 2020
doi: 10.3389/fimmu.2020.535147

Endothelial Barrier Integrity Is Disrupted *In Vitro* by Heme and by Serum From Sickle Cell Disease Patients

*Vanessa Araujo Gomes Santaterra[1], Maiara Marx Luz Fiusa[1], Bidossessi Wilfried Hounkpe[1], Francine Chenou[1], Wouitchekpo Vincent Tonasse[1], Loredana Nilkenes Gomes da Costa[1,2], Diego Garcia-Weber[3], Igor de Farias Domingos[4,5], Franciele de Lima[1], Ivanio Teixeira Borba-Junior[1], Aderson da Silva Araújo[6], Antonio Roberto Lucena-Araújo[4], Marcos André Cavalcante Bezerra[4], Magnun Nueldo Nunes dos Santos[1], Fernando Ferreira Costa[1,7], Jaime Millán[3] and Erich Vinicius De Paula[1,7]**

[1] School of Medical Sciences, University of Campinas, Campinas, Brazil, [2] Department of Biomedicine, Federal University of Piaui, Parnaiba, Brazil, [3] Centro de Biologia Molecular Severo Ochoa, Consejo Superior de Investigaciones Cientificas, Universidad Autonoma de Madrid, Madrid, Spain, [4] Genetics Postgraduate Program, Federal University of Pernambuco, Recife, Brazil, [5] Department of Clinical and Toxicological Analysis, Federal University of Rio Grande do Norte, Natal, Brazil, [6] Department of Internal Medicine, Hematology and Hemotherapy Foundation of Pernambuco (HEMOPE), Recife, Brazil, [7] Hematology and Hemotherapy Center, University of Campinas, Campinas, Brazil

Free extracellular heme has been shown to activate several compartments of innate immunity, acting as a danger-associated molecular pattern (DAMP) in hemolytic diseases. Although localized endothelial barrier (EB) disruption is an important part of inflammation that allows circulating leukocytes to reach inflamed tissues, non-localized/deregulated disruption of the EB can lead to widespread microvascular hyperpermeability and secondary tissue damage. In mouse models of sickle cell disease (SCD), EB disruption has been associated with the development of a form of acute lung injury that closely resembles acute chest syndrome (ACS), and that can be elicited by acute heme infusion. Here we explored the effect of heme on EB integrity using human endothelial cell monolayers, in experimental conditions that include elements that more closely resemble *in vivo* conditions. EB integrity was assessed by electric cell-substrate impedance sensing in the presence of varying concentrations of heme and sera from SCD patients or healthy volunteers. Heme caused a dose-dependent decrease of the electrical resistance of cell monolayers, consistent with EB disruption, which was confirmed by staining of junction protein VE-cadherin. In addition, sera from SCD patients, but not from healthy volunteers, were also capable to induce EB disruption. Interestingly, these effects were not associated with total heme levels in serum. However, when heme was added to sera from SCD patients, but not from healthy volunteers, EB disruption could be elicited, and this effect was associated with hemopexin serum levels. Together our *in vitro* studies provide additional support to the concept of heme as a DAMP in hemolytic conditions.

Keywords: endothelial barrier, heme, sickle cell disease, electric cell-substrate impedance sensing, danger-associated molecular pattern, hemopexin

OPEN ACCESS

Edited by:
Caroline Le Van Kim, Université Paris Diderot, France

Reviewed by:
Philippe Connes, Université Claude Bernard Lyon 1, France
Olivier Blanc-Brude, INSERM U970 Paris-Centre de Recherche Cardiovasculaire (PARCC), France

***Correspondence:**
Erich Vinicius De Paula
erich@unicamp.br

Specialty section:
This article was submitted to Inflammation, a section of the journal Frontiers in Immunology

Received: *14 February 2020*
Accepted: *04 November 2020*
Published: *14 December 2020*

Citation:
Santaterra VAG, Fiusa MML, Hounkpe BW, Chenou F, Tonasse WV, da Costa LNG, Garcia-Weber D, Domingos IdF, Lima Fd, Borba-Junior IT, Araújo AS, Lucena-Araújo AR, Bezerra MAC, dos Santos MNN, Costa FF, Millán J and De Paula EV (2020) Endothelial Barrier Integrity Is Disrupted In Vitro by Heme and by Serum From Sickle Cell Disease Patients. Front. Immunol. 11:535147. doi: 10.3389/fimmu.2020.535147

INTRODUCTION

Heme is a ubiquitous molecule present in almost all forms of life, that is normally found conjugated to hemoproteins such as hemoglobin (Hb), the most abundant pool of heme in mammals. However, despite its importance in biological pathways such as oxygen transportation, several lines of evidence demonstrate that free extracellular heme (FEH) can also be toxic to cells, a concept supported by the selection of extremely effective extracellular scavenging mechanisms (e.g., hemopexin) that preclude the circulation of FEH (1–3).

The toxicity of FEH is particularly important for the pathogenesis of conditions associated with increased intravascular hemolysis (hence, high free Hb levels), since oxidation of free Hb has been shown to increase the rate of heme release to the extracellular space (4). FEH toxicity can be caused by direct (i.e., intercalation of heme in cellular membranes) or indirect (i.e., immune-mediated) mechanisms, and in regard to the latter, several studies demonstrated that heme can activate a myriad of innate immunity compartments such as TLR4-dependent pathways (5), neutrophil/neutrophil extracellular trap release (6, 7), complement (8, 9), inflammasomes (10), and hemostasis (11–13). Together, these studies support the notion that heme can act as a danger-associated molecular pattern (DAMP) in diseases characterized by high hemolytic rates such as malaria, sepsis, hemolytic uremic syndrome and sickle cell disease (SCD), where FEH could trigger and/or contribute to the underlying inflammatory response (14–17).

Localized endothelial barrier (EB) disruption is an important and finely regulated part of innate immune response that allows circulating leukocytes to reach inflamed tissues (18). However, deregulated EB disruption can lead to widespread microvascular hyperpermeability and secondary tissue damage (19, 20). While this possibility is more evident in conditions such as sepsis-associated acute lung injury (ALI) and cerebral malaria, studies in mice models of SCD recently demonstrated that EB disruption could contribute to the pathogenesis of acute chest syndrome (ACS), a form of ALI that figures among the main causes of death in SCD (21). Moreover, these studies demonstrated that FEH can cause a severe and fatal form of ALI in SCD mice, preceded by congestion and edema of alveolar spaces (22). In fact, the barrier-disrupting effects of heme have been demonstrated more than 15 years ago (23), and were recently confirmed in studies using endothelial cell cultures stimulated by FEH by independent groups, using different experimental designs (24–26). However, to the best of our knowledge no study evaluated the effect of sera from SCD patients with varying levels of heme on EB integrity. Moreover, one of the caveats of studying the pathological relevance of heme refers to the unstable nature of FEH in biological systems due to its fast binding kinetics to circulating proteins (such as hemopexin and albumin), allowing some authors to question the concept that heme can act as a DAMP in living organisms (27). Here we explored the effect of heme on human endothelial cell monolayers in experimental conditions designed to address some of these caveats, using a robust functional assay (28, 29) that has been previously used in studies of EB function in other inflammatory conditions (30, 31).

MATERIALS AND METHODS

Reagents, Antibodies, and Cells

Heme was obtained from Frontier Scientific (Frontier Scientific, USA) and TNFα from Biolegend (Biolegend, USA). Endothelial basal medium (EBM-2), endothelial cell growth medium supplement (EGM-2), and primary human umbilical vein endothelial cells (HUVEC) were obtained from Lonza (Walkersville, MD, USA). Rabbit monoclonal anti–VE-cadherin antibody was from Cell Signaling Technology (Boston, MA, USA), and Alexa fluor 555-phalloidin was obtained from Life Technologies (Gaithersburg, MD, USA).

Cell Culture

HUVECs were grown in fibronectin (10 μg/ml) pre-coated 75 cm^2 flasks in EBM-2 medium supplemented with 2% fetal bovine serum and with EGM-2, at 37°C in an atmosphere of 5% CO_2/95% air, as previously described (32). Medium was replaced every 48 h until confluence (approximately 80%) was reached. All experiments were performed in HUVECs between passages 3 to 5.

In Vitro Evaluation of Endothelial Barrier Function

EB integrity was measured using ECIS, an electric cell-substrate impedance sensing system (ECIS Zθ, Applied BioPhysics, Troy, NY) (28, 29, 33). Cells were seeded (2.5×10^5 cells/well) and grown to confluency on fibronectin-coated (10 μg/ml) eight-well arrays (8WE10, Applied BioPhysics, Troy, NY) containing interdigitated gold electrodes, specific for this system. The system is based on the application of a weak alternating current through the electrode array, and on the continuous measurement of the ability of the cell monolayer to impede the movement of electrons between adjacent endothelial cells. This resistance is expressed by the parameter R (resistance), a component of the impedance measured by ECIS (34). As previously shown, at low frequencies the movement of current between cells is mostly restricted by the presence of intercellular junctions (35, 36). Endothelial cells were normally seeded 48 h before experiments and R was recorded after 48 h. Only wells with R > 1,500 ohms and stable impedance/resistance readings were used. Before stimulation, resistance was continuously monitored for 2 h, to confirm EB stability represented by a plateau in the R curve. Stimuli were then added to wells under continuous impedance/resistance monitoring, for the time indicated in each experiment. A baseline R value was recorded immediately prior to the addition of each stimuli, and results were then expressed as a ratio from baseline resistance (normalized R). The lower the normalized R value, the higher the magnitude of EB disruption of cell monolayers.

Stimulation of Endothelial Cells

Heme was diluted to an initial working concentration of 5 mM in NaOH 0.1 M. This solution was filtrated through a 0.22-μm filter

and immediately used in experiments, at concentrations from 5 to 100 μM (diluted in serum free EBM-2 medium). Of note, the final concentration of NaOH in these solutions varied from 0.01 to 0.2 μM respectively. NaOH solutions with concentrations equivalent to those used to in heme dilutions of 30, 50, and 100 μM were used as negative controls (vehicle), as detailed in figure legends. TNFα was diluted in serum free EBM-2 medium and immediately added to cell monolayers. Sera from patients or healthy volunteers were diluted (20% v/v) in EBM-2, as previously described (37). The protein concentration of final sera preparations corresponded to 20% of serum total protein concentration from each subject (shown in **Table S1**) and varied from varied from 1.24 to 1.98 g/dl in patients, and 1.22 to 1.54 g/dl in healthy volunteers.

Patients and Healthy Volunteers

The study was performed in accordance with the Declaration of Helsinki and approved by the local Institutional Review Boards of both HEMOPE and University of Campinas (protocols 510.517 and 3.291.418 respectively). Written informed consent was obtained from all subjects or their legal representatives prior to enrollment. The study population consisted of 20 patients with SCD (all with sickle cell anemia—HbSS) followed at HEMOPE Foundation (Recife, PE, Brazil) and 10 healthy volunteers from the same geographic region and ethnic background. These individuals were part of a cohort from an ongoing collaborative study aimed to investigate the association of haptoglobin polymorphisms with markers of endothelial activation in SCD. Patients were selected from this cohort based on pre-determined serum heme levels measured by a colorimetric assay (QuantiChrom Heme Assay Kit, BioAssay Systems, USA), so that patients with highest and lowest heme levels were represented in sample. All included SCD patients were in steady state (i.e., at least 3 months from the last vaso-occlusive crisis or red blood cell transfusion), and 8/20 were using hydroxyurea. Whole blood samples were obtained by venipuncture and allowed to clot at room temperature for 30 min, and then centrifuged at 1,000*g* (4°C, 15 min) for serum separation, which was stored at −80°C until analysis. Subject characteristics were recorded at the time of sample collection. Based on ECIS results from a previous study from our laboratory with sepsis patients, a sample size of 20 patients and 10 controls was planned, to obtain a power of 80% and a type II error rate of 0.05.

Immunofluorescence

Cells were grown to confluence for 48 h on fibronectin (10 μg/ml) pre-coated microscopy-grade glass coverslips, serum starved for 2 h, and stimulated with heme 30 μM for 6 h. HUVECs were then fixed in paraformaldehyde (4% for 20 min), washed with phosphate-buffered saline (PBS), treated (5 min) with 10 mM glycine, permeabilized with 0.2% Triton-X in PBS, rinsed and blocked with 3% bovine serum albumin in PBS (15 min). Cells were then incubated with anti VE-cadherin antibody (30 min), rinsed and incubated with Alexa Fluor-coupled secondary antibodies (30 min). Actin filaments were detected with fluorescent phalloidin. Confocal laser scanning microscopy was carried out using a Zeiss LSM 510 microscope, equipped with a 63 × 1.3 oil immersion objective. Intercellular gaps were quantified using Image J, by an investigator blinded to experimental condition, as previously described (38). Briefly, a total of 10 images, each containing approximately twenty cells were analyzed for each experiment. Image contrast was adjusted semi-automatically until saturation, so that areas of the confluent monolayer that yielded no signal in all fluorescence channels could be identified as gaps, and selected by creating a threshold. Then, the proportion of empty areas in respect to total image area was calculated. To show the empty areas, the region obtained with the threshold was blue-colored and flattened to the original image.

Measurement of Hemopexin and sVCAM-1 Levels

Hemopexin and sVCAM-1 levels were measured in serum by Elisa in accordance with manufacturer's instructions (Abcam ab171576, Cambridge, UK; and R&D #DY809, Minneapolis, USA, respectively).

Statistical Analysis

Differences in continuous variables were analyzed using Student's t-test/Anova or Mann-Whitney/Kruskal-Wallis tests according to: variable distribution (Gaussian or non-Gaussian respectively) assessed by the D'Agostino & Pearson normality test, and to the number of groups in each comparison. Correlation was calculated using the Spearman correlation coefficient. Data are expressed as mean ± SEM or median and range, as specified. A P-value ≤ 0.05 was considered statistically significant. All statistical analysis was performed with GraphPad Prism 7.0 Software (GraphPad Inc., San Diego, CA, USA).

RESULTS

Heme Induces a Transient and Dose-Dependent Disruption of EB

We first demonstrated that heme is capable to induce a dose-dependent disruption of EB in HUVECs, which attains statistical significance as early as 10 min after stimulation, and that persists for 30 min with heme concentrations between 20 and 30 μM, for 60 min with heme 50 μM, returning to baseline values after these timepoints except for heme 100 μM concentration (**Figure 1A**). Of note, the effect vehicle (NaOH) caused no changes in EB integrity measured by ECIS (**Figure S1A**). In order to confirm if these functional changes were associated with morphological changes, we selected a representative heme concentration (30 μM) to stimulate HUVECs, which increased intercellular gap counts in VE-cadherin stained slides (**Figures 1B, C**).

Sera From SCD Patients Cause EB Disruption *In Vitro*

Next, we investigated whether sera from patients with SCD, containing varying levels of heme, could elicit changes in EB

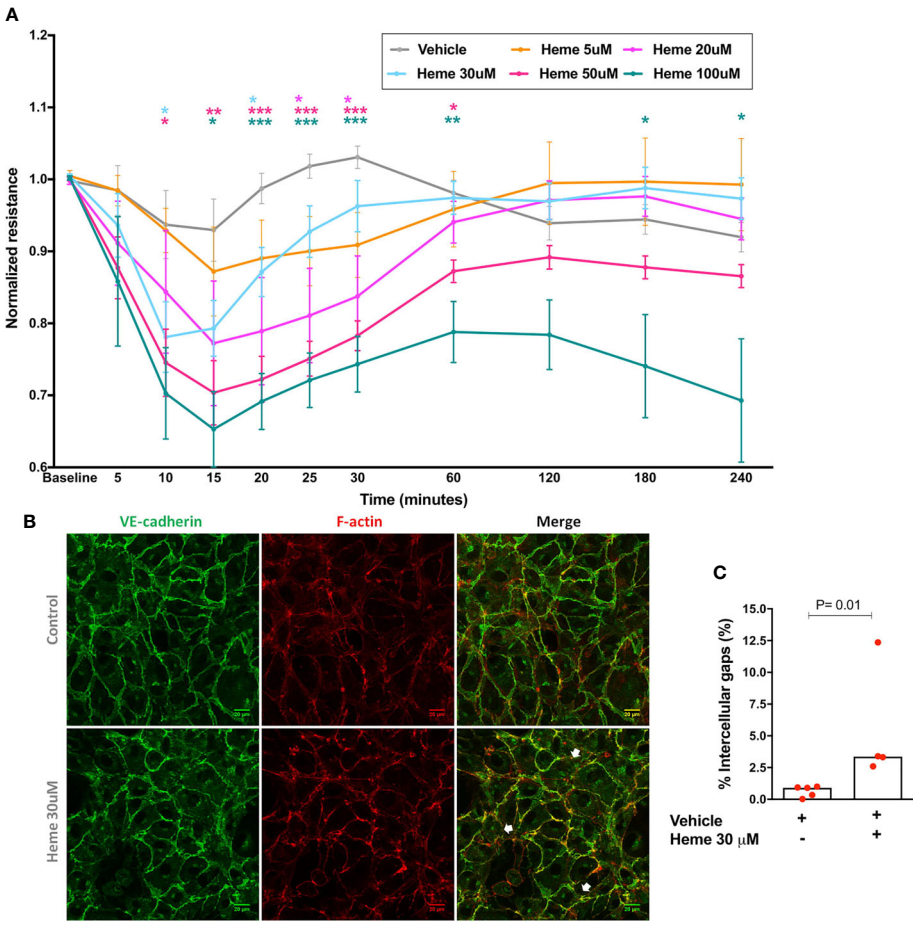

FIGURE 1 | Endothelial barrier integrity after heme stimulation. **(A)** Each line represents the mean ± SEM of the normalized resistance of HUVECs stimulated with heme in serum-free solutions measured by ECIS at 4,000 Hz. Differences between vehicle and heme-stimulated cells were compared using the Kruskal-Wallis test with the Dunn's posttest. Statistical significant differences are indicated by colored asterisks on each timepoint. *P= 0.01 to 0.05; **P<0.01; ***P< 0.001; n = 5 to 15 independent experiments in at least three different days per heme concentration. **(B)** HUVECs were treated for 6 h with vehicle or heme 30 μM, and stained for the cell-cell junction marker VE-cadherin and for filamentous actin (F-actin). White arrows indicate intercellular gaps. **(C)** Semi-automated image processing identified intercellular gaps in the images that were quantified respect to the total area of the cell monolayer (n= 4 to 5 per group in two independent experiments). Mann-Whitney test; *P =0.01. Vehicle corresponds to the same solution used to dilute heme (NaOH 0.1 M), without heme. The final NaOH concentration in each heme dilution varied from 0.01 to 0.2 μM for heme 5 μM to heme 100 μM. In vehicles, higher NaOH concentrations were used (0.06 to 0.2 μM in panel **A**, and 0.06 μM in panel **B**).

integrity in HUVECs. Characteristics of our study population are shown in **Table S1**. First, we compared the effect of sera from all SCD patients with those from healthy volunteers. As shown in **Figure 2**, after a period of EB stability observed in both groups, SCD sera elicited a significant decrease in normalized resistance, consistent with EB disruption (**Figure 2A**). This effect persisted for at least 4 h. We then separated patients in two groups according to median levels of total heme in serum (63.0 μM). However, no differences could be observed between these two patient subgroups (**Figure 2B**). It should be noted that while statistically significant, the effects of serum presented a lower magnitude than the effects of heme in aqueous solutions. Of note, no difference could be observed between HU users and non-users (**Figure S1B**).

Sera From Healthy Volunteers, but Not From SCD Patients, Inhibit EB-Disrupting Effects of Heme

Since total serum heme (which includes mainly the protein-bound fraction of this molecule) was not a significant determinant of the magnitude of EB disruption, we hypothesized that an acute increase in heme levels would be necessary to reproduce the effect of heme shown in **Figure 1**, based on the assumption that FEH might not be available in a protein-rich matrix such as serum. In order to test this hypothesis, cells were incubated with serum from healthy volunteers or SCD patients for 24 h in ECIS arrays, and then challenged with heme to a final concentration of 30 μM. While the presence of sera from healthy volunteers prevented the effects

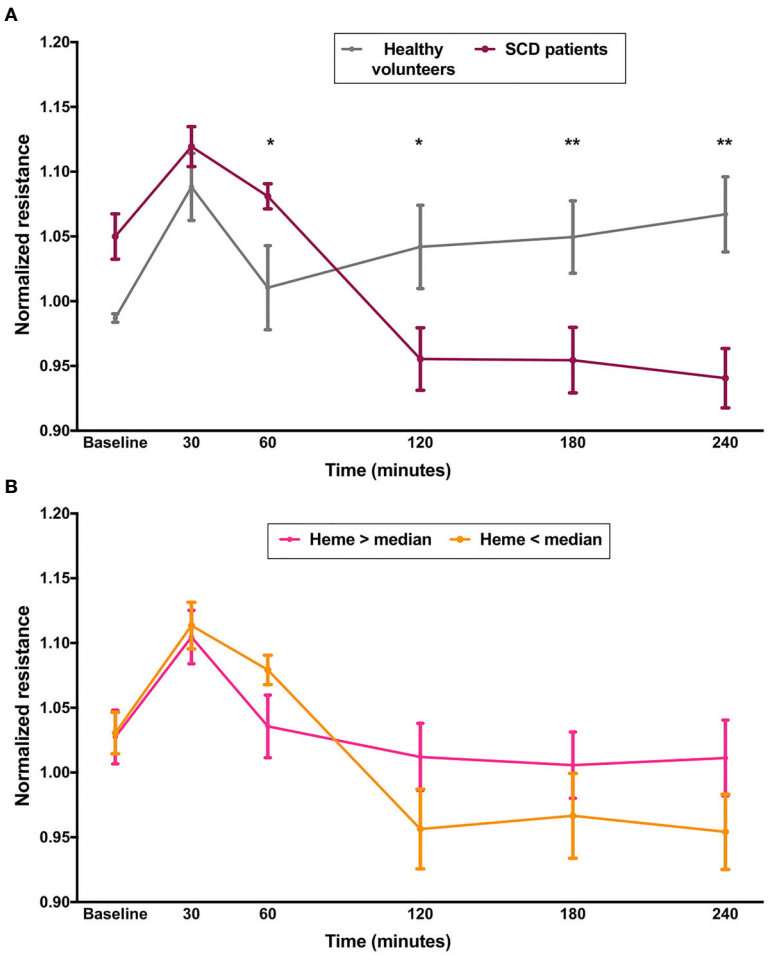

FIGURE 2 | Effect of sera from SCD on EB integrity. Confluent HUVEC monolayers were incubated with sera (20% v/v) from SCD patients (n=20) or healthy volunteers (n=10) and normalized resistance was recorded at 4,000 Hz. Each line represents the mean ± SEM in the specified time points from experiments comparing **(A)** patients and healthy volunteers; or **(B)** patients subgrouped by total levels of heme in serum. Differences were compared using the Mann-Whitney test. Statistical significant differences are indicated by colored asterisks on each timepoint. *P= 0.01 to 0.05; **P<0.01.

of heme on EB integrity, a milder, yet significant disruption of EB was observed when heme was added to cells incubated with sera from SCD patients (**Figure 3**).

Heme-Induced EB Disruption Is Associated With Hemopexin Levels

Since free heme is quickly removed from the circulation by hemopexin, we hypothesized that the induction of EB disruption by the addition of heme to SCD sera could be associated with lower hemopexin levels when compared to healthy volunteers. In fact, hemopexin levels were significantly lower in SCD patients compared to controls (0.33 ± 0.32 vs 1.29 ± 0.23; P< 0.001) (**Figure 4A**). As expected, a strong correlation (R_s = 0.90; P < 0.0001) was observed between heme and hemopexin levels (**Figure 4B**). Interestingly, when all participants were divided according to median hemopexin levels (0.59 mg/ml), lower values of normalized resistance (which indicate heme-induced EB disruption) were observed in individuals with lower hemopexin levels (**Figure 4C**). Moreover, the magnitude of heme-induced EB disruption at 12 min (the timepoint when this effect was more evident) were correlated with hemopexin levels (R_s = 0.68; P < 0.0001) (**Figure 4D**). Of note, a strong correlation was observed between hemopexin and sVCAM-1 (R_s = −0.72; P< 0.001). However, while levels of sVCAM-1 were also associated with normalized resistance, the correlation coefficient was weak (Rs = −0.42; P = 0.03).

DISCUSSION

EB disruption is a hallmark of several inflammatory diseases (39–42), and studies in animal models suggest that this process is involved in the pathogenesis of acute complications of SCD, namely ACS (21, 22). Accordingly, the effects of hemolysis byproducts such as free hemoglobin and heme on EB integrity in endothelial cell monolayers have been recently investigated, with consistent data supporting an EB-disrupting effect of heme

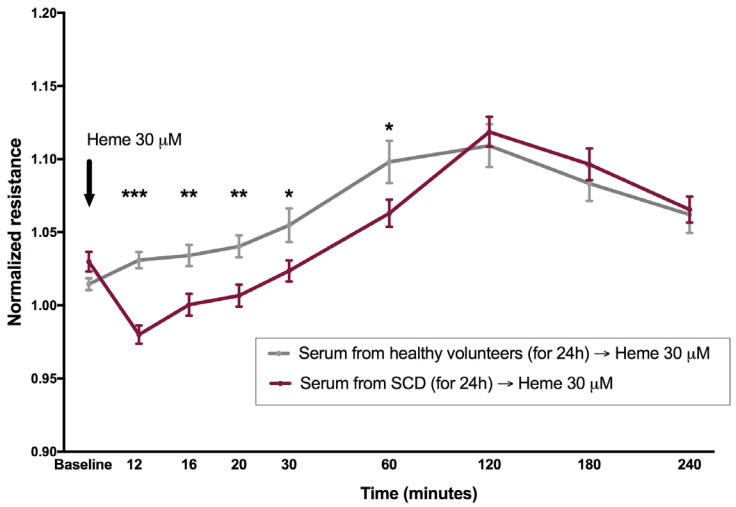

FIGURE 3 | Heme is capable to induce EB disruption in the presence of serum from patients with SCD, but not from healthy volunteers. Confluent HUVEC monolayers were incubated with sera (20% v/v) from SCD patients (n = 20) or healthy volunteers (n = 10) for 24 h, followed by challenge with heme 30 μM (black arrow). Normalized resistance was recorded at 4,000 Hz. Each line represents the mean ± SEM in the specified time points. Differences were compared using the Mann-Whitney test. Statistical significant differences are indicated by colored asterisks on each timepoint. *P= 0.01 to 0.05; **P<0.01; ***P<0.001. Heme was diluted in NaOH, and the final NaOH concentration in heme dilutions was 0.06 μM.

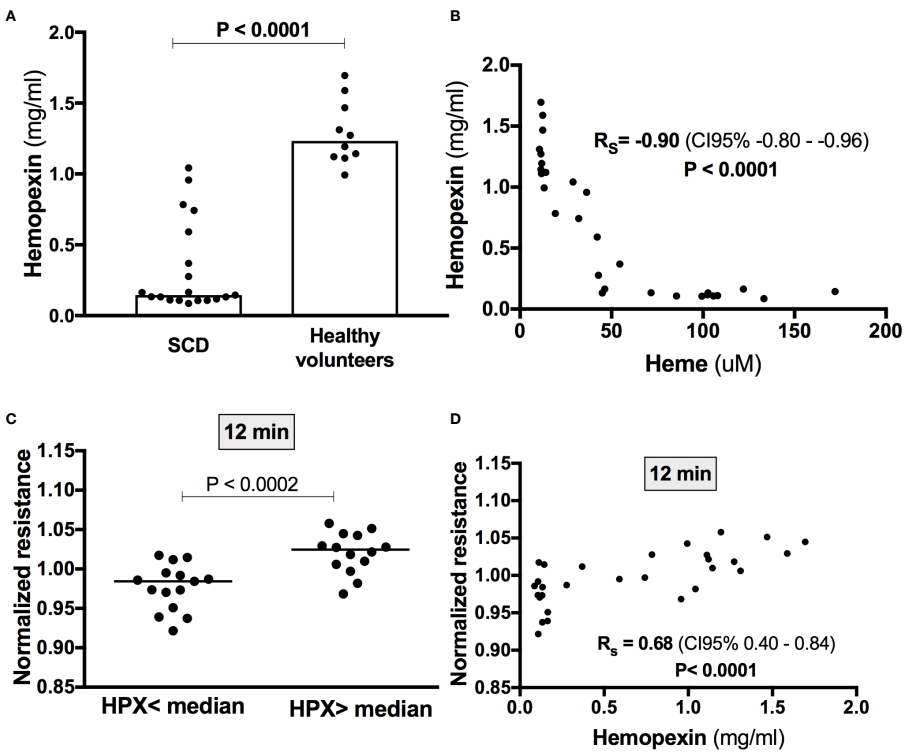

FIGURE 4 | Heme-induced EB disruption in the presence of serum is associated with hemopexin levels. **(A)** Hemopexin levels were measured by Elisa and were lower in SCD patients (n=19) compared to healthy volunteers (n=10) (Mann-Whitney test). **(B)** A strong negative correlation was observed between hemopexin and heme levels (Spearman correlation coefficient). **(C)** Lower values of normalized resistance at the timepoint of peak heme-induced EB disruption were observed in individuals with lower hemopexin levels (t test). Accordingly, peak heme-induced EB disruption (i.e., after 12 min) was statistically correlated with hemopexin levels (Spearman correlation coefficient) **(D)**.

(24–26). However, due to the strong affinity of heme to circulating proteins, coupled with the possible interplay of heme with other inflammatory mediators, it is important to confirm these effects in experimental conditions that more closely resemble those observed in the clinic. The most important result of our study was the demonstration that heme is capable to induce EB disruption even in the presence of serum proteins, but that this effect only occurs with serum from SCD patients, but not from healthy volunteers, and is associated with hemopexin levels.

Based on the demonstration that heme can trigger innate immunity activation (1, 13–15), excess heme was associated with the pathogenesis of vaso-occlusion (43) and ACS (22, 44) in SCD. Accordingly, a growing interest emerged on whether alterations of the alveolar-capillary barrier participated in the pathogenesis of ACS, as well as if heme was capable to induce EB disruption. In regard to the former, studies using mice models of SCD suggested that EB disruption was involved in the pathogenesis of ACS (21, 22). Moreover, isolated pulmonary endothelial cells from homozygous sickle mice (SS) were shown to be more sensitive to the EB-disrupting effects of LPS (measured by ECIS) than cells from heterozygous (AS) mice (45). In regard to the latter question, the first demonstration that heme could elicit EB disruption was published almost 20 years ago in a study that demonstrated the accumulation of radiolabeled liposomes in different organs of C57Bl/6 mice treated with heme (46), a finding that was also demonstrated using other *in vivo* assays of EB integrity in mice (11). In the last 4 years this observation was confirmed and further explored in cell-based assays, in which the exposure of pulmonary or microvascular endothelial cells to heme (diluted in aqueous solutions of NaOH) consistently induced EB disruption in both static and flow-based (microfluidic) assays (24–26). These studies also demonstrated that these effects occurred in the context of the effects of heme on innate immunity, since they were TLR4-dependent. However, one of the caveats of studies about the effects of heme on innate immunity is the strong affinity of this molecule for proteins that are abundant in serum such as hemopexin and albumin, so that some authors recently questioned their biological relevance at all (27). Of note, all of the recent cell-based studies about the effects of heme on EB disruption used heme diluted in protein-free solutions.

In our study we first confirmed that heme can disrupt EB, in a dose dependent (in our system, in concentrations above 10 μM) and transient fashion. Barrier integrity returned to normal within 25 to 60 min in cells exposed to the lower range of heme concentrations used in our study (below 30 μM), which more closely resemble the concentrations of FEH in contact to cells in humans. This transient nature indicates that heme-induced barrier disruption is not caused by cell death, and raises the question on which of the signaling pathways involved in the regulation of EB integrity are modulated by heme. This observation is also consistent with a previous study that also showed a dose-dependent effect of heme on EB integrity, and that showed that heme used at a higher concentration (40μM) was associated with a more delayed disruption of EB integrity that was attributed to necroptotic cell death (25), but other pathways that are modulated by heme such as autophagy (47–49) and MKK3/p38MAPK (50) have also been recently associated with EB changes. It should be noted that our results also confirm that the EB of HUVECs behave similarly to pulmonary and microvascular endothelial cells in response to heme, supporting their use in our subsequent experiments.

We also demonstrated that sera from patients with SCD, but not from healthy volunteers, induce EB disruption of HUVEC monolayers. Regulation of EB integrity is a complex process that involves cellular and humoral mediators (51–53), both altered in SCD. In this regard, our results suggest that soluble inflammatory mediators contribute at least in part to EB disruption in SCD, and that their identification could generate important insights about the pathogenesis of this disease. Given the complex nature of this process, high-throughput strategies such as proteomics or metabolomics would possibly be more adequate than the testing of isolated candidate modulators by immunological methods. As far as we are aware, only one group studied evaluated the effect of specific plasma components on EB integrity in SCD. This study showed that exosomes from SCD patients with a higher frequency of ACS (mainly derived from red blood cells), induced a more pronounced disturbance of the EB on human microvascular endothelia cells than exosomes from patients with no history of ACS (54). Of note, the same group had previously shown that these exosomes were mainly derived from endothelial cells, and had a miRNA cargo capable to discriminate mild from severe clinical phenotypes (55). As in our study, all patients from the former study were in steady-state when samples were collected, and EB function was measured by ECIS. Since our study was focused on the role of heme as an EB-disrupting agent in SCD, we first investigated whether total heme levels in these serum samples influenced the magnitude of EB disruption, which was not confirmed. Our negative results can be probably explained by the fact that total heme levels encompass not only FEH, but mainly heme bound to hemopexin, albumin and hemoglobin (56), which is not capable to activate the immune system. Accordingly, it is likely that levels of FEH in stored serum samples are extremely low, or even absent, as suggested by others (56). So, we added heme to cells in the presence of serum to investigate whether an acute increase in serum heme concentrations could reproduce the effects of heme on EB. By doing this, we were able to show that proteins present in serum from patients with SCD are not sufficient to inhibit the EB-disruption induced by an acute challenge with heme. Interestingly, addition of heme to sera from healthy volunteers did not elicit any effect on EB, suggesting that the inflammatory milieu characteristic of serum from SCD patients is required for heme-induced EB disruption.

Of all heme scavenging proteins present in serum, hemopexin is the one with the highest affinity, recognized as a critical line of defense against FEH. As expected, hemopexin levels were markedly lower in SCD patients compared to healthy volunteers. Moreover, hemopexin levels were also correlated with both heme and sVCAM-1, which is a marker of endothelial activation in SCD. Interestingly, we demonstrated that peak heme-induced EB disruption in the presence of serum was associated with hemopexin levels, which as far as we are aware represent the first time when human hemopexin levels were associated with

modulation of EB function. Together these results provide additional support for the concept that FEH can directly contribute to EB disruption in SCD. Of note, in a recent study, the mechanisms by which heme disrupts the EB were further elucidated and shown to involve endothelial cytoskeleton remodeling (50), paving the way for the study of these pathways in SCD. Finally, our results also demonstrate that the effects of heme on endothelial cells are not restricted to serum free conditions.

Our study has limitations that need to be acknowledged. First, although the ECIS method has been validated as a method to assess the integrity of intercellular junctions by both empirical data (35, 36), as well as by its use in the description of several key features of endothelial barrier function (57–61), it only evaluates the response of endothelial cells to a discrete stimulus, compared to the much more complex regulation of endothelial function *in vivo*. On the other hand, this very characteristic represents an advantage to answer focused research questions such as the one from our study. Another limitation is the use of HUVECs as opposed to other adult organ-specific endothelial cell types, since phenotypic differences have been reported between different endothelial cell types. It should be noted however, that HUVECs have been a valuable tool for studies of vascular phenotype for several decades, including studies about central aspects of endothelial barrier biology during inflammation (62, 63). In addition, in the first part of our study using heme in NaOH solutions we demonstrated that HUVECs respond to heme in a similar fashion compared to pulmonary and microvascular endothelial cells in regard to EB function. We should also mention that although our results demonstrate a yet unknown association of serum hemopexin levels with heme-induced *in vitro* EB disruption in SCD, this association does not allow us to claim for a causal relationship between hemopexin deficiency and EB disruption, which requires additional studies investigating whether hemopexin can reverse these changes. Another limitation of our study is related to the fact that methods used to measure heme in most studies involving SCD are not capable to separate total or cell free heme, from protein-free heme (i.e., not bound to hemopexin, albumin or other proteins). This fraction, referred in our study as FEH, is the one that is expected to be toxic to cells and tissues. This methodological limitation could explain why total heme levels were not associated with EB disruption, whereas hemopexin levels, which is consumed by the release of free heme, were. Studies using recently described methods capable to measure protein-free heme (64, 65) are warranted to address this issue. Another limitation that deserves to be discussed is the relevance of adding NaOH-solubilized heme to cell cultures, as a model of heme release. In fact, important details about the kinetics of heme release from damaged red blood cells in patients with hemolytic disorders are yet to be clarified, and the very existence of FEH *in vivo* has been discussed (27). Although the role of red blood cell microparticles as mediators of heme transfer has been recently demonstrated (66), one cannot exclude that other aspects of the interaction of heme with blood components that are not included in our model may be key to its pathological effects *in vivo*. Nevertheless, we believe that our strategy of adding heme to patient serum, and measuring EB function in real time can overcome at least some of these limitations, potentially representing a closer model to the pathological effects of heme *in vivo*. Since all our experiments were performed with serum, we should also mention the fact that some of the pro-inflammatory effects of heme in cell models were only observed in serum free conditions (1). Finally, the relatively low sample size of our study should also be considered when interpreting our results.

In conclusion, we demonstrated that the previously described transient disruption of EB by heme is also observed in the presence of sera from SCD patients, corroborating the role of FEH in the pathogenesis of this condition, through the demonstration that its effects are not restricted to serum free conditions. The fact that the effects of heme on EB are only observed in serum from SCD and that this effect is associated with hemopexin levels support the concept that heme could directly contribute to EB disruption in SCD, thus warranting additional studies to confirm this causal relationship. Together our *in vitro* studies provide additional support to the concept that heme may act as a danger-associated molecular pattern (DAMP) in hemolytic conditions.

DATA AVAILABILITY STATEMENT

The datasets generated for this study are available on request to the corresponding author.

ETHICS STATEMENT

The studies involving human participants were reviewed and approved by Institutional Review Boards HEMOPE (protocol 510.517) and of University of Campinas (protocol 3.291.418). The patients/participants provided their written informed consent to participate in this study.

AUTHOR CONTRIBUTIONS

VS and MF designed the study, performed endothelial cell assays, and analyzed data. LC performed endothelial cell assays. DG-W revised and analyzed confocal data. BH and FC contributed to study design and measured heme levels. WT and FL contributed to hemopexin and sVCAM-1 measurements. ID, AA, AL-A, MB, and MN recruited and monitored patients. IB-J performed ECIS studies with NaOH and thrombin. FFC contributed with reagents and laboratory infrastructure. JM supervised ECIS experiments and contributed with reagents and laboratory infrastructure. EP designed the study, reviewed, and analyzed data and drafted the manuscript. All authors contributed to the article and approved the submitted version.

FUNDING

This study was funded by the Sao Paulo Research Foundation (FAPESP), grants 2016/14172-6 to EP, and 2014/00984-3 to FFC, respectively; Conselho Nacional de Desenvolvimento Cientifico e Tecnologico (CNPq) Brazil; Coordenacao de Aperfeicoamento

de Pessoal de Nivel Superior – Brasil (CAPES), finance code 001; and FAEPEX-UNICAMP.

SUPPLEMENTARY MATERIAL

The Supplementary Material for this article can be found online at: https://www.frontiersin.org/articles/10.3389/fimmu.2020.535147/full#supplementary-material

SUPPLEMENTARY FIGURE 1 | Exploration of the effects of NaOH and hydroxyurea (HU) on EB. In **(A)**, different concentrations of NaOH, which was the vehicle used to dilute heme, were used under the same experimental conditions. Each line represents the mean ± SEM of the normalized resistance of HUVECs stimulated with either NaOH or thrombin used as a positive control. Normalized resistance was measured by ECIS at 4,000 Hz. As shown in the upper panel, NaOH at different concentrations did not affect EB. In **(B)**, data from SCD patients used in **Figure 3** were subdivided according to the use or not of hydroxyurea (HU). No difference in ECIS readings after heme stimulation could be detected between these two subgroups. Kruskall Wallis and Dunn's posttest.

REFERENCES

1. Dutra FF, Bozza MT. Heme on innate immunity and inflammation. *Front Pharmacol* (2014) 5:115. doi: 10.3389/fphar.2014.00115
2. Tolosano E, Fagoonee S, Morello N, Vinchi F, Fiorito V. Heme Scavenging and the Other Facets of Hemopexin. *Antioxid Redox Signal* (2010) 12:305–20. doi: 10.1089/ars.2009.2787
3. Chiabrando D, Vinchi F, Fiorito V, Mercurio S, Tolosano E. Heme in pathophysiology: a matter of scavenging, metabolism and trafficking across cell membranes. *Front Pharmacol* (2014) 5:61. doi: 10.3389/fphar.2014.00061
4. Hebbel RP, Morgan WT, Eaton JW, Hedlund BE. Accelerated autoxidation and heme loss due to instability of sickle hemoglobin. *Proc Natl Acad Sci USA* (1988) 85:237–41. doi: 10.1073/pnas.85.1.237
5. Porto BN, Alves LS, Fernández PL, Dutra TP, Figueiredo RT, Graça-Souza AV, et al. Heme induces neutrophil migration and reactive oxygen species generation through signaling pathways characteristic of chemotactic receptors. *J Biol Chem* (2007) 282:24430–6. doi: 10.1074/jbc.M703570200
6. Graça-Souza AV, Arruda MAB, de Freitas MS, Barja-Fidalgo C, Oliveira PL. Neutrophil activation by heme: implications for inflammatory processes. *Blood* (2002) 99:4160–5. doi: 10.1182/blood.V99.11.4160
7. Chen G, Zhang D, Fuchs TA, Manwani D, Wagner DD, Frenette PS. Heme-induced neutrophil extracellular traps contribute to the pathogenesis of sickle cell disease. *Blood* (2014) 123:3818–27. doi: 10.1182/blood-2013-10-529982
8. Frimat M, Tabarin F, Dimitrov JD, Poitou C, Halbwachs-Mecarelli L, Fremeaux-Bacchi V, et al. Complement activation by heme as a secondary hit for atypical hemolytic uremic syndrome. *Blood* (2013) 122:282–92. doi: 10.1182/blood-2013-03-489245
9. Merle NS, Grunenwald A, Rajaratnam H, Gnemmi V, Frimat M, Figueres M-L, et al. Intravascular hemolysis activates complement via cell-free heme and heme-loaded microvesicles. *JCI Insight* (2018) 3:1–17. doi: 10.1172/jci.insight.96910
10. Dutra FF, Alves LS, Rodrigues D, Fernandez PL, de Oliveira RB, Golenbock DT, et al. Hemolysis-induced lethality involves inflammasome activation by heme. *Proc Natl Acad Sci USA* (2014) 111:E4110–8. doi: 10.1073/pnas.1405023111
11. Sparkenbaugh EM, Chantrathammachart P, Wang S, Jonas W, Kirchhofer D, Gailani DD, et al. Excess of heme induces tissue factor-dependent activation of coagulation in mice. *Haematologica* (2015) 100:308–14. doi: 10.3324/haematol.2014.114728
12. de Souza GR, Hounkpe BW, Fiusa MML, Colella MP, Annichino-Bizzacchi JM, Traina F, et al. Tissue factor-dependent coagulation activation by heme: A thromboelastometry study. *PloS One* (2017) 12:e0176505. doi: 10.1371/journal.pone.0176505
13. Hounkpe BW, Fiusa MML, Colella MP, da Costa LNG, Benatti R de O, Saad STO, et al. Role of innate immunity-triggered pathways in the pathogenesis of Sickle Cell Disease: a meta-analysis of gene expression studies. *Sci Rep* (2015) 5:17822. doi: 10.1038/srep17822
14. Soares MP, Bozza MT. Red alert: labile heme is an alarmin. *Curr Opin Immunol* (2016) 38:94–100. doi: 10.1016/j.coi.2015.11.006
15. Mendonça R, Silveira AAA, Conran N. Red cell DAMPs and inflammation. *Inflammation Res* (2016) 65:665–78. doi: 10.1007/s00011-016-0955-9
16. Roumenina LT, Rayes J, Lacroix-Desmazes S, Dimitrov JD. Heme: Modulator of Plasma Systems in Hemolytic Diseases. *Trends Mol Med* (2016) 22:200–13. doi: 10.1016/j.molmed.2016.01.004
17. Conran N, De Paula EV. Thromboinflammatory mechanisms in sickle cell disease - challenging the hemostatic balance. *Haematologica* (2020) 105 (10):2380–90. doi: 10.3324/haematol.2019.239343
18. Goswami D, Vestweber D. How leukocytes trigger opening and sealing of gaps in the endothelial barrier. *F1000Research* (2016) 5:2321. doi: 10.12688/f1000research.9185.1
19. Seeley EJ, Matthay MA, Wolters PJ. Inflection points in sepsis biology: from local defense to systemic organ injury. *Am J Physiol Lung Cell Mol Physiol* (2012) 303:L355–63. doi: 10.1152/ajplung.00069.2012
20. Higgins SJ, Purcell LA, Silver KL, Tran V, Crowley V, Hawkes M, et al. Dysregulation of angiopoietin-1 plays a mechanistic role in the pathogenesis of cerebral malaria. *Sci Transl Med* (2016) 8:358ra128. doi: 10.1126/scitranslmed.aaf6812
21. Ghosh S, Tan F, Ofori-Acquah SF. Spatiotemporal dysfunction of the vascular permeability barrier in transgenic mice with sickle cell disease. *Anemia* (2012) 2012:582018. doi: 10.1155/2012/582018
22. Ghosh S, Adisa OA, Chappa P, Tan F, Jackson KA, Archer DR, et al. Extracellular hemin crisis triggers acute chest syndrome in sickle mice. *J Clin Invest* (2013) 123:4809–20. doi: 10.1172/JCI64578
23. Wagener FA, Eggert A, Boerman OC, Oyen WJ, Verhofstad A, Abraham NG, et al. Heme is a potent inducer of inflammation in mice and is counteracted by heme oxygenase. *Blood* (2001) 98:1802–11. doi: 10.1182/blood.V98.6.1802
24. Qiu Y, Ahn B, Sakurai Y, Hansen CE, Tran R, Mimche PN, et al. Microvasculature-on-a-chip for the long-term study of endothelial barrier dysfunction and microvascular obstruction in disease. *Nat BioMed Eng* (2018) 2:453–63. doi: 10.1038/s41551-018-0224-z
25. Singla S, Sysol JR, Dille B, Jones N, Chen J, Machado RF. Hemin Causes Lung Microvascular Endothelial Barrier Dysfunction by Necroptotic Cell Death. *Am J Respir Cell Mol Biol* (2017) 57(3):307–14. doi: 10.1165/rcmb.2016-0287OC rcmb.2016-0287OC.
26. Wagener BM, Hu PJ, Oh J-Y, Evans CA, Richter JR, Honavar J, et al. Role of heme in lung bacterial infection after trauma hemorrhage and stored red blood cell transfusion: A preclinical experimental study. *PloS Med* (2018) 15: e1002522. doi: 10.1371/journal.pmed.1002522
27. Vallelian F, Schaer CA, Deuel JW, Ingoglia G, Humar R, Buehler PW, et al. Revisiting the putative role of heme as a trigger of inflammation. *Pharmacol Res Perspect* (2018) 6:e00392. doi: 10.1002/prp2.392
28. Bischoff I, Hornburger MC, Mayer BA, Beyerle A, Wegener J, Fürst R. Pitfalls in assessing microvascular endothelial barrier function: impedance-based devices versus the classic macromolecular tracer assay. *Sci Rep* (2016) 6:23671. doi: 10.1038/srep23671
29. Szulcek R, Bogaard HJ, van Nieuw Amerongen GP. Electric cell-substrate impedance sensing for the quantification of endothelial proliferation, barrier function, and motility. *J Vis Exp* (2014) 85:1–12. doi: 10.3791/51300
30. Xie Z, Ghosh CC, Patel R, Iwaki S, Gaskins D, Nelson C, et al. Vascular endothelial hyperpermeability induces the clinical symptoms of Clarkson disease (the systemic capillary leak syndrome). *Blood* (2012) 119:4321–32. doi: 10.1182/blood-2011-08-375816
31. Tramontini FG de SC, Baimukanova G, Lanteri MC, Keating SM, Moraes Ferreira F, Heitman J, et al. Serum from dengue virus-infected patients with and without plasma leakage differentially affects endothelial cells barrier function in vitro. *PloS One* (2017) 12:e0178820. doi: 10.1371/journal.pone.0178820
32. Millán J, Cain RJ, Reglero-Real N, Bigarella C, Marcos-Ramiro B, Fernández-Martín L, et al. Adherens junctions connect stress fibres between adjacent endothelial cells. *BMC Biol* (2010) 8:1–13. doi: 10.1186/1741-7007-8-11
33. Tiruppathi C, Malik AB, Del Vecchio PJ, Keese CR, Giaever I. Electrical method for detection of endothelial cell shape change in real time: assessment of endothelial barrier function. *Proc Natl Acad Sci USA* (1992) 89:7919–23. doi: 10.1073/pnas.89.17.7919

34. Stolwijk JA, Matrougui K, Renken CW, Trebak M. Impedance analysis of GPCR-mediated changes in endothelial barrier function: overview and fundamental considerations for stable and reproducible measurements. *Pflugers Arch* (2015) 467:2193–218. doi: 10.1007/s00424-014-1674-0
35. Moy AB, Winter M, Kamath A, Blackwell K, Reyes G, Giaever I, et al. Histamine alters endothelial barrier function at cell-cell and cell-matrix sites. *Am J Physiol Lung Cell Mol Physiol* (2000) 278:L888–98. doi: 10.1152/ajplung.2000.278.5.L888
36. Robilliard L, Kho D, Johnson R, Anchan A, O'Carroll S, Graham E. The Importance of Multifrequency Impedance Sensing of Endothelial Barrier Formation Using ECIS Technology for the Generation of a Strong and Durable Paracellular Barrier. *Biosensors* (2018) 8:64. doi: 10.3390/bios8030064
37. Zheng Y, Zhou B, Ding G, Wang Z-C, Wang X-Q, Wang Y-L, et al. Effect of Serum From Patients With Severe Acute Pancreatitis on Vascular Endothelial Permeability. *Pancreas* (2013) 42:633–9. doi: 10.1097/MPA.0b013e318273066b
38. Marcos-Ramiro B, Oliva Nacarino P, Serrano-Pertierra E, Blanco-Gelaz MTMAMT, Weksler BB, Romero IAIAIA, et al. Microparticles in multiple sclerosis and clinically isolated syndrome: effect on endothelial barrier function. *BMC Neurosci* (2014) 15:110. doi: 10.1186/1471-2202-15-110
39. Park-Windhol C, D'Amore PA. Disorders of Vascular Permeability. *Annu Rev Pathol* (2016) 11:251–81. doi: 10.1146/annurev-pathol-012615-044506
40. Opal SM, van der Poll T. Endothelial barrier dysfunction in septic shock. *J Intern Med* (2015) 277:277–93. doi: 10.1111/joim.12331
41. Gavard J. Endothelial permeability and VE-cadherin: a wacky comradeship. *Cell Adh Migr* (2014) 8:158–64. doi: 10.4161/cam.29026
42. Dejana E, Orsenigo F. Endothelial adherens junctions at a glance. *J Cell Sci* (2013) 126:2545–9. doi: 10.1242/jcs.124529
43. Belcher JJD, Chen C, Nguyen J, Milbauer L, Abdulla F, Alayash AIAAI, et al. Heme triggers TLR4 signaling leading to endothelial cell activation and vaso-occlusion in murine sickle cell disease. *Blood* (2014) 123:377–90. doi: 10.1182/blood-2013-04-495887
44. Adisa OA, Hu Y, Ghosh S, Aryee D, Osunkwo I, Ofori-Acquah SF. Association between plasma free haem and incidence of vaso-occlusive episodes and acute chest syndrome in children with sickle cell disease. *Br J Haematol* (2013) 162:702–5. doi: 10.1111/bjh.12445
45. Umapathy NS, Gonzales J, Makala LH, Xu H, Biddinger P, Pace BS. Impaired pulmonary endothelial barrier function in sickle cell mice. *Haematologica* (2017) 102:e26–9. doi: 10.3324/haematol.2016.153098
46. Wagener FADTG, Eggert A, Boerman OC, Oyen WJG, Verhofstad A, Abraham NG, et al. Heme is a potent inducer of inflammation in mice and is counteracted by heme oxygenase. *Blood* (2001) 98:1802–11. doi: 10.1182/blood.V98.6.1802
47. Zhang D, Zhou J, Ye LC, Li J, Wu Z, Li Y, et al. Autophagy maintains the integrity of endothelial barrier in LPS-induced lung injury. *J Cell Physiol* (2018) 233:688–98. doi: 10.1002/jcp.25928
48. Fader CM, Salassa BN, Grosso RA, Vergara AN, Colombo MI. Hemin induces mitophagy in a leukemic erythroblast cell line. *Biol Cell* (2016) 108:77–95. doi: 10.1111/boc.201500058
49. Grosso RA, Caldarone PVS, Sánchez MC, Chiabrando GA, Colombo MI, Fader CM. Hemin induces autophagy in a leukemic erythroblast cell line through the LRP1 receptor. *Biosci Rep* (2019) 39:1–17. doi: 10.1042/BSR20181156
50. James J, Srivastava A, Valuparampil Varghese M, Eccles CA, Zemskova M, Rafikova O, et al. Heme induces rapid endothelial barrier dysfunction via the MKK3/p38MAPK axis. *Blood* (2020) 136(6):749–54. doi: 10.1182/blood.2019003986
51. Trani M, Dejana E. New insights in the control of vascular permeability: vascular endothelial-cadherin and other players. *Curr Opin Hematol* (2015) 22:267–72. doi: 10.1097/MOH.0000000000000137
52. Dejana E, Tournier-Lasserve E, Weinstein BM. The control of vascular integrity by endothelial cell junctions: molecular basis and pathological implications. *Dev Cell* (2009) 16:209–21. doi: 10.1016/j.devcel.2009.01.004
53. Rahimi N. Defenders and Challengers of Endothelial Barrier Function. *Front Immunol* (2017) 8:1847. doi: 10.3389/FIMMU.2017.01847
54. Lapping-Carr G, Khalyfa A, Rangel S, Darlington W, Beyer EC, Peddinti R, et al. Exosomes contribute to endothelial integrity and acute chest syndrome risk: Preliminary findings. *Pediatr Pulmonol* (2017) 52:1478–85. doi: 10.1002/ppul.23698
55. Khalyfa A, Khalyfa AA, Akbarpour M, Connes P, Romana M, Lapping-Carr G, et al. Extracellular microvesicle microRNAs in children with sickle cell anaemia with divergent clinical phenotypes. *Br J Haematol* (2016) 174:786–98. doi: 10.1111/bjh.14104
56. Oh J-Y, Hamm J, Xu X, Genschmer K, Zhong M, Lebensburger J, et al. Absorbance and redox based approaches for measuring free heme and free hemoglobin in biological matrices. *Redox Biol* (2016) 9:167–77. doi: 10.1016/j.redox.2016.08.003
57. Keil JM, Liu X, Antonetti DA. Glucocorticoid Induction of Occludin Expression and Endothelial Barrier Requires Transcription Factor p54 NONO. *Invest Opthalmol Vis Sci* (2013) 54:4007. doi: 10.1167/iovs.13-11980
58. Taylor SL, Wahl-Jensen V, Copeland AM, Jahrling PB, Schmaljohn CS. Endothelial Cell Permeability during Hantavirus Infection Involves Factor XII-Dependent Increased Activation of the Kallikrein-Kinin System. *PloS Pathog* (2013) 9:e1003470. doi: 10.1371/journal.ppat.1003470
59. Ortega MC, Santander-García D, Marcos-Ramiro B, Barroso S, Cox S, Jiménez-Alfaro I, et al. Activation of Rac1 and RhoA Preserve Corneal Endothelial Barrier Function. *Invest Ophthalmol Vis Sci* (2016) 57:6210–22. doi: 10.1167/iovs.16-20031
60. Marcos-Ramiro B, García-Weber D, Barroso S, Feito J, Ortega MC, Cernuda-Morollón E, et al. RhoB controls endothelial barrier recovery by inhibiting Rac1 trafficking to the cell border. *J Cell Biol* (2016) 213:385–402. doi: 10.1083/jcb.201504038
61. Argraves KM, Gazzolo PJ, Groh EM, Wilkerson BA, Matsuura BS, Twal WO, et al. High density lipoprotein-associated sphingosine 1-phosphate promotes endothelial barrier function. *J Biol Chem* (2008) 283:25074–81. doi: 10.1074/jbc.M801214200
62. González-González A, González A, Rueda N, Alonso-González C, Menéndez-Menéndez J, Gómez-Arozamena J, et al. Melatonin Enhances the Usefulness of Ionizing Radiation: Involving the Regulation of Different Steps of the Angiogenic Process. *Front Physiol* (2019) 10:879. doi: 10.3389/fphys.2019.00879
63. Esser S, Lampugnani MG, Corada M, Dejana E, Risau W. Vascular endothelial growth factor induces VE-cadherin tyrosine phosphorylation in endothelial cells. *J Cell Sci* (1998) 111:1853–65. doi: 10.1016/j.jpba.2019.05.013
64. Noé R, Bozinovic N, Lecerf M, Lacroix-Desmazes S, Dimitrov JD. Use of cysteine as a spectroscopic probe for determination of heme-scavenging capacity of serum proteins and whole human serum. *J Pharm BioMed Anal* (2019) 172:311–9. doi: 10.1016/j.jpba.2019.05.013
65. Gouveia Z, Carlos AR, Yuan X, Aires-da-Silva F, Stocker R, Maghzal GJ, et al. Characterization of plasma labile heme in hemolytic conditions. *FEBS J* (2017) 284:3278–301. doi: 10.1111/febs.14192
66. Camus SM, De Moraes JA, Bonnin P, Abbyad P, Le Jeune S, Lionnet F, et al. Circulating cell membrane microparticles transfer heme to endothelial cells and trigger vaso-occlusions in sickle cell disease. *Blood* (2015) 125:blood-2014-07-589283. doi: 10.1182/blood-2014-07-589283

Conflict of Interest: The authors declare that the research was conducted in the absence of any commercial or financial relationships that could be construed as a potential conflict of interest.

frontiers in Immunology

ORIGINAL RESEARCH
published: 19 January 2021
doi: 10.3389/fimmu.2020.613278

Endothelial TLR4 Expression Mediates Vaso-Occlusive Crisis in Sickle Cell Disease

Joan D. Beckman†, Fuad Abdullah, Chunsheng Chen, Rachel Kirchner, Dormarie Rivera-Rodriguez, Zachary M. Kiser, Aithanh Nguyen, Ping Zhang, Julia Nguyen, Robert P. Hebbel, John D. Belcher and Gregory M. Vercellotti**

Department of Medicine, Division of Hematology, Oncology and Transplantation, University of Minnesota, Minneapolis, MN, United States

OPEN ACCESS

Edited by:
Renata Sesti-Costa, Campinas State University, Brazil

Reviewed by:
Alessandro Matte, University of Verona, Italy
Toshiyuki Murai, Osaka University, Japan

***Correspondence:**
Gregory M. Vercellotti
verce001@umn.edu
John D. Belcher
belcher@umn.edu

†ORCID
Joan D. Beckman
orcid.org/0000-0001-7903-944X

Specialty section:
This article was submitted to Inflammation, a section of the journal Frontiers in Immunology

Received: *01 October 2020*
Accepted: *04 December 2020*
Published: *19 January 2021*

Citation:
Beckman JD, Abdullah F, Chen C, Kirchner R, Rivera-Rodriguez D, Kiser ZM, Nguyen A, Zhang P, Nguyen J, Hebbel RP, Belcher JD and Vercellotti GM (2021) Endothelial TLR4 Expression Mediates Vaso-Occlusive Crisis in Sickle Cell Disease. Front. Immunol. 11:613278. doi: 10.3389/fimmu.2020.613278

Heme, released from red blood cells in sickle cell disease (SCD), interacts with toll-like receptor 4 (TLR4) to activate NF-κB leading to the production of cytokines and adhesion molecules which promote inflammation, pain, and vaso-occlusion. In SCD, TLR4 inhibition has been shown to modulate heme-induced microvascular stasis and lung injury. We sought to delineate the role of endothelial verses hematopoietic TLR4 in SCD by developing a TLR4 null transgenic sickle mouse. We bred a global *Tlr4*$^{-/-}$ deficiency state into Townes-AA mice expressing normal human adult hemoglobin A and Townes-SS mice expressing sickle hemoglobin S. SS-*Tlr4*$^{-/-}$ had similar complete blood counts and serum chemistries as SS-*Tlr4*$^{+/+}$ mice. However, SS-*Tlr4*$^{-/-}$ mice developed significantly less microvascular stasis in dorsal skin fold chambers than SS-*Tlr4*$^{+/+}$ mice in response to challenges with heme, lipopolysaccharide (LPS), and hypoxia/reoxygenation (H/R). To define a potential mechanism for decreased microvascular stasis in SS-*Tlr4*$^{-/-}$ mice, we measured pro-inflammatory NF-κB and adhesion molecules in livers post-heme challenge. Compared to heme-challenged SS-*Tlr4*$^{+/+}$ livers, SS-*Tlr4*$^{-/-}$ livers had lower adhesion molecule and cytokine mRNAs, NF-κB phospho-p65, and adhesion molecule protein expression. Furthermore, lung P-selectin and von Willebrand factor immunostaining was reduced. Next, to establish if endothelial or hematopoietic cell TLR4 signaling is critical to vaso-occlusive physiology, we created chimeric mice by transplanting SS-*Tlr4*$^{-/-}$ or SS-*Tlr4*$^{+/+}$ bone marrow into AA-*Tlr4*$^{-/-}$ or AA-*Tlr4*$^{+/+}$ recipients. Hemin-stimulated microvascular stasis was significantly decreased when the recipient was AA-*Tlr4*$^{-/-}$. These data demonstrate that endothelial, but not hematopoietic, TLR4 expression is necessary to initiate vaso-occlusive physiology in SS mice.

Keywords: sickle cell disease, heme, Toll-like receptor 4, endothelium, vaso-occlusive events

INTRODUCTION

Sickle cell disease (SCD), which is caused by a single point mutation in the β-globin gene of hemoglobin, manifests with chronic intra- and extravascular hemolysis, oxidative stress, inflammation, and vaso-occlusive crisis (VOC). Recently, the role of the innate immune system in perpetuating SCD inflammation and vaso-occlusive physiology has been recognized (1–9). Specifically, heme, which is released during intravascular hemolysis, is able to serve as a damage-associated molecular pattern (DAMP) to stimulate TLR4 signaling on blood cells and the vasculature leading to vaso-occlusion and pulmonary injury (8–11). Heme mediates pain *via* TLR4 in SCD mice and blockade or knockout of TLR4 attenuates hyperalgesia suggesting heme -induced microglial activation *via* TLR4 in the central nervous system contributes to the initiation and maintenance of sickle pain (12). Consequentially, downstream of TLR4, activation of the pro-inflammatory transcription factor NF-κB leads to the production of cytokines and adhesion molecules that promote inflammation, coagulation, and vaso-occlusion (8, 9). Additionally, work done in drug-induced hemolysis models suggests that TLR4-mediated P-selectin release increases complement activation to further drive endothelial activation (13). Collectively, these studies have raised speculation that TLR4 and complement-targeted therapies may reduce severity of VOC in SCD.

Several critical questions regarding the consequences of TLR4 inhibition in SCD remain. Our prior work demonstrated that knockout of TLR4 in the vessel wall was sufficient to ablate SCD VOC physiology (8). However, those transplant studies of SS bone marrow into TLR4 knockout mice could not examine the effects of TLR4 knockout in hematopoietic cells on VOC. We previously showed that monocytes isolated from SCD patients can activate endothelial monolayers and others have shown that heterocellular aggregates play an important role in vaso-occlusion (14–16). Here we asked the question, does knockout of TLR4 in circulating hematopoietic-derived cells, but not the vessel wall, ablate microvascular stasis?

Therefore, we bred a global *Tlr4*$^{-/-}$ deficiency state into Townes-AA mice expressing normal human adult hemoglobin A and Townes-SS mice expressing sickle hemoglobin S. We demonstrate that loss of TLR4 in SCD does not alter chronic hemolysis, but does decrease response to an acute stimulus with hemin, LPS or ischemia through loss of downstream NF-κB signaling. Downstream of NF-κB, SS-*Tlr4*$^{-/-}$ mice exhibit decreased pro-inflammatory and adhesive protein expression. Importantly, using bone marrow chimeras, we demonstrated that endothelial, but not hematopoietic, TLR4 signaling is critical in mediating SCD VOC.

MATERIALS AND METHODS

Mice

All animal experiments were approved by the University of Minnesota's Institutional Animal Care and Use Committee. These studies used male and female Townes-AA and -SS mice on a 129/B6 mixed genetic background (17) and *Tlr4*$^{-/-}$ mice (TLR4$^{lps\text{-}del}$, Jackson Labs) with knockout of the entire *Tlr4* gene, expressing murine alpha and beta globins on a C57B6 genetic background. We bred a global *Tlr4*$^{-/-}$ deficiency state into Townes-AA mice expressing normal human adult hemoglobin A and Townes-SS mice expressing sickle hemoglobin S. These *Tlr4*$^{-/-}$ Townes mice were backcrossed 10 generations to homogenize their genetic background with our *Tlr4*$^{+/+}$ Townes mouse colony. All animals were housed in specific pathogen-free rooms to limit infections and kept on a 12 hour (h) light/dark cycle at 21°C. All animals were monitored daily for health problems, food and water levels, and cage conditions. All animals were included in each endpoint analysis and there were no unexpected adverse events that required modification of the protocol. Mice were aged 8–24 weeks.

Bone Marrow Transplants

Chimeric mice were generated by harvesting bone marrow (BM) from SS-*Tlr4*$^{+/+}$ or SS-*Tlr4*$^{-/-}$ mice followed by transplant into lethally irradiated AA-*Tlr4*$^{+/+}$ or AA-*Tlr4*$^{-/-}$ mice. Recipients (8–10 weeks of age) were irradiated with 2 doses of 5 Gy (X-RAD 320 Biological Irradiator) 3 hours apart. During the 3-hour interval, BM donors were sacrificed and BM was collected from both femurs. Ten million BM cells were injected *via* tail vein into each irradiated recipient. Drinking water containing 0.2% neomycin sulfate (Sigma-Aldrich) was given to transplanted mice for 3 weeks immediately after transplantation. Eight weeks post-transplant, globin phenotype was confirmed by hemoglobin isoelectric focusing and *Tlr4* genotype was verified by PCR. Chimeric mice were employed 16 to 24 weeks after transplant.

Blood Analysis

Blood was collected *via* cardiac puncture at the time of euthanasia from mice into sodium EDTA or serum separator tubes at time points indicated. Complete blood counts with differential, hematocrit levels, and reticulocytes were measured in EDTA blood by the University of Minnesota Veterinary Diagnostic Laboratory.

Measurement of Vaso-Occlusion (Microvascular Stasis)

Mice were anesthetized with a mixture of ketamine (106 mg/kg) and xylazine (7.2 mg/kg) and implanted with dorsal skin-fold chambers (**Supplemental Figure 1**). After implantation, mice were placed on an intravital microscopy stage and 20–24 flowing subcutaneous venules in the chamber window were selected and mapped as previously described (18). After baseline selection of flowing venules, mice were infused with a bolus infusion *via* tail vein with the indicated doses of hemin (3.2 μmol/kg) or lipopolysaccharide (LPS, 1 mg/kg; Escherichia coli, serotype O111:B4; Sigma-Aldrich) or exposed to H/R which consisted of 1-hour hypoxia (7%O_2/93%N_2) followed by 4-hours normoxia. Each of the same venules selected and mapped at baseline were visually re-examined for stasis (no flow) at 1, 2, 3, and 4 hours after infusion or H/R. The static venules in each mouse were counted and percent stasis at 1–4 h was calculated by

dividing the number of static venules by the total (static + flowing) number of venules.

Western Blots

Microsomes and nuclear extracts were isolated from tissues of mice as previously described (19). Immunoblots of cellular subfractions (15–30 μg of protein) were immunostained with primary antibodies to NF-κB phospho-p65 (Ser536, Cell Signaling #3031), total p65 (Cell Signaling #3034), VCAM-1 (Abcam #174279), ICAM-1 (Abcam #ab124759), E-selectin (BioVision #3631) and loading control GAPDH (Sigma-Aldrich #G9545). Primary antibodies were detected with appropriate secondary antibodies conjugated to alkaline phosphatase and visualized with ECF substrate (GE Healthcare) and a Typhoon FLA 9500 imager (GE Healthcare).

RNA Analysis

RNA was extracted using RNeasy kit (Qiagen), followed by cDNA generation according to the manufacturer's protocol (Bio-Rad). Prime PCR RNA array was used for genes. Each reaction contained 20 ng of cDNA, lyophilized primers, SSoAdvanced SYBR Green QPCR master mix (BioRad). The PCR conditions included activating the DNA polymerase at 95°C for 10 min, followed by 40 cycles of three step PCR (95°C for 10 s, 60°C for 30 s). Melt curves for each primer set was run and verified. The cycle threshold (*Ct*) values from samples of each gene and the internal control (GAPDH) were obtained and the relative quantification for each gene was calculated using the $\Delta\Delta Ct$ method (20).

Immunohistology

Mice were infused with hemin (3.2 μmol/kg) 4 hours before tissue collection. Lungs were collected and placed in optimal cutting temperature (OCT) compound, snap-frozen in liquid nitrogen and stored at -85°C prior to frozen sectioning in a microtome-cryostat into 6 μm sections. Tissues were stained with primary antibodies to P-selectin (R&D Systems #AF737) and von Willebrand factor (vWF, Cedarlane #CL20176A-R), and with the nuclear stain DAPI (Sigma-Aldrich). Primary antibodies in tissues were identified with the appropriate fluorescent-labeled secondary antibodies (Jackson Immunoresearch). Slides were mounted using DPX mounting medium (Electron Microscope Sciences #13514), visualized, and images acquired using a FluoView FV1000 BX2 upright confocal microscope (Olympus, Center Valley, PA) with UPlanSApo 20X/0.80 and UPlanApo N 60X/1.42 objectives with zoom (Z) 2. Images were processed with FluoView (Olympus) and Adobe Photoshop software (San Jose, CA).

Statistics

Descriptive statistics are presented as mean ± standard error. Normality assessments were conducted for groups. Analysis for each experiment is included in legends, with multiple comparisons analyzed using ANOVA with the Holm-Sidak method or Kruskal-Wallis with the Dunn's test for multiple comparisons using GraphPad Prism (v 8).

RESULTS

Generating Townes-AA and –SS *Tlr4* Knockout Mice

In SCD mice, inhibition of TLR4 signaling using the small molecule inhibitor TAK-242 reduces microvascular stasis in presence of hemin, LPS, and hypoxia/reoxygenation (H/R) (8, 9). Furthermore, TLR4 inhibition prevents hemin-mediated lethality. Therefore, to determine if knockout of *Tlr4* in mice carrying human hemoglobin S (Townes-SS) would reduce hemolysis and inflammation, we generated Townes-SS mice with $Tlr4^{-/-}$ genotype. $Tlr4^{-/-}$ mice ($TLR4^{lps\text{-}del}$, Jackson Labs) with knockout of the entire *Tlr4* gene, expressing murine alpha and beta globins on a C57B6 genetic background were breed with Townes-AA $Tlr4^{+/+}$ mice expressing human alpha- and beta-globins on a mixed 129/B6 genetic background. Male and female heterozygous offspring were bred together and pups expressing exclusively human alpha- and beta-globins and at least one deleted *Tlr*4 gene were selected for backcrossing 9 generations with Townes-AA $Tlr4^{+/+}$ mice from our colony with AA mice heterozygous for *Tlr*4 knockout selected for breeding with AA-$Tlr4^{+/+}$ mice at each new generation. After 9 backcrosses, heterozygous AA-$Tlr4^{+/-}$ were bred with SS-$Tlr4^{+/+}$ mice from the colony for the 10^{th} backcross. AS-$Tlr4^{+/-}$ offspring were breed together and AA, AS and SS-$Tlr4^{-/-}$ offspring were selected for breeding to expand the Townes-AA-, AS-, and SS-$Tlr4^{-/-}$ colony and generate mice for experimentation (**Supplemental Figure 2**).

Compared to SS-$Tlr4^{+/+}$ mice, SS-$Tlr4^{-/-}$ mice had no differences in white blood cell counts or in markers of hemolysis (**Table 1**). Likewise, there was no difference in organ function, as demonstrated by serum chemistries (**Table 1**). Therefore, knockout of the *Tlr4* gene in SS mice does not appear to reduce chronic hemolysis.

Tlr4 Knockout Reduced Microvascular Stasis in Sickle Cell Mice

We have previously demonstrated that compared to AA mice, SS mice exhibit a chronic baseline hemolysis that leads to increased occlusion of skin venules (8). However, SS, but not AA mice, also exhibit robust microvascular vaso-occlusion when stimulated with excess hemin, LPS, or H/R (8). Therefore, to determine if TLR4 knockout would protect SS mice from vaso-occlusion, we used dorsal skin fold chambers to assess microvascular stasis at 1h, 2h, 3h, and 4h post-stimulation with hemin, LPS or H/R in SS-$Tlr4^{+/+}$ and SS-$Tlr4^{-/-}$ mice (**Supplemental Figure 1**). Compared to hemin-stimulated SS-$Tlr4^{+/+}$ mice, hemin-stimulated SS-$Tlr4^{-/-}$ mice had a significant reduction in % venules occluded at 1–4 h post-infusion ($Tlr4^{+/+}$ % occluded range 17.5%-28.7% versus $Tlr4^{-/-}$ % occluded range 1.8%-3.9%, $p < 0.005$, **Figure 1A**). With LPS stimulation, compared the SS-$Tlr4^{+/+}$ mice, SS-$Tlr4^{-/-}$ mice also exhibited decreased % venules occluded at 1–4 h post-infusion ($Tlr4^{+/+}$ % occluded range 17.7–37.1% vs. $Tlr4^{-/-}$ % occluded range 3.3–11.3%, $p < 0.02$, **Figure 1B**). After H/R, compared to SS-$Tlr4^{+/+}$, SS-$Tlr4^{-/-}$ exhibited decreased occlusion at 1 h ($Tlr4^{+/+}$ % occluded 20.1 vs. $Tlr4^{-/-}$ % occluded 3.2%, $p < 0.01$, **Figure 1C**) and 2 h time points

TABLE 1 | Complete blood count and serum chemistries from AA-*Tlr4*$^{+/+}$, AA-*Tlr4*$^{-/-}$, SS-*Tlr4*$^{+/+}$ and SS-*Tlr4*$^{-/-}$ mice.

Complete Blood Count	AA-*Tlr4*$^{+/+}$ (n = 4–5, ± std dev)	AA-*Tlr4*$^{-/-}$ (n = 5–6, ± std dev)	SS-*Tlr4*$^{+/+}$ (n = 5–6, ± std dev)	SS-*Tlr4*$^{-/-}$ (n = 4, ± std dev)
White blood cells (WBC), 10^3/µl	1.68 ± 0.68	2.04 ± 1.20	36.62 ± 19.0	33.24 ± 9.66
Neutrophils (%)	22.8	19.4	9.8	14.5
Lymphocytes (%)	72.8	76.6	87.3	80.8
Monocytes (%)	1.3	1.8	2.5	3.3
Eosinophils (%)	2.5	1.8	0.0	0.8
Basophils (%)	0.8	0.4	0.3	0.8
Red blood cells (RBC), 10^6/µL	10.8 ± 1.1	11.3 ± 1.8	5.1 ± 1.1	4.4 ± 1.1
Hemoglobin (Hgb). g/dL	9.5 ± 0.9	9.8 ± 1.5	4.8 ± 1.0	3.9 ± 1.1
Hematocrit (Hct), %	32.1 ± 5.6	35.2 ± 6.1	20.6 ± 4.8	20.3 ± 3.0
Platelets, 10^3/µl	700 ± 112	1012 ± 74	480.1 ± 65.3	445.5 ± 63.3
Reticulocytes (%)	6.6 ± 1.4	11.8 ± 7.9	40.2 ± 29.1	44.9 ± 26.9
Serum Chemistries	AA-*Tlr4*$^{+/+}$	AA-*Tlr4*$^{-/-}$	SS-*Tlr4*$^{+/+}$	SS-*Tlr4*$^{-/-}$
AST	169 ± 43.5	132.7 ± 45.8	653.4 ± 422	416.5 ± 299
ALT	73.2 ± 22.6	57.2 ± 25.7	515.8 ± 478	617.3 ± 720
Total bilirubin	0.1 ± 0.05	0.2 ± 0.11	1.5 ± 0.80	1.2 ± 0.25
Albumin	2.5 ± 0.14	2.5 ± 0.23	2.9 ± 0.13	2.6 ± 0.23
Blood urea nitrogen	26.4 ± 4.3	22.8 ± 4.4	22.0 ± 2.9	25.0 ± 3.2
Creatinine	0.2 ± 0.08	0.1 ± 0.09	0.1 ± 0.1	0.2 ± 0.08

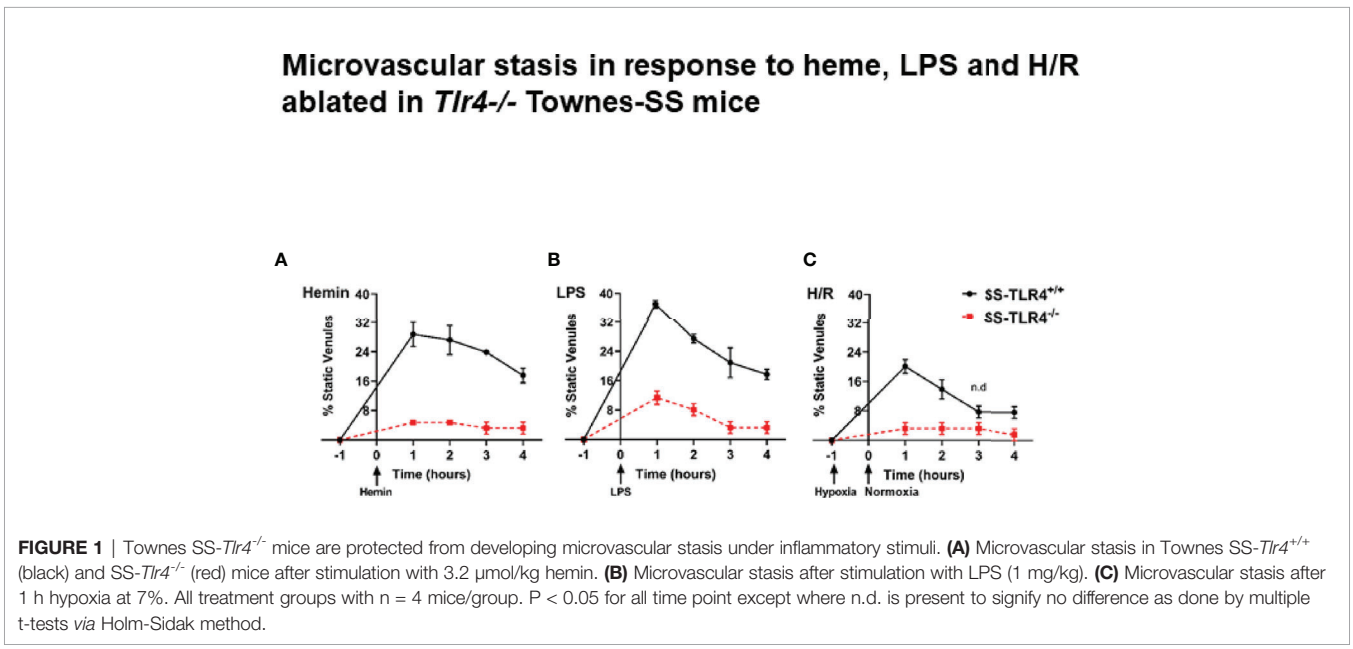

FIGURE 1 | Townes SS-*Tlr4*$^{-/-}$ mice are protected from developing microvascular stasis under inflammatory stimuli. **(A)** Microvascular stasis in Townes SS-*Tlr4*$^{+/+}$ (black) and SS-*Tlr4*$^{-/-}$ (red) mice after stimulation with 3.2 µmol/kg hemin. **(B)** Microvascular stasis after stimulation with LPS (1 mg/kg). **(C)** Microvascular stasis after 1 h hypoxia at 7%. All treatment groups with n = 4 mice/group. $P < 0.05$ for all time point except where n.d. is present to signify no difference as done by multiple t-tests *via* Holm-Sidak method.

(*Tlr4*$^{+/+}$ % occluded 13.9 vs. *Tlr4*$^{-/-}$ % occluded 3.2%, $p < 0.01$, **Figure 1C**). Collectively, these data suggest that loss of TLR4 in SS mice does not reduce baseline hemolysis, but does eliminate microvascular stasis after challenge with hemin, LPS, or H/R.

Loss of TLR4 Reduces NF-κB Signaling

The innate immune system activates signaling cascades within cells in order to promote inflammation. The TLR4 and NADPH oxidase (NOX)-dependent signaling cascades converge to increase pro-inflammatory NF-κB signaling (21). When stimulated with hemin, *Tlr4*$^{-/-}$ mouse pulmonary vein endothelial cells demonstrate reduced NF-κB activation (8). Likewise, treatment of human umbilical vein endothelial cells with the TLR4 inhibitor TAK-242 also reduces NF-κB signaling. To evaluate if knockout of TLR4 reduces NF-κB signaling in SS mice, we performed western blots on nuclear extracts from livers isolated from hemin-stimulated SS-*Tlr4*$^{+/+}$ and SS-*Tlr4*$^{-/-}$ mice. Compared to hemin-stimulated SS-*Tlr4*$^{+/+}$, hemin-stimulated SS-*Tlr4*$^{-/-}$ mice lacked phosphorylation of NF-κB p65 (**Figure 2**). This suggests that loss of TLR4 reduces inflammation through abrogation of NF-κB signaling.

SS-*Tlr4*$^{-/-}$ Mice Challenged With Hemin Exhibit Reduced Pro-Inflammatory Cytokine and Adhesion Molecule mRNA

Vaso-occlusion requires both inflammation and adhesion to occur, with NF-κB signaling serving as a crucial transcription signaling for numerous pro-inflammatory and adhesive genes.

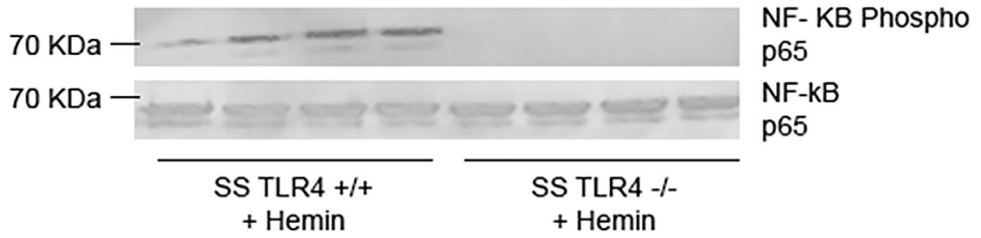

FIGURE 2 | Hemin-stimulated Townes SS-*Tlr4*$^{-/-}$ mice do not activate NF-κβ signaling. Western blot of liver nuclear extracts isolated from hemin-stimulated Townes SS-*Tlr4*$^{+/+}$ and SS-*Tlr4*$^{-/-}$ mice probed for NF-κB phopsho-p65 and total p65. (n = 4 per group).

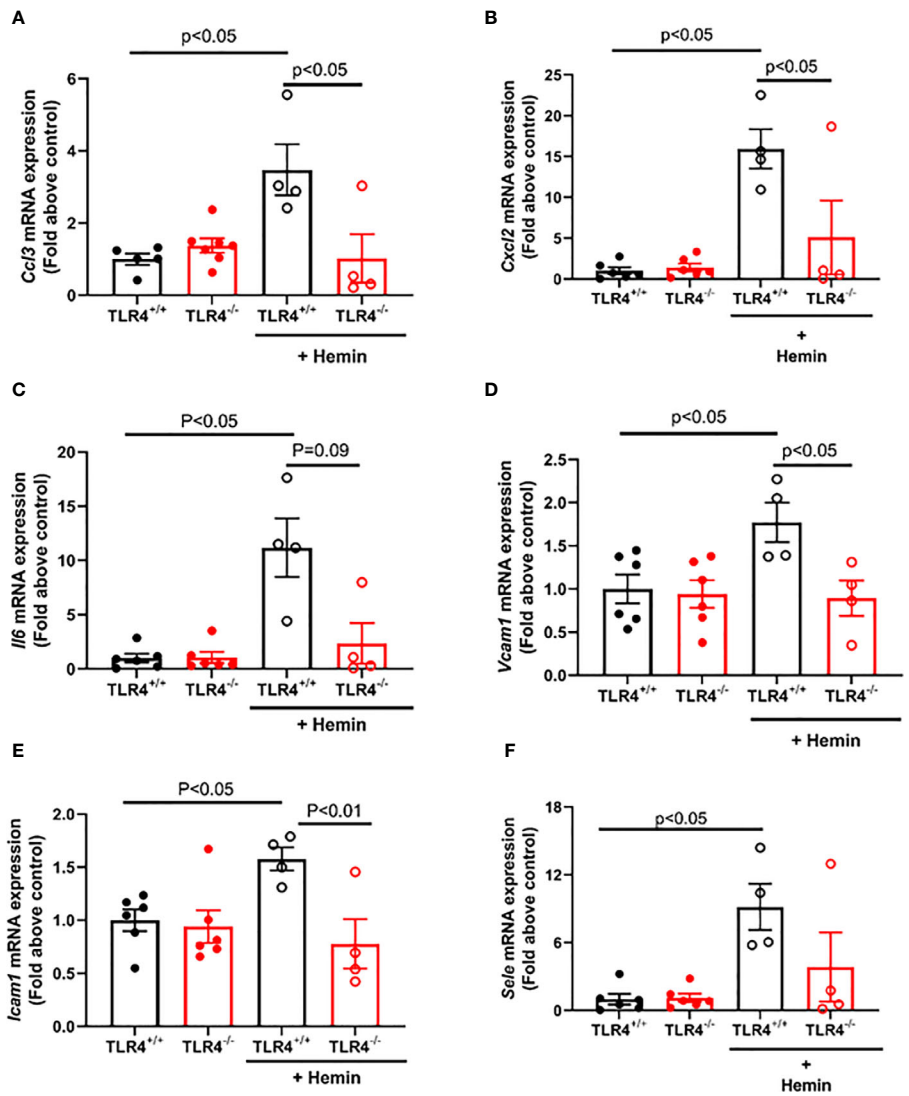

FIGURE 3 | Hemin-stimulated Townes SS-*Tlr4*$^{-/-}$ mice do not upregulate pro-inflammatory cytokine and adhesive genes. Liver mRNA was extracted and underwent qRT-PCR analysis. **(A)** Macrophage inflammatory protein 1-α (MIP-1α, *Ccl3*). **(B)** Macrophage inflammatory 2-α (MIP-2α, *Cxcl2*) mRNA. **(C)** IL-6 *(Il6)* mRNA. **(D)** *Vcam1* mRNA **(E)** *Icam1* mRNA. **(F)** E-selectin (*Sele*) mRNA. Values are mean ± standard error of mean (SEM), with p-values determined by one-way analysis of variance with Holm-Sidak's multiple comparison testing.

Therefore, we sought to evaluate the downstream consequences of reduced NF-κB activation in hemin-stimulated SS-*Tlr4*$^{-/-}$ mice by assessing the livers of SS-*Tlr4*$^{+/+}$ and SS-*Tlr4*$^{-/-}$ mice for changes in pro-inflammatory and adhesion gene expression. First, compared to untreated SS-*Tlr4*$^{+/+}$ mice, hemin-treated SS-*Tlr4*$^{+/+}$ mice have significant upregulation of macrophage inflammatory protein 1-α (MIP-1α, *Ccl3*) and macrophage inflammatory 2-α (MIP-2α, *Cxcl2*) mRNA by 3.5-fold (*Ccl3*, $P < 0.004$, n = 4–5 mice per group, **Figure 3A**) and 16-fold respectively (*Cxcl2*, $P < 0.0004$, n = 4–5 mice per group, **Figure 3B**). Compared to untreated SS-*Tlr4*$^{-/-}$ mice, hemin-stimulated SS-*Tlr4*$^{-/-}$ mice do not upregulate either *Ccl3* mRNA (**Figure 3A**) or *Cxcl2* mRNA (**Figure 3B**). Moreover, for both chemokines, comparison between hemin-treated SS-*Tlr4*$^{+/+}$ mice to hemin-treated SS-*Tlr4*$^{-/-}$ mice demonstrated significant loss of *Ccl3* and *Cxcl2* mRNA upregulation in absence of TLR4. Next, we assessed IL-6 (Il6) mRNA expression. Similar to *Ccl3* and *Cxcl2*, compared to untreated SS-*Tlr4*$^{+/+}$ mice, hemin-treated SS-*Tlr4*$^{+/+}$ mice had an 11-fold increase in *Il6* mRNA ($P < 0.03$, n = 4–6 mice per group, **Figure 3C**). In untreated and hemin-stimulated SS-*Tlr4*$^{-/-}$, there was no difference in *Il6* mRNA (n = 4–6 mice per group, **Figure 3C**). Additionally, comparison between hemin-treated SS-*Tlr4*$^{+/+}$ mice to hemin-treated SS-*Tlr4*$^{-/-}$ mice demonstrated a reduced *Il6* mRNA upregulation (p=0.09) in absence of TLR4. This was also seen in the kidneys (**Supplemental Figure 3A**). Collectively, these data suggest that loss of TLR4 in SCD leads to decreased inflammation-mediated cytokine gene expression.

Next, to determine if loss of TLR4 reduces hemin-mediated upregulation of endothelial adhesion molecules, we assessed mRNA expression of *Vcam1*, *Icam1*, and E-selectin (*Sele*). Compared to untreated SS-*Tlr4*$^{+/+}$ mice, hemin-stimulated SS-*Tlr4*$^{+/+}$ mice had a significant 1.8-fold upregulation of *Vcam1* mRNA ($P < 0.05$, **Figure 3D**) and 1.6-fold upregulation of *Icam1* mRNA ($P < 0.05$, **Figure 3E**). In SS-*Tlr4*$^{-/-}$ mice, compared to untreated, hemin-stimulated SS-*Tlr4*$^{-/-}$ mice had no difference in *Vcam1* mRNA (**Figure 3D**) or *Icam1* mRNA (**Figure 3E**). Similar to pro-inflammatory markers, comparison between hemin-treated SS-*Tlr4*$^{+/+}$ mice and SS-*Tlr4*$^{-/-}$ mice demonstrated significant loss of *Vcam1* mRNA and *Icam1* mRNA upregulation in absence of TLR4. Last, for *Sele*, compared to untreated SS-*Tlr4*$^{+/+}$ mice, hemin-stimulated SS-*Tlr4*$^{+/+}$ mice upregulated *Sele* mRNA 9-fold ($P < 0.05$, **Figure 3F**), whereas compared to untreated SS-*Tlr4*$^{-/-}$mice, hemin-stimulated SS-*Tlr4*$^{-/-}$mice did not upregulate *Sele* mRNA (**Figure 3F**). Similar pattern of mRNA expression changes were also observed for these genes in the kidney (**Supplemental Figures 3B–D**). Collectively, these data suggest that in SS mice, loss of TLR4 reduces upregulation of both pro-inflammatory and endothelial adhesion genes.

Hemin-Stimulated SS-*Tlr4*$^{-/-}$ Mice Do Not Upregulate Endothelial Adhesion Proteins

In SCD, upregulation of endothelial adhesion proteins contributes to vaso-occlusion. Therefore, to evaluate if endothelial adhesion molecule protein expression is reduced in SS mice by TLR4 knockout, we performed western blots on liver microsomes isolated from SS-*Tlr4*$^{+/+}$ and SS-*Tlr4*$^{-/-}$ mice after hemin stimulation. Consistent with mRNA data, compared to hemin-stimulated SS-*Tlr4*$^{+/+}$ mice, hemin-stimulated SS-*Tlr4*$^{-/-}$ mice do not increase VCAM-1 (**Figure 4A**). Likewise, compared to hemin-stimulated SS-*Tlr4*$^{+/+}$ mice, hemin-stimulated SS-*Tlr4*$^{-/-}$ mice do not increase ICAM-1 or E-selectin (**Figures 4B–D**). Together with mRNA data, these data suggest that loss of TLR4 in SS mice reduces heme-mediated endothelial cell activation leading to reduced adhesion molecule expression and decreased inflammation.

Hemin-Stimulated SS-*Tlr4*$^{-/-}$ Mice Exhibit Reduced P-Selectin and VWF Release From Endothelium

TLR4 blockade reduces heme-mediated release of P-selectin and VWF from endothelial cell Weibel Palade bodies (8). Therefore, we performed immunofluorescence of SS-*Tlr4*$^{-/-}$ and SS-*Tlr4*$^{+/+}$ lungs in mice treated with and without hemin to evaluate heme-mediated P-selectin and VWF release. Compared to SS-*Tlr4*$^{+/+}$ mice, SS-*Tlr4*$^{-/-}$ treated with hemin exhibit decreased P-selectin and VWF release (**Figure 5**). Collectively, these data confirm that loss of TLR4 signaling in SS mice reduces pro-adhesive and

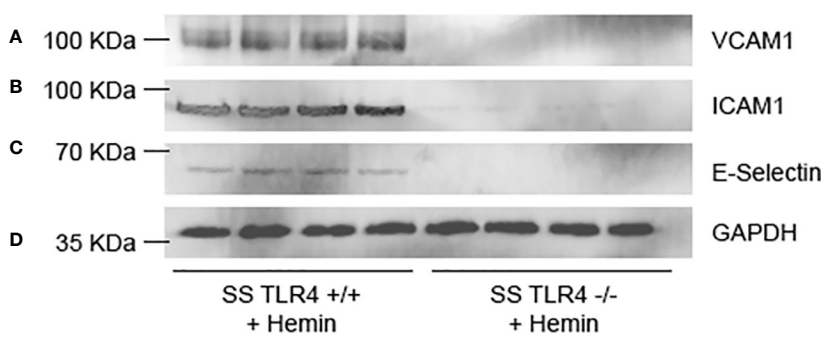

FIGURE 4 | Hemin-stimulated Townes SS-*Tlr4*$^{-/-}$ mice lose upregulation of adhesion proteins. Western blot of liver microsomes isolated from hemin-stimulated Townes SS-*Tlr4*$^{+/+}$ and SS-*Tlr4*$^{-/-}$ mice probed for **(A)** VCAM-1, **(B)** ICAM-1, **(C)** E-selectin, and **(D)** GAPDH loading control. (n = 4 per group).

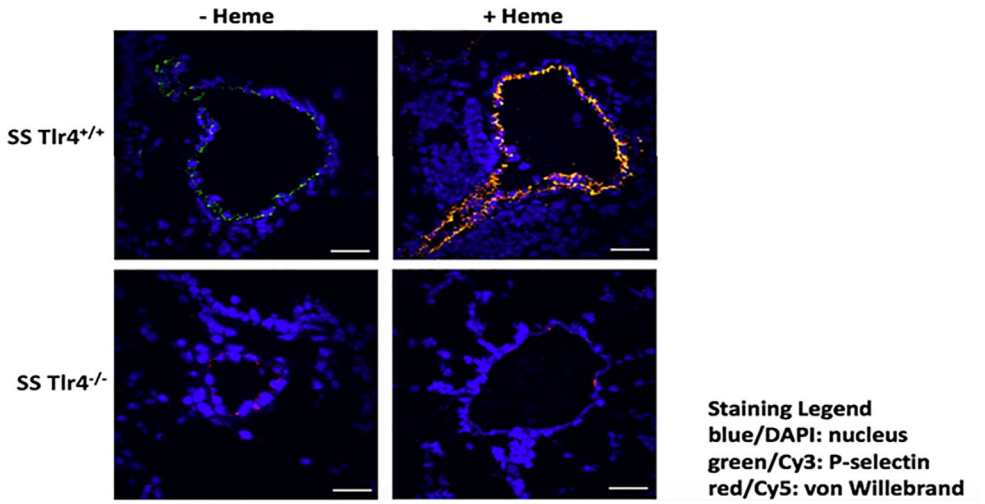

FIGURE 5 | Hemin-stimulated Townes SS-*Tlr4*$^{-/-}$ mice have decreased pulmonary expression of VWF and P-selectin. Immunostaining of surface P-selectin (green) and von Willebrand factor (red) on blood vessels in the lungs of hemin-infused Townes-SS *Tlr4*$^{+/+}$ and *Tlr4*$^{-/-}$ mice (3.2 μmol/kg and lungs removed at 1h). Scale bars (white) 30 μm. Representative images are presented.

thrombotic P-selectin and VWF secretion from endothelial Weibel-Palade bodies.

Endothelial, Not Hematopoietic, TLR4 Drives SS Vaso-Occlusion

Several groups have demonstrated that knockdown of TLR4 in endothelial cells reduces monocyte and neutrophil adhesion (22, 23). Further, prior work demonstrated that knockout of TLR4 in the vessel wall was sufficient to ablate SCD VOC physiology (1). However, those studies transplanted SS BM into TLR4 knockout mice and therefore could not examine the effects of TLR4 knockout in circulating hematopoietic cells on VOC. This is an important question because monocytes isolated from SCD patients can activate endothelial monolayers (14) and heterocellular aggregates play an important role in vaso-occlusion (15, 16). Here we addressed the question does knockout of TLR4 in circulating hematopoietic-derived cells ablate microvascular stasis? Therefore, we performed BM chimera studies using the SS-*Tlr4*$^{-/-}$ and SS-*Tlr4*$^{+/+}$ mice into AA-*Tlr4*$^{-/-}$ or AA *Tlr4*$^{+/+}$ recipients followed by assessment of hemin-stimulated vaso-occlusion in dorsal skin fold chambers (**Figures 6A, C**). First, to assess the contribution of hematopoietic expression of TLR4, we compared chimeras generated from SS-*Tlr4*$^{-/-}$ mice transplanted into AA-*Tlr4*$^{+/+}$ or AA-*Tlr4*$^{-/-}$ recipients (**Figure 6A**). Hemin-stimulated SS or SS-*Tlr4*$^{+/+}$ mice exhibit average % occlusion of ~30% (historic and **Figure 1A**); loss of TLR4 in hematopoietic cells (SS-*Tlr4*$^{-/-}$ mice into AA-*Tlr4*$^{+/+}$ recipients) lead to no change in % venules occluded (range % occluded 21.0–31.6%, **Figure 6B**). Comparatively, and consistent with SS-*Tlr4*$^{-/-}$ mice, transplant of SS-*Tlr4*$^{-/-}$ marrow into AA-*Tlr4*$^{-/-}$ recipients significantly reduced the % venules occluded (range 3.1–11.0% occluded vessels, $p < 0.001$, **Figure 6B**). Overall, these data suggest that hematopoietic TLR4 signaling is not essential in triggering vaso-occlusive response. Next, to assess effects of endothelial TLR4 knockout, we created chimeras transplanting SS-*Tlr4*$^{+/+}$ hematopoietic cells into AA-*Tlr4*$^{+/+}$ and AA-*Tlr4*$^{-/-}$ recipients (**Figure 6C**). Similar to SS and SS-*Tlr4*$^{+/+}$ mice, transplant of SS-*Tlr4*$^{+/+}$ hematopoietic cells into AA-*Tlr4*$^{+/+}$ lead to vaso-occlusion (range 17.2–31.3% occluded vessels **Figure 6D**). Strikingly, transplant of SS-*Tlr4*$^{+/+}$ marrow into AA-*Tlr4*$^{-/-}$ mice abrogated vessel occlusion (range 1.6–7.2% occluded vessels, $p < 0.001$, **Figure 6D**). Collectively, these data demonstrate that endothelial, but not hematopoietic, TLR4 expression is necessary to initiate vaso-occlusive physiology in SS mice.

DISCUSSION

Intravascular hemolysis of sickle red blood cells release hemoglobin S (HbS) into the plasma which is promptly oxidized to methemoglobin, which readily releases free heme. Heme is a DAMP that can activate the innate immune pattern recognition receptor complex of CD14, MD-2 and TLR4 (8–10); this process promotes a pro-inflammatory and pro-adhesive phenotype, which ultimately leads to VOC (1, 8–10). Herein, we demonstrate that loss of TLR4 signaling in SCD leads to decreased VOC stimulated by numerous agonists, including heme, LPS and H/R. Importantly, we also demonstrate that endothelial, but not hematopoietic, TLR4 expression is necessary to initiate vaso-occlusion in SS mice. Collectively, these data illustrate the indispensable role of the endothelium in mediating the crosstalk between hemolysis and the innate immune system in SCD VOC physiology.

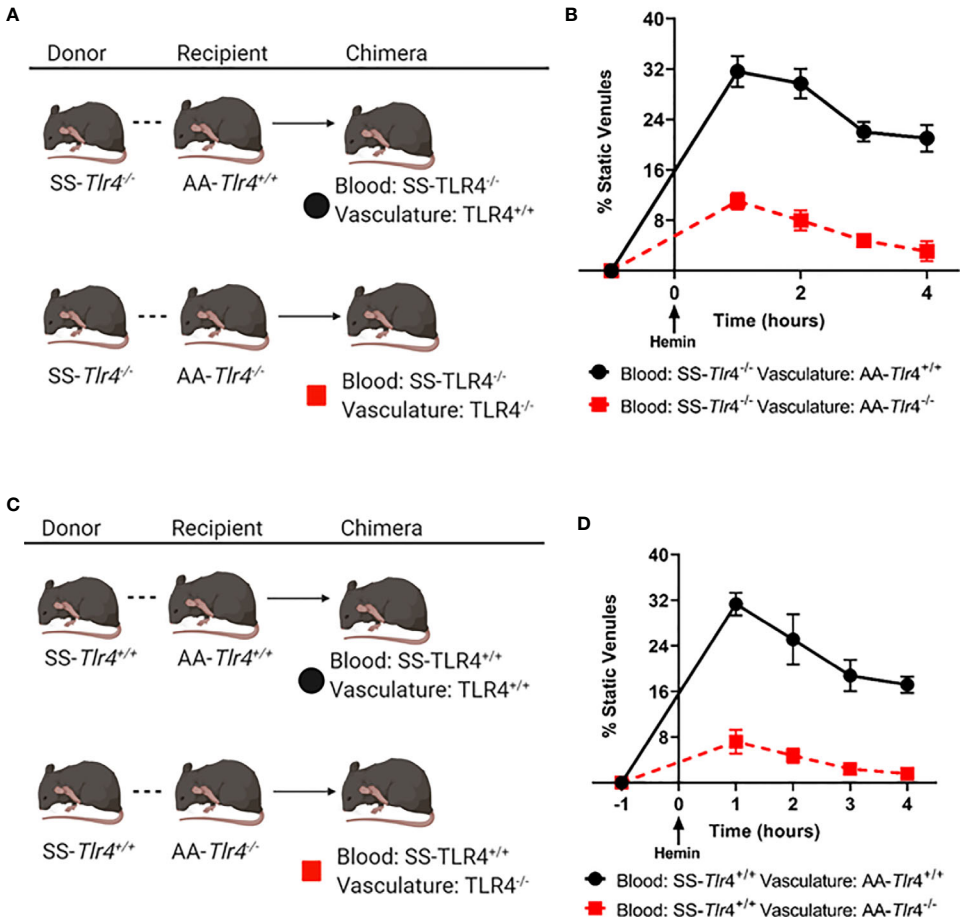

FIGURE 6 | Loss of endothelial, but not hematopoietic, TLR4 expression prevents microvascular stasis. **(A)** Schematic for bone marrow chimera crosses using SS-*Tlr4*$^{-/-}$ donor marrow into AA-*Tlr4*$^{+/+}$ or AA-*Tlr4*$^{-/-}$ recipients. **(B)** Hemin-stimulated microvascular stasis in chimeric AA-*Tlr4*$^{+/+}$ (black) and AA-*Tlr4*$^{-/-}$ (red) recipients that received SS-*Tlr4*$^{-/-}$ marrow. **(C)** schematic for bone marrow chimera crosses using SS-*Tlr4*$^{+/+}$ donor marrow into AA-*Tlr4*$^{+/+}$ or AA-*Tlr4*$^{-/-}$ recipients. **(D)** Hemin-stimulated microvascular stasis in chimeric AA-*Tlr4*$^{+/+}$ (black) and AA-*Tlr4*$^{-/-}$ (red) that received SS-*Tlr4*$^{+/+}$ marrow. All treatment groups with n = 4 mice/group. $P < 0.05$ for all time points analyzed by multiple t-tests *via* Holm-Sidak method.

In SCD, chronic hemolysis leads to organ dysfunction due to recurrent cycles of I/R physiology. However, VOC occurs when pro-inflammatory stimuli are present, such as heme or LPS and the compensatory mechanisms responsible for rebalancing the system are overcome (24). Therefore, when approaching SCD pathogenesis, acute verses chronic stimulation of the innate immune system should be considered. Our work demonstrates that compared to Townes SS-*Tlr4*$^{+/+}$ mice, Townes SS-*Tlr4*$^{-/-}$ mice did not have changes in baseline hemolytic markers. However, importantly, our studies demonstrate that in response to an acute increase in heme, such as would be expected during an acute VOC, loss of TLR4 signaling results in decreased pro-inflammatory and adhesive gene expression and ultimately decreased stasis. Therefore, we speculate that during VOC, strategies to target TLR4 may reduce incidence and perhaps duration of VOC.

In SCD, the prominent end-organ damage is associated with the vasculature, including pulmonary hypertension, strokes, and priapism and retinal disease. However, renal failure, liver damage and hyposplenism are also manifestations of chronic, progressive I/R damage (25). Therefore, we performed analysis of inflammatory markers and adhesion markers in the liver, lungs and kidneys. In the liver, resident hepatic macrophages, also known as Kupffer cells, and hepatic stellate cells are key mediators of hepatic fibrogenesis. Hepatic stellate cells are the main target of TLR4 ligands in the liver (26). Once stimulated, hepatic stellate cells stimulate chemokine secretion, which drives Kupffer cell chemotaxis and pro-fibrotic TGF-β production. Overall, it has been found that loss of hepatic stellate cell TLR4-MyD88 signaling reduces development of hepatic fibrosis. Of note, during chimera generation, hepatic stellate cells are not replaced by BM-derived cells, and without clodraonate-mediated depletion, only a proportion of Kupffer cells become replaced by BM-derived cells (26, 27). Therefore, in our chimera studies, the AA-*Tlr4*$^{-/-}$ recipients lack hepatic stellate cells responsive to TLR4 ligands. Of note, when comparing SS-*Tlr4*$^{-/-}$ mice to hemin-treated SS-*Tlr4*$^{-/-}$ mice, there was a trend toward decreased pro-fibrotic TGF-β expression in both liver

and kidney samples (**Supplemental Figure 4**). Therefore one may speculate that long-term SS-*Tlr4*$^{-/-}$ mice may be protected from fibrosis.

In other I/R models, such as cardiac transplant, loss of endothelial TLR4/Trif-mediated signaling reduces neutrophil adhesion and recruitment (23). Our data is consistent with these models, as the livers of hemin-treated Townes SS-*Tlr4*$^{-/-}$ mice demonstrate loss of *Ccl3* and *Cxcl2* gene upregulation, two chemokines important for the initiation of selectin-mediated rolling and leukocyte recruitment. Of note, in our kidney mRNA assessment, we did not see a significant change in *Ccl3* or *Cxcl2* mRNA changes; this likely reflects that kidneys lack cells similar to stellate cells and that renal disease in SCD is not characterized by inflammatory cell infiltrates. Last, our data demonstrates loss of heme-mediated release of Weibel-Palade bodies from the lung endothelium in SS *Tlr4*$^{-/-}$ mice. This is important as surface expression of von Willebrand factor and P-selectin are involved in platelet binding, leukocyte recruitment, and stasis (8, 28–31). Collectively, these data suggest that endothelial TLR4 response to heme leads to increased leukocyte recruitment, rolling, and adhesion to amplify I/R physiology.

With the advent of gene-therapy on the horizon for SCD, the importance of hematopoietic verses non-hematopoietic TLR4 signaling is a crucial distinction as TLR4 expression on hematopoietic cells is essential for bacterial clearance. As current transplant paradigms incorporate myelo-ablation, which increases risk of infections, strategies that reduce VOC but maintain effective pathogen clearance in SCD are desirable. Therefore, within the context of SCD, targeting of heme-mediated vascular TLR4 signaling, but not LPS-mediated TLR4 signaling, may be a strategy to prevent or decrease I/R injury while maintaining immune function.

One limitation of this work is we did not quantitate leukocyte recruitment during VOC physiology; however, we have previously demonstrated reduced leukocyte rolling in *Tlr4*$^{-/-}$ mice transplanted with SS BM (8). Second, our studies have not evaluated SS-*Tlr4*$^{-/-}$ mice for reductions in acute pain but recent studies by Lei et al. used BERK- SS-*Tlr4*$^{-/-}$ mice to demonstrate a causal role of free heme in the genesis of acute and chronic sickle pain (12).

In conclusion, endothelial TLR4 signaling triggered by heme is critical for SCD VOC. We demonstrate the knockout of vascular, not hematopoietic, TLR4 signaling reduces heme-mediated inflammation and VOC. Overall, these data suggest that targeted inhibition of heme-mediated vascular endothelial TLR4 signaling may be a potential strategy to break the inflammatory cycle of I/R that is initiated by HbS-driven hemolysis.

DATA AVAILABILITY STATEMENT

The raw data supporting the conclusions of this article will be made available by the authors, without undue reservation.

ETHICS STATEMENT

The animal study was reviewed and approved by University of Minnesota Institutional Animal Care and Use Committee.

AUTHOR CONTRIBUTIONS

JBec designed and performed experiments, analyzed results, and wrote the manuscript. FA performed experiments and analyzed results. CC performed experiments and analyzed results. RK performed experiments and analyzed results. DR-R performed experiments and analyzed results. ZK performed experiments and analyzed results. AN performed experiments and analyzed results. PZ performed experiments and analyzed results. JN performed experiments and analyzed results. RH designed experiments and reviewed manuscript. JBel designed experiments, analyzed results and wrote the manuscript. GV designed experiments, analyzed results, and wrote the manuscript. All authors contributed to the article and approved the submitted version.

FUNDING

Research funding from NIH 5R01HL114567. ZK was supported by the Hematology Research Training Grant T32 L007062/HL/NHLBI. RK and DR-R received funding from University of Minnesota Life Sciences Undergraduate Research Program (LSSURP) 5R25HL088728-14.

ACKNOWLEDGMENTS

The authors would like to thank Elena Aronovich, Jacob Lloyd, and Kristine Nachbor for assistance with laboratory work.

SUPPLEMENTARY MATERIAL

The Supplementary Material for this article can be found online at: https://www.frontiersin.org/articles/10.3389/fimmu.2020.613278/full#supplementary-material

REFERENCES

1. Hebbel RP, Belcher JD, Vercellotti GM. The multifaceted role of ischemia/reperfusion in sickle cell anemia. *J Clin Invest* (2020) 130(3):1062–72. doi: 10.1172/JCI133639
2. Matte A, Recchiuti A, Federti E, Koehl B, Mintz T, El Nemer W, et al. Resolution of sickle cell disease-associated inflammation and tissue damage with 17R-resolvin D1. *Blood* (2019) 133(3):252–65. doi: 10.1182/blood-2018-07-865378
3. Vercellotti GM, Dalmasso AP, Schaid TRJr., Nguyen J, Chen C, Ericson ME, et al. Critical role of C5a in sickle cell disease. *Am J Hematol* (2018) 94:327–37. doi: 10.1002/ajh.25384
4. Ataga KI, Kutlar A, Kanter J, Liles D, Cancado R, Friedrisch J, et al. Crizanlizumab for the Prevention of Pain Crises in Sickle Cell Disease. *New Engl J Med* (2017) 376(5):429–39. doi: 10.1056/NEJMoa1611770
5. Zhao Y, Schwartz EA, Palmer GM, Zennadi R. MEK1/2 inhibitors reverse acute vascular occlusion in mouse models of sickle cell disease. *FASEB J Off*

Publ Fed Am Societies Exp Biol (2016) 30(3):1171–86. doi: 10.1096/fj.15-278481
6. Zhang D, Xu C, Manwani D, Frenette PS. Neutrophils, platelets, and inflammatory pathways at the nexus of sickle cell disease pathophysiology. *Blood* (2016) 127(7):801–9. doi: 10.1182/blood-2015-09-618538
7. Chen G, Zhang D, Fuchs TA, Manwani D, Wagner DD, Frenette PS. Heme-induced neutrophil extracellular traps contribute to the pathogenesis of sickle cell disease. *Blood* (2014) 123(24):3818–27. doi: 10.1182/blood-2013-10-529982
8. Belcher JD, Chen C, Nguyen J, Milbauer L, Abdulla F, Alayash AI, et al. Heme triggers TLR4 signaling leading to endothelial cell activation and vaso-occlusion in murine sickle cell disease. *Blood* (2014) 123(3):377–90. doi: 10.1182/blood-2013-04-495887
9. Nath KA, Belcher JD, Nath MC, Grande JP, Croatt AJ, Ackerman AW, et al. Role of TLR4 signaling in the nephrotoxicity of heme and heme proteins. *Am J Physiol Renal Physiol* (2018) 314(5):F906–f14. doi: 10.1152/ajprenal.00432.2017
10. Belcher JD, Zhang P, Nguyen J, Kiser ZM, Nath KA, Hu J, et al. Identification of a Heme Activation Site on the MD-2/TLR4 Complex. *Front Immunol* (2020) 11(1370):10. doi: 10.3389/fimmu.2020.01370
11. Figueiredo RT, Fernandez PL, Mourao-Sa DS, Porto BN, Dutra FF, Alves LS, et al. Characterization of heme as activator of Toll-like receptor 4. *J Biol Chem* (2007) 282(28):20221–9. doi: 10.1074/jbc.M610737200
12. Lei J, Paul J, Wang Y, Gupta M, Vang D, Thompson S, et al. Heme Causes Pain in Sickle Mice via Toll-Like Receptor 4-Mediated Reactive Oxygen Species- and Endoplasmic Reticulum Stress-Induced Glial Activation. *Antioxid Redox Signal* (2020). doi: 10.1089/ars.2019.7913
13. Merle NS, Paule R, Leon J, Daugan M, Robe-Rybkine T, Poillerat V, et al. P-selectin drives complement attack on endothelium during intravascular hemolysis in TLR-4/heme-dependent manner. *Proc Natl Acad Sci* (2019) 116(13):6280. doi: 10.1073/pnas.1814797116
14. Belcher JD, Marker PH, Weber JP, Hebbel RP, Vercellotti GM. Activated monocytes in sickle cell disease: potential role in the activation of vascular endothelium and vaso-occlusion. *Blood* (2000) 96(7):2451–9. doi: 10.1182/blood.V96.7.2451.h8002451_2451_2459
15. Frenette PS. Sickle cell vaso-occlusion: multistep and multicellular paradigm. *Curr Opin Hematol* (2002) 9(2):101–6. doi: 10.1097/00062752-200203000-00003
16. Bennewitz MF, Vats R, Tutuncuoglu E, Gladwin MT, Sundd P. Lung Vaso-Occlusion in Sickle Cell Disease Mediated By Arteriolar Neutrophil-Platelet Micro-Emboli. *Blood* (2016) 128(22):159–. doi: 10.1182/blood.V128.22.159.159
17. Wu LC, Sun CW, Ryan TM, Pawlik KM, Ren J, Townes TM. Correction of sickle cell disease by homologous recombination in embryonic stem cells. *Blood* (2006) 108(4):1183–8. doi: 10.1182/blood-2006-02-004812
18. Kalambur VS, Mahaseth H, Bischof JC, Kielbik MC, Welch TE, Vilback A, et al. Microvascular blood flow and stasis in transgenic sickle mice: Utility of a dorsal skin fold chamber for intravital microscopy. *Am J Hematol* (2004) 77(2):117–25. doi: 10.1002/ajh.20143
19. Belcher J, Vineyard J, Bruzzone C, Chen C, Beckman J, Nguyen J, et al. Heme oxygenase-1 gene delivery by Sleeping Beauty inhibits vascular stasis in a murine model of sickle cell disease. *J Mol Med* (2010) 88(7):665–75. doi: 10.1007/s00109-010-0613-6
20. Schmittgen TD. Analyzing real-time PCR data by the comparative C(T) method. *Nat Protoc* (2008) 3(6):1101–8. doi: 10.1038/nprot.2008.73
21. Park HS, Jung HY, Park EY, Kim J, Lee WJ, Bae YS. Cutting edge: direct interaction of TLR4 with NAD(P)H oxidase 4 isozyme is essential for lipopolysaccharide-induced production of reactive oxygen species and activation of NF-kappa B. *J Immunol* (2004) 173(6):3589–93. doi: 10.4049/jimmunol.173.6.3589
22. Qu D, Wang L, Huo M, Song W, Lau C-W, Xu J, et al. Focal TLR4 activation mediates disturbed flow-induced endothelial inflammation. *Cardiovasc Res* (2019) 116(1):226–36. doi: 10.1093/cvr/cvz046
23. Li W, Feng G, Gauthier JM, Lokshina I, Higashikubo R, Evans S, et al. Ferroptotic cell death and TLR4/Trif signaling initiate neutrophil recruitment after heart transplantation. *J Clin Invest* (2019) 129(6):2293–304. doi: 10.1172/JCI126428
24. Belcher JD, Chen C, Nguyen J, Abdulla F, Zhang P, Nguyen H, et al. Haptoglobin and hemopexin inhibit vaso-occlusion and inflammation in murine sickle cell disease: Role of heme oxygenase-1 induction. *PloS One* (2018) 13(4):e0196455. doi: 10.1371/journal.pone.0196455
25. Piel FB, Steinberg MH, Rees DC. Sickle Cell Disease. *New Engl J Medicine* (2017) 376(16):1561–73. doi: 10.1056/NEJMra1510865
26. Seki E, De Minicis S, Osterreicher CH, Kluwe J, Osawa Y, Brenner DA, et al. TLR4 enhances TGF-beta signaling and hepatic fibrosis. *Nat Med* (2007) 13(11):1324–32. doi: 10.1038/nm1663
27. Yang L, Miura K, Zhang B, Matsushita H, Yang YM, Liang S, et al. TRIF Differentially Regulates Hepatic Steatosis and Inflammation/Fibrosis in Mice. *Cell Mol Gastroenterol Hepatol* (2017) 3(3):469–83. doi: 10.1016/j.jcmgh.2016.12.004
28. Gotsch U, Jager U, Dominis M, Vestweber D. Expression of P-selectin on endothelial cells is upregulated by LPS and TNF-alpha in vivo. *Cell Adhesion Communication* (1994) 2(1):7–14. doi: 10.3109/15419069409014198
29. Frenette PS, Subbarao S, Mazo IB, von Andrian UH, Wagner DD. Endothelial selectins and vascular cell adhesion molecule-1 promote hematopoietic progenitor homing to bone marrow. *Proc Natl Acad Sci U S A* (1998) 95(24):14423–8. doi: 10.1073/pnas.95.24.14423
30. Frenette PS, Moyna C, Hartwell DW, Lowe JB, Hynes RO, Wagner DD. Platelet-endothelial interactions in inflamed mesenteric venules. *Blood* (1998) 91(4):1318–24. doi: 10.1182/blood.V91.4.1318
31. Frenette PS, Denis CV, Weiss L, Jurk K, Subbarao S, Kehrel B, et al. P-Selectin glycoprotein ligand 1 (PSGL-1) is expressed on platelets and can mediate platelet-endothelial interactions in vivo. *J Exp Med* (2000) 191(8):1413–22. doi: 10.1084/jem.191.8.1413

Conflict of Interest: JBec receives funding from Bayer not related to work herein. JBel and GV receive research funding from CSL Behring and Mitobridge (Astellas).

The remaining authors declare that the research was conducted in the absence of any commercial or financial relationships that could be construed as a potential conflict of interest.

frontiers in Immunology

REVIEW
published: 27 January 2021
doi: 10.3389/fimmu.2020.561917

The Worst Things in Life are Free: The Role of Free Heme in Sickle Cell Disease

Oluwabukola T. Gbotosho[1,2†], *Maria G. Kapetanaki*[2,3†] *and Gregory J. Kato*[1,2*]

[1] *Division of Hematology-Oncology, Department of Medicine, University of Pittsburgh School of Medicine, Pittsburgh, PA, United States,* [2] *Pittsburgh Heart, Lung, Blood, and Vascular Medicine Institute, Department of Medicine, University of Pittsburgh School of Medicine, Pittsburgh, PA, United States,* [3] *Division of Pulmonary, Allergy and Critical Care Medicine, Department of Medicine, University of Pittsburgh School of Medicine, Pittsburgh, PA, United States*

Hemolysis is a pathological feature of several diseases of diverse etiology such as hereditary anemias, malaria, and sepsis. A major complication of hemolysis involves the release of large quantities of hemoglobin into the blood circulation and the subsequent generation of harmful metabolites like labile heme. Protective mechanisms like haptoglobin-hemoglobin and hemopexin-heme binding, and heme oxygenase-1 enzymatic degradation of heme limit the toxicity of the hemolysis-related molecules. The capacity of these protective systems is exceeded in hemolytic diseases, resulting in high residual levels of hemolysis products in the circulation, which pose a great oxidative and proinflammatory risk. Sickle cell disease (SCD) features a prominent hemolytic anemia which impacts the phenotypic variability and disease severity. Not only is circulating heme a potent oxidative molecule, but it can act as an erythrocytic danger-associated molecular pattern (eDAMP) molecule which contributes to a proinflammatory state, promoting sickle complications such as vaso-occlusion and acute lung injury. Exposure to extracellular heme in SCD can also augment the expression of placental growth factor (PlGF) and interleukin-6 (IL-6), with important consequences to enthothelin-1 (ET-1) secretion and pulmonary hypertension, and potentially the development of renal and cardiac dysfunction. This review focuses on heme-induced mechanisms that are implicated in disease pathways, mainly in SCD. A special emphasis is given to heme-induced PlGF and IL-6 related mechanisms and their role in SCD disease progression.

Keywords: hemolysis, sickle cell disease, free heme, inflammation, oxidative stress, IL-6, placental growth factor, pulmonary hypertension

OPEN ACCESS

Edited by:
Wilma Barcellini,
IRCCS Ca 'Granda Foundation Maggiore Policlinico Hospital, Italy

Reviewed by:
Claudio Canetti,
Federal University of Rio de Janeiro, Brazil
Iqbal Hamza,
University of Maryland, College Park, United States
Xiaojing Yuan,
University of Maryland, College Park, United States,
in collaboration with reviewer IH

****Correspondence:***
Gregory J. Kato
gregorykatomd@gmail.com

†These authors share first authorship

Specialty section:
This article was submitted to Inflammation, a section of the journal Frontiers in Immunology

Received: *14 May 2020*
Accepted: *04 December 2020*
Published: *27 January 2021*

Citation:
Gbotosho OT, Kapetanaki MG and Kato GJ (2021) The Worst Things in Life are Free: The Role of Free Heme in Sickle Cell Disease. Front. Immunol. 11:561917. doi: 10.3389/fimmu.2020.561917

INTRODUCTION

Sickle Cell Disease (SCD) is an inherited hematological disorders, with a multi-organ complication affecting millions of people worldwide, especially in sub-Saharan Africa (1). In the United States, there are about 100,000 people with SCD. There are variability and often concurrent complications related to the disease, which may differ in frequency and severity. Accumulating evidence suggests that intravascular hemolysis and hemolysis byproducts including hemoglobin and heme instigate a series of events leading to vascular damage. While hemolysis is a prominent feature of SCD, it is certainly not unique to this disease. Red cell destruction may occur as a result of a hereditary hemolytic disorder, an infection, a medication, cancer, an autoimmune disorder, a cardiomyopathy, a hemorrhagic stroke, trauma or even a blood transfusion, to mention a few (2). The current review focuses on the heme-induced mechanisms that are implicated in disease pathways, mainly in SCD and downstream effects of non-bound (free) heme as a result of intravascular hemolysis caused by sickle cell anemia and other hemolytic disorders (**Figure 1**).

Heme as a Signaling Molecule in Normal Physiology

Heme synthesis, transport and turnover occurs under normal physiological conditions, and it exerts a physiological signal that helps to control these pathways. For example, heme feeds back to the first committed step in porphyrin synthesis, α-levulinic acid synthase. Heme regulates the Ras-Mitogen Activated Protein Kinase (MAPK) pathway, and it regulates the BACH1 transcriptional repressor, impacting expression of HMOX-1 and β-globin. Heme-regulated inhibitor (HRI) is a eukaryotic initiation factor 2α kinase that coordinates protein synthesis with heme availability in reticulocytes (3). Heme is a crucial prosthetic group for activity of many hemoproteins, include oxygen transport, electron transport, oxygen reduction, and others (4). Heme modulates macrophage differentiation of monocytes to tissue-resident macrophages and stimulates macrophage inflammatory response (5). In sickle cell disease, heme from red cells is turned over *via* both intravascular and extravascular hemolysis pathways that leads to extensive pathology described in the remainder of this review.

OXIDATIVE STRESS AND HEMOLYSIS IN SICKLE CELL DISEASE

Reactive Oxygen Species Production in SCD Contributes to Hemolysis

Oxidative stress occurs due to dysregulation between production of reactive oxygen species (ROS) and antioxidants. ROS are vital for cell signaling and homeostasis and are produced as a natural by-product of the normal metabolism of oxygen or exogenously by ionizing radiation and xenobiotic compounds (6–8). Oxidative stress contributes to pathophysiological pathways that underlie inflammation in many hemolytic disorders including SCD (8), β-thalassemia (9, 10), paroxysmal nocturnal hemoglobinuria (11, 12), hereditary spherocytosis (13), and glucose-6-phosphate dehydrogenase deficiency (14–16). RBCs are constantly subjected to oxidative stress due to their role as an oxygen transporter and continuous exposure to both endogenous and exogenous sources of ROS that can damage the RBC and alter blood rheology in SCD patients (17, 18). ROS is generated in SCD through several pathways. Sickle hemoglobin (HbS) produces ROS such as superoxide anion ($O2^{-}$), hydrogen peroxide (H_2O_2), peroxynitrite ($OONO^{-}$) and hydroxyl radical (OH.) following auto-oxidation (19). Auto-oxidation is a normal physiological process that generates methemoglobin (metHb, Hb oxidized to Fe^{3+} state with no ability to bind O_2) and O_2^- in about 3% of the total Hb every day (19). A small rate of auto-oxidation can produce substantial levels of ROS due to the high concentration of oxygenated Hb (about 5 mM), which can cause enormous damage to the RBC itself, because RBCs make up 40% of the blood volume (20). Moreover, $O2^{-}$ is spontaneously converted to H_2O_2 by superoxide dismutase, thereby increasing ROS in the system (19). Excessive amounts of reactive oxygen metabolites is produced due to the unstable

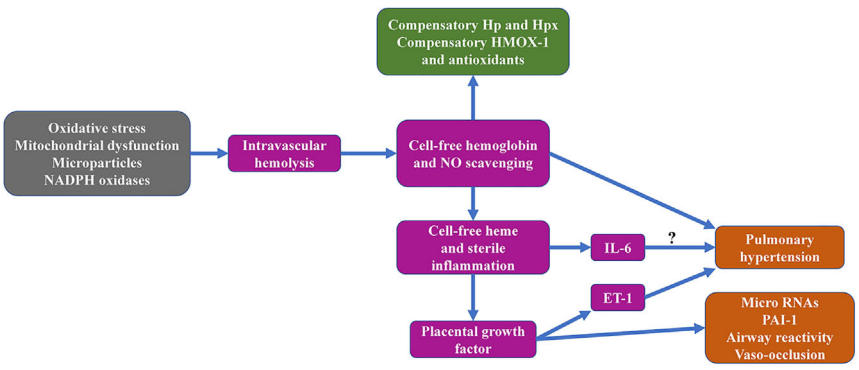

FIGURE 1 | Graphical overview of sickle cell hemolysis-associated topics addressed in the current review manuscript.

nature of HbS resulting in conformational change in the Hb in low O_2 environment and the continuous auto-oxidation of iron in heme released from Hb (6–8). This heme can oxidize membrane lipids and proteins (21), as evidenced by elevated levels of products of lipid peroxidation including malondialdehyde (MDA) in the plasma of SCD patients (22). Other Hb oxidation products such as ferryl Hb which is also formed in RBCs under conditions of oxidative stress also occurs in HbS (23–25), causing actin remodeling, thereby compromising membrane integrity and transport (26, 27).

Mitochondrial Dysfunction

The major source of intracellular ROS is the mitochondria in most cells (28) but mature red blood cells (RBCs) from healthy individuals extrude their mitochondria and other organelles during the terminal process of erythropoiesis (29–32). In contrast, a higher percentage of mature RBCs from SCD patients and mice retain their mitochondria leading to excessive ROS accumulation and oxidative stress (25, 33, 34). It has been shown that treatment with products of hemolysis including ferric Hb, ferryl Hb or heme causes bioenergetics changes, abnormal membrane permeability and ROS-induced lipid peroxidation in endothelial and alveolar cells mitochondria (35, 36), which may contribute to inflammatory process and lung injury (37, 38). Additionally, platelets from SCD patients have abnormal mitochondrial activity resulting in oxidant generation and increased activation during vaso-occlusive crisis (VOC) (39). Exposure to cell-free hemoglobin exacerbates this aberrant platelet mitochondrial activity and correlates with markers of hemolysis, NO scavenging and severity of pulmonary arterial hypertension (40).

Microparticles

Another source of oxidative stress in SCD is erythrocyte-derived submicron membrane vesicles called microparticles (eMPs) (41–44). Plasma eMPs are elevated in sickle cell mice (25), in SCD patients at steady state (41, 44) and during vaso occlusive crisis (45, 46). These eMPs are generated during reoxygenation of sickled erythrocyte (42, 43) or during hemolysis (41, 47). Additionally, thrombospondin-1 (TSP1) may trigger shedding of phosphatidylserine positive eMPs and injection of these eMPs into SCD mice caused vaso occlusion in the kidney (48). These hemoglobin-laden eMPs can transfer heme to endothelial cells, adhere to vascular endothelium and scavenge NO thereby mediating oxidative stress (49–51). Staining of human renal biopsies has been shown to contain hemoglobin-laden eMPs adherent to the capillary endothelium in kidney tissue samples from hyperalbuminuric SCD patients, suggesting that eMPs may contribute to renal injury in SCD (51). Finally, other blood cells such as neutrophils and macrophages also release ROS into the plasma which are neutralized by anti-oxidants such as superoxide dismutase before they can be taken up by RBCs (52).

Nicotinamide Adenine Dinucleotide Phosphate Oxidases

Vascular smooth muscle and phagocytic cells express nicotinamide adenine dinucleotide phosphate (NADPH) oxidases, which can generate endogenous ROS (53). NADPH oxidase activity is mediated by activation of the small Ras-like GTPase Rac *via* protein kinase C (PKC) stimulation (53). Some plasma factors such as transforming growth factor β1 (TGFβ1) and endothelin-1 (ET-1) have also been shown to stimulate NADPH oxidase activity in neutrophils, monocytes and endothelial cells and many of these factors are present at higher levels in the plasma of SCD patients as a result of persistent inflammatory state associated with SCD (54). RBCs from SCD patients also contain NADPH oxidases, which can generate endogenous ROS, thereby contributing to RBC rigidity and fragility (55).

Oxidant–Antioxidant Balance

Accumulation of oxidative injury to the erythrocyte distorts membrane integrity, alters blood flow rheology, membrane transport abnormalities, exposure of phosphatidylserine, and cell death (56–58). Despite the numerous pathways by which ROS is generated in SCD, oxidative stress in patients appears to be compensated at steady state, and only becomes deleterious when the balance between ROS production and antioxidants is perturbed due to excessive ROS generation, low antioxidant levels or during crisis (59). Likewise, ROS production becomes markedly amplified in low antioxidant microenvironments, as found in SCD, resulting in damage of macromolecules including lipids (60, 61), DNA (62, 63), and proteins (64, 65).

However, studies of antioxidant levels in SCD patients have yielded variable results, with several studies reporting low (66–69) and others reporting high levels (70, 71) of activity of antioxidant enzymes including glutathione peroxidase (66, 67), superoxide dismutase (67, 70, 72), and catalase (68, 72). These differences may be due to variations in level of disease severity including hemolysis, lipid peroxidation, VOC, acute splenic sequestration and pulmonary hypertension reported in these patients (73–78). Irrespective of the levels detected, the total antioxidant capacity in SCD patients is insufficient to neutralize excess ROS, resulting in oxidative stress (79). Other non-enzymatic antioxidants such as vitamin C and E (80, 81), zinc (76), and selenium (69, 77, 80) are also decreased in SCD patients.

Several approaches to mitigate the harmful effects of oxidative stress in SCD have been proposed such as use of antioxidants (82), neutralization of products of hemolysis with haptoglobin (Hp) and hemopexin (Hpx) (83) and moderate strength and endurance exercise therapy (84). Recent studies showed that increase in physical activity improves blood rheology, increases NO bioavailability and reduction in oxidative stress and hemolysis in mice (85–87) and SCD patients (88).

Intravascular Hemolysis, Free Hemoglobin, and NO Deficiency

Intravascular and extravascular hemolysis, due in large part to recurrent sickling and unsickling and oxidative stress discussed above, causes premature destruction of RBCs, and contributes to anemia in SCD (56, 89). Rapid production of RBCs ensues to compensate for anemia, resulting in an increased proportion of

reticulocytes and younger RBCsin the circulation. Younger RBCs have a higher content of arginase, and with lysis of these younger cells, arginase is released into the plasma during hemolysis (90). This ectopic plasma arginase consumes plasma L-arginine (substrate needed for NO production), and together with consumption of endothelial NO by cell-free plasma Hb contributes to decreased NO bioavailability (91–93). Although consequences of hemolysis in SCD are multifactorial, induction of NO deficiency and oxidative stress by acute and chronic release of products of hemolysis into circulation are major sequelae of hemolysis (94). Depletion of NO promotes a chronic vasculopathy endophenotype that predisposes to pre-capillary pulmonary hypertension, leg ulceration, cerebrovascular arteriopathy, chronic kidney disease and priapism. Details of nitric oxide deficiency and pulmonary hypertension are beyond the scope of this review and have been reviewed in detail elsewhere (94–96).

Compensatory Mechanisms

Several distinct and overlapping mechanisms have evolved to mitigate the cytotoxic effect of products of hemolysis. Hb dimers are avidly bound by the serum glycoprotein **haptoglobin** (Hp), in the plasma to form Hb-Hp complex, which protects against oxidative damage (97–100). The Hb-Hp complex is recognized and internalized *via* its receptor, CD163, and subsequently cleared by the phagocytic cells in the reticuloendothelial system (97–99). Continuous formation of Hb-Hp complexes in diseases with severe intravascular hemolysis including SCD and paroxysmal nocturnal hemoglobinuria results in depletion of Hp to undetectable levels, leading to some accumulation in plasma of cell-free Hb (101, 102).

Heme Scavenging Proteins

Cell-free Hb that becomes oxidized or denatured prior to clearance is prone to release free heme. Plasma free heme becomes elevated in SCD patients (103, 104). About 80% of total heme initially binds to plasma lipoproteins including low-density lipoproteins (LDLs) (105, 106) and high-density lipoproteins (HDLs) (107, 108), before being transferred to albumin and Hpx (107, 109). Low levels of these lipoproteins are reported in SCD patients which may be due to increased catabolism or decreased synthesis (110, 111), as low plasma levels also negatively correlated with markers of hemolysis in SCD patients (112–114). Free heme reversibly binds to albumin to form **metalbumin** (115–117), or with high affinity to **hemopexin** (Hpx) (118, 119), and **α1-microglobulin** (120–122).

Hemopexin

Of all these plasma proteins, Hpx, a plasma glycoprotein produced in the liver has the highest affinity for binding free heme (118, 119, 123), resulting in the formation of Hpx-heme complexes that are removed by endocytosis *via* the Hpx receptor (CD91) in hepatocytes and macrophages (124, 125). After delivering heme to CD91-expressing cells for internalization and degradation by heme oxygenase 1 (HMOX-1), at least some of the Hpx molecules can be recycled back into plasma. Elevated eMPs also correlated with increase in hemolysis markers and low Hpx in SCD patients (126). In the same patients cohort, high eMPs positively correlated with elevated TRV, linking Hpx depletion to increased eMPs and hemolysis, which may predispose patients to pulmonary hypertension (126). In another study, low Hpx negatively correlated with lipid oxidation in human and mice with SCD, with postmortem analysis in SCD patients showing oxidized LDL deposits in the pulmonary artery (127). These reports showed that delayed clearance of heme in circulation due to low plasma Hpx may activate deleterious downstream pathological pathways that may contribute to morbidity and mortality in SCD patients.

Heme Oxygenase-1

HMOX-1 is an evolutionarily conserved and rate limiting enzyme that degrades heme into equimolar amount of iron, biliverdin and carbon monoxide (108, 128, 129). HMOX-1 is highly expressed in human and mice with SCD and further upregulated on exposure to heme (130, 131). Heme-induced oxidative stress exceeds the capacity of HMOX-1 to prevent cellular and organ injury in transgenic murine model of SCD. Augmentation of HMOX-1 level and activity *via* gene transfer approaches, or pharmacological activation through NRF2 (132), the transcription factor that regulates HMOX-1 expression, conferred protection from heme-induced lung injury (133), vaso-occlusion (134), liver injury (135), kidney injury (136), erythrocyte membrane damage (137), endothelium activation and adherence (135), activation of immune cells and production of inflammatory cytokines (138). Still, the effect of NRF2 activation on hemolysis, γ-globin levels or stress erythropoiesis in mouse model of SCD is controversial (136–138). Not all heme and Hb are bound to proteins or other macromolecules. Unbound heme or hemoglobin in circulation causes erythrocyte membrane damage and injury, activates proinflammatory signaling pathways in RBCs, immune and endothelial cells, hepatocytes, macrophages and neutrophils (105, 139).

Antioxidant Enzymes

Heme induces a program of antioxidant enzymes that compensate for its intrinsic oxidant stress. These include glutathione S-transferase pi (GSTpi) and NAD(P)H dehydrogenase [quinone] 1 (NQO1) (140).

HEME AND STERILE INFLAMMATION IN SICKLE CELL DISEASE

Hemolysis is a major driver of sterile inflammation in pathological conditions including SCD (94, 103, 141), malaria (142, 143), sepsis (144, 145), and also a marker of severity and survival in these patients (146–149). Following hemolysis, Hb is oxidized to unstable methemoglobin resulting in release of free heme (139), which can intercalate into cell membrane and alter cellular structures or taken up by cells (150, 151).

Intravascular Hemolysis Releases Cell-Free Heme

Free heme accumulates in the plasma in both acute and chronic hemolysis when the rate of intravascular hemolysis exceeds the

capacity of circulating heme-binding proteins (152), including Hp and Hpx, which are depleted in human and mice with SCD patients (59, 104, 114, 126, 127, 153–156). There is an emerging concept of small molecular weight scavenging protein such as α1-microglobulin, becoming the predominant heme scavenger when plasma Hpx is low (59). Binding of free heme to different scavenger impacts clinical manifestation of excess heme in circulation as heme-Hpx is trafficked to and recycled primarily in the liver while heme-bound α1-microglobulin are taken to the kidney (59). This phenomenon was demonstrated in a recent publication from Ofori-Acquah and colleagues. They showed that hemopexin deficiency correlates with a compensatory increase in α1-microglobulin in both human and mice with SCD (155). Elevated α1-microglobulin and low hemopexin was also associated with increase in acute kidney injury biomarkers urinary KIM-1 and serum NGAL in SCD patients. The authors showed that this heme-bound α1-microglobulin is directed to the kidney for clearance resulting in acute kidney injury in sickle cell mice (155). Also, acute kidney injury may occur *via* complement deposition in the kidney during intravascular hemolysis and in Hpx deficient condition in SCD mice (157). Patients with SCD with higher plasma levels of free heme also have greater frequency of VOC and acute chest syndrome (158). Accumulation of free heme in plasma is not only cytotoxic, but also mediates generation of free radicals *via* the Fenton pathway (159–161).

Detection of Heme and Hemoglobin

Assay of cell-free heme and Hb may be an important tool for diagnosis in disease conditions characterized by hemolysis (152, 162). Accurate quantification of heme species may result in early therapeutic intervention before irreversible damage to organs occurs. Currently, most commercially available assays measure total heme (free heme and heme bound to proteins) and are not specific for measuring cell-free heme or Hb. There is a possibility of overestimating or underestimating these heme species. Moreover, free heme is likely a more potent mediator of organ injury and signal transductions, its accurate quantification as a biomarker in disease conditions may be vital. Researchers have developed detection methods using the spectral deconvolution method, antibody capture ELISA or western blotting, reversed-high-performance liquid chromatography, and fluorescence-based assays to measure Hb and CFH (103, 152, 162–165). Although these are not commercially available currently, they present an opportunity to quantify different heme species in relation to pathogenesis and therapeutic efficacy in hemolytic conditions.

Cell-Free Heme in Inflammation

Free heme can induce inflammation *via* direct activation of RBCs (166, 167), macrophages (168–170), neutrophils (171), and endothelial cells (139, 172–174) to secret proinflammatory cytokines including toll-like receptors (TLRs), tumor necrosis factor (TNF), interleukin-6 (IL-6), placenta growth factor (PlGF), interleukin 1 beta (IL-1β) (105, 139, 169, 175, 176) and release of erythroid damage-associated molecular patterns (eDAMPs) that potentiates inflammation (177, 178). Heme has been shown to induce production of IL-1β by activated monocytes/macrophages, endothelial and smooth muscle cells through a nucleotide-binding domain and leucine-rich repeat-containing protein 3 (NLRP3) inflammasome dependent mechanism (139, 169, 172). High mobility group box 1 (HMGB1), a nuclear protein released during systemic inflammatory response, has also been shown to mediate ROS-dependent activation of endothelial cells to secrete IL-1β *via* NLRP3 activation (179, 180). Elevated circulating HMGB1 is associated with inflammation in hemolytic disorders including SCD and sepsis (181–184), suggesting a shared inflammatory signaling pathway through TLR4/Bruton tyrosine kinase for both heme and HMGB1 in SCD (185, 186). Heme can also directly affect the vasculature in mice, as recently shown with loss of heme exporter, feline leukemia virus subgroup C receptor 1a (FLVCR1a) in endothelial cells resulted in disruption of microvessel architecture (187).

Cell Adhesion Pathways

Cell-free heme also contributes to inflammation by activating cell adhesion pathways. This includes activation of adhesion molecules such as vascular cell adhesion molecule-1 (VCAM-1), intercellular adhesion molecule 1 (ICAM-1), selectins (L, P and E), all involved in mediating cell adhesion to the vascular endothelium *via* activation of integrin αMβ2 on neutrophils (188–192). Besides, several studies in the last decade have associated hemolysis and selectins expression with RBCs adhesion to endothelial cells (193–195), acute lung injury (196), vaso occlusion (197), pain (198, 199), liver injury (200–202), and kidney injury in SCD (83).

P-selectin is associated with platelet-neutrophil aggregate formation that contributes to inflammation, pulmonary dysfunction and lung vaso occlusion in SCD (200, 203). In addition, a recent study by Merle and colleagues, showed a direct link between heme-induced TLR4 and complement system activation on liver endothelium mediated by P-selectin, with genetic or pharmacological blockade of P-selectin or complement system ameliorating liver injury in mice (202). This expansive body of works culminated in clinical trial and eventual FDA approval of P-selectin blockade therapy for the prevention of pain crises in SCD (198, 199). Furthermore, persistent inducibility of endothelium-derived adhesion molecules by proinflammatory cytokines such as TNF-α and IL-6 coupled with chronic hemolysis in SCD patients ultimately results in VOC, organ dysfunction and early mortality (101, 204–208). There are several ongoing clinical trials in SCD looking at mediating the effect of inflammation-induced organ damage *via* some of the mechanisms discussed above.

Hemolysis, Inflammation, and microRNAs

Recent evidence supports a potential role of microRNAs (miRNAs) in complications of SCD (209, 210) and malaria (211, 212), both pathological conditions with hemolysis, suggesting a role for heme modulation of miRNAs. miRNAs are noncoding RNAs of 22 nucleotides in length that regulate the expression of their target genes post-transcriptionally (213). miRNAs are involved in important biological processes

including apoptosis (214), hematopoietic differentiation (215) and cell proliferation (216). miRNAs are important regulatory molecules and activation of immune response during initiation and progression of many diseases inflammatory diseases such as cancer, Crohn's disease, rheumatoid arthritis, systemic lupus erythematosus, and asthma, *via* expression of proinflammatory cytokines including TNF-α and TLRs (217–222). There are studies linking heme and miRNAs processing in mammalian cells. Heme binds directly to the RNA-binding protein DiGeorge critical region-8 (DGCR8), which is essential for the first miRNA processing step (213, 223–225). Hemolysis elevates the expression of several miRNAs found in RBCs including miR-16, miR-92a, miR-451, and miR-486 (226, 227). There is upregulation of some miRNAs including miR-16, miR-451 and miR-144 in reticulocytes from SCD patients (228, 229). Conversely, elevated levels of these miRNAs also correlated with severe anemia, increased sensitivity to oxidative stress, downregulation of NRF2 and decreased intracellular glutathione levels (230, 231). On the other hand, members of the miR-154, the miR-329 and miR-376 family, involved in TGF-β signaling pathway are downregulated in platelets of SCD patients (210). Although few numbers of studies have reported the involvement of miRNAs in complications of SCD (232), however, there is a gap in knowledge of how stress or heme regulation of these miRNAs and exposure of immune cells to proinflammatory cytokines that are elevated in SCD might play a role in organ dysfunction. Targeting these miRNAs in SCD might offer novel therapeutic strategy in preventing hemolysis-induced inflammation and end organ damage, especially in the heart, lung, liver, and kidney where miRNAs are abundant (222, 233–240).

HEMOLYSIS AND ORGAN DAMAGE IN SICKLE CELL DISEASE

SCD patients on average live longer today than 50 years ago. This is due to progress in understanding the mechanisms and risk factors of several complications of the disease, associated clinical findings and mouse models, approval of new treatment therapies, multi-disciplinary approach to care, penicillin prophylaxis and high-tech diagnostic tools (241). However, this reduction in childhood mortality gives rise to an older population of patients that develop age-related chronic organ damage, driven in part by hemolysis (94). Hemolysis-induced extensive and sometimes irreversible organ damage continues to be a major source of morbidity and mortality in SCD. Even transplanted organs are also at risk of failure in SCD patients due to hemolysis and sickling (242). Therefore, there is a need for research to understand the fundamental mechanisms involved in heme-mediated organ damage in SCD patients. Over the years, several studies in the general population as well as in SCD suggest that hemolysis causes injury to the kidney (243–245), lung (246), heart, and liver. We have summarized some of the impacts of hemolysis on different organs in **Table 1**.

PLACENTA GROWTH FACTOR

In addition to its role as a DAMP, heme promotes the expression and secretion of placenta growth factor (PlGF), a pleiotropic growth factor already known to influence multiple pathways contributing to the pathophysiology of SCD (167, 176, 280). PlGF is a member of the Vascular Endothelial Growth Factor (VEGF) family. It was originally cloned from a human placenta cDNA library in 1991 (281), hence the name, but since then it has been detected in a wide variety of tissues (282). PlGF has a partial sequence similarity to VEGF-A but the two molecules share a remarkable topological identity (283). There are four human isoforms (PlGF 1–4), which are generated by alternative splicing and are slightly different in size. PlGF-1 (131 aa) and PlGF-2 (152 aa) are the predominant isoforms in humans. On the contrary, mice carry a single isoform, PlGF-2 (140 aa).

PlGF exists as a homodimer or as a heterodimer with VEGF. PlGF is a ligand for the transmembrane and soluble form of the vascular endothelial growth factor receptor 1 (VEGFR-1, Flt-1) (284), which can also bind VEGF. Distinct from VEGF, PlGF does not bind vascular endothelial growth factor receptor 2 (VEGFR-2, Flk-1) but it can affect VEGFR-2 signaling in an indirect manner (285–287). PlGF-2 can also bind heparin and the transmembrane neuropilin receptors 1 and 2 (NRP1 and NRP2) (288, 289). In addition to its role as a receptor binding competitor of VEGF (284), PlGF can exert its own biological effect upon binding to VEGFR-1. Depending on the cell type, PlGF binding upregulates VEGF, fibroblast growth factor 2 (FGF2), platelet derived growth factor beta (PDGFB) and matrix metalloproteases (MMPs) (290, 291). Furthermore, PlGF receptor binding is shown to activate an intermolecular crosstalk regulator between VEGFR-1 and VEGFR-2, often resulting in enhancing VEGF/VEGFR-2 signaling (287). It is important to emphasize here that PlGF or VEGF binding to FLT1 results in discernible receptor phosphorylation patterns and induction of distinct signaling pathways (287, 292, 293). PlGF expression is induced by hypoxia, probably in a cell specific manner, but the exact mechanism remains elusive in the absence of hypoxia responsive elements (HRE) at the gene's promoter region (294, 295). So far, the association of only a few transcription factors has been verified for the PlGF promoter: metal transcription factor 1 (MTF-1) (295), NF-kB (296), forkhead box D1 (FoxD) (297), erythroid Kruppel-like factor (EKLF) (167), nuclear factor erythroid 2 like 2 (NRF2) (176), glial cell missing 1 (GCM1) (298). Posttrascriptional regulation of PlGF has also been reported through the regulation of the protein kinase C (PKC), p38 mitogen activated protein kinases (p38 MAPK), c-jun N-terminal kinase (JNK) and Ras-dependent extracellular signal-regulated kinase 1/2 (ERK1/2) signaling pathways (299, 300).

Surprisingly, PlGF seems to have a redundant role under normal conditions (285) but becomes very important in disease situations, where fluctuations of its levels cause a variety of issues in multiple biological processes. Because of that reason, PlGF-based therapeutic approaches have been proposed as disease specific with minimal impact for healthy cells (301). The most

TABLE 1 | Summary of current literature supporting a damaging role of hemolysis in different organs.

Organ	Impact of heme damage	References	Disease/model
Kidney	Proximal tubule dysfunction and impaired vitamin D metabolism	(247, 248)	Cell culture/mice
	Proteinuria, acute and chronic injury, and iron deposition	(244, 245, 249–253)	Human
	Acute renal failure, oxidative stress, inflammation, and toxicity	(254–257)	Human/mice
	Acute renal vasoconstriction *via* TLR4 signaling	(258, 259)	Cell culture/Mice
	Apoptosis in proximal tubular epithelial cells *via* caspase-dependent/-independent pathways	(260, 261)	Cell culture
	Endothelial apoptosis and vaso occlusion	(262)	Human/cell culture/mice
Lung	Acute chest syndrome *via* TLR4, NRF2 and p-selectin signaling	(133, 196, 263)	Cell culture/mice
	Oxidative injury and progression of pulmonary hypertension (PH)	(262)	Cell culture/mice
	Angioproliferative PH *via* accelerated purine metabolism	(264)	Rats
	Acute lung injury *via* increased alveolar capillary barrier dysfunction	(265, 266)	Human/cell culture/mice
	Oxidation and mitochondrial dysfunction in epithelial lung cells	(36)	Cell culture
Liver	Increased vascular ICAM-1 expression on blood vessels and vaso occlusion	(267)	Cell culture/mice
	Advanced fibrosis and iron overload	(268)	
	Oxidative stress, neutrophil infiltration, and extravasation through NF-κB activation	(269)	
Heart	Impaired nitric oxide bioavailability and pulmonary hypertension	(270, 271)	Mice
	Smooth muscle proliferation *via* NADPH oxidase activity, atherosclerosis, and hypertension	(101, 272)	Cell culture
	Increased risk of cardiovascular disease	(273, 274)	Human
	Endothelial activation and altered cardiac function	(275, 276)	Mice
	Mitochondria dysfunction	(277)	Human/cell line
	Ischemic injury	(278)	Human/cell culture/mice
	Contractile dysfunction due to altered contractile proteins	(279)	Human primary cardiomyocytes

well established role of PlGF is in angiogenesis and more specifically in neo-angiogenesis in pathological conditions such as ischemia or cancer (285, 302, 303). PlGF's pleiotropic nature in evident in its angiogenic role where it exerts a paracrine or autocrine effect on endothelial cells, smooth-muscle cells, fibroblasts, bone marrow progenitor cells and monocytes, to orchestrate vessel growth and maturation (304). The description of the full spectrum of PlGF's biological role is beyond the scope of this review but to mention a few, PlGF plays a role in inflammatory response (305, 306), promotes bone repair (307), sustains the proangiogenic M2 phenotype of tumor associated macrophages (308), affects dendritic cell differentiation and maturation (309), supports the generation of an inflammatory status driving adaptive cardiac remodeling (310). To summarize, all the evidence to date supports a role for PlGF in pathogenic angiogenesis and inflammation well outside the realm of pregnancy. Through mitogen and migratory effects on endothelial cells as well as macrophage activation and chemoattraction, PlGF emerges as a driver and marker of a plethora of seemingly diverse pathologies, especially angiogenesis and inflammation.

HEMOLYSIS, PLGF, AND COMPLICATIONS OF SICKLE CELL DISEASE

One of the least appreciated roles of PlGF is the one that it has in hematopoiesis (311, 312) and in hemoglobinopathies (313) (**Figure 2**). Plasma PlGF is elevated in SCD patients and the increase correlates with the severity of hemolysis, endothelin 1 (ET-1) expression, the occurrence of pulmonary hypertension (167, 280, 314, 315) and VOC (316, 317).

Pulmonary Hypertension

PH is a serious complication in sickle cell patients, which is associated with high mortality (318). A variety of biological pathways and disease related pathologies contribute to the development of PH and many of them involve free heme and upregulation of PlGF. Along with PlGF, ET-1, a potent vasoconstrictor, is significantly higher in the blood of sickle patients (167, 316, 319, 320) suggesting a mechanistic link between the two factors. In support of this connection, the overexpression of PlGF in healthy mice using lentiviral gene transfer results in increased ET-1, increased right ventricle pressure and right ventricle hypertrophy as early as 8 weeks after PlGF gene transfer (280). In vitro PlGF stimulation of cultured human pulmonary microvascular endothelial cells (HPMVEC) revealed that ET-1 induction was mediated by PI-3 Kinase, NADPH-oxidase, and HIF-1a (314). Interestingly, HIF-1a stimulation of the ET-1 promoter is hypoxia independent and occurs upon the direct binding of HIF-1a on the HRE elements of the ET-1 promoter. In a similar manner, PlGF upregulates endothelin-B receptor (ET-BR) in monocytes, priming them to be over-stimulated by ET-1 and produce higher levels of chemokines MCP-1 and IL-8 (314). Both MCP-1 and IL-8 are elevated in SCD patients (321) supporting the PlGF-ET-1 synergy as another contributing factor to the development of PH in SCD.

Regulation of miRNAs

On a post-transcriptional level, PlGF attenuates miR-648 and miR-454, which recognize and bind the 3' UTR of ET-1 mRNA. The association of low miR-648/miR-454 with high ET-1 and PlGF levels is supported in both *in vivo* and *in vitro* studies (322, 323). Furthermore, PlGF attenuates miR-199-5p, which binds the 3'UTR of HIF-1a mRNA, creating another level of control over ET-1 expression (324). The molecular repression of miR-

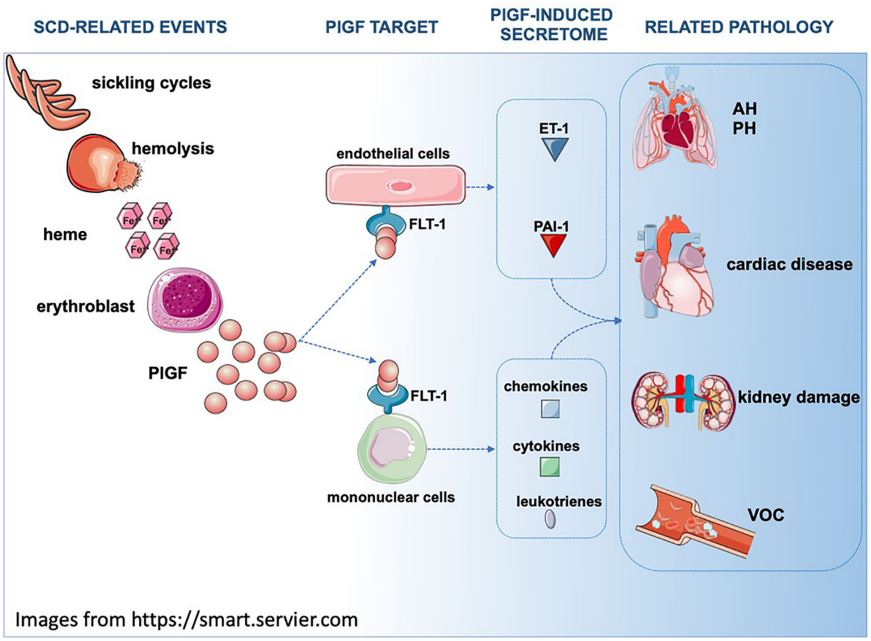

FIGURE 2 | In SCD, repeating sickling cycles result in increased hemolysis. Hemolysis byproducts such as heme induce PlGF expression in multiple cell types (for simplicity purposes only erythroblasts are depicted). Secreted PlGF is a ligand for FLT-1 receptor and triggers the expression of ET-1, PAI-1, leukotrienes and cytochemokines, affecting the physiology of multiple organs. AH, Airway hyperreactivity; PH, Pulmonary hypertension; FLT1/VEGFR1, Fms related receptor tyrosine kinase 1; PlGF, placenta growth factor; ET-1, endothelin 1; PAI-1/Serpine1, plasminogen activator inhibitor 1.

199-5p by PlGF is mediated by the upregulation of the activating transcription factor 3 (ATF3) which upon binding causes deacetylation and chromatin condensation at the miR-199-5p locus (325). Similar to miR-648, the association of low miR-199-5p levels with high PlGF and ET-1 levels is supported by *in vivo* and *in vitro* studies (324).

Plasminogen Activator Inhibitor 1

PlGF is also linked to the increase in PAI-1 levels in the plasma and lungs of sickle cell patients and humanized sickle mice respectively (326). PAI-1 is increased during steady state SCD but its expression is exacerbated during VOC. Elevation of PAI-1 levels is associated with decreased fibrinolytic capacity (327) and is believed to contribute to the SCD prothrombotic state and the development of PH (328). In vitro PlGF stimulation induced PAI-1 expression in pulmonary microvascular endothelial cells and monocytes through the activation of c-jun N-terminal kinase (JNK), hypoxia inducible factor 1a (HIF-1a) and nicotinamide adenine dinucleotide phosphate (NADPH) oxidase (326). In addition, PlGF expression affects the stability of PAI-1 mRNA by downregulating microRNAs miR-454, miR-301a, and miR-30c which recognize and bind the PAI-1 3'-UTR. PlGF regulation of miR-454 and miR-301 is mediated by PPARa and HIF-1a (323). All of these microRNAs are detected in significantly lower levels in SCD patients compared to healthy controls (323, 329). In vivo experiments using PlGF null and SS sickle mice as well as adenoviral overexpression of PlGF, have confirmed that PlGF plays a significant role in PAI-1 regulation (326).

Inflammation and Airway Hyper-Reactivity

Airway hyper-reactivity is a common complication in SCD, especially in younger patients (330), and correlates with biomarkers of hemolysis (331). Patients show elevated levels of circulating leukotrienes (332) and their monocytes express higher levels of 5-lipoxygenase (5-LO) and 5-lipoxygenase activating protein (FLAP), both involved in leukotriene synthesis (333). Consistent to its proinflammatory nature, PlGF induces leukotriene production which in turn increases inflammation and airway hyper-reactivity, both key features of SCD. As in the case of PAI-1, the induction is mediated by HIF-1a and NADPH oxidase (333). Further studies have confirmed PlGF as an important regulator of leukotriene production and airway hyperactivity in SCD and asthma (332).

Vaso-Occlusion

Activated leukocytes in sickle cell patients are considered a significant promoting factor for VOC (334). Activated mononuclear cells from SCD patients express high levels of the cytochemokines VEGF, IL-1β, monocyte chemotactic protein 1 (MCP-1), IL-8 and macrophage inflammatory protein-1 beta (MIP-1β). In vitro studies have shown that monocytes from healthy individuals can be activated by PlGF to increase the expression of proinflammatory cytokines and chemokines such

as TNF-α, IL-1β, MCP-1, IL-8, and MIP-1β (316, 335). This activation is achieved by the PlGF-VEGFR-1 interaction and involves the PI-3 kinase/AKT and ERK-1/2 signaling pathways (335). Because VOC in SCD is promoted by inflammation and leukocyte adhesion stimulated by cytokines (197, 336, 337), antibody neutralization of PlGF was tried successfully for reduction of inflammation and vaso-occlusive complications in murine SCD models (317). Regulation of PlGF levels could also be achieved by manipulating factors that control its transcriptional or translational expression. Per instance, pharmacological upregulation of miR-214 which is known to bind PlGF 3'-UTR, could be engaged to reduce PlGF levels (338).

Renal Dysfunction

PlGF is significantly upregulated in the serum of patients with chronic kidney disease and decreased renal function, supporting a potential mechanistic link between PlGF and kidney function (339, 340). Sickle cell nephropathy (SCN) is an complex phenotype which encompasses almost every physiological process in the kidney, leading to complications that may range from common and relatively mild to rare and life-limiting (243). In SCD patients markers of renal dysfunction are associated with elevated ET-1 serum levels (341) and studies in sickle cell mice have shown that ET-1 can cause renal injury, likely mediated by ROS (342). Although it has not been shown experimentally, sickle cell-related elevated PlGF levels could possibly contribute to higher ET-1 levels (167, 314) driving renal dysfunction. However, administration of exogenous heme in control and sickle cell mice has been shown to result in the upregulation of PlGF in the murine kidneys in agreement with heme uptake from renal cells and HMOX-1induction (343). In addition to ET-1, PAI-1 has also been shown to play a role in nephropathies (344) but its role in SCD or its potential regulation by PlGF remains unexplored.

Cardiac Dysfunction

Cardiac complications are common in SCD patients and along with the pulmonary complications raise their morbidity and mortality risk (94, 345). There has been accumulating evidence that PlGF dysregulation is present in multiple heart conditions although it is often unclear if it is only a disease biomarker or it actively promotes disease pathogenesis. In patients with chronic kidney disease, PlGF levels are associated with higher incidence of cardiovascular events and mortality (340). In the same disease, PlGF is an independent risk predictor for left ventricular diastolic dysfunction (346). In human atherosclerotic plaques, the expression of PlGF is associated with plaque destabilization and disease manifestation (347). The pro-atherosclerotic role of PlGF is corroborated in rabbits where PlGF adenoviral expression promotes atherogenic intimal thickening and macrophage accumulation in the carotid artery (348). PlGF is also elevated in the plasma of patients with acute coronary syndromes where it can be used as a risk predicting biomarker (349). PlGF promotes cardiac hypertrophy *via* endothelial cell release of NO which induces cardiomyocyte growth (350) and by inducing the secretion of paracrine factors (IL-6, IL-1b, Cxcl1) from endothelia and fibroblasts that promote cardiac adaptation and hypertrophy (351–353). In the case of ischemic cardiomyopathy, PlGF has been reported both as promoting the disease (354) and as a potential therapeutic (355). The apparent controversy could be due to differences between a local and acute administration of an angiogenic factor (355) compared to a more systemic and chronic upregulation (354). Our research has shown that PlGF is elevated in the hearts of sickle mice and it is further induced after administering exogenous heme (343). Surprisingly, the level of PlGF induction is comparable to that of the liver which is considered the major heme detoxifying organ (343). An interesting finding of this study is that mouse hearts have high levels of HMOX-1, which are further increased by heme induction, and that they show no heme accumulation unless NRF2 is depleted. These data suggest that cardiac tissue has the ability to detoxify heme *via* the NRF2 antioxidant response pathway.

HEMOLYSIS, INTERLEUKIN-6, AND CARDIOVASCULAR DYSFUNCTION

IL-6 is a ubiquitous and pleiotropic proinflammatory cytokine produced by many cells including macrophages (356, 357), neutrophils (358, 359), endothelial and smooth muscle cells (360, 361), cardiomyocytes (362) and fibroblasts (363), when stimulated by ligands for toll-like receptors or other pattern recognition receptors. IL-6 is a glycoprotein composed of 184 amino acids and of 26 kDa in molecular weight (364). Currently, there are ten cytokines belonging to the IL-6 family; IL-6, IL-11, ciliary neurotrophic factor (CNTF), leukemia inhibitory factor (LIF), oncostatin M (OSM), cardiotropin-1 (CT-1), cardiotrophin-like cytokine (CLC), IL-27, neuropoietin (NP), and IL-31 (365). IL-6 regulates many biological functions including hematopoiesis (366), oncogenesis (367) and differentiation of B cells (368), induction of acute phase proteins and immune regulation (369). Additionally, IL-6 plays a vital role in chronic inflammatory processes in various cells and disease conditions (364). IL-6 signaling is through two pathways; classic/cis-mediated signaling *via* membrane-bound IL-6 receptor (mIL-6R) or trans-mediated signaling *via* the soluble form of IL-6R (sIL-6R) (364, 369). Classic/cis-signaling occurs in cells that express IL-6R such as hepatocytes, neutrophils and monocytes (365, 369). Conversely, trans-mediated signaling occurs after secretion of sIL-6R by RNA alternative splicing, ectodomain shedding or proteolytic cleavage of mIL-6R (370), which in turn stimulate cells (365, 369). Once IL-6 binds to mIL-6R or sIL-6R, the cytokine forms a complex with the ubiquitously expressed membrane protein gp130, a shared signal-transducing receptor of all IL-6 type cytokines (370). Dimerization of the receptor complex activates Janus kinases (JAKs) resulting in phosphorylation of the tyrosine residues in the cytoplasmic domain of gp130 (364, 371). Activation of JAKs triggers the extracellular-signal-regulated kinase (ERK), mitogen-activated protein kinase (MAPK) and signal transducer and activator of

transcription (STAT) signaling pathways (370, 371). However, IL-6 role in pathophysiology of chronic inflammation and diseases is driven *via* IL-6 trans-signaling because classic/cis-signaling *via* the mIL-6R is limited to few cells that express IL-6R (372). Blockade of IL-6 trans-signaling is effective in attenuating proinflammatory activities of IL-6 in several disease conditions (365).

Several studies in human and rodents found hemolysis and elevated IL-6 occurring concurrently. Hemolysis and elevated IL-6 are associated with disease severity in malaria (373, 374), sepsis (375) and pre-eclampsia (376), with cardiac dysfunction as an additional comorbidity in these diseases. Besides, elevated cardiac IL-6 is also associated with cardiac hypertrophy and fibrosis in the general population (362, 377) and in rodents (378, 379). In malaria, elevated IL-6 is found in patients with severe *Plasmodium falciparum/vivax* malaria and associated with development of cardiac complications (373, 374). Sepsis patients with elevated IL-6 are at a higher risk of developing cardiac dysfunction which may be due to direct negative inotropic effect of IL-6 mediated *via* altered production of myocardial nitric oxide (375), altered calcium homeostasis (380, 381) and impaired β-adrenergic signaling (382–384). Elevated IL-6 in pre-eclampsia patients result in reduced anti-inflammatory protection in the maternal vascular system (385) and stimulation of vasoactive substances including angiotensin II type 1 receptor and endothelin-1 (386). Although, elevated plasma IL-6 have been reported in human and mice with SCD (168, 387, 388), and hemolysis is a major comorbidity of SCD (94), however, there has been no direct link between these two processes. Conversely, left ventricular hypertrophy (LVH) is found in over 60% of children and 37% in adults with SCD (389, 390), with cardiopulmonary complications accounting for about 26% of deaths in adults with SCD (391). In this current issue and for the first time, our group investigated the expression of plasma and cardiac IL-6 and its inducibility by heme in Townes sickle cell (SS) mouse model (392). We observed significantly elevated cardiac IL-6 and direct heme induction of circulating and cardiac IL-6 transcripts and protein in SS mice compared to controls. We showed that this heme-induced IL-6 is NRF2-independent in the heart. Our results of heme-induced IL-6 is in agreement with elevated levels of IL-6 reported in cardiac cells treated with Hpx and in heart isolated from Hpx deficient mice (393). Because our data showed upregulation of cardiac hypertrophy genes following heme treatment in SS mice, there is a possibility that heme is inducing IL-6 in the heart and prolonged activation and exposure to IL-6 could contribute to LVH in SCD patients. We are currently investigating potential mechanism(s) and specific cell-types secreting IL-6 in the heart of SS mice. There are several pathways through which heme may induce IL-6 expression. It is possible that parallel heme-induced pathways are activating IL-6 indirectly and with continuous hemolysis forming a feedback loop. With elevated cardiac PlGF at baseline in SCD mice and further inducibility by heme (343), cardiac hypertrophy may develop *via* IL-6 signaling (350). Therefore, it can be envisaged that prolonged hemolysis induced PlGF and IL-6 in SCD feeds the vicious cycle of inflammation *via* an autocrine feedback system resulting in reactivation of genetic cardiac hypertrophy program.

THERAPEUTIC INTERVENTION IN HEMOLYSIS AND INFLAMMATION

The role of hemolysis and its attendant oxidant stress and inflammatory activation in SCD has been supported by the success of therapies that normalize these pathways. Hydroxyurea has pleiotropic effects that reduce hemolysis and offset its pathobiological consequences. The approval of hydroxyurea by the FDA in 1998 provided a watershed moment in the history of SCD (394, 395). Hydroxyurea treatment yielded an improved quality of life for SCD patients attributable to induction of fetal hemoglobin, slowing of chronic damage to several organs, including the brain (394–400). More than twenty years later, three new drugs; L-glutamine (Endari; reduction of pain-related hospital visit and length of stay) and crizanlizumab-tmca (Adakveo; reduction of frequency of VOC) and voxelotor (Oxbryta; inhibition of deoxygenated sickle hemoglobin polymerization), have been approved by the FDA for treatment of SCD (401). L-glutamine is thought to reverse the redox imbalance imposed by hemolysis and other sources of oxidative stress. Crizanlizumab blocks the inflammation-activated P-selection adhesive pathway. Voxelotor inhibits polymerization of sickle hemoglobin, with the most apparent effect of reduced hemolysis. Curative intent therapies have also shown evidence of reduced hemolysis. Although permanent cure afforded to patients through bone marrow transplant and gene therapy would be ideal, it would be quite expensive and the majority of patients with SCD live in areas lacking both economic and human resources needed to make these curative therapies broadly accessible (402). Importantly, the global majority of SCD patients live in resource-poor countries, with minimal access to these newer therapies and limited capacity for hematological monitoring requirements and other diagnostic equipment (1, 403). High childhood mortality rate ranging from 50–90% still prevail in these areas and acceptance of hydroxyurea as therapy is very low compared to developed countries (403–405).

Encouragingly, recent studies show the efficacy, safety and feasibility of using hydroxyurea treatment in children and adults with sickle cell anemia living in sub-Saharan Africa (406–408).

Clinical trials are underway to assess the potential of hemopexin intravenous infusion in the treatment of SCD (Clinicaltrials.gov identifier NCT04285827). In the Townes SCD mouse model, infusion of hemopexin reduced microvascular occlusion induced by hemoglobin infusion, hypoxia-reoxygenation, or lipopolysaccharide (83). Hemopexin mitigated induction of ICAM-1 and VCAM-1 *via* inhibition of NF-κB activation (83). In another study, treatment with Hpx attenuated free heme activation of complement pathways and kidney injury caused by complement deposition and inflammation in mice during hemolysis (157). Hemopexin also significantly decreased plasma heme concentration, pulmonary neutrophil extracellular trap (NET) formation, plasma DNA, neutrophil activation and NET-associated hypothermia in SCD mice (171).

CONCLUSION

Hemolysis is a feature of many diseases, and in most cases occurring with acute and chronic inflammation that contributes to organ injury. Products of hemolysis activate several inflammatory pathways in many cell types, including cells in the innate immune system. Hemolysis appears to serve as a priming stimulus that combines with TLR4 signaling to a cascade of production of inflammatory cytokines which activate downstream pathophysiology. Therapeutic intervention targeting the upstream effects of hemolysis has potential to mitigate downstream innate immune system response and inflammation in treating patients with intravascular hemolytic disease.

AUTHOR CONTRIBUTIONS

All authors drafted the review. The first two authors contributed equally. GK approved the final version of this review. All authors contributed to the article and approved the submitted version.

FUNDING

GK received support from NIH grants HL133864, MD009162 and from the Institute for Transfusion Medicine Hemostasis and Vascular Biology Research Institute at the University of Pittsburgh School of Medicine. OTG is supported by the American Society of Hematology Scholar Award.

REFERENCES

1. Piel FB, Hay SI, Gupta S, Weatherall DJ, Williams TN. Global burden of sickle cell anaemia in children under five, 2010-2050: modelling based on demographics, excess mortality, and interventions. *PloS Med* (2013) 10(7): e1001484. doi: 10.1371/journal.pmed.1001484
2. Phillips J, Henderson AC. Hemolytic Anemia: Evaluation and Differential Diagnosis. *Am Fam Physician* (2018) 98(6):354–61.
3. Mense SM, Zhang L. Heme: a versatile signaling molecule controlling the activities of diverse regulators ranging from transcription factors to MAP kinases. *Cell Res* (2006) 16(8):681–92. doi: 10.1038/sj.cr.7310086
4. Shimizu T, Lengalova A, Martinek V, Martinkova M. Heme: emergent roles of heme in signal transduction, functional regulation and as catalytic centres. *Chem Soc Rev* (2019) 48(24):5624–57. doi: 10.1039/C9CS00268E
5. Pradhan P, Vijayan V, Gueler F, Immenschuh S. Interplay of Heme with Macrophages in Homeostasis and Inflammation. *Int J Mol Sci* (2020) 21 (3):1–14. doi: 10.3390/ijms21030740
6. Hebbel R, Morgan W, Eaton J, Hedlund B. Accelerated autoxidation and heme loss due to instability of sickle hemoglobin. *Proc Natl Acad Sci USA* (1988) 85(1):237–41. doi: 10.1073/pnas.85.1.237
7. Hebbel R. Beyond hemoglobin polymerization: The red blood cell membrane and sickle disease pathophysiology. *Blood* (1991) 77:214–37. doi: 10.1182/blood.V77.2.214.214
8. Hebbel R, Eaton J, Balasingam M, Steinberg M. Spontaneous oxygen radical generation by sickle erythrocytes. *J Clin Investigation* (1982) 70(6):1253–9. doi: 10.1172/JCI110724
9. Fibach E, Rachmilewitz E. The role of oxidative stress in hemolytic anemia. *Curr Mol Med* (2008) 8(7):609–19. doi: 10.2174/156652408786241384
10. Advani R, Rubin E, Mohandas N, Schrier SL. Oxidative red blood cell membrane injury in the pathophysiology of severe mouse beta-thalassemia. *Blood* (1992) 79(4):1064–7. doi: 10.1182/blood.V79.4.1064.1064
11. Amer J, Zelig O, Fibach E. Oxidative status of red blood cells, neutrophils, and platelets in paroxysmal nocturnal hemoglobinuria. *Exp Hematol* (2008) 36(4):369–77. doi: 10.1016/j.exphem.2007.12.003
12. Fibach E, Dana M. Oxidative stress in paroxysmal nocturnal hemoglobinuria and other conditions of complement-mediated hemolysis. *Free Radical Biol Med* (2015) 88(Pt A):63–9. doi: 10.1016/j.freeradbiomed.2015.04.027
13. Caprari P, Bozzi A, Ferroni L, Strom R, Salvati AM. Oxidative erythrocyte membrane damage in hereditary spherocytosis. *Biochem Int* (1992) 26 (2):265–74.
14. Cappellini MD, Fiorelli G. Glucose-6-phosphate dehydrogenase deficiency. *Lancet* (2008) 371(9606):64–74. doi: 10.1016/S0140-6736(08)60073-2
15. Pandolfi PP, Sonati F, Rivi R, Mason P, Grosveld F, Luzzatto L. Targeted disruption of the housekeeping gene encoding glucose 6-phosphate dehydrogenase (G6PD): G6PD is dispensable for pentose synthesis but essential for defense against oxidative stress. *EMBO J* (1995) 14(21):5209–15. doi: 10.1002/j.1460-2075.1995.tb00205.x
16. Schrier SL, Mohandas N. Globin-chain specificity of oxidation-induced changes in red blood cell membrane properties. *Blood* (1992) 79(6):1586–92. doi: 10.1182/blood.V79.6.1586.1586
17. Mohanty J, Nagababu E, Rifkind J. Red blood cell oxidative stress impairs oxygen delivery and induces red blood cell aging. *Front Physiol* (2014) 5 (84):1–6. doi: 10.3389/fphys.2014.00084
18. Caprari P, Massimi S, Diana L, Sorrentino F, Maffei L, Materazzi S, et al. Hemorheological Alterations and Oxidative Damage in Sickle Cell Anemia. *Front Mol Biosciences* (2019) 6:142. doi: 10.3389/fmolb.2019.00142
19. Nagababu E, Fabry M, Nagel R, Rifkind J. Heme degradation and oxidative stress in murine models for hemoglobinopathies: Thalassemia, sickle cell disease and hemoglobin C disease. *Blood Cells Molecules Diseases* (2008) 41 (1):60–6. doi: 10.1016/j.bcmd.2007.12.003
20. Johnson R, Goyette GJ, Ravindranath Y, Ho Y. Hemoglobin autoxidation and regulation of endogenous H2O2 levels in erythrocytes. *Free Radical Biol Med* (2005) 39(11):1407–17. doi: 10.1016/j.freeradbiomed.2005.07.002
21. Rank B, Carlsson J, Hebbel R. Abnormal redox status of membrane-protein thiols in sickle erythrocytes. *J Clin Investigation* (1985) 75:1531–7. doi: 10.1172/JCI111857
22. Wood K, Hsu L, Gladwin M. Sickle cell disease vasculopathy: a state of nitric oxide resistance. *Free Radical Biol Med* (2008) 44(8):1506–28. doi: 10.1016/j.freeradbiomed.2008.01.008
23. Svistunenko D, Patel R, Voloshchenko S, Wilson M. The globin-based free radical of ferryl hemoglobin is detected in normal human blood. *J Biol Chem* (1997) 272(11):7114–21. doi: 10.1074/jbc.272.11.7114
24. Giulivi C, Davies KJ. A novel antioxidant role for hemoglobin. The comproportionation of ferrylhemoglobin with oxyhemoglobin. *J Biol Chem* (1990) 265:19453–60.
25. Jana S, Strader MB, Meng F, Hicks W, Kassa T, Tarandovskiy I, et al. Hemoglobin oxidation-dependent reactions promote interactions with band 3 and oxidative changes in sickle cell-derived microparticles. *JCI Insight* (2018) 3(21):1–20. doi: 10.1172/jci.insight.120451
26. Farah M, Sirotkin V, Haarer B, Kakhniashvili D, Amberg D. Diverse protective roles of the actin cytoskeleton during oxidative stress. *Cytoskeleton* (2011) 68:340–54. doi: 10.1002/cm.20516
27. Cyrklaff M, Sanchez C, Kilian N, Bisseye C, Simpore J, Frischknecht F, et al. Hemoglobins S and C interfere with actin remodeling in Plasmodium falciparum-infected erythrocytes. *Science* (2011) 334(6060):1283–6. doi: 10.1126/science.1213775
28. Turrens J. Mitochondrial formation of reactive oxygen species. *J Physiol* (2003) 552(Pt 2):335–44. doi: 10.1113/jphysiol.2003.049478
29. Schweers RL, Zhang J, Randall MS, Loyd MR, Li W, Dorsey FC, et al. NIX is required for programmed mitochondrial clearance during reticulocyte maturation. *Proc Natl Acad Sci USA* (2007) 104(49):19500–5. doi: 10.1073/pnas.0708818104
30. Zhang J, Loyd MR, Randall MS, Waddell MB, Kriwacki RW, Ney PA. A short linear motif in BNIP3L (NIX) mediates mitochondrial clearance in reticulocytes. *Autophagy* (2012) 8(9):1325–32. doi: 10.4161/auto.20764

31. Kundu M, Lindsten T, Yang CY, Wu J, Zhao F, Zhang J, et al. Ulk1 plays a critical role in the autophagic clearance of mitochondria and ribosomes during reticulocyte maturation. *Blood* (2008) 112(4):1493–502. doi: 10.1182/blood-2008-02-137398
32. Gnanapragasam MN, McGrath KE, Catherman S, Xue L, Palis J, Bieker JJ. EKLF/KLF1-regulated cell cycle exit is essential for erythroblast enucleation. *Blood* (2016) 128(12):1631–41. doi: 10.1182/blood-2016-03-706671
33. Jagadeeswaran R, Vazquez BA, Thiruppathi M, Ganesh BB, Ibanez V, Cui S, et al. Pharmacological inhibition of LSD1 and mTOR reduces mitochondrial retention and associated ROS levels in the red blood cells of sickle cell disease. *Exp Hematol* (2017) 50:46–52. doi: 10.1016/j.exphem.2017.02.003
34. Jagadeeswaran R, Rivers A. Evolving treatment paradigms in sickle cell disease. *Hematol Am Soc Hematol Educ Program* (2017) 2017(1):440–6. doi: 10.1182/asheducation-2017.1.440
35. Higdon AN, Benavides GA, Chacko BK, Ouyang X, Johnson MS, Landar A, et al. Hemin causes mitochondrial dysfunction in endothelial cells through promoting lipid peroxidation: the protective role of autophagy. *Am J Physiol Heart Circ Physiol* (2012) 302(7):H1394–409. doi: 10.1152/ajpheart.00584.2011
36. Kassa T, Jana S, Strader MB, Meng F, Jia Y, Wilson MT, et al. Sickle Cell Hemoglobin in the Ferryl State Promotes betaCys-93 Oxidation and Mitochondrial Dysfunction in Epithelial Lung Cells (E10). *J Biol Chem* (2015) 290(46):27939–58. doi: 10.1074/jbc.M115.651257
37. Chintagari NR, Jana S, Alayash AI. Oxidized Ferric and Ferryl Forms of Hemoglobin Trigger Mitochondrial Dysfunction and Injury in Alveolar Type I Cells. *Am J Respir Cell Mol Biol* (2016) 55(2):288–98. doi: 10.1165/rcmb.2015-0197OC
38. Jana S, Meng F, Hirsch RE, Friedman JM, Alayash AI. Oxidized Mutant Human Hemoglobins S and E Induce Oxidative Stress and Bioenergetic Dysfunction in Human Pulmonary Endothelial Cells. *Front Physiol* (2017) 8:1082. doi: 10.3389/fphys.2017.01082
39. Cardenes N, Corey C, Geary L, Jain S, Zharikov S, Barge S, et al. Platelet bioenergetic screen in sickle cell patients reveals mitochondrial complex V inhibition, which contributes to platelet activation. *Blood* (2014) 123(18):2864–72. doi: 10.1182/blood-2013-09-529420
40. Villagra J, Shiva S, Hunter LA, Machado RF, Gladwin MT, Kato GJ. Platelet activation in patients with sickle disease, hemolysis-associated pulmonary hypertension, and nitric oxide scavenging by cell-free hemoglobin. *Blood* (2007) 110(6):2166–72. doi: 10.1182/blood-2006-12-061697
41. Westerman M, Pizzey A, Hirschman J, Cerino M, Weil-Weiner Y, Ramotar P, et al. Microvesicles in haemoglobinopathies offer insights into mechanisms of hypercoagulability, haemolysis and the effects of therapy. *Br J Haematol* (2008) 142(1):126–35. doi: 10.1111/j.1365-2141.2008.07155.x
42. Allan D, Limbrick AR, Thomas P, Westerman MP. Release of spectrin-free spicules on reoxygenation of sickled erythrocytes. *Natur* (1982) 295(5850):612–3. doi: 10.1038/295612a0
43. Lane PA, O'Connell JL, Marlar RA. Erythrocyte membrane vesicles and irreversibly sickled cells bind protein S. *Am J Hematol* (1994) 47(4):295–300. doi: 10.1002/ajh.2830470409
44. Mahfoudhi E, Lecluse Y, Driss F, Abbes S, Flaujac C, Garcon L. Red cells exchanges in sickle cells disease lead to a selective reduction of erythrocytes-derived blood microparticles. *Br J Haematol* (2012) 156(4):545–7. doi: 10.1111/j.1365-2141.2011.08897.x
45. van Tits LJ, van Heerde WL, Landburg PP, Boderie MJ, Muskiet FA, Jacobs N, et al. Plasma annexin A5 and microparticle phosphatidylserine levels are elevated in sickle cell disease and increase further during painful crisis. *Biochem Biophys Res Commun* (2009) 390(1):161–4. doi: 10.1016/j.bbrc.2009.09.102
46. van Beers EJ, Schaap MC, Berckmans RJ, Nieuwland R, Sturk A, van Doormaal FF, et al. Circulating erythrocyte-derived microparticles are associated with coagulation activation in sickle cell disease. *Haematologica* (2009) 94(11):1513–9. doi: 10.3324/haematol.2009.008938
47. Platt OS, Brambilla DJ, Rosse WF, Milner PF, Castro O, Steinberg MH, et al. Mortality in sickle cell disease. Life expectancy and risk factors for early death. *New Engl J Med* (1994) 330(23):1639–44. doi: 10.1056/NEJM199406093302303
48. Camus SM, Gausseres B, Bonnin P, Loufrani L, Grimaud L, Charue D, et al. Erythrocyte microparticles can induce kidney vaso-occlusions in a murine model of sickle cell disease. *Blood* (2012) 120(25):5050–8. doi: 10.1182/blood-2012-02-413138
49. Donadee C, Raat NJ, Kanias T, Tejero J, Lee JS, Kelley EE, et al. Nitric oxide scavenging by red blood cell microparticles and cell-free hemoglobin as a mechanism for the red cell storage lesion. *Circulation* (2011) 124(4):465–76. doi: 10.1161/CIRCULATIONAHA.110.008698
50. Liu C, Zhao W, Christ GJ, Gladwin MT, Kim-Shapiro DB. Nitric oxide scavenging by red cell microparticles. *Free Radical Biol Med* (2013) 65:1164–73. doi: 10.1016/j.freeradbiomed.2013.09.002
51. Camus SM, De Moraes JA, Bonnin P, Abbyad P, Le Jeune S, Lionnet F, et al. Circulating cell membrane microparticles transfer heme to endothelial cells and trigger vasoocclusions in sickle cell disease. *Blood* (2015) 125(24):3805–14. doi: 10.1182/blood-2014-07-589283
52. Nagababu E, Rifkind J. Formation of fluorescent heme degradation products during the oxidation of hemoglobin by hydrogen peroxide. *Biochem Biophys Res Commun* (1998) 247(3):592–6. doi: 10.1006/bbrc.1998.8846
53. Bedard K, Krause K. The NOX family of ROS-generating NADPH oxidases: physiology and pathophysiology. *Physiol Rev* (2007) 87(1):245–313. doi: 10.1152/physrev.00044.2005
54. Lanaro C, Franco-Penteado C, Albuqueque D, Saad S, Conran N, Costa F. Altered levels of cytokines and inflammatory mediators in plasma and leukocytes of sickle cell anemia patients and effects of hydroxyurea therapy. *J Leukocyte Biol* (2009) 85(2):235–42. doi: 10.1189/jlb.0708445
55. George A, Pushkaran S, Konstantinidis DG, Koochaki S, Malik P, Mohandas N, et al. Erythrocyte NADPH oxidase activity modulated by Rac GTPases, PKC, and plasma cytokines contributes to oxidative stress in sickle cell disease. *Blood* (2013) 121(11):2099–107. doi: 10.1182/blood-2012-07-441188
56. Lew, Bookchin R. Ion transport pathology in the mechanism of sickle cell dehydration. *Physiol Rev* (2005) 85(1):179–200. doi: 10.1152/physrev.00052.2003
57. Lang KS, Lang PA, Bauer C, Duranton C, Wieder T, Huber SM, et al. Mechanisms of suicidal erythrocyte death. *Cell Physiol Biochem Int J Exp Cell Physiol Biochem Pharmacol* (2005) 15(5):195–202. doi: 10.1159/000086406
58. Gbotosho OT, Cytlak UM, Hannemann A, Rees DC, Tewari S, Gibson JS. Inhibitors of second messenger pathways and Ca(2+)-induced exposure of phosphatidylserine in red blood cells of patients with sickle cell disease. *Pflugers Archiv Eur J Physiol* (2014) 466(7):1477–85. doi: 10.1007/s00424-013-1343-8
59. Detterich JA, Liu H, Suriany S, Kato RM, Chalacheva P, Tedla B, et al. Erythrocyte and plasma oxidative stress appears to be compensated in patients with sickle cell disease during a period of relative health, despite the presence of known oxidative agents. *Free Radical Biol Med* (2019) 141:408–15. doi: 10.1016/j.freeradbiomed.2019.07.004
60. Tappel AL. The mechanism of the oxidation of unsaturated fatty acids catalyzed by hematin compounds. *Arch Biochem Biophys* (1953) 44(2):378–95. doi: 10.1016/0003-9861(53)90056-3
61. Vincent SH, Grady RW, Shaklai N, Snider JM, Muller-Eberhard U. The influence of heme-binding proteins in heme-catalyzed oxidations. *Arch Biochem Biophys* (1988) 265(2):539–50. doi: 10.1016/0003-9861(88)90159-2
62. Aft RL, Mueller GC. Hemin-mediated DNA strand scission. *J Biol Chem* (1983) 258(19):12069–72.
63. Gao JL, Lu Y, Browne G, Yap BC, Trewhella J, Hunter N, et al. The role of heme binding by DNA-protective protein from starved cells (Dps) in the Tolerance of Porphyromonas gingivalis to heme toxicity. *J Biol Chem* (2012) 287(50):42243–58. doi: 10.1074/jbc.M112.392787
64. Vasconcellos LR, Dutra FF, Siqueira MS, Paula-Neto HA, Dahan J, Kiarely E, et al. Protein aggregation as a cellular response to oxidative stress induced by heme and iron. *Proc Natl Acad Sci USA* (2016) 113(47):E7474–E82. doi: 10.1073/pnas.1608928113
65. Aft RL, Mueller GC. Hemin-mediated oxidative degradation of proteins. *J Biol Chem* (1984) 259(1):301–5.
66. Biswal S, Rizwan H, Pal S, Sabnam S, Parida P, Pal A. Oxidative stress, antioxidant capacity, biomolecule damage, and inflammation symptoms of sickle cell disease in children. *Hematol (Amsterdam Netherlands)* (2019) 24(1):1–9. doi: 10.1080/10245332.2018.1498441
67. Alsultan AI, Seif MA, Amin TT, Naboli M, Alsuliman AM. Relationship between oxidative stress, ferritin and insulin resistance in sickle cell disease. *Eur Rev Med Pharmacol Sci* (2010) 14(6):527–38.

68. Ama Moor VJ, Pieme CA, Chetcha Chemegne B, Manonji H, Njinkio Nono BL, Tchoula Mamiafo C, et al. Oxidative profile of sickle cell patients in a Cameroonian urban hospital. *BMC Clin Pathol* (2016) 16:15. doi: 10.1186/s12907-016-0037-5
69. Natta CL, Chen LC, Chow CK. Selenium and glutathione peroxidase levels in sickle cell anemia. *Acta Haematol* (1990) 83(3):130–2. doi: 10.1159/000205188
70. Renoux C, Joly P, Faes C, Mury P, Eglenen B, Turkay M, et al. Association between Oxidative Stress, Genetic Factors, and Clinical Severity in Children with Sickle Cell Anemia. *J Pediatrics* (2018) 195:228–35. doi: 10.1016/j.jpeds.2017.12.021
71. Mockesch B, Connes P, Charlot K, Skinner S, Hardy-Dessources MD, Romana M, et al. Association between oxidative stress and vascular reactivity in children with sickle cell anaemia and sickle haemoglobin C disease. *Br J Haematol* (2017) 178(3):468–75. doi: 10.1111/bjh.14693
72. Antwi-Boasiako C, Dankwah GB, Aryee R, Hayfron-Benjamin C, Donkor ES, Campbell AD. Oxidative Profile of Patients with Sickle Cell Disease. *Med Sci (Basel Switzerland)* (2019) 7(2):1–8. doi: 10.3390/medsci7020017
73. Schacter L, Warth JA, Gordon EM, Prasad A, Klein BL. Altered amount and activity of superoxide dismutase in sickle cell anemia. *FASEB J* (1988) 2 (3):237–43. doi: 10.1096/fasebj.2.3.3350236
74. Farias ICC, Mendonca-Belmont TF, da Silva AS, do OK, Ferreira F, Medeiros FS, et al. Association of the SOD2 Polymorphism (Val16Ala) and SOD Activity with Vaso-occlusive Crisis and Acute Splenic Sequestration in Children with Sickle Cell Anemia. *Mediterranean J Hematol Infect Diseases* (2018) 10(1):e2018012. doi: 10.4084/mjhid.2018.012
75. Armenis I, Kalotychou V, Tzanetea R, Moyssakis I, Anastasopoulou D, Pantos C, et al. Reduced peripheral blood superoxide dismutase 2 expression in sickle cell disease. *Ann Hematol* (2019) 98(7):1561–72. doi: 10.1007/s00277-019-03709-8
76. Smith OS, Ajose OA, Adegoke SA, Adegoke OA, Adedeji TA, Oderinu KA. Plasma level of antioxidants is related to frequency of vaso-occlusive crises in children with sickle cell anaemia in steady state in Nigeria. *Pediatr Hematol Oncol J* (2019) 4(1):17–22. doi: 10.1016/j.phoj.2019.03.003
77. Delesderrier E, Cople-Rodrigues CS, Omena J, Kneip Fleury M, Barbosa Brito F, Costa Bacelo A, et al. Selenium Status and Hemolysis in Sickle Cell Disease Patients. *Nutrients* (2019) 11(9):1–11. doi: 10.3390/nu11092211
78. Manfredini V, Lazzaretti LL, Griebeler IH, Santin AP, Brandao VD, Wagner S, et al. Blood antioxidant parameters in sickle cell anemia patients in steady state. *J Natl Med Assoc* (2008) 100(8):897–902. doi: 10.1016/S0027-9684(15)31402-4
79. Morris C, Suh J, Hagar W, Larkin S, Bland D, Steinberg M, et al. Erythrocyte glutamine depletion, altered redox environment, and pulmonary hypertension in sickle cell disease. *Blood* (2008) 111(1):402–10. doi: 10.1182/blood-2007-04-081703
80. Hamdy MM, Mosallam DS, Jamal AM, Rabie WA. Selenium and Vitamin E as antioxidants in chronic hemolytic anemia: Are they deficient? A case-control study in a group of Egyptian children. *J Adv Res* (2015) 6(6):1071–7. doi: 10.1016/j.jare.2015.01.002
81. Arruda MM, Mecabo G, Rodrigues CA, Matsuda SS, Rabelo IB, Figueiredo MS, et al. and E supplementation increases markers of haemolysis in sickle cell anaemia patients: a randomized, double-blind, placebo-controlled trial. *Br J Haematol* (2013) 160(5):688–700. doi: 10.1111/bjh.12185
82. Muhammad A, Waziri AD, Forcados GE, Sanusi B, Sani H, Malami I, et al. Sickling-preventive effects of rutin is associated with modulation of deoxygenated haemoglobin, 2,3-bisphosphoglycerate mutase, redox status and alteration of functional chemistry in sickle erythrocytes. *Heliyon* (2019) 5(6):e01905. doi: 10.1016/j.heliyon.2019.e01905
83. Belcher JD, Chen C, Nguyen J, Abdulla F, Zhang P, Nguyen H, et al. Haptoglobin and hemopexin inhibit vaso-occlusion and inflammation in murine sickle cell disease: Role of heme oxygenase-1 induction. *PloS One* (2018) 13(4):e0196455. doi: 10.1371/journal.pone.0196455
84. Gellen B, Messonnier LA, Galacteros F, Audureau E, Merlet AN, Rupp T, et al. Moderate-intensity endurance-exercise training in patients with sickle-cell disease without severe chronic complications (EXDRE): an open-label randomised controlled trial. *Lancet Haematol* (2018) 5(11):e554–e62. doi: 10.1016/S2352-3026(18)30163-7
85. Chatel B, Messonnier LA, Barge Q, Vilmen C, Noirez P, Bernard M, et al. Endurance training reduces exercise-induced acidosis and improves muscle function in a mouse model of sickle cell disease. *Mol Genet Metab* (2018) 123 (3):400–10. doi: 10.1016/j.ymgme.2017.11.010
86. Charrin E, Aufradet E, Douillard A, Romdhani A, Souza GD, Bessaad A, et al. Oxidative stress is decreased in physically active sickle cell SAD mice. *Br J Haematol* (2015) 168(5):747–56. doi: 10.1111/bjh.13207
87. Gouraud E, Charrin E, Dube JJ, Ofori-Acquah SF, Martin C, Skinner S, et al. Effects of Individualized Treadmill Endurance Training on Oxidative Stress in Skeletal Muscles of Transgenic Sickle Mice. *Oxid Med Cell Longevity* (2019) 2019:3765643. doi: 10.1155/2019/3765643
88. Grau M, Nader E, Jerke M, Schenk A, Renoux C, Dietz T, et al. Impact of A Six Week Training Program on Ventilatory Efficiency, Red Blood Cell Rheological Parameters and Red Blood Cell Nitric Oxide Signaling in Young Sickle Cell Anemia Patients: A Pilot Study. *J Clin Med* (2019) 8 (12):1–16. doi: 10.3390/jcm8122155
89. Kato G, McGowan V, Machado R, Little J, Taylor J, Morris C, et al. Lactate dehydrogenase as a biomarker of hemolysis-associated nitric oxide resistance, priapism, leg ulceration, pulmonary hypertension, and death in patients with sickle cell disease. *Blood* (2006) 107(6):2279–85. doi: 10.1182/blood-2005-06-2373
90. Morris C, Kato G, Poljakovic M, Wang X, Blackwelder W, Sachdev V, et al. Dysregulated arginine metabolism, hemolysis-associated pulmonary hypertension, and mortality in sickle cell disease. *J Am Med Assoc* (2005) 294(1):81–90. doi: 10.1001/jama.294.1.81
91. Reiter C, Wang X, Tanus-Santos J, Hogg N, Cannon RR, Schechter A, et al. Cell-free hemoglobin limits nitric oxide bioavailability in sickle-cell disease. *Nat Med* (2002) 8(12):1383–9. doi: 10.1038/nm1202-799
92. Palmer R, Ferrige A, Moncada S. Nitric oxide release accounts for the biological activity of endothelium-derived relaxing factor. *Nature* (1987) 327:524 – 6. doi: 10.1038/327524a0
93. Arnold W, Mittal C, Katsuki S, Murad F. Nitric oxide activates guanylate cyclase and increases guanosine 3′:5′-cyclic monophosphate levels in various tissue preparations. *Proc Natl Acad Sci USA* (1977) 74:3203–7. doi: 10.1073/pnas.74.8.3203
94. Kato GJ, Steinberg MH, Gladwin MT. Intravascular hemolysis and the pathophysiology of sickle cell disease. *J Clin Invest* (2017) 127(3):750–60. doi: 10.1172/JCI89741
95. Potoka KP, Gladwin MT. Vasculopathy and pulmonary hypertension in sickle cell disease. *Am J Physiol Lung Cell Mol Physiol* (2015) 308(4):L314–24. doi: 10.1152/ajplung.00252.2014
96. Gordeuk VR, Castro OL, Machado RF. Pathophysiology and treatment of pulmonary hypertension in sickle cell disease. *Blood* (2016) 127(7):820–8. doi: 10.1182/blood-2015-08-618561
97. Kristiansen M, Graversen JH, Jacobsen C, Sonne O, Hoffman HJ, Law SK, et al. Identification of the haemoglobin scavenger receptor. *Nature* (2001) 409(6817):198–201. doi: 10.1038/35051594
98. Schaer DJ, Schaer CA, Buehler PW, Boykins RA, Schoedon G, Alayash AI, et al. CD163 is the macrophage scavenger receptor for native and chemically modified hemoglobins in the absence of haptoglobin. *Blood* (2006) 107 (1):373–80. doi: 10.1182/blood-2005-03-1014
99. Nielsen MJ, Andersen CB, Moestrup SK. CD163 binding to haptoglobin-hemoglobin complexes involves a dual-point electrostatic receptor-ligand pairing. *J Biol Chem* (2013) 288(26):18834–41. doi: 10.1074/jbc.M113.471060
100. Smith A, McCulloh RJ. Hemopexin and haptoglobin: allies against heme toxicity from hemoglobin not contenders. *Front Physiol* (2015) 6:187. doi: 10.3389/fphys.2015.00187
101. Rother RP, Bell L, Hillmen P, Gladwin MT. The clinical sequelae of intravascular hemolysis and extracellular plasma hemoglobin: a novel mechanism of human disease. *JAMA* (2005) 293(13):1653–62. doi: 10.1001/jama.293.13.1653
102. Immenschuh S, Vijayan V, Janciauskiene S, Gueler F. Heme as a Target for Therapeutic Interventions. *Front Pharmacol* (2017) 8:146. doi: 10.3389/fphar.2017.00146
103. Oh JY, Hamm J, Xu X, Genschmer K, Zhong M, Lebensburger J, et al. Absorbance and redox based approaches for measuring free heme and free hemoglobin in biological matrices. *Redox Biol* (2016) 9:167–77. doi: 10.1016/j.redox.2016.08.003
104. Thomas AM, Gerogianni A, McAdam MB, Floisand Y, Lau C, Espevik T, et al. Complement Component C5 and TLR Molecule CD14 Mediate Heme-

Induced Thromboinflammation in Human Blood. *J Immunol* (2019) 203 (6):1571–8. doi: 10.4049/jimmunol.1900047
105. Balla J, Vercellotti GM, Jeney V, Yachie A, Varga Z, Eaton JW, et al. Heme, heme oxygenase and ferritin in vascular endothelial cell injury. *Mol Nutr Food Res* (2005) 49(11):1030–43. doi: 10.1002/mnfr.200500076
106. Grinshtein N, Bamm VV, Tsemakhovich VA, Shaklai N. Mechanism of low-density lipoprotein oxidation by hemoglobin-derived iron. *Biochemistry* (2003) 42(23):6977–85. doi: 10.1021/bi020647r
107. Miller YI, Shaklai N. Kinetics of hemin distribution in plasma reveals its role in lipoprotein oxidation. *Biochim Biophys Acta* (1999) 1454(2):153–64. doi: 10.1016/S0925-4439(99)00027-7
108. Gozzelino R, Jeney V, Soares MP. Mechanisms of cell protection by heme oxygenase-1. *Annu Rev Pharmacol Toxicol* (2010) 50:323–54. doi: 10.1146/annurev.pharmtox.010909.105600
109. Fasano M, Mattu M, Coletta M, Ascenzi P. The heme-iron geometry of ferrous nitrosylated heme-serum lipoproteins, hemopexin, and albumin: a comparative EPR study. *J Inorganic Biochem* (2002) 91(3):487–90. doi: 10.1016/S0162-0134(02)00473-7
110. Sasaki J, Waterman MR, Buchanan GR, Cottam GL. Plasma and erythrocyte lipids in sickle cell anaemia. *Clin Lab Haematol* (1983) 5(1):35–44. doi: 10.1111/j.1365-2257.1983.tb00494.x
111. Akinlade KS, Adewale CO, Rahamon SK, Fasola FA, Olaniyi JA, Atere AD. Defective lipid metabolism in sickle cell anaemia subjects in vaso-occlusive crisis. *Nigerian Med J J Nigeria Med Assoc* (2014) 55(5):428–31. doi: 10.4103/0300-1652.140388
112. Zorca S, Freeman L, Hildesheim M, Allen D, Remaley AT, JGt T, et al. Lipid levels in sickle-cell disease associated with haemolytic severity, vascular dysfunction and pulmonary hypertension. *Br J Haematol* (2010) 149 (3):436–45. doi: 10.1111/j.1365-2141.2010.08109.x
113. Yalcinkaya A, Unal S, Oztas Y. Altered HDL particle in sickle cell disease: decreased cholesterol content is associated with hemolysis, whereas decreased Apolipoprotein A1 is linked to inflammation. *Lipids Health Disease* (2019) 18(1):225. doi: 10.1186/s12944-019-1174-5
114. Vendrame F, Olops L, Saad STO, Costa FF, Fertrin KY. Differences in heme and hemopexin content in lipoproteins from patients with sickle cell disease. *J Clin Lipidol* (2018) 12(6):1532–8. doi: 10.1016/j.jacl.2018.08.002
115. Fasano M, Fanali G, Leboffe L, Ascenzi P. Heme binding to albuminoid proteins is the result of recent evolution. *IUBMB Life* (2007) 59(7):436–40. doi: 10.1080/15216540701474523
116. Ascenzi P, Fasano M. Serum heme-albumin: an allosteric protein. *IUBMB Life* (2009) 61(12):1118–22. doi: 10.1002/iub.263
117. Bunn HF, Jandl JH. Exchange of heme among hemoglobins and between hemoglobin and albumin. *J Biol Chem* (1968) 243(3):465–75.
118. Hvidberg V, Maniecki MB, Jacobsen C, Hojrup P, Moller HJ, Moestrup SK. Identification of the receptor scavenging hemopexin-heme complexes. *Blood* (2005) 106(7):2572–9. doi: 10.1182/blood-2005-03-1185
119. Tolosano E, Fagoonee S, Morello N, Vinchi F, Fiorito V. Heme scavenging and the other facets of hemopexin. *Antioxidants Redox Signaling* (2010) 12 (2):305–20. doi: 10.1089/ars.2009.2787
120. Allhorn M, Berggard T, Nordberg J, Olsson ML, Akerstrom B. Processing of the lipocalin alpha(1)-microglobulin by hemoglobin induces heme-binding and heme-degradation properties. *Blood* (2002) 99(6):1894–901. doi: 10.1182/blood.V99.6.1894
121. Meining W, Skerra A. The crystal structure of human alpha(1)-microglobulin reveals a potential haem-binding site. *Biochem J* (2012) 445 (2):175–82. doi: 10.1042/BJ20120448
122. Allhorn M, Klapyta A, Akerstrom B. Redox properties of the lipocalin alpha1-microglobulin: reduction of cytochrome c, hemoglobin, and free iron. *Free Radical Biol Med* (2005) 38(5):557–67. doi: 10.1016/j.freeradbiomed.2004.12.013
123. Hahl P, Hunt R, Bjes ES, Skaff A, Keightley A, Smith A. Identification of oxidative modifications of hemopexin and their predicted physiological relevance. *J Biol Chem* (2017) 292(33):13658–71. doi: 10.1074/jbc.M117.783951
124. Paoli M, Anderson BF, Baker HM, Morgan WT, Smith A, Baker EN. Crystal structure of hemopexin reveals a novel high-affinity heme site formed between two beta-propeller domains. *Nat Struct Biol* (1999) 6(10):926–31. doi: 10.1038/13294
125. Gkouvatsos K, Papanikolaou G, Pantopoulos K. Regulation of iron transport and the role of transferrin. *Biochim Biophys Acta* (2012) 1820(3):188–202. doi: 10.1016/j.bbagen.2011.10.013
126. Olatunya OS, Lanaro C, Longhini AL, Penteado CFF, Fertrin KY, Adekile A, et al. Red blood cells microparticles are associated with hemolysis markers and may contribute to clinical events among sickle cell disease patients. *Ann Hematol* (2019) 98(11):2507–21. doi: 10.1007/s00277-019-03792-x
127. Yalamanoglu A, Deuel JW, Hunt RC, Baek JH, Hassell K, Redinius K, et al. Depletion of haptoglobin and hemopexin promote hemoglobin-mediated lipoprotein oxidation in sickle cell disease. *Am J Physiol Lung Cell Mol Physiol* (2018) 315(5):L765–L74. doi: 10.1152/ajplung.00269.2018
128. Soares MP, Bach FH. Heme oxygenase-1: from biology to therapeutic potential. *Trends Mol Med* (2009) 15(2):50–8. doi: 10.1016/j.molmed.2008.12.004
129. Wagener FA, Volk HD, Willis D, Abraham NG, Soares MP, Adema GJ, et al. Different faces of the heme-heme oxygenase system in inflammation. *Pharmacol Rev* (2003) 55(3):551–71. doi: 10.1124/pr.55.3.5
130. Alam J, Killeen E, Gong P, Naquin R, Hu B, Stewart D, et al. Heme activates the heme oxygenase-1 gene in renal epithelial cells by stabilizing Nrf2. *Am J Physiol Renal Physiol* (2003) 284(4):F743–52. doi: 10.1152/ajprenal.00376.2002
131. Belcher JD, Beckman JD, Balla G, Balla J, Vercellotti G. Heme degradation and vascular injury. *Antioxidants Redox Signaling* (2010) 12(2):233–48. doi: 10.1089/ars.2009.2822
132. Boyle JJ, Johns M, Lo J, Chiodini A, Ambrose N, Evans PC, et al. Heme induces heme oxygenase 1 via Nrf2: role in the homeostatic macrophage response to intraplaque hemorrhage. *Arteriosclerosis thrombosis Vasc Biol* (2011) 31(11):2685–91. doi: 10.1161/ATVBAHA.111.225813
133. Ghosh S, Hazra R, Ihunnah CA, Weidert F, Flage B, Ofori-Acquah SF. Augmented NRF2 activation protects adult sickle mice from lethal acute chest syndrome. *Br J Haematol* (2018) 182(2):271–5. doi: 10.1111/bjh.15401
134. Belcher JD, Vineyard JV, Bruzzone CM, Chen C, Beckman JD, Nguyen J, et al. Heme oxygenase-1 gene delivery by Sleeping Beauty inhibits vascular stasis in a murine model of sickle cell disease. *J Mol Med (Berlin Germany)* (2010) 88(7):665–75. doi: 10.1007/s00109-010-0613-6
135. Belcher JD, Mahaseth H, Welch TE, Otterbein LE, Hebbel RP, Vercellotti GM. Heme oxygenase-1 is a modulator of inflammation and vaso-occlusion in transgenic sickle mice. *J Clin Investig* (2006) 116(3):808–16. doi: 10.1172/JCI26857
136. Belcher JD, Chen C, Nguyen J, Zhang P, Abdulla F, Nguyen P, et al. Control of Oxidative Stress and Inflammation in Sickle Cell Disease with the Nrf2 Activator Dimethyl Fumarate. *Antioxidants Redox Signaling* (2017) 26 (14):748–62. doi: 10.1089/ars.2015.6571
137. Krishnamoorthy S, Pace B, Gupta D, Sturtevant S, Li B, Makala L, et al. Dimethyl fumarate increases fetal hemoglobin, provides heme detoxification, and corrects anemia in sickle cell disease. *JCI Insight* (2017) 2(20):1–16. doi: 10.1172/jci.insight.96409
138. Keleku-Lukwete N, Suzuki M, Otsuki A, Tsuchida K, Katayama S, Hayashi M, et al. Amelioration of inflammation and tissue damage in sickle cell model mice by Nrf2 activation. *Proc Natl Acad Sci USA* (2015) 112(39):12169–74. doi: 10.1073/pnas.1509158112
139. Balla J, Jacob HS, Balla G, Nath K, Eaton JW, Vercellotti GM. Endothelial-cell heme uptake from heme proteins: induction of sensitization and desensitization to oxidant damage. *Proc Natl Acad Sci USA* (1993) 90 (20):9285–9. doi: 10.1073/pnas.90.20.9285
140. Iwasaki K, Mackenzie EL, Hailemariam K, Sakamoto K, Tsuji Y. Hemin-mediated regulation of an antioxidant-responsive element of the human ferritin H gene and role of Ref-1 during erythroid differentiation of K562 cells. *Mol Cell Biol* (2006) 26(7):2845–56. doi: 10.1128/MCB.26.7.2845-2856.2006
141. Conran N, Belcher JD. Inflammation in sickle cell disease. *Clin Hemorheol Microcirc* (2018) 68(2-3):263–99. doi: 10.3233/CH-189012
142. Pamplona A, Ferreira A, Balla J, Jeney V, Balla G, Epiphanio S, et al. Heme oxygenase-1 and carbon monoxide suppress the pathogenesis of experimental cerebral malaria. *Nat Med* (2007) 13(6):703–10. doi: 10.1038/nm1586
143. Pereira MLM, Marinho CRF, Epiphanio S. Could Heme Oxygenase-1 Be a New Target for Therapeutic Intervention in Malaria-Associated Acute Lung

Injury/Acute Respiratory Distress Syndrome? *Front Cell Infection Microbiol* (2018) 8:161. doi: 10.3389/fcimb.2018.00161
144. Ekregbesi P, Shankar-Hari M, Bottomley C, Riley EM, Mooney JP. Relationship between Anaemia, Haemolysis, Inflammation and Haem Oxygenase-1 at Admission with Sepsis: a pilot study. *Sci Rep* (2018) 8 (1):11198. doi: 10.1038/s41598-018-29558-5
145. Adamzik M, Hamburger T, Petrat F, Peters J, de Groot H, Hartmann M. Free hemoglobin concentration in severe sepsis: methods of measurement and prediction of outcome. *Crit Care* (2012) 16(4):R125. doi: 10.1186/cc11425
146. Clark IA, Awburn MM, Harper CG, Liomba NG, Molyneux ME. Induction of HO-1 in tissue macrophages and monocytes in fatal falciparum malaria and sepsis. *Malaria J* (2003) 2(1):41. doi: 10.1186/1475-2875-2-41
147. Kato G, Gladwin M, Steinberg M. Deconstructing sickle cell disease: reappraisal of the role of hemolysis in the development of clinical subphenotypes. *Blood Rev* (2007) 21(1):37–47. doi: 10.1016/j.blre.2006.07.001
148. Takaki S, Takeyama N, Kajita Y, Yabuki T, Noguchi H, Miki Y, et al. Beneficial effects of the heme oxygenase-1/carbon monoxide system in patients with severe sepsis/septic shock. *Intensive Care Med* (2010) 36 (1):42–8. doi: 10.1007/s00134-009-1575-4
149. Janz DR, Bastarache JA, Sills G, Wickersham N, May AK, Bernard GR, et al. Association between haptoglobin, hemopexin and mortality in adults with sepsis. *Crit Care* (2013) 17(6):R272. doi: 10.1186/cc13108
150. Balla G, Jacob HS, Eaton JW, Belcher JD, Vercellotti GM. Hemin: a possible physiological mediator of low density lipoprotein oxidation and endothelial injury. *Arterioscler Thromb J Vasc Biol* (1991) 11(6):1700–11. doi: 10.1161/01.ATV.11.6.1700
151. Dutra FF, Bozza MT. Heme on innate immunity and inflammation. *Front Pharmacol* (2014) 5:115. doi: 10.3389/fphar.2014.00115
152. Gouveia Z, Carlos AR, Yuan X, Aires-da-Silva F, Stocker R, Maghzal GJ, et al. Characterization of plasma labile heme in hemolytic conditions. *FEBS J* (2017) 284(19):3278–301. doi: 10.1111/febs.14192
153. Santiago RP, Guarda CC, Figueiredo CVB, Fiuza LM, Aleluia MM, Adanho CSA, et al. Serum haptoglobin and hemopexin levels are depleted in pediatric sickle cell disease patients. *Blood Cells Mol Dis* (2018) 72:34–6. doi: 10.1016/j.bcmd.2018.07.002
154. Vercellotti GM, Zhang P, Nguyen J, Abdulla F, Chen C, Nguyen P, et al. Hepatic Overexpression of Hemopexin Inhibits Inflammation and Vascular Stasis in Murine Models of Sickle Cell Disease. *Mol Med (Cambridge Mass)* (2016) 22:1–15. doi: 10.2119/molmed.2016.00063
155. Ofori-Acquah SF, Hazra R, Orikogbo OO, Crosby D, Flage B, Ackah EB, et al. Hemopexin deficiency promotes acute kidney injury in sickle cell disease. *Blood* (2020) 135(13):1044–8. doi: 10.1182/blood.2019002653
156. Muller-Eberhard U, Javid J, Liem HH, Hanstein A, Hanna M. Plasma concentrations of hemopexin, haptoglobin and heme in patients with various hemolytic diseases. *Blood* (1968) 32(5):811–5. doi: 10.1182/blood.V32.5.811.811
157. Merle NS, Grunenwald A, Rajaratnam H, Gnemmi V, Frimat M, Figueres ML, et al. Intravascular hemolysis activates complement via cell-free heme and heme-loaded microvesicles. *JCI Insight* (2018) 3(12):1–17. doi: 10.1172/jci.insight.96910
158. Adisa OA, Hu Y, Ghosh S, Aryee D, Osunkwo I, Ofori-Acquah SF. Association between plasma free haem and incidence of vaso-occlusive episodes and acute chest syndrome in children with sickle cell disease. *Br J Haematol* (2013) 162(5):702–5. doi: 10.1111/bjh.12445
159. Sadrzadeh SM, Graf E, Panter SS, Hallaway PE, Eaton JW. Hemoglobin. A biologic fenton reagent. *J Biol Chem* (1984) 259(23):14354–6.
160. Thomas DD, Espey MG, Vitek MP, Miranda KM, Wink DA. Protein nitration is mediated by heme and free metals through Fenton-type chemistry: an alternative to the NO/O2- reaction. *Proc Natl Acad Sci USA* (2002) 99(20):12691–6. doi: 10.1073/pnas.202312699
161. Winterbourn CC. Toxicity of iron and hydrogen peroxide: the Fenton reaction. *Toxicol Lett* (1995) 82-83:969–74. doi: 10.1016/0378-4274(95)03532-x
162. Meng F, Alayash AI. Determination of extinction coefficients of human hemoglobin in various redox states. *Anal Biochem* (2017) 521:11–9. doi: 10.1016/j.ab.2017.01.002
163. Hanna DA, Harvey RM, Martinez-Guzman O, Yuan X, Chandrasekharan B, Raju G, et al. Heme dynamics and trafficking factors revealed by genetically encoded fluorescent heme sensors. *Proc Natl Acad Sci USA* (2016) 113 (27):7539–44. doi: 10.1073/pnas.1523802113
164. Newton LD, Pascu SI, Tyrrell RM, Eggleston IM. Development of a peptide-based fluorescent probe for biological heme monitoring. *Org Biomol Chem* (2019) 17(3):467–71. doi: 10.1039/C8OB02290A
165. Hargrove MS, Whitaker T, Olson JS, Vali RJ, Mathews AJ. Quaternary structure regulates hemin dissociation from human hemoglobin. *J Biol Chem* (1997) 272(28):17385–9. doi: 10.1074/jbc.272.28.17385
166. Anderson HL, Brodsky IE, Mangalmurti NS. The Evolving Erythrocyte: Red Blood Cells as Modulators of Innate Immunity. *J Immunol* (2018) 201 (5):1343–51. doi: 10.4049/jimmunol.1800565
167. Wang X, Mendelsohn L, Rogers H, Leitman S, Raghavachari N, Yang Y, et al. Heme-bound iron activates placenta growth factor in erythroid cells via erythroid Krüppel-like factor. *Blood* (2014) 124(6):946–54. doi: 10.1182/blood-2013-11-539718
168. Vinchi F, Costa da Silva M, Ingoglia G, Petrillo S, Brinkman N, Zuercher A, et al. Hemopexin therapy reverts heme-induced proinflammatory phenotypic switching of macrophages in a mouse model of sickle cell disease. *Blood* (2016) 127(4):473–86. doi: 10.1182/blood-2015-08-663245
169. Dutra FF, Alves LS, Rodrigues D, Fernandez PL, de Oliveira RB, Golenbock DT, et al. Hemolysis-induced lethality involves inflammasome activation by heme. *Proc Natl Acad Sci USA* (2014) 111(39):E4110–8. doi: 10.1073/pnas.1405023111
170. Sparkenbaugh EM, Chantrathammachart P, Wang S, Jonas W, Kirchhofer D, Gailani D, et al. Excess of heme induces tissue factor-dependent activation of coagulation in mice. *Haematologica* (2015) 100(3):308–14. doi: 10.3324/haematol.2014.114728
171. Chen G, Zhang D, Fuchs TA, Manwani D, Wagner DD, Frenette PS. Heme-induced neutrophil extracellular traps contribute to the pathogenesis of sickle cell disease. *Blood* (2014) 123(24):3818–27. doi: 10.1182/blood-2013-10-529982
172. Erdei J, Toth A, Balogh E, Nyakundi BB, Banyai E, Ryffel B, et al. Induction of NLRP3 Inflammasome Activation by Heme in Human Endothelial Cells. *Oxid Med Cell Longevity* (2018) 2018:4310816. doi: 10.1155/2018/4310816
173. Belcher JD, Chen C, Nguyen J, Milbauer L, Abdulla F, Alayash AI, et al. Heme triggers TLR4 signaling leading to endothelial cell activation and vaso-occlusion in murine sickle cell disease. *Blood* (2014) 123(3):377–90. doi: 10.1182/blood-2013-04-495887
174. Deuel JW, Vallelian F, Schaer CA, Puglia M, Buehler PW, Schaer DJ. Different target specificities of haptoglobin and hemopexin define a sequential protection system against vascular hemoglobin toxicity. *Free Radical Biol Med* (2015) 89:931–43. doi: 10.1016/j.freeradbiomed.2015.09.016
175. Figueiredo RT, Fernandez PL, Mourao-Sa DS, Porto BN, Dutra FF, Alves LS, et al. Characterization of heme as activator of Toll-like receptor 4. *J Biol Chem* (2007) 282(28):20221–9. doi: 10.1074/jbc.M610737200
176. Kapetanaki MG, Gbotosho OT, Sharma D, Weidert F, Ofori-Acquah SF, Kato GJ. Free heme regulates placenta growth factor through NRF2-antioxidant response signaling. *Free Radic Biol Med* (2019) 143:300–8. doi: 10.1016/j.freeradbiomed.2019.08.009
177. Gladwin MT, Ofori-Acquah SF. Erythroid DAMPs drive inflammation in SCD. *Blood* (2014) 123(24):3689–90. doi: 10.1182/blood-2014-03-563874
178. Mendonca R, Silveira AA, Conran N. Red cell DAMPs and inflammation. *Inflammation Res* (2016) 65(9):665–78. doi: 10.1007/s00011-016-0955-9
179. Xiang M, Shi X, Li Y, Xu J, Yin L, Xiao G, et al. Hemorrhagic shock activation of NLRP3 inflammasome in lung endothelial cells. *J Immunol* (2011) 187 (9):4809–17. doi: 10.4049/jimmunol.1102093
180. Vogel S, Thein SL. Platelets at the crossroads of thrombosis, inflammation and haemolysis. *Br J Haematol* (2018) 180(5):761–7. doi: 10.1111/bjh.15117
181. Maeda R, Kawasaki Y, Kume Y, Go H, Suyama K, Hosoya M. Involvement of high mobility group box 1 in the pathogenesis of severe hemolytic uremic syndrome in a murine model. *Am J Physiol Renal Physiol* (2019) 317(6): F1420–F9. doi: 10.1152/ajprenal.00263.2019
182. Ataga KI, Orringer EP. Hypercoagulability in sickle cell disease: a curious paradox. *Am J Med* (2003) 115(9):721–8. doi: 10.1016/j.amjmed.2003.07.011
183. Wang H, Bloom O, Zhang M, Vishnubhakat JM, Ombrellino M, Che J, et al. HMG-1 as a late mediator of endotoxin lethality in mice. *Science* (1999) 285 (5425):248–51. doi: 10.1126/science.285.5425.248

184. Xu H, Wandersee NJ, Guo Y, Jones DW, Holzhauer SL, Hanson MS, et al. Sickle cell disease increases high mobility group box 1: a novel mechanism of inflammation. *Blood* (2014) 124(26):3978–81. doi: 10.1182/blood-2014-04-560813
185. Vogel S, Arora T, Wang X, Mendelsohn L, Nichols J, Allen D, et al. The platelet NLRP3 inflammasome is upregulated in sickle cell disease via HMGB1/TLR4 and Bruton tyrosine kinase. *Blood Adv* (2018) 2(20):2672–80. doi: 10.1182/bloodadvances.2018021709
186. Murthy P, Durco F, Miller-Ocuin JL, Takedai T, Shankar S, Liang X, et al. The NLRP3 inflammasome and bruton's tyrosine kinase in platelets co-regulate platelet activation, aggregation, and in vitro thrombus formation. *Biochem Biophys Res Commun* (2017) 483(1):230–6. doi: 10.1016/j.bbrc.2016.12.161
187. Petrillo S, Chiabrando D, Genova T, Fiorito V, Ingoglia G, Vinchi F, et al. Heme accumulation in endothelial cells impairs angiogenesis by triggering paraptosis. *Cell Death Differ* (2018) 25(3):573–88. doi: 10.1038/s41418-017-0001-7
188. Wagener FA, Feldman E, de Witte T, Abraham NG. Heme induces the expression of adhesion molecules ICAM-1, VCAM-1, and E selectin in vascular endothelial cells. *Proc Soc Exp Biol Med Soc Exp Biol Med* (1997) 216 (3):456–63. doi: 10.3181/00379727-216-44197
189. Telen MJ. Cellular adhesion and the endothelium: E-selectin, L-selectin, and pan-selectin inhibitors. *Hematology/Oncology Clinics North America* (2014) 28(2):341–54. doi: 10.1016/j.hoc.2013.11.010
190. Hidalgo A, Chang J, Jang JE, Peired AJ, Chiang EY, Frenette PS. Heterotypic interactions enabled by polarized neutrophil microdomains mediate thromboinflammatory injury. *Nat Med* (2009) 15(4):384–91. doi: 10.1038/nm.1939
191. Gee BE, Platt OS. Sickle reticulocytes adhere to VCAM-1. *Blood* (1995) 85 (1):268–74. doi: 10.1182/blood.V85.1.268.bloodjournal851268
192. Kucukal E, Ilich A, Key NS, Little JA, Gurkan UA. Red Blood Cell Adhesion to Heme-Activated Endothelial Cells Reflects Clinical Phenotype in Sickle Cell Disease. *Am J Hematol* (2018) 93(8):1050–60. doi: 10.1002/ajh.25159
193. Matsui NM, Borsig L, Rosen SD, Yaghmai M, Varki A. Embury SH. P-selectin mediates the adhesion of sickle erythrocytes to the endothelium. *Blood* (2001) 98(6):1955–62. doi: 10.1182/blood.V98.6.1955
194. Matsui NM, Varki A, Embury SH. Heparin inhibits the flow adhesion of sickle red blood cells to P-selectin. *Blood* (2002) 100(10):3790–6. doi: 10.1182/blood-2002-02-0626
195. Embury SH, Matsui NM, Ramanujam S, Mayadas TN, Noguchi CT, Diwan BA, et al. The contribution of endothelial cell P-selectin to the microvascular flow of mouse sickle erythrocytes in vivo. *Blood* (2004) 104(10):3378–85. doi: 10.1182/blood-2004-02-0713
196. Ghosh S, Flage B, Weidert F, Ofori-Acquah SF. P-selectin plays a role in haem-induced acute lung injury in sickle mice. *Br J Haematol* (2019) 186 (2):329–33. doi: 10.1111/bjh.15807
197. Chang J, Patton JT, Sarkar A, Ernst B, Magnani JL, Frenette PS. GMI-1070, a novel pan-selectin antagonist, reverses acute vascular occlusions in sickle cell mice. *Blood* (2010) 116(10):1779–86. doi: 10.1182/blood-2009-12-260513
198. Ataga KI, Kutlar A, Kanter J, Liles D, Cancado R, Friedrisch J, et al. Crizanlizumab for the Prevention of Pain Crises in Sickle Cell Disease. *New Engl J Med* (2017) 376(5):429–39. doi: 10.1056/NEJMoa1611770
199. Kutlar A, Kanter J, Liles DK, Alvarez OA, Cancado RD, Friedrisch JR, et al. Effect of crizanlizumab on pain crises in subgroups of patients with sickle cell disease: A SUSTAIN study analysis. *Am J Hematol* (2019) 94(1):55–61. doi: 10.1002/ajh.25308
200. Polanowska-Grabowska R, Wallace K, Field JJ, Chen L, Marshall MA, Figler R, et al. P-selectin-mediated platelet-neutrophil aggregate formation activates neutrophils in mouse and human sickle cell disease. *Arteriosclerosis thrombosis Vasc Biol* (2010) 30(12):2392–9. doi: 10.1161/ATVBAHA.110.211615
201. Keleku-Lukwete N, Suzuki M, Panda H, Otsuki A, Katsuoka F, Saito R, et al. Nrf2 activation in myeloid cells and endothelial cells differentially mitigates sickle cell disease pathology in mice. *Blood Adv* (2019) 3(8):1285–97. doi: 10.1182/bloodadvances.2018017574
202. Merle NS, Paule R, Leon J, Daugan M, Robe-Rybkine T, Poillerat V, et al. P-selectin drives complement attack on endothelium during intravascular hemolysis in TLR-4/heme-dependent manner. *Proc Natl Acad Sci USA* (2019) 116(13):6280–5. doi: 10.1073/pnas.1814797116
203. Bennewitz MF, Jimenez MA, Vats R, Tutuncuoglu E, Jonassaint J, Kato GJ, et al. Lung vaso-occlusion in sickle cell disease mediated by arteriolar neutrophil-platelet microemboli. *JCI Insight* (2017) 2(1):e89761. doi: 10.1172/jci.insight.89761
204. Kato GJ, Martyr S, Blackwelder WC, Nichols JS, Coles WA, Hunter LA, et al. Levels of soluble endothelium-derived adhesion molecules in patients with sickle cell disease are associated with pulmonary hypertension, organ dysfunction, and mortality. *Br J Haematol* (2005) 130(6):943–53. doi: 10.1111/j.1365-2141.2005.05701.x
205. Antwi-Boasiako C, Donkor ES, Sey F, Dzudzor B, Dankwah GB, Otu KH, et al. Levels of Soluble Endothelium Adhesion Molecules and Complications among Sickle Cell Disease Patients in Ghana. *Diseases* (2018) 6(2):1–7. doi: 10.3390/diseases6020029
206. Setty BN, Stuart MJ, Dampier C, Brodecki D, Allen JL. Hypoxaemia in sickle cell disease: biomarker modulation and relevance to pathophysiology. *Lancet* (2003) 362(9394):1450–5. doi: 10.1016/S0140-6736(03)14689-2
207. Elmariah H, Garrett ME, De Castro LM, Jonassaint JC, Ataga KI, Eckman JR, et al. Factors associated with survival in a contemporary adult sickle cell disease cohort. *Am J Hematol* (2014) 89(5):530–5. doi: 10.1002/ajh.23683
208. Keikhaei B, Mohseni AR, Norouzirad R, Alinejadi M, Ghanbari S, Shiravi F, et al. Altered levels of pro-inflammatory cytokines in sickle cell disease patients during vaso-occlusive crises and the steady state condition. *Eur Cytokine Netw* (2013) 24(1):45–52. doi: 10.1684/ecn.2013.0328
209. Khalyfa A, Khalyfa AA, Akbarpour M, Connes P, Romana M, Lapping-Carr G, et al. Extracellular microvesicle microRNAs in children with sickle cell anaemia with divergent clinical phenotypes. *Br J Haematol* (2016) 174(5):786–98. doi: 10.1111/bjh.14104
210. Jain S, Kapetanaki MG, Raghavachari N, Woodhouse K, Yu G, Barge S, et al. Expression of regulatory platelet microRNAs in patients with sickle cell disease. *PloS One* (2013) 8(4):e60932. doi: 10.1371/journal.pone.0060932
211. Barker KR, Lu Z, Kim H, Zheng Y, Chen J, Conroy AL, et al. miR-155 Modifies Inflammation, Endothelial Activation and Blood-Brain Barrier Dysfunction in Cerebral Malaria. *Mol Med (Cambridge Mass)* (2017) 23:24–33. doi: 10.2119/molmed.2016.00139
212. Cohen A, Zinger A, Tiberti N, Grau GER, Combes V. Differential plasma microvesicle and brain profiles of microRNA in experimental cerebral malaria. *Malaria J* (2018) 17(1):192. doi: 10.1186/s12936-018-2330-5
213. Faller M, Matsunaga M, Yin S, Loo JA, Guo F. Heme is involved in microRNA processing. *Nat Struct Mol Biol* (2007) 14(1):23–9. doi: 10.1038/nsmb1182
214. Cimmino A, Calin GA, Fabbri M, Iorio MV, Ferracin M, Shimizu M, et al. miR-15 and miR-16 induce apoptosis by targeting BCL2. *Proc Natl Acad Sci USA* (2005) 102(39):13944–9. doi: 10.1073/pnas.0506654102
215. Chen CZ, Li L, Lodish HF, Bartel DP. MicroRNAs modulate hematopoietic lineage differentiation. *Science* (2004) 303(5654):83–6. doi: 10.1126/science.1091903
216. Brennecke J, Hipfner DR, Stark A, Russell RB, Cohen SM. bantam encodes a developmentally regulated microRNA that controls cell proliferation and regulates the proapoptotic gene hid in Drosophila. *Cell* (2003) 113(1):25–36. doi: 10.1016/S0092-8674(03)00231-9
217. Guo Z, Wu R, Gong J, Zhu W, Li Y, Wang Z, et al. Altered microRNA expression in inflamed and non-inflamed terminal ileal mucosa of adult patients with active Crohn's disease. *J Gastroenterol Hepatology* (2015) 30 (1):109–16. doi: 10.1111/jgh.12644
218. Lu J, Getz G, Miska EA, Alvarez-Saavedra E, Lamb J, Peck D, et al. MicroRNA expression profiles classify human cancers. *Nature* (2005) 435 (7043):834–8. doi: 10.1038/nature03702
219. Alevizos I, Illei GG. MicroRNAs as biomarkers in rheumatic diseases. *Nat Rev Rheumatol* (2010) 6(7):391–8. doi: 10.1038/nrrheum.2010.81
220. Nakasa T, Miyaki S, Okubo A, Hashimoto M, Nishida K, Ochi M, et al. Expression of microRNA-146 in rheumatoid arthritis synovial tissue. *Arthritis Rheumatism* (2008) 58(5):1284–92. doi: 10.1002/art.23429
221. Pekow JR, Kwon JH. MicroRNAs in inflammatory bowel disease. *Inflammatory bowel Diseases* (2012) 18(1):187–93. doi: 10.1002/ibd.21691
222. Tomankova T, Petrek M, Kriegova E. Involvement of microRNAs in physiological and pathological processes in the lung. *Respiratory Res* (2010) 11:159. doi: 10.1186/1465-9921-11-159

223. Weitz SH, Gong M, Barr I, Weiss S, Guo F. Processing of microRNA primary transcripts requires heme in mammalian cells. *Proc Natl Acad Sci USA* (2014) 111(5):1861–6. doi: 10.1073/pnas.1309915111
224. Nguyen TA, Park J, Dang TL, Choi YG, Kim VN. Microprocessor depends on hemin to recognize the apical loop of primary microRNA. *Nucleic Acids Res* (2018) 46(11):5726–36. doi: 10.1093/nar/gky248
225. Barr I, Smith AT, Chen Y, Senturia R, Burstyn JN, Guo F. Ferric, not ferrous, heme activates RNA-binding protein DGCR8 for primary microRNA processing. *Proc Natl Acad Sci USA* (2012) 109(6):1919–24. doi: 10.1073/pnas.1114514109
226. Kirschner MB, Edelman JJ, Kao SC, Vallely MP, van Zandwijk N, Reid G. The Impact of Hemolysis on Cell-Free microRNA Biomarkers. *Front Genet* (2013) 4:94. doi: 10.3389/fgene.2013.00094
227. Pizzamiglio S, Zanutto S, Ciniselli CM, Belfiore A, Bottelli S, Gariboldi M, et al. A methodological procedure for evaluating the impact of hemolysis on circulating microRNAs. *Oncol Lett* (2017) 13(1):315–20. doi: 10.3892/ol.2016.5452
228. Chen SY, Wang Y, Telen MJ, Chi JT. The genomic analysis of erythrocyte microRNA expression in sickle cell diseases. *PloS One* (2008) 3(6):e2360. doi: 10.1371/journal.pone.0002360
229. Byon JC, Papayannopoulou T. MicroRNAs: Allies or foes in erythropoiesis? *J Cell Physiol* (2012) 227(1):7–13. doi: 10.1002/jcp.22729
230. Sangokoya C, Telen MJ, Chi JT. microRNA miR-144 modulates oxidative stress tolerance and associates with anemia severity in sickle cell disease. *Blood* (2010) 116(20):4338–48. doi: 10.1182/blood-2009-04-214817
231. Li B, Zhu X, Ward CM, Starlard-Davenport A, Takezaki M, Berry A, et al. MIR-144-mediated NRF2 gene silencing inhibits fetal hemoglobin expression in sickle cell disease. *Exp Hematol* (2019) 70:85–96 e5. doi: 10.1016/j.exphem.2018.11.002
232. Desai AA, Zhou T, Ahmad H, Zhang W, Mu W, Trevino S, et al. A novel molecular signature for elevated tricuspid regurgitation velocity in sickle cell disease. *Am J Respir Crit Care Med* (2012) 186(4):359–68. doi: 10.1164/rccm.201201-0057OC
233. Ha TY. MicroRNAs in Human Diseases: From Lung, Liver and Kidney Diseases to Infectious Disease, Sickle Cell Disease and Endometrium Disease. *Immune Netw* (2011) 11(6):309–23. doi: 10.4110/in.2011.11.6.309
234. Lu M, Zhang Q, Deng M, Miao J, Guo Y, Gao W, et al. An analysis of human microRNA and disease associations. *PloS One* (2008) 3(10):e3420. doi: 10.1371/journal.pone.0003420
235. Small EM, Frost RJ, Olson EN. MicroRNAs add a new dimension to cardiovascular disease. *Circulation* (2010) 121(8):1022–32. doi: 10.1161/CIRCULATIONAHA.109.889048
236. Barringhaus KG, Zamore PD. MicroRNAs: regulating a change of heart. *Circulation* (2009) 119(16):2217–24. doi: 10.1161/CIRCULATIONAHA.107.715839
237. Latronico MV, Condorelli G. MicroRNAs and cardiac pathology. *Nat Rev Cardiol* (2009) 6(6):419–29. doi: 10.1038/nrcardio.2009.56
238. Jopling CL, Yi M, Lancaster AM, Lemon SM, Sarnow P. Modulation of hepatitis C virus RNA abundance by a liver-specific MicroRNA. *Science* (2005) 309(5740):1577–81. doi: 10.1126/science.1113329
239. Wang K, Zhang S, Marzolf B, Troisch P, Brightman A, Hu Z, et al. Circulating microRNAs, potential biomarkers for drug-induced liver injury. *Proc Natl Acad Sci USA* (2009) 106(11):4402–7. doi: 10.1073/pnas.0813371106
240. Pandey P, Brors B, Srivastava PK, Bott A, Boehn SN, Groene HJ, et al. Microarray-based approach identifies microRNAs and their target functional patterns in polycystic kidney disease. *BMC Genomics* (2008) 9:624. doi: 10.1186/1471-2164-9-624
241. Chaturvedi S, DeBaun MR. Evolution of sickle cell disease from a life-threatening disease of children to a chronic disease of adults: The last 40 years. *Am J Hematol* (2016) 91(1):5–14. doi: 10.1002/ajh.24235
242. Huang E, Parke C, Mehrnia A, Kamgar M, Pham PT, Danovitch G, et al. Improved survival among sickle cell kidney transplant recipients in the recent era. *Nephrol Dial Transplant Off Publ Eur Dialysis Transplant Assoc - Eur Renal Assoc* (2013) 28(4):1039–46. doi: 10.1093/ndt/gfs585
243. Nath KA, Hebbel RP. Sickle cell disease: renal manifestations and mechanisms. *Nat Rev Nephrol* (2015) 11(3):161–71. doi: 10.1038/nrneph.2015.8
244. Day TG, Drasar ER, Fulford T, Sharpe CC, Thein SL. Association between hemolysis and albuminuria in adults with sickle cell anemia. *Haematologica* (2012) 97(2):201–5. doi: 10.3324/haematol.2011.050336
245. Plewes K, Kingston HWF, Ghose A, Maude RJ, Herdman MT, Leopold SJ, et al. Cell-free hemoglobin mediated oxidative stress is associated with acute kidney injury and renal replacement therapy in severe falciparum malaria: an observational study. *BMC Infect Dis* (2017) 17(1):313. doi: 10.1186/s12879-017-2373-1
246. Gaggar A, Patel RP. There is blood in the water: hemolysis, hemoglobin, and heme in acute lung injury. *Am J Physiol Lung Cell Mol Physiol* (2016) 311(4):L714–L8. doi: 10.1152/ajplung.00312.2016
247. Gliozzi ML, Rbaibi Y, Long KR, Vitturi DA, Weisz OA. Hemoglobin alters vitamin carrier uptake and vitamin D metabolism in proximal tubule cells: implications for sickle cell disease. *Am J Physiol Cell Physiol* (2019) 317(5):C993–C1000. doi: 10.1152/ajpcell.00287.2019
248. van Swelm RP, Wetzels JF, Verweij VG, Laarakkers CM, Pertijs JC, van der Wijst J, et al. Renal Handling of Circulating and Renal-Synthesized Hepcidin and Its Protective Effects against Hemoglobin-Mediated Kidney Injury. *J Am Soc Nephrol JASN* (2016) 27(9):2720–32. doi: 10.1681/ASN.2015040461
249. Schein A, Enriquez C, Coates TD, Wood JC. Magnetic resonance detection of kidney iron deposition in sickle cell disease: a marker of chronic hemolysis. *J Magn Reson Imaging* (2008) 28(3):698–704. doi: 10.1002/jmri.21490
250. Vasavda N, Gutierrez L, House MJ, Drasar E, St Pierre TG, Thein SL. Renal iron load in sickle cell disease is influenced by severity of haemolysis. *Br J Haematol* (2012) 157(5):599–605. doi: 10.1111/j.1365-2141.2012.09093.x
251. Gurkan S, Scarponi KJ, Hotchkiss H, Savage B, Drachtman R. Lactate dehydrogenase as a predictor of kidney involvement in patients with sickle cell anemia. *Pediatr Nephrol* (2010) 25(10):2123–7. doi: 10.1007/s00467-010-1560-8
252. Saraf SL, Zhang X, Kanias T, Lash JP, Molokie RE, Oza B, et al. Haemoglobinuria is associated with chronic kidney disease and its progression in patients with sickle cell anaemia. *Br J Haematol* (2014) 164(5):729–39. doi: 10.1111/bjh.12690
253. Barber BE, Grigg MJ, Piera KA, William T, Cooper DJ, Plewes K, et al. Intravascular haemolysis in severe Plasmodium knowlesi malaria: association with endothelial activation, microvascular dysfunction, and acute kidney injury. *Emerging microbes Infect* (2018) 7(1):106. doi: 10.1038/s41426-018-0105-2
254. Nath KA, Grande JP, Haggard JJ, Croatt AJ, Katusic ZS, Solovey A, et al. Oxidative stress and induction of heme oxygenase-1 in the kidney in sickle cell disease. *Am J Pathol* (2001) 158(3):893–903. doi: 10.1016/S0002-9440(10)64037-0
255. Nath KA, Haggard JJ, Croatt AJ, Grande JP, Poss KD, Alam J. The indispensability of heme oxygenase-1 in protecting against acute heme protein-induced toxicity in vivo. *Am J Pathol* (2000) 156(5):1527–35. doi: 10.1016/S0002-9440(10)65024-9
256. Nath KA, Vercellotti GM, Grande JP, Miyoshi H, Paya CV, Manivel JC, et al. Heme protein-induced chronic renal inflammation: suppressive effect of induced heme oxygenase-1. *Kidney Int* (2001) 59(1):106–17. doi: 10.1046/j.1523-1755.2001.00471.x
257. Rubio-Navarro A, Vazquez-Carballo C, Guerrero-Hue M, Garcia-Caballero C, Herencia C, Gutierrez E, et al. Nrf2 Plays a Protective Role Against Intravascular Hemolysis-Mediated Acute Kidney Injury. *Front Pharmacol* (2019) 10:740. doi: 10.3389/fphar.2019.00740
258. Nath KA, Belcher JD, Nath MC, Grande JP, Croatt AJ, Ackerman AW, et al. Role of TLR4 signaling in the nephrotoxicity of heme and heme proteins. *Am J Physiol Renal Physiol* (2018) 314(5):F906–F14. doi: 10.1152/ajprenal.00432.2017
259. Piazza M, Damore G, Costa B, Gioannini TL, Weiss JP, Peri F. Hemin and a metabolic derivative coprohemin modulate the TLR4 pathway differently through different molecular targets. *Innate Immun* (2011) 17(3):293–301. doi: 10.1177/1753425910369020
260. Wei Q, Hill WD, Su Y, Huang S, Dong Z. Heme oxygenase-1 induction contributes to renoprotection by G-CSF during rhabdomyolysis-associated acute kidney injury. *Am J Physiol Renal Physiol* (2011) 301(1):F162–70. doi: 10.1152/ajprenal.00438.2010
261. Gonzalez-Michaca L, Farrugia G, Croatt AJ, Alam J, Nath KA. Heme: a determinant of life and death in renal tubular epithelial cells. *Am J Physiol Renal Physiol* (2004) 286(2):F370–7. doi: 10.1152/ajprenal.00300.2003

262. Irwin DC, Baek JH, Hassell K, Nuss R, Eigenberger P, Lisk C, et al. Hemoglobin-induced lung vascular oxidation, inflammation, and remodeling contribute to the progression of hypoxic pulmonary hypertension and is attenuated in rats with repeated-dose haptoglobin administration. *Free Radical Biol Med* (2015) 82:50–62. doi: 10.1016/j.freeradbiomed.2015.01.012
263. Ghosh S, Adisa OA, Chappa P, Tan F, Jackson KA, Archer DR, et al. Extracellular hemin crisis triggers acute chest syndrome in sickle mice. *J Clin Investig* (2013) 123(11):4809–20. doi: 10.1172/JCI64578
264. Bilan VP, Schneider F, Novelli EM, Kelley EE, Shiva S, Gladwin MT, et al. Experimental intravascular hemolysis induces hemodynamic and pathological pulmonary hypertension: association with accelerated purine metabolism. *Pulmonary circulation* (2018) 8(3):1–15. doi: 10.1177/2045894018791557
265. Shaver CM, Upchurch CP, Janz DR, Grove BS, Putz ND, Wickersham NE, et al. Cell-free hemoglobin: a novel mediator of acute lung injury. *Am J Physiol Lung Cell Mol Physiol* (2016) 310(6):L532–41. doi: 10.1152/ajplung.00155.2015
266. Singla S, Sysol JR, Dille B, Jones N, Chen J, Machado RF. Hemin Causes Lung Microvascular Endothelial Barrier Dysfunction by Necroptotic Cell Death. *Am J Respir Cell Mol Biol* (2017) 57(3):307–14. doi: 10.1165/rcmb.2016-0287OC
267. Liu Y, Jing F, Yi W, Mendelson A, Shi P, Walsh R, et al. HO-1(hi) patrolling monocytes protect against vaso-occlusion in sickle cell disease. *Blood* (2018) 131(14):1600–10. doi: 10.1182/blood-2017-12-819870
268. Feld JJ, Kato GJ, Koh C, Shields T, Hildesheim M, Kleiner DE, et al. Liver injury is associated with mortality in sickle cell disease. *Alimentary Pharmacol Ther* (2015) 42(7):912–21. doi: 10.1111/apt.13347
269. Dey S, Bindu S, Goyal M, Pal C, Alam A, Iqbal MS, et al. Impact of intravascular hemolysis in malaria on liver dysfunction: involvement of hepatic free heme overload, NF-kappaB activation, and neutrophil infiltration. *J Biol Chem* (2012) 287(32):26630–46. doi: 10.1074/jbc.M112.341255
270. Hsu L, Champion H, Campbell-Lee S, Bivalacqua T, Manci E, Diwan B, et al. Hemolysis in sickle cell mice causes pulmonary hypertension due to global impairment in nitric oxide bioavailability. *Blood* (2007) 109(7):3088–98. doi: 10.1182/blood-2006-08-039438
271. Gladwin MT, Kato GJ. Cardiopulmonary complications of sickle cell disease: role of nitric oxide and hemolytic anemia. *Hematol Am Soc Hematol Educ Program* (2005) 2005:51–7. doi: 10.1182/asheducation-2005.1.51
272. Moraes JA, Barcellos-de-Souza P, Rodrigues G, Nascimento-Silva V, Silva SV, Assreuy J, et al. Heme modulates smooth muscle cell proliferation and migration via NADPH oxidase: a counter-regulatory role for heme oxygenase system. *Atherosclerosis* (2012) 224(2):394–400. doi: 10.1016/j.atherosclerosis.2012.07.043
273. Qi L, van Dam RM, Rexrode K, Hu FB. Heme iron from diet as a risk factor for coronary heart disease in women with type 2 diabetes. *Diabetes Care* (2007) 30(1):101–6. doi: 10.2337/dc06-1686
274. Fang X, An P, Wang H, Wang X, Shen X, Li X, et al. Dietary intake of heme iron and risk of cardiovascular disease: a dose-response meta-analysis of prospective cohort studies. *Nutrition metabolism Cardiovasc Dis NMCD* (2015) 25(1):24–35. doi: 10.1016/j.numecd.2014.09.002
275. Ingoglia G, Sag CM, Rex N, De Franceschi L, Vinchi F, Cimino J, et al. Hemopexin counteracts systolic dysfunction induced by heme-driven oxidative stress. *Free Radical Biol Med* (2017) 108:452–64. doi: 10.1016/j.freeradbiomed.2017.04.003
276. Vinchi F, De Franceschi L, Ghigo A, Townes T, Cimino J, Silengo L, et al. Hemopexin therapy improves cardiovascular function by preventing heme-induced endothelial toxicity in mouse models of hemolytic diseases. *Circulation* (2013) 127(12):1317–29. doi: 10.1161/CIRCULATIONAHA.112.130179
277. Khechaduri A, Bayeva M, Chang HC, Ardehali H. Heme levels are increased in human failing hearts. *J Am Coll Cardiol* (2013) 61(18):1884–93. doi: 10.1016/j.jacc.2013.02.012
278. Sawicki KT, Shang M, Wu R, Chang HC, Khechaduri A, Sato T, et al. Increased Heme Levels in the Heart Lead to Exacerbated Ischemic Injury. *J Am Heart Assoc* (2015) 4(8):e002272. doi: 10.1161/JAHA.115.002272
279. Alvarado G, Jeney V, Toth A, Csosz E, Kallo G, Huynh AT, et al. Heme-induced contractile dysfunction in human cardiomyocytes caused by oxidant damage to thick filament proteins. *Free Radical Biol Med* (2015) 89:248–62. doi: 10.1016/j.freeradbiomed.2015.07.158
280. Sundaram N, Tailor A, Mendelsohn L, Wansapura J, Wang X, Higashimoto T, et al. High levels of placenta growth factor in sickle cell disease promote pulmonary hypertension. *Blood* (2010) 116(1):109–12. doi: 10.1182/blood-2009-09-244830
281. Maglione D, Guerriero V, Viglietto G, Delli-Bovi P, Persico MG. Isolation of a human placenta cDNA coding for a protein related to the vascular permeability factor. *Proc Natl Acad Sci U S A* (1991) 88(20):9267–71. doi: 10.1073/pnas.88.20.9267
282. Persico MG, Vincenti V, DiPalma T. Structure, expression and receptor-binding properties of placenta growth factor (PlGF). *Curr Top Microbiol Immunol* (1999) 237:31–40. doi: 10.1007/978-3-642-59953-8_2
283. Iyer S, Leonidas DD, Swaminathan GJ, Maglione D, Battisti M, Tucci M, et al. The crystal structure of human placenta growth factor-1 (PlGF-1), an angiogenic protein, at 2.0 A resolution. *J Biol Chem* (2001) 276(15):12153–61. doi: 10.1074/jbc.M008055200
284. Park JE, Chen HH, Winer J, Houck KA, Ferrara N. Placenta growth factor. Potentiation of vascular endothelial growth factor bioactivity, in vitro and in vivo, and high affinity binding to Flt-1 but not to Flk-1/KDR. *J Biol Chem* (1994) 269(41):25646–54. doi: 10.1074/jbc.M008055200
285. Carmeliet P, Moons L, Luttun A, Vincenti V, Compernolle V, De Mol M, et al. Synergism between vascular endothelial growth factor and placental growth factor contributes to angiogenesis and plasma extravasation in pathological conditions. *Nat Med* (2001) 7(5):575–83. doi: 10.1038/87904
286. Tarallo V, Vesci L, Capasso O, Esposito MT, Riccioni T, Pastore L, et al. A placental growth factor variant unable to recognize vascular endothelial growth factor (VEGF) receptor-1 inhibits VEGF-dependent tumor angiogenesis via heterodimerization. *Cancer Res* (2010) 70(5):1804–13. doi: 10.1158/0008-5472.CAN-09-2609
287. Autiero M, Waltenberger J, Communi D, Kranz A, Moons L, Lambrechts D, et al. Role of PlGF in the intra- and intermolecular cross talk between the VEGF receptors Flt1 and Flk1. *Nat Med* (2003) 9(7):936–43. doi: 10.1038/nm884
288. Mamluk R, Gechtman Z, Kutcher ME, Gasiunas N, Gallagher J, Klagsbrun M. Neuropilin-1 binds vascular endothelial growth factor 165, placenta growth factor-2, and heparin via its b1b2 domain. *J Biol Chem* (2002) 277(27):24818–25. doi: 10.1074/jbc.M200730200
289. Gaur P, Bielenberg DR, Samuel S, Bose D, Zhou Y, Gray MJ, et al. Role of class 3 semaphorins and their receptors in tumor growth and angiogenesis. *Clin Cancer Res* (2009) 15(22):6763–70. doi: 10.1158/1078-0432.CCR-09-1810
290. Roy H, Bhardwaj S, Babu M, Jauhiainen S, Herzig KH, Bellu AR, et al. Adenovirus-mediated gene transfer of placental growth factor to perivascular tissue induces angiogenesis via upregulation of the expression of endogenous vascular endothelial growth factor-A. *Hum Gene Ther* (2005) 16(12):1422–8. doi: 10.1089/hum.2005.16.1422
291. Marcellini M, De Luca N, Riccioni T, Ciucci A, Orecchia A, Lacal PM, et al. Increased melanoma growth and metastasis spreading in mice overexpressing placenta growth factor. *Am J Pathol* (2006) 169(2):643–54. doi: 10.2353/ajpath.2006.051041
292. Huang XX, McCaughan GW, Shackel NA, Gorrell MD. Up-regulation of proproliferative genes and the ligand/receptor pair placental growth factor and vascular endothelial growth factor receptor 1 in hepatitis C cirrhosis. *Liver Int* (2007) 27(7):960–8. doi: 10.1111/j.1478-3231.2007.01542.x
293. Clauss M, Weich H, Breier G, Knies U, Röckl W, Waltenberger J, et al. The Vascular Endothelial Growth Factor Receptor Flt-1 Mediates Biological Activities: Implications For A Functional Role Of Placenta Growth Factor In Monocyte Activation And Chemotaxis. *J Biol Chem* (1996) 271(30):17629–34. doi: 10.1074/jbc.271.30.17629
294. Kelly BD, Hackett SF, Hirota K, Oshima Y, Cai Z, Berg-Dixon S, et al. Cell type-specific regulation of angiogenic growth factor gene expression and induction of angiogenesis in nonischemic tissue by a constitutively active form of hypoxia-inducible factor 1. *Circ Res* (2003) 93(11):1074–81. doi: 10.1161/01.RES.0000102937.50486.1B
295. Green CJ, Lichtlen P, Huynh NT, Yanovsky M, Laderoute KR, Schaffner W, et al. Placenta growth factor gene expression is induced by hypoxia in

fibroblasts: a central role for metal transcription factor-1. *Cancer Res* (2001) 61(6):2696–703. doi: 10.1074/jbc.271.30.17629
296. Cramer M, Nagy I, Murphy BJ, Gassmann M, Hottiger MO, Georgiev O, et al. NF-kappaB contributes to transcription of placenta growth factor and interacts with metal responsive transcription factor-1 in hypoxic human cells. *Biol Chem* (2005) 386(9):865–72. doi: 10.1515/BC.2005.101
297. Zhang H, Palmer R, Gao X, Kreidberg J, Gerald W, Hsiao L, et al. Transcriptional activation of placental growth factor by the forkhead/winged helix transcription factor FoxD1. *Curr Biol* (2003) 13(18):1625–9. doi: 10.1016/j.cub.2003.08.054
298. Chiu YH, Yang MR, Wang LJ, Chen MH, Chang GD, Chen H. New insights into the regulation of placental growth factor gene expression by the transcription factors GCM1 and DLX3 in human placenta. *J Biol Chem* (2018) 293(25):9801–11. doi: 10.1074/jbc.RA117.001384
299. Yao YG, Yang HS, Cao Z, Danielsson J, Duh EJ. Upregulation of placental growth factor by vascular endothelial growth factor via a post-transcriptional mechanism. *FEBS Lett* (2005) 579(5):1227–34. doi: 10.1016/j.febslet.2005.01.017
300. Shaw JH, Lloyd PG. Post-transcriptional regulation of placenta growth factor mRNA by hydrogen peroxide. *Microvasc Res* (2012) 84(2):155–60. doi: 10.1016/j.mvr.2012.05.009
301. Dewerchin M, Carmeliet P. PlGF: A Multitasking Cytokine with Disease-Restricted Activity. *Cold Spring Harbor Perspect Med* (2012) 2(8):1227–34. doi: 10.1101/cshperspect.a011056
302. Rakic JM, Lambert V, Devy L, Luttun A, Carmeliet P, Claes C, et al. Placental growth factor, a member of the VEGF family, contributes to the development of choroidal neovascularization. *Invest Ophthalmol Vis Sci* (2003) 44 (7):3186–93. doi: 10.1167/iovs.02-1092
303. Luttun A, Tjwa M, Moons L, Wu Y, Angelillo-Scherrer A, Liao F, et al. Revascularization of ischemic tissues by PlGF treatment, and inhibition of tumor angiogenesis, arthritis and atherosclerosis by anti-Flt1. *Nat Med* (2002) 8(8):831–40. doi: 10.1038/nm731
304. De Falco S. The discovery of placenta growth factor and its biological activity. *Exp Mol Med* (2012) 44(1):1–9. doi: 10.3858/emm.2012.44.1.025
305. Oura H, Bertoncini J, Velasco P, Brown LF, Carmeliet P, Detmar M. A critical role of placental growth factor in the induction of inflammation and edema formation. *Blood* (2003) 101(2):560–7. doi: 10.1182/blood-2002-05-1516
306. Yoo SA, Yoon HJ, Kim HS, Chae CB, De Falco S, Cho CS, et al. Role of placenta growth factor and its receptor flt-1 in rheumatoid inflammation: a link between angiogenesis and inflammation. *Arthritis Rheumatol* (2009) 60 (2):345–54. doi: 10.1002/art.24289
307. Maes C, Coenegrachts L, Stockmans I, Daci E, Luttun A, Petryk A, et al. Placental growth factor mediates mesenchymal cell development, cartilage turnover, and bone remodeling during fracture repair. *J Clin Invest* (2006) 116(5):1230–42. doi: 10.1172/JCI26772
308. Rolny C, Mazzone M, Tugues S, Laoui D, Johansson I, Coulon C, et al. HRG inhibits tumor growth and metastasis by inducing macrophage polarization and vessel normalization through downregulation of PlGF. *Cancer Cell* (2011) 19(1):31–44. doi: 10.1016/j.ccr.2010.11.009
309. Lin YL, Liang YC, Chiang BL. Placental growth factor down-regulates type 1 T helper immune response by modulating the function of dendritic cells. *J Leukoc Biol* (2007) 82(6):1473–80. doi: 10.1189/jlb.0307164
310. Carnevale D, Cifelli G, Mascio G, Madonna M, Sbroggio M, Perrino C, et al. Placental growth factor regulates cardiac inflammation through the tissue inhibitor of metalloproteinases-3/tumor necrosis factor-alpha-converting enzyme axis: crucial role for adaptive cardiac remodeling during cardiac pressure overload. *Circulation* (2011) 124(12):1337–50. doi: 10.1161/CIRCULATIONAHA.111.050500
311. Hattori K, Heissig B, Wu Y, Dias S, Tejada R, Ferris B, et al. Placental growth factor reconstitutes hematopoiesis by recruiting VEGFR1(+) stem cells from bone-marrow microenvironment. *Nat Med* (2002) 8(8):841–9. doi: 10.1038/nm740
312. Carlo-Stella C, Di Nicola M, Longoni P, Cleris L, Lavazza C, Milani R, et al. Placental growth factor-1 potentiates hematopoietic progenitor cell mobilization induced by granulocyte colony-stimulating factor in mice and nonhuman primates. *Stem Cells* (2007) 25(1):252–61. doi: 10.1634/stemcells.2006-0020
313. Kalra VK, Zhang S, Malik P, Tahara SM. Placenta growth factor mediated gene regulation in sickle cell disease. *Blood Rev* (2018) 32(1):61–70. doi: 10.1016/j.blre.2017.08.008
314. Patel N, Gonsalves CS, Malik P, Kalra VK. Placenta growth factor augments endothelin-1 and endothelin-B receptor expression via hypoxia-inducible factor-1α. *Blood* (2008) 112(3):856–65. doi: 10.1182/blood-2007-12-130567
315. Brittain JE, Hulkower B, Jones SK, Strayhorn D, De Castro L, Telen MJ, et al. Placenta growth factor in sickle cell disease: association with hemolysis and inflammation. *Blood* (2010) 115(10):2014–20. doi: 10.1182/blood-2009-04-217950
316. Perelman N, Selvaraj SK, Batra S, Luck LR, Erdreich-Epstein A, Coates TD, et al. Placenta growth factor activates monocytes and correlates with sickle cell disease severity. *Blood* (2003) 102(4):1506–14. doi: 10.1182/blood-2002-11-3422
317. Gu J-M, Yuan S, Sim D, Abe K, Liu P, Rosenbruch M, et al. Blockade of placental growth factor reduces vaso-occlusive complications in murine models of sickle cell disease. *Exp Hematol* (2018) 60:73–82.e3. doi: 10.1016/j.exphem.2018.01.002
318. Gladwin MT, Sachdev V, Jison ML, Shizukuda Y, Plehn JF, Minter K, et al. Pulmonary hypertension as a risk factor for death in patients with sickle cell disease. *New Engl J Med* (2004) 350(9):886–95. doi: 10.1056/NEJMoa035477
319. Graido-Gonzalez E, Doherty JC, Bergreen EW, Organ G, Telfer M, McMillen MA. Plasma endothelin-1, cytokine, and prostaglandin E2 levels in sickle cell disease and acute vaso-occlusive sickle crisis. *Blood* (1998) 92(7):2551–5. doi: 10.1182/blood.V92.7.2551
320. Rybicki AC, Benjamin LJ. Increased levels of endothelin-1 in plasma of sickle cell anemia patients. *Blood* (1998) 92(7):2594–6. doi: 10.1182/blood.V92.7.2594.2594_2594_2596
321. Qari MH, Dier U, Mousa SA. Biomarkers of inflammation, growth factor, and coagulation activation in patients with sickle cell disease. *Clin Appl Thromb Hemost* (2012) 18(2):195–200. doi: 10.1177/1076029611420992
322. Li C, Gonsalves CS, Eiymo Mwa Mpollo MS, Malik P, Tahara SM, Kalra VK. MicroRNA 648 Targets ET-1 mRNA and is cotranscriptionally regulated with MICAL3 by PAX5. *Mol Cell Biol* (2015) 35(3):514–28. doi: 10.1128/MCB.01199-14
323. Gonsalves CS, Li C, Malik P, Tahara SM, Kalra VK. Peroxisome proliferator-activated receptor-alpha-mediated transcription of miR-301a and miR-454 and their host gene SKA2 regulates endothelin-1 and PAI-1 expression in sickle cell disease. *Biosci Rep* (2015) 35(6):195–200. doi: 10.1042/BSR20150190
324. Li C, Mpollo MS, Gonsalves CS, Tahara SM, Malik P, Kalra VK. Peroxisome proliferator-activated receptor-alpha-mediated transcription of miR-199a2 attenuates endothelin-1 expression via hypoxia-inducible factor-1alpha. *J Biol Chem* (2014) 289(52):36031–47. doi: 10.1074/jbc.M114.600775
325. Li C, Zhou Y, Loberg A, Tahara SM, Malik P, Kalra VK. Activated Transcription Factor 3 in Association with Histone Deacetylase 6 Negatively Regulates MicroRNA 199a2 Transcription by Chromatin Remodeling and Reduces Endothelin-1 Expression. *Mol Cell Biol* (2016) 36(22):2838–54. doi: 10.1128/MCB.00345-16
326. Patel N, Sundaram N, Yang M, Madigan C, Kalra VK, Malik P. Placenta Growth Factor (PlGF), a Novel Inducer of Plasminogen Activator Inhibitor-1 (PAI-1) in Sickle Cell Disease (SCD). *J Biol Chem* (2010) 285(22):16713–22. doi: 10.1074/jbc.M110.101691
327. Nsiri B, Gritli N, Mazigh C, Ghazouani E, Fattoum S, Machghoul S. Fibrinolytic response to venous occlusion in patients with homozygous sickle cell disease. *Hematol Cell Ther* (1997) 39(5):229–32. doi: 10.1007/s00282-997-0229-7
328. Hillery CA, Panepinto JA. Pathophysiology of stroke in sickle cell disease. *Microcirculation* (2004) 11(2):195–208. doi: 10.1080/10739680490278600
329. Patel N, Tahara SM, Malik P, Kalra VK. Involvement of miR-30c and miR-301a in immediate induction of plasminogen activator inhibitor-1 by placental growth factor in human pulmonary endothelial cells. *Biochem J* (2011) 434(3):473–82. doi: 10.1042/BJ20101585
330. Leong MA, Dampier C, Varlotta L, Allen JL. Airway hyperreactivity in children with sickle cell disease. *J Pediatr* (1997) 131(2):278–83. doi: 10.1016/S0022-3476(97)70166-5

331. Field JJ, Stocks J, Kirkham FJ, Rosen CL, Dietzen DJ, Semon T, et al. Airway hyperresponsiveness in children with sickle cell anemia. *Chest* (2011) 139 (3):563–8. doi: 10.1378/chest.10-1243
332. Eiymo Mwa Mpollo M-S, Brandt EB, Shanmukhappa SK, Arumugam PI, Tiwari S, Loberg A, et al. Placenta growth factor augments airway hyperresponsiveness via leukotrienes and IL-13. *J Clin Invest* (2016) 126 (2):571–84. doi: 10.1172/JCI77250
333. Patel N, Gonsalves CS, Yang M, Malik P, Kalra VK. Placenta growth factor induces 5-lipoxygenase-activating protein to increase leukotriene formation in sickle cell disease. *Blood* (2009) 113(5):1129–38. doi: 10.1182/blood-2008-07-169821
334. Turhan A, Weiss LA, Mohandas N, Coller BS, Frenette PS. Primary role for adherent leukocytes in sickle cell vascular occlusion: a new paradigm. *Proc Natl Acad Sci USA* (2002) 99(5):3047–51. doi: 10.1073/pnas.052522799
335. Selvaraj SK, Giri RK, Perelman N, Johnson C, Malik P, Kalra VK. Mechanism of monocyte activation and expression of proinflammatory cytochemokines by placenta growth factor. *Blood* (2003) 102(4):1515–24. doi: 10.1182/blood-2002-11-3423
336. Kaul DK, Liu XD, Choong S, Belcher JD, Vercellotti GM, Hebbel RP. Anti-inflammatory therapy ameliorates leukocyte adhesion and microvascular flow abnormalities in transgenic sickle mice. *Am J Physiol - Heart Circulatory Physiol* (2004) 287(1 56-1):H293–301. doi: 10.1152/ajpheart.01150.2003
337. Mousavi Z, Yazdani Z, Moradabadi A, Hoseinpourkasgari F, Hassanshahi G. Role of some members of chemokine/cytokine network in the pathogenesis of thalassemia and sickle cell hemoglobinopathies: a mini review. *Exp Hematol Oncol* (2019) 8(1):21. doi: 10.1186/s40164-019-0145-x
338. Gonsalves CS, Li C, Mpollo MS, Pullarkat V, Malik P, Tahara SM, et al. Erythropoietin-mediated expression of placenta growth factor is regulated via activation of hypoxia-inducible factor-1alpha and post-transcriptionally by miR-214 in sickle cell disease. *Biochem J* (2015) 468(3):409–23. doi: 10.1042/BJ20141138
339. Zakiyanov O, Kalousová M, Zima T, Tesař V. Placental Growth Factor in Patients with Decreased Renal Function. *Renal Failure* (2011) 33(3):291–7. doi: 10.3109/0886022X.2011.560402
340. Matsui M, Uemura S, Takeda Y, Samejima K, Matsumoto T, Hasegawa A, et al. Placental Growth Factor as a Predictor of Cardiovascular Events in Patients with CKD from the NARA-CKD Study. *J Am Soc Nephrol* (2015) 26 (11):2871–81. doi: 10.1681/ASN.2014080772
341. Ataga KI, Derebail VK, Caughey M, Elsherif L, Shen JH, Jones SK, et al. Albuminuria Is Associated with Endothelial Dysfunction and Elevated Plasma Endothelin-1 in Sickle Cell Anemia. *PloS One* (2016) 11(9): e0162652. doi: 10.1371/journal.pone.0162652
342. Heimlich JB, Speed JS, O'Connor PM, Pollock JS, Townes TM, Meiler SE, et al. Endothelin-1 contributes to the progression of renal injury in sickle cell disease via reactive oxygen species. *Br J Pharmacol* (2016) 173(2):386–95. doi: 10.1111/bph.13380
343. Gbotosho OT, Ghosh S, Kapetanaki MG, Lin Y, Weidert F, Bullock GC, et al. Cardiac expression of HMOX1 and PGF in sickle cell mice and haem-treated wild type mice dominates organ expression profiles via Nrf2 (Nfe2l2). *Br J Haematol* (2019) 187(5):666–75. doi: 10.1111/bjh.16129
344. Malgorzewicz S, Skrzypczak-Jankun E, Jankun J. Plasminogen activator inhibitor-1 in kidney pathology (Review). *Int J Mol Med* (2013) 31(3):503–10. doi: 10.3892/ijmm.2013.1234
345. Gladwin MT, Sachdev V. Cardiovascular abnormalities in sickle cell disease. *J Am Coll Cardiol* (2012) 59(13):1123–33. doi: 10.1016/j.jacc.2011.10.900
346. Peiskerová M, Kalousová M, Danzig V, Míková B, Hodková M, Němeček E, et al. Placental growth factor may predict increased left ventricular mass index in patients with mild to moderate chronic kidney disease–a prospective observational study. *BMC Nephrol* (2013) 14:142–. doi: 10.1186/1471-2369-14-142
347. Pilarczyk K, Sattler KJ, Galili O, Versari D, Olson ML, Meyer FB, et al. Placenta growth factor expression in human atherosclerotic carotid plaques is related to plaque destabilization. *Atherosclerosis* (2008) 196(1):333–40. doi: 10.1016/j.atherosclerosis.2006.10.038
348. Khurana R, Moons L, Shafi S, Luttun A, Collen D, Martin JF, et al. Placental growth factor promotes atherosclerotic intimal thickening and macrophage accumulation. *Circulation* (2005) 111(21):2828–36. doi: 10.1161/CIRCULATIONAHA.104.495887
349. Heeschen C, Dimmeler S, Fichtlscherer S, Hamm CW, Berger J, Simoons ML, et al. Prognostic Value of Placental Growth Factor in Patients With Acute Chest Pain. *JAMA* (2004) 291(4):435–41. doi: 10.1001/jama.291.4.435
350. Jaba IM, Zhuang ZW, Li N, Jiang Y, Martin KA, Sinusas AJ, et al. NO triggers RGS4 degradation to coordinate angiogenesis and cardiomyocyte growth. *J Clin Invest* (2013) 123(4):1718–31. doi: 10.1172/JCI65112
351. Accornero F, van Berlo JH, Benard MJ, Lorenz JN, Carmeliet P, Molkentin JD. Placental growth factor regulates cardiac adaptation and hypertrophy through a paracrine mechanism. *Circ Res* (2011) 109(3):272–80. doi: 10.1161/CIRCRESAHA.111.240820
352. Harada E, Nakagawa O, Yoshimura M, Harada M, Nakagawa M, Mizuno Y, et al. Effect of interleukin-1 beta on cardiac hypertrophy and production of natriuretic peptides in rat cardiocyte culture. *J Mol Cell Cardiol* (1999) 31 (11):1997–2006. doi: 10.1006/jmcc.1999.1030
353. Wang L, Zhang YL, Lin QY, Liu Y, Guan XM, Ma XL, et al. CXCL1-CXCR2 axis mediates angiotensin II-induced cardiac hypertrophy and remodelling through regulation of monocyte infiltration. *Eur Heart J* (2018) 39(20):1818–31. doi: 10.1093/eurheartj/ehy085
354. Nakamura T, Funayama H, Kubo N, Yasu T, Kawakami M, Momomura S, et al. Elevation of plasma placental growth factor in the patients with ischemic cardiomyopathy. *Int J Cardiol* (2009) 131(2):186–91. doi: 10.1016/j.ijcard.2007.10.050
355. Kolakowski SJr., Berry MF, Atluri P, Grand T, Fisher O, Moise MA, et al. Placental growth factor provides a novel local angiogenic therapy for ischemic cardiomyopathy. *J Card Surg* (2006) 21(6):559–64. doi: 10.1111/j.1540-8191.2006.00296.x
356. Rolla S, Ingoglia G, Bardina V, Silengo L, Altruda F, Novelli F, et al. Acute-phase protein hemopexin is a negative regulator of Th17 response and experimental autoimmune encephalomyelitis development. *J Immunol* (2013) 191(11):5451–9. doi: 10.4049/jimmunol.1203076
357. Morse D, Pischke SE, Zhou Z, Davis RJ, Flavell RA, Loop T, et al. Suppression of inflammatory cytokine production by carbon monoxide involves the JNK pathway and AP-1. *J Biol Chem* (2003) 278(39):36993–8. doi: 10.1074/jbc.M302942200
358. Zimmermann M, Aguilera FB, Castellucci M, Rossato M, Costa S, Lunardi C, et al. Chromatin remodelling and autocrine TNFalpha are required for optimal interleukin-6 expression in activated human neutrophils. *Nat Commun* (2015) 6:6061. doi: 10.1038/ncomms7061
359. Zimmermann M, Arruda-Silva F, Bianchetto-Aguilera F, Finotti G, Calzetti F, Scapini P, et al. IFNalpha enhances the production of IL-6 by human neutrophils activated via TLR8. *Sci Rep* (2016) 6:19674. doi: 10.1038/srep19674
360. Chi L, Li Y, Stehno-Bittel L, Gao J, Morrison DC, Stechschulte DJ, et al. Interleukin-6 production by endothelial cells via stimulation of protease-activated receptors is amplified by endotoxin and tumor necrosis factor-alpha. *J interferon cytokine Res Off J Int Soc Interferon Cytokine Res* (2001) 21 (4):231–40. doi: 10.1089/107999001750169871
361. Zampetaki A, Zhang Z, Hu Y, Xu Q. Biomechanical stress induces IL-6 expression in smooth muscle cells via Ras/Rac1-p38 MAPK-NF-kappaB signaling pathways. *Am J Physiol Heart Circ Physiol* (2005) 288(6):H2946–54. doi: 10.1152/ajpheart.00919.2004
362. Fredj S, Bescond J, Louault C, Delwail A, Lecron JC, Potreau D. Role of interleukin-6 in cardiomyocyte/cardiac fibroblast interactions during myocyte hypertrophy and fibroblast proliferation. *J Cell Physiol* (2005) 204 (2):428–36. doi: 10.1002/jcp.20307
363. Sano M, Fukuda K, Kodama H, Pan J, Saito M, Matsuzaki J, et al. Interleukin-6 family of cytokines mediate angiotensin II-induced cardiac hypertrophy in rodent cardiomyocytes. *J Biol Chem* (2000) 275(38):29717–23. doi: 10.1074/jbc.M003128200
364. Fontes JA, Rose NR, Cihakova D. The varying faces of IL-6: From cardiac protection to cardiac failure. *Cytokine* (2015) 74(1):62–8. doi: 10.1016/j.cyto.2014.12.024
365. Su H, Lei CT, Zhang C. Interleukin-6 Signaling Pathway and Its Role in Kidney Disease: An Update. *Front Immunol* (2017) 8:405. doi: 10.3389/fimmu.2017.00405

366. Peters M, Muller AM, Rose-John S. Interleukin-6 and soluble interleukin-6 receptor: direct stimulation of gp130 and hematopoiesis. *Blood* (1998) 92 (10):3495–504. doi: 10.1182/blood.V92.10.3495.422k47_3495_3504
367. Guo Y, Xu F, Lu T, Duan Z, Zhang Z. Interleukin-6 signaling pathway in targeted therapy for cancer. *Cancer Treat Rev* (2012) 38(7):904–10. doi: 10.1016/j.ctrv.2012.04.007
368. Hirano T, Yasukawa K, Harada H, Taga T, Watanabe Y, Matsuda T, et al. Complementary DNA for a novel human interleukin (BSF-2) that induces B lymphocytes to produce immunoglobulin. *Nature* (1986) 324(6092):73–6. doi: 10.1038/324073a0
369. Lacroix M, Rousseau F, Guilhot F, Malinge P, Magistrelli G, Herren S, et al. Novel Insights into Interleukin 6 (IL-6) Cis- and Trans-signaling Pathways by Differentially Manipulating the Assembly of the IL-6 Signaling Complex. *J Biol Chem* (2015) 290(45):26943–53. doi: 10.1074/jbc.M115.682138
370. Scheller J, Garbers C, Rose-John S. Interleukin-6: from basic biology to selective blockade of pro-inflammatory activities. *Semin Immunol* (2014) 26 (1):2–12. doi: 10.1016/j.smim.2013.11.002
371. Mihara M, Hashizume M, Yoshida H, Suzuki M, Shiina M. IL-6/IL-6 receptor system and its role in physiological and pathological conditions. *Clin Sci (Lond)* (2012) 122(4):143–59. doi: 10.1042/CS20110340
372. Jones SA, Scheller J, Rose-John S. Therapeutic strategies for the clinical blockade of IL-6/gp130 signaling. *J Clin Invest* (2011) 121(9):3375–83. doi: 10.1172/JCI57158
373. Lyke KE, Burges R, Cissoko Y, Sangare L, Dao M, Diarra I, et al. Serum levels of the proinflammatory cytokines interleukin-1 beta (IL-1beta), IL-6, IL-8, IL-10, tumor necrosis factor alpha, and IL-12(p70) in Malian children with severe Plasmodium falciparum malaria and matched uncomplicated malaria or healthy controls. *Infection Immunity* (2004) 72(10):5630–7. doi: 10.1128/IAI.72.10.5630-5637.2004
374. Nayak KC, Meena SL, Gupta BK, Kumar S, Pareek V. Cardiovascular involvement in severe vivax and falciparum malaria. *J Vector Borne Dis* (2013) 50(4):285–91. doi: 10.1074/jbc.M115.682138
375. Finkel MS, Oddis CV, Jacob TD, Watkins SC, Hattler BG, Simmons RL. Negative inotropic effects of cytokines on the heart mediated by nitric oxide. *Science* (1992) 257(5068):387–9. doi: 10.1126/science.1631560
376. Burwick RM, Rincon M, Beeraka SS, Gupta M, Feinberg BB. Evaluation of Hemolysis as a Severe Feature of Preeclampsia. *Hypertension (Dallas Tex 1979)* (2018) 72(2):460–5. doi: 10.1161/HYPERTENSIONAHA.118.11211
377. Kumar S, Wang G, Zheng N, Cheng W, Ouyang K, Lin H, et al. HIMF (Hypoxia-Induced Mitogenic Factor)-IL (Interleukin)-6 Signaling Mediates Cardiomyocyte-Fibroblast Crosstalk to Promote Cardiac Hypertrophy and Fibrosis. *Hypertension (Dallas Tex 1979)* (2019) 73(5):1058–70. doi: 10.1161/HYPERTENSIONAHA.118.12267
378. Melendez GC, McLarty JL, Levick SP, Du Y, Janicki JS, Brower GL. Interleukin 6 mediates myocardial fibrosis, concentric hypertrophy, and diastolic dysfunction in rats. *Hypertension (Dallas Tex 1979)* (2010) 56 (2):225–31. doi: 10.1161/HYPERTENSIONAHA.109.148635
379. Dinh W, Futh R, Nickl W, Krahn T, Ellinghaus P, Scheffold T, et al. Elevated plasma levels of TNF-alpha and interleukin-6 in patients with diastolic dysfunction and glucose metabolism disorders. *Cardiovasc Diabetol* (2009) 8:58. doi: 10.1186/1475-2840-8-58
380. Sugishita K, Kinugawa K, Shimizu T, Harada K, Matsui H, Takahashi T, et al. Cellular basis for the acute inhibitory effects of IL-6 and TNF- alpha on excitation-contraction coupling. *J Mol Cell Cardiol* (1999) 31(8):1457–67. doi: 10.1006/jmcc.1999.0989
381. Hagiwara Y, Miyoshi S, Fukuda K, Nishiyama N, Ikegami Y, Tanimoto K, et al. SHP2-mediated signaling cascade through gp130 is essential for LIF-dependent I CaL, [Ca2+]i transient, and APD increase in cardiomyocytes. *J Mol Cell Cardiol* (2007) 43(6):710–6. doi: 10.1016/j.yjmcc.2007.09.004
382. Drosatos K, Lymperopoulos A, Kennel PJ, Pollak N, Schulze PC, Goldberg IJ. Pathophysiology of sepsis-related cardiac dysfunction: driven by inflammation, energy mismanagement, or both? *Curr Heart failure Rep* (2015) 12(2):130–40. doi: 10.1007/s11897-014-0247-z
383. Zhang W, Qu X, Chen B, Snyder M, Wang M, Li B, et al. Critical Roles of STAT3 in beta-Adrenergic Functions in the Heart. *Circulation* (2016) 133 (1):48–61. doi: 10.1161/CIRCULATIONAHA.115.017472
384. de Montmollin E, Aboab J, Mansart A, Annane D. Bench-to-bedside review: Beta-adrenergic modulation in sepsis. *Crit Care* (2009) 13(5):230. doi: 10.1186/cc8026
385. Wang Y, Lewis DF, Gu Y, Zhao S, Groome LJ. Elevated maternal soluble Gp130 and IL-6 levels and reduced Gp130 and SOCS-3 expressions in women complicated with preeclampsia. *Hypertension (Dallas Tex 1979)* (2011) 57(2):336–42. doi: 10.1161/HYPERTENSIONAHA.110.163360
386. Lamarca B, Brewer J, Wallace K. IL-6-induced pathophysiology during pre-eclampsia: potential therapeutic role for magnesium sulfate? *Int J interferon cytokine Mediator Res* (2011) 2011(3):59–64. doi: 10.2147/IJICMR.S16320
387. Sarray S, Saleh LR, Lisa Saldanha F, Al-Habboubi HH, Mahdi N, Almawi WY. Serum IL-6, IL-10, and TNFalpha levels in pediatric sickle cell disease patients during vasoocclusive crisis and steady state condition. *Cytokine* (2015) 72(1):43–7. doi: 10.1016/j.cyto.2014.11.030
388. Taylor SC, Shacks SJ, Mitchell RA, Banks A. Serum interleukin-6 levels in the steady state of sickle cell disease. *J interferon cytokine Res Off J Int Soc Interferon Cytokine Res* (1995) 15(12):1061–4. doi: 10.1089/jir.1995.15.1061
389. Lester LA, Sodt PC, Hutcheon N, Arcilla RA. Cardiac abnormalities in children with sickle cell anemia. *Chest* (1990) 98(5):1169–74. doi: 10.1378/chest.98.5.1169
390. Faro GB, Menezes-Neto OA, Batista GS, Silva-Neto AP, Cipolotti R. Left ventricular hypertrophy in children, adolescents and young adults with sickle cell anemia. *Rev Bras Hematol Hemoter* (2015) 37(5):324–8. doi: 10.1016/j.bjhh.2015.07.001
391. Crocker P, Werb Z, Gordon S, Bainton D. Ultrastructural localization of a macrophage-restricted sialic acid binding hemagglutinin, SER, in macrophage-hematopoietic cell clusters. *Blood* (1990) 76(6):1131–8. doi: 10.1182/blood.V76.6.1131.bloodjournal7661131
392. Gbotosho OT, Kapetanaki MG, Ghosh S, Villanueva FS, Ofori-Acquah SF, Kato GJ. Heme Induces IL-6 and Cardiac Hypertrophy Genes Transcripts in Sickle Cell Mice. *Front Immunol* (2020) 72(1):43–7. doi: 10.3389/fimmu.2020.01910
393. Ingoglia G, Sag CM, Rex N, De Franceschi L, Vinchi F, Cimino J, et al. Data demonstrating the anti-oxidant role of hemopexin in the heart. *Data Brief* (2017) 13:69–76. doi: 10.1016/j.dib.2017.05.026
394. Strouse JJ, Heeney MM. Hydroxyurea for the treatment of sickle cell disease: efficacy, barriers, toxicity, and management in children. *Pediatr Blood Cancer* (2012) 59(2):365–71. doi: 10.1002/pbc.24178
395. Kato GJ. New insights into sickle cell disease: mechanisms and investigational therapies. *Curr Opin Hematol* (2016) 23(3):224–32. doi: 10.1097/MOH.0000000000000241
396. Rees D, Williams T, Gladwin M. Sickle-cell disease. *Lancet* (2010) 376 (9757):2018–31. doi: 10.1016/S0140-6736(10)61029-X
397. Kato GJ, Piel FB, Reid CD, Gaston MH, Ohene-Frempong K, Krishnamurti L, et al. Sickle cell disease. *Nat Rev Dis Primers* (2018) 4:18010. doi: 10.1038/nrdp.2018.10
398. Zimmerman SA, Schultz WH, Burgett S, Mortier NA, Ware RE. Hydroxyurea therapy lowers transcranial Doppler flow velocities in children with sickle cell anemia. *Blood* (2007) 110(3):1043–7. doi: 10.1182/blood-2006-11-057893
399. Platt OS. Hydroxyurea for the treatment of sickle cell anemia. *New Engl J Med* (2008) 358(13):1362–9. doi: 10.1056/NEJMct0708272
400. Wang WC, Ware RE, Miller ST, Iyer RV, Casella JF, Minniti CP, et al. Hydroxycarbamide in very young children with sickle-cell anaemia: a multicentre, randomised, controlled trial (BABY HUG). *Lancet* (2011) 377 (9778):1663–72. doi: 10.1016/S0140-6736(11)60355-3
401. Voelker R. New Option for Sickle Cell Disease. *JAMA* (2020) 323(1):18. doi: 10.1001/jama.2019.20640
402. Gluckman E. Allogeneic transplantation strategies including haploidentical transplantation in sickle cell disease. *Hematol Am Soc Hematol Educ Program* (2013) 2013:370–6. doi: 10.1182/asheducation-2013.1.370
403. Makani J, Ofori-Acquah SF, Nnodu O, Wonkam A, Ohene-Frempong K. Sickle cell disease: new opportunities and challenges in Africa. *TheScientificWorldJournal* (2013) 2013:193252. doi: 10.1155/2013/193252
404. Rogers DW, Clarke JM, Cupidore L, Ramlal AM, Sparke BR, Serjeant GR. Early deaths in Jamaican children with sickle cell disease. *Br Med J* (1978) 1 (6126):1515–6. doi: 10.1136/bmj.1.6126.1515

405. Grosse SD, Odame I, Atrash HK, Amendah DD, Piel FB, Williams TN. Sickle cell disease in Africa: a neglected cause of early childhood mortality. *Am J Preventive Med* (2011) 41(6 Suppl 4):S398–405. doi: 10.1016/j.amepre.2011.09.013
406. Tshilolo L, Tomlinson G, Williams TN, Santos B, Olupot-Olupot P, Lane A, et al. Hydroxyurea for Children with Sickle Cell Anemia in Sub-Saharan Africa. *New Engl J Med* (2019) 380(2):121–31. doi: 10.1056/NEJMoa1813598
407. Tayo BO, Akingbola TS, Saraf SL, Shah BN, Ezekekwu CA, Sonubi O, et al. Fixed Low-Dose Hydroxyurea for the Treatment of Adults with Sickle Cell Anemia in Nigeria. *Am J Hematol* (2018) 377(9778):1663–72. doi: 10.1002/ajh.25412
408. Lagunju I, Brown BJ, Sodeinde O. Hydroxyurea lowers transcranial Doppler flow velocities in children with sickle cell anaemia in a Nigerian cohort. *Pediatr Blood Cancer* (2015) 62(9):1587–91. doi: 10.1002/pbc.25529

Conflict of Interest: GK is an employee of CSL Behring, LLC.

The remaining authors declare that the research was conducted in the absence of any commercial or financial relationships that could be construed as a potential conflict of interest.

frontiers in Immunology

ORIGINAL RESEARCH
published: 04 February 2021
doi: 10.3389/fimmu.2020.617962

Inflammatory Dendritic Cells Contribute to Regulate the Immune Response in Sickle Cell Disease

Renata Sesti-Costa, Marina Dorigatti Borges, Carolina Lanaro, Dulcinéia Martins de Albuquerque, Sara Terezinha Olalla Saad and Fernando Ferreira Costa*

Hematology and Hemotherapy Center, University of Campinas, UNICAMP, Campinas, Brazil

Sickle cell disease (SCD), one of the most common hemoglobinopathies worldwide, is characterized by a chronic inflammatory component, with systemic release of inflammatory cytokines, due to hemolysis and vaso-occlusive processes. Patients with SCD demonstrate dysfunctional T and B lymphocyte responses, and they are more susceptible to infection. Although dendritic cells (DCs) are the main component responsible for activating and polarizing lymphocytic function, and are able to produce pro-inflammatory cytokines found in the serum of patients with SCD, minimal studies have thus far been devoted to these cells. In the present study, we identified the subpopulations of circulating DCs in patients with SCD, and found that the bloodstream of the patients showed higher numbers and percentages of DCs than that of healthy individuals. Among all the main DCs subsets, inflammatory DCs ($CD14^+$ DCs) were responsible for this rise and correlated with higher reticulocyte count. The patients had more activated monocyte-derived DCs (mo-DCs), which produced MCP-1, IL-6, and IL-8 in culture. We found that a $CD14^+$ mo-DC subset present in culture from some of the patients was the more activated subset and was mainly responsible for cytokine production, and this subset was also responsible for IL-17 production in co-culture with T lymphocytes. Finally, we suggest an involvement of heme oxygenase in the upregulation of CD14 in mo-DCs from the patients, indicating a potential mechanism for inducing inflammatory DC differentiation from circulating monocytes in the patients, which correlated with inflammatory cytokine production, T lymphocyte response skewing, and reticulocyte count.

Keywords: dendritic cell, sickle cell disease, heme oxygenase, inflammation, monocyte

OPEN ACCESS

Edited by:
Daniela Bosisio, University of Brescia, Italy

Reviewed by:
Gregory J. Kato, CSL, United States
Jeanne Elise Hendrickson, Yale University School of Medicine, United States

****Correspondence:***
Renata Sesti-Costa
renata.sesti@gmail.com

Specialty section:
This article was submitted to Inflammation, a section of the journal Frontiers in Immunology

Received: *15 October 2020*
Accepted: *21 December 2020*
Published: *04 February 2021*

Citation:
Sesti-Costa R, Borges MD, Lanaro C, Albuquerque DM, Saad STO and Costa FF (2021) Inflammatory Dendritic Cells Contribute to Regulate the Immune Response in Sickle Cell Disease. Front. Immunol. 11:617962. doi: 10.3389/fimmu.2020.617962

INTRODUCTION

Sickle cell disease (SCD) is a condition that affects millions of people worldwide. It is caused by a mutation in the β-globin gene that results in the replacement of a single glutamic acid with valine. As a consequence, an abnormal hemoglobin, HbS, is produced, which polymerizes under deoxygenation conditions. HbS polymerization causes changes in the shape and physical properties of erythrocytes, resulting in hemolytic anemia and the occlusion of small blood vessels (1, 2). Such crises are spontaneous and recurrent complications, in which microvascular infarction

leads to episodes of extreme pain, multiple organ dysfunction, and infection (3–5). The vaso-occlusion process that occurs in patients with SCD is a complex phenomenon that involves the aggregation of erythrocytes, which interact with the endothelium and other blood cells, decreased nitric oxide (NO) bioavailability, oxidative stress, and the release of inflammatory cytokines into the bloodstream, such as TNF-α, IL-6, and IL-8 (6–8).

Patients with SCD are more susceptible to infection due to splenic hypofunction and impaired immune function (9–11). In addition to the deficiency described in innate immunity, including insufficient opsonization and phagocytosis of bacteria (12, 13), evidence of T and B lymphocyte dysfunction in SCD has also been reported in both patients and animal models. These changes include reduction in the proportion of circulating $CD4^+$ and $CD8^+$ T cells (14), defects in regulatory T cells (Tregs) (15), the polarization of cells to a T helper (Th)2 profile (16), and the loss of immunoglobulin (Ig)M-secreting memory B lymphocytes (17).

Dendritic cells (DCs) are the main cells responsible for adaptive immune response activation, polarization, and regulation. They are activated by both the pathogen- and damage-associated molecular patterns, which can be released by tissue necrosis or hemolysis (18–20), which are frequent occurrences in patients with SCD. Changes in DC activation or function may, therefore, be responsible for previously observed dysfunction in the T lymphocyte response. DCs can produce pro- or anti-inflammatory mediators depending on the tissue, the situation, and the cell subpopulation, as DCs form a heterogeneous population of cells with different functions. There are four main subsets of DCs, which share some roles, such as presenting antigens to lymphocytes, but they also have unique functions. Conventional type 1 DCs (cDC1) express the CD141 and Clec9a markers and are mainly responsible for $CD8^+$ T lymphocyte activation and for polarizing the response to the Th1 profile. Conventional type 2 DCs (cDC2) express CD1c and Clec4a4 and are involved in lymphocyte differentiation to Th2 and Th17 profiles. Plasmacytoid DCs (pDCs), in turn, express the IL-3 receptor, CD123, and BDCA2, and produce large amounts of type I IFN. Finally, inflammatory DCs are derived from circulating monocytes during inflammation; they produce pro-inflammatory cytokines and are difficult to distinguish from cDCs2 (18, 21–23). Depending on the activation pattern and expression of inhibitory molecules, DCs are also essential in Treg differentiation, thus participating in the regulation of the immune response. The development of DCs and their differentiation to a specific cell subtype depends on the cytokines released in the microenvironment (24, 25), and the bloodstream of patients with SCD contains greater amounts of GM-CSF and IL-3, which are determinants in the development of cDCs and pDCs, respectively (8, 26). Nevertheless, the landscape of DC subsets in SCD remains unknown.

In the present study, we identified the subsets of circulating DCs in patients with SCD at steady state and showed that inflammatory DCs are elevated in the patients' bloodstream, which correlated with hemolysis and IL-17–producing lymphocytes. Monocyte-derived DCs from patients produced inflammatory cytokines and skewed T lymphocyte responses towards a Th17 profile. Moreover, the inflammatory DCs arose from the patients' monocytes in a heme oxygenase (HO)–dependent pathway. The present data provide new information on the initiation of the immune response in SCD, which may be related to susceptibility to infection and the sustained inflammatory component of the disease.

METHODS

Human Samples

Patients with SCD (n = 47) and healthy controls (n = 46) aged 20 to 59 years were enrolled in the present study. Participants with HbSS or $HbS\beta^0$ genotypes were included as patients with SCD, and hemoglobin patterns were confirmed by high-performance liquid chromatography (HPLC) (Bio-Rad) and DNA sequence analysis. Patients who had received blood transfusions in the past 3 months, in vaso-occlusive crises and with apparent infection were excluded from the study. No patient was being treated with antibiotics or corticosteroids, and all patients were under treatment with folic acid, calcium, and vitamin D. Moreover, most patients were under treatment with hydroxyurea. Blood samples were obtained from the participants during regular consultation at the Unicamp Hematology and Hemotherapy Center, São Paulo, Brazil. Complete blood counts with reticulocyte counts were performed on blood collected with EDTA in a hematology analyzer (Beckman Coulter). The study was approved by the Unicamp Human Research Ethics Committee (protocol number CAAE: 85061318.0.0000.5404). All patients and controls had agreed to participate and had signed informed consent forms.

Separation of Peripheral Blood Mononuclear Cells (PBMCs) and Isolation of Monocytes and T Lymphocytes

Blood was collected from all participants in heparin-coated tubes. The fresh blood was diluted in phosphate-buffered saline (PBS), and PBMCs were obtained by density gradient centrifugation on Ficoll-Hypaque (GE Healthcare) at 400*g* for 30 min at room temperature. The mononuclear leukocyte layer was separated and washed. The pellet with the remaining aggregated red blood cells was lysed with lysis buffer and washed with PBS. PBMCs were resuspended in RPMI 1640 medium (Gibco) supplemented with 10% fetal bovine serum, penicillin and streptomycin, and L-glutamine. Monocytes were isolated from the PBMCs by anti-CD14-coated magnetic beads (Miltenyi Biotec), and T lymphocytes were isolated using human a pan-T cell isolation kit (Miltenyi Biotec) according to the manufacturer instructions.

Cell Phenotyping by Flow Cytometry

PBMCs were incubated in staining buffer (PBS; ACD; 10% BSA) and stained with monoclonal antibodies conjugated to PE, PE-Cy7, FITC, APC, APC-Cy7, PerCP-Cy5, BV451, BV605, or BV650 for 30 min at 4°C. DCs were stained using antibodies

against CD3, CD19, CD56, CD14, HLA-DR, CD1c, CD141, CD123, and CD135 (BD Biosciences and BioLegend). The absolute number of DCs per μl of blood was calculated by multiplying the percentages by the complete blood leukocyte count. Monocytes were analyzed using antibodies against CD14 and CD16. Cells were washed and evaluated by flow cytometry (Cytoflex, Beckman Counter). For analyzing Tregs, surface marker staining was performed as described above with anti-CD3 and anti-CD4 antibodies, and then the cells were washed, fixed, and permeabilized with a Foxp3 Cytofix/Cytoperm kit (BD Biosciences) according to the manufacturer's instructions, and stained with anti-FOXP3 antibody for an additional 30 min at 4°C. The cells were washed before acquisition in flow cytometry. To evaluate intracellular cytokines in lymphocytes, PBMCs were stimulated with 500 μg/ml PMA and 50 μg/ml ionomycin in the presence of GolgiStop (BD Biosciences) for 4 h, then stained with conjugated antibodies against CD3, CD4, and CD8. The cells were washed, fixed, and permeabilized using a Cytofix/Cytoperm kit (BD Biosciences) using the manufacturer's instructions. Then, the cells were incubated with monoclonal antibodies against IFN-γ, IL-10, or IL-17 for 30 min at 4°C, washed, and evaluated by flow cytometry. Data were analyzed using FlowJo (BD Biosciences).

Generation of Monocyte-Derived DCs

DCs were differentiated from isolated monocytes in culture by incubation in RPMI 1640 medium (Gibco) supplemented with 10% fetal bovine serum, L-glutamine, penicillin, streptomycin, and containing 20 ng/ml GM-CSF and 20 ng/ml IL-4 (R&D Systems) for 7 days. The medium containing the cytokines was replenished on the third day. In some experiments, monocytes were incubated with the HO-1 inhibitor SnPP (tin protoporphyrin IX dichloride, R&D Systems; 50 μM) for 1 h before and during DC differentiation. The cells were analyzed by flow cytometry, and the cytokine levels in the supernatant were quantified. Monocyte-derived DCs (mo-DCs) were stained using antibodies against CD14, CD209, CD1c, CD86, HLA-DR, and CD83 (BD Biosciences and BioLegend). In other experiments, the cells were counted and incubated with T lymphocytes to perform co-culture.

Co-culture of DCs and T Lymphocytes

The mo-DCs were counted, and 5×10^4 cells were plated in 96-well culture plates. After 24 h, T lymphocytes were isolated from the PBMCs from the healthy controls and stained with 2.5 μM CFSE (carboxyfluorescein succinimidyl ester) for 15 min at room temperature. T lymphocytes (5×10^5) were incubated with mo-DCs for an additional 5 days. Lymphocyte proliferation was evaluated by flow cytometry based on CFSE dilution in the CD4 or CD8 gates after staining with antibodies against CD4 and CD8. The co-culture supernatant was harvested and used to measure cytokine levels.

Cytokine Measurement

The cytokines IL-1β, IFN-α2, IFN-γ, TNF-α, MCP-1, IL-6, IL-8, IL-10, IL-12p70, IL-17A, IL-18, IL-23, and IL-33 were measured in the supernatant of DCs and co-cultures using the LEGENDplex Human Inflammation Panel 1 (BioLegend) according to the manufacturer's instructions. The acquisition was performed by flow cytometry (Cytoflex, Beckman Coulter), and the results were analyzed by LEGENDplex software.

Quantitative Real-Time PCR

Total RNA was extracted from monocytes using an RNeasy Mini Kit (Qiagen), and genomic DNA was digested with DNase I (Fermentas). Reverse transcription was performed using a RevertAid H Minus First Strand cDNA Synthesis Kit (Thermo Scientific), and *Hmox1* expression was analyzed using SYBR Green PCR master mix (Applied Biosystems). The following primers were used: *Hmox1* forward: 5′-GACGGCTTCAAGCTG GTGAT-3′ and reverse: 5′-GTTGCGCTCAATCTCCTCCT-3′; *Rplpo* (ribosomal protein lateral stalk subunit P0) forward: 5′-GGAAGGCTGTGGTGCTGATG-3′ and reverse 5′-GAGGCAGCAGTTTCTCCAGAG-3′.

Statistical Analyses

The mean ± SEM values are presented in the graphs, and the pair of groups were compared using the Mann-Whitney test for non-Gaussian distributed data. Pairs of cells sorted from the culture of the same patient were analyzed using paired Student's *t*-tests. P values < 0.05 were considered statistically significant. All data were analyzed using Prism 5.1 software (GraphPad).

RESULTS

Patients With SCD Had Increased Total DCs and Altered Ratio of DC Subsets

To characterize the main DC subsets in the bloodstream of the patients, we isolated PBMCs from their blood and performed multicolor flow cytometry. The gating strategy used for identifying the DC population (**Figure 1A**), was to gate on lymphocyte and monocyte populations by forward scatter and side scatter plots, followed by gating in single cells. Next, total DCs were detected as negative for lineage markers (CD3/CD19/CD56/CD14) and HLA-DR$^+$. Within the total DC population, additional gates were designed to distinguish the different DC subsets and pre-DC population. Pre-DCs were considered lineage$^-$HLA-DR$^+$CD1c$^-$CD141$^-$CD123$^-$CD135$^+$; cDC1 as lineage$^-$HLA-DR$^+$CD1c$^-$CD141$^+$CD123$^-$; cDC2 as lineage$^-$HLA-DR$^+$CD1c$^+$CD141$^-$CD123$^-$; and pDC as lineage$^-$HLA-DR$^+$CD1c$^-$CD141$^-$ CD123$^+$ (19, 27, 28). A subset of DCs expressing CD14, henceforth referred to as inflammatory DCs (iDCs), was identified as negative for lineage markers (CD3/CD19/CD56) and were HLA-DR$^+$CD1c$^+$CD14$^+$ (29).

The patients had total DCs increased in the blood (**Figure 1B**). The result was very heterogeneous among the patients, some of them had very high numbers of DCs, whereas others presented numbers similar to controls. The development of DCs from the bone marrow is possible to be, at least in part, responsible for this increase, as the percentage and total number of DC precursors were augmented in the patients' blood (**Figure 1C**). Notably, the increased amount of DCs is

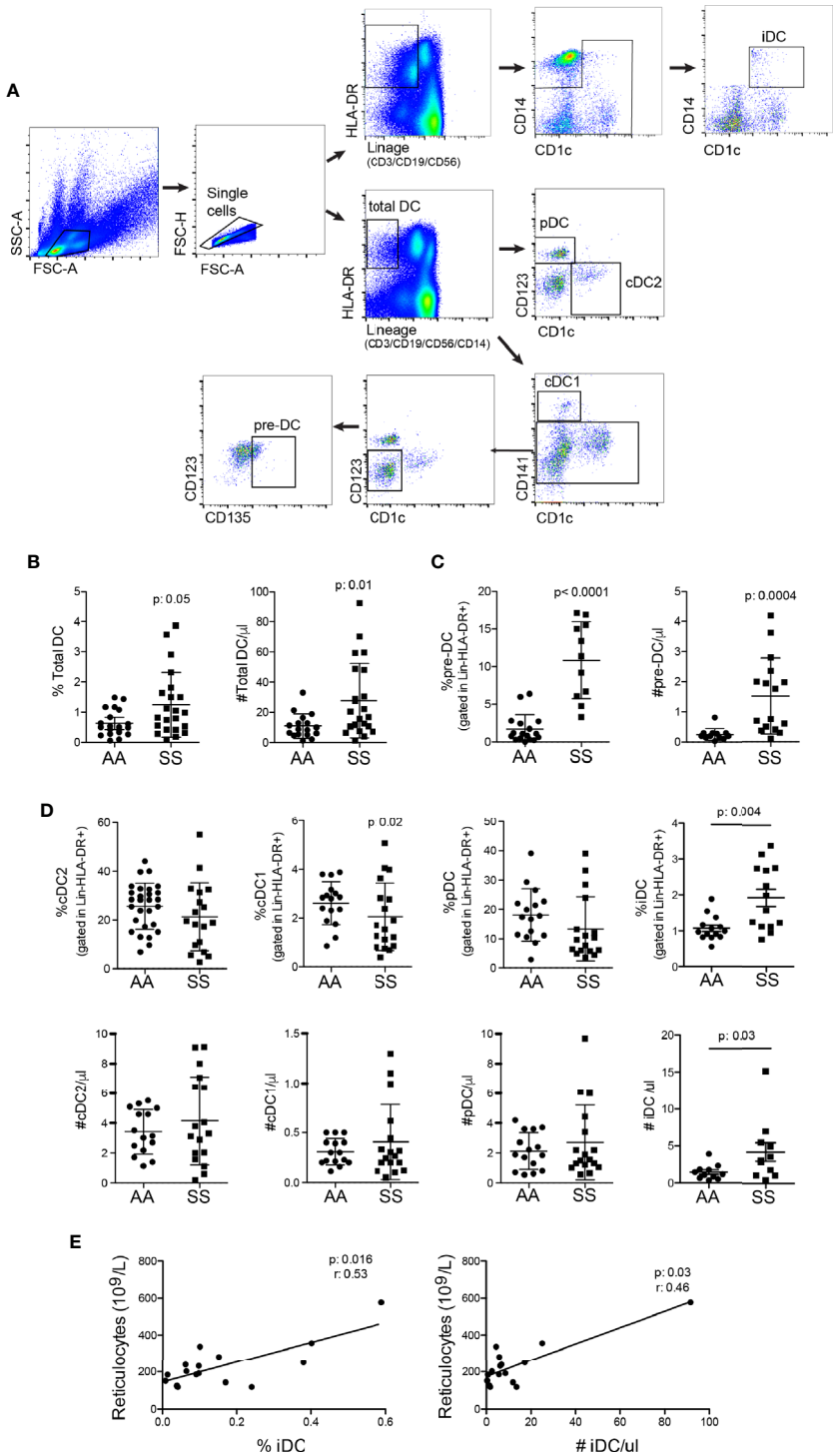

FIGURE 1 | Patients with SCD have an increased number of total DCs in the bloodstream and distinct proportions of DC subsets. The different DC subsets were identified in the blood from the patients (SS: hemoglobin S) and controls (AA: hemoglobin A) by flow cytometry. **(A)** The gating strategy used to identify total DCs, namely, lineage$^-$ (CD3/CD19/CD56/CD14) HLA-DR$^+$; pre-DCs (lineage$^-$HLA-DR$^+$CD1c$^-$CD141$^-$CD123$^-$CD135$^+$); cDC1 (lineage$^-$HLA-DR$^+$CD1c$^-$CD141$^+$CD123$^-$); cDC2 (lineage$^-$HLA-DR$^+$CD1c$^+$CD141$^-$CD123$^-$); pDC (lineage$^-$HLA-DR$^+$CD1c$^-$CD141$^-$CD123$^+$), and iDC is lineage$^-$ (CD3/CD19/CD56), HLA-DR$^+$CD1c$^+$CD14$^+$. **(B)** The percentage of total DCs in PBMCs and their absolute number per µl blood. **(C)** The percentage of pre-DCs in total DCs and their absolute number per µl blood. **(D)** The percentage within total DCs (top panel) and the absolute number per µl (bottom panel) cDC2, cDC1, pDC, and iDC. N: AA = 20; SS = 22. *P*-values were obtained using the Mann-Whitney test. **(E)** Spearman correlation between %iDC (left panel) and #iDC (right panel) with circulating reticulocyte numbers.

unlikely to be only a result of leukocyte redistribution due to splenic hypofunction, as the percentage of DCs among white blood cells was also increased (**Figure 1B**). The discrimination of DC subsets revealed that the ratio of cDC1 was reduced, whereas that of iDC was increased in the patients relative to the controls. The percentages of cDC2 and pDC were similar between the groups (**Figure 1D**). iDC was the only subset with a significantly higher total number in the patients' blood. None of the other three main subsets alone accounted for the increase in total DCs. Their numbers were slightly higher in the patients than in the controls, but the difference was not statistically significant (**Figure 1D**), suggesting that all subsets together and pre-DCs may contribute to the higher number of circulating DCs. Notably, both the percentage and total number of iDCs were significantly correlated with the number of reticulocytes in the blood (**Figure 1E**), a *bona fide* hemolysis parameter.

Mo-DCs From Patients With SCD Showed an Activated Phenotype and Produced Inflammatory Cytokines

iDCs are cells mainly derived from activated monocytes present in the circulation. Thus, we characterized the DCs differentiated *in vitro* in the presence of GM-CSF and IL-4 from monocytes (mo-DCs) isolated from the PBMCs of the patients and the controls. More mo-DCs from the patients presented an activated phenotype, as shown in the higher expression of the presenting antigen molecule HLA-DR and the co-stimulator CD86. No difference was seen in the expression of the DC marker CD209 and the maturation molecule CD83 (**Figure 2A**). Interestingly, DCs from the patients produced two- to three-fold more MCP-1, IL-6, and IL-8 compared to the controls even with no *in vitro* stimulation (**Figure 2B**), indicating a potential role for these cells in monocyte and neutrophil recruitment to the inflammatory microenvironment. A more detailed analysis of mo-DCs revealed the expression of the monocyte marker CD14 in some patients (**Figure 2C**). These cells expressed the DC markers CD209 (**Figure 2C**) and CD1c, and were smaller than monocytes (data not shown), which characterized them as iDCs. Furthermore, $CD14^+$ DCs showed higher expression of the DC maturation marker CD83, and the activation markers HLA-DR and CD86 than $CD14^-$ DCs from the same patient (**Figure 2D**). Next, we sorted $CD14^+$ DCs and $CD14^-$ DCs and incubated them for 24 h without any additional stimulation. Surprisingly, the $CD14^+$ DCs were among the mo-DCs responsible for the production of MCP-1, IL-6, and IL-8 in the culture supernatant (**Figure 2E**).

Patients With SCD Had More Activated T Lymphocytes and More IL-17 Production

DCs are the major cells responsible for modulating lymphocyte function (20, 30, 31). Thus, the next step was to determine T cell responses in the circulation of this cohort of patients to associate them with the alterations in DC numbers and ratios. We observed a greater percentage of T lymphocytes from the patients as compared to that from the controls, especially $CD8^+$ T lymphocytes, which presented a statistically significant difference in CD69 expression, a T cell activation marker (**Figures 3A, B**). Although SCD is a chronic inflammatory disease, the T lymphocytes did not present an exhaustion profile, as PD-1 expression by both $CD4^+$ and $CD8^+$ T cells was comparable to that of the controls (**Figure 3B**). Tregs are important cells involved in regulating exacerbated inflammation *via* several mechanisms (32). Compared with the controls, the patients had reduced Tregs, as demonstrated by the lower percentages of $FOXP3^+CD4^+$ T lymphocytes in their bloodstream (**Figure 3C**). Then, we stimulated PBMCs *in vitro* with PMA and ionomycin in the presence of brefeldin to analyze the profile of cytokines produced by the T cells. Both $CD4^+$ and $CD8^+$ T lymphocytes from the patients produced higher amounts of IL-17 (**Figures 3D, E**). No difference was seen in IFN-γ production by T lymphocytes in this cohort (**Figure 3E**), and IL-10 production by *in vitro* stimulation was very low and similar between the groups (data not shown). Altogether, these data suggest that the lower ratio of Tregs and the skewed T cell response to Th17 and Tc17 (IL-17–secreting CD8 T cells) profiles can cooperate for the inflammatory phenotype and altered adaptive immune response seen in the patients.

Mo-Derived DCs From the Patient with SCD Stimulated T Lymphocyte Proliferation and IL-17 Production

To address whether DCs are responsible for the T cell phenotype observed in the patients, we performed a co-culture assay of mo-DCs from the patients or controls with allogeneic T cells stained with CFSE. Mo-DCS from the patients induced higher-intensity proliferation of total T lymphocytes as compared to that of the controls. When the analysis was stratified in $CD4^+$ and $CD8^+$ T lymphocytes, we observed that both cells contributed to the higher proliferation of the T cell population (**Figures 4A, B**), showing that mo-DCs from the patients had additional capability for stimulating both $CD4^+$ and $CD8^+$ T cells, absent in those from the controls. Notably, when the sorted $CD14^+$ and $CD14^-$ DCs from the same patient were used in co-culture, the $CD14^+$ DCs induced higher IL-17 production than their counterparts, whereas IFN-γ and IL-10 were induced with the same intensity (**Figure 4C**), indicating that $CD14^+$ DCs are, at least in part, responsible for the Th17/Tc17 phenotype in patients with SCD.

Upregulation of HO-1 by Monocytes Induced $CD14^+$ DC Differentiation in Patients With SCD

In an attempt to unveil the mechanisms by which monocytes from some patients differentiate into $CD14^+$ DCs, we evaluated the distribution of monocyte subtypes in the bloodstream. In the present cohort, we did not find any difference in the monocyte subtype ratio between the patients and the controls (**Figure 5A**), suggesting no role for subset-specific monocytes in iDC differentiation and no correlation of a monocyte subset with DCs compartment changes. Monocytes from patients with SCD are constantly exposed to heme released during hemolysis, and there is evidence that they can upregulate HO-1, which metabolizes heme into CO (carbon monoxide), Fe (iron), and

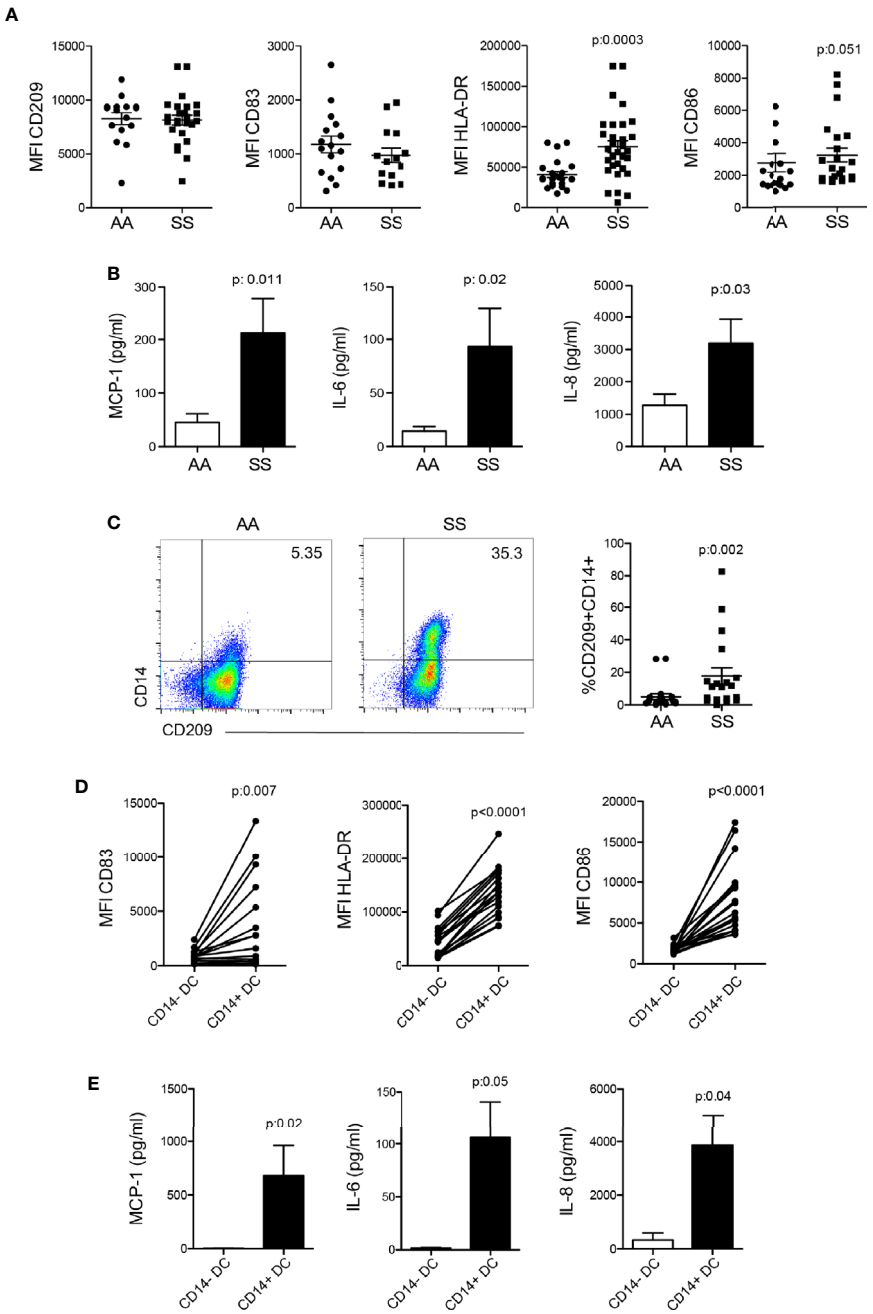

FIGURE 2 | Activation profile and inflammatory cytokine production by mo-derived DCs from patients with SCD. Monocytes were isolated from the PBMCs of the patients (SS) and controls (AA) and cultured with 20 ng/ml GM-CSF and IL-4 for 6 to 7 days for DC differentiation. **(A)** Flow cytometry analysis of DC activation marker expression. **(B)** LEGENDplex measurement and flow cytometry acquisition of cytokine secretion in the supernatant after 24 h. **(C)** CD14 expression in $CD209^{+}HLA\text{-}DR^{+}$ DCs after differentiation. **(D)** Analysis of DC activation markers in the $CD14^{+}$ and $CD14^{-}$ DC subpopulations. *P*-values were obtained using the Mann-Whitney test. **(E)** $CD14^{+}$ and $CD14^{-}$ DCs from the same patient were sorted by flow cytometry and incubated for 24 h. Cytokines were measured in the supernatant by LEGENDplex. *P*-values were obtained using the paired Student's *t*-test.

biliverdin (33, 34). Thus, we evaluated HO-1 expression by monocytes, and found that monocytes from the patients overall demonstrated upregulation of HO-1 compared to that from the controls. Notably, monocytes from the patients that differentiated *in vitro* into $CD14^{+}$ DCs (SS $CD14^{+}$ DC) showed even higher upregulation of HO-1 expression than the monocytes that differentiated only into $CD14^{-}$ DCs (SS $CD14^{-}$ DC) (**Figure 5B**). Hence, to reveal the role of HO-1 in $CD14^{+}$ DC differentiation, we treated monocytes from the patients with the HO-1 inhibitor, SnPP, for 1 h before and during *in vitro* DC

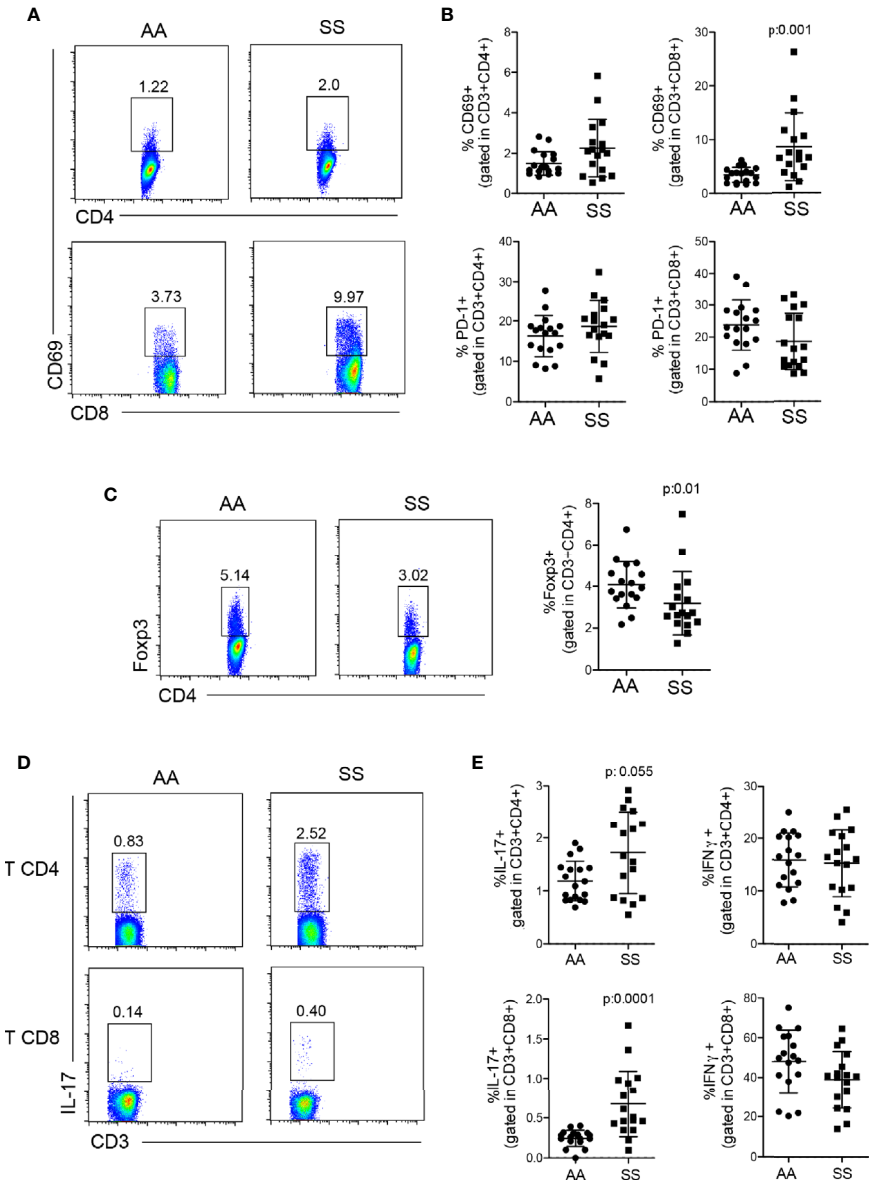

FIGURE 3 | Profile of T lymphocyte response in patients with SCD. **(A, B)** Activation and exhaustion of $CD4^+$ and $CD8^+$ T lymphocytes were quantified by staining of PBMCs from the patients (SS) and controls (AA) with CD69 and PD-1, respectively, within $CD3^+CD4^+$ or $CD3^+CD8^+$ populations. **(A)** Representative dot plots of CD69. **(B)** The percentage of CD69 (top) and PD-1 (bottom)-stained cells within $CD4^+$ (left) and $CD8^+$ (right) T lymphocytes. **(C)** Tregs were identified in PBMCs by the percentage of $FOXP3^+CD4^+$ T lymphocytes. The left panel shows the representative dot plots; the right panel shows the percentage of Tregs in the patients (SS) and controls (AA). **(D, E)** PBMCs were stimulated *in vitro* with PMA and ionomycin in the presence of brefeldin for 4 h, then stained for intracellular cytokines. **(D)** Representative dot plots of IL-17. **(E)** The percentage of IL-17 (left) and IFN-γ (right)-producing $CD4^+$ (top) and $CD8^+$ (bottom) T lymphocytes. N: AA = 17; SS = 17. *P*-values were obtained using the Mann-Whitney test.

differentiation. SnPP treatment increased the percentage of DCs differentiated in culture, as seem by HLA-DR^+ $CD209^+$ cells ratio (**Figure 5C**). However, the treatment decreased both the percentage and mean fluorescence of CD14 on mo-DCs (**Figure 5C**), indicating a previously unknown mechanism of HO-1 in iDC differentiation in patients with SCD.

Altogether, the data show that the number and ratio of DCs are increased in the circulation of patients with SCD and that the amount of iDCs correlates with hemolysis. DCs from patients with SCD, especially $CD14^+$ DCs, show an activated phenotype and produce inflammatory cytokines seen to be responsible for monocyte and neutrophil recruitment, indicating that they may cooperate in the inflammatory milieu. In addition, they demonstrated an association with T lymphocyte activation and IL-17 production. Finally, we found that the differentiation of iDCs from monocytes may occur through an HO-1–dependent pathway.

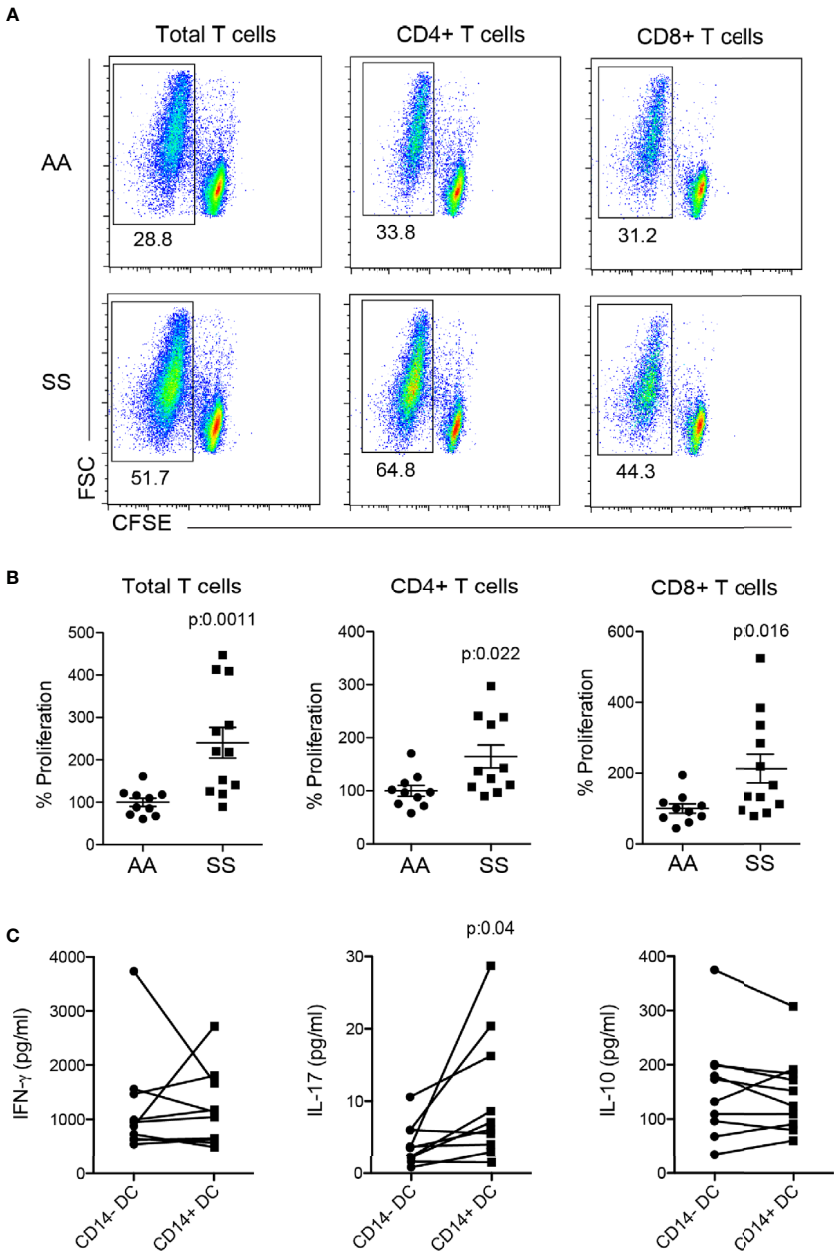

FIGURE 4 | Co-culture of mo-derived DCs and T lymphocytes. Monocytes were isolated from PBMCs of the patients (SS) and controls (AA) and cultured with 20 ng/ml GM-CSF and IL-4 for 6–7 days for DC differentiation. Mo-DCs were co-cultured (1:10) with allogeneic T lymphocytes from healthy individuals; the T lymphocytes had been previously stained with CFSE for 5 days. **(A, B)** T lymphocyte proliferation was evaluated by CFSE dilution and CD4 and CD8 staining. **(A)** Representative dot plots and **(B)** graphs of the percentage of proliferation measured by $CFSE^{-}$ gating. AA was considered 100%. *P*-values were obtained using a Student's *t*-test. **(C)** $CD14^{+}$ and $CD14^{-}$ mo-DCs were sorted by flow cytometry before co-culture with T lymphocytes. Cytokines were measured in co-culture supernatant by flow cytometry. *P*-values were obtained using a paired Student's *t*-test.

DISCUSSION

Despite exceptional advances in the last decade in SCD therapy, including new drugs, bone marrow transplantation, and gene therapy (35–37), both basic and clinical research is ongoing to obtain greater knowledge of the cells and mediators involved in the disease, and to develop new and better therapies that improve patient quality of life.

DCs are key players in the initiation of the immune response to pathogens and also of tolerance to self, microbiota, and dietary antigens (20, 38). Changes in DC function can result in prevention of the fight against infection or in the development

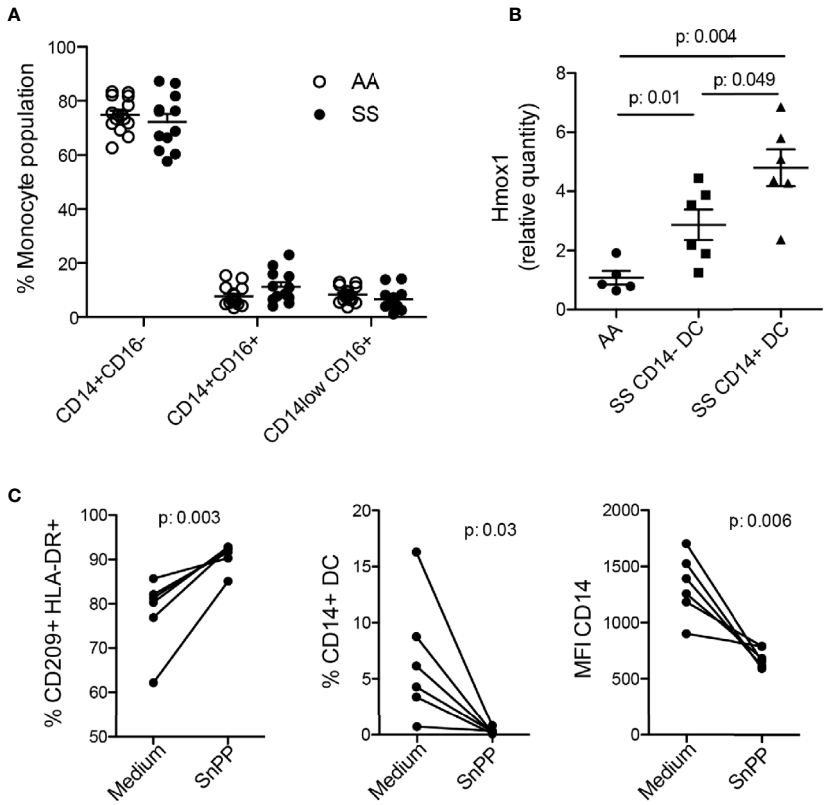

FIGURE 5 | The role of HO-1 in iDC differentiation. **(A)** Phenotyping of monocyte subsets in the controls (AA) and patients (SS) by flow cytometry**. (B)** Monocytes were isolated from the PBMCs of the patients (SS) and controls (AA). A portion was cultured with 20 ng/ml GM-CSF and IL-4 for 6 to 7 days for DC differentiation and evaluation of CD14 expression. The other portion underwent RNA extraction for RT-PCR evaluation of HO-1 transcript expression (*Hmox1*). The graph shows data separately from patients with (SS $CD14^+$ DC) or without (SS $CD14^-$ DC) $CD14^+$ DC differentiation. *P*-values were obtained using the Mann-Whitney test. **(C)** Monocytes isolated from the PBMCs of the patients were treated with SnPP (50 μM) for 1 h, then induced to differentiate into DCs. The percentage and mean fluorescence intensity (MFI) were measured by flow cytometry. *P*-values were obtained using a paired Student's *t*-test.

of autoimmune and inflammatory diseases (39–41). The role of DCs and their specific subsets in the chronic inflammatory component or adaptive immune dysfunction of SCD remains elusive. In the present work, we show for the first time that circulating DCs are increased and that the ratio of DC subsets is altered in patients with SCD. The higher numbers of circulating pre-DCs may indicate intensification in DC development from the bone marrow. In addition, as iDCs can arise from circulating monocytes, they are likely to be another source of DC expansion in the bloodstream, as our data show higher numbers of this DC subpopulation. We also observed a reduction in the circulating cDC1 in the patients. It remains uncertain whether the development of this subpopulation is reduced or whether they are being activated and subsequently migrate to the lymph nodes, where they prime T lymphocytes. These hypotheses are difficult to address in humans; nevertheless, they warrant future investigation. Notably, we found a heterogeneity among the patients regarding circulating DCs ratios and a correlation between iDC percentage and number with reticulocyte counts, suggesting that changes in DCs compartment may be present only in patients with certain degree of disease severity. Although we could not establish a clear cause and effect relationship, we observed that the percentage of DCs was also increased in the patients, suggesting a skewing towards DC development rather than a general leukocyte increase or redistribution.

Here, *in vitro* differentiation of monocytes into DCs revealed that the patients' monocytes could derive more activated and inflammatory iDCs, as they produced MCP-1, IL-6, and IL-8 even without stimulation. No difference was observed in the DC or maturation markers CD209 and CD83, respectively, which was also shown in an investigation of mo-DCs in the context of SCD alloimmunization (42). That study also suggests that mo-DCs from patients with SCD produce more inflammatory cytokines, as the authors showed that SCD mo-DCs produced more IL-12 than those from healthy individuals after stimulation with LPS, LPS +IFN-γ, or R848. Additionally, some of the patients' mo-DCs expressed the monocyte marker CD14. Despite this, they had the DC phenotype, expressed CD209 and CD1c, and were smaller than monocytes. $CD14^+$ mo-DCs are more mature and activated than $CD14^-$ mo-DCs, and are responsible for inflammatory cytokine production. Patients with SCD present an expansion of monocyte and neutrophil counts, which interact with the activated endothelium, cooperating in vaso-occlusion (43, 44). Although our *in vitro* system did not allow us to estimate the contribution of

DCs to inflammatory cytokine production *in vivo* in the bloodstream compared to other cells, the present data indicate that the DCs of patients with SCD, especially $CD14^+$ DCs, produce these cytokines, which may be associated with their systemic amounts and the migration of monocytes and neutrophils to DC sites. Thus, it is important to determine whether DCs are present and participate in the vaso-occlusion process.

As the T lymphocyte response in patients with SCD varies according to the cohort evaluated and the parameter analyzed, we assessed T cells in the present cohort to associate to the DC phenotype. We found that the patients had more $CD4^+$ and $CD8^+$ T lymphocytes and higher IL-17 production. Several studies have shown the involvement of IL-17 in neutrophil activation and recruitment and in the development of autoimmune and inflammatory disease (45–48); thus, IL-17 may participate in the inflammatory process in patients with SCD and can alter their immune response to a subsequent infection. Depending on the context, previous studies have shown variable results for the production of IFN-γ and Th1-biased responses in patients with SCD (16, 49, 50). In our cohort, IFN-γ production by both $CD4^+$ and $CD8^+$ T cells was similar between the patients and the controls. In addition, the patients showed a reduced percentage of Tregs, which may contribute to the inflammatory state. We demonstrate the role of DCs in some T lymphocyte responses in the patients. Our results show that the DCs of patients with SCD are more capable of inducing both $CD4^+$ and $CD8^+$ T cell proliferation, and that $CD14^+$ DCs stimulated higher IL-17 production in co-culture than $CD14^-$ DCs. The mechanisms by which $CD14^+$ DCs induce IL-17 production are still unknown. IL-6, IL-23, and TGF-β production by DCs polarizes T lymphocytes to a Th17 profile (51). In our co-culture system, although we observed higher IL-6 production by the patients' DCs, especially $CD14^+$ DCs, IL-23 was undetectable in the supernatant of unstimulated DCs (data not shown), suggesting no participation of these cytokines in the process.

Although other groups have found changes in monocyte subpopulations in patients with SCD (52), our patient cohort did not show any difference in the monocyte subpopulations compared with the controls, which indicates that no specific monocyte subset is responsible for $CD14^+$ DC differentiation. The difference between previous data and ours may be because, for most of the experiments, all patients from our cohort were under hydroxyurea treatment, which may directly or indirectly reverse the changes in monocyte subset ratio caused by the disease, as previously shown (53). Due to changes in membrane lesion secondary to HbS polymerization into erythrocytes, SCD is characterized by a percentage of intravascular hemolysis (54), which results in the release of free hemoglobin and free heme in circulation. Free heme can modulate monocyte and mo-DC functions in SCD (42, 55) and in several other diseases (56) through the TLR4 or HO-1 pathways. In our work, we found that HO-1 expression in the patients' monocytes was upregulated compared to that from the controls, as previously reported (33). Surprisingly, patients whose monocytes could differentiate into $CD14^+$ DCs in culture expressed even more HO-1 than the patients whose monocytes differentiated only into $CD14^-$ DCs. The inhibition of HO-1 enzymatic activity in the patients' monocytes prevented CD14 expression in the posteriorly derived DCs, indicating a possible mechanism by which the monocytes from some patients differentiate into these iDCs. Further investigation is still need to confirm this possibility and would provide more important information about the stimulus responsible for HO-1 upregulation, the signaling pathways downstream to HO-1 involved in DCs differentiation, and the changes in DCs functions observed. In summary, the present study reports novel findings regarding the role of DCs in SCD and provides new insights into the chronic inflammation and the immune dysfunction observed in patients with SCD.

DATA AVAILABILITY STATEMENT

The raw data supporting the conclusions of this article will be made available by the authors, without undue reservation.

ETHICS STATEMENT

The studies involving human participants were reviewed and approved by Unicamp Human Research Ethics Committee (protocol number CAAE: 85061318.0.0000.5404). The patients/participants provided their written informed consent to participate in this study.

AUTHOR CONTRIBUTIONS

RS-C and FFC designed the experiments and wrote the manuscript. RS-C and MDB performed the experiments. CL and DMA collaborated in some experiments. STOS and FFC assisted the patients. FFC supervised the work. All authors contributed to the article and approved the submitted version.

ACKNOWLEDGMENTS

We acknowledge the participants that agreed to contribute to this work; Irene Santos, for the assistance with flow cytometry; and FAPESP for financial support (process numbers: 2017/21892-8 and 2014/00984-3).

REFERENCES

1. Steinberg MH. Genetic etiologies for phenotypic diversity in sickle cell anemia. *Sci World J* (2009) 9:46–67. doi: 10.1100/tsw.2009.10
2. Steinberg MH, Rodgers GP. Pathophysiology of sickle cell disease: role of cellular and genetic modifiers. *Semin Hematol* (2001) 38(4):299–306. doi: 10.1016/s0037-1963(01)90023-x
3. Madigan C, Malik P. Pathophysiology and therapy for haemoglobinopathies. Part I: sickle cell disease. *Expert Rev Mol Med* (2006) 8(9):1–23. doi: 10.1017/S1462399406010659
4. Ramakrishnan M, Moisi JC, Klugman KP, Iglesias JM, Grant LR, Mpoudi-Etame M, et al. Increased risk of invasive bacterial infections in African people with sickle-cell disease: a systematic review and meta-analysis. *Lancet Infect Dis* (2010) 10(5):329–37. doi: 10.1016/S1473-3099(10)70055-4

5. Kato GJ, Piel FB, Reid CD, Gaston MH, Ohene-Frempong K, Krishnamurti L, et al. Sickle cell disease. *Nat Rev Dis Primers* (2018) 4:18010. doi: 10.1038/nrdp.2018.10
6. Conran N, Saad ST, Costa FF, Ikuta T. Leukocyte numbers correlate with plasma levels of granulocyte-macrophage colony-stimulating factor in sickle cell disease. *Ann Hematol* (2007) 86(4):255–61. doi: 10.1007/s00277-006-0246-6
7. Keikhaei B, Mohseni AR, Norouzirad R, Alinejadi M, Ghanbari S, Shiravi F, et al. Altered levels of pro-inflammatory cytokines in sickle cell disease patients during vaso-occlusive crises and the steady state condition. *Eur Cytokine Netw* (2013) 24(1):45–52. doi: 10.1684/ecn.2013.0328
8. Lanaro C, Franco-Penteado CF, Albuqueque DM, Saad ST, Conran N, Costa FF. Altered levels of cytokines and inflammatory mediators in plasma and leukocytes of sickle cell anemia patients and effects of hydroxyurea therapy. *J Leukoc Biol* (2009) 85(2):235–42. doi: 10.1189/jlb.0708445
9. Booth C, Inusa B, Obaro SK. Infection in sickle cell disease: a review. *Int J Infect Dis* (2010) 14(1):e2–e12. doi: 10.1016/j.ijid.2009.03.010
10. Balandya E, Reynolds T, Obaro S, Makani J. Alteration of lymphocyte phenotype and function in sickle cell anemia: Implications for vaccine responses. *Am J Hematol* (2016) 91(9):938–46. doi: 10.1002/ajh.24438
11. Brousse V, Buffet P, Rees D. The spleen and sickle cell disease: the sick(led) spleen. *Br J Haematol* (2014) 166(2):165–76. doi: 10.1111/bjh.12950
12. Anyaegbu CC, Okpala IE, Akren'Ova YA, Salimonu LS. Peripheral blood neutrophil count and candidacidal activity correlate with the clinical severity of sickle cell anaemia (SCA). *Eur J Haematol* (1998) 60(4):267–8. doi: 10.1111/j.1600-0609.1998.tb01036.x
13. Humbert JR, Winsor EL, Githens JM, Schmitz JB. Neutrophil dysfunctions in sickle cell disease. *BioMed Pharmacother* (1990) 44(3):153–8. doi: 10.1016/0753-3322(90)90002-q
14. Koffi KG, Sawadogo D, Meite M, Nanho DC, Tanoh ES, Attia AK, et al. Reduced levels of T-cell subsets CD4+ and CD8+ in homozygous sickle cell anaemia patients with splenic defects. *Hematol J* (2003) 4(5):363–5. doi: 10.1038/sj.thj.6200310
15. Vingert B, Tamagne M, Desmarets M, Pakdaman S, Elayeb R, Habibi A, et al. Partial dysfunction of Treg activation in sickle cell disease. *Am J Hematol* (2014) 89(3):261–6. doi: 10.1002/ajh.23629
16. Musa BO, Onyemelukwe GC, Hambolu JO, Mamman AII, Isa AH. Pattern of serum cytokine expression and T-cell subsets in sickle cell disease patients in vaso-occlusive crisis. *Clin Vaccine Immunol* (2010) 17(4):602–8. doi: 10.1128/CVI.00145-09
17. Rautonen N, Martin NL, Rautonen J, Rooks Y, Mentzer WC, Wara DW. Low number of antibody producing cells in patients with sickle cell anemia. *Immunol Lett* (1992) 34(3):207–11. doi: 10.1016/0165-2478(92)90215-a
18. Satpathy AT, Wu X, Albring JC, Murphy KM. Re(de)fining the dendritic cell lineage. *Nat Immunol* (2012) 13(12):1145–54. doi: 10.1038/ni.2467
19. Villani AC, Satija R, Reynolds G, Sarkizova S, Shekhar K, Fletcher J, et al. Single-cell RNA-seq reveals new types of human blood dendritic cells, monocytes, and progenitors. *Science* (2017) 356(6335):eaah4573. doi: 10.1126/science.aah4573
20. Durai V, Murphy KM. Functions of Murine Dendritic Cells. *Immunity* (2016) 45(4):719–36. doi: 10.1016/j.immuni.2016.10.010
21. Murphy TL, Grajales-Reyes GE, Wu X, Tussiwand R, Briseno CG, Iwata A, et al. Transcriptional Control of Dendritic Cell Development. *Annu Rev Immunol* (2016) 34:93–119. doi: 10.1146/annurev-immunol-032713-120204
22. Patente TA, Pinho MP, Oliveira AA, Evangelista GCM, Bergami-Santos PC, Barbuto JAM. Human Dendritic Cells: Their Heterogeneity and Clinical Application Potential in Cancer Immunotherapy. *Front Immunol* (2018) 9:3176. doi: 10.3389/fimmu.2018.03176
23. Swiecki M, Colonna M. The multifaceted biology of plasmacytoid dendritic cells. *Nat Rev Immunol* (2015) 15(8):471–85. doi: 10.1038/nri3865
24. Mildner A, Jung S. Development and function of dendritic cell subsets. *Immunity* (2014) 40(5):642–56. doi: 10.1016/j.immuni.2014.04.016
25. Swiecki M, Wang Y, Gilfillan S, Colonna M. Plasmacytoid dendritic cells contribute to systemic but not local antiviral responses to HSV infections. *PloS Pathog* (2013) 9(10):e1003728. doi: 10.1371/journal.ppat.1003728
26. Croizat H. Circulating cytokines in sickle cell patients during steady state. *Br J Haematol* (1994) 87(3):592–7.doi: 10.1111/j.1365-2141.1994.tb08318.x
27. MacDonald KP, Munster DJ, Clark GJ, Dzionek A, Schmitz J, Hart DN. Characterization of human blood dendritic cell subsets. *Blood* (2002) 100(13):4512–20. doi: 10.1182/blood-2001-11-0097
28. Alcantara-Hernandez M, Leylek R, Wagar LE, Engleman EG, Keler T, Marinkovich MP, et al. High-Dimensional Phenotypic Mapping of Human Dendritic Cells Reveals Interindividual Variation and Tissue Specialization. *Immunity* (2017) 47(6):1037–50.e6. doi: 10.1016/j.immuni.2017.11.001
29. Dutertre CA, Becht E, Irac SE, Khalilnezhad A, Narang V, Khalilnezhad S, et al. Single-Cell Analysis of Human Mononuclear Phagocytes Reveals Subset-Defining Markers and Identifies Circulating Inflammatory Dendritic Cells. *Immunity* (2019) 51(3):573–89.e8. doi: 10.1016/j.immuni.2019.08.008
30. Kapsenberg ML. Dendritic-cell control of pathogen-driven T-cell polarization. *Nat Rev Immunol* (2003) 3(12):984–93. doi: 10.1038/nri1246
31. Steinman RM, Gutchinov B, Witmer MD, Nussenzweig MC. Dendritic cells are the principal stimulators of the primary mixed leukocyte reaction in mice. *J Exp Med* (1983) 157(2):613–27. doi: 10.1084/jem.157.2.613
32. Wing K, Sakaguchi S. Regulatory T cells exert checks and balances on self tolerance and autoimmunity. *Nat Immunol* (2010) 11(1):7–13. doi: 10.1038/ni.1818
33. Liu Y, Jing F, Yi W, Mendelson A, Shi P, Walsh R, et al. HO-1(hi) patrolling monocytes protect against vaso-occlusion in sickle cell disease. *Blood* (2018) 131(14):1600–10. doi: 10.1182/blood-2017-12-819870
34. Liu Y, Zhong H, Bao W, Mendelson A, An X, Shi P, et al. Patrolling monocytes scavenge endothelial-adherent sickle RBCs: a novel mechanism of inhibition of vaso-occlusion in SCD. *Blood* (2019) 134(7):579–90. doi: 10.1182/blood.2019000172
35. Charache S, Terrin ML, Moore RD, Dover GJ, McMahon RP, Barton FB, et al. Design of the multicenter study of hydroxyurea in sickle cell anemia. Investigators of the Multicenter Study of Hydroxyurea. *Control Clin Trials* (1995) 16(6):432–46. doi: 10.1016/s0197-2456(95)00098-4
36. Steinberg MH, Barton F, Castro O, Pegelow CH, Ballas SK, Kutlar A, et al. Effect of hydroxyurea on mortality and morbidity in adult sickle cell anemia: risks and benefits up to 9 years of treatment. *JAMA* (2003) 289(13):1645–51. doi: 10.1001/jama.289.13.1645
37. Brawley OW, Cornelius LJ, Edwards LR, Gamble VN, Green BL, Inturrisi CE, et al. NIH consensus development statement on hydroxyurea treatment for sickle cell disease. *NIH Consens State Sci Statements* (2008) 25(1):1–30.
38. Schraml BU, Reis e Sousa C. Defining dendritic cells. *Curr Opin Immunol* (2015) 32:13–20. doi: 10.1016/j.coi.2014.11.001
39. Coutant F, Miossec P. Altered dendritic cell functions in autoimmune diseases: distinct and overlapping profiles. *Nat Rev Rheumatol* (2016) 12(12):703–15. doi: 10.1038/nrrheum.2016.147
40. Chu CC, Di Meglio P, Nestle FO. Harnessing dendritic cells in inflammatory skin diseases. *Semin Immunol* (2011) 23(1):28–41. doi: 10.1016/j.smim.2011.01.006
41. Shale M, Ghosh S. How intestinal epithelial cells tolerise dendritic cells and its relevance to inflammatory bowel disease. *Gut* (2009) 58(9):1291–9. doi: 10.1136/gut.2006.098475
42. Godefroy E, Liu Y, Shi P, Mitchell WB, Cohen D, Chou ST, et al. Altered heme-mediated modulation of dendritic cell function in sickle cell alloimmunization. *Haematologica* (2016) 101(9):1028–38. doi: 10.3324/haematol.2016.147181
43. Belcher JD, Marker PH, Weber JP, Hebbel RP, Vercellotti GM. Activated monocytes in sickle cell disease: potential role in the activation of vascular endothelium and vaso-occlusion. *Blood* (2000) 96(7):2451–9. doi: 10.1182/blood.V96.7.2451
44. Finnegan EM, Turhan A, Golan DE, Barabino GA. Adherent leukocytes capture sickle erythrocytes in an in vitro flow model of vaso-occlusion. *Am J Hematol* (2007) 82(4):266–75. doi: 10.1002/ajh.20819
45. Kasten KR, Prakash PS, Unsinger J, Goetzman HS, England LG, Cave CM, et al. Interleukin-7 (IL-7) treatment accelerates neutrophil recruitment through gamma delta T-cell IL-17 production in a murine model of sepsis. *Infect Immun* (2010) 78(11):4714–22. doi: 10.1128/IAI.00456-10
46. Hoshino H, Laan M, Sjostrand M, Lotvall J, Skoogh BE, Linden A. Increased elastase and myeloperoxidase activity associated with neutrophil recruitment by IL-17 in airways in vivo. *J Allergy Clin Immunol* (2000) 105(1 Pt 1):143–9. doi: 10.1016/s0091-6749(00)90189-1
47. Ambrosi A, Espinosa A, Wahren-Herlenius M. IL-17: a new actor in IFN-driven systemic autoimmune diseases. *Eur J Immunol* (2012) 42(9):2274–84. doi: 10.1002/eji.201242653

48. Miossec P. IL-17 and Th17 cells in human inflammatory diseases. *Microbes Infect* (2009) 11(5):625–30. doi: 10.1016/j.micinf.2009.04.003
49. Raghupathy R, Haider MZ, Azizieh F, Abdelsalam R, D'Souza TM, Adekile AD. Th1 and Th2 cytokine profiles in sickle cell disease. *Acta Haematol* (2000) 103(4):197–202. doi: 10.1159/000041049
50. ElAlfy MS, Adly AAM, Ebeid FSE, Eissa DS, Ismail EAR, Mohammed YH, et al. Immunological role of CD4(+)CD28(null) T lymphocytes, natural killer cells, and interferon-gamma in pediatric patients with sickle cell disease: relation to disease severity and response to therapy. *Immunol Res* (2018) 66 (4):480–90. doi: 10.1007/s12026-018-9010-y
51. McGeachy MJ, Cua DJ. Th17 cell differentiation: the long and winding road. *Immunity* (2008) 28(4):445–53. doi: 10.1016/j.immuni.2008.03.001
52. Singhal R, Rathore DK, Bhakuni T, Seth T, Guchhait P. Absence of Nonclassical Monocytes in Hemolytic Patients: Free Hb and NO-Mediated Mechanism. *J Immunol Res* (2019) 2019:1409383. doi: 10.1155/2019/1409383
53. Guarda CC, Silveira-Mattos PSM, Yahouedehou S, Santiago RP, Aleluia MM, Figueiredo CVB, et al. Hydroxyurea alters circulating monocyte subsets and dampens its inflammatory potential in sickle cell anemia patients. *Sci Rep* (2019) 9(1):14829. doi: 10.1038/s41598-019-51339-x
54. Kato GJ, Steinberg MH, Gladwin MT. Intravascular hemolysis and the pathophysiology of sickle cell disease. *J Clin Invest* (2017) 127(3):750–60. doi: 10.1172/JCI89741
55. Zhong H, Bao W, Friedman D, Yazdanbakhsh K. Hemin controls T cell polarization in sickle cell alloimmunization. *J Immunol* (2014) 193(1):102–10. doi: 10.4049/jimmunol.1400105
56. Dutra FF, Bozza MT. Heme on innate immunity and inflammation. *Front Pharmacol* (2014) 5:115. doi: 10.3389/fphar.2014.00115

Conflict of Interest: The authors declare that the research was conducted in the absence of any commercial or financial relationships that could be construed as a potential conflict of interest.

frontiers in Immunology

ORIGINAL RESEARCH
published: 11 March 2021
doi: 10.3389/fimmu.2021.559925

Immunological Hallmarks of Inflammatory Status in Vaso-Occlusive Crisis of Sickle Cell Anemia Patients

*Alexander Leonardo Silva-Junior[1,2], Nadja Pinto Garcia[2], Evilázio Cunha Cardoso[1,2], Stephanny Dias[2], Andrea Monteiro Tarragô[1,2,3], Nelson Abrahim Fraiji[1,2], Matheus Souza Gomes[4], Laurence Rodrigues Amaral[4], Andréa Teixeira-Carvalho[1,5], Olindo Assis Martins-Filho[1,5], Erich Vinicius De Paula[1,6], Allyson Guimarães Costa[1,2,3,7,8,9] and Adriana Malheiro[1,2,3,7]**

[1] Programa de Pós-Graduação em Ciências Aplicadas à Hematologia, Universidade do Estado do Amazonas (UEA), Manaus, Brazil, [2] Diretoria de Ensino e Pesquisa, Fundação Hospitalar de Hematologia e Hemoterapia do Amazonas (HEMOAM), Manaus, Brazil, [3] Programa de Pós-Graduação em Imunologia Básica e Aplicada, Instituto de Ciências Biológicas, Universidade Federal do Amazonas (UFAM), Manaus, Brazil, [4] Laboratório de Bioinformática e Análises Moleculares, Rede Multidisciplinar de Pesquisa, Ciência e Tecnologia, Universidade Federal de Uberlândia, Patos de Minas, Brazil, [5] Grupo Integrado de Pesquisas em Biomarcadores de Diagnóstico e Monitoração, Centro de Pesquisas René Rachou, Fundação Oswaldo Cruz (FIOCRUZ), Belo Horizonte, Brazil, [6] Escola de Ciências Médicas, Universidade de Campinas, Campinas, Brazil, [7] Programa de Pós-Graduação em Medicina Tropical, Universidade do Estado do Amazonas (UEA), Manaus, Brazil, [8] Instituto de Pesquisa Clínica Carlos Borborema, Fundação de Medicina Tropical Dr. Heitor Vieira Dourado (FMT-HVD), Manaus, Brazil, [9] Escola de Enfermagem de Manaus, Universidade Federal do Amazonas (UFAM), Manaus, Brazil

OPEN ACCESS

Edited by:
Caroline Le Van Kim,
Université Paris Diderot, France

Reviewed by:
Antonio Riva,
Institute of Hepatology London, United Kingdom
John D. Belcher,
University of Minnesota Twin Cities, United States

***Correspondence:**
Adriana Malheiro
malheiroadriana@yahoo.com.br

Specialty section:
This article was submitted to Inflammation, a section of the journal Frontiers in Immunology

Received: 07 May 2020
Accepted: 15 February 2021
Published: 11 March 2021

Citation:
Silva-Junior AL, Garcia NP, Cardoso EC, Dias S, Tarragô AM, Fraiji NA, Gomes MS, Amaral LR, Teixeira-Carvalho A, Martins-Filho OA, De Paula EV, Costa AG and Malheiro A (2021) Immunological Hallmarks of Inflammatory Status in Vaso-Occlusive Crisis of Sickle Cell Anemia Patients. Front. Immunol. 12:559925. doi: 10.3389/fimmu.2021.559925

Sickle Cell Anemia (SCA) is the most common genetic disorder around the world. The mutation in the β-globin gene is responsible for a higher hemolysis rate, with further involvement of immunological molecules, especially cytokines, chemokines, growth factors, and anaphylatoxins. These molecules are responsible for inducing and attracting immune cells into circulation, thus contributing to increases in leukocytes and other pro-inflammatory mediators, and can culminate in a vaso-occlusive crisis (VOC). This study aimed to characterize the levels of these molecules in SCA patients in different clinical conditions in order to identify potential hallmarks of inflammation in these patients. An analytical prospective study was conducted using the serum of SCA patients in steady-state (StSt; $n = 27$) and VOC ($n = 22$), along with 53 healthy donors (HD). Samples from the VOC group were obtained on admission and on discharge, in the convalescent phase (CV). Levels of chemokines (CXCL8, CXCL10, CL2, CLL3, CCL4, CL5, and CCL11), cytokines (IL-1β, IL-1ra, IL-2, IL-4, IL-5, IL-6, IL-7, IL-10, IL-12p70, IL-13, IL-17A, TNF-α, and IFN-γ) and growth factors (VEGF, FGFb, PDGF-BB, GM-CSF, and G-CSF) were measured using a Luminex assay, and anaphylatoxins (C3a, C4a, and C5a) were measured using Cytometric Bead Array. SCA patients in StSt showed a pro-inflammatory profile, and were indicated as being higher producers of CCL2, IL-1β, IL-12p70, IFN-γ, IL-17A, and GM-CSF, while VOC is highlighted by molecules IL-4 and IL-5, but also IL-2, IL-7, PDGF-BB, and G-CSF. PDGF-BB and IL-1ra seemed to be two important hallmarks for the acute-to-chronic stage, due to their significant decrease after crisis inflammation and statistical difference in VOC and CV groups. These molecules

show higher levels and a strong correlation with other molecules in VOC. Furthermore, they remain at higher levels even after crisis recovery, which suggest their importance in the role of inflammation during crisis and participation in immune cell adhesion and activation. These results support a relevant role of cytokines, neutrophil and monocytes, since these may act as markers of VOC inflammation in SCA patients.

Keywords: molecules, hemolytic anemia, Brazilian Amazon, immune profile, biomarkers, inflammation

INTRODUCTION

Sickle cell anemia (SCA) is the most prevalent hemoglobinopathy around the world and the most severe form of a set of genetic disorders that involve the β-globin gene (1, 2). It is caused by the homozygous form of a single mutation (adenine > thymine) on 17th nucleotide from region 15.5 of the long arm of chromosome 11, and results in production of a valine (instead of glutamic acid) and formation of a tetrameric protein known as hemoglobin S (HbS) (1, 3–7).

The mutation induces major alterations in the structure of red blood cells (RBC) secondary to the polymerization of HbS in areas of low oxygen tensions (8). These alterations lead to changes in the interaction of RBC with platelets, leukocytes and endothelial cells, contribute to both vaso-occlusion of small capillaries, and ischemia-reperfusion injury, and result in chronic hemolysis (1, 3). Accordingly, SCA is considered a chronic sterile inflammatory disease that occurs through ischemic injuries that contribute to the inflammatory process through the release of free hemoglobin during RBC hemolysis, besides other damage-associated molecular pattern (DAMP), such as heme and HMGB1. This leads to a stimulus of TLR4 and further promotes a chronic and sterile inflammation, adhesion of immune cells and vaso-occlusion process. The cellular response to this chronic stimulus contributes to the activation of neutrophils, monocytes, mast cells, endothelial cells, dendritic cells and NK cells, which are all regulated by levels of inflammatory mediator's that are driven mainly by immunological molecules (1, 8–14).

Although caused by a single mutation, the clinical presentation of SCA is modulated by the manner in which the immune system responds to chronic hemolysis and ischemia-reperfusion injury. Moreover, the disease is characterized by chronic progressive organ damage during periods known as steady-state (StSt), intercalated with acute episodes of vaso-occlusion, termed VOC, which are considered exacerbations of the pro-inflammatory condition of SCA with further formation of aggregates with immune cells, sickle RBCs and platelets (1, 8–10).

The aggregate rate is related to increase in the risk of VOC, and consequences of this include tissue injury, hypoxia, ischemia-reperfusion, renal dysfunction, acute chest syndrome, stroke, and finally, a decrease on the patient's life expectancy (3, 8, 10, 11, 15, 16). Even though many studies have analyzed immunological patterns in SCA (17–21), the relationship between these molecules and VOC inflammatory status and clinical presentation, there are still some knowledge gaps.

This study aimed to evaluate whether and to what point cytokines, chemokines, anaphylatoxins, and growth factors are hallmarks of inflammatory status for SCA patients in different clinical conditions treated at a hematological reference hospital in the Brazilian Amazon. We show here that even after clinical recovery from VOC, SCA patients still presented a higher concentration of pro-inflammatory mediators.

MATERIALS AND METHODS

Ethics Statement

The present study was submitted to and approved by the Ethical Committee at Fundação Hospitalar de Hematologia e Hemoterapia do Amazonas (CEP-HEMOAM), via the processes #1.864.640 and #2.478.469. All participants enrolled in the present investigation read and signed the informed consent form in accordance with the Declaration of Helsinki and Resolution 466/2012 of the Brazilian National Health Council for research involving human subjects.

Subjects and Samples

Whole blood samples were collected through venipuncture from 53 healthy donors (HD) that were eligible for blood donation and had no infectious or genetic disease. Samples were also collected from 27 patients with SCA in steady-state (StSt) condition (defined as the absence of clinical symptoms associated with VOC), who had not received a blood transfusion in the 90 days prior to recruitment, and had negative serology tests for HIV, HCV, HBV, HTLV and Syphilis. In addition, samples were also obtained from 22 patients with SCA in VOC (characterized by acute pain located at lumbar, hip, bone, articulation or abdominal with no other cause), which had been confirmed by health professionals at HEMOAM; the reference hospital in the Amazonas state for treatment of patients with hematological diseases. An additional blood sample was obtained from patients in the VOC group, in the period between the patients' discharge and their first outpatient visit, within 90 days from enrollment. These samples were identified as the convalescence (CV) group. Clinical and epidemiological data was obtained from medical records. In regards to treatment, the following medications were recorded: folic acid, hydroxyurea, analgesics, corticoids, and anti-inflammatory drugs for more than 1 year prior to sample collection.

From all healthy donors and patients, 8 ml of whole blood was collected and divided equally into EDTA (BD Vacutainer® EDTA K2) tubes and Gel separator (Gel BD SST® II Advance) tubes. Whole blood in EDTA tubes was used for acquisition

of hematological data for red blood cells (RBCs), white blood cells (WBCs) and platelets, which were obtained using an automatic hematological counter (ADVIA 2120i, Siemens, USA) at HEMOAM. Using centrifugation, serum was obtained from the tubes with separator gel and was then stored at −80°C until further assays.

Quantification of Immunological Molecules

Serum was used for quantifying chemokines (CXCL8, CXCL10, CCL2, CCL3, CCL4, CCL5, and CCL11), cytokines (IL-1β, IL-1ra, IL-2, IL-4, IL-5, IL-6, IL-7, IL-10, IL-12p70, IL-13, IL-17A, IFN-γ, and TNF-α) and growth factors [G-CSF, GM-CSF, PDGF-BB, VEGF, and FGF Basic (FGFb)], and was performed using the Luminex technique at Instituto René Rachou (FIOCRUZ-MG). The Bioplex-Pro Human Cytokine 27-Plex Kit (Bio-Rad, California, USA) was used following the manufacturer's instructions and protocol. Data acquisition and molecule levels were measured on a Luminex 200 System and Bioplex Manager Software, respectively, using the Five Parameters Logistic Regression, with results expressed in pg/ml. The detection limit of molecules is as follows: CXCL8 = 42,150 pg/ml; CXCL10 = 31,236 pg/ml; CCL2 = 24,282 pg/ml; CCL3 = 960 pg/ml; CCL4 = 11,233 pg/ml; PDGF-BB = 24,721 pg/ml, CCL5 = 16,533 pg/ml; CCL11 = 26,842; IL-1β = 8,608 pg/ml; IL-1ra = 91,661 pg/ml; IL-2 = 18,297 pg/ml; IL-4 = 4,789 pg/ml; IL-5 = 23,105 pg/ml; IL-6 = 37,680 pg/ml; IL-7 = 16,593 pg/ml; IL-10 = 35,170 pg/ml; IL-12p70 = 37,684 pg/ml; IL-13 = 8,090 pg/ml; IL-17A = 28,850 pg/ml; IFN-γ = 25,411 pg/ml; TNF-α = 64,803 pg/ml; FGFb = 16,046 pg/ml; G-CSF = 40,049 pg/ml; GM-CSF = 12,844 pg/ml; and VEGF = 29,464 pg/ml. Due to bead analysis issues, IL-9 and IL-15 levels could not be performed. In addition, quantification of anaphylatoxins C3a, C4a, and C5a were performed using EDTA plasma samples with the BD™ CBA (Cytometric Bead Array) Human Anaphylatoxin kit (BD® Biosciences, San Diego, CA, USA). A FACSCanto II flow cytometer was used for sample acquisition. The analysis of the concentration of anaphylatoxin molecules was conducted using FCAP-Array software v.3 (Soft Flow Inc., USA). The detection limits are as follows: C3a = 0.45 pg/ml; C4a = 0.70 pg/ml; C5a = 1.15 pg/ml.

Statistical Analysis

Data analysis and graphs were performed using GraphPad Prism v.5.0 software (San Diego, CA, USA). The Shapiro-Wilk normality test was conducted for analysis of normality distribution and acquisition of median and (25th and 75th). The epidemiological data was compared for the groups using the Chi-square test (χ^2). The median of hematological parameters and molecule levels was used for comparison of HD, StSt, and VOC using the Kruskal-Wallis test, followed by Dunn's Multiple Comparison Test. For VOC and CV group comparison, the Wilcoxon matched pair test was used. A p-value of < 0.05 was considered significant for all statistical tests.

Signature of Immunological Molecules

The median of each molecule for HD, StSt and VOC groups was calculated, as previously described (22), and used as the cut-off point. This was expressed in pg/ml (CXCL8 = 2.64; PDGF-BB = 292.0; CCL3 = 0.96; CCL4 = 10.74; CCL2 = 9.07; CCL5 = 57.0; IL-1β = 1.12; IL-1ra = 29.11; TNF-α = 12.12; IL-6 = 1.12; IL-7 = 2.82; IL-12p70 = 2.40; IL-2 = 0.44; IFN-γ = 15.85; IL-4 = 0.53; IL-5 = 2.93; IL-13 = 0.70; IL-17A = 6.74; IL-10 = 5.20; CXCL10 = 69.68; VEGF = 9.08; GM-CSF = 7.81; G-CSF = 1.24; FGFb = 3.64; CCL11 = 23.14; C3a = 10.03; C4a = 7.61; C5a = 316.9). This value was employed to classify the patients for each group as being either "High" or "Low" molecule producers. The percentage value was obtained, and presented in a Venn diagram when higher than the 50th percentile, and obtained using a public website (http://bioinformatics.psb.ugent.be/webtools/Venn/).

Immunological Hallmarks Network

The correlation analysis was conducted using Spearman test in GraphPad Prism v.5.0 software (San Diego, CA, USA), and employed all molecules and blood cell parameters for each group. The data was transferred to a spreadsheet (Microsoft Excel 2010), and the cytokine network was visualized on the open access software Cytoscape v.3.7.2. For all networks, each parameter was represented by a circular node, while a significant correlation was represented by a line connecting both correlated nodes. Absolute values of the correlation index (r) was used in order to classify correlation strength as weak ($r < 0$), moderate ($r \geq 0.36$ and ≤ 0.68), or strong ($r > 0.68$), which is represented by line thickness, while positive and negative correlation was represented by continuous and dashed lines, respectively, as previously proposed (23).

Heatmap and Decision Tree Analysis

The heatmap analyses were performed using the serum concentration levels of each biomarker evaluated using heatmap.2 function in R software (Project for Statistical Computing Version 3.0.1) and the gplots package. The decision trees were built using the WEKA software (Waikato Environment for Knowledge Analysis, version 3.6.11, University of Waikato, New Zealand) in order to classify SCA patients based on immunological markers. Leave-one-out-cross-validation (LOOCV) was applied in order to estimate the classification accuracy and to test the generalizability of the model.

RESULTS

Epidemiological and Laboratorial Data

SCA patients presented a median of 22 years of age in StSt and VOC groups, while the median age of the control group was 30 years ($p = 0.0324$). Males were the majority gender in the HD group (70%), while females were the majority in the StSt group (67%). Data regarding place of residence and chronic pharmacological treatment is described in **Table 1**.

Hematological values of each group, the medians and the results of the statistical analysis are described in **Table 2**. Patients in StSt had lower RBC, hemoglobin and hematocrit levels, when compared to the healthy donors. In addition, SCA patients (both StSt and VOC) showed increased levels of reticulocytes. The VOC group was marked by higher WBC counts, which

TABLE 1 | Epidemiological data of HD and SCA patients, showing age, gender, city of residence, and chronic pharmacological treatment.

Variable	HD $n = 53$	StSt $n = 27$	VOC $n = 22$	CV $n = 22$	*p*-value
Age (years, median [IQR])	30 [23–42]	30 [22–34]	22 [14–34]	22 [14–34]	***0.032***
Gender, *n (%)*					
Male	37 (70)	9 (37)	11 (50)	11 (50)	***0.016***[a]
Female	16 (30)	18 (67)	11 (50)	11 (50)	
Place of residence, *n (%)*					
Manaus, AM	53 (100)	23 (85)	20 (91)	20 (91)	0.063
Interior of Amazonas state	–	4 (15)	2 (9)	2 (9)	
Chronic pharmacological treatment, *n (%)*					
Folic acid	–	25 (93)	17 (77)	17 (77)	0.219
Hydroxyureia	–	22 (81)	14 (63)	14 (63)	0.202
Analgesic	–	12 (44)	12 (54)	12 (54)	0.570
Corticoid	–	2 (7)	–	–	1
Anti-inflammatory	–	1 (4)	5 (23)	5 (23)	0.077

HD, Healthy Donors; StSt, Steady-state; VOC, Vaso-Occlusive Crisis; CV, Convalescence.
[a]*Significant difference for HD vs. StSt.*
Statistical analysis performed by Kruskal-Wallis with Dunn's Multiple Comparison Test for the variable of age in order to compare HD, and SS and VOC. In addition, Wilcoxon test was performed for VOC and CV comparison. Gender and city of residence was compared using a Chi-Square (χ^2) test. For both analyses, p was considered significant when < 0.05. Bold-type font indicates statistical significance.

seem to be driven by neutrophil and monocyte involvement, although only the neutrophil level was statistically lower after crisis. Basophil levels decreased in conditions of StSt to VOC, but no significant difference was observed in conditions of VOC and the convalescent phase. Even though platelet level had no statistical difference in SCA patients, it was higher than in the HD group. SCA patients, regardless of inflammatory status, showed higher involvement of lymphocytes and platelets.

SCA Is Marked by an Inflammatory Molecule Profile Regardless of Clinical Condition

With the aim of characterizing the profile of serum biomarkers in SCA patients, a range of soluble mediators were quantified in StSt, VOC groups, and compared to the HD group. Significantly higher levels of chemokines (CXCL8, CXCL10, CCL3, CCL4, CCL5), cytokines (IL-1β, IL-12p70, IL-17A, IL-10), growth factors (VEGF and GM-CSF) and anaphylatoxin C4a were found in SCA patients, when compared to the HD group, as shown in **Figure 1**. Chemokines seemed to be more involved in VOC, when compared to StSt, through increased levels of CCL3, CCL5, and CCL11 (**Figure 1A**). Furthermore, IL-4 and IL-5 levels were higher (**Figure 1B**). The inflammatory status observed in the StSt group was characterized by an increased concentration of the pro-inflammatory molecules IL-1β, TNF-α, IL12p70, IFN-γ, and IL-17A, despite there being higher circulating levels of IL-10, GM-CSF, C4a, and C5a, when compared to the VOC group (**Figures 1A,C,D**). In addition, in our molecule analysis we observed that patients in the VOC group have significantly higher median values of cell proliferation markers.

Signature of Immune Molecules Presented by HD, StSt, and VOC Groups

Figure 2 summarizes the biomarker signatures and presents the Venn diagram of immunological molecules, with respective intersections and elements for the HD, StSt, and VOC groups. Our aim was to describe which group was classified as being the highest producer of molecules, and which belong exclusively to each group (**Figure 2A**). Inflammatory status in the StSt group showed that the majority of patients have increased levels of 22 soluble immune molecules, while the StSt group presented as higher producers of only six: CCL2, IL-1β, IL-12p70, IFN-γ, IL-17A, and GM-CSF, based on the majority of patients and the global median (**Figure 2B**). Our analysis did not identify any molecule that all three groups share as high producers, however, the HD and StSt groups both showed higher production of TNF-α, C5a, and IL-6, and SCA patients, regardless of inflammatory status presented themselves as higher producers of 13 immune molecules (**Figure 2B**). Although 19 molecules were identified as having higher production in VOC, only six were shown exclusively in this stage: IL-2, IL-7, IL-4, IL-5, PDGF-BB, and G-CSF, which suggests that the VOC condition is orchestrated not just by anti-inflammatory cytokines, but also by intense cell proliferation (**Figure 2B**).

Potential of Immunological Markers IL-1β, IL-10, IL-1ra, and IL-6 for Distinguishing Clinical Conditions (StSt, VOC, and CV) in SCA Patients

The heatmap analysis was performed with the serum levels of the immune molecules of SCA patients to demonstrate the components used in the clustering of the StSt or VOC subgroups when compared to the healthy individuals. Even

TABLE 2 | Laboratorial data of hematological parameters from HD, StSt, VOC and CV groups.

Variables	HD $n = 53$	StSt $n = 27$	VOC $n = 22$	CV $n = 22$	*p*-value
RBC ($\times 10^6/\mu L$, median [IQR])	4.99 [4.59–5.40]	2.51 [2.19–2.75]	2.39 [2.09–2.94]	2.65 [2.29–3.12]	**<0.0001[a,b]**
Hemoglobin (g/dL, median [IQR])	14.90 [13.55–15.95]	8.0 [7.10–9.0]	7.50 [6.20–8.45]	8.30 [7.20–8.70]	**<0.0001[a,b]**
Hematocrit (%, median [IQR])	43.70 [40.45–47.30]	24.50 [21.70-28.50]	22.0 [18.60–25.0]	24.80 [21.95–26.68]	**<0.0001[a,b,d]**
MCV (fL, median [IQR])	87.80 [84.85–90.4]	99.90 [92.80–110.2]	91.30 [79.60–99.80]	90.55 [86.83–99.15]	**<0.0001 [a,c]**
MCH (pg, median [IQR])	29.70 [28.90–30.60]	32.10 [30.30–36.70]	31.10 [27.35–33.20]	29.70 [27.58–34.03]	**0.0008[a]**
MCHC (g/dL, median [IQR])	34.10 [33.10–34.60]	32.70 [31.90–34.10]	33.60 [32.90–34.05]	33.15 [32.40–33.95]	**0.0057[a]**
RDW (fL, median [IQR])	13.70 [12.95-13.95]	18.20 [17.30–19.80]	21.20 [19.65–23.80]	19.95 [18.08–22.90]	**<0.0001[a,b]**
Reticulocyte ($\times 10^3/\mu L$, median [IQR])	72.70 [56.90–88.80]	367.6 [226.0–529.9]	257.4 [134.3–349.2]	248.6 [134.5–332.8]	**<0.0001[a,b]**
WBC ($\times 10^6/\mu L$, median [IQR])	6.33 [5.27–7.10]	7.42 [5.95–9.44]	11.39 [8.82–15.17]	9.51 [8.07–11.38]	**<0.0001[b,c]**
Neutrophil ($x10^3/\mu L$, median [IQR])	3.43 [2.80–4.18]	3.39 [2.13–4.81]	6.90 [4.87–9.46]	4.88 [3.05–6.43]	**<0.0001[b,c,d]**
Lymphocyte ($v10^3/\mu L$, median [IQR])	1.84 [1.55–2.16]	2.41 [2.13–3.36]	3.02 [2.32–4.78]	3.28 [2.43–4.96]	**<0.0001[a,b]**
Monocyte ($\times 10^3/\mu L$, median [IQR])	0.38 [0.29–0.41]	0.43 [0.33–0.69]	0.66 [0.52–0.86]	0.60 [0.41–0.83]	**< 0.0001[b,c]**
Basophil ($\times 10^3/\mu L$, median [IQR])	0.03 [0.02–0.05]	0.03 [0.03–0.05]	0.00 [0.00–0.03]	0.00 [0.00–0.04]	**0.0002[b,c]**
Eosinophil ($\times 10^3/\mu L$, median [IQR])	0.19 [0.12–0.41]	0.24 [0.13–0.50]	0.22 [0.10–0.62]	0.42 [0.24–0.62]	0.6031
Platelet count ($\times 10^3/\mu L$, median [IQR])	244 [213–281.5]	420 [372–533]	411 [326–530]	460.5 [339.8–642.0]	**<0.0001[a,b]**

[a] *Significant difference for HD vs. StSt.*
[b] *Significant difference for HD vs. VOC.*
[c] *Significant difference for StSt vs. VOC.*
[d] *Significant difference for VOC vs. CV. Statistical analysis performed using Kruskal-Wallis with Dunn's Multiple Comparison Test in order to compare HD, StSt and VOC. In addition, Wilcoxon test was performed for VOC and CV comparison. For both analyses, p was considered significant when <0.05.*
Bold-type font indicates statistical significance.

though histograms of the comparison of the HD (top bar yellow) group with the SCA StSt (top bar red) group (**Figure 3A**) and the VOC (top bar green) group (**Figure 3B**) had better clustering when compared to SCA patients, our tree decision analysis for SCA subgroups highlighted IL-10 and IL-1ra levels as the major attributes for characterizing healthy individuals and patients in StSt based on molecule profile, with a global accuracy of 100%, which reached 96% after LOOCV (**Figure 3C**). Analysis showed that circulating levels of IL-10 when ≤17.56 pg/ml indicated an HD group, while when >17.56 pg/ml, a further analysis contributed to identify HD if IL-1ra >62.88 pg/ml or StSt if IL-1ra ≤62.88 pg/ml (**Figure 3C**). In order to characterize the HD and VOC groups, the serum biomarker levels contributed to cluster the HD group if IL-1β >0.43 pg/ml or VOC if IL-1β ≤0.43 pg/ml with 100% accuracy, which reached 98% after LOOCV (**Figure 3D**). Under SCA subgroups, IL-1β can also be used to categorize StSt patients, when >0.43 pg/ml, or if <0.43 pg/ml, a further analysis contribute to identify VOC if IL-6 >2.66 pg/ml or CV if IL-6 ≤2.66 pg/ml (**Figure 3E**).

Hallmarks of Immune Molecules in Acute-to-Chronic SCA Patients After VOC

A follow-up was performed in patients during the VOC condition, which compared samples obtained on admission and after convalescence. By analyzing the results obtained, we could identify the most sensitive markers of SCA physiopathology after VOC recovery. The median time between sample collection was 53 days. However, our results show that the inflammatory profile did not change significantly. Both the VOC and the CV states maintained a similar immunological profile, with the exception of CXCL8, CCL4, IL-1ra, and PDGF-BB (**Figures 4A–C**). Even though CXCL8 and CCL4 had significantly lower levels in CV, there was no observed difference in median values in StSt and VOC groups, which was different from IL-1ra and PDGF-BB. As shown in **Figures 1**, **4**, hallmarks of acute-to-chronic transition

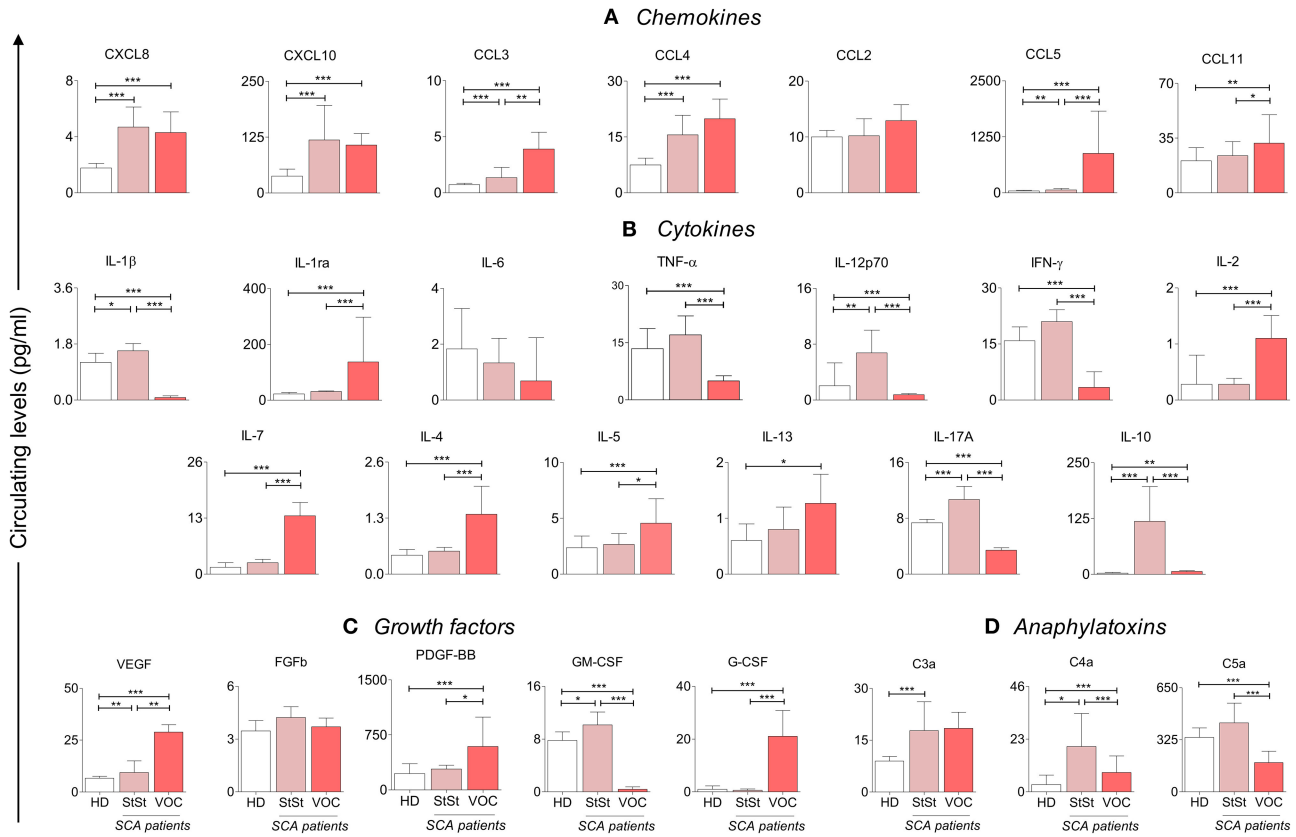

FIGURE 1 | SCA patients in VOC (■) condition show an anti-inflammatory cytokine profile, when compared to StSt (■) and HD (□) groups. Statistically significant values were considered when $p < 0.05$, and are presented as $^{*}p < 0.05$; $^{**}p < 0.01$; $^{***}p < 0.001$. Chemokines **(A)**, cytokines **(B)** and growth factors **(C)** were measured using Luminex, and anaphylatoxins **(D)** measured using CBA. Data is presented as median values and interquartile range in pg/ml. Statistical analysis was performed using Kruskal-Wallis and Dunn's Multiple Comparison Test. HD, healthy donors; StSt, Steady-state; VOC, vaso-occlusive crisis.

can be marked by all four of these molecules, although only IL-1ra and PDGF-BB showed significant differences in both states.

SCA Patients Display a Complex Correlation Network With Different Involvement in Immune Molecules Based on Inflammatory Status

Despite the function of most immune molecules being already known, correlation analysis allows us to observe interaction among the groups. Thus, we observed that correlation analysis in the HD group and the SCA StSt and VOC patients had different patterns. While StSt patients have less interactions, a chronic inflammatory condition mediated by monocyte, driven by IL-17A, IL-12p70, CXCL10, and CCL4 (**Figure 5B**) can be seen when compared to the HD group (**Figure 5A**). In contrast, the VOC group had an increase in correlation molecules, which was highlighted by the inflammatory pattern and polarized to an anti-inflammatory response, and showed a main interaction of IL-1β, IL-2, IL-7, IL-4, IL-5, IL-13, IL-17A, FGFb, and GM-CSF (**Figure 5C**). Besides the strong and positive correlations observed, GM-CSF and IL-1ra had a strong but negative correlation. The CV group network had a lower correlation index (**Figure 5D**), although the molecules described in VOC still seemed to have higher participation in the acute-to-chronic inflammation process.

Correlation matrices further corroborate these findings and highlight that while HD (**Figure 6A**) displayed a hallmark network with an overall moderate connectivity and the StSt group (**Figure 6B**) presented a panoramic network with less neighborhood connections, the VOC patients exhibited a higher level of immune marker connectivity, particularly within the cytokine axis (**Figure 6C**). As the VOC group shift toward the CV group (**Figure 6D**) a clear downregulation of biomarker connectivity can be observed.

DISCUSSION

SCA is marked by intense inflammation that is secondary to systemic injury and clinical status. The inflammatory process is evidenced by several interactions of cells, such as neutrophils, monocytes, platelets, and RBCs, which are involved in the pathogenesis of this condition. Accordingly, immunological molecules, especially cytokines, chemokines, growth factors, and anaphylatoxins are also relevant as regulators of this process.

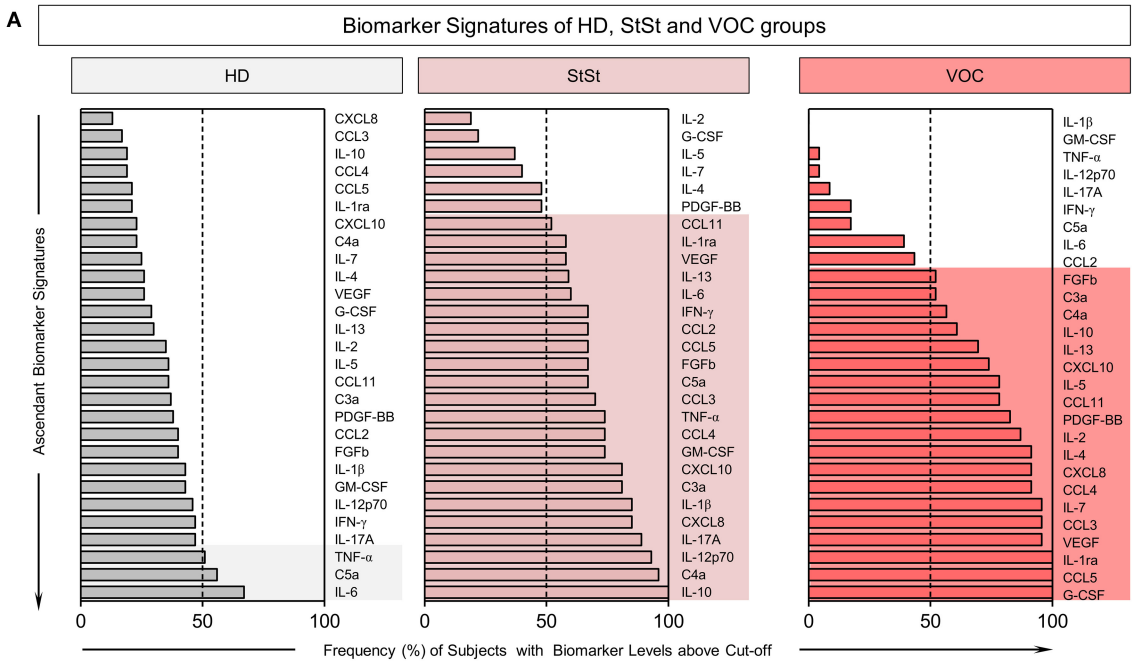

Groups	Intersections	Elements
StSt	6	CCL2, IL-1β, L-12p70, IFN-γ, IL-17A and GM-CSF
HD / StSt	3	IL-6, TNF-α and C5a
StSt / VOC	13	CXCL8, CXCL10, CCL3, CCL4, CCL5, CCL11, IL-1ra, IL-13, IL-10, VEGF, FGFb, C3a and C4a
VOC	**6**	**IL-4, IL-5, IL-2, IL-7, PDGF-BB, G-CSF**

FIGURE 2 | Immunological molecules in VOC clinical condition of SCA patients presented in a Venn diagram. **(A)** Ascendant Biomarker Signature of HD, StSt and VOC groups based on frequency of subjects with biomarker levels above Cut-off. **(B)** Venn Diagram with respective groups, intersections, and elements reported as potential hallmarks. The elements describe which molecules are potential hallmarks for each clinical condition and controls. Molecules were measured using Luminex and CBA. The global median for each soluble molecule was calculated and used as a cut-off point in order to classify groups as low (<50%) or high (>50%) producers of chemokines, cytokines, growth factors and anaphylatoxins. HD, healthy donors; StSt, steady-state; VOC, vaso-occlusive crisis.

Although several studies have evaluated the levels of these molecules and their association with clinical characteristics of SCA, little evidence is available regarding the interaction of these molecules in the individuals with SCA, particularly during VOC and in the transition from the acute-to-chronic state after a VOC. The main finding of our study was the ability to use IL-1β, IL-10, and IL-1ra levels to segregate subgroups of SCA patients.

Patients in StSt have less disease severity and show no threatening clinical symptoms, in comparison to those patients in crisis. Even with no severe symptoms, inflammatory markers are still present, in comparison to healthy controls. In addition, these molecules are involved in immune response that contributes to vaso-occlusion episodes (3, 8, 24). The chronic inflammation in StSt seem to be characterized by increased levels in the pro-inflammatory cytokines IL-1β, TNF-α, IL-12p70, IFN-γ, and circulating cells but with less endothelial involvement, similarly to what has been observed in other studies (18, 25–28). It has already been established that neutrophils, monocytes and pro-inflammatory molecules, together with platelets, play an important role in disease severity (3, 9, 26, 29). Increased levels of IL-10 in the StSt has been described as part of T-cell differentiation (30), VOC development and disease severity (31), suggesting that this cytokine participates in the process of regulating the pro-inflammatory state. Furthermore, other factors, such as infectious or other genetic diseases, influence inflammatory response and contribute to vaso-occlusion, thus, reducing patient's life expectancy (1, 10).

Acute inflammation is characterized by local ischemia/reperfusion injury, leukocyte recruitment and circulating cell activation, which contribute to severe

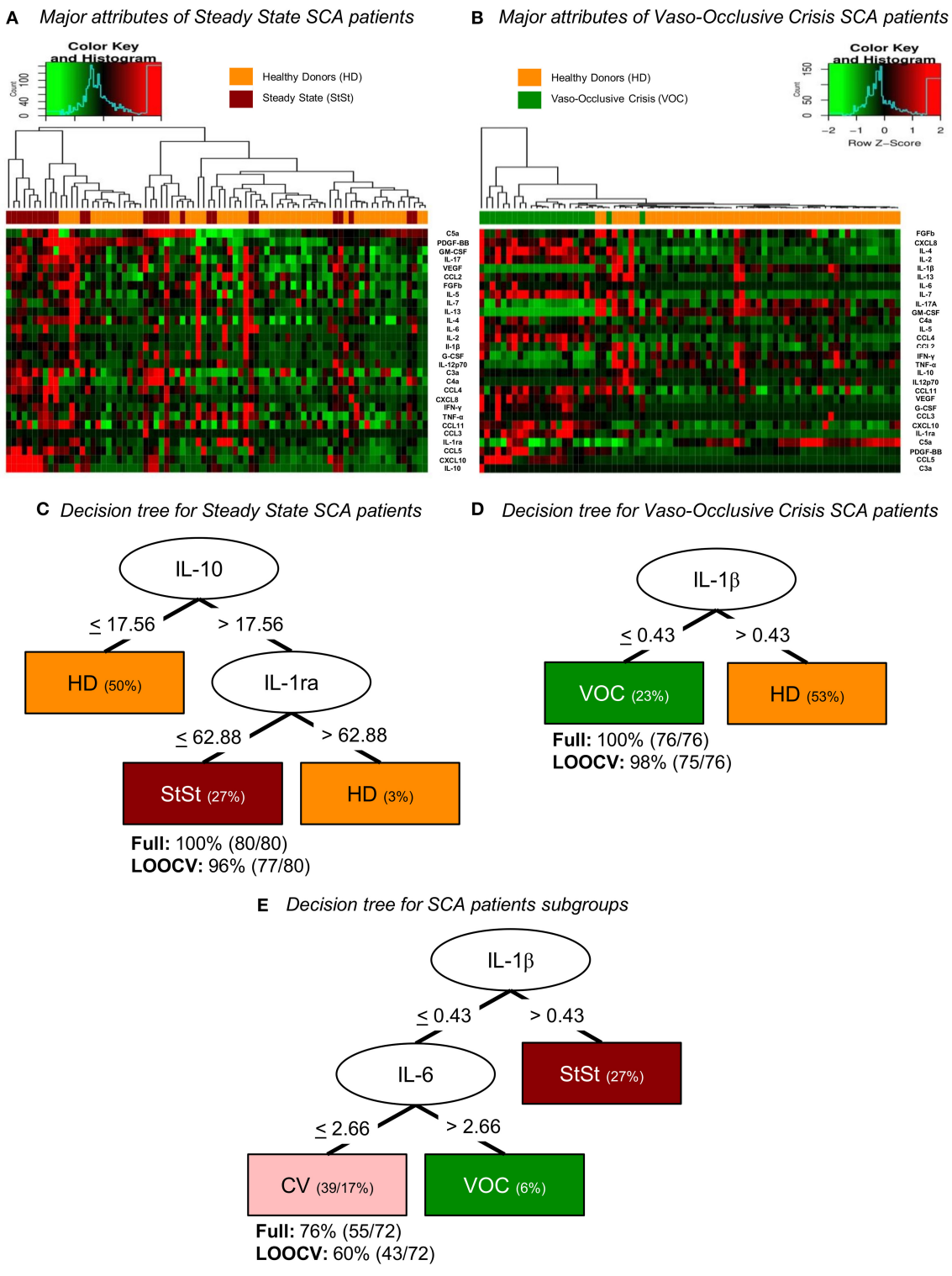

FIGURE 3 | Bioinformatic analysis of serum molecules divided into the attributes of the control group and SCA subgroups according to clinical condition, represented by heatmaps **(A,B)** and decision trees **(C–E)** of z-score normalized events. **(A)** Molecule attributes showed the ability to cluster healthy individuals and steady-state SCA patients. **(B)** Heatmap analysis also shows high ability to distinguish controls and vaso-occlusive SCA patients. **(C)** Decision tree analysis provides the clustering based on IL-10 circulating levels in order to classify individuals as HD if ≤ 17.56 pg/ml or if > 17.56 pg/ml, analyze IL-1ra level to categorize as HD if > 62.88 pg/ml or as StSt if ≤ 62.88 pg/ml. **(D)** Decision tree analysis provides clustering of HD and VOC groups based on IL-1β circulating levels in order to categorize individuals as HD if > 0.43 pg/ml or as VOC if ≤ 0.43 pg/ml. **(E)** Decision tree analysis provides clustering of SCA patients based on IL-1β circulating levels in order to classify individuals as StSt if > 0.43 pg/ml or if ≤ 0.43 pg/ml, analyze IL-6 level to categorize as VOC if > 2.66 pg/ml or as CV if ≤ 2.66 pg/ml. HD, healthy donors; StSt, steady-state; VOC, Vaso-occlusive crisis; CV, Convalescence; LOOCV, Leave-One-Out Cross Validation.

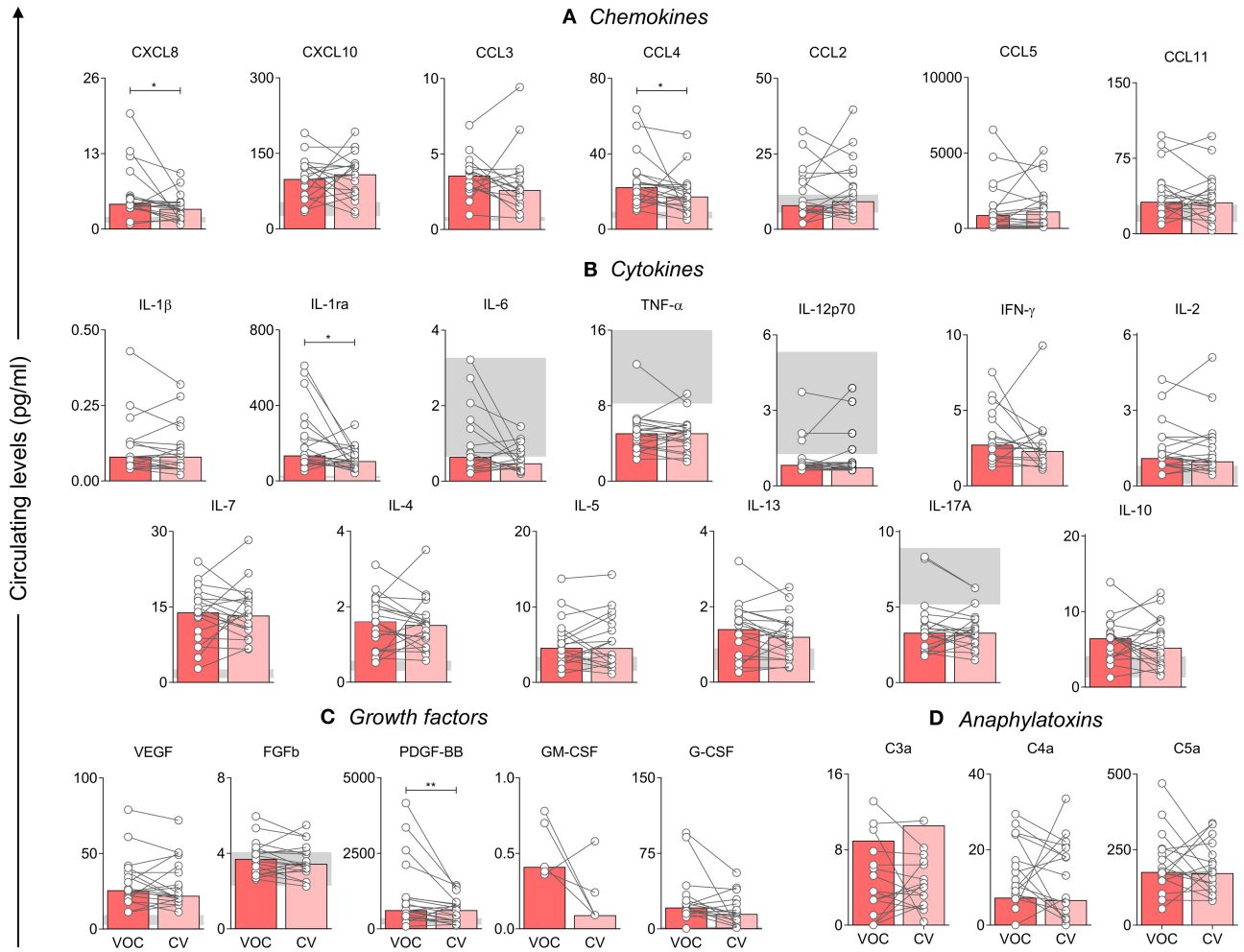

FIGURE 4 | Analysis of the first molecules that decrease after crisis, when compared with VOC (■) and CV (■) groups. Statistical analysis was performed using the Wilcoxon test. A p-value < 0.05 was considered statistically significant and was presented as $^{*}p < 0.05$; $^{**}p < 0.01$. Chemokines **(A)**, cytokines **(B)**, and growth factors **(C)** were measured using Luminex, and anaphylatoxins **(D)** using CBA. Data is shown as median values and interquartile range, using data in pg/ml. VOC, Vaso-occlusive crisis; CV, Convalescence.

clinical symptoms in a VOC (3, 8). Some studies describe the participation of anti-inflammatory cytokines in this condition (8, 20, 24, 30) and, in addition, our results show that it is marked mainly by IL-1ra and IL-4 molecules, with involvement of adherent neutrophils and monocytes. Many studies have focused on differences in molecule levels in StSt and VOC (17–19, 32), However few studies have focused on immunological hallmarks, which can be used to describe the transition between inflammatory states (StSt, VOC, and convalescence). Increased levels of IL-2 and IL-7, together with growth factors, have been previously observed (20) and contribute to proliferation and maturation of granulocytes. In addition, the findings regarding chemokines support the statement that these circulating cells show a higher capacity to adhere to endothelial cells and form cell-to-cell and cell-endothelium aggregates in VOC, which contributes to endothelial injury, inflammatory marker production, immune cell recruitment, vaso-occlusion and consequently severe clinical complications, as described by other authors (3, 10, 29, 30, 33). Our data demonstrated that VOC patients displayed a lack of canonical pro-inflammatory factors and a clear increase in regulatory mediators. This may suggest that VOC is not an anti-inflammatory condition *per se*, but it may be linked to a skew in the "type" of inflammation rather than its magnitude/strength. The analysis of biomarker networks and the correlation matrices between pairs of soluble mediators demonstrated that there is strong connectivity between pro-inflammatory/regulatory cytokines in VOC. The strength of IL-1β connections in VOC was noteworthy and may suggest that the inflammasome activation may participate in SCA pathophysiology.

We identified that the alternative pathway of the complement system is not that different under StSt or VOC, contrary to what has been described by other authors. IL-1β and IL-17A might be indirectly related to classical activation of the complement

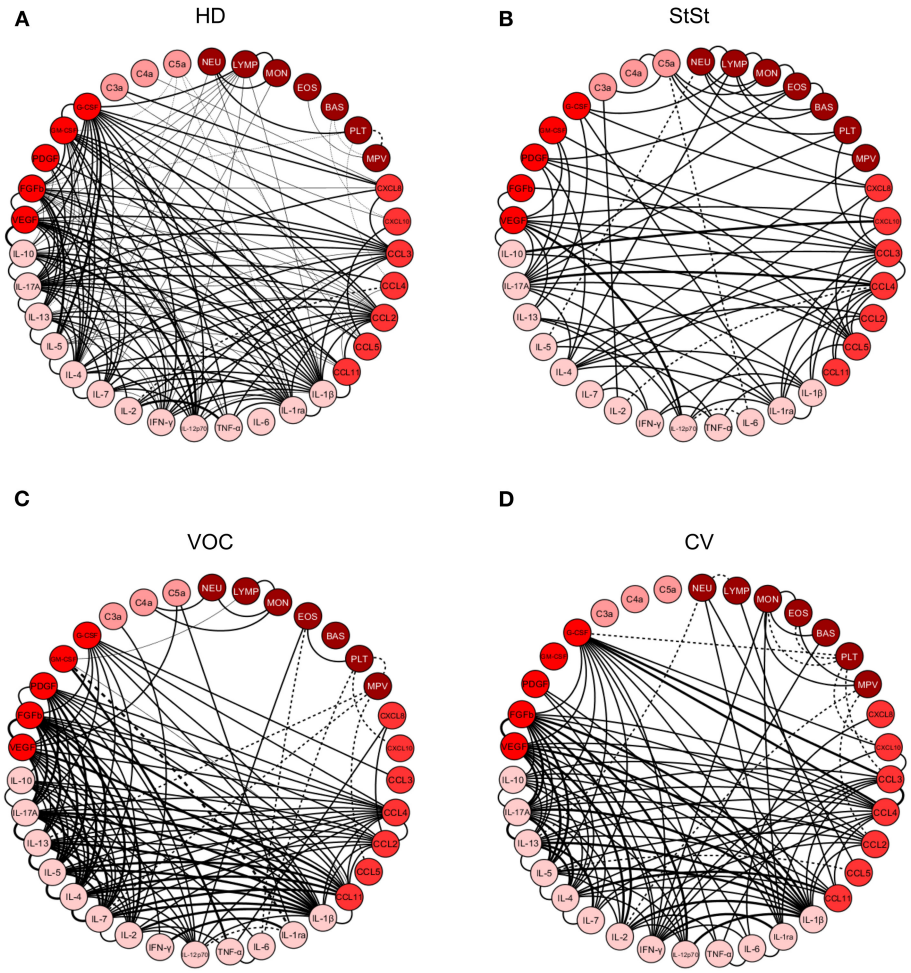

FIGURE 5 | Correlation analysis presented as a network of immunological cytokines, chemokines, growth factors, anaphylatoxins, and leukocytes in healthy donors **(A)**, steady-state **(B)** vaso-occlusive crisis **(C)**, and convalescence **(D)** stages. Each parameter is shown in a node. Statistical analysis was performed using the Spearman correlation test and the significant correlations ($p < 0.05$) are represented by a line connecting both nodes. The correlation was classified as weak ($r < 0$), moderate ($0.36 < r < 0.68$) and strong ($r > 0.68$), based on absolute value of correlation index r, represented by line thickness. Positive correlation is expressed by a continuous line, while negative correlation by dashed lines. NEU, Neutrophil; LYMP, Lymphocytes; MON, Monocytes; EOS, Eosinophils; BAS, Basophils; PLT, Platelets; MPV, Mean platelet volume; chemokines (CXCL8; CXCL10; CCL3; CCL4; CCL2; CCL5; CCL11), cytokines (IL-1β; IL-1ra; IL-6; TNF-α; IL-12p70; IFN-γ; IL-2; IL-7; IL-4; IL-5; IL-13; IL-17A; IL-10), growth factors (VEGF; FGFb; PDGF; GM-CSF; G-CSF) and anaphylatoxins (C3a; C4a; C5a). HD, Healthy donors; StSt, Steady-state; VOC, vaso-occlusive crisis; CV, convalescence.

system through C-reactive protein (CRP) production from the liver (32, 34–36), and further interaction with natural antibodies (37), culminating in higher C4 cleavage rate. Free heme interacts with C1q ligands (CRP and immunoglobulin) and leads to less classical complement activation in VOC (38); and with C3, culminating on higher C3 cleavage rate (39, 40). Free heme availability and its direct and indirect interaction to complement molecules may explain why the SCA groups had no significant difference in C3a levels. This increased activation of the complement pathway has already been described in StSt patients and observed in our results (41). Little information related to the involvement of the complement system in SCA is available, but even though the production of anaphylatoxins is well defined, the function of anaphylatoxins as inflammatory or regulatory molecules remains unclear in SCA pathophysiology.

Surprisingly, both HD and StSt groups were identified as higher producers of the pro-inflammatory molecules TNF-α and IL-6, although only TNF-α levels were significantly higher in VOC, though not IL-6, as observed in some studies (18, 27, 28) and in contrast to others (17, 20, 32, 36, 42–44). VOC was characterized as being a higher producer of anti-inflammatory and immune cell proliferation cytokines. It is important to notice that IL-4 and IL-5 are also produced by activated mast cells, in which have been reported during VOC in mice, and are important contributor on pain (14). Even though higher levels of some cytokines have been described by other authors, this characterization has never been described before for SCA patients.

Complementarily, our bioinformatic analysis permitted the segregation of SCA patients based on circulating IL-1β, IL-10,

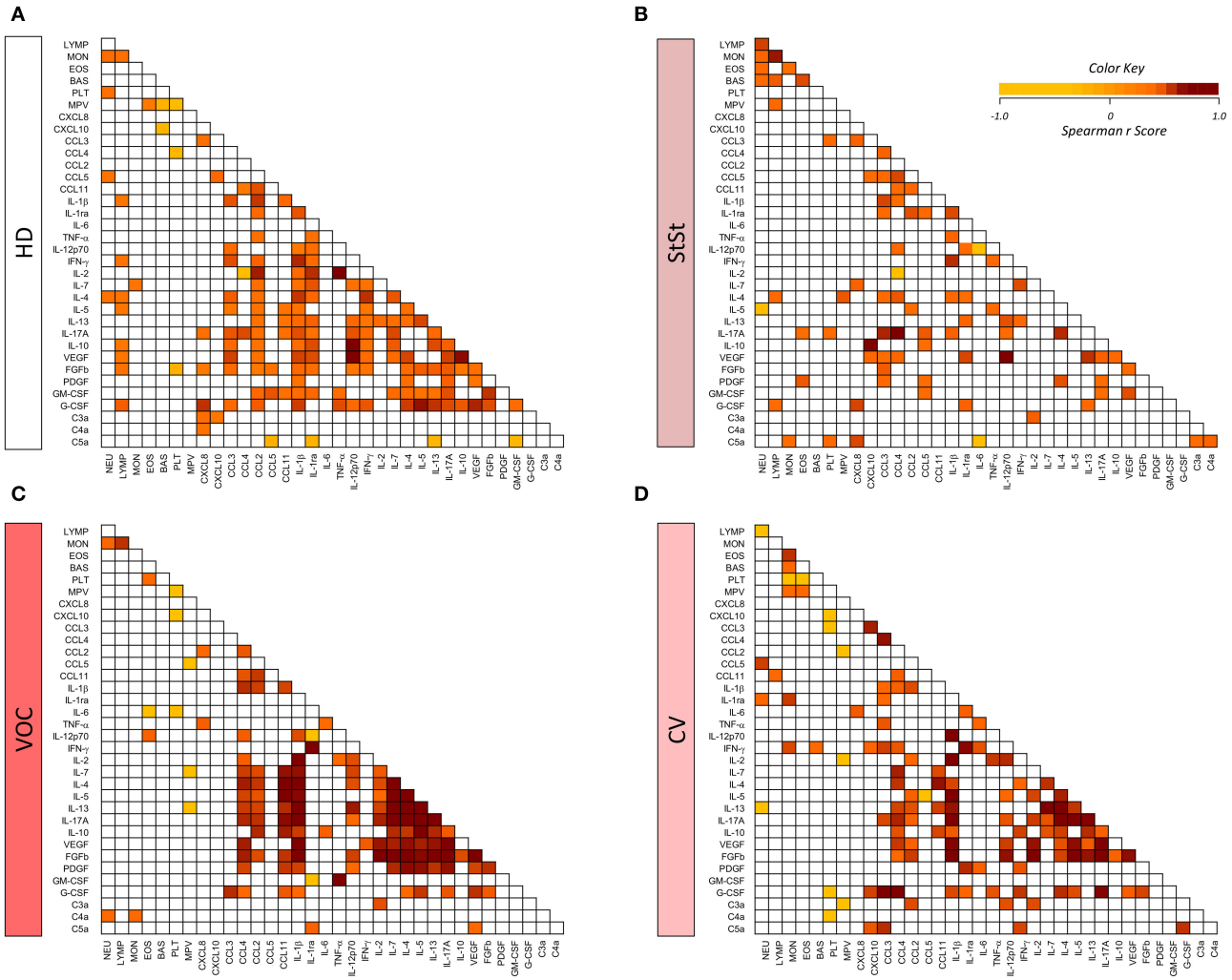

FIGURE 6 | Biomarker correlation matrices illustrate distinct patterns of biomarker connectivity in healthy donors **(A)**, steady-state **(B)**, vaso-occlusive crisis **(C)** and convalescence **(D)** stages. Biomarker networks were based on the Spearman's correlation indices (*r*). Correlation matrices display significant association ($p < 0.05$) between biomarker pairs based on the rank indices, which are tagged by color keys, ranging from −1.0 to 1.0 to underscore the correlation strength, according to the color key provided in the figure. NEU, Neutrophil; LYMP, Lymphocytes; MON, Monocytes; EOS, Eosinophils; BAS, Basophils; PLT, Platelets; MPV, Mean platelet volume; chemokines (CXCL8; CXCL10; CCL3; CCL4; CCL2; CCL5; CCL11), cytokines ((IL-1β; IL-1ra; IL-6; TNF-α; IL-12p70; IFN-γ; IL-2; IL-7; IL-4; IL-5; IL-13; IL-17A; IL-10), growth factors (VEGF; FGFb; PDGF; GM-CSF; G-CSF), and anaphylatoxins (C3a; C4a; C5a). HD, healthy donors; StSt, steady-state; VOC, vaso-occlusive crisis; CV, convalescence.

IL-1ra, and IL-6 levels, and regardless of their role, we described these molecules as potential hallmarks for segregating these patients into StSt, VOC, and CV groups. The decision trees show novel proposals for biomarkers that should to be investigated in further studies for a better comprehension of SCA physiopathology and thus may contribute to better clinical decisions.

The CV group was an intermediary period in VOC and StSt stages, for which we observed that the first inflammatory mediators to decrease were CXCL8, CCL4, IL-1ra, and PDGF-BB after hospital release after a VOC episode. However, only IL-1ra and PDGF-BB presented statistical differences in VOC and StSt groups. Even though IL-1ra is known to be an anti-inflammatory marker, its concentration was related to increased events of pain (45). As such, we believe that these results may contribute to the SCA patient's follow-up after treatment for VOC episodes. In addition, the correlations allowed us to identify that, during this acute-to-chronic transition, some interactions in the main molecules responsible for cell proliferation still remain, which indicates that there still is stimulus for leukocytosis, even though the inflammation pattern does not differ that much from VOC.

A strong and positive correlation under TNF-α and GM-CSF in VOC was identified in our analysis, which sustains a positive inflammatory pattern, with further leukocyte recruitment and activation, especially neutrophils and monocytes (9, 33). Negative feedback is observed in both StSt and VOC conditions, the

first is mediated by IL-10, while the second by IL-1ra, which is an inactive antagonist of IL-1β. This statement is supported by the IL-10/CXCL10 and IL-1ra/GM-CSF axis in StSt and VOC, respectively. IL-10's role as a biomarker in SCA is still controversial, since some authors describe lower levels in StSt, when compared to the control group, together with CXCL10 (43), while others found increased levels (20, 30, 46, 47) and some show no difference (17).

The present study has some limitations. Since SCA is considered a sterile inflammatory disease, the assessment of the TLRs expression, as well as the analysis of checkpoints in immune cell subsets along with quantification of other cytokines (IL-1a, IL-18, and IL-33), would provide a more detailed description regarding the inflammasome activation in order to more fully understand SCA pathophysiology and allow for the identification of novel prognostic factors. These aspects remain to be elucidated in future investigations.

Our study brought new perspectives for inflammatory knowledge of SCA. In fact, the role of many molecules in SCA is still discussable whether inflammatory or regulatory, as well as their association to a VOC development or as a consequence of a VOC.

CONCLUSION

Herein, we highlight the interactions of IL-4 and IL-2 cytokines in VOC, as well as the efficacy of IL-1ra and PDGF-BB as markers of clinical recovery post-VOC. In addition, we describe the ability of IL-10 and IL-1ra levels to cluster patients into HD or StSt, and IL-1β levels to cluster patients into HD or VOC. Our results contribute to novel markers in the Brazilian Amazon SCA population, and suggest their potential in prognosis and follow-up after hospital recovery from VOC. The present study is the first report on inflammatory hallmarks in VOC and CV in sickle cell anemia patients and supports greater understanding of disease pathophysiology mechanisms in order to identify novel inflammatory biomarkers and contribute to therapeutic perspectives.

DATA AVAILABILITY STATEMENT

The original contributions presented in the study are included in the article/supplementary material, further inquiries can be directed to the corresponding author/s.

ETHICS STATEMENT

The studies involving human participants were reviewed and approved by the Ethical Committee at Fundação Hospitalar de Hematologia e Hemoterapia do Amazonas (CEP-HEMOAM), via the processes #1.864.640 and #2.478.469. All participants enrolled in the present investigation read and signed the informed consent form in accordance with the Declaration of Helsinki and Resolution 466/2012 of the Brazilian National Health Council for research involving human subjects. The patients/participants provided their written informed consent to participate in this study.

AUTHOR CONTRIBUTIONS

AS-J, AC, and AM designed, performed the experiments, analyzed data, and wrote the manuscript. AS-J, MG, LA, OM-F, and AC analyzed data. AS-J, NG, EC, SD, and AT recruited all individuals, performed the experiments, and revised the manuscript. NF, AT-C, and ED revised the manuscript. AS-J, NG, AT, OM-F, AT-C, and AM supervised the project development, designed the experiments, interpreted the data, wrote, and revised the manuscript. All authors read and approved the final manuscript.

FUNDING

This study was funded by Fundação de Amparo à Pesquisa do Estado do Amazonas (FAPEAM) (Pró-Estado Program—#002/2008, #007/2018, and #005/2019, PAMEQ Program—#004/2019 and PAPAC Program—#005/2019), Conselho Nacional de Desenvolvimento Científico e Tecnológico (CNPq), Coordenação de Aperfeiçoamento de Pessoal de Nível Superior (CAPES) (PROCAD-Amazônia 2018 Program—#88881.200581/2018-01). AS-J, EC, SD had fellowship from CAPES and FAPEAM (PhD, Master and SI students). OM-F was level 1 research fellow from CNPq and a research fellow from FAPEAM (PVN-II, Pró-Estado Program—#002/2008, #007/2018 and #005/2019). AT-C and AM were level 2 research fellows from CNPq. The funders had no participation in study design, sample and data collection, analysis and manuscript development.

ACKNOWLEDGMENTS

The authors also thank the Program for Technological Development in Tools for Health (PDTIS-FIOCRUZ) for the use of its facilities and Flow Cytometry Platform at HEMOAM. We are grateful to Grupo Integrado de Pesquisas em Biomarcadores at Instituto René Rachou, Fundação Oswaldo Cruz of Minas Gerais state (FIOCRUZ-MG) for excellent technical assistance and support with the assays (collaboration of the technical assistants Ana Carolina Campi-Azevedo and Elaine Spezziali).

REFERENCES

1. Piel FB, Steinberg MH, Rees DC. Sickle cell disease. *N Engl J Med*. (2017) 376:1561–73. doi: 10.1056/NEJMra1510865
2. Faes C, Sparkenbaugh EM, Pawlinski R. Hypercoagulable state in sickle cell disease. *Clin Hemorheol Microcirc*. (2018) 68:301–18. doi: 10.3233/CH-189013
3. Sundd P, Gladwin MT, Novelli EM. Pathophysiology of sickle cell disease. *Ann Rev Pathol*. (2018) 14:261–90. doi: 10.1146/annurev-pathmechdis-012418-012838
4. Rees DC, Williams TN, Gladwin MT. Sickle-cell disease. *Lancet*. (2010) 376:2018–31. doi: 10.1016/S0140-6736(10)61029-X

5. Naoum PC. Interferentes eritrocitários e ambientais na anemia falciforme. *Rev Bras Hematol Hemoter*. (2000) 22:5–22. doi: 10.1590/S1516-84842000000100003
6. Vekilov PG. Sickle-cell haemoglobin polymerization: is it the primary pathogenic event of sickle-cell anaemia? *Br J Haematol*. (2007) 139:173–84. doi: 10.1111/j.1365-2141.2007.06794.x
7. Neto GC de G, Pitombeira M da S. Aspectos moleculares da anemia falciforme. *J Bras Patol Med Lab*. (2003) 39:51–6. doi: 10.1590/S1676-24442003000100011
8. Zhang D, Xu C, Manwani D, Frenette PS. Neutrophils, platelets, and inflammatory pathways at the nexus of sickle cell disease pathophysiology. *Blood J*. (2016) 127:801–10. doi: 10.1182/blood-2015-09-618538
9. Garcia NP, Júnior ALS, Soares GAS, Costa TCC, Santos APC dos, Costa AG, et al. Sickle cell anemia patients display an intricate cellular and serum biomarker network highlighted by $TCD4^{+}CD69^{+}$ lymphocytes, IL-17/MIP-1β, IL-12/VEGF, and IL-10/IP-10 axis. *J Immunol Res.* (2020) 2020:4585704. doi: 10.1155/2020/4585704
10. Kato GJ, Piel FB, Reid CD, Gaston MH, Ohene-Frempong K, Krishnamurti L, et al. Sickle cell disease. *Nat Rev Dis Prim*. (2018) 4:1–22. doi: 10.1038/nrdp.2018.10
11. Xu H, Wandersee NJ, Guo Y, Jones DW, Holzhauer SL, Hanson MS, et al. Sickle cell disease increases high mobility group box 1: a novel mechanism of in flammation. *Blood*. (2014) 124:3978–82. doi: 10.1182/blood-2014-04-560813
12. Park JS, Gamboni-Robertson F, He Q, Svetkauskaite D, Kim J-Y, Strassheim D, et al. High mobility group box 1 protein interacts with multiple Toll-like receptors. *Am J Physiol Cell Physiol.* (2006) 290:917–24. doi: 10.1152/ajpcell.00401.2005
13. Conran N, de Paula E V. Thromboinflammatory mechanisms in sickle cell disease—challenging the hemostatic balance. *Haematologica*. (2020) 105:1–11. doi: 10.3324/haematol.2019.239343
14. Vincent L, Vang D, Nguyen J, Gupta M, Luk K, Ericson ME, et al. Mast cell activation contributes to sickle cell pathobiology and pain in mice. *Blood*. (2013) 122:1853–62. doi: 10.1182/blood-2013-04-498105
15. Merle NS, Boudhabhay I, Leon J, Fremeaux-Bacchi V, Roumenina LT. Complement activation during intravascular hemolysis: implication for sickle cell disease and hemolytic transfusion reaction. *Transfus Clin Biol.* (2019) 26:116–24. doi: 10.1016/j.tracli.2019.02.008
16. Adisa OA, Hu Y, Ghosh S, Aryee D, Osunkwo I, Ofori-Acquah SF. Association between plasma free haem and incidence of vaso-occlusive episodes and acute chest syndrome in children with sickle cell disease. *Br J Haematol.* (2013) 162:702–5. doi: 10.1111/bjh.12445
17. Cavalcante JEA, Machado RPG, Laurentino MR, dos Santos TEJ, Bandeira ICJ, Filho PAM, et al. Clinical events and their relation to the tumor necrosis factor-alpha and interleukin-10 genotypes in Sickle-Cell- Anemia patients. *Hematol Oncol Stem Cell Ther*. (2016) 9:14–9. doi: 10.1016/j.hemonc.2015.11.002
18. Barbu EA, Mendelsohn L, Samsel L, Thein SL. Pro-inflammatory cytokines associate with NETosis during sickle cell vaso-occlusive crises. *Cytokine*. (2020) 127:1–5. doi: 10.1016/j.cyto.2019.154933
19. Adegoke SA, Kuti BP, Omole KO, Smith OS, Oyelami OA, Oyewole O. Acute chest syndrome in sickle cell anaemia : higher serum levels of interleukin-8 and highly sensitive C-reactive proteins are associated with impaired lung function. *Paediatr Int Child Health*. (2018) 38:244–50. doi: 10.1080/20469047.2018.1519988
20. Rees DC, Gibson JS. Biomarkers in sickle cell disease. *Br J Haematol.* (2011) 156:433–45. doi: 10.1111/j.1365-2141.2011.08961.x
21. Asare K, Gee BE, Stiles JK, Wilson NO, Driss A, Quarshie A, et al. Plasma interleukin-1β concentration is associated with stroke in sickle cell disease. *Cytokine*. (2010) 49:39–44. doi: 10.1016/j.cyto.2009.10.002
22. Ibiapina HNS, Costa AG, Sachett JAG, Silva IM, Tarragô AM, Neves JCF, et al. An immunological stairway to severe tissue complication assembly in bothrops atrox snakebites. *Front Immunol*. (2019) 10:1–12. doi: 10.3389/fimmu.2019.01882
23. Taylor R. Interpretation of the correlation coefficient: a basic review. *J Diagnostic Med Sonogr*. (1990) 6:35–9. doi: 10.1177/875647939000600106
24. Pathare A, Kindi SAL, Daar S, Dennison D. Cytokines in sickle cell disease. *Hematology*. (2003) 8:329–37. doi: 10.1080/10245330310001604719
25. Vilas-boas W, Cerqueira BAV, Figueiredo CVB, Santiago RP, Guarda CC da, Pitanga TN, et al. Association of homocysteine and inflammatory-related molecules in sickle cell anemia. *Hematology*. (2015) 21:126–31. doi: 10.1179/1607845415Y.0000000048
26. da Silva RR, Pereira MC, Rêgo MJBM, Hatzlhofer BLD, da Araújo AS, Bezerra MAC, et al. Cytokine evaluation of Th17 related cytokines associated with clinical and laboratorial parameters in sickle cell anemia patients with leg ulcers. *Cytokine*. (2014) 65:143–7. doi: 10.1016/j.cyto.2013.11.012
27. Keikhaei B, Mohseni AR, Norouzirad R, Alinejadi M, Ghanbari S, Shiravi F, et al. Altered levels of pro-inflammatory cytokines in sickle cell disease patients during vaso-occlusive crises and the steady state condition. *Eur Cytokine Netw*. (2013) 24:45–52. doi: 10.1684/ecn.2013.0328
28. Veiga PC, Schroth RJ, Guedes R, Freire SM, Nogueira-Filho G. Serum cytokine profile among Brazilian children of African descent with periodontal inflammation and sickle cell anaemia. *Arch Oral Biol*. (2013) 58:505–10. doi: 10.1016/j.archoralbio.2012.11.006
29. Villagra J, Shiva S, Hunter LA, Machado RF, Gladwin MT, Kato GJ. Platelet activation in patients with sickle disease, hemolysis-associated pulmonary hypertension, and nitric oxide scavenging by cell-free hemoglobin. *Blood*. (2007) 110:2166–73. doi: 10.1182/blood-2006-12-061697
30. Musa BOP, Onyemelukwe GC, Hambolu JO, Mamman AI, Isa AH. Pattern of serum cytokine expression and T-cell subsets in sickle cell disease patients in vaso-occlusive crisis. *Clin Vaccine Immunol*. (2010) 17:602–8. doi: 10.1128/CVI.00145-09
31. Sarray S, Saleh LR, Saldanha FL, Al-habboubi HH, Mahdi N, Almawi WY. Cytokine serum IL-6, IL-10, and TNFα levels in pediatric sickle cell disease patients during vasoocclusive crisis and steady state condition. *Cytokine*. (2015) 72:43–7. doi: 10.1016/j.cyto.2014.11.030
32. Pathare A, Al Kindi S, Alnaqdy AA, Daar S, Knox-Macaulay H, Dennison D. Cytokine profile of sickle cell disease in Oman. *Am J Hematol*. (2004) 77:323–8. doi: 10.1002/ajh.20196
33. Makis AC, Hatzimichael EC, Bourantas KL. The role of cytokines in sickle cell disease. *Ann Hematol*. (2000) 79:407–13. doi: 10.1007/s002770000173
34. Van Beers EJ, Yang Y, Raghavachari N, Tian X, Allen D, Nichols J, et al. Iron, inflammation and early death with sickle cell disease. *Circ Res*. (2015) 116:298–306. doi: 10.1161/CIRCRESAHA.116.304577
35. Eklund CM. Proinflammatory cytokines in crp baseline regulation. *Adv Clin Chem*. (2009) 48:111–36. doi: 10.1016/S0065-2423(09)48005-3
36. Damanhouri GA, Jarullah J, Marouf S, Hindawi SI, Mushtaq G, Kamal MA. Clinical biomarkers in sickle cell disease. *Saudi J Biol Sci*. (2015) 22:24–31. doi: 10.1016/j.sjbs.2014.09.005
37. Abbas AK, Lichtman AH, Pillai S. *Cellular and Molecular Immunology*. Rio de Janeiro: Elsevier. Vol. 8. (2015).
38. Roumenina LT, Rayes J, Lacroix-Desmazes S, Dimitrov JD. Heme: modulator of plasma systems in hemolytic diseases. *Trends Mol Med.* (2016) 22:200–13. doi: 10.1016/j.molmed.2016.01.004
39. Merle NS, Noe R, Halwachs-Mecarelli L, Fremeaux-Bacchi V, Roumenina LT. Complement system part II: role in immunity. *Front Immunol*. (2015) 6:1–26. doi: 10.3389/fimmu.2015.00257
40. Merle NS, Grunenwald A, Rajaratnam H, Gnemmi V, Frimat M, Figueres M, et al. Intravascular hemolysis activates complement via cell-free heme and heme-loaded microvesicles. *JCI Insight*. (2018) 3:1–17. doi: 10.1172/jci.insight.96910
41. Gavriilaki E, Mainou M, Christodoulou I, Koravou E-E, Paleta A, Touloumenidou T, et al. *In vitro* evidence of complement activation in patients with sickle cell disease. *Haematologica*. (2017) 102:481–2. doi: 10.3324/haematol.2017.174201
42. Qari MH, Dier U, Mousa SA. Biomarkers of inflammation, growth factor, and coagulation activation in patients with sickle cell Disease. *Clin Appl Thromb*. (2012) 18:195–200. doi: 10.1177/1076029611420992
43. Hibbert JM, Hsu LL, Bhathena SAMJ, Irune I, Sarfo B, Creary MS, et al. Proinflammatory cytokines and the hypermetabolism of children with sickle cell disease. *Exp Biol Med.* (2004) 230:68–74. doi: 10.1177/153537020523000109
44. Lanaro C, Franco-Penteado CF, Albuqueque DM, Saad STO, Conran N, Costa FF. Altered levels of cytokines and inflammatory mediators in plasma and leukocytes of sickle cell anemia patients and effects of hydroxyurea therapy. *J Leukoc Biol*. (2009) 85:235–42. doi: 10.1189/jlb.0708445

45. Zhang J-M, An J. Cytokines, inflammation and pain. *Int Anesth Clin*. (2007) 45:27–37. doi: 10.1097/AIA.0b013e318034194e
46. Pitanga TN, Oliveira RR, Zanette DL, Guarda CC, Santiago RP, Santana SS, et al. Sickle red cells as danger signals on proinflammatory gene expression, leukotriene B4 and interleukin-1 beta production in peripheral blood mononuclear cell. *Cytokine*. (2016) 83:75–84. doi: 10.1016/j.cyto.2016.03.016
47. Safaya S, Steinberg MH, Klings ES. Monocytes from sickle cell disease patients induce differential pulmonary endothelial gene expression via activation of NF-kB signaling pathway. *Mol Immunol*. (2012) 50:117–23. doi: 10.1016/j.molimm.2011.12.012

Conflict of Interest: The authors declare that the research was conducted in the absence of any commercial or financial relationships that could be construed as a potential conflict of interest.

frontiers in Immunology

ORIGINAL RESEARCH
published: 26 March 2021
doi: 10.3389/fimmu.2021.632709

Soluble MD-2 and Heme in Sickle Cell Disease Plasma Promote Pro-Inflammatory Signaling in Endothelial Cells

Ping Zhang[1], *Julia Nguyen*[1], *Fuad Abdulla*[1], *Alexander T. Nelson*[2], *Joan D. Beckman*[1], *Gregory M. Vercellotti*[1] *and John D. Belcher*[1]*

[1] Division of Hematology, Oncology and Transplantation, Department of Medicine, University of Minnesota, Minneapolis, MN, United States, [2] University of Minnesota School of Medicine, Minneapolis, MN, United States

Recent evidence indicates that hemolysis in sickle cell disease (SCD) promotes inflammation *via* innate immune signaling through toll-like receptor 4 (TLR4). Free heme released by hemolyzed red blood cells can bind to myeloid differentiation factor-2 (MD-2) and activate TLR4 pro-inflammatory signaling on endothelium to promote vaso-occlusion and acute chest syndrome in murine models of SCD. MD-2 is co-expressed with TLR4 on cell membranes, but in inflammatory conditions, soluble MD-2 (sMD-2) is elevated in plasma. sMD-2 levels were significantly increased in human and murine sickle (SS) plasma as compared to normal (AA) plasma. Human umbilical vein endothelial cells (HUVEC) and human lung microvascular endothelial cells incubated with human SS plasma had significant increases in pro-inflammatory IL-8, IL-6, and soluble VCAM-1 secretion compared to endothelial cells incubated with AA plasma. The increase in HUVEC IL-8 secretion was blocked by depletion of sMD-2 from SS plasma and enhanced by the addition of sMD-2 to AA plasma. The TLR4 signaling inhibitor, TAK-242, inhibited HUVEC IL-8 secretion in response to SS plasma by 85%. Heme-agarose pull-down assays and UV/Vis spectroscopy demonstrated that heme binds to sMD-2. Hemopexin, a high affinity heme-binding protein, inhibited HUVEC IL-8 secretion induced by SS plasma or SS and AA plasma supplemented with sMD-2. These data suggest that sMD-2 bound to heme might play an important role in pro-inflammatory signaling by endothelium in SCD.

Keywords: soluble MD-2, sickle cell disease, IL-8, endothelial cell, TLR4, heme, hemopexin, IL-6

OPEN ACCESS

Edited by:
Nicola Conran,
State University of Campinas, Brazil

Reviewed by:
Samit Ghosh,
University of Pittsburgh, United States
Margaret Bennewitz,
West Virginia University, United States

***Correspondence:**
John D. Belcher
belcher@umn.edu

Specialty section:
This article was submitted to Inflammation, a section of the journal Frontiers in Immunology

Received: *23 November 2020*
Accepted: *10 March 2021*
Published: *26 March 2021*

Citation:
Zhang P, Nguyen J, Abdulla F, Nelson AT, Beckman JD, Vercellotti GM and Belcher JD (2021) Soluble MD-2 and Heme in Sickle Cell Disease Plasma Promote Pro-Inflammatory Signaling in Endothelial Cells. Front. Immunol. 12:632709. doi: 10.3389/fimmu.2021.632709

INTRODUCTION

Sickle cell disease (SCD) is caused by a single point mutation (Glu->Val) at position 6 in the β-globin gene that leads to polymerization of deoxy-hemoglobin S (HbS) and the characteristic sickling of red blood cells. The ongoing polymerization of HbS promotes hemolysis, inflammation, and vaso-occlusive pain crises (1). During hemolysis, HbS is released into the vasculature and readily oxidized to methemoglobin, which can release free heme (2, 3). Normally, free hemoglobin

and heme in plasma are safely cleared by haptoglobin and hemopexin (4, 5). However in SCD, chronic hemolysis depletes circulating haptoglobin and hemopexin (6, 7), allowing free heme to activate toll-like receptor 4 (TLR4) signaling on endothelial and inflammatory cells (3, 8–10). TLR4 signaling on endothelium leads to NF-κB activation, rapid release of Weibel-Palade bodies, discharge of P-selectin and von Willebrand factor, and vaso-occlusion in murine models of SCD (3).

TLR4 signaling induced by heme or its canonical ligand, lipopolysaccharide (LPS), requires cofactors CD14 and MD-2 (3, 8, 11–15). The transduction mechanism for TLR4 activation is well characterized for LPS from gram negative bacteria. CD14 delivers LPS to MD-2, which forms a stable heterodimer with the extracellular domain of TLR4 (16), leading to dimerization of the TLR4-MD-2 complex (17). This brings the toll/interleukin-1 receptor (TIR) domains on the cytoplasmic tails of TLR4 together allowing recruitment of cytoplasmic adapter molecules that promote oxidant production by NADPH oxidase and activation of downstream signaling pathways, leading to activation of pro-inflammatory transcription factors, such as NF-κB and AP-1, as well as the production of type 1 interferons (18).

MD-2 is co-expressed with TLR4 on the cell membrane of various cell types including leukocytes and endothelium (11, 19, 20), but soluble MD-2 (sMD-2) is elevated in plasma from patients with inflammatory conditions, such as sepsis, HIV infection, and endotoxemia (21–23). Epithelial cells in the gut and the airways express TLR4, but not MD-2, and are therefore entirely reliant on sMD-2 for TLR4 signaling (24–26). sMD-2 circulates in plasma of healthy individuals primarily as disulfide-linked oligomers (27). During experimental human endotoxemia, sMD-2 in septic plasma increases rapidly like an acute phase reactant and contains both sMD-2 oligomers and monomers. The monomeric form of sMD-2 represents the biologically active form of MD-2 (28).

In addition to being a required co-factor for TLR4 responses to LPS, MD-2 is also a required cofactor for TLR4 responses to heme (15). Heme binds to MD-2 at amino acids W23 and Y34 on MD-2, at a site independent of the LPS-binding site, to activate TLR4 pro-inflammatory signaling (15). Since SCD is a pro-inflammatory condition with an activated endothelium and elevated plasma heme, we examined sMD-2 levels in SCD plasma and its potential role in endothelial cell activation. We tested the hypothesis that sMD-2 is increased in SCD plasma and, by binding heme, contributes to pro-inflammatory signaling by endothelial cells.

MATERIALS AND METHODS

Collection of Human and Mouse Blood

Human EDTA blood was obtained from healthy adult volunteers and SCD patients in steady-state after informed consent and according to protocols approved by the University of Minnesota's Institutional Review Board in accordance with the Declaration of Helsinki. Mouse EDTA blood was collected from the inferior vena cava from homozygous Townes mice (29) expressing human HbS or HbA in accordance with protocols approved by University of Minnesota's Institutional Animal Care and Use Committee. Human and mouse platelet-free plasma was stored at -85°C before use.

sMD-2 ELISA

Human MD-2 ELISA kit (Millipore) was used to measure sMD-2 levels in human normal control and SCD plasma following the manufacturer's instructions.

sMD-2 Western Blots

Plasma samples were diluted with PBS (1:2 dilution for mouse plasma, and 1:5 dilution for human plasma). 2 μl of the diluted plasma was separated under denaturing conditions on 4-15% SDS-PAGE (Bio-Rad) and transferred to PVDF membranes (Millipore). Membranes were incubated with MD-2 primary antibody (Abcam) and fluorescent secondary antibodies (LI-COR). Fluorescence was quantitated with an Odyssey Image System (LI-COR). An IgG western blot or a total protein stain using AzureRed Fluorescent Total Protein Stain (Azure Biosystems) was used as a loading control.

Endothelial IL-8, IL-6, and Soluble VCAM-1 Secretion

HUVEC were isolated and cultured as described previously (30). Human lung microvascular endothelial cells (HMVEC-L, Lonza) were cultured with microvascular endothelial cell growth medium-2 (Lonza) with 10% FBS. HUVEC or HMVEC-L in 24 well plates were treated with 2% of human AA or SS plasma in RPMI-1640 for 18 hours. IL-8, IL-6, and sVCAM-1 in the medium was measured using IL-8 and IL-6 ELISA kits (BioLegend), and a human VCAM-1 Quantikine ELISA kit (R&D Systems).

Expression and Purification of N-Flag-Tagged Recombinant hMD-2

pFlag-CMV1–hMD-2 (a gift from Dr. Doug Golenbock, Addgene #13028) was sub-cloned into a Caggs expression plasmid. Chinese Hamster Ovary (CHO) cells were transfected with pT2/Caggs-Flag-hMD-2 to produce recombinant sMD-2 as described (31). CHO cells were maintained in RPMI-1640 with L-glutamine (Gibco) plus 10% fetal bovine serum in 5% CO_2 at 37°C. Sixteen T225 flasks of CHO cells were used for each purification. Cells were transfected with polyethylenimine (PEI, linear, MW 2500, Polysciences) using 4:1 PEI to DNA (w/w). After 18 hours, cells were changed to ProCHO-AT protein-free media (Lonza). After 2-4 days, conditioned media were collected and centrifuged at 6000g for 30 minutes at 4°C and filtered using a 0.22 μm Stercup vacuum filter (Corning). Media collected after two days were used to treat HUVECs; media collected after four days were applied to an anti-Flag M2-affinity-gel (Sigma-Aldrich) column for sMD-2 purification. MD-2 was eluted with Flag peptide and concentrated using 10k centrifugal filter units (Amicon). The purity and concentration of the protein was determined by using 4-15% SDS-PAGE. Recombinant hMD-2 was confirmed by Western blot.

Heme-Agarose Pull-Down Assays

To determine the physical interaction between sMD-2 and heme, human SS plasma was incubated overnight at 4°C with heme-agarose or control agarose (Sigma-Aldrich). After incubation, agarose beads were pelleted by centrifugation, washed, subjected to SDS-PAGE, and anti-MD-2 Western blot (15).

Depletion of sMD-2 From SS Plasma

Anti-hMD-2 antibody (ab24182, Abcam) was coupled to CNBr-Sepharose (600 μg/ml gel; Sigma-Aldrich). Human SS plasma was diluted 5-fold in PBS and incubated at 4°C for 18 hours with the antibody-conjugated Sepharose. MD-2-depleted plasma was collected after pelleting the antibody-coated Sepharose by centrifugation and the MD-2 depletion was confirmed by western blot.

Detecting sMD-2-Heme Binding by UV/Vis Absorbance

UV/Vis absorption spectra (250–550 nm) of heme, sMD-2, and heme plus sMD-2 were measured using a Nanophotometer (Implen). Rat hemopexin (HPX) (Athens Research & Technology) or recombinant hFlag-HPX was used as a heme-binding control (15).

Statistical Analysis

Results are presented as means ± standard deviation. Comparisons of multiple treatment groups were made using One-Way ANOVA with the Holm-Sidak multiple comparison test (Sigma Stat). Significance testing between 2 groups was performed using Student's paired or unpaired t-test as appropriate. Statistical significance was $p < 0.05$.

RESULTS

sMD-2 Is Increased in SCD Plasma

As plasma sMD-2 is elevated in various inflammatory conditions and SCD is pro-inflammatory, we assessed plasma levels of sMD-2 in sickle (SS) and normal (AA) humans and mice by Western blot. sMD-2 was increased by 2.5-fold in human SS plasma compared to healthy AA plasma ($p<0.02$, **Figures 1A, B**). Similarly, in Townes SS mice, plasma sMD-2 was increased 7.6-fold compared to Townes control AA mice ($p<0.002$, **Figures 1C, D**). In addition, we measured human plasma sMD-2 level using an MD-2 ELISA kit. Mean sMD-2 levels were 35.6 ± 45.5 ng/ml in SS plasma, compared to 4.9 ± 6.3 ng/ml in AA control plasma ($p<0.02$, **Figure 1E**). The characteristics of human control and SCD subjects are summarized in **Supplementary Data Table 1**. Complete blood counts and serum chemistries of Townes AA and SS mice were published in a recent report from our lab (32).

Endothelial Cells Secrete sMD-2 in Response to Heme

Potential sources of sMD-2 in plasma include the liver, monocyte-derived dendritic cells, and endothelial cells (22, 33, 34). LPS and TNF-α induce sMD-2 secretion by HUVEC (21, 22). To determine whether heme can induce sMD-2 secretion by endothelial cells, HUVEC were incubated with heme (0-30 μM) for 18 hours, and sMD-2 accumulation in the media was measured. sMD-2 in HUVEC culture media increased in a dose-responsive manner (**Supplemental Figure 1**). LPS (100 ng/ml), a positive control, also increased sMD-2 in HUVEC media.

SCD Plasma Activates Endothelial Cells

SCD plasma contains a number of pro-inflammatory molecules (35–39). Platelets can contaminate plasma and release pro-inflammatory molecules into plasma that can activate endothelial cells. Therefore platelet-free plasma was used for these experiments to minimize their effects on endothelial cells. To determine whether SCD plasma could activate endothelial cells, we incubated HUVEC and HMVEC-L for 18 hours with media containing 2% AA or SS human platelet-free plasma and measured IL-8, IL-6 and sVCAM-1 in the media by ELISAs. IL-8 content in RPMI basal medium containing 2% AA or SS plasma before addition to HUVEC was too low to be measured by ELISA. IL-8 was 2-fold higher in the media of HUVEC treated with SS plasma (525.5 ± 167.0 pg/ml) compared to the media of HUVEC treated with AA plasma (260.9 ± 68.2 pg/ml, $p<0.002$, **Figure 2A**). In addition, sVCAM-1 was significantly increased in the media of HUVEC treated with SS plasma (13.42 ± 6.93 ng/ml) compared to HUVEC treated with AA plasma (5.48 ± 2.83 ng/ml, $p<0.05$, **Supplementary Figure S2A**). IL-6 was also significantly increased in the media of HUVEC treated with SS plasma (254.25 ± 33.18 pg/ml) compared to HUVEC treated with AA plasma (194.56 ± 46.04 pg/ml, $p<0.005$, **Supplementary Figure S2B**).

Like HUVEC, incubation of HMVEC-L with 2% SS plasma for 18 hours significantly increased IL-8, sVCAM-1 and IL-6 levels in the media compared to AA plasma (**Supplementary Figures S3A–C**). In subsequent experiments, we used IL-8 secretion by HUVEC to measure endothelial cell activation.

SCD Plasma Activates TLR4 Signaling in Endothelial Cells

We have previously shown that heme binds to MD-2 and activates TLR4 signaling (3, 15). To determine whether SCD plasma activates endothelial cells through TLR4 signaling, we incubated HUVEC with media containing 2% SS or AA human plasma in the presence or absence of the TLR4 inhibitor TAK-242 and measured IL-8 in the media by ELISA. We found TAK-242 decreased IL-8 secretion induced by HUVEC incubated with SS plasma by 85% ($p<0.005$, **Figure 2B**). TAK-242 had no significant effects on IL-8 secretion in HUVEC incubated with AA plasma (145.1 ± 33.2 with TAK-242 and 152.1 ± 33. 8 without TAK-242, n=6). These results indicate that SS plasma increased IL-8 through TLR4 signaling.

sMD-2 Contributes to SS Plasma-Induced IL-8 Secretion by HUVEC

Plasma from SCD patients has many elevated pro-inflammatory molecules, such as IL-1β, IL-18, IL-6, and HMGB1 (35–39). Any of these could contribute to the increased IL-8 secretion by

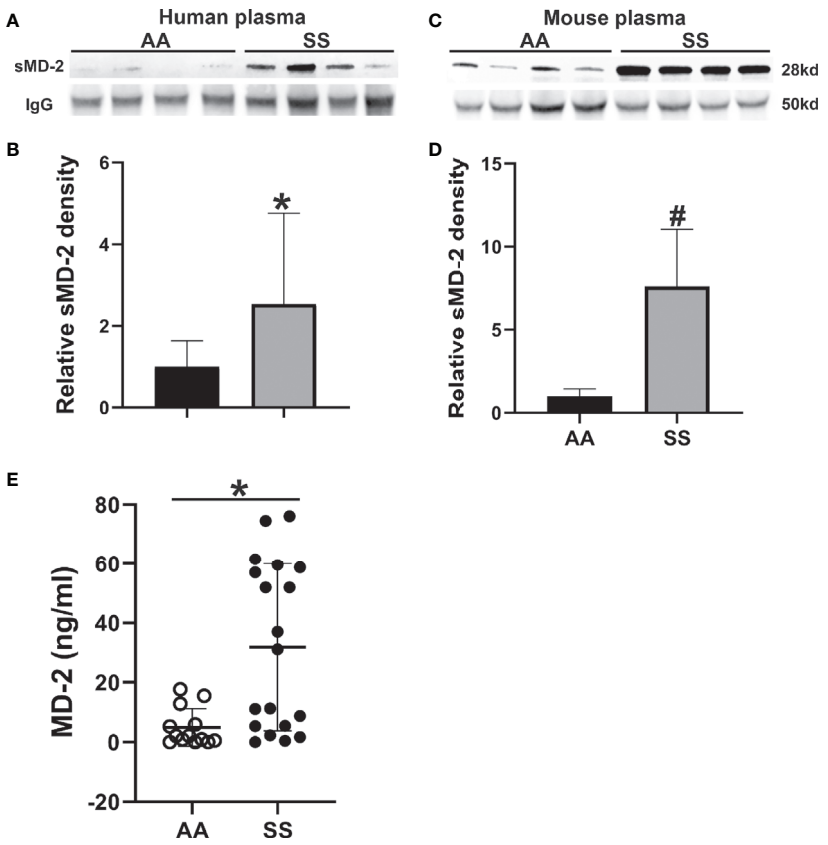

FIGURE 1 | sMD-2 is increased in SCD plasma from humans and mice. **(A, C)** Representative western blots of sMD-2 from sickle (SS) and normal control (AA) plasma from humans and Townes mice. **(B, D)** Relative plasma sMD-2 on Western blots is calculated as the density ratios of sMD-2 bands compared to IgG in SS (n=17 for human, n=9 for mice) and AA (n=16 for human, n=7 for mice) plasma. **(E)** sMD-2 levels in human AA (n=13) and SS (n=19) plasma measured by ELISA. Bars are means ± SD, **p*<0.02 and #*p*<0.002.

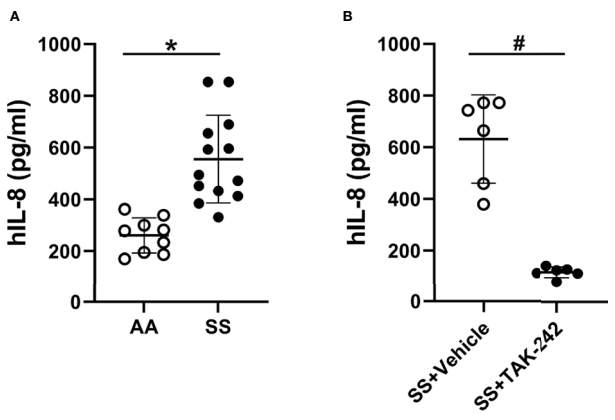

FIGURE 2 | Human SS plasma induces IL-8 secretion in HUVEC through TLR4 signaling. **(A)** HUVEC were cultured with 2% AA (n=9) or SS (n=13) plasma in RPMI-1640 media for 18 hours. The IL-8 content in the conditioned medium was measured by ELISA. **(B)** HUVEC were cultured with 2% SS plasma plus vehicle or TLR4 signaling inhibitor, TAK-242 (1 μM) for 18 hours and IL-8 secretion into the media was measured by ELISA (n=6). Bars are means ± SD, **p*<0.002, #*p*<0.005.

HUVEC incubated with SS plasma. To determine whether sMD-2 contributes to increased IL-8 secretion by HUVEC incubated with SS plasma, we used two approaches: depletion of sMD-2 from SS plasma and addition of sMD-2 to AA plasma (**Figure 3A**). Plasma samples from these two approaches were then incubated with HUVEC to determine their effects on IL-8 secretion. When sMD-2 was removed from SS plasma using an anti-MD-2 affinity column (**Figure 3B**), the sMD-2-depleted SS plasma reduced IL-8 secretion by 34.3% as compared to the same SS plasma without MD-2 depletion ($p<0.05$, **Figure 3C**). When conditioned CHO medium containing recombinant sMD-2 (**Figure 3D**) was added to AA plasma, the sMD-2-treated AA plasma increased IL-8 secretion by 1.8-fold ($p<0.01$, **Figure 3E**), and the TLR4 inhibitor, TAK-242, inhibited this increase ($p<0.05$, **Figure 3E**). Together, these results suggest that sMD-2 contributes to SS plasma-induced IL-8 secretion by HUVECs through TLR4 signaling.

Polymyxin B Does Not Inhibit HUVEC IL-8 Secretion

Polymyxin B inhibits LPS-mediated TLR4 signaling (40). To determine whether the observed increased IL-8 secretion in

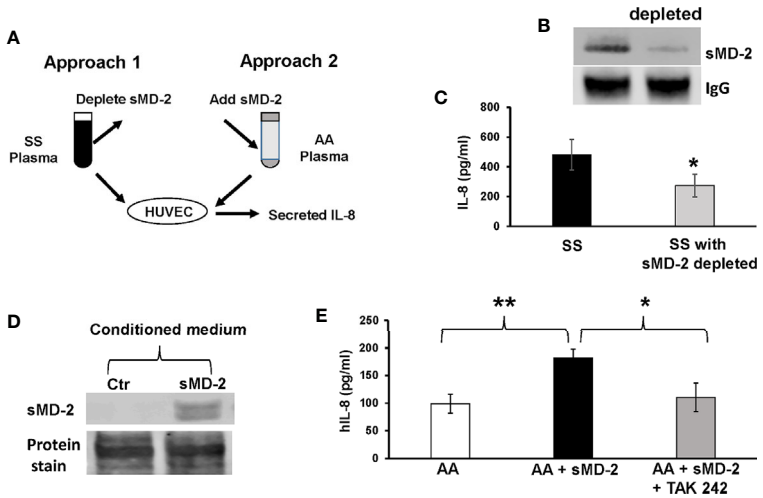

FIGURE 3 | sMD-2 in plasma mediates IL-8 secretion by HUVEC. **(A)** Diagram shows two approaches to study sMD-2's contribution to HUVEC IL-8 secretion. In approach 1, sMD-2 is depleted from SS plasma and in approach 2, sMD-2 is added to AA plasma. Plasma (2%) from both approaches were incubated with HUVEC for 18 hours and IL-8 secretion into the media was measured by ELISA. **(B)** Representative western blot of SS plasma after sMD-2 depletion. The IgG western blot was shown as loading controls. **(C)** IL-8 secretion by HUVEC after incubation with MD-2-depleted SS plasma. **(D)** Western blot of recombinant sMD-2 in conditioned medium from CHO cells transfected with MD-2-containing plasmids or non-transfected control CHO media. The total protein stain was shown as loading controls **(E)** sMD-2 CHO-conditioned medium or control CHO medium (10%) were added to HUVEC culture media along with 2% AA plasma in the presence or absence of TLR4 inhibitor, TAK-242 (1 μM), and incubated with HUVEC for 18 hours. The secreted IL-8 was measured by ELISA. Bars in C and E are means ± SD (n=3). *p<0.05, **p<0.01.

HUVEC with SS plasma and recombinant sMD-2 was caused by LPS contamination, we added polymyxin B (Sigma-Aldrich) to our HUVEC culture media. LPS (10 ng/ml) induced IL-8 secretion in HUVEC that was inhibited by polymyxin B in a dose-responsive manner (**Supplemental Figure 4A**). Importantly, polymyxin B (1000 U/ml) did not inhibit IL-8 secretion in HUVEC treated with SS plasma or AA plasma + sMD-2 (**Supplemental Figures 4B, C**). Thus, HUVEC IL-8 secretion induced by SS plasma or AA plasma + sMD-2 was not mediated by LPS contamination.

sMD-2 Binds Heme

We have previously shown that heme binds to MD-2 to initiate TLR4 signaling (15). We confirmed heme-binding to sMD-2 in plasma using heme-agarose pull-down followed by MD-2 Western blots. Heme-agarose or control agarose was incubated with SS plasma overnight, and then the agarose was pelleted by centrifugation. The proteins pulled-downed with the agarose beads were washed and eluted from the beads with SDS-containing buffer and run on MD-2 Western blots. Heme-agarose, but not control agarose, pulled down sMD-2 from SS human and mouse plasma (**Figure 4A**). To obtain additional evidence of heme binding to sMD-2, a standard heme–binding assay was performed as described previously (31). Heme binding to recombinant sMD-2 was assessed by scanning UV/Vis absorption spectrometry (250-550 nm, **Figure 4B**). Heme binding to recombinant hemopexin (HPX) was used as a positive control (**Figure 4C**). Absorbance spectra show scans of heme alone (black dashed line), recombinant protein alone (blue line), and recombinant protein plus heme (red line). The Soret peak at 414 nm, indicative of heme binding, increased in the presence of added heme (red line) for HPX and sMD-2. In the absence of added heme, both recombinant proteins appeared to have some bound heme as indicated by the Soret peak at 414 nm (blue line).

Hemopexin Inhibits HUVEC IL-8 Secretion Induced by SS Plasma and AA Plasma Plus sMD-2

We have previously demonstrated that the high-affinity heme-binding protein hemopexin (HPX) blocks endothelial cell activation induced by heme-mediated TLR4 signaling (3). We examined whether heme plays a role in plasma sMD-2 stimulation of HUVEC IL-8 secretion. HPX has the highest heme-binding affinity (K_d ~10^{-13} M) among the known heme-binding proteins and can readily remove heme from other heme-binding proteins with lower heme affinity (41–43). When HPX was added to SS plasma, IL-8 secretion by HUVEC was reduced by 31.6% (p<0.05, **Figure 5A**). Adding HPX to AA plasma had no significant effect on IL-8 secretion. In addition, When HPX was added to AA or SS plasma plus recombinant sMD-2, HUVEC IL-8 secretion was significantly inhibited (AA p<0.05 and SS p<0.01, **Figure 5B**). Taken together, these results indicate that heme is necessary for enhanced HUVEC IL-8 secretion induced by SS plasma or AA plasma supplemented with sMD-2.

DISCUSSION

These data demonstrate that SCD plasma has increased levels of sMD-2 that can bind plasma heme and activate pro-inflammatory

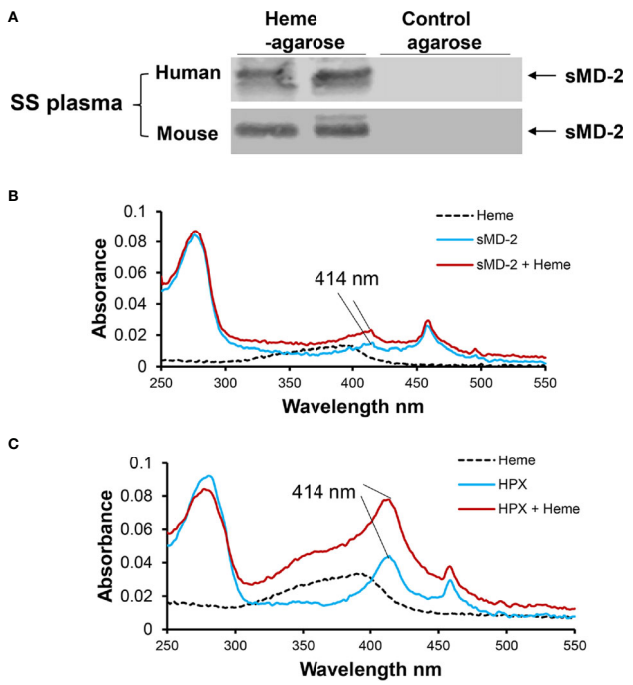

FIGURE 4 | sMD-2 binds heme. **(A)** To determine the physical interaction between sMD-2 and heme, human SS plasma was incubated overnight at 4°C with heme-agarose or control agarose beads. The pelleted beads were washed with PBS 6 times. The pull-down proteins bound to the beads were then run on an SDS-PAGE Western bot using anti-MD-2 IgG as the primary detection antibody. Six SS plasmas were examined in independent experiments with similar results. Representative Western blots of 2 SS human and mouse plasmas are shown. **(B, C)** UV/Vis absorption spectra (250 - 550 nm) of recombinant **(B)** sMD-2 and **(C)** hemopexin (HPX, positive control), with and without added heme. Absorbance spectra show scans of heme alone (black dashed line), recombinant protein alone (blue line) and recombinant protein plus heme (red line). The Soret peak at 414 nm, indicative of heme binding, increases in the presence of added heme (red) for sMD-2 and HPX. In the absence of added heme, both recombinant proteins appear to have some bound heme (blue line) as shown by the Soret peak at 414 nm. The UV/Vis scans **(B, C)** are representative of 3 independent experiments.

IL-8 secretion by endothelial cells through TLR4 signaling. The combination of heme-induced oxidative stress, inflammation, and adhesion of circulating blood cells to vascular endothelium is a key driver of the pro-inflammatory and prothrombotic vasculature that promotes sludging and stasis of blood flow in the post-capillary venules and ongoing ischemia-reperfusion physiology (44–46). Nature provides complicated systems to respond to heme overload, such as heme oxygenase-1 (HO-1) induction to degrade heme and heme-binding proteins to neutralize and transport heme (43, 47). Among the known heme-binding proteins, plasma HPX sequesters and transports heme to the liver for catabolism and detoxification *via* induction of HO-1 and ferritin (48, 49). Plasma HPX levels are depleted in SCD patients and mice because of chronic intravascular hemolysis (6, 7, 31). We have previously shown that increasing HPX through supplementation (3, 5) or gene transfer (31) prevents heme-induced inflammation and vaso-occlusion in SS mice. In this study, HPX-treated SS plasma lost its enhanced ability to induce IL-8 secretion in HUVEC, while adding HPX to AA plasma had no effect on basal IL-8 secretion. These findings demonstrate that heme can bind to sMD-2 and suggest that the addition of HPX to SS plasma sequesters heme away from sMD-2, thereby preventing TLR4-mediated IL-8 production by endothelial cells.

MD-2 expression can be regulated in specific tissue responses to sterile inflammatory stimuli and bacteria. In human hepatocytes, IL-6 induces the expression of MD-2 (34). In monocytes, corneal and intestinal epithelial cells, IL-10 or INF-γ can induce MD-2 expression (23, 50–52). Using immunohistochemical analysis, Wolfs et al. found MD-2 is expressed by endothelial cells and inflammatory cells in the livers and lungs of septic patients and suggested these cells are a source of the enhanced circulating sMD-2 levels during acute systemic inflammatory diseases such as endotoxemia and sepsis (22). In a recently published study, we found both MD-2 and MIP-2α (a murine IL-8 homologue) mRNA levels were increased in the livers of Townes SS mice compared to control AA mice, these differences are consistent with markedly increased hemolysis in Townes SS mice (32). In this study, we showed that HUVEC secreted sMD-2 in response to heme or LPS. We speculate that endothelial cells might be a potential source of some of the sMD-2 in SCD plasma, which will need further studies to validate.

MD-2 is a required accessory molecule for TLR4 signaling, indispensable for LPS recognition and signaling (25, 53). MD-2 knockout mice are hypo-responsive to LPS and are able to survive endotoxic shock, supporting a significant role of MD-2 in TLR4-dependent inflammatory responses *in vivo* (54). As a pattern recognition protein, MD-2 has been shown to bind to various ligands besides LPS to activate TLR4 signaling and promote inflammation, including heme (15), palmitic acid (55), angiotensin (56), and some synthetic compounds with no similarity to LPS (57). In our study, we found that heme agarose pulls-down sMD-2 from SCD plasma and recombinant sMD-2 has a Soret band at 414 nm, which indicates that sMD-2 binds heme.

Heme-induced microvascular stasis in SS mice requires endothelial TLR4 signaling (3). Heme activates TLR4 signaling on endothelial cells, leading to delivery of Weibel-Palade body constituents P-selectin and VWF to the surface of the vessel wall and the activation of the pro-inflammatory transcription factor NF-κB (3). Our finding that sMD-2-heme in SS plasma induces TLR4-dependent IL-8 secretion is in congruence with these previous observations. Thus, sMD-2 in plasma provides a potential pathway for heme-MD-2-mediated activation of TLR4 signaling to induce activation of the endothelium and vaso-occlusion in SCD.

The low level of IL-8, s-VCAM-1 and IL-6 production in HUVEC and HMVEC-L incubated with AA plasma and the incomplete inhibition of IL-8 secretion by HUVEC incubated with SS plasma depleted of sMD-2 or SS plasma plus TAK-242 indicates that other pro-inflammatory molecules in SS plasma might also induce HUVEC IL-8 secretion (35, 37, 39). A basal level TLR4 receptor activity induced by AA plasma has been reported before. Using a TLR4 reporter cell line that specifically

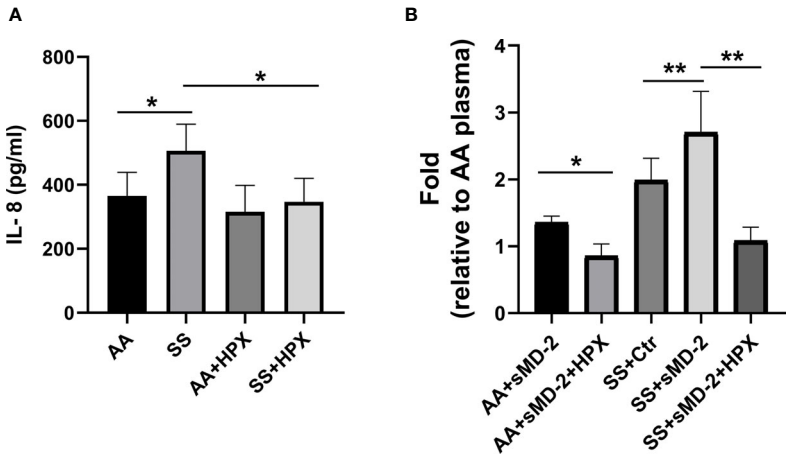

FIGURE 5 | Hemopexin inhibits IL-8 secretion by HUVEC stimulated with human SS-plasma and AA-plasma plus sMD-2. **(A)** HUVEC media containing human AA or SS plasma (2%) was pre-incubated with recombinant hemopexin (HPX, 10 μM) for 30 minutes before being added to HUVEC for 18 hours. The IL-8 secreted into the HUVEC media was measured by ELISA (n=4). **(B)** CHO cells expressing recombinant MD-2 were cultured in protein-free medium for 2 days, the medium was collected as sMD-2-conditioned medium. HUVEC media containing AA (n=7) or SS (n=5) plasma (2%) plus sMD-2-conditioned medium (10%) was pre-incubated with HPX (10 μM) for 30 minutes before being added to HUVEC for 18 hours. The secreted IL-8 was measured by ELISA and presented as fold-change compared to AA-plasma +control conditioned medium without HPX. Bars are means ± SD. *$p<0.05$ and **$p<0.01$.

recognizes ligands that bind and activate TLR4 (TLR4/NF-kB/SEAP Stable Reporter Cells), Xu et al. (39) found plasma from healthy AA control subjects induced low levels of TLR4 receptor activity; about 10% of the total TLR4 receptor activity induced by AA plasma was from HMGB1-dependent TLR4 receptor activity. In our study we found the TLR4 inhibitor TAK-242 had no significant effects on AA plasma-induced IL-8 secretion, suggesting other non-TLR4 pathways are likely contributing to the low level of IL-8 secretion induced by AA plasma. In SS plasma, 85% of IL-8 production by HUVEC was inhibited by TAK-242. The remaining IL-8 production induced by SS plasma could have been induced by other pro-inflammatory molecules that do not require TLR4 such as IL-1β, IL-18, and IL-6 (35–39).

The function of sMD-2 has been extensively studied in LPS-TLR4 signaling. Following synthesis, MD-2 is either secreted directly into the medium as a soluble, active protein, or binds directly to TLR4 in the endoplasmic reticulum before migrating to the cell surface (12). Heme activates TLR4 signaling by binding to a site on MD-2 that is independent and distinct from the LPS binding site on MD-2 (15). As shown in other studies (3, 8), heme-MD-2/TLR4-mediated pro-inflammatory effects are not due to LPS contamination. In this study, endothelial cell IL-8 secretion in response to SS plasma was not blocked by the LPS antagonist, polymyxin B.

SCD patients are known to be at higher risk for contracting bacterial infections compared to healthy humans (58, 59). The molecular pathophysiology that contributes to this infection susceptibility is incompletely understood. Because lung epithelial cells express TLR4 without MD-2, they remain resistant to endotoxin (25). sMD-2, produced either by neighboring cells or brought to the epithelial cells by plasma exudate, is required for LPS activation of lung epithelial cells (60). Increased circulating sMD-2 in SCD plasma could make SCD patients more susceptible to pulmonary infections and acute chest syndrome, especially in response to enhanced hemolysis (9, 61).

There are several limitations of this study. Although we found SS plasma increased IL-8, sVCAM-1, and IL-6 secretion in both HUVEC and HMVEC-L, endothelial cells vary widely among vascular beds such as lung and brain. The functions of sMD-2-heme in different endothelial cell beds and non-endothelial cells with TLR4 receptors, such as platelets and macrophages need be defined by separate studies.

In conclusion, SCD is considered a chronic inflammatory disease with hemolysis, vaso-occlusion, and ischemia-reperfusion, resulting in activation of the innate immune system and persistent activation of leukocytes, platelets, and endothelial cells. Therapeutic approaches for SCD include targeting HbS polymerization and the inflammatory processes that trigger vaso-occlusion (1, 35, 62). Clinical studies targeting TLR4 signaling as a therapeutic approach for sepsis and septic shock have brought several compounds and antibodies to clinical trials, with unsuccessful results. One such unsuccessful therapeutic is TAK-242, a small-molecule inhibitor of TLR4 signaling, that failed to suppress cytokine levels in patients with sepsis or respiratory failure in a phase III study (63). The LPS-MD-2/TLR4 antagonist, eritoran, also failed to reduce mortality among patients with severe sepsis (64). Nevertheless, targeting MD-2 to interfere with MD-2–TLR4 signaling has been extensively explored, and the results support the concept that MD-2 is an effective target to treat inflammatory disorders such as sepsis and acute lung injury (53, 65–68). We provide evidence that sMD-2 is increased in SCD, contributes to pro-inflammatory signaling in endothelial cells, and therefore, might be a potential therapeutic target for SCD and other hemolytic conditions.

DATA AVAILABILITY STATEMENT

The original contributions presented in the study are included in the article/**Supplementary Material**. Further inquiries can be directed to the corresponding author.

ETHICS STATEMENT

The studies involving human participants were reviewed and approved by University of Minnesota's Institutional Review Board. The patients/participants provided their written informed consent to participate in this study. The animal study was reviewed and approved by University of Minnesota's Institutional Animal Care and Use Committee.

AUTHOR CONTRIBUTIONS

PZ, GMV, and JDBel designed the study, wrote, and edited the manuscript. PZ and JDBel prepared the figures. PZ, JN, and FA performed the experiments. JDBec and ATN collected data, analyzed results, and reviewed the manuscript. All authors contributed to the article and approved the submitted version.

FUNDING

This work was funded by NIH grant R01 HL114567.

ACKNOWLEDGMENTS

We would like to thank Michael Franklin for his superb editorial assistance.

SUPPLEMENTARY MATERIAL

The Supplementary Material for this article can be found online at: https://www.frontiersin.org/articles/10.3389/fimmu.2021.632709/full#supplementary-material

REFERENCES

1. Telen MJ, Malik P, Vercellotti GM. Therapeutic strategies for sickle cell disease: towards a multi-agent approach. *Nat Rev Drug Discov* (2019) 18 (2):139–58. doi: 10.1038/s41573-018-0003-2
2. Bunn HF, Jandl JH. Exchange of heme among hemoglobins and between hemoglobin and albumin. *J Biol Chem* (1968) 243(3):465–75. doi: 10.1016/S0021-9258(18)93628-8
3. Belcher JD, Chen C, Nguyen J, Milbauer L, Abdulla F, Alayash AI, et al. Heme triggers TLR4 signaling leading to endothelial cell activation and vaso-occlusion in murine sickle cell disease. *Blood* (2014) 123(3):377–90. doi: 10.1182/blood-2013-04-495887
4. Schaer DJ, Buehler PW, Alayash AI, Belcher JD, Vercellotti GM. Hemolysis and free hemoglobin revisited: exploring hemoglobin and hemin scavengers as a novel class of therapeutic proteins. *Blood* (2013) 121(8):1276–84. doi: 10.1182/blood-2012-11-451229
5. Belcher JD, Chen C, Nguyen J, Abdulla F, Zhang P, Nguyen H, et al. Haptoglobin and hemopexin inhibit vaso-occlusion and inflammation in murine sickle cell disease: Role of heme oxygenase-1 induction. *PLoS One* (2018) 13(4):e0196455. doi: 10.1371/journal.pone.0196455
6. Muller-Eberhard U, Javid J, Liem HH, Hanstein A, Hanna M. Plasma concentrations of hemopexin, haptoglobin and heme in patients with various hemolytic diseases. *Blood* (1968) 32(5):811–5. doi: 10.1182/blood.V32.5.811.811
7. Santiago RP, Guarda CC, Figueiredo CVB, Fiuza LM, Aleluia MM, Adanho CSA, et al. Serum haptoglobin and hemopexin levels are depleted in pediatric sickle cell disease patients. *Blood Cells Mol Diseases* (2018) 72:34–6. doi: 10.1016/j.bcmd.2018.07.002
8. Figueiredo RT, Fernandez PL, Mourao-Sa DS, Porto BN, Dutra FF, Alves LS, et al. Characterization of heme as activator of Toll-like receptor 4. *J Biol Chem* (2007) 282(28):20221–9. doi: 10.1074/jbc.M610737200
9. Ghosh S, Adisa OA, Chappa P, Tan F, Jackson KA, Archer DR, et al. Extracellular hemin crisis triggers acute chest syndrome in sickle mice. *J Clin Invest* (2013) 123(11):4809–20. doi: 10.1172/JCI64578
10. Lin S, Yin Q, Zhong Q, Lv F-L, Zhou Y, Li J-Q, et al. Heme activates TLR4-mediated inflammatory injury via MyD88/TRIF signaling pathway in intracerebral hemorrhage. *J Neuroinflamm* (2012) 9(1):46. doi: 10.1186/1742-2094-9-46
11. Shimazu R, Akashi S, Ogata H, Nagai Y, Fukudome K, Miyake K, et al. MD-2, a molecule that confers lipopolysaccharide responsiveness on Toll-like receptor 4. *J Exp Med* (1999) 189(11):1777–82. doi: 10.1084/jem.189.11.1777
12. Kennedy MN, Mullen GE, Leifer CA, Lee C, Mazzoni A, Dileepan KN, et al. A complex of soluble MD-2 and lipopolysaccharide serves as an activating ligand for Toll-like receptor 4. *J Biol Chem* (2004) 279(33):34698–704. doi: 10.1074/jbc.M405444200
13. Elson G, Dunn-Siegrist I, Daubeuf B, Pugin J. Contribution of Toll-like receptors to the innate immune response to Gram-negative and Gram-positive bacteria. *Blood* (2007) 109(4):1574–83. doi: 10.1182/blood-2006-06-032961
14. Fernandez PL, Dutra FF, Alves L, Figueiredo RT, Mourao-Sa D, Fortes GB, et al. Heme amplifies the innate immune response to microbial molecules through spleen tyrosine kinase (Syk)-dependent reactive oxygen species generation. *J Biol Chem* (2010) 285(43):32844–51. doi: 10.1074/jbc.M110.146076
15. Belcher JD, Zhang P, Nguyen J, Kiser ZM, Nath KA, Hu J, et al. Identification of a Heme Activation Site on the MD-2/TLR4 Complex. *Front Immunol* (2020) 11:1370. doi: 10.3389/fimmu.2020.01370
16. Kim SJ, Kim HM. Dynamic lipopolysaccharide transfer cascade to TLR4/MD2 complex via LBP and CD14. *BMB Rep* (2017) 50(2):55–7. doi: 10.5483/BMBRep.2017.50.2.011
17. Park BS, Song DH, Kim HM, Choi BS, Lee H, Lee JO. The structural basis of lipopolysaccharide recognition by the TLR4-MD-2 complex. *Nature* (2009) 458(7242):1191–5. doi: 10.1038/nature07830
18. Ohnishi H, Tochio H, Kato Z, Orii KE, Li A, Kimura T, et al. Structural basis for the multiple interactions of the MyD88 TIR domain in TLR4 signaling. *Proc Natl Acad Sci* (2009) 106(25):10260–5. doi: 10.1073/pnas.0812956106
19. Kim HM, Park BS, Kim JI, Kim SE, Lee J, Oh SC, et al. Crystal structure of the TLR4-MD-2 complex with bound endotoxin antagonist Eritoran. *Cell* (2007) 130(5):906–17. doi: 10.1016/j.cell.2007.08.002
20. Yamamoto S, Niida S, Azuma E, Yanagibashi T, Muramatsu M, Huang TT, et al. Inflammation-induced endothelial cell-derived extracellular vesicles modulate the cellular status of pericytes. *Sci Rep* (2015) 5:8505. doi: 10.1038/srep08505
21. Pugin J, Stern-Voeffray S, Daubeuf B, Matthay MA, Elson G, Dunn-Siegrist I. Soluble MD-2 activity in plasma from patients with severe sepsis and septic shock. *Blood* (2004) 104(13):4071–9. doi: 10.1182/blood-2003-04-1290

22. Wolfs TG, Dunn-Siegrist I, van't Veer C, Hodin CM, Germeraad WT, van Zoelen MA, et al. Increased release of sMD-2 during human endotoxemia and sepsis: a role for endothelial cells. *Mol Immunol* (2008) 45(11):3268–77. doi: 10.1016/j.molimm.2008.02.014
23. Sandanger O, Ryan L, Bohnhorst J, Iversen AC, Husebye H, Halaas O, et al. IL-10 enhances MD-2 and CD14 expression in monocytes and the proteins are increased and correlated in HIV-infected patients. *J Immunol* (2009) 182 (1):588–95. doi: 10.4049/jimmunol.182.1.588
24. Ohnishi T, Muroi M, Tanamoto K. The lipopolysaccharide-recognition mechanism in cells expressing TLR4 and CD14 but lacking MD-2. *FEMS Immunol Med Microbiol* (2007) 51(1):84–91. doi: 10.1111/j.1574-695X.2007.00281.x
25. Jia HP, Kline JN, Penisten A, Apicella MA, Gioannini TL, Weiss J, et al. Endotoxin responsiveness of human airway epithelia is limited by low expression of MD-2. *Am J Physiol Lung Cell Mol Physiol* (2004) 287(2): L428–37. doi: 10.1152/ajplung.00377.2003
26. Abreu MT, Vora P, Faure E, Thomas LS, Arnold ET, Arditi M. Decreased expression of Toll-like receptor-4 and MD-2 correlates with intestinal epithelial cell protection against dysregulated proinflammatory gene expression in response to bacterial lipopolysaccharide. *J Immunol* (2001) 167(3):1609–16. doi: 10.4049/jimmunol.167.3.1609
27. Mullen GE, Kennedy MN, Visintin A, Mazzoni A, Leifer CA, Davies DR, et al. The role of disulfide bonds in the assembly and function of MD-2. *Proc Natl Acad Sci U S A* (2003) 100(7):3919–24. doi: 10.1073/pnas.0630495100
28. Visintin A, Halmen KA, Latz E, Monks BG, Golenbock DT. Pharmacological inhibition of endotoxin responses is achieved by targeting the TLR4 coreceptor, MD-2. *J Immunol* (2005) 175(10):6465–72. doi: 10.4049/jimmunol.175.10.6465
29. Wu LC, Sun CW, Ryan TM, Pawlik KM, Ren J, Townes TM. Correction of sickle cell disease by homologous recombination in embryonic stem cells. *Blood* (2006) 108(4):1183–8. doi: 10.1182/blood-2006-02-004812
30. Balla J, Jacob HS, Balla G, Nath K, Eaton JW, Vercellotti GM. Endothelial-cell heme uptake from heme proteins: induction of sensitization and desensitization to oxidant damage. *Proc Natl Acad Sci U S A* (1993) 90 (20):9285–9. doi: 10.1073/pnas.90.20.9285
31. Vercellotti GM, Zhang P, Nguyen J, Abdulla F, Chen C, Nguyen P, et al. Hepatic Overexpression of Hemopexin Inhibits Inflammation and Vascular Stasis in Murine Models of Sickle Cell Disease. *Mol Med (Cambridge Mass)* (2016) 22:437–51. doi: 10.2119/molmed.2016.00063
32. Beckman JD, Abdullah F, Chen C, Kirchner R, Rivera-Rodriguez D, Kiser ZM, et al. Endothelial TLR4 Expression Mediates Vaso-Occlusive Crisis in Sickle Cell Disease. *Front Immunol* (2021) 11:613278. doi: 10.3389/fimmu.2020.613278
33. Visintin A, Mazzoni A, Spitzer JA, Segal DM. Secreted MD-2 is a large polymeric protein that efficiently confers lipopolysaccharide sensitivity to Toll-like receptor 4. *Proc Natl Acad Sci U S A* (2001) 98(21):12156–61. doi: 10.1073/pnas.211445098
34. Tissieres P, Dunn-Siegrist I, Schappi M, Elson G, Comte R, Nobre V, et al. Soluble MD-2 is an acute-phase protein and an opsonin for Gram-negative bacteria. *Blood* (2008) 111(4):2122–31. doi: 10.1182/blood-2007-06-097782
35. Conran N, Belcher JD. Inflammation in sickle cell disease. *Clin Hemorheol Microcirculation* (2018) 68(2-3):263–99. doi: 10.3233/CH-189012
36. Pitanga TN, Oliveira RR, Zanette DL, Guarda CC, Santiago RP, Santana SS, et al. Sickle red cells as danger signals on proinflammatory gene expression, leukotriene B4 and interleukin-1 beta production in peripheral blood mononuclear cell. *Cytokine* (2016) 83:75–84. doi: 10.1016/j.cyto.2016.03.016
37. Hounkpe B, Fiusa M, Colella M, da Costa LN, Benatti Rde O, Saad ST, et al. Role of innate immunity-triggered pathways in the pathogenesis of Sickle Cell Disease: a meta-analysis of gene expression studies. *Sci Rep* (2015) 5:17822. doi: 10.1038/srep17822
38. Qari MH, Dier U, Mousa SA. Biomarkers of inflammation, growth factor, and coagulation activation in patients with sickle cell disease. *Clin Appl Thromb/Hemostasis* (2012) 18(2):195–200. doi: 10.1177/1076029611420992
39. Xu H, Wandersee NJ, Guo Y, Jones DW, Holzhauer SL, Hanson MS, et al. Sickle cell disease increases high mobility group box 1: a novel mechanism of inflammation. *Blood* (2014) 124(26):3978–81. doi: 10.1182/blood-2014-04-560813
40. Guo YB, Chen LP, Cao HW, Wang N, Zheng J, Xiao GX. Polymyxin B antagonizing biological activity of lipopolysaccharide. *Chin J Traumatol = Zhonghua chuang shang za zhi* (2007) 10(3):180–3.
41. Hrkal Z, Vodrazka Z, Kalousek I. Transfer of heme from ferrihemoglobin and ferrihemoglobin isolated chains to hemopexin. *Eur J Biochem / FEBS* (1974) 43(1):73–8. doi: 10.1111/j.1432-1033.1974.tb03386.x
42. Morgan WT, Liem HH, Sutor RP, Muller-Ebergard U. Transfer of heme from heme-albumin to hemopexin. *Biochim Biophys Acta* (1976) 444(2):435–45. doi: 10.1016/0304-4165(76)90387-1
43. Smith A, McCulloh RJ. Hemopexin and haptoglobin: allies against heme toxicity from hemoglobin not contenders. *Front Physiol* (2015) 6:187. doi: 10.3389/fphys.2015.00187
44. Kaul DK, Hebbel RP. Hypoxia/reoxygenation causes inflammatory response in transgenic sickle mice but not in normal mice. *J Clin Invest* (2000) 106 (3):411–20. doi: 10.1172/JCI9225
45. Telen MJ. Cellular adhesion and the endothelium: E-selectin, L-selectin, and pan-selectin inhibitors. *Hematol Oncol Clin North Am* (2014) 28(2):341–54. doi: 10.1016/j.hoc.2013.11.010
46. Hebbel RP, Belcher JD, Vercellotti GM. The multifaceted role of ischemia/reperfusion in sickle cell anemia. *J Clin Invest* (2020) 130(3):1062–72. doi: 10.1172/JCI133639
47. Belcher JD, Mahaseth H, Welch TE, Otterbein LE, Hebbel RP, Vercellotti GM. Heme oxygenase-1 is a modulator of inflammation and vaso-occlusion in transgenic sickle mice. *J Clin Invest* (2006) 116(3):808–16. doi: 10.1172/JCI26857
48. Smith A, Morgan WT. Haem transport to the liver by haemopexin. Receptor-mediated uptake with recycling of the protein. *Biochem J* (1979) 182(1):47–54. doi: 10.1042/bj1820047
49. Alam J, Smith A. Receptor-mediated transport of heme by hemopexin regulates gene expression in mammalian cells. *J Biol Chem* (1989) 264 (30):17637–40. doi: 10.1016/S0021-9258(19)84616-1
50. Wang Y, Li T, Wu B, Liu H, Luo J, Feng D, et al. STAT1 regulates MD-2 expression in monocytes of sepsis via miR-30a. *Inflammation* (2014) 37 (6):1903–11. doi: 10.1007/s10753-014-9922-1
51. Roy S, Sun Y, Pearlman E. Interferon-gamma-induced MD-2 protein expression and lipopolysaccharide (LPS) responsiveness in corneal epithelial cells is mediated by Janus tyrosine kinase-2 activation and direct binding of STAT1 protein to the MD-2 promoter. *J Biol Chem* (2011) 286(27):23753–62. doi: 10.1074/jbc.M111.219345
52. Abreu MT, Arnold ET, Thomas LS, Gonsky R, Zhou Y, Hu B, et al. TLR4 and MD-2 expression is regulated by immune-mediated signals in human intestinal epithelial cells. *J Biol Chem* (2002) 277(23):20431–7. doi: 10.1074/jbc.M110333200
53. Park SH, Kim ND, Jung JK, Lee CK, Han SB, Kim Y. Myeloid differentiation 2 as a therapeutic target of inflammatory disorders. *Pharmacol Ther* (2012) 133 (3):291–8. doi: 10.1016/j.pharmthera.2011.11.001
54. Nagai Y, Akashi S, Nagafuku M, Ogata M, Iwakura Y, Akira S, et al. Essential role of MD-2 in LPS responsiveness and TLR4 distribution. *Nat Immunol* (2002) 3(7):667–72. doi: 10.1038/ni809
55. Wang Y, Qian Y, Fang Q, Zhong P, Li W, Wang L, et al. Saturated palmitic acid induces myocardial inflammatory injuries through direct binding to TLR4 accessory protein MD2. *Nat Commun* (2017) 8:13997. doi: 10.1038/ncomms13997
56. Han J, Zou C, Mei L, Zhang Y, Qian Y, You S, et al. MD2 mediates angiotensin II-induced cardiac inflammation and remodeling via directly binding to Ang II and activating TLR4/NF-kappaB signaling pathway. *Basic Res Cardiol* (2017) 112(1):9. doi: 10.1007/s00395-016-0599-5
57. Wang Y, Su L, Morin MD, Jones BT, Whitby LR, Surakattula MM, et al. TLR4/MD-2 activation by a synthetic agonist with no similarity to LPS. *Proc Natl Acad Sci U S A* (2016) 113(7):E884–93. doi: 10.1073/pnas.1525639113
58. Gladwin MT, Vichinsky E. Pulmonary complications of sickle cell disease. *N Engl J Med* (2008) 359(21):2254–65. doi: 10.1056/NEJMra0804411
59. Vichinsky EP, Neumayr LD, Earles AN, Williams R, Lennette ET, Dean D, et al. Causes and outcomes of the acute chest syndrome in sickle cell disease. National Acute Chest Syndrome Study Group. *N Engl J Med* (2000) 342 (25):1855–65. doi: 10.1056/NEJM200006223422502
60. Hadina S, Weiss JP, McCray PB Jr, Kulhankova K, Thorne PS. MD-2-dependent pulmonary immune responses to inhaled lipooligosaccharides:

effect of acylation state. *Am J Respir Cell Mol Biol* (2008) 38(6):647–54. doi: 10.1165/rcmb.2007-0418OC
61. Sundd P, Gladwin MT, Novelli EM. Pathophysiology of Sickle Cell Disease. *Annu Rev Pathol* (2019) 14:263–92. doi: 10.1146/annurev-pathmechdis-012418-012838
62. Owusu-Ansah A, Ihunnah CA, Walker AL, Ofori-Acquah SF. Inflammatory targets of therapy in sickle cell disease. *Trans Res J Lab Clin Med* (2016) 167 (1):281–97. doi: 10.1016/j.trsl.2015.07.001
63. Rice TW, Wheeler AP, Bernard GR, Vincent JL, Angus DC, Aikawa N, et al. A randomized, double-blind, placebo-controlled trial of TAK-242 for the treatment of severe sepsis. *Crit Care Med* (2010) 38(8):1685–94. doi: 10.1097/CCM.0b013e3181e7c5c9
64. Opal SM, Laterre PF, Francois B, LaRosa SP, Angus DC, Mira JP, et al. Effect of eritoran, an antagonist of MD2-TLR4, on mortality in patients with severe sepsis: the ACCESS randomized trial. *JAMA J Am Med Assoc* (2013) 309 (11):1154–62. doi: 10.1001/jama.2013.2194
65. Gradisar H, Keber MM, Pristovsek P, Jerala R. MD-2 as the target of curcumin in the inhibition of response to LPS. *J leukocyte Biol* (2007) 82(4):968–74. doi: 10.1189/jlb.1206727
66. Chen L, Jin Y, Chen H, Sun C, Fu W, Zheng L, et al. Discovery of caffeic acid phenethyl ester derivatives as novel myeloid differentiation protein 2 inhibitors for treatment of acute lung injury. *Eur J Med Chem* (2018) 143:361–75. doi: 10.1016/j.ejmech.2017.11.066
67. Wang Y, Shan X, Chen G, Jiang L, Wang Z, Fang Q, et al. MD-2 as the target of a novel small molecule, L6H21, in the attenuation of LPS-induced inflammatory response and sepsis. *Br J Pharmacol* (2015) 172(17):4391–405. doi: 10.1111/bph.13221
68. Zhang Y, Xu T, Wu B, Chen H, Pan Z, Huang Y, et al. Targeting myeloid differentiation protein 2 by the new chalcone L2H21 protects LPS-induced acute lung injury. *J Cell Mol Med* (2017) 21(4):746–57. doi: 10.1111/jcmm.13017

Conflict of Interest: JDBec receives funding from Bayer not related to work herein. JDBel and GMV receive research funding from CSL Behring and Mitobridge (Astellas).

The remaining authors declare that the research was conducted in the absence of any commercial or financial relationships that could be construed as a potential conflict of interest.

Advantages of publishing in Frontiers

OPEN ACCESS
Articles are free to read for greatest visibility and readership

FAST PUBLICATION
Around 90 days from submission to decision

HIGH QUALITY PEER-REVIEW
Rigorous, collaborative, and constructive peer-review

TRANSPARENT PEER-REVIEW
Editors and reviewers acknowledged by name on published articles

Frontiers
Avenue du Tribunal-Fédéral 34
1005 Lausanne | Switzerland

Visit us: www.frontiersin.org
Contact us: frontiersin.org/about/contact

REPRODUCIBILITY OF RESEARCH
Support open data and methods to enhance research reproducibility

DIGITAL PUBLISHING
Articles designed for optimal readership across devices

FOLLOW US
@frontiersin

IMPACT METRICS
Advanced article metrics track visibility across digital media

EXTENSIVE PROMOTION
Marketing and promotion of impactful research

LOOP RESEARCH NETWORK
Our network increases your article's readership